



Stéphanie Pereira Oliveira

**Serotonergic signaling modulation as a  
therapeutic strategy for Machado-Joseph  
disease: finding the molecular traits**

**Universidade do Minho**  
Escola de Medicina







**Universidade do Minho**

Escola de Medicina

Stéphanie Pereira Oliveira

**Serotonergic signaling modulation as a  
therapeutic strategy for Machado-Joseph  
disease: finding the molecular traits**

Tese de Doutoramento

Doutoramento em Envelhecimento e Doenças Crónicas

Trabalho efetuado sob a orientação da

**Doutora Andreia Cristiana Teixeira de Castro**

e da

**Professora Doutora Ana Luísa Monteiro de  
Carvalho**

## **DIREITOS DE AUTOR E CONDIÇÕES DE UTILIZAÇÃO DO TRABALHO POR TERCEIROS**

Este é um trabalho académico que pode ser utilizado por terceiros desde que respeitadas as regras e boas práticas internacionalmente aceites, no que concerne aos direitos de autor e direitos conexos.

Assim, o presente trabalho pode ser utilizado nos termos previstos na licença abaixo indicada.

Caso o utilizador necessite de permissão para poder fazer um uso do trabalho em condições não previstas no licenciamento indicado, deverá contactar o autor, através do RepositóriUM da Universidade do Minho.



**Atribuição-NãoComercial-SemDerivações**  
**CC BY-NC-ND**

<https://creativecommons.org/licenses/by-nc-nd/4.0/>



## Agradecimentos/Acknowledgments

---

*Things always seem impossible until they are done.*

Uma tese de doutoramento é uma longa caminhada cheia de desafios e de muita aprendizagem. Cada contributo foi indispensável e, por esta razão, gostaria de expressar o meu sincero agradecimento a todos os que de alguma forma contribuíram para a realização deste trabalho. • À Andreia Castro, pela orientação, pela confiança e pela paciência, desde o primeiro dia (muito antes deste doutoramento). Pelo entusiasmo e honestidade com que fazes investigação, pelas ideias, espírito crítico e rigor, pelos valores que transmites e porque arranjas sempre uma maneira e uma solução. • À Professora Ana Luísa Carvalho, por ter aceitado orientar este trabalho e por me ter recebido no seu laboratório, dando-me a oportunidade de aprender novas técnicas. • Ao PhD e à coordenadora deste programa na Escola de Medicina (EM) da Universidade do Minho (UM), Professora Margarida Correia Neves, por todo o apoio. • À Professora Patrícia Maciel, pelo acompanhamento, sugestões e incentivos ao longo destes anos. À Sara Silva, pela inabalável disponibilidade e amabilidade, por me introduzires ao mundo das “ratices” e pelo auxílio em tudo no laboratório. À Marta Costa, pela simplicidade e companhia nos cafés (e chocolates), pelo tempo para tirar uma dúvida e dar-me uma sugestão. Ao Jorge Silva, pela tua alegre personalidade, sempre em grande estilo, e pela partilha de conhecimento. Às “pessoas da serotonina”, Joana Sousa, Bruna Lomba, André Mira, Cármen Vieira, pela partilha e cooperação nesta aventura. À Daniela Garcia, Daniela Monteiro, Joana Correia, Jorge Fernandes, Daniela Campos, pela disponibilidade em ajudar, sempre! À Andreia Carvalho, pelas inúmeras dicas. A todos os (ex-)membros do lab, Bruno Almeida, Catarina Ferreira, Liliana Costa, Ana Bela Campos, Ana Jalles, Anabela Silva, Carlos Bessa, Fátima Lopes, Liliana Santos, com quem aprendi e continuo a aprender. À Sofia Neves, pela ajuda na análise de dados e pelas sugestões. Aos NeRDs, pelo bom ambiente e comentários construtivos! Aos funcionários/técnicos da EM, em especial à Manuela Carneiro, Goreti Pinto e Eduarda Correia. To Jian Li, for all the help kindly provided. • Aos meus amigos: à Ana e à Sónia, por todos os momentos e pelo incentivo ao longo de todos estes anos; à Aurélie, porque provas que a distância geográfica não significa nada; à Isabel, ao Ricardo, à Liliana, ao André, à Flávia e às pequenas traquinas, uma segunda família, obrigada pelas aventuras partilhadas. • Aos meus pais, a quem devo tudo o que sou, pelo amor, pela compreensão e suporte incondicional, porque sempre acreditaram em mim, e as minhas vitórias são também vossas; ao meu avô (*Papi*) que, onde quer que esteja, sei que está a olhar por mim. • Ao Joel, por seres o companheiro de todos os momentos. Pelas horas infundáveis passadas comigo durante a escrita da tese a ajudar-me, pelo apoio técnico/gráfico imprescindível também. Por dizeres incansavelmente: “Vais conseguir!”. Por ouvires todos os meus desabafos, por teres sempre uma nova perspetiva e me arrancares as melhores gargalhadas. Por seres o meu porto-seguro. Por todo o amor, carinho, paciência... Esta tese também é tua!

## Funding

---

The work presented in this thesis was performed in the Life and Health Sciences Research Institute (ICVS), University of Minho. Financial support was provided by grants from the Portuguese Foundation for Science and Technology (FCT): Inter-University Doctoral Programme in Ageing and Chronic Disease fellowship (PD/BD/127818/2016) to S. Oliveira; and by FEDER, through the Competitiveness Internationalization Operational Programme (POCI) under the scope of the project POCI-01-0145-FEDER-031987 to A. Teixeira-Castro, supported by North Portugal Regional Operational Programme (NORTE 2020), under the PORTUGAL 2020 Partnership Agreement, through the European Regional Development Fund (ERDF); and by National funds, through the FCT - project UIDB/50026/2020 and UIDP/50026/2020. This work was also funded through the National Ataxia Foundation (NAF), USA, and by the U.S. Department of Defense (DoD) - grant award number: W81XWH-19-1-0638.



## **STATEMENT OF INTEGRITY**

I hereby declare having conducted this academic work with integrity. I confirm that I have not used plagiarism or any form of undue use of information or falsification of results along the process leading to its elaboration.

I further declare that I have fully acknowledged the Code of Ethical Conduct of the University of Minho.

## **Modulação da sinalização serotoninérgica como estratégia terapêutica para a doença de Machado-Joseph: à procura dos determinantes moleculares**

---

### **Resumo**

A doença de Machado-Joseph (DMJ) é uma doença autossômica dominante incurável, de início tardio. Caracteriza-se por uma expansão de repetições do triplete CAG no gene *MJD1/ATXN3*, que origina proteínas com conformação nativa alterada, promovendo agregação e perda neuronal. É uma doença incapacitante, tendo grande impacto económico e social, sendo urgente o desenvolvimento de terapias.

Nesta tese, procurámos estudar o potencial terapêutico da modulação da sinalização serotoninérgica pelo citalopram, um inibidor seletivo da recaptção da serotonina (ISRS), e dos seus mecanismos de ação na DMJ. Investigou-se se o tratamento com citalopram iniciado pós-sintomaticamente seria eficaz em ratinhos transgênicos da DMJ. Observámos que este melhorou a função motora, apesar deste ser menos eficaz que o tratamento pré-sintomático, mostrando impacto limitado na agregação da ATXN3 e na neuroproteção. Para identificar determinantes moleculares subjacentes à supressão da proteotoxicidade via sinalização serotoninérgica, foi realizada uma análise transcriptómica no estriado de ratinhos CMVMJD135 tratados pré-sintomaticamente. Verificou-se uma alteração na sinalização serotoninérgica neste modelo, envolvendo o receptor 5-HT<sub>1A</sub> e respetivas vias de sinalização, incluindo a proteína de ligação ao elemento de resposta cAMP - CREB, que poderá ser relevante na patogénese e no tratamento desta doença. Também se observou que o citalopram altera os níveis de expressão de genes relacionados com o controlo de qualidade proteico (CQP) e vias auxiliares (ex., degradação, manutenção da conformação e resposta antioxidante), melhorando a homeostase proteica. Estes dados foram corroborados num modelo genético em *C. elegans* com neurotransmissão serotoninérgica aumentada, via ablação do transportador de serotonina *mod-5* em nematodes que expressam a ATXN3 mutante. Foi observada uma recuperação total do perfil transcriptómico dos animais mutantes, confirmando-se este gene como um modificador genético da DMJ em *C. elegans*. Demonstrou-se ainda a ativação de respostas de defesa e de CQP (ex., via lisossomal e autofagia) nestes animais duplos mutantes, incluindo algumas vias comuns a animais com longevidade aumentada.

Resumindo, demonstrou-se que a modulação serotoninérgica foi protetora na DMJ mesmo após início dos sintomas, constituindo o citalopram uma estratégia promissora a ser avaliada em ensaios clínicos humanos. Este trabalho também levantou a hipótese duma alteração na transmissão serotoninérgica na DMJ e apontou vias candidatas que contribuem para o efeito benéfico da modulação desta sinalização em contrabalançar os efeitos proteotóxicos mediados pela ATXN3 mutante.

**Palavras-chave:** citalopram, Doença de Machado-Joseph (DMJ), proteotoxicidade, serotonina

## **Serotonergic signaling modulation as a therapeutic strategy for Machado-Joseph disease: finding the molecular traits**

---

### **Abstract**

Machado-Joseph disease (MJD) is an autosomal dominantly inherited late onset disorder with no disease-modifying treatment available. It is characterized by an expansion of the CAG repeat in the *MJD1/ATXN3* gene, triggering the appearance of misfolded protein species, leading to aggregation and neuronal loss. It is an incapacitant disease, requiring full-time care of the patient, with consequent strong economic and social impact, being urgent to find to new therapies to improve patients' quality of life.

In this thesis, we aimed at further addressing the therapeutic potential of serotonergic signaling modulation by citalopram treatment, a selective serotonin reuptake inhibitor (SSRI), and to uncover its mechanism(s) of action in MJD. We investigated whether post-symptomatic citalopram treatment initiation in MJD transgenic mice would show efficacy. We observed that it still improved motor behavior, although not as strongly as pre-symptomatic treatment, with limited impact on ATXN3 aggregation and neuroprotection. To find the molecular determinants underlying serotonergic signaling-mediated suppression of proteotoxicity, a transcriptomic analysis of the striatum of pre-symptomatically citalopram- and vehicle-treated MJD mice was performed. Results indicated that serotonergic signaling is altered in MJD mice and that the serotonin 5-HT<sub>1A</sub> receptor and its signal-transduction pathways, including the cAMP response element-binding protein (CREB) transcription factor, could be relevant in MJD pathogenesis and treatment. It showed that citalopram can alter the levels of several protein quality control (PQC)-related genes and auxiliary pathways (e.g., degradation, folding, and antioxidant response), enhancing proteostasis capacity. This was further confirmed by RNA-sequencing of a genetic *C. elegans* model of increased serotonergic neurotransmission, in which the serotonin transporter *mod-5* was ablated in the background of MJD pathology, mimicking citalopram action. This ablation rescued the transcriptomic profile of mutant ATXN3 animals, establishing *mod-5* as genetic modifier of MJD in *C. elegans*. Activation of defense responses and PQC-related machinery (e.g., lysosomal pathway and autophagy) were observed in double mutant animals, a subset of which are also found in long-lived animals.

In summary, this work demonstrated that modulation of serotonergic signaling protected against MJD pathogenesis even after symptom onset, evidencing citalopram as a promising therapeutic compound to be evaluated in human clinical trials. It also raised the hypothesis of an altered serotonergic transmission in the disease and suggested candidate pathways which contribute to the beneficial effect of serotonergic signaling modulation in offsetting mutant ATXN3-mediated proteotoxicity.

**Keywords:** citalopram, Machado-Joseph disease (MJD), proteotoxicity, serotonin

## Table of Contents

---

Direitos de Autor e Condições de Utilização do Trabalho por Terceiros.....	ii
Agradecimentos/Acknowledgments .....	iii
Statement of Integrity .....	iv
Resumo.....	v
Abstract.....	vi
Table of Contents .....	vii
List of Abbreviations .....	xi
List of Figures.....	xiii
List of Tables.....	xv
Thesis Outline .....	xvii
<b>Chapter 1: General introduction .....</b>	<b>1</b>
1.1 Neurodegenerative diseases .....	2
1.2 Polyglutamine disorders.....	3
1.3 Machado-Joseph disease (MJD) or Spinocerebellar ataxia type 3 (SCA3).....	6
1.3.1 Clinical presentation and pathological features .....	7
1.3.2 MJD genetic origin .....	10
1.3.3 Ataxin-3 (ATXN3): the MJD protein .....	11
1.3.3.1 ATXN3 activity, functions, and molecular interactions .....	12
1.3.4 MJD pathogenic mechanisms .....	14
1.3.4.1 Protein misfolding as a central feature in MJD pathogenesis .....	14
1.3.4.2 Toxicity-mediating mechanisms in MJD .....	15
1.3.5 Animal models of MJD pathogenesis.....	26
1.3.6 Therapeutic approaches and clinical trials .....	36
1.4 Serotonergic system in the brain.....	46
1.4.1 Serotonergic signaling.....	48
1.4.2 Serotonin signaling in the treatment of depression.....	55
1.4.3 Selective Serotonin Reuptake Inhibitors (SSRIs): mode of action .....	56
1.4.3.1 The specific case of citalopram .....	56
1.4.4 Serotonergic signaling in the context of neurodegenerative disorders.....	57
1.5 Aims of the thesis.....	59
References .....	61

<b>Chapter 2: Preclinical evidence supporting early initiation of citalopram treatment in Machado-Joseph disease</b> .....	109
Supplementary data.....	123
Manuscript published in <i>Molecular Neurobiology (Mol Neurobiol</i> 56, 3626–3637 (2019))	
<b>Chapter 3: Finding the molecular determinants of serotonergic signaling modulation in a mouse model of MJD</b> .....	129
<b>Chapter 3.1: Possible role of the dysregulation of the serotonin 1A receptor signaling in MJD pathogenesis and its reestablishment by citalopram treatment</b> .....	131
Abstract.....	133
1. Introduction.....	134
2. Materials and methods .....	135
2.1 Animal research: ethics statement .....	135
2.2 Mouse samples: transgenic mouse model maintenance and drug administration .....	136
2.3 RNA sequencing (RNA-seq) of mouse striatum.....	137
2.4 RNA-seq analysis .....	138
2.5 Quantitative Reverse Transcriptase PCR (qRT-PCR).....	138
2.6 Nematode strains and general methods .....	139
2.7 Generation of <i>C. elegans</i> mutant and double mutant strains .....	140
2.8 Chronic treatment of the nematodes with citalopram (drug assay) .....	142
2.9 <i>C. elegans</i> motility assay.....	143
2.10 Statistical analysis .....	143
3. Results .....	144
3.1 Transcriptomic analysis of mouse MJD model reveals alterations in serotonergic signaling. 144	
3.2 Alterations in genes associated to <i>5-HT<sub>1A</sub>R</i> transduction pathways upon citalopram chronic treatment.....	148
3.3 Possible role of CREB transcriptional program in citalopram-mediated suppression of ATXN3-mediated pathogenesis .....	152
4. Discussion.....	156
5. Conclusion .....	160
Final considerations.....	160
Acknowledgments.....	160
Funding.....	161
References .....	162

<b>Chapter 3.2: Exploring the modulation of protein homeostasis by citalopram chronic treatment in a MJD mouse model</b> .....	173
Abstract.....	175
1. Introduction.....	176
2. Materials and methods.....	178
2.1 Transcriptomic data.....	178
2.2 Transcriptomic data analysis: protein quality control (PQC) network.....	179
3. Results.....	180
3.1 Gene expression changes of components of the core of the PQC network in MJD mice and upon citalopram treatment.....	180
3.2 Gene expression changes of stress responses auxiliary to the PQC network in MJD mice and upon citalopram treatment.....	186
3.3 Involvement of CREB transcription program in citalopram-induced alterations of the PQC machinery.....	188
4. Discussion.....	190
5. Conclusions.....	194
Final considerations.....	194
Acknowledgments.....	195
Funding.....	195
References.....	196
Supplementary data.....	207

<b>Chapter 4: Serotonin transporter ablation restores the transcriptomic profile and induces protective responses in a <i>C. elegans</i> MJD model</b> .....	210
Abstract.....	212
1. Introduction.....	213
2. Materials and methods.....	214
2.1 <i>C. elegans</i> strains and generation of double mutants.....	214
2.2 Worm preparation for RNA extraction.....	216
2.3 RNA extraction.....	217
2.4 Transcriptomic analysis by RNA-sequencing.....	217
2.5 Transcriptomic data: gene, phenotype and tissue enrichment analyses.....	218
2.6 Transcriptomic data analysis: protein quality control (PQC); suppressors and enhancers of polyQ aggregation and CREB targets.....	219
3. Results.....	219

3.1 <i>C. elegans</i> serotonin transporter ablation restores the transcriptomic profile of mutant ATXN3-expressing worms resembling WT animals.....	219
3.2 Serotonin signaling modulation triggers protective responses in ATXN3 mutant animals .....	223
3.3 Alterations in proteome homeostasis-related genes are induced by <i>mod-5</i> serotonin transporter ablation in a <i>C. elegans</i> model of MJD.....	229
3.4 Serotonin transporter <i>mod-5</i> ablation in ATXN3 background alters the expression level of polyQ aggregation regulators.....	232
3.5 CREB role in <i>mod-5</i> ablation-induced proteostasis in ATXN3 mutant animals .....	234
4. Discussion.....	236
5. Conclusions.....	240
Acknowledgments.....	240
Funding.....	241
References .....	242
Supplementary data.....	248
<b>Chapter 5: General discussion and future perspectives</b> .....	250
5.1 Citalopram as a valid therapeutic approach: preclinical trials' design and lessons .....	251
5.2 RNA-sequencing as a tool to explore cellular mechanisms: general and technical considerations .....	257
5.3 Serotonergic signaling in MJD: a new perspective.....	261
5.4 Serotonergic signaling modulation by citalopram in MJD: mode of action .....	263
5.4.1 Serotonergic signaling modulation by citalopram in MJD: protein homeostasis and neuroprotection .....	268
5.5 Serotonin signaling modulation in MJD: future perspectives.....	271
References .....	273
<b>Annexes</b> .....	282
Annex I: Ethical approval for the use of animal models in research by the University of Minho (Parecer da Subcomissão de Ética para as Ciências da Vida e da Saúde) .....	283



## List of Abbreviations

---

<b>5-HT:</b> Serotonin	<b>ERAD:</b> Endoplasmic Reticulum-Associated Degradation
<b>5-HT<sub>1A</sub>R:</b> 5-HT <sub>1A</sub> Receptor	<b>ERK:</b> Extracellular signal-Regulated Kinase
<b>AC:</b> Adenylyl Cyclase	<b>FC:</b> Fold Change
<b>AD:</b> Alzheimer's Disease	<b>FDA:</b> Food and Drug Administration
<b>ALS:</b> Amyotrophic Lateral Sclerosis	<b>FDR:</b> False Discovery Rate
<b>ANOVA:</b> Analysis of Variance	<b>FELASA:</b> Federation of European Laboratory Animal Science Associations
<b>ARRIVE:</b> Animal Research: Reporting of <i>In Vivo</i> Experiments	<b>FTD:</b> Frontotemporal Dementia
<b>ASOs:</b> Antisense Oligonucleotides	<b>GEA:</b> Gene Enrichment Analysis
<b>ATXN3:</b> Ataxin-3	<b>GFP:</b> Green Fluorescent Protein
<b><i>C. elegans:</i></b> <i>Caenorhabditis elegans</i>	<b>GIRK:</b> G protein-coupled Inwardly Rectifying Potassium
<b>CAG:</b> Cytosine-Adenosine-Guanine	<b>GLM:</b> Generalized Linear Model
<b>cAMP:</b> Cyclic Adenosine Monophosphate	<b>GO:</b> Gene Ontology
<b>CBD:</b> Corticobasal Degeneration	<b>GP:</b> Globus Pallidus
<b>CBP:</b> CREB-Binding Protein	<b>GPCRs:</b> G Protein-Coupled Receptors
<b>cDNA:</b> Complementary DNA	<b>HD:</b> Huntington's Disease
<b>CGC:</b> <i>Caenorhabditis</i> Genetics Center	<b>HDAC:</b> Histone Deacetylase
<b>CNS:</b> Central Nervous System	<b>HSF1:</b> Heat Shock Factor 1
<b>CREB:</b> cAMP Response Element-Binding protein	<b>HSPs:</b> Heat Shock Proteins
<b>CRISPR:</b> Clustered Regularly Interspaced Short Palindromic repeats	<b>HSR:</b> Heat Shock Response
<b>CSF:</b> Cerebrospinal Fluid	<b>ID:</b> Identification
<b>CTRL:</b> Control	<b>IPA:</b> Ingenuity Pathway Analysis
<b>DEGs:</b> Differentially Expressed Genes	<b>iPSCs:</b> Induced Pluripotent Stem Cells
<b>DN:</b> Dentate Nucleus	<b>KO:</b> Knockout
<b>DNA:</b> Deoxyribonucleic Acid	<b>LB:</b> Luria Broth
<b>DR:</b> Dorsal Raphe	<b>LCN:</b> Lateral Cuneate Nucleus
<b>DRPLA:</b> DentatoRubral-Pallidolusian Atrophy	<b>MAOIs:</b> Monoamine Oxidase Inhibitors
<b>DUB:</b> Deubiquitylating enzyme	<b>MAPK:</b> Mitogen-Activated Protein Kinases
<b>ER:</b> Endoplasmic Reticulum	

**MDD:** Major Depressive Disorder

**MDS:** Multidimensional Scaling Analysis

**MJD:** Machado-Joseph Disease

**MOA:** Mechanism of Action

**MR:** Median Raphe

**MRI:** Magnetic Resonance Imaging

**mRNA:** Messenger RNA

**MSA:** Multiple System Atrophy

**NES:** Nuclear Export Signals

**NGM:** Nematode Growth Medium

**NLS:** Nuclear Localization Signal

**OCD:** Obsessive-Compulsive Disorder

**p300:** E1A binding protein

**PCR:** Polymerase Chain Reaction

**PD:** Parkinson's Disease

**PDE:** Phosphodiesterase

**PEA:** Phenotype Enrichment Analysis

**PI3K:** Phosphoinositide 3-Kinase

**PKA:** Protein Kinase A

**PLC:** Phospholipase C

**PN:** Pontine Nucleus

**PolyQ:** Polyglutamine

**PQC:** Protein Quality Control

**PSP:** Progressive Supranuclear Palsy

**qRT-PCR:** Quantitative Reverse-Transcriptase Polymerase Chain Reaction

**RN:** Red Nucleus

**RNA:** Ribonucleic Acid

**RNAi:** Ribonucleic Acid interference

**RNA-seq:** Ribonucleic Acid sequencing

**ROS:** Reactive Oxygen Species

**RQI:** RNA Quality Indicator

**RT:** Room Temperature

**SBMA:** Spinal and Bulbar Muscular Atrophy

**SCAs:** Spinocerebellar Ataxias

**SCAx:** Spinocerebellar Ataxia type x

**SD:** Standard Deviation

**SEM:** Standard Error of the Mean

**SERT:** Serotonin Transporter

**shRNA:** Short hairpin Ribonucleic Acid

**sHsp:** Small Heat shock protein

**siRNA:** Small interference Ribonucleic Acid

**SN:** Substantia Nigra

**ssODN:** Single-stranded Oligodeoxynucleotide

**SSRI:** Selective Serotonin Reuptake Inhibitor

**STN:** Subthalamic Nucleus

**STR:** Striatum

**SUMO:** Small Ubiquitin-related Modifier

**TCAs:** Tricyclic Antidepressants

**TEA:** Tissue Enrichment Analysis

**Tg:** Transgenic

**TPR:** Tetratricopeptide Repeat

**UPR:** Unfolded Protein Response

**Ub:** Ubiquitin

**UIMs:** Ubiquitin-Interacting Motifs

**UPR<sup>mt</sup>:** Unfolded Protein Response of the mitochondria

**UPS:** Ubiquitin-Proteasome System

**WT:** Wild-Type

**YFP:** Yellow Fluorescent Protein

## List of Figures

---

### Chapter 1: General introduction

Figure 1.1 Overview of the main features of different neurodegenerative disorders .....	3
Figure 1.2 Polyglutamine (polyQ) disease proteins .....	5
Figure 1.3 Brain regions classically affected in MJD .....	9
Figure 1.4 Ataxin-3 protein architecture .....	11
Figure 1.5 Molecular mechanisms and cellular pathways of ATXN3-mediated pathogenesis .....	20
Figure 1.6 Serotonergic system and effects in the organism .....	47
Figure 1.7 Serotonergic system of the mouse brain .....	48

### Chapter 2: Preclinical evidence supporting early initiation of citalopram treatment in Machado-Joseph disease

Figure S2.1 CMVMJD135hi transgenic mice show defects in motor coordination and balance at 10 weeks of age .....	125
Figure S2.2 No effect of chronic post-symptomatic citalopram treatment in CMVMJD135hi mice foot dragging .....	126
Figure S2.3 Vehicle-treated and not citalopram-treated CMVMJD135hi mice present increased phenotype severity related to higher (CAG) <sub>n</sub> repeat length .....	126
Figure S2.4 Impact of citalopram post-symptomatic treatment on ATXN3 aggregation and ChAT- and NeuN-positive cells in CMVMJD135hi mice .....	127
Figure S2.5 Impact of post-symptomatic citalopram treatment of CMVMJD135hi mice on brain ATXN3 protein levels .....	128

### Chapter 3.1: Possible role of the dysregulation of the serotonin 1A receptor signaling in MJD pathogenesis and its reestablishment by citalopram treatment

Figure 3.1.1 Different mRNA expression profile between groups in the striatum of MJD mice .....	145
Figure 3.1.2 Expression profile of CMVMJD135 transgenic (Tg) mice is altered upon citalopram treatment .....	146
Figure 3.1.3 Serotonergic signaling and other pathways alterations in transgenic mice and upon citalopram chronic treatment .....	147
Figure 3.1.4 Serotonin receptor <i>Htr1a</i> /5-HT <sub>1A</sub> R gene expression is altered in CMVMJD135 mice and restored upon citalopram treatment .....	149
Figure 3.1.5 Citalopram-induced molecular alterations in the 5-HT <sub>1A</sub> R transduction signaling pathways in MJD transgenic mice .....	151
Figure 3.1.6 Presence of CREB target genes in the mouse striatum transcriptomic analysis .....	153

Figure 3.1.7 Citalopram is dependent on CREB/CRH-1 transcription factor to improve motility on ATXN3 animals.....	156
---	-----

**Chapter 3.2: Exploring the modulation of protein homeostasis by citalopram chronic treatment in a MJD mouse model**

Figure 3.2.1 Components of the degradation branch of the protein quality control (PQC) network show altered expression in the striatum of MJD transgenic mice, mostly upon citalopram treatment .....	183
---	-----

**Chapter 4: Serotonin transporter ablation restores the transcriptomic profile and induces protective responses in a *C. elegans* MJD model**

Figure 4.1 Deletion of <i>mod-5</i> in Q130 worms alters their transcriptome to become more similar to WT .....	221
Figure 4.2 Substantial and contrasting changes in transcript expression are observed in WT <i>vs</i> Q130 and Q130 <i>vs mod-5</i> ; Q130 comparisons.....	222
Figure 4.3 Organism defense responses are altered in ATXN3 animals and upon serotonin transporter ablation .....	224
Figure 4.4 Modulation of different responses by serotonin transporter <i>mod-5</i> ablation .....	225
Figure 4.5 Alterations in worm phenotype triggered by ATXN3-mediated proteotoxicity and serotonin signaling modulation.....	227
Figure 4.6 Alterations in worm tissues triggered by ATXN3-mediated proteotoxicity and serotonin signaling modulation.....	228
Figure 4.7 Representativity of the protein quality control (PQC) machinery in the <i>C. elegans</i> transcriptomic analysis .....	230
Figure 4.8 Representativity of the CREB targets in the transcriptomic analysis.....	235
Figure S4.1 Contrasting alterations in the expression of the common genes between WT <i>vs</i> Q130 and Q130 <i>vs mod-5</i> ; Q130 comparisons.....	249

**Chapter 5: General discussion and future perspectives**

Figure 5.1 Model for serotonergic-signaling modulation by citalopram in MJD models .....	267
--	-----

## List of Tables

---

### Chapter 1: General introduction

Table 1.1 PolyQ-associated diseases: molecular and clinical features.....	4
Table 1.2 Principal MJD subtypes according to symptoms, prevalence, and age of onset .....	8
Table 1.3 MJD animal models: <i>C. elegans</i> , <i>Drosophila melanogaster</i> and <i>Danio rerio</i> (Zebrafish) ...	33
Table 1.3 (continued) MJD animal models: mouse ( <i>Mus musculus</i> ).....	34
Table 1.3 (continued) MJD animal models: mouse ( <i>Mus musculus</i> ), rat ( <i>Rattus norvegicus</i> ) and marmoset ( <i>Callithrix jacchus</i> ).....	35
Table 1.4 Clinical (interventional) trials for MJD or that include MJD patients .....	43
Table 1.4 (continued) Clinical (interventional) trials for MJD or that include MJD patients .....	44
Table 1.5 Overview of serotonin receptors .....	49

### Chapter 2: Preclinical evidence supporting early initiation of citalopram treatment in Machado-Joseph disease

Table S2.1 Age at which phenotypic differences are first detected in CMVMJD135 and CMVMJD135hi mice.....	125
--	-----

### Chapter 3.1: Possible role of the dysregulation of the serotonin 1A receptor signaling in MJD pathogenesis and its reestablishment by citalopram treatment

Table 3.1.1 List of primers used for the determination of gene expression by qRT-PCR .....	139
Table 3.1.2 Primers used for <i>crh-1</i> mutation screening.....	141
Table 3.1.3 <i>C. elegans</i> strains used in this study .....	142
Table 3.1.4 List of a subset of CREB target genes found in the transcriptomic analysis .....	154

### Chapter 3.2: Exploring the modulation of protein homeostasis by citalopram chronic treatment in a MJD mouse model

Table 3.2.1 List of a subset of the DEGs found in the different PQC core categories, according to each comparison analyzed .....	184
Table 3.2.2 List of the DEGs found in the different PQC accessory pathways, according to each comparison analyzed .....	187
Table 3.2.3 Proportion of PQC components that are also CREB targets in the mouse transcriptomic analysis .....	189
Table S3.2.1 List of the DEGs found among all RNA-seq comparison analyzed belonging to the different PQC accessory pathways .....	208

## **Chapter 4: Serotonin transporter ablation restores the transcriptomic profile and induces protective responses in a *C. elegans* MJD model**

Table 4.1 <i>C. elegans</i> strains used in this study .....	215
Table 4.2 Primers used for <i>mod-5</i> mutation screening.....	216
Table 4.3 List of the DEGs found in the different PQC categories, according to the main comparisons performed .....	231
Table 4.4 List of known regulators of polyQ aggregation showing differential expression in our dataset .....	233

## Thesis Outline

---

The present dissertation is organized in 6 chapters. The first chapter is the general introduction, followed by four chapters corresponding to the experimental work conducted, in the format of research articles. The manuscript presented in chapter 2 is published, while sub-chapters 3.1, 3.2 and chapter 4 are *in preparation*. Chapter 5 is the general discussion of the work.

**Chapter 1.** Before addressing the aims of this dissertation, an overview of MJD is provided, describing the present understanding of the disease from a clinical to a molecular perspective. A description of the existing animal models is presented, mechanisms of disease and therapeutic strategies are provided, as well as clinical trials performed and/or still ongoing for this disease. In a second part, an overview of the serotonergic system is presented, including a description of serotonergic signaling players. Lastly, we describe the impact of the modulation of the serotonergic system by antidepressants, namely of selective serotonin reuptake inhibitors (SSRIs) in the context of neurodegenerative diseases, focusing on previous work of our laboratory that shows a striking therapeutic impact of pre-symptomatic citalopram treatment on MJD animal models, establishing the premise for the current dissertation.

**Chapter 2.** In this chapter, the work entitled "*Preclinical evidence supporting early initiation of citalopram treatment in Machado-Joseph disease*" is presented. It describes a preclinical trial performed to assess the effect of citalopram post-symptomatic treatment on the motor performance and neuropathology of the CMVMJD135 MJD mouse model. A cohort of animals with higher CAG repeat number and consequent increased severity and faster disease progression was evaluated, to better mimic the clinical context of symptom-driven diagnosis and treatment initiation. Citalopram administration after symptom installation ameliorated motor coordination and balance, still mitigating disease progression, although the therapeutic effect was less pronounced when compared to pre-symptomatic treatment initiation. Limited impact on aggregation and neuroprotection was observed, with increased cerebellar calbindin staining and increased number of motor neurons and of NeuN-positive cells in certain brain regions upon treatment, however not reaching statistical significance. The results obtained further confirmed the potential of this treatment to be applied in the clinical context of MJD and perhaps other neurodegenerative diseases, suggesting that early intervention would be an ideal approach.

**Chapter 3.** This chapter under the theme "*Finding the molecular determinants of serotonergic signaling modulation in a mouse model of MJD*" is sub-divided in two (sub-chapters 3.1 and 3.2), aiming at understanding which molecule(s) and signaling pathway(s) are essential for the positive impact of

serotonergic signaling modulation in the CMVMJD135 mouse model through transcriptomic (RNA-sequencing) analysis.

**Chapter 3.1** entitled *“Possible role of the dysregulation of the serotonin 1A receptor signaling in MJD pathogenesis and its reestablishment by citalopram treatment”* describes a transcriptomic analysis, using RNA-sequencing, performed in the striatum of CMVMJD135 mice pre-symptomatically treated with vehicle or citalopram. This analysis revealed a basal dysregulation in serotonergic signaling of CMVMJD135 mice, mediated by the 5-HT<sub>1A</sub>R, supported by a decrease in the expression of this receptor in transgenic mice, which was restored to wild-type (WT) levels upon citalopram treatment. Alterations in the expression of several components of 5-HT<sub>1A</sub>R transduction signaling pathways were also observed, pointing to a possible involvement of the cAMP-response-element binding protein (CREB) in the mechanism of action of citalopram in MJD.

**Chapter 3.2.** This sub-chapter, entitled *“Exploring the modulation of the protein homeostasis by citalopram chronic treatment in a MJD mouse model”*, is an extension of the RNA-seq data analysis conducted in sub-chapter 3.1, focusing on the proteostasis alterations triggered by the chronic administration of citalopram in CMVMJD135 mice. The analysis revealed that core modules of the protein quality control (PQC) network, such as degradation and folding/conformational maintenance, as well as PQC auxiliary pathways, including the antioxidant response, are modulated by citalopram. Additionally, several genes associated to those modules/pathways are identified as CREB targets, which reinforces the idea that the effects of citalopram could be mediated through this transcription factor.

**Chapter 4.** In this last section of results, entitled *“Serotonin transporter ablation restores the transcriptomic profile and induces protective responses in a C. elegans MJD model”*, a genetic approach was taken to further unveil the molecular determinants underlying serotonergic signaling-mediated suppression of proteotoxicity. For this, ablation of the serotonin transporter SERT/MOD-5 in the background of mutant ATXN3-expressing nematodes was performed, genetically mimicking citalopram-mediated serotonin recapture inhibition. Strikingly, the transcriptomic analysis (RNA-seq) showed that *mod-5* ablation restored the transcriptomic profile of mutant expressing ATXN3 animals to that of WT. Moreover, protection and PQC-related responses were triggered by this serotonin signaling modulation, overlapping with the results observed in previous chapters in the mouse model.

**Chapter 5.** This chapter integrates a discussion of the results obtained throughout this thesis describing the relevance of our findings to the field, as well as the advantages and limitations of the experiments conducted, and envisaging future perspectives.



# Chapter 1

---

## General introduction

## 1.1 Neurodegenerative diseases

Life expectancy has been increasing globally and, for the first time, most people can expect to reach their sixties and beyond [1]. For all living creatures, ageing is a challenging process and Humans are no exception to that. The organism reaches a certain point where damage in cells increase, sub products of the metabolism accumulate, and cellular mechanisms of repair become less reliable, making the organism more susceptible to disease. Among those age-related conditions, are the neurodegenerative diseases, that affect millions of people worldwide [2]. Nowadays, these disorders represent a critical economic and social burden, mostly due to their irreversibility, their impact on emotional and social dimensions (for the patient and for the family), and the lack of effective treatment [3].

Neurodegenerative diseases include a wide range of conditions which primarily affect neurons, leading to their loss-of-function and progressive cell death in the central nervous system (CNS). Examples of the most common disorders of this category are Alzheimer's disease (AD), Parkinson's disease (PD), Huntington's disease (HD), frontotemporal dementia (FTD), amyotrophic lateral sclerosis (ALS), progressive supranuclear palsy (PSP), corticobasal degeneration (CBD) and multiple system atrophy (MSA) (generally described in [2, 4]). These disorders vary in their pathophysiology and can affect cognition, memory, movement, and other abilities. They can be hereditary or sporadic and despite their diverse clinical manifestations, they share common mechanisms and features (Figure 1.1).

Two major features define neurodegenerative diseases: i) the deposition of cytosolic and nuclear proteins, also known as misfolded proteins, into inclusions and/or plaques, related to abnormal processing [5]; and ii) the loss of specific neurons, that are thought to be more vulnerable, in different brain regions, generating the characteristic clinical manifestation of each disease. In order to understand this neurodegenerative process, several biological models have been created, *in vivo* and *in vitro*, with the ultimate goal to find new therapeutic strategies to be used [6]. Despite those efforts and the current knowledge, the molecular mechanisms underlying each of these disorders remain mostly unclear and we still lack effective treatment for the patients.

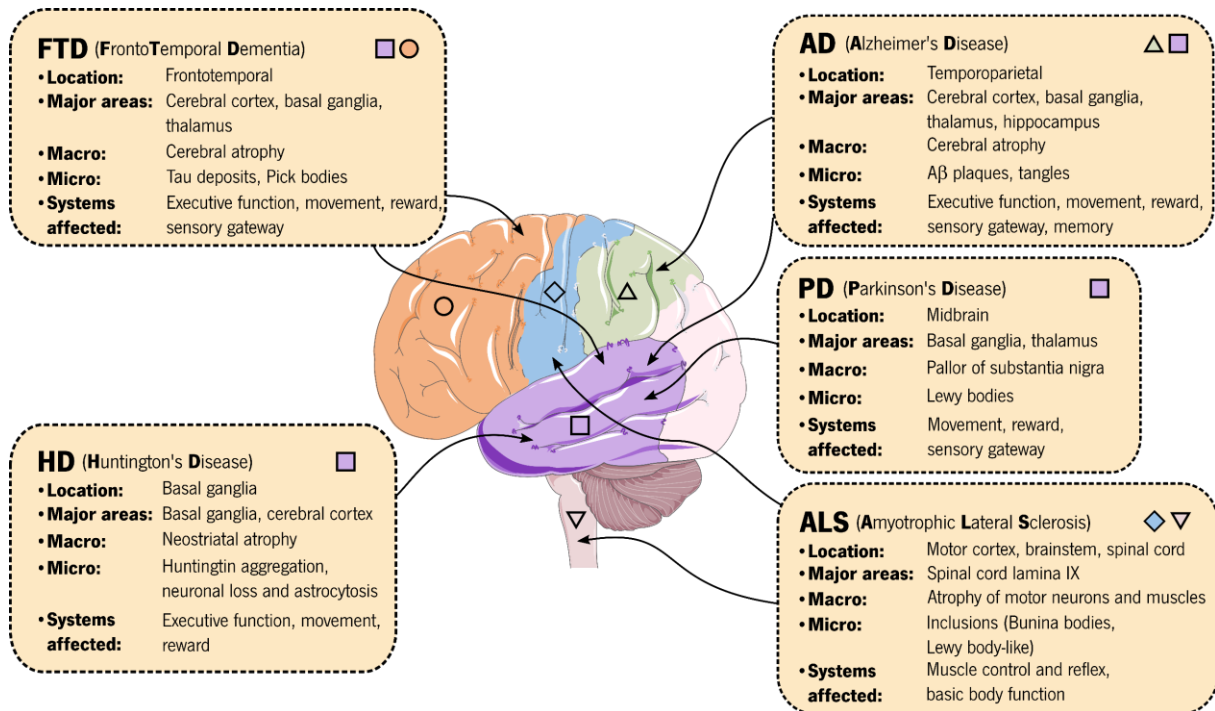


**Figure 1.1 Overview of the main features of different neurodegenerative disorders.** Brief description of several neurodegenerative disorders in terms of major affected brain regions, macro- (Macro) and micro- (Micro)scopic alterations, and systems/circuits affected related to them. Note that the pathological characterization of the diseases represented is more complex than depicted here. Based on [7, 8].

## 1.2 Polyglutamine disorders

Polyglutamine (polyQ) disorders are a family of nine late-onset progressive neurodegenerative conditions that are caused by the expansion of the cytosine-adenosine-guanine (CAG) triplet repeat within the coding regions of the disease-associated genes, producing expanded glutamine tracts in the expressed protein [9]. The first condition connected to a CAG repeat expansion was the spinal and bulbar muscular atrophy (SBMA) or Kennedy's disease, in 1991 [10]. PolyQ disorders include eight other pathologies: HD [11], dentatorubral-pallidoluysian atrophy (DRPLA) [12, 13] and several spinocerebellar ataxias (SCAs), SCA 1, 2, 3 (or Machado-Joseph disease - MJD), 6, 7, and 17, as described in Table 1.1 [14-20].

Those disorders are rare and their impact is unequal to their prevalence, which is estimated to be between 1 to 10 cases per 100 000 people [21]. Among them, HD is the best studied and the most prevalent, ranging from 10.6 to 13.7/100 000 individuals in western populations [22], followed by SCA3. Worldwide, the prevalence of the SCA family combined is estimated to be 1 to 5 in 100 000 persons, depending on geographic localization [23, 24]. Although SCA3 is rare globally (1-2/100 000 individuals), it represents 15-45 % of SCAs in different countries and ethnicities [25, 26].

**Table 1.1 PolyQ-associated diseases: molecular and clinical features.** Based on [27-29].

Disease	Gene (Locus)	Protein	Normal CAG repeat #	Pathological CAG repeat #	Function	Most affected areas	Clinical manifestations
DRPLA	<i>ATN1</i> (12p13.31)	Atrophin-1	3-38	49-88	Transcriptional corepressor	Cerebellum, red nucleus, globus pallidus, subthalamic nucleus, cerebral cortex	Ataxia, chorea, dementia, myoclonic epilepsy
HD	<i>HTT</i> (4p16.3)	Huntingtin	6-35	36-121	Likely scaffold protein, signaling, transcription, cellular trafficking	Striatum, cerebellar cortex	Dystonia, chorea, dementia
SBMA	<i>AR</i> (Xq12)	Androgen receptor	6-36	38-70	Steroid-hormone receptor	Spinal cord, brainstem	Muscular atrophy, weakness, bulbar palsy, fasciculations, gynecomastia
SCA1	<i>ATXN1</i> (6p22.3)	Ataxin-1	6-34	39-88	Chromatin binding factor, transcriptional corepressor	Cerebellum, brainstem	Ataxia, spasticity, bulbar palsy, polyneuropathy, cognitive impairment
SCA2	<i>ATXN2</i> (12q24.12)	Ataxin-2	14-31	32-77	RNA metabolism	Cerebellum, brainstem	Ataxia, polyneuropathy, parkinsonism, slow saccades
SCA3 /MJD	<i>ATXN3</i> (14q32.12)	Ataxin-3	12-40	55-86	Deubiquitylating enzyme	Cerebellum, brainstem, basal ganglia, spinal cord	Ataxia, dysarthria, spasticity, dystonia, diplopia, polyneuropathy
SCA6	<i>CACNA1A</i> (19p13.13)	Calcium voltage-gated channel subunit $\alpha 1A$	4-18	21-33	Calcium channel	Cerebellum	Ataxia, down-beating nystagmus, dysarthria
SCA7	<i>ATXN7</i> (3p14.1)	Ataxin-7	7-18	38-200	Transcription (SAGA complex)	Cerebellum, retina, brainstem, visual cortex	Ataxia, ophthalmoplegia, retinal degeneration
SCA17	TBP (6q27)	TATA-box-binding protein	25-43	45-63	Transcription factor	Cerebellum, striatum	Ataxia, seizures, extrapyramidal signs, dementia, psychosis

All polyQ pathologies are inherited in an autosomal dominant form, except for SBMA, which is X-linked. The proteins associated to these diseases lack sequence similarity, other than the polyQ tract, and are not related to each other being different in size and in the polyQ location within the protein (Figure 1.2). They are expressed in the CNS and in peripheral tissues, each one of them originating a specific neurodegeneration pattern [30, 31]. Expansion of CAG tracts over the pathogenic threshold are unstable

across generations, changing in size when transmitted from parents to offspring, phenomena known as generational instability or meiotic instability. Furthermore, the generational instability seems to be sensitive to the gender of the parents. It is frequent to observe that maternal meiosis leads to contractions of CAG tracts, in contrast with the paternal one which leads to expansions [32]. Variations in CAG tract length within the different tissues of the same individual can also occur (phenomenon called somatic mosaicism or mitotic instability), and are thought to be the result of cellular proliferation and differentiation during early development of the individual or later on during ageing [33]. Intergenerational instability underlies anticipation, or the earlier onset of disease manifestations in succeeding generations, with increased severity of symptoms, characteristic of polyQ diseases [34-36]. This association of a certain polyQ repeat length threshold, that is necessary for disease penetrance, and the inverse correlation between the age at disease onset and CAG repeat length point towards the expansion of the trinucleotide repeat as the primary driver of neurodegeneration [37]. Of notice, it has recently been reported that the size of the uninterrupted CAG repeat itself, excluding the non-CAG coded polyQ, drives HD onset [38].

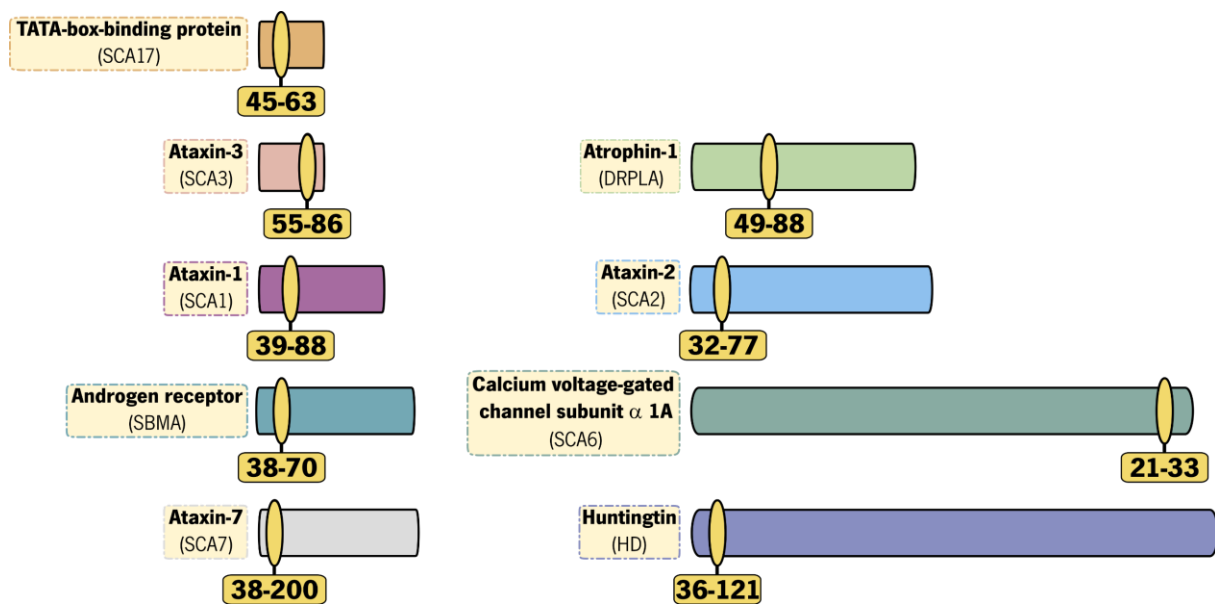


**Figure 1.2 Polyglutamine (polyQ) disease proteins.** The causative proteins of the nine polyQ diseases are represented, their relative size compared to other polyQ proteins is depicted in addition to the relative localization of the CAG/polyQ repeat tract (yellow marker) within the protein, with the pathological repeat range associated to each disease. Based on [28, 31].

It is believed that the expanded polyQ domain highly contributes to the toxic properties of the proteins involved in polyQ diseases. In fact, the presence of polyQ expansions and the absence of cases associated with deletions or point mutations in the polyQ-associated genes (except in the atypical case of SCA6 [39]) replicating the polyQ disease, suggest that these disorders do not result from a pure

loss-of-function, but rather arise from a gain of toxic function. Moreover, the presence of polyQ expansions in several functionally unrelated genes is another compelling argument of a toxic gain-of-function disease. This hypothesis is endorsed by several other lines of evidence, including the fact that null mice for several of these proteins are embryonic lethal (as for huntingtin mice) or do not display characteristic features of these disease [40-42].

### **1.3 Machado-Joseph disease (MJD) or Spinocerebellar ataxia type 3 (SCA3)**

The 1970s marked the start of the Machado-Joseph disease history. It was first described among three families of Azorean (Portuguese) descent in the United States of America (Machado - Thomas - Joseph families). William Machado, of Portuguese/Azorean ancestry, was the first patient described by Nakano and collaborators, in 1972, as having an *autosomal dominant ataxia*, which they named *Machado disease* [43]. In the same year, Woods and Schaumburg described the Thomas family, whose symptomatology was very similar to the first description, but with some additional features, which they named *Nigro-spino-dentatal degeneration with nuclear ophthalmoplegia* [44]. Four years later, an *autosomal dominant striatonigral degeneration* was described by Rosenberg and colleagues, as a new genetic disorder in the family of Antone Joseph [45]. It was not until 1978 that Coutinho and Andrade, by studying 40 patients among 15 families in the Azores Islands, evidenced that the previous descriptions could be a single genetic disease, with variable phenotypic expression [46]. Later on, the same authors proposed, for the first time, the name Machado-Joseph disease (MJD) for the clinical entity encompassing the phenotypes previously described and introduced a criteria for its diagnosis [47]. MJD was defined as a single entity with high clinical variability, and three clinical types were defined, grouping all the variability observed. The union was totally achieved in 1983-84, when among the patients examined by Rosenberg and Barbeau, siblings showed characteristics of different types of MJD [48, 49].

Today, MJD is also known as spinocerebellar ataxia type 3 (SCA3) and although it is rare, its known to exist worldwide as the most common form of dominant spinocerebellar ataxia. Its relative frequency among other SCAs is variable. A higher frequency has been reported in Portugal (49 %) [50], Germany (42-50 %) [51, 52], the Netherlands (44 %) [24], Brazil (ranging from 44 % [53] to 92 % in specific regions [54]), Chinese mainland (49 %) [55] and Japan (43 %) [56]. A lower relative frequency was observed in France (33 %) [57], the United Kingdom (15 %) [58], Australia (12 %) [59] and the United States of America (21 %) [60]; even more rare in Italy (1 %) [61] and India (< 3 %) [62].

Within each country the geographic distribution of MJD is heterogenous. For example, in Portugal, MJD is relatively rare in the mainland (1:100 000) [63] with some exceptions, as the Tagus River Valley

with 1 case per 1 000 habitants [64]. However, it is highly present in the Azores Islands, where 1 per 239 habitants are affected in Flores Island, being the highest prevalence worldwide [65].

### **1.3.1 Clinical presentation and pathological features**

The discovery of MJD demonstrates the difficulty of defining a disease into a single entity when a wide range of symptoms are hallmarks of the pathology. The central clinical feature of MJD is progressive ataxia caused by dysfunction of the cerebellum and the brainstem. The average age of onset is around 40 years and survival after disease ranges from 21 to 25 years [66], with preservation of the intellectual functions [46]. Ataxia is never the unique characteristic. MJD is a multisystem pathology and several other clinical problems are a reflection of the progressive dysfunction of the brainstem, pyramidal and extrapyramidal pathways, oculomotor system, lower motor neurons and peripheral nerves [67]. MJD patients usually present progressive ataxia (lack of voluntary coordination of muscle movement), ophthalmoplegia (paralysis or weakness of the eye muscles), spasticity (stiff muscles, preventing normal movement), dystonia (involuntary contraction of the muscles), dysarthria (difficulty with speech articulation and with swallowing due to muscle weakness). Some patients present twitching (fasciculation) of the face or tongue and/or bulging eyes [46, 47, 49].

Based on the phenotypic variability of MJD, an organization in disease sub-types was proposed, sorted by the age of clinical onset and major symptoms presented [47], as summarized in Table 1.2 for the most common ones. **MJD type I** includes early onset forms of the disease, with faster disease progression and severe extrapyramidal and pyramidal signs, such as dystonia. **MJD type II** is characterized by an intermediate age at onset, with moderate progression rate and patients predominantly exhibiting ataxia and ophthalmoplegia. This is the most frequent form of MJD. **MJD type III** include the latest age at onset, slow disease progression and more peripheral signs. **MJD type IV** was added in 1983 by Rosenberg, being the rarest form of the disease and includes patients with Parkinson's symptoms in association to other characteristic symptoms of MJD [48, 68]. **MJD subtype V** was proposed by Sakai and Kawakami, in 1996, by observation of two siblings presenting spastic paraplegia without cerebellar ataxia [69].

Clinical presentation and age of onset correlates with CAG repeat length [35]. Other non-motor symptoms have been reported in MJD patients, such as sleep disorders [70, 71], mood disorders (mostly depression and anxiety) [72, 73], olfactory malfunction [74], chronic pain [75], cramps [76, 77], fatigue [78] and nutritional problems [79, 80], the latter being associated with dysphagia (difficulty in swallowing) only in late disease stages.

**Table 1.2 Principal MJD subtypes according to symptoms, prevalence, and age of onset.** Based on [47, 48, 68, 81].

MJD subtype	Age of onset (years)	Prevalence	Clinical manifestations
I	10-30	Typical in patients with long repeats	Ataxia, severe dystonia, ophthalmoplegia, spasticity, pyramidal signs, faster disease progression
II	20-50	Most frequent	Ataxia, cerebellar pyramidal signs, ophthalmoplegia
III	40-70	Second most frequent	Cerebellar signs, peripheral neuropathy, ophthalmoplegia, slow disease progression
IV	38-47	Rare (typical in patients with short CAG repeat expansions)	Prominent parkinsonism responsive to L-DOPA, fasciculations, peripheral neuropathy

Pathological evaluation of *post-mortem* brain tissue from MJD patients revealed neuronal degeneration in specific areas of the brain (Figure 1.3), namely in the cerebellar dentate nucleus, substantia nigra, globus pallidus, subthalamic nucleus, brainstem oculomotor nuclei (III) and other select cranial nerve nuclei (IV, VI, VIII and XI), red and pontine nucleus, spinal cord (anterior spinocerebellar tract, anterior horn and Clarke's column), and the nucleus ambiguus and dorsal nucleus of the vagus nerve can also be affected [82-87]. However, conflicting results have been observed regarding the inferior olivary nucleus and Purkinje cells [88-90]. Later, a series of pathoanatomical studies, using thick serial brain tissue slices allowing the observation of more cells per section and thus revealing subtle pathological changes, exposed widespread neurodegeneration in the thalamus, cerebellum, pons, midbrain, medulla oblongata and spinal cord [91-98]. This pattern of neurodegeneration included the vestibular, visual, auditory, somatosensory, ingestion-related, dopaminergic, and cholinergic systems, correlated with clinical findings and helped to explain the variety of MJD symptoms observed in patients.

The weight of MJD patient brains, with a disease span over 15 years, was found to be considerably reduced in comparison to healthy individuals (without medical record of neurological or psychiatric diseases) [99]. In accordance, magnetic resonance imaging (MRI)-based and other neuroimaging studies have shown significant atrophy and other abnormalities of the cerebellum, brainstem, putamen, caudate, frontal and temporal lobes, vermis, basal ganglia, pons and spinal cord [100-102]. A more recent study showed that pre-symptomatic patients had white matter microstructural abnormalities mostly in the cerebellar and cerebral peduncles, as well as a reduction in the volume of the midbrain, spinal cord and substantia nigra [103]. Moreover, after assessing disease progression, the same authors found that the initial stages of MJD would be characterized by cerebellar peduncles, substantia nigra and spinal cord damage, followed by brainstem and basal ganglia involvement in an intermediated stage, ending with the manifestation of cerebellar cortex damage in final stages of the disease. The same effect on cerebellum and basal ganglia was reported in another longitudinal study, although progressive spinal cord



abnormalities were not detected [104]. Regarding brain functionality/metabolism, glucose hypometabolism was observed in the occipital/temporal cortex, vermis, brainstem, cerebellum, thalamus, putamen, and striatum, suggesting the presence of neuronal and axonal dysfunction within these brain regions in MJD [105-109].

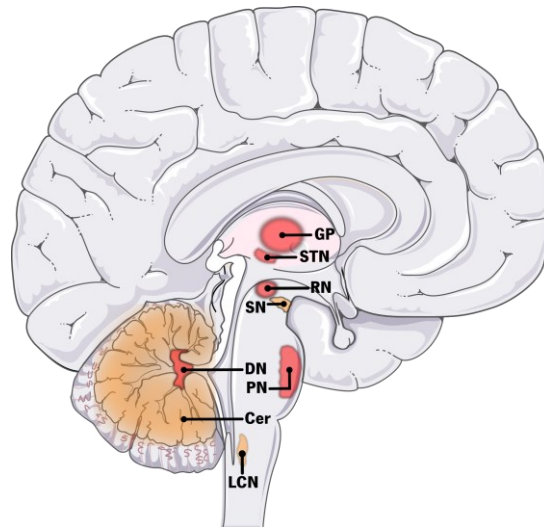


**Figure 1.3 Brain regions classically affected in MJD.** Red indicates severe/selective neuronal loss; orange indicates moderate/variable cell loss. GP - globus pallidus; STN - subthalamic nucleus, RN - red nucleus; SN - substantia nigra; DN - dentate nucleus; PN - pontine nucleus; Cer - cerebellar cortex; LCN - lateral cuneate nucleus. Based on [110].

As it happens with other polyQ diseases, one of the hallmarks of MJD is the presence of neuronal ataxin-3 (ATXN3) ubiquitylated inclusions. Mutant ataxin-3 aggregation is mostly described to be intranuclear [111]. Nevertheless, widespread axonal aggregates were found in fiber tracts known to undergo neurodegeneration in MJD, the aggregates or inclusions being ubiquitylated and immunopositive for the proteasome- and autophagy-associated protein p62 [112]. Inside inclusions other components have been discovered such as proteasomal proteins, molecular chaperones, transcription factors, besides normal and expanded ATXN3 [113-115]. Further detailed analysis, however, demonstrated the presence of ATXN3 inclusions in degenerated and spared brain areas of MJD patients [86, 96-98, 113] and MJD mouse models [116-118], pointing to a lack of correlation between their occurrence and the pattern of neurodegeneration [86, 96, 97, 113]. Additionally, an inverse correlation between the frequency of intranuclear inclusions and neurodegeneration was observed in the brainstem of MJD patients, suggesting a possible protective role for such structures [119].

### 1.3.2 MJD genetic origin

MJD, as other polyQ disorders, is inherited in an autosomal dominant manner and is caused by a mutation in the *MJD1/ATXN3* gene, localized in the long arm of the chromosome 14 (14q32.1) [120]. Cloning of the gene was achieved in 1994, one year after its mapping, by Kawaguchi and colleagues [17].

*MJD1/ATXN3* gene is about 48 kb and was first described to be composed by 11 exons [121]. Two others exons were described in 2010, in a total of 13 exons, and this gene harbors the (CAG)<sub>n</sub> tract in exon 10 [122]. After the identification and cloning of the gene, MJD molecular diagnosis became possible. The presence of the mutation was confirmed in families of different origins and, as expected, the expanded CAG tract (mutation) was detected only in patients [35, 123]. In healthy individuals, CAG repeat numbers range from 12 to 44 repeats, whereas expanded alleles, with full disease penetrance, range between 52 to 86 repeats [64, 124, 125]. Persons carrying intermediate CAG repeat numbers, between 45 to 51, may or may not manifest the disease [64, 125, 126].

At least four different species of transcripts, of approximately 1.4, 1.8, 4.5 and 7.5 kb, were described to be encoded by the *MJD1/ATXN3* gene, with ubiquitous expression in human tissues (neuronal and non-neuronal), probably due to differential splicing (of exons 2, 10 and 11) and polyadenylation (at exon 11) events [121, 127]. Those four transcripts were described to be encoded by five cDNA clones: MJD1a, MJD1-1, MJD2-1, MJD5-1 and H2. MJD1a variant was the first described [17] and uses exon 10 to provide the 3'-terminal sequence [121]. MJD2-1 is equal to MJD1a variant except for a single nucleotide substitution in the exon 10 stop codon. MJD1-1 and MJD5-1 sequences only change in the size of their 3' UTR and use exon 11 as the 3'-terminal sequence [127]. In H2 variant the exon 2 is skipped [121].

A few years later, in 2010, together with the description of the two new exons, 50 new alternative splicing variants of *ATXN3* gene were found [122], suggesting a role for alternative splicing in the regulation of *ATXN3* expression, and raising the possibility that it might contribute to the MJD pathogenic process. The biological and clinical relevance of these variants remain to be fully understood. More recent studies demonstrated that, at the physiological level, alternative splicing and the presence of premature stop codons altered *ATXN3* stability, and that the different isoforms differed in their enzymatic activity, subcellular localization and in protein-protein interactions. Pathologically, the expansion of the polyQ repeats stabilized *ATXN3*, the variants showed different aggregation propensities, and functional interactions between normal and expanded *ATXN3* isoforms were also observed [128, 129].

### 1.3.3 Ataxin-3 (ATXN3): the MJD protein

#### Structure and domains

The central gene of MJD encodes for the ataxin-3 (ATXN3) protein, essentially composed by a globular N-terminal Josephin domain and a flexible C-terminal tail (Figure 1.4) [130]. The Josephin domain contains a catalytic triad of amino acids characteristic of cysteine proteases (namely papain): cysteine (C14), histidine (H119) and asparagine (N134), displaying ubiquitin protease activity [131]. Following this domain are two or three ubiquitin-interacting motifs (UIMs), according to the protein isoform. The longest isoform of ATXN3 has an approximate molecular weight of 42 kDa [17, 127]. Particularly, the most common isoform found in the brain has a third UIM localized in the C-terminal region, after the polyQ stretch [129]. The polyQ segment, located at the C-terminus of the protein, has a variable length [132]. ATXN3 proteins also harbor a conserved nuclear localization signal (NLS), which may determine its transport rate into the nucleus [131, 133]. Nuclear export signals (NES) have also been found within ataxin-3 primary structure. *In vitro* studies showed that, of the six previously predicted NES sites [131, 133], only one was weakly functional, and revealed the presence of two novel NES [134].

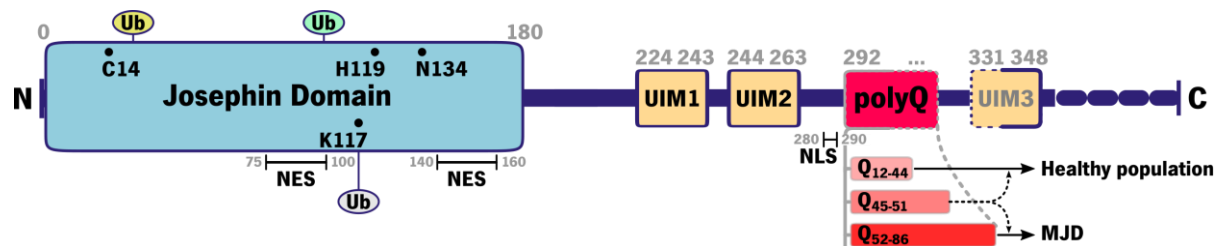


**Figure 1.4 Ataxin-3 protein architecture.** Ataxin-3 protein contains a N-terminal (N) catalytic domain, the Josephin domain (light blue), followed by a C-terminal (C) tail, composed by two or three ubiquitin-interacting motifs (UIM, yellow), depending on the isoform (dotted line). The deubiquitylating (DUB) catalytic center of the Josephin domain is represented by C14, H119 and N134 amino acids (marked with points). This domain also contains two ubiquitin (Ub) binding sites (site 1 and site 2, represented by a Ub in yellow and green, respectively). Ataxin-3 DUB activity can be enhanced by monoubiquitylation on lysine 117 (K117, marked with a point and a Ub). The polyglutamine tract (in red) can vary in the number of glutamine (Q) repeats found in healthy population and Machado-Joseph disease (MJD) carriers. In the intermediate range, people can either manifest or not the disease. NES - nuclear export signal; NLS - nuclear localization signal. Based on [135].

#### Distribution and ubiquity

ATXN3 is a protein widely distributed among eukaryotes and has been identified in plants and animals (from nematodes to vertebrates). A high level of homology has been observed between human ATXN3 and the mouse [136], rat [137], chicken [138], *C. elegans* [139], frog and *Drosophila* [140]

proteins; a lower percentage of homology was also described in plants such as rice and *Arabidopsis thaliana* [140]. This is suggestive of an evolutionary conserved function and properties, however, the polyQ expanded tract seem to be specific to primates/humans, since it is nearly absent in other species. For instance, rat, mouse and worms have three, six and no glutamines, respectively, in their ATXN3 protein homologue [136, 137, 139], indicating that this stretch could be necessary for specific acquired functions of the wild-type (WT) protein in higher species.

In humans, mice and worms, ATXN3 has a ubiquitous expression among different body tissues and cell types [113, 121, 136, 141, 142]. Wide expression throughout the brain was observed with variable expression levels in different regions [142].

Ataxin-3 is abundantly present in the cytoplasm of cells. It may also be found in the nucleus and in association with the nuclear matrix, the mitochondria and the endoplasmic reticulum (ER) [113, 133, 141-143]. As in other polyQ disorders, normal and expanded allele products were described to be equally expressed, both in lymphoblastoid cells and in the brain of MJD patients [113, 144]. Moreover, normal and mutant ATXN3 proteins were found to be expressed throughout the body and in affected and spared brain regions in MJD patients [113].

### **1.3.3.1 ATXN3 activity, functions, and molecular interactions**

A large amount of *in vitro* experimental evidence has pointed to the involvement of ATXN3 in the ubiquitin-proteasome system (UPS), leading to the important discovery of its deubiquitylating (DUB) activity [132, 145, 146]. DUBs belong to the superfamily of proteases and based on the mechanism of catalysis, they are divided into five main classes: aspartic, metallo, serine, threonine, and cysteine proteases. ATXN3 is included in the cysteine protease class, belonging to the MJD protein domain protease subclass, that includes proteins harboring a Josephin domain [147, 148]. The enzymatic activity of cysteine proteases relies on the catalytic triad of the amino acids described above (see structure and domains in the previous section) [148]. The primary role of DUBs consists in substrate deubiquitylation (i.e., cleavage of ubiquitin from proteins). Still, some research suggested that DUBs can have other functions, such as: (i) the processing of inactive ubiquitin precursors; (ii) to proofread ubiquitin-protein conjugates; (iii) to reverse ubiquitylation or ubiquitin-like modifications of target proteins, rescuing off-target proteins from the proteasome; and (iv) to disassemble unanchored ubiquitin oligomers [149-151].

The ability of ATXN3 proteins to bind and cleave polyubiquitin chains and polyubiquitylated proteins has been observed experimentally [132, 152]. Importantly, the inhibition of ATXN3 catalytic

activity led to an increase in polyubiquitylated proteins, resembling the effects of proteasome inhibition [153], indicating its involvement in protein degradation pathways. On the other hand, the expression of WT ATXN3, and not of the catalytic inactive form, reduced the ubiquitylation level of valosin-containing protein (VCP)/p97 substrates, suggesting that ATXN3 can remove ubiquitin from proteins *in vitro* [154]. The role of ATXN3 in the UPS was also supported by the observation of its interaction with the ubiquitin-like domain homologs of the yeast DNA repair protein Rad23, or human HHR23A and HHR23B [145, 155-157], and with VCP/97 [145, 154, 158] (known to be involved in the endoplasmic reticulum-associated degradation - ERAD) and with the ubiquitin ligase E4B, a ubiquitin chain assembly factor [159].

Although DUBs are habitually promiscuous, specific substrates have been reported for ATXN3, such as proteins involved in ERAD pathways. This is the case of CD3 $\delta$ , degradation of which is decreased in the presence of ATXN3, without altering the levels of other non-ERAD substrates [154]. Other specific substrates have been attributed to ATXN3 such as the  $\alpha$ 5 integrin subunit [160] and parkin [161, 162]. More recently, mediator of DNA damage checkpoint 1 (MDC1) [163], beclin-1 [164] and possibly the autophagy adaptors LC3C and GABARAP [165] were described as ATXN3 substrates, supporting a role in the DNA damage response and in the autophagic process.

Other biological functions have been proposed for ATXN3. A role in cell structure and/or motility has been demonstrated for mouse ATXN3 protein, due to its abundance in all types of muscle and in epithelial ciliated cells [136]. In accordance, ATXN3 was shown to interact with tubulin [166] and to regulate ciliogenesis and phagocytosis in the mouse/zebrafish retina, by modulation of microtubule polymerization and microtubule-dependent retrograde transport [167]. Remarkably, data obtained using *C. elegans* ATXN3, not only strengthened the argument of a possible function in structure and motility, but also pointed to an involvement in signal transduction [139]. For instance, very recently, ATXN3 was reported to impact on the dynamics of clathrin-coated pits [168], that can be important for neuronal receptors internalization [169].

A different role for the *MJD1/ATXN3* gene product concerns its possible involvement in transcription regulation. ATXN3 has been shown to regulate the expression of several genes [139, 170]. The transcriptomic analysis of two different ATXN3 knockout (KO) *C. elegans* strains in comparison to WT led to the identification of 290 differentially expressed genes that could be grouped according to their biological roles: cell structure/mobility, signal transduction, the ubiquitin-proteasome pathway, and other cell processes involving enzymes, transporters, receptors, and channels. Although there was a clear transcriptional dysregulation in the KO strains, animals were viable and presenting no obvious phenotype [139] (the same is observed in ATXN3 mice KO [41]). The presumed role of ATXN3 in transcriptional

regulation is proposed to involve the modulation of histone acetylation and deacetylation at specific promoters. In fact, ATXN3 is known to interact with three transcription activators: cAMP-response-element binding protein (CREB)-binding protein (CBP), p300 and p300/CREB-binding-associated factor (PCAF/KAT2B), through its C-terminal region, in a polyQ size-dependent manner [171]. ATXN3 also interacts with two transcription repressors: histone deacetylase 3 (HDAC3) and nuclear receptor co-repressor (NCOR1), by interaction with its UIMs [172]; and with histones H3 and H4, through the N-terminal region [171]. Consequently, it has been proposed that ATXN3 represses transcription by binding to CBP, p300 and PCAF/KAT2B co-activators or either by stopping access to histone acetylation sites (through binding of histones) or by the recruitment of HDAC3 and NCOR1 repressors [171, 172].

### **1.3.4 MJD pathogenic mechanisms**

As briefly referred in previous sections, several cellular and molecular mechanisms seem to underlie the pathology of polyQ disorders and are indicative of a toxic gain-of-function of the protein harboring an expanded polyQ tract and, in some cases, also associated with a partial loss-of-function of the disease proteins. The principal molecular mechanisms and cellular pathways thought to contribute to MJD pathogenesis (generally represented in Figure 1.5) will be more comprehensively detailed in the following pages.

#### **1.3.4.1 Protein misfolding as a central feature in MJD pathogenesis**

A common feature of polyQ diseases, including MJD, is the presence of neuronal insoluble ubiquitylated intranuclear inclusions containing the disease protein, within the neurons of affected and spared brain regions. Their discovery in MJD and other polyQ disorders suggested that protein misfolding was central to pathogenesis [31].

Ataxin-3 is a protein ubiquitously expressed in the brain, present in the cytoplasm [113] and in the nucleus of cells [141, 143, 173, 174] in association with the nuclear matrix [133]. It has also been associated with the mitochondria [142] and the ER [175]. The expansion of the polyQ tract leads to conformational alterations, which impair the proper folding of the protein [111, 176]. In accordance, mutant polyQ proteins adopted amyloid-like conformations and deposited into aggregates *in vitro* [176]. The existing knowledge of ATXN3 folding, self-assembly and aggregation is mostly based on *in vitro* studies (reviewed in [177]). A two-stage model has been proposed for ATXN3 aggregation, by Ellisdon and coworkers [178]. The first step is mediated by self-association of the Josephin domain, in both WT and polyQ-expanded ATXN3, leading to the formation of SDS-sensitive oligomers and protofibrils. The second

step is polyQ-expanded-dependent and generates long-straight, mature, and SDS-resistant ATXN3 fibrils [176, 179, 180].

Intracellular inclusions have been linked to the pathogenesis of MJD and other polyQ disorders, as a major contributor for toxicity due to their ability to sequester different molecules that have different cellular roles and could be involved in: transcription regulation [181], cellular quality control (molecular chaperones and proteasome components) and UPS [115, 182-184], axonal transport [112, 185], among other cellular processes [114]. The role of these aggregates in disease pathogenesis may, however, appear contradictory. Contributing to this is the fact that inclusions were detected in brain regions described to be affected by neurodegeneration but also in regions normally spared in the disease [86, 96, 97, 113]. In this way, the role of inclusions could be pleiotropic and even unspecific. Many authors suggested that these structures could be protective, resulting from a cellular mechanism triggered to cope with the toxicity of polyQ-expanded proteins, holding the aggregates in a restricted cellular area. There is also the possibility that aggregates are only formed or become visible when cells reach a certain level of general dysfunction or that only cells containing aggregates survive and are therefore the ones that are visible. The current understanding attributes higher toxicity to the soluble oligomers that precede the formation of inclusion bodies in the aggregation process [27, 186]. Nevertheless, it could also be that there is a precise cellular and temporal regulation of the aggregation process, during which the formation of visible inclusions precedes toxicity and cell death in some cells, while in others, aggregate formation does not occur because toxicity overrules aggregation. In spared brain regions, the aggregation process could be assisted and controlled by cellular quality control mechanisms limiting toxicity at a subthreshold level, delaying or even preventing cell dysfunction and death [187].

#### **1.3.4.2 Toxicity-mediating mechanisms in MJD**

##### ATXN3 proteolytic cleavage and other post-translational modifications

Several studies suggest that proteolytic cleavage of polyQ disease proteins into toxic polyQ-containing fragments is relevant and contributes to pathogenesis, this being referred as the *toxic fragment hypothesis* [188]. This hypothesis claims that fragment formation is required for the initiation of the aggregation process and it has been suggested that polyQ-containing fragments may translocate to the nucleus and exert toxic effects [189].

Although proteolysis can be activated in an unspecific manner during several stress responses and upon activation of death pathways, making the presence of proteolysis products often hard to interpret, proteolytic cleavage of ATXN3 has been observed in several cell and animal models as well as

in the brain of MJD patients [190-193]. ATXN3 cleavage, namely by calpains, caspases, aspartic endopeptidases and/or other enzymes, was observed to produce polyQ-bearing C-terminal fragments of around 36 kDa, having similar fragments been detected in affected brain regions of MJD patients and transgenic mice [190, 194]. In addition, the expression of C-terminal ATXN3 fragments, containing the polyQ expansion, led to strong ATXN3 aggregation and cell death [111, 191, 195, 196]. Mutant ATXN3 was shown to be a substrate for proteolytic cleavage of caspases [197, 198] (cysteine proteases that cleave proteins at specific aspartate residues [199]). However, caspase inhibitors were unable to completely stop ATXN3 fragment formation, indicating the involvement of other enzymes in this process [193, 196, 197]. Calpains, calcium-activated cysteine proteases [200], were also found to mediate ATXN3 proteolysis, generating ATXN3 fragments that contributed to aggregation and neurodegeneration and which calpastatin (a calpain inhibitor) was able to abrogate [192, 201]. Additionally, It has been demonstrated that L-glutamate-induced excitation of MJD patient-specific induced pluripotent stem cell (iPSC)-derived neurons initiated a Ca<sup>2+</sup>-dependent proteolysis of ATXN3, resulting in aggregate formation, which was abolished by calpain inhibition, further supporting the contribution of proteolytic cleavage to pathogenesis [202].

Altogether, these results suggest that ATXN3 proteolysis and the consequent formation of aggregates are important in disease pathogenesis: cleavage of the protein may increase the ability of the fragments to form toxic oligomers and/or perturb ATXN3 function and interactions, leading to the dysregulation of normal cellular mechanisms.

Besides proteolysis, other post-translational modifications of mutant ATXN3 protein have been associated to modulation of its pathogenesis. For instance, phosphorylation of ATXN3 by glycogen synthase kinase 3 $\beta$  (GSK3 $\beta$ ), at serine 256, reduced mutant ATXN3 aggregation *in vitro* [203]. The same was observed upon ATXN3 phosphorylation at serine 12, which led to a reduction of defects observed in rat neuronal cultures, as well as a suppression of aggregation, and neuronal and synapse loss, *in vitro* and *in vivo* [204]. In another study, ATXN3 stability and nuclear localization, of both normal and expanded forms, were shown to be modulated by casein kinase 2 (CK2)-dependent phosphorylation of serine 340 and 352 [205]. Ubiquitylation can also modify ATXN3, as it has been shown to enhance its enzymatic activity; both WT and expanded forms were activated by this mechanism [206]. The lysine 117 residue was identified as the main ubiquitylation site in ATXN3 and ubiquitylation of ATXN3 at this residue was important for the reduction of ubiquitylated aggregates and for the induction of aggresome formation in mammalian cells [207]. Other studies, using a *Drosophila* model, demonstrated that WT ATXN3 protein has a protective role in flies and is able to suppress neuronal degeneration induced by polyQ-expanded



proteins (including itself) [208], and that this protection was enhanced when WT ATXN3 was ubiquitylated at Lys-117, supporting the importance of ubiquitylation for regulation of its catalytic activity *in vivo* [209]. Although these studies suggested beneficial effects of the non-expanded ATXN3 allele in MJD, other works using rodent models did not support this conclusion [210, 211].

SUMOylation is a covalent and reversible connection of the small ubiquitin-related modifier (SUMO) proteins to the side chain of protein lysine residues [212]. SUMOylation of ATXN3 was observed at lysine 166 and was shown to promote an increase of mutant ATXN3 stability and cytotoxicity in cells [213]. SUMOylation, at lysine 356, of the predominantly expressed ATXN3 isoform in the brain (cDNA variants MJD1.1 and MJD5.1, isoform with 3 UIMs) promoted differences in the protein self-assembly, modulated ATXN3 affinity for VCP/p97, and decreased the percentage of cortical neurons presenting ATXN3 inclusions [214].

Although more studies are needed to further explore transglutamination (protein cross-linking between glutamine and lysine residues) in MJD [215], inhibition of transglutaminase enzymes was found to exacerbate neurotoxicity by increasing mutant ATXN3 aggregation in *Drosophila* [216]. This was unexpected as transglutamination had initially been put forward as contributing to the toxicity of polyQ proteins [217].

To date, other post-translational modifications have been associated with polyQ disease proteins, such as acetylation and palmitoylation, but no evidence has been obtained for a direct modification of this structure for ataxin-3 [218]. Other types of post-translational modifications, linked to monoamines, such as serotonylation and dopaminylation have been described but none explored in the context of polyglutamine disorders yet [219, 220].

### Proteostasis disturbance

Besides ATXN3 aggregation itself, the idea that cellular homeostasis is perturbed in MJD was also based on the observation of the sequestration of molecular chaperones and other proteostasis components into ATXN3 aggregates, which could consequently further increase protein misfolding and reduce the normal clearance of other important proteins, leading to a disequilibrium in cellular proteostasis [115, 182, 183].

**UPS dysfunction.** Alterations in the normal DUB activity of ATXN3 by the presence of an expanded polyQ tract could compromise UPS activity, resulting in inefficient degradation of misfolded proteins, as it can alter the interaction with UPS components [154, 161]. Moreover, the proteasome appears to be irreversibly recruited into polyQ aggregates, possibly “trapped” while attempting to degrade misfolded

proteins, also being unable to efficiently degrade polyQ-containing proteins due to their intrinsic properties [221]. Indeed, components of the proteasome complex were found in ATXN3 inclusions in MJD patients [182, 183]. Furthermore, UPS impairment in MJD was reinforced by the evidence that an aberrant form of ubiquitin (UBB<sup>-1</sup>) accumulates in neuronal inclusions in patients, indicating inhibition of the proteasome [222]. UPS activity was also seen to be inhibited by protein aggregation in cells with transient expression of two unrelated aggregation-prone proteins [223], culminating into cellular malfunction and possibly cellular death. Indeed, several reports showing that decreasing or impairing proteasomal activity was sufficient for neuronal death to occur [224-226]. In MJD, proteasome inhibition was also shown to cause a repeat length-dependent increase in aggregate formation in cells [182].

**Molecular chaperones.** The induction of chaperones in cellular and whole-organism models of polyQ diseases was found to modify the toxicity phenotype and to be beneficial [227-231]. Heat shock protein 70 and 40, Hsp70 and Hsp40, respectively, were shown to be associated with expanded ATXN3 inclusions in both transfected cells and in the brain of MJD patients [115]. The initial observation that molecular chaperones were sequestered into the aggregates was challenged by the discovery that there was only a transient association between chaperones and cellular inclusions [232]. Nevertheless, recent reports showed that aggregate-driven chaperone competition led to both gain- and loss-of-function phenotypes due to chaperone depletion from several client proteins, therefore impacting on multiple cellular processes [169].

**Autophagy.** Impairments in the autophagic process have been strongly linked with neurodegeneration [233]. In MJD, mutant ATXN3 has been shown to be cleared by autophagy, and activation of this pathway through temsirolimus treatment reduced the number of aggregates and levels of soluble mutant ATXN3, in mouse brains [234]. Brain tissue (putamen) analyses of MJD patients revealed abnormal immunoreactivity for autophagic markers (p62, ATg16L and LC3); also using MJD transgenic mice and a MJD lentiviral rat model, abnormal expression of autophagic markers, accumulation of autophagosomes and decreased levels of beclin-1 were detected [235]. In the rat model, stimulation of the autophagic flux by beclin-1 overexpression led to mutant ATXN3 clearance and to neuroprotection in neuronal cultures [235]. It was also shown that WT ataxin-3 deubiquitylates beclin-1, protecting it from proteasomal degradation, thus enabling the autophagic process [164]. This was mediated by the normal polyQ length tract and abolished in the presence of a longer polyQ mutation in the disease protein [164]. More recently, autophagy adaptors (LC3C and GABARAP) have been shown to interact with the Josephin domain of ATXN3, and a role in stimulation of autophagic degradation by prevention of superfluous autophagosome initiation was proposed in *C. elegans* [165]. It is not completely understood which proteins are degraded

by autophagy or the UPS, but it was recently suggested that ATXN3 isoforms lacking the third UIM (less stable) were primarily degraded by the UPS, while the ATXN3 isoform containing the third UIM was mainly degraded by autophagy [129].

#### Mitochondrial impairment and oxidative stress

Mitochondrial dysfunction has been associated with age-related diseases, particularly neurodegenerative disorders [236]. Mitochondria are known to play central functions in cells including energy (ATP) generation, maintaining intracellular  $\text{Ca}^{2+}$  homeostasis, formation of reactive oxygen species (ROS) and apoptosis. Neurons are particularly dependent on mitochondria due to their high energy demands, so it is fair to hypothesize that this type of cells are relatively vulnerable to mitochondrial dysfunction. *In vitro* studies using cellular models of MJD showed that the expression of mutant ATXN3 induced mitochondrial-mediated cell death (apoptosis), increased oxidative stress, and reduced the copy number of mitochondrial DNA, suggestive of an alteration in mitochondrial function in the disease [237-239]. In fact, the decrease in mitochondrial copy numbers was also observed in blood and brain samples of a transgenic MJD mouse model [240, 241]. Recently, it was reported that preataxic MJD patients accumulated a common mitochondrial DNA deletion and exhibited a decreased BCL2/BAX ratio, indicative of alterations in the apoptotic pathway [242].

Both normal and expanded ATXN3 proteins were found to be localized in the mitochondria besides the expected cytoplasmic and nuclear localizations. Normal ATXN3 (but not its fragments) localized in both mitochondrial matrix and membranes, while pathological ATXN3 and its cleaved fragments were present in both locations, unaggregated in membranes and presenting SDS-resistant aggregates only in the mitochondrial matrix, suggesting a potential mitochondria damaging role for these fragments [243]. More recently, studies have shown that N- and C-terminal calpain-mediated cleavage fragments may lead to a mitochondrial phenotype, independently of the polyQ tract [244, 245]. Dysfunctional mitochondria were also observed in a MJD mouse model, involving a substantial decrease in mitochondrial complex II activity, which might be at the origin of the cell death observed in disease models [246].

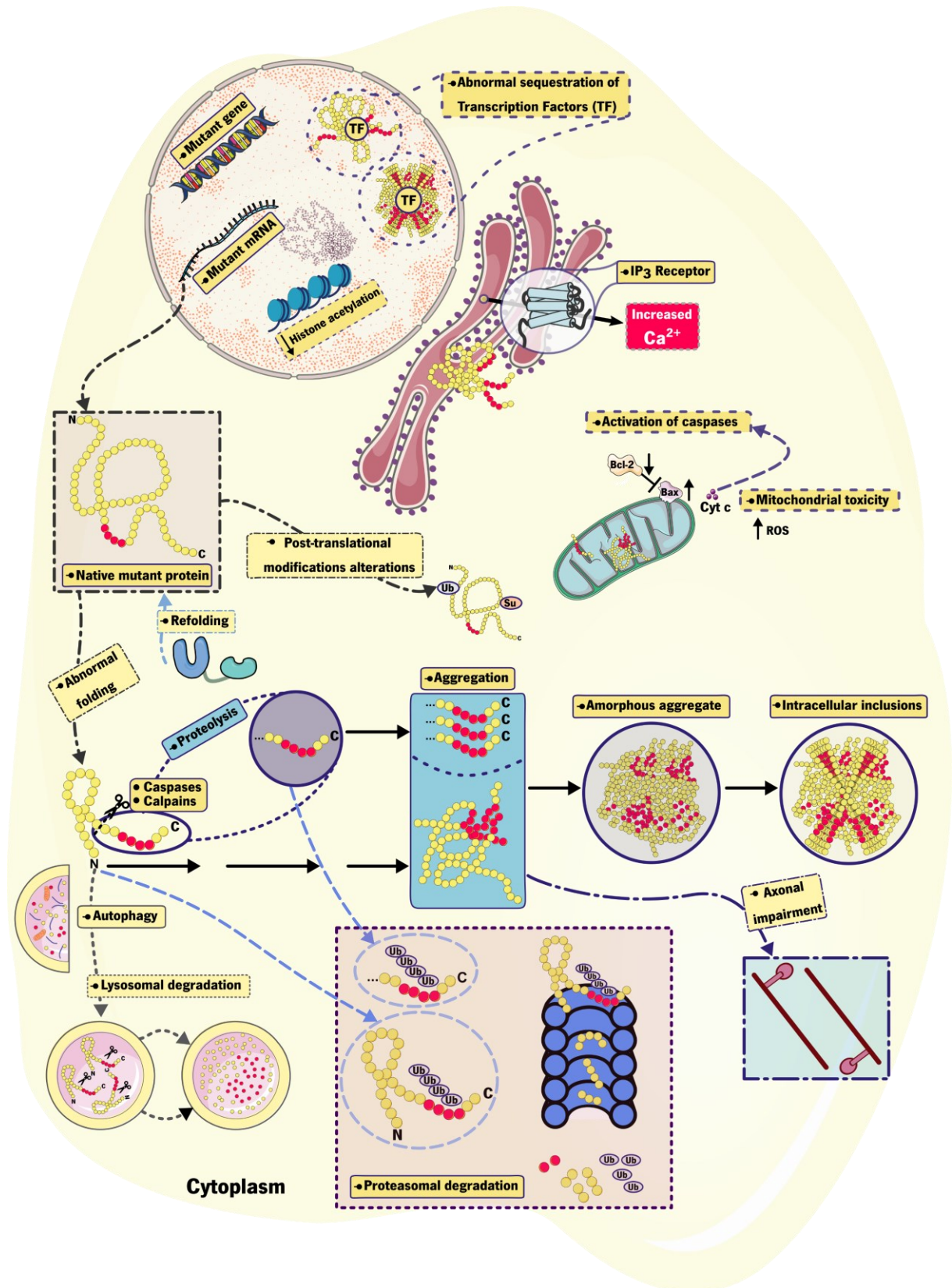


**Figure 1.5 Molecular mechanisms and cellular pathways of ATXN3-mediated pathogenesis.** The polyQ expansion in mutant ataxin-3 protein triggers several events thought to contribute to MJD pathogenesis as represented in this simplified scheme. The pathogenic process initiates with the synthesis of the native mutant ATXN3 protein containing an expanded CAG

repeat tract, altering its conformation. The cellular machinery (chaperones) actively attempts to retrieve the proper folding of the protein. Part of the abnormally folded mutant proteins can be degraded by several cellular processes (lysosomal degradation, autophagy and/or proteasomal degradation). The non-degraded fraction can suffer post-translational modifications, including protein cleavage (by the action of calpains and caspases). The full mutant protein or cleavage products can associate and aggregate, ultimately leading to the formation of intracellular inclusions, which constitute the last step of the aggregation process. Aggregates might contribute to pathology through abnormal interactions with cellular proteins or might represent a self-defense mechanism aiming at reducing the toxicity of aggregation intermediates. The presence of those fragments or inclusions can impact on several cellular mechanism. Aggregates/inclusions can translocate to the nucleus, where they can recruit transcription factors (TF), coactivators and corepressors altering transcription. In the endoplasmic reticulum, aggregation intermediates can bind inositol 1,4,5-trisphosphate receptor (IP<sub>3</sub>R) and increase calcium release into the cytoplasm. In the mitochondria, they disrupt its function, activate caspases, and lead to increased reactive oxygen species (ROS) production. Additionally, they can impair proteasomal degradation and impair axonal transport machinery.

Mutant ATXN3 has been reported to decrease the activity of antioxidant enzymes causing mitochondrial DNA damage [239]. More recently, it was shown that ATXN3 truncated forms disrupted mitochondria dynamics (reduction in membrane potential) and increased ROS levels [244]. Interestingly, ataxin-3 was shown to interact with the forkhead box O (FOXO) transcription factor FOXO4, regulating the expression of manganese superoxide dismutase (SOD2), which acts as an antioxidant enzyme [247]. Mutant ATXN3 had reduced capability to activate *SOD2* gene expression, thus limiting the response to oxidative stress. Indeed, lymphoblastoid cell lines of MJD patients showed lowered levels of SOD2, an increased ROS formation and cytotoxicity under oxidative stress [247]. Other studies in MJD subjects have shown alterations in peripheral oxidative stress biomarkers [248, 249], suggesting that this phenomenon may be relevant in the context of the disease.

### Defects on axonal transport

It has been suggested that defects in the axonal transport may contribute to the pathogenesis of polyQ diseases and other neurodegenerative disorders (reviewed in [250-252]), being an interesting hypothesis to explain neuronal vulnerability. The mechanism underlying axonal transport impairment is not completely understood but it has been proposed that (i) disease-causing proteins may have a normal function in axonal transport system and may cause blockages when mutated; (ii) protein aggregates may physically obstruct transport within axons; and (iii) disturbed organelles and cellular mechanisms, such as mitochondrial damage, may be the causative effect for axonal transport defects.

In 2010, Seidel and collaborators showed the presence of mutant ATXN3 aggregates in axons belonging to neurons from different brain regions and postulated that those could be detrimental for

axonal transport, contributing to neurodegeneration [112]. Hindrance of axonal transport was observed in a *Drosophila* model overexpressing huntingtin and ATXN3 constructs [185]; although, one year later, another study did not report any effects in axonal trafficking disruption for ATXN3, suggesting that axonal defects occurring downstream of cytoplasmic aggregate formation are probably specific to other polyQ diseases, such as HD [253]. Interestingly, ATXN3 was found to interact with dynein, which is required for aggresome formation and for the transport of misfolded proteins [154, 254]. Also, cytoskeletal disorganization was verified in cells lacking ATXN3 [255, 256] and this could be putatively reflecting altered interaction with tubulin,  $\alpha 5$  integrin or dynein, reinforcing the idea that ATXN3 plays a significant role in cytoskeleton organization, which was proven to be true in neuronal cultures [256]. Recently, a proteome analysis of a knock-in mouse model of MJD revealed the disturbance of proteins involved in cytoskeletal architecture, vesicular and axonal transport, among others, making axons as a central subcellular structure in MJD pathogenesis [257]. Therefore, over the years, a building amount of evidence has emerged and implicated axonal transport in MJD pathology.

#### Deregulation of calcium ( $\text{Ca}^{2+}$ ) homeostasis

Calcium is an important signaling ion in the cell. In neurons,  $\text{Ca}^{2+}$  homeostasis is crucial for processes like the release of neurotransmitters, synaptic structure and function, and neurite outgrowth. Disruption of the  $\text{Ca}^{2+}$  signaling may impair key cellular pathways contributing to the neurodegeneration process [258-260]. In MJD, it has been demonstrated that mutant ATXN3 specifically associates with an intracellular  $\text{Ca}^{2+}$  release channel - inositol 1,4,5-trisphosphate receptor type 1 ( $\text{InsP}_3\text{R1}$ ) - present in the endoplasmic reticulum (ER), augmenting its sensitivity towards activation by  $\text{InsP}_3$  and potentiating  $\text{Ca}^{2+}$  release from the ER [261]. Moreover, dantrolene, an inhibitor of  $\text{Ca}^{2+}$  release, administered to YACMJD84.2 MJD transgenic mice was able to improve motor coordination, gait deficits and to prevent neuronal death [261]. Also, ATXN3 aggregates increased intracellular  $\text{Ca}^{2+}$  levels in the granule neurons of rat cerebellum. Cellular interaction with ATXN3 oligomers, in this context, also involved lipid raft ganglioside GM1, glutamatergic receptors and voltage dependent calcium channels [262].

Intracellular  $\text{Ca}^{2+}$  excess can cause cell death by activation of multiple mechanisms, such as mitochondria permeabilization, oxidative stress, cytoskeletal disorganization and calcium-dependent protein activation (e.g., calpains) [263] and, as above referred, this process could be implicated in the pathogenic mechanism of MJD.

### Transcriptional regulation disturbance

There is a strong evidence for alterations in transcription that occur in polyQ diseases [264, 265]. Three main mechanisms have been suggested to underlie transcriptional dysregulation: (i) the sequestration by nuclear inclusions of transcription factors; (ii) the inhibition of acetyltransferase activity of transcription regulators and (iii) the direct suppression of the transcriptional machinery by the mutant proteins.

In MJD, the expanded ATXN3 has been shown to be involved in transcriptional perturbation, contributing to disease pathogenesis [114, 181, 266]. The ability of expanded ataxin-3 (polyQ) rich nuclear inclusions to recruit specific transcription factors, such as CBP and TATA-binding protein (TBP), has been reported [114, 171], suggesting that an altered transcription mediated by these factors might contribute to neurotoxicity. Moreover, normal and expanded ATXN3 interact with CBP, p300 and PCAF/KAT2B, inhibiting transcription, with the C-terminal part of the protein harboring the expanded polyQ tract binding more efficiently to those transcription factors than normal polyQ, indicative of a possible pathological function for ATXN3 [171]. In addition, expanded ATXN3 compared to the normal form of the protein, displayed a reduced ability to activate the FOXO4-mediated SOD2 expression during oxidative stress conditions, which led to cytotoxicity [247].

Transcription dysregulation, in a MJD mouse model, also affected the expression of proteins involved in several cellular processes such as: intracellular calcium signaling/mobilization, glutamatergic neurotransmission, MAPK pathways, GABAA/B receptor subunits, heat shock proteins, but also transcription factors regulating neuronal survival and differentiation; all of those with downregulated mRNA expression. In contrary, upregulated expression of neurodegeneration mediators (*Bax*, *Ccnd1* -cyclin D1, and *Cdk5-p39*) was also observed in ataxin-3-Q79 transgenic mice [267]. Other studies have shown transcription alterations of inflammatory and cell-surface associated proteins [170, 268].

The contribution of transcription perturbations for the initiation of the pathology is still a matter of debate. While a study reported transcriptional abnormalities in transgenic MJD animals prior to the appearance of a neurological phenotype [267], another only found major changes in transcription in old mice [269].

A study aiming at investigating the transcriptomic profiles of WT and ATXN3 null mice embryonic fibroblasts, revealed alterations in signal transduction pathways. In absence of ATXN3, they found that Eph receptor A3 (EFNA3) upregulation was connected to the hyperacetylation of histones H3 and H4 and to reduced levels of HDAC3 and NCOR [270]. Additionally, another report of transcriptional profiling of the YACMJD84.2 MJD mouse model, demonstrated that most of the mRNA expression changes

occurred in the brainstem and the striatum, with alteration in the phosphoinositide 3-kinase (PI3K) signaling cascade and cholesterol biosynthesis pathways, and in the axon guidance and synaptic transmission pathways, respectively. When combining all the brain regions under study (brainstem, cerebellum, striatum and cortex), only alterations in the  $\alpha$ -adrenergic and CREB pathways were found [271].

Evidence for a dysfunction of the endogenous microRNA system in MJD was also described. An abnormal downregulation of genes involved in microRNA biogenesis and silencing activity was reported for different biological MJD models [272], with the overexpression of certain microRNAs being beneficial to the disease.

Overall, these findings support a key role of transcriptional perturbations in the progression of the pathogenesis of this polyQ disease.

#### Involvement of the cellular localization of mutant ATXN3 in the pathogenic mechanism

The different localization of polyQ proteins in cells has been thought to be a significant factor for disease pathogenesis. Although nuclear accumulation of the mutant protein into inclusion bodies is prominently found in MJD patient studies, inclusions have also been found in the cytoplasm, namely in axons, of neurons from affected brain regions [86, 111-113, 119].

It has been suggested that a nuclear localization of ATXN3 is required for symptom manifestation *in vivo*, whereas the induced export of ATXN3 from the nucleus prevents the phenotype manifestation [173]. Since then, it has been shown that CK2-dependent phosphorylation controlled the nuclear localization of ATXN3 and that phosphorylation of ATXN3 increased the formation of nuclear inclusions [205]. More recently, the use of the HDAC inhibitor, valproic acid, was shown to rescue cytotoxicity in cell cultures expressing different constructs of human ATXN3, particularly by preventing the heat shock-dependent nuclear transport of ATXN3 [273]. Moreover, it has been shown that the KO of karyopherin alpha 3 (KPNA3), which recognizes the NLS signal within the primary sequence of ATXN3, alleviated the neurological phenotypes induced by mutant ATXN3. In fact, in mice, the absence of KPNA3 kept mutant ATXN3 in the cytoplasm, therefore preventing its aggregation [274].

Overall, it seems that favoring cytoplasmic localization of ATXN3 could help in preventing, at least, some of the deleterious effects associated to the polyQ expansion in ATXN3.



### Ageing-mediated malfunction

Ageing is the principal risk factor for neurodegenerative disorders, and it can be defined as a natural time-dependent process associated with a progressive decline of biological functions. During ageing, alterations due to the formation of secondary products of metabolism and building up of cellular damage can lead to the development of pathologies or accelerate the progression of the ones that are already present. There are nine biological hallmarks (changes) associated to ageing: genomic instability, telomere attrition, epigenetic alterations, loss of proteostasis, mitochondrial dysfunction, cellular senescence, deregulated nutrient sensing, stem cell exhaustion, and altered intercellular communication [275, 276]. Those manifest during normal ageing and their aggravation speeds up ageing, while their mitigation is likely to delay the normal aging process and increase healthspan.

In MJD, as in the ageing process, as previously mentioned, quality-control pathways, such as the UPS, molecular chaperones and autophagy are dysregulated; consequently, ageing can further contribute to the deterioration of the cell's capacity to remove misfolded proteins [277-281]. Interestingly, it has been demonstrated, in *C. elegans*, that the threshold for polyQ-expanded protein aggregation, as well as cytotoxicity, is flexible and strongly influenced by ageing [282]. Plus, the collapse of proteostasis mechanisms seems to be an early adulthood event, that certainly contributes to magnify protein damage in age-related diseases of protein conformation [283]. Besides that, studies have identified transcriptional alterations in components of mitochondrial, lysosomal degradation, inflammatory, cell cycle, cell senescence and apoptotic processes, in microarray analysis of tissues from young and older individuals from several species [284]. As detailed in previous sections, alterations in several of these processes are thought to contribute to MJD pathogenesis. For example, evidence connected neuronal death to transcriptional abnormalities in MJD transgenic mice, since altered mRNA levels of *Bax*, *Ccnd1*-cyclin D1, and *Cdk5-p39* were observed [267]. Additionally, mutant ATXN3 caused upregulation of inflammatory genes in MJD cell lines and human pontine neurons and tissues [170, 268]. Thus, transcriptional mechanisms that normally become altered with age, might already be compromised during MJD pathogenic process.

Several signaling pathways that influence ageing have been described: the insulin/insulin-like growth factor 1 (IGF-1) signaling, target of rapamycin (TOR) signaling, mitochondrial function, sirtuins and caloric restriction [285, 286]. Interestingly, alterations in all these pathways have been observed in MJD. A downregulation of the insulin/IGF-1 signaling was able to improve ATXN3-mediated phenotypes in *C. elegans* [231]. The insulin/IGF-1 system was also described to be involved in MJD as serum components of this system were found to be altered in patients, such as lower levels of insulin and IGFBP3

and high levels of insulin sensitivity (HOMA2), IGF-1, and IGFBP1 in comparison to controls [80]. Also, the modulation of the same pathway, through subcutaneous IGF-1 treatment, improved scores in the scale for the assessment and rating of ataxia (SARA) in MJD patients [287]. Of note, the insulin/IGF-1 pathway works differently in vertebrates and in invertebrates, as vertebrates acquired more complex metabolic pathways (with multiple ligands, binding protein and receptors) over evolution (as reviewed in [288]). For instance, mammals have insulin/IGF-1 receptors spread in all tissues and those have different roles depending on their location (in the CNS - catabolic effects, or in the periphery - anabolic effects). In addition, mammals have distinct and specific receptors for insulin and IGF-1, signaling through different pathways and having various functions [289]. On the opposite, in lower species, the signaling of those receptors occurs through the nervous system and translates into anabolism and longevity [290], explaining why different outcomes can be obtained regarding this signaling pathway in different species. An abnormal accumulation of TOR (a negative regulator of autophagy) was reported in the brain of MJD patients [291]. Changes in mitochondrial function have been observed in MJD studies in cells and in a mouse model of the disease, revealing that expanded ATXN3 was able to enhance mitochondrial-mediated cell death, lead to mitochondrial DNA damage, alter levels of mitochondrial porin, and decrease antioxidant activity [238, 239, 292]. A decreased expression of the sirtuin SIRT1 was observed in transgenic MJD mice and both the re-establishment of SIRT1 levels through gene delivery approach and the caloric restriction were able to improve neuropathology in these mice [293].

Indeed, several aging-related processes are implicated in MJD pathogenic mechanisms, reinforcing the idea that ageing-related changes potentiate the polyQ-derived toxic gain-of-function.

### **1.3.5 Animal models of MJD pathogenesis**

Animal models are important tools to study the mechanisms and pathophysiology associated with neurodegenerative disorders. Since the first description of the MJD-causing gene, several *in vivo* models have been generated. While simpler organisms made important contributions to the identification of pathogenic mechanisms and were further used for the identification of modifier genes and drug screening approaches, mammalian models recapitulate the main clinical features of the disease in humans and constitute valuable tools to validate mechanisms and to conduct preclinical validations of therapeutic strategies.

Until now, MJD models in worms (*C. elegans*), flies (*Drosophila melanogaster*), zebrafish (*Danio rerio*), mouse (*Mus musculus*), rat (*Rattus norvegicus*) and even marmoset (*Callithrix jacchus*) have been

developed (see a summary of the principal model features in Table 1.3). Here, we will mainly focus on the general features of *C. elegans* and mouse models, as these were used in this thesis.

As a model system, *C. elegans* is versatile, considered a good compromise between the complexity found in vertebrates and the simplicity of unicellular models. It has characteristics that make it very suitable to be used in the lab, such as its size (1 mm in length), short generation time (about 3-4 days) and its transparency. A two-week lifespan is convenient when studying aging-related diseases. It is unexpensive to maintain (mostly at 20 °C and can be kept in glycerol stocks (at -80 °C) for long term storage. *C. elegans* are self-fertilizing hermaphrodites (more than 99 %), with males arising spontaneously but infrequently.

Worms are a great model to study polyQ proteins, because, as a transparent multicellular organism with multiple tissue types, the *in vivo* dynamics of these proteins (when labeled) can be assessed noninvasively in aging animals. It is possible to examine individual neurons, while in the context of a multicellular organism. One extremely important feature is that all cells from this organism have been mapped and characterized in terms of their developmental relationships and functions. The worm has a total of 959 somatic cells (1031 in the adult male), 302 of them being neurons (383 in the adult male), that have been mapped [294-296]. Although the worm nervous system is relatively small, animals display quite complex behaviors that provide good readouts to assess neuronal function [297, 298]. In addition, *C. elegans* also possess 56 glial cells [299]. Worm behavioral analyses with laser-deleted neurons have shed light onto the function of individual and/or small groups of neurons including chemosensory, mechanosensory and motor neurons [297, 300]. By taking advantage of its transparency, behavioral and biophysical assays can be combined with *in vivo* imaging to assess protein solubility and protein interaction, in neurons of interest in the context of polyQ diseases [301, 302].

Another strength of *C. elegans*, as a small model organism, is its aptness for screening methodologies. *C. elegans* MJD models (Table 1.3) became especially useful for screening of compound libraries and drug target validations [303, 304].

About 65 % of human disease genes have homologs in *C. elegans* [305], including *ATXN3*. The endogenous ortholog of human *ATXN3* is called *atx-3* in the worm, consisting in four exons and lacking a CAG repeat [139]. The knockout (KO) of the gene does not trigger any significant phenotype in worms under normal growth conditions, but leads to differences in the expression of genes linked to the UPS, signal transduction, cell structure and motility, and an altered response to heat stress [139].

The main MJD *C. elegans* models generated by laboratories differ in terms of the type of transgene used (different isoform, full-length or truncated expression of the protein), promoter and polyQ

repeat size. The model developed by Teixeira-Castro *et al.* (in our lab), in 2011, harbored a human WT or mutant full-length ATXN3, with pan-neuronal expression, under the control of the *rgef-1* promoter. ATXN3 C-terminus was tagged with YFP. Strains with different polyQ repeat sizes were generated (14Q, 75Q and 130Q), which led to a polyQ length-dependent, neuron-specific aggregation and neuronal dysfunction. AT3q14 and AT3q75 showed a diffuse neuronal distribution of ATXN3 proteins, however AT3q130 worms presented discrete foci detected in some neurons and a diffuse distribution in others. While AT3q14 and AT3q75 did not exhibit any motility impairment at adulthood, AT3q130 worms had a significant reduction in motility. Additionally, the AT3q130 strain had a slight reduction in lifespan whereas AT3q14 and AT3q75 were similar to WT N2 worms. A model expressing a C-terminal fragment of ATXN3 was also generated, having a similar aggregation profile, but a more severe effect on motility than the full-length ATXN3 model [231].

Before the generation of this model, another one had been created by Khan *et al.* in 2006, to induce an MJD-like phenotype and aggregation in worms. The constructs were generated under the pan-neuronal promoter *unc-119*, with either full-length or truncated expression of ATXN3 with a different number of polyQ repeats and tagged with fluorescent proteins. Only worms expressing long repeats of 130Q in full-length ATXN3 developed aggregation and movement deficits, but not before six days of age [306]. In comparison with the Teixeira-Castro *et al.* model, the full-length ATXN3 with 130Q was able to induce an earlier motor phenotype in worms (at least at day four of age), foci formation was detected as early as day 1 post-hatching, and reduced lifespan was also observed [231]. This might be explained either by the use of a different promoter (*rgef-1* versus *unc-119*) or the use of a different ATXN3 isoform (the MJD1-1/ataxin-3c isoform, containing three UIMs, was used by Teixeira-Castro *et al.*, while the MJD1a short isoform with two UIMs was used in the work of Khan *et al.*). In both works, the expression of truncated forms of ATXN3 (C-terminal fragment) led to an increased phenotype severity when compared to the full-length expression.

The other existing MJD *C. elegans* model, created by Christie *et al.*, in 2014, expressed the C-terminal region of the ATXN3 protein with various polyQ lengths in body wall muscle cells, under the *unc-54* promoter and was tagged with YFP [307]. Expression in non-neuronal cells is the major difference between the two other existing models. Formation of aggregates in body wall muscle cells was polyQ length-dependent and aggregation correlated with toxicity revealed by motor defects. Intriguingly, ageing was not found as a modifier of aggregation and motility (thrashing) in this model, unlike the neuronal models as reported by Teixeira-Castro *et al.* and by Khan *et al.*

Although more difficult to generate and less genetically manipulable than invertebrates, rodent models have important molecular, physiological, and anatomical resemblances with humans which make them extremely relevant for drug discovery during preclinical studies.

Several MJD mouse and rat models have been generated in the past years, comprising transgenic [117, 118, 173, 190, 194, 195, 267, 308-313], lentiviral [116] and knock-in models [314-317] (see Table 1.3). Also, two KO models have been generated [41, 318]. Overall, *ATXN3* KO mice had normal viability, fertility, and showed no major motor dysfunction, however, a reduced exploratory behavior might be suggestive of heightened anxiety, and they also presented higher level of ubiquitylated proteins, in accordance to the function of *ATXN3* as a deubiquitylating enzyme [41]. Switonski and colleagues also serendipitously generated a KO model, in the attempt to generate a knock-in model, as a result of alternative splicing events [318]. The mouse generated was viable, fertile and had no reduction in lifespan or neurological anomalies, but it also showed higher quantity of ubiquitylated proteins [318].

The first transgenic MJD mouse model was developed by Ikeda and collaborators in 1996. Mice were generated using full-length and truncated *ATXN3* cDNA (MJD1a isoform), using the L7 promoter to direct expression specifically in Purkinje cells. Expression of full-length forms of *ATXN3* did not trigger any pathological alterations, while truncated forms led to an early and severe ataxic phenotype starting at 4 weeks of age in which a prominent atrophy of the cerebellum, and an extensive degeneration of Purkinje cells was observed [195].

Later, in the attempt of generating a model that replicated more precisely the temporal and spatial expression of the human gene, a mouse model was generated using yeast artificial chromosome (YAC) constructs. These carried the full-length *ATXN3* gene (in addition to 35 kb upstream and 170 kb downstream flanking genomic sequences) with different sizes of polyQ repeat expansions and, importantly, they contained all the long-regulatory elements and enhancers thought to be necessary for a cell-specific expression at physiological levels although, the *ATXN3* gene was not at its proper genomic location, and they also overexpressed two additional genes. Heterozygous mice harboring expanded alleles displayed mild and slow progressive deficits, starting at the age of 4 weeks, including abnormal gait, hypoactivity, tremors, limb claspings, reduced grip strength and an inability to correct geotaxis. Also, with disease progression pelvic elevation became lowered, toe pinch response became abnormal, and balance deficits and a progressive weight loss was observed. The symptoms aggravated with higher repeat length and gene dosage. Homozygous mice presented earlier onset and faster disease progression. Pathologically, animals presented neuronal intranuclear inclusions, marked neuronal loss and gliosis [117].

In the following years, five additional mouse models were generated by different laboratories, expressing either a full-length or truncated pathogenic form of *ATXN3* (MJD1a or MJD1-1/ataxin-3c isoforms), under the control of a prion protein (*Prnp*) promoter [173, 190, 194, 267, 308]. Regarding phenotype, these models were quite similar. Early onset motor dysfunction and the reproduction of many MJD features such as gait and limb ataxia, postural instability, weight loss, and premature death were reported for these models. The presence of neuronal intranuclear inclusions in neurons was also found, however neurodegeneration was not very significant in any of these models. Other pathological findings were reported in these transgenic mice, such as decreased tyrosine hydroxylase-positive neurons in the substantia nigra [190] and Purkinje cell abnormal morphology and loss [173, 267]. The creation of these models helped to better understand some mechanisms that contribute to disease and to envisage some new therapeutic strategies. For instance, with the use of the model generated by Goti *et al.*, the authors suggested that enhancing the activity of the C-terminus of Hsp70-interacting protein (CHIP) could be beneficial in MJD [190]. Additionally, Bichelmeier and colleagues demonstrated that the severity of the MJD phenotype increased along with the increase in polyQ repeat number, and that the nuclear presence of *ATXN3* was necessary for the development of symptoms [173]. Chou and collaborators further showed that there was a transcriptional dysregulation in MJD mice before the emergence of symptom, involving glutamatergic neurotransmission, intracellular calcium signaling/mobilization or MAPK pathways, transcription factors regulating neuronal survival and differentiation, heat shock proteins and GABAA/B receptor subunits [267].

During that time, Torashima and coworkers generated a new model with the Purkinje cell specific promoter L7, which controlled the expression of a human truncated form of *ATXN3*, to test a new potential therapeutic approach: guanosine triphosphatase (Crag), a compound previously found by the authors to facilitate the degradation of polyQ aggregates through the UPS in cultured cells. Mice developed early onset ataxia, impaired performance in rotarod, a reduction in weight and a severe cerebellar atrophy. They detected inclusions in the cytoplasm and in the nuclei of Purkinje cells. The lentiviral vector-mediated expression of Crag in the Purkinje cells of this mouse model was able to clear inclusions and rescue the ataxic phenotype [312].

The first conditional model of MJD was generated in 2009 by Boy *et al.* using a Tet-Off system with the expression of full-length human *ATXN3* cDNA (under the *PrP* promoter). Mice developed a progressive neurological phenotype comprising impaired motor coordination and balance, hyperactivity, reduced anxiety, cerebellar neuronal dysfunction, and reduced body weight gain. Mice also had *ATXN3*-positive nuclear inclusions in the brain. When expanded *ATXN3* expression was turned off, in early

symptomatic ages, a complete reversal of the phenotype was observed [309]. Recently, using this responder mouse line, a new Tet-Off transgenic mice was generated but under the control of the *CamKII* promoter [313].

One year later, Boy *et al.* published another MJD transgenic mice model expressing ATXN3 with 148 CAG repeats, under the control of a fragment of the huntingtin promoter, promoting ubiquitous expression of the protein throughout the brain. Many features of MJD disease in humans were also recapitulated by this model, such as the late onset of symptoms and the instability of CAG repeats transmission to the offspring. A decline in motor coordination was observed in rotarod after about one year of age, and ATXN3 inclusions were not detected before 18 months of age [308].

In the same year, another transgenic model was created (in our lab), using the cytomegalovirus (CMV) promoter to drive the ubiquitous expression of an *ATXN3* construct (MJD1-1 isoform) with 83 and 94 CAG repeat tracts. This novel model of MJD resembled many characteristics of the human disease. Impairment of motor function (motor uncoordination phenotype and reduced locomotor activity), neuronal dysfunction and CAG repeat instability were observed in CMVMJD94 mice, whereas CMVMJD83 mice had no detectable phenotype. Neuronal atrophy and astrogliosis were found in the model, but no presence of neuronal inclusions was detected, neither any type of cell death [311]. In 2014, the same authors described a similar model in which the CAG repeat stretch was increased to 135 repeats (CMVMJD135), which recapitulated more closely MJD progression in humans. In CMVMJD135 mice a progressive motor phenotype starting at 6 weeks of age was observed, as well as reduced body weight gain, intergenerational repeat length variation, and the presence of intranuclear inclusions, in different regions of the CNS known to be affected in humans [118]. This new mouse model proved to be useful to test new therapeutic strategies for MJD [303, 319].

In 2011, Hübener *et al.* developed a mouse model of MJD, by gene trap integration, in which an ATXN3 fusion protein harboring 259 N-terminal amino acids but missing the C-terminal polyQ tract and other regulatory regions was used. In initial stages, mice developed with no major abnormality until they reached 9 months of age, where a deficient motor coordination and body weight loss were observed, culminating in premature death at 12 months of age. Mice also presented extranuclear ATXN3 inclusions and neuronal cell death was seen in the cerebellum. With this model, the authors concluded that the N-terminal region of ATXN3 could contribute to MJD pathogenesis [310].

In 2015, two different knock-in MJD mouse models were reported. The first, a humanized knock-in model, resulted in CAG repeat instability in transmission to offspring, late onset impairment of motor coordination and loss of Purkinje cells [314]. The second, although displaying prominent aggregate

pathology, missed behavioral deficits or neuropathological changes [315]. This model was later corrected due to an erroneous insertion of a tandem copy of the original targeting vector, resulting in the insertion of two copies of mutant exon 10, harboring the CAG repeat tract [316]. Very recently, a study describing a new knock-in MJD mouse model harboring 304 CAACAG repeats, presenting protein aggregation, impairments of Purkinje cells, body weight reduction, and gait and balance instability, was issued [317].

Alves *et al.* developed another rodent (rat) model, in 2008, by lentivirus injection with expression of human ATXN3 in the striatum. It reproduced several characteristics of MJD neuropathology, such as the formation of neuronal intranuclear inclusions and neuronal loss [116].

The first transgenic non-human primate (marmoset) model of MJD was generated very recently, using a lentiviral approach. It displayed several motor and neurological symptoms, protein aggregation, neurodegeneration, and degeneration of skeletal muscles. Nevertheless, studies in non-humane primates are expensive and time-consuming and until now only a limited number of animals were analyzed [320].

Mouse models continue to be the most popular model to study age-related neurodegenerative disorders since they are mammals, phylogenetically close to humans, and their nervous system is more related to ours. When experimenters are aware of their models' strengths, weaknesses and limitations, these models can be useful and successfully predictive of clinical outcomes. Although some promising results can be obtained in preclinical trials, the failure of translation to humans is often observed. Accounting for this are common limitations associated to these models: (i) the putative limited relevance of models based on the expression of rare genetic mutations/variants to understand sporadic forms of the disease (particularly in the case of neurodegenerative disorders predominantly of non-genetic origin such as AD and PD); (ii) the methodology used for the animal model generation (e.g., artificial overexpression of proteins and adeno-associated viral vector-mediated models); (iii) the short lifespan of the model species, that might contribute to the incomplete development of disease pathology; (iv) inherent differences between mice and humans, particularly regarding brain functions (e.g., in cognitive and emotional paradigms); (v) genomic differences (e.g., binding sites for RNA-binding proteins that are not well conserved and RNA-processing changes not entirely recapitulated in mice); (vi) the use of inbred animals that do not reflect the variability within a human population [321, 322].

All the MJD mouse models referred in Table 1.3 have been vital to decipher general mechanisms of the disease. Therefore, their importance is undeniable, despite their differences, and the pros and cons regarding the methodology used to generate them. Some of these models recapitulate major phenotypic and pathological hallmarks of MJD, whereas others do it only partially. Even the last ones can be important to answer more specific questions.



Table 1.3 MJD animal models: *C. elegans*, *Drosophila melanogaster* and *Danio rerio* (Zebrafish).

Organism	Model designation	Transgene	Promoter	Pathology	Phenotype
<b><i>C. elegans</i></b> <i>Khan et al.</i> , 2006 [306]	MJD1-(17/91/130)Q-GFP (19/33/63/127)Q-GFP (19/127)Q-CFP (19/127)Q-RFP	Full-length and C-terminal truncated MJD1a cDNA	<i>unc-119</i> (pan-neuronal)	No neurodegeneration. Presence of inclusions.	Uncoordination.
	Teixeira-Castro <i>et al.</i> , 2011 [231]	AT3q(14/75/130) 257cAT3q(14/75/80/128)	<i>zgef-1</i> (pan-neuronal)	Presence of inclusions.	Uncoordination. Shortened lifespan.
<b><i>Drosophila</i></b> <i>Warrick et al.</i> , 1998 [323]	AT3CT(Q45) AT3CT(Q63)	C-terminal truncated MJD1-1 cDNA (YFP)	<i>unc-54</i> (body wall muscle)	Presence of inclusions.	Uncoordination. Reduced thrashing rate.
	MJDtr-Q27 MJDtr-Q78	C-terminal truncated MJD1a cDNA	gmr-GAL4 (eye) elav-GAL4 (pan-neuronal)	Neurodegeneration. Presence of inclusions.	Progressive eye degeneration. Defects in eye morphology and pigmentation.
<i>Kretzshmar et al.</i> , 2004 [324]	AppI-X/elav/AppI-II-Q27 AppI-X/elav/AppI-II-Q78w(w/m/s) M1B/loco-II/loco-III-Q27 M1B/loco-II/loco-III-Q78(w/m/s)	C-terminal truncated MJD1a cDNA (w-weak; m-medium; s-strong expression strength)	elav, AppI-X, and AppI-III (neuronal) M1B, loco-II, and loco-III (glial)	Glial cell death only. Presence of inclusions.	Behavioral deficits (fast-phototaxis and walking behavior in Buridan's Paradigm). Shortened lifespan.
	SCA3-Q(27/84) SCA3-Q78 SCA3-Q(27/80)-UIM* SCA3-Q(27/88)-C14A SCA3-delta	Full-length, N-terminal and C-terminal truncated MJD1a cDNA	gmr-GAL4 (eye) elav-GAL4 (pan-neuronal)	Neurodegeneration. Presence of inclusions.	Retinal degeneration. Disruption of photoreceptor pattern. Early adult death.
<i>Jung et al.</i> 2009 [193]	Myc-Atx3Q(27/84) Myc-Atx3Q84-Flag (WT) Myc-Atx3Q84-Flag (6 M)	Full-length MJD1a cDNA	elav-GAL4 (neuronal) rh1-GAL4 (photoreceptor) gmr-GAL4 (eye)	Presence of inclusions. Neurodegeneration.	Eye degeneration.
	<b><i>Danio rerio</i></b> <i>Watchon et al.</i> 2017 [325]	EGFP-Ataxin3 (23/84)Q	elav-GAL4 (neuronal) mir218-enhancer-Kal4 (motor neuron)	Presence of inclusions.	Impaired motor function. Reduced survival.

Description of isoforms: the isoform 1a (MJD1a), the short isoform of ATXN3, contains two UIMs (ubiquitin-interacting motifs) and a premature stop. The 1a long isoform contains two UIM and 1.6 additional amino acids at its C-terminus (MJD2-1; GenBank: U6421; GenBank: U6421); the 3c isoform contains a third UIM in the C-terminus (MJD1-1/MJD5-1; GenBank: U64820/U64822).

**Table 1.3 (continued) MJD animal models: mouse (*Mus musculus*).**

Organism	Model designation	Transgene	Promoter	Pathology	Phenotype
<i>Mus musculus</i> /Keda et al., 1996 [195]	MJD79 / Q79 Q <sub>(57/79)</sub> C	Full-length and C-terminal truncated MJD1a cDNA	L7 (Purkinje cells)	Cb atrophy. Neurodegeneration in three layers of the cerebellum.	Ataxia. Gait perturbation. Absence of rearings.
Cemal et al., 2002 [117]	MJD15.1/15.4 MJD64-84 (various)	Full-length (human locus, 15Q and 64-84Q)	ATXN3 YAC (ubiquitous)	Neurodegeneration in the PN and DN. Peripheral nerve demyelination.	Ataxia. Weight loss. Flattened pelvic elevation. Hypotonia. Motor/sensory loss.
Goti et al., 2004 [190]	Q20-(A/B) Q71-(A/B/C)	Full-length MJD1a cDNA	<i>Pmp</i> (ubiquitous)	Neuronal inclusions. ↓tyrosine hydroxylase-positive neurons in the SN.	Postural instability. Gait and limb ataxia. Weight loss. Premature death.
Colomer Gould et al., 2007 [194]	deltaQ20 deltaQ71	MJD1a cDNA (Δaa190-220)	<i>Pmp</i> (ubiquitous)	Inclusions in the cerebellum.	Tremors. Hunchback. Abnormal gait. Weight loss. Premature death.
Bichelmeier et al. 2007 [173]	(15/70/148)Q 148Q.NES/NLS	Full-length MJD1-1 cDNA	<i>Pmp</i> (ubiquitous)	Ubiquitin- and ATXN3-positive intranuclear inclusion bodies.	Tremors. Reduced motor and exploratory activity. Hunchback. Premature death.
Chou et al. 2008 [267]	ataxin-3-Q22 ataxin-3-Q79	Full-length and C-terminal truncated MJD1a cDNA	<i>Pmp</i> (ubiquitous)	Intranuclear inclusions (DN, PN, SN).	Motor dysfunction. Ataxia. Limb claspings.
Torashima et al., 2008 [312]	ataxin-3[Q69]	C-terminal truncated MJD1a cDNA	L7 (Purkinje cells)	Presence of inclusions. Poor dendritic arborization of Purkinje cells.	Severe ataxia.
Boy et al., 2009 [309]	Prp/MJD77	Full-length MJD1-1 cDNA	<i>Pmp</i> (ubiquitous) Tet-Off	Presence of inclusions in cerebral cortex.	Reduced anxiety. Hyperactivity. Altered gait. Lower body weight gain.
Boy et al., 2010 [308]	HDPromMJD148	Full-length MJD1-1 cDNA	Rat <i>Htt</i> (ubiquitous)	Late formation of inclusions in the RN, pons, Cb and Purkinje cells.	Hyperactivity. Motor uncoordination.
Silva-Fernandes et al., 2010 [311]	CMVMJD83/94	Full-length MJD1-1 cDNA	CMV (ubiquitous)	Neuronal atrophy (PN, DN, thalamus). Astrogliosis (VN and SN).	Motor uncoordination.
Silva-Fernandes et al., 2014 [118]	CMVMJD135	Full-length MJD1-1 cDNA	CMV (ubiquitous)	Presence of intranuclear inclusions in PN, RtTg and SC.	Abnormal gait. Limb claspings and tonus deficit. Lower body weight gain.
Hübener et al. 2011 [310]	ataxin-3(wt/gt) ataxin-3(gt/gt)	ATXN3 (aa 1-259) lacZ-neoR	ATXN3 (ubiquitous)	Extranuclear protein aggregates. Neurodegeneration.	Abnormal gait. Limb claspings Motor uncoordination. Body weight loss.
Switonski et al. 2015 [314]	Ki91	Mouse ex 1-6 mouse/human ex 7 human ex 8-11	ATXN3 (ubiquitous)	Neurodegeneration. Intranuclear inclusions in Cb. Astrogliosis.	Late disease onset. Motor uncoordination.
Ramani et al. 2015 [315]	ATXN3Q82/Q6 ATXN3Q82/Q82	Full length mouse ATXN3	ATXN3 (ubiquitous)	Intranuclear inclusions. Extranuclear Aggregates in neuritic processes.	Absence of behavioral deficits.

Decrease (↓); PN - pontine nuclei; DN - dentate nuclei; SN - substantia nigra; Cb - cerebellum; RN - red nucleus; VN - vestibular nuclei; SC - spinal cord; RtTg - reticulotegmental nuclei of pons; STR - striatum.

**Table 1.3 (continued) MJD animal models: mouse (*Mus musculus*), rat (*Rattus norvegicus*) and marmoset (*Callithrix jacchus*).**

Organism	Model designation	Transgene	Promoter	Pathology	Phenotype
<b><i>Mus musculus</i></b> Ramani <i>et al.</i> , 2017 [316]	ATXN3Q82/Q6	Full length mouse ATXN3	ATXN3 (ubiquitous)	Intranuclear inclusions in brainstem neurons of Ki-homozygous mice.	Absence of behavioral deficits.
	ATXN3Q82/Q82 (Ki line: "corrected" dupKi line)				
Schmidt <i>et al.</i> , 2019 [313]	CamKII/MJD77	Full-length MJD3c cDNA	CamKII (neuron-specific, mainly forebrain) Tet-Off	Ataxin-3- and ubiquitin-positive inclusions in forebrain regions (cortex, STR, hippocampus). Neurodegeneration.	Progressive deficits in motor coordination. Defective learning of new motor tasks. Hyperactivity.
Haas <i>et al.</i> , 2021 [317]	WT/304Q 304Q/304Q	Full length mouse ATXN3	ATXN3 (ubiquitous)	Massive aggregation formation. Mild loss of Purkinje cells.	Reduced body weight. Gait and balance instability.
<b><i>Rattus norvegicus</i></b> Alves <i>et al.</i> , 2008 [116]	atx3-27Q	Full-length MJD1a cDNA	Lentivirus (PGK) (injection SN, STR or cortex.)	Inclusions. Loss of dopaminergic markers in SN. Degeneration in STR.	Apomorphine-induced turning behavior when induced in SN.
	atx3-72Q				
<b><i>Callithrix jacchus</i></b> Tomioka <i>et al.</i> 2017 [320]	PQD (CMV-ataxin-3- 120Q-(IRES/2A)- Venus	Full-length human MJD1 cDNA	Lentivirus (CMV). (Ubiquitous)	Loss of Purkinje cells. Gliosis in Cb. Degeneration of lower motor neurons. Intranuclear inclusions.	Movement disability. Contractures of the legs and arms. Lower body weight. Difficulty in eating.

PN - pontine nuclei; DN - dentate nuclei; SN - substantia nigra; Cb - cerebellum; RN - red nucleus; VN - vestibular nuclei; SC - spinal cord; RTg - reticulotegmental nuclei of pons; STR - striatum.

### 1.3.6 Therapeutic approaches and clinical trials

Over the years, several therapeutic strategies for MJD and other polyQ diseases have been tested and focused mostly on (i) the targeting of the mutant polyQ proteins themselves, and (ii) the targeting of downstream effects of these mutant proteins.

#### (i) Therapies directed at the polyQ proteins

**DNA-targeting approaches.** The ideal treatment for MJD and other polyQ diseases would be to directly correct the mutant *ATXN3* allele, thus suppressing the production of all types of toxic *ATXN3* gene products. Genome editing in induced pluripotent stem cells (iPSCs) derived from SCA3 patients has been achieved. A research group described a successful deletion of the expanded polyQ-encoding region of *ATXN3*, through clustered regularly interspaced short palindromic repeats (CRISPR) and CRISPR-associated protein 9 (Cas9) - CRISPR/Cas9 - technology, in which the ubiquitin binding property of the protein was maintained [326]. In a recent study performed in cells of HD patients and in the striatum of HD mice, researchers made use of a newly identified small-molecule (naphthyridine-azaquinolone) that specifically binds to CAG repeats, to induce its contraction. This led to a reduction in mutant huntingtin protein aggregation [327]. These are promising therapeutic strategies that need further testing and validation in preclinical trials for MJD.

**RNA-targeting approaches.** Strategies focused on downregulating the expression of the mutant gene using RNA interference (RNAi) or antisense oligonucleotides (ASOs) have been very efficacious in preclinical settings. The type of RNAi molecules used have been different, including short hairpin RNA (shRNA) [328-331], small interference RNA (siRNAs) [332], microRNAs [333-335] and ASOs [336-340] to suppress *ATXN3* expression in the brain.

Back in 2008, an innovative study by Alves and collaborators, demonstrated that allele-specific silencing of *ATXN3*, by the delivery of shRNA directed at a specific single nucleotide polymorphism (present in 70 % of MJD patients [64]), was able to decrease neuropathological deficiencies derived from mutant *ATXN3* expression in rat striatum [328]. Since then, several efforts have been developed by the same team, using shRNA, with positive results, mitigating behavioral impairments and reducing neuropathological features in *ATXN3* transgenic mice [329]. Importantly, long term treatment of WT mice with shRNAs did not cause toxicity [331]. Later on, they showed that siRNAs were also a valid strategy to attenuate behavioral and pathological hallmarks of the disease in both lentiviral and transgenic mouse models [332]. Another study showed that delivery of microRNAs directed at *ATXN3* transcripts in mouse cerebellum led to a suppression of mutant *ATXN3* expression, but was ineffective in rescuing motor

deficits, thus suggesting that delivery to all MJD affected regions would be necessary to attain therapeutic efficacy [333]. Two recent ASO technologies, targeting either *ATXN3* transcripts [338] and or the CAG repeat [337], were effective in reducing mutant ATXN3 levels in the brains of MJD mice and rescued behavior deficits, with no major signs of toxicity [338].

RNA-targeting strategies have progressed and revealed to be promising therapeutic strategies for MJD and other polyQ diseases. Nevertheless, more preclinical studies are needed to apply these technologies to human clinical trials, assuring that the effects of depleting mutant and often also wild-type *ATXN3* transcripts, and potential off-target effects, in a long-term treatment, show therapeutic efficacy and have low toxicity.

**Protein quality control approaches (targeting protein proteolysis, aggregation, and degradation).** Other possible strategies for MJD therapeutic interventions are related to the modulation of processes such as proteolytic cleavage (to decrease the levels of toxic protein fragments); chaperone machinery (to decrease ATXN3 misfolding and aggregation); and UPS and autophagy (to induce the clearance of toxic ATXN3 species).

As suggested by the *toxic fragment hypothesis* [188], proteolytic cleavage of polyQ-expanded proteins could generate smaller fragments which are more toxic and prone to aggregation [191]. Most of the studies intended at the inhibition of ATXN3 proteolysis targeted calpains and caspases. For instance, Haacke and collaborators showed that calpain inhibition, using calpeptin, prevented ATXN3 fragmentation and aggregate formation in cells [192]. The same strategy has proven efficient in MJD zebrafish [325] and mouse models [116, 341, 342]. A study using iPSC-derived neurons of a patient with MJD also demonstrated that calpain inhibition prevented the formation of ATXN3 aggregates, caused by glutamate-induced ATXN3 proteolysis [202]. However, a later study failed to reproduce this glutamate-induced ATXN3 aggregation on iPSC-derived neurons [343]. Although these methodologies showed good results in model systems, their clinical translation is still limited by possible toxicity, arising from the lack of target specificity, possibly impairing the normal function of cellular proteases on other target proteins.

Inhibition or prevention of aggregation was one of the first therapeutic strategies used in the field of protein conformation disorders. Modulation of molecular chaperones has been used for that purpose. Inhibition of HSP90 activity, through 17-DMAG treatment, restored motor function and reduced neuropathology of CMVMJD135 mouse model [118]. Overexpression of DNAJC8, in mutant ATXN3 SH-SY5Y neuroblastoma cells, led to a reduction in polyQ aggregation and apoptosis [344]. Additionally, *in vitro* studies showed that overexpression of two Hsp40 chaperones, DNAJ-1 and DNAJ-2, suppressed

mutant ATXN3 aggregation [115]. The use of small heat shock proteins (sHsp) inhibited the first step of ataxin-3 aggregation, but not the polyQ-dependent step [345]. The use of chemical chaperones, i.e., reagents that stabilize proteins, also decreased aggregate formation and toxicity in an *in vitro* model of MJD [346]. Treatment with trehalose, initially thought to act as a chemical chaperone but then shown to induce autophagy, also improved motor function and neuropathology in MJD mouse models [347].

As expected, acting on ATXN3 degradation processes also proved to be effective in reducing ATXN3 levels, hence this became a topic of interest. It was found that ATXN3 turnover is regulated by its catalytic activity [348]. Moreover, ATXN3 turnover does not require ubiquitylation, but is regulated by the ubiquitin-binding site 2 (UbS2) on its N-terminus. It was shown that mutating this site decreases ATXN3 levels, increasing its degradation [349]. Manipulation of components of the UPS, for instance by overexpression, was one strategy also tested. In 2004, it was shown that the expression of the ubiquitin chain assembly factor E4B was able to induce mutant ATXN3 degradation *in vitro* and to suppress neurodegeneration in a *Drosophila* model [159]. One year later, Jana and collaborators showed that the transient overexpression of the C-terminus of Hsp70-interacting protein (CHIP) increased the ubiquitylation and the degradation rate of polyQ-expanded ATXN3 [350]. Indeed, the importance of CHIP was further demonstrated in another study, since its reduction accelerated disease progression, increasing ATXN3 microaggregation levels in a MJD mouse model [351]. The overexpression of p45, an ATPase subunit of the 19S proteasome, also stimulated ATXN3 degradation [352]. Intriguingly, a more recent study showed that increasing levels of the proteasome shuttle protein Rad23 (an ATXN3 interactor), increased the toxicity of mutant ATXN3, whereas its reduction alleviated toxicity, suggesting that this interaction could be an interesting therapeutic target for MJD [353].

Autophagy is the principal cellular pathway involved in the degradation of aggregated polyQ proteins [354]. The implication of autophagy in MJD pathogenesis became clearer when it was reported that WT ATXN3 interacts with the autophagic protein beclin-1 [164]. In 2010, it was shown that the administration of an inhibitor of TOR - temsirolimus, upregulating autophagy, led to a reduction in aggregated and soluble mutant ATXN3 in a transgenic MJD mouse model [234]. In the same line, autophagy activation through 17-DMAG (a Hsp90 inhibitor) had a beneficial effect in a MJD mouse model, decreasing levels and intranuclear aggregation of mutant ataxin-3 [118]. Activation of autophagy through different targets, in other MJD animal models, has also proven to be effective [293, 325]. However, other studies failed to see improvements, having even reported toxicity. In 2014, Duarte-Silva and colleagues reported that lithium chloride, in spite of autophagy induction, did not reduce the protein levels of mutant ataxin-3, neither impacted on motor phenotype of an MJD transgenic mouse model [355]. Later, the

same authors showed that combined administration of two autophagy inducers, temsirolimus and lithium, acting through complementary pathways, was neurotoxic in WT and ATXN3 transgenic mice and ineffective in the latter [356]. The different models used and different approaches to achieve autophagy induction could explain the contradictory results. Gene therapy strategies have also been used to modulate autophagy. Overexpression of beclin-1 had neuroprotective effects in neuronal cultures and in a MJD lentiviral-based rat model [235]. In a follow-up study, beclin-1 overexpression rescued motor and neuropathological defects when administered at pre- and post-symptomatic stages of the disease [357]. Overall, autophagy could constitute a relevant therapeutic target if specificity is achieved, and exaggerated activation of this mechanism with consequent over-degradation of other targets important for cellular function is avoided. Perhaps a novel targeted approach, such as the one developed by Li and collaborators, seeking to directly target mutant huntingtin for macroautophagic degradation, through linker compounds that interact both with the mutant huntingtin protein and the autophagosome protein LC3, could show therapeutic potential for other polyQ pathologies, as shown also for MJD [358], although this needs to be adequately tested *in vivo*.

#### (ii) Therapies directed at the polyQ proteins-mediated downstream effects

**Transcriptional modulation approaches.** Several studies focused on targeting the transcriptional dysregulation suggested to occur in MJD [265]. One of the methods tested consisted in the use of HDAC inhibitors. An initial report by Jung and Binini, in 2007, evidenced that trichostatin A treatment normalized histone acetylation and suppressed repeat instability [359]. Administration of another HDAC inhibitor, sodium butyrate, reversed histone hypoacetylation and downregulated transcription in the cerebellum of an MJD mouse model, contributing to prevent mutant ATXN3-induced pathology [360, 361]. Valproic acid alleviated ATXN3-mediated pathology in a *Drosophila* model [362]. However, limited effects of this HDAC inhibitor were observed in a preclinical study in the CMVMJD135 MJD mouse model [319]. Further studies are needed to overcome the limitations found in preclinical trials for future clinical applications of HDAC inhibitors.

**Mitochondrial and oxidative stress-directed approaches.** Many lines of evidence support mitochondria dysfunction and oxidative stress to play a role in neurodegenerative disorders, including MJD [236, 239]. Coenzyme Q10 (CoQ10), a cofactor of the electron transport chain and a potent antioxidant was found to reduce cell death, to increase the monomer fraction and decrease aggregates *in vitro* [363]. Duarte-Silva and colleagues showed that supplementation with creatine (known as a cellular energy buffer), in a MJD transgenic mouse model, improved motor function, slowed disease progression

and ameliorated disease-associated neuropathology [292]. Unpublished data from the same author showed that tauroursodeoxycholic acid (TUDCA), which also has antioxidant properties, improved the motor phenotype of the CMVMJD135 mouse model and exhibited neuroprotective effects [364]. Compounds (caffeine and resveratrol), acting through the nuclear factor erythroid-derived-2-like 2 (Nrf2) pathway, a master transcription factor that upregulates the expression of antioxidant defense genes, shown beneficial effects *in vivo* and *in vitro* in MJD models [365]. More recently, plant extracts (from *Brassica napus* (rapeseed) pomace and *Hyptis spp.*), with antioxidant properties, demonstrated to be neuroprotective in a *C. elegans* MJD model, improving motor function [366, 367]. Together these results suggest that targeting mitochondria and oxidative stress might be a promising therapeutic approach for MJD, perhaps in combination with other therapies.

**Calcium/ion homeostasis approaches.** Although a limited number of studies focused on the role of calcium homeostasis in MJD, this was shown to be dysregulated [261]. Dantrolene, a stabilizer of calcium signaling, was reported to be able to ameliorate the motor function and prevent neurodegeneration in the substantia nigra and pontine nuclei of transgenic MJD mice [261]. However, dantrolene might not be a good therapeutic option since its relaxing effects in muscles can be overwhelming for patients, and might lead to prolonged respiratory insufficiency, principally in patients suffering from a neuromuscular disease like MJD [368].

MJD models also display potassium channel dysfunction [369, 370]. Based on this, riluzole (a mixed action anti-glutamatergic agent) and the calcium-activated potassium (SK) channel activator SKA-31 were proposed as possible MJD therapeutic strategies. Riluzole protected MJD-iPSC-derived neurons and contributed to reduce their cell death [371], while SKA-31 improved motor function and partially corrected abnormal Purkinje cell firing in MJD mice [370]. However, when tested in a conditional MJD mouse model riluzole had no beneficial effect, leading instead to a reduction in the calbindin expression of Purkinje cells [372].

**Neuronal/cellular homeostasis approaches.** MJD pathogenesis is complex and affects several cellular mechanisms, depleting cells from crucial components that play a role in homeostasis maintenance. More holistic and new therapeutic approaches have been tried to counteract MJD-associated features and reestablish cellular equilibrium. Among those, we can find approaches involving cellular transplantation therapy [373], gene therapy to restore reduced levels of downstream proteins [374-376], caloric restriction [293], and the use of specific compounds [303, 377-382].



Transplantation of cerebellar neural stem cells into the cerebellum of MJD transgenic mice, as a new cellular therapy, was able to alleviate motor phenotype, reducing also neuropathological hallmarks of the disease [373].

Duarte-Neves and colleagues observed that lentiviral-mediated overexpression of neuropeptide Y rescued motor deficits and neuropathological abnormalities in two mouse models of MJD. The effect was associated to the increase in the levels of brain neurotrophic factors and to a decrease in inflammatory markers [374]. Another study found that ataxin-2 mRNA levels were decreased in MJD patients and in transgenic mice (probably due to its recruitment into inclusions, as previously observed [383]), and that the re-establishment of their levels also led to a reduction in the levels of mutant ATXN3, while decreasing motor deficits and ATXN3-associated neuropathology [375]. Interestingly, more recently, it was demonstrated that restoring brain cholesterol 24-hydroxylase (CYP46A1), responsible for brain cholesterol turnover, exerted beneficial effects on motor and pathological abnormalities in adult MJD mice [376].

Caloric restriction has also proven to be very effective in counteracting ATXN3-associated impairments in a transgenic mouse model of the disease. The effect seemed to be mediated by an increase in SIRT1 levels as reported by the authors [293].

Other studies have focused on specific compounds, either supported by previous evidence or found upon broad range drug screenings to find new therapeutic approaches for MJD. For instance, the treatment with the non-selective adenosine receptor antagonist caffeine and the selective adenosine A<sub>2A</sub> receptor inactivation were reported to reduce pathological findings associated to MJD in a lentiviral mouse model [377]. Later, the caffeine beneficial effect was confirmed in a MJD transgenic mouse model [379]. In accordance, Chou and collaborators, also tested an adenosine A<sub>2A</sub> receptor agonist, T1-11, and its synthetic analogue JMF1907, in a transgenic MJD mouse model, finding that both were able to ameliorate motor dysfunction, reducing mutant ATXN3 levels and mitigating neurodegeneration [378].

In the same line, compounds that modulate neurotransmission were identified in screenings of FDA-approved drugs. Citalopram, an antidepressant, was found to rescue neuronal dysfunction and reduce aggregation in *C. elegans* and mouse models of MJD [303] (this will further be discussed in section 1.4.4 of this chapter). Another screening identified the antipsychotic drug aripiprazole, which was tested in *Drosophila* and transgenic mice, and led to the reduction of mutant ATXN3 aggregation [381]. More recently, still in the optic of drug repurposing, Ibuprofen was found to confer neuroprotection, leading to ATXN3 inclusions size reduction and improving motor performance in two MJD mouse models [382].

Although the mode of action of most compounds above mentioned is not fully understood in the context of MJD, drug repurposing approaches have been useful to identify novel cellular targets for MJD therapy.

#### Clinical trials in MJD patients

Currently, there is no disease-modifying treatment for MJD, only a few symptomatic therapeutic options are available (as reviewed in [384]). A successful translation of the findings from model systems to MJD patients is critical. Although a considerable number of models and therapeutic strategies have been developed, the lack of knowledge about key aspects of the pathogenic mechanisms, the clinical and molecular variability of MJD patients, as well as the insufficient biological material from patients available for research, make the translation step a very hard process. Nevertheless, some approaches were tested in human clinical trials for MJD or for ataxia phenotypes, that included MJD patients. Table 1.4 summarizes information on completed and ongoing trials.

**Table 1.4 Clinical (interventional) trials for MJD or that include MJD patients.**

Drug/Intervention	Reference	Identifier	Target/Mechanism	Design	Patients no.	Treatment duration	Status	Outcome
Bupropion	Friedman <i>et al.</i> , 1997 [385]	-	Serotonin 5-HT <sub>1A</sub> receptor partial agonist	Case-study	1	15 weeks	Completed	Improved gait ataxia.
Trimethoprim and sulfamethoxazole	Schulte <i>et al.</i> , 2001 [386]	-	Antibiotics	Double-blind	22	2 weeks	Completed	No significant effects.
Tandospirone	Takei <i>et al.</i> 2002 [387]	-	Serotonin 5-HT <sub>1A</sub> receptor partial agonist	Case-study	1	8 weeks	Completed	Ataxia, leg pain, insomnia, anorexia, and depression eased.
Fluoxetine	Monte <i>et al.</i> , 2003 [388]	-	Serotonin selective reuptake inhibitor (SSRI)	Open-label	13	6 weeks	Completed	No significant improvement in motor abilities.
Tandospirone	Takei <i>et al.</i> 2004 [389]	-	Serotonin 5-HT <sub>1A</sub> receptor partial agonist	Open-label Double-blind	10	7 weeks	Completed	Ataxia, leg pain, insomnia, anorexia, and depression eased.
Lamotrigine	Liu <i>et al.</i> , 2005 [390]	-	Sodium channel blocking agent	Open-label Double-blind	6	9 weeks	Completed	One leg standing test (OLST) and tandem gait index (TGI) improved.
Insulin-like growth factor-1 (IGF-1)	Arpa <i>et al.</i> , 2011 [287]	-	Neuromodulatory functions	Open-label	7*	8 months	Completed	SARA improved after 8 months and worsened after 20 months.
Varenicline (Chantix)	Zesiewicz <i>et al.</i> , 2012 [391]	NCT00992771	Agonist of $\alpha 4\beta 2$ sub-type of the nicotinic receptor	Double-blind	20	8 weeks	Phase II completed	Improved axial symptoms and rapid alternating movements.
Sodium phenylbutyrate		NCT01096095	Histone deacetylase (HDAC) inhibitor	-	-	-	Withdrawn #	-
Valproic acid	Lei <i>et al.</i> , 2016 [392]	ChiCTR-TRC10000754	Histone deacetylase (HDAC) inhibitor	Double-blind	36	12 weeks	Phase I completed	Improvement in locomotor function (decrease in SARA score).
Lithium carbonate	Saute <i>et al.</i> , 2014 [393]	NCT01096082	Inhibition of GSK3 $\beta$ / Autophagy inducer	Double-blind	62	48 weeks	Phase II/III completed	No effect on NESSCA and SARA scales.
Riluzole	Romano <i>et al.</i> , 2015 [394]	NCT01104649	Glutamate release inhibitor	Double-blind	60* (40 SCAs)	12 months	Phase II/III completed	50 % patient with a decrease in SARA score.

\*Includes diseases other than MJD/SCA3. # Regulatory authorities did not allow the entrance of the study drug in the country. SARA - Scale for the Assessment and Rating of Ataxia; NESSCA - Neurological Examination Score for the Assessment of Spinocerebellar Ataxia; ICARS - International Cooperative Ataxia Rating Scale; T25FW - timed 25-foot walk; MSCs - mesenchymal stem cells; Ad - adipose; TRH - thyrotropin releasing hormone.

Table 1.4 (continued) Clinical (interventional) trials for MJD or that include MJD patients.

Drug/Intervention	Reference	Identifier	Target/Mechanism	Design	Patients no.	Treatment duration	Status	Outcome
Weight in lower limbs	-	NCT02906046	Gait	Single	20	-	Completed	-
Ad-MSC	Tsai <i>et al.</i> , 2017 [395]	NCT01649687	Neuroprotection	Open-label	7* (6 MJD)	1 administration	Phase I/II completed	Increased brain glucose metabolism.
Cabaletta (trehalose)	Zaltman <i>et al.</i> , 2020 [396]	NCT02147886	Chemical chaperone	Double-blind	15	24 weeks	Phase II completed	Stable on the SARA scale.
Oral trehalose	-	NCT04426149	Chemical chaperone	Open-label	13	6 months	Completed	-
Oral trehalose	-	NCT04399265	Chemical chaperone	Double-blind	40	3 months	Recruiting	-
Dalfampridine	-	NCT01811706	Potassium channel blocker	Double-blind	20*	4 weeks	Completed	No difference in change of T25FW and SARA score.
Deep Repetitive Transcranial Magnetic Stimulation (TMS)	-	NCT02039206	-	Open label	20	-	Phase II completed	-
Cerebellar transcranial direct current stimulation (tDCS)	Benussi <i>et al.</i> , 2018 [397]	NCT03120013	-	Double-blind	21*	2 weeks	-	Significant improvement in SARA and ICARS scores.
Stemchymal®	-	NCT02540655	Neuroprotection	Double-Blind	.*	-	Phase II unknown	-
Umbilical Cord MSCs	-	NCT03378414	-	Open label	.*	-	Not yet recruiting	-
Troriluzole	-	NCT03701399	Glutamate release inhibitor	Double-blind	.*	-	Phase III recruiting	-
BHV-4157 (pro-drug of riluzole)	-	NCT03408080	Glutamate release inhibitor	Open Label	.*	-	Phase III, active, not recruiting	-
Nilotinib (Tasigna®)	Lee <i>et al.</i> , 2017 [398]	NCT03932669	Inhibitor of tyrosine kinase BCR-ABL/Autophagy enhancer	Open label	.*	5-16 weeks	Phase II, active, not recruiting	Improvement in modified Rankin scale (mRS)
C-Trelin OD Tab	-	NCT04107740	Analogue of TRH/Inhibition of activation of glutamate	Double-blind	.*	-	Phase IV recruiting	-

\*Includes diseases other than MJD/SCA3. # Regulatory authorities did not allow the entrance of the study drug in the country. SARA - Scale for the Assessment and Rating of Ataxia; NESSCA - Neurological Examination Score for the Assessment of Spinocerebellar Ataxia; ICARS - International Cooperative Ataxia Rating Scale; T25FW - timed 25-foot walk. MSCs - mesenchymal stem cells; Ad - adipose; TRH - thyrotropin releasing hormone; TMS - transcranial magnetic stimulation; tDCS - transcranial direct current stimulation.

The therapeutic approaches tested or under evaluation in clinical trials include neurotransmission modulators, antibiotics, growth factors, ion modulators, HDAC inhibitors, autophagy enhancers, cell therapy and other approaches such as physical activity, the deep repetitive transcranial magnetic stimulation (TMS) and the cerebellar transcranial direct current stimulation (tDCS). While multiple compounds and therapeutic strategies have been suggested to date [135, 384, 399], few adequately designed interventional studies have been carried out in MJD or that included patients with the disease (Table 1.4). Indeed, most of them were completed using very few patients and only short-term effects were analyzed, which might interfere with the evaluation outcome. From all the interventions tested, none has proven to be reliably efficient. One reason for that could be that the interventions/compounds tested lack strong preclinical evidence to guide protocol design of the clinical trial. Also, most of the strategies tested did not aim at the modulation of the causes of disease (e.g., silencing of the mutant gene or protein misfolding), but rather at the downstream consequences. For instance, several neuromodulators, including buspirone, tandospirone, fluoxetine, varenicline, valproic acid and riluzole, have been tested achieving moderate results in improving major symptomatology [385, 387-389, 391, 392, 394]. The same was observed for the autophagy inducer Lithium carbonate [393], which showed no significant beneficial effect in a preclinical trial [355]. Maybe, betting on compounds that can act on the aggregation or related protein quality control mechanisms could be the way to find disease-modifying treatment for MJD patients. Remarkably, compounds such as citalopram and creatine which were proven to reduce mutant ATXN3 aggregation in MJD mouse preclinical trials [292, 303, 380] and are thought to also target downstream effects of it, could constitute good candidates for translation. The great advantage of such compounds is their safety profile and therefore are well tolerated by humans, having few or no major side effects. This would accelerate their transition into the clinics and their repurposing for MJD.

Nevertheless, ensuring that the drugs proposed to enroll in clinical trials have been robustly studied in terms of mode of action and downstream mechanisms in a particular disease context, and that sufficient preclinical evidence have been gathered is vital to increase efficacy. Clearly, an increase in the number of participating patients, in treatment duration, and follow up time will be determinant to assess if strategies proven to be promising in preclinical trials are effective or not at the clinical stage.

## 1.4 Serotonergic system in the brain

The monoamine neurotransmitter serotonin (5-hydroxytryptamine, 5-HT) is the most widely distributed neurotransmitter in the brain [400-402]. About 95 % of the 5-HT production is localized in the intestine (enterochromaffin cells), whereas in the brain the raphe nuclei neurons represent the main source of 5-HT production [403, 404]. 5-HT is involved in a multitude of physiological processes, ranging from basic physiology (respiratory drive, body temperature, sleep/circadian rhythms, feeding, reproduction, locomotion, nociception, gastrointestinal motility, cardiac function, etc.) to emotion, cognition and social behavior (Figure 1.6) [405-408].

The 5-HT system in the mammalian brain originates from the raphe nuclei (located in the midline of the hindbrain) and the reticular formation, where 5-HT producing neurons are clustered into nine nuclei numbered from B1 to B9. These clusters are subdivided into rostral (comprising the caudal linear (CLi, B8), median raphe (MR: B5 and B8), dorsal raphe (DR: B6, B7), B9 and B4 nuclei, although this last one is not consensual [409]) and caudal sections (B1, B2, B3) [400, 409, 410]. The neurons from the rostral section project axons primarily to the forebrain, innervating essentially all regions (hypothalamus, amygdala, thalamus, striatum, frontal cortex, hippocampus, cerebellum, etc.) and neurons from the caudal group project mainly to the medulla, spinal cord and cerebellum [400, 409] (Figure 1.7). The widespread reach of 5-HT neurons throughout the brain allows the modulations of several neuronal networks whose activity is required for various organismal functions.

Serotonin synthesis is derived from tryptophan obtained from the diet. The initial and rate-limiting step is the conversion of L-tryptophan to 5-hydroxy-L-tryptophan (5-HTP) [411]. This conversion is ensured by tryptophan 5-hydroxylase (TPH), which has two isoforms, TPH1 and TPH2. The first isoform is primarily localized in the enterochromaffin cells, in peripheral tissues, while TPH2 is principally found in the CNS [412, 413]. The second and last step is the conversion of 5-HTP into 5-HT by an aromatic L-amino acid decarboxylase [414]. Once formed, it rapidly gets transported into vesicles via a vesicular monoamine transporter (VMAT), which exists in two isoforms: VMAT1 present in neuroendocrine cells and VMAT2 present in neurons [415]. Serotonin is then released via exocytosis into the synaptic cleft by a  $\text{Ca}^{2+}$ -dependent process, where it can bind pre- and/or post-synaptic serotonin receptors. Serotonin reuptake from the extracellular space to 5-HT neurons is mediated by the membrane-bound 5-HT transporter (SERT, SLC6A4, 5HTT), a  $\text{Na}^+/\text{Cl}^-$ -dependent transporter, located in cellular bodies, dendrites and/or axons of those [416, 417]. Upon reuptake, serotonin is catabolized by monoamine oxidase (MAO) enzyme into 5-hydroxyindoleacetic acid (5-HIAA) or, alternatively, converted into melatonin by acetylation and subsequent methylation (this conversion occurring primarily in the pineal gland) [418].

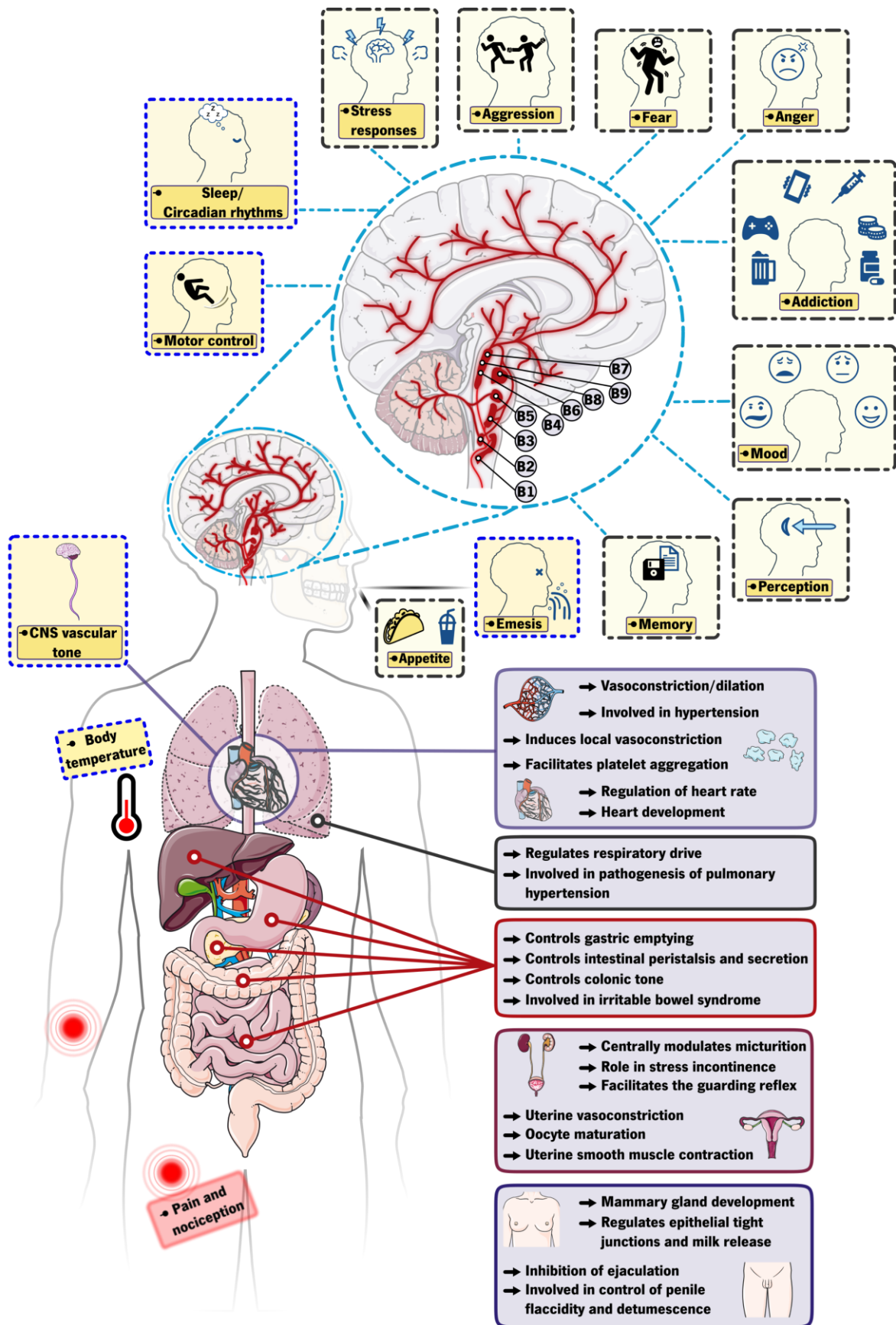


**Figure 1.6 Serotonergic system and effects in the organism.** In the central nervous system (CNS), serotonergic neuronal projections arise from neurons originating in the raphe nuclei, in the midline of the brainstem (represented in red).

This region is further subdivided into 9 nuclei: B1-B9. Serotonergic projections enervate essentially all brain regions, controlling nearly all behaviors and numerous other brain functions. Dashed line boxes represent CNS behavioral effects (— — —) and other CNS effects (- - - - -). Effects outside the CNS are also represented (boxes without dashed lines). Figure design was based in the following references: [405, 419].

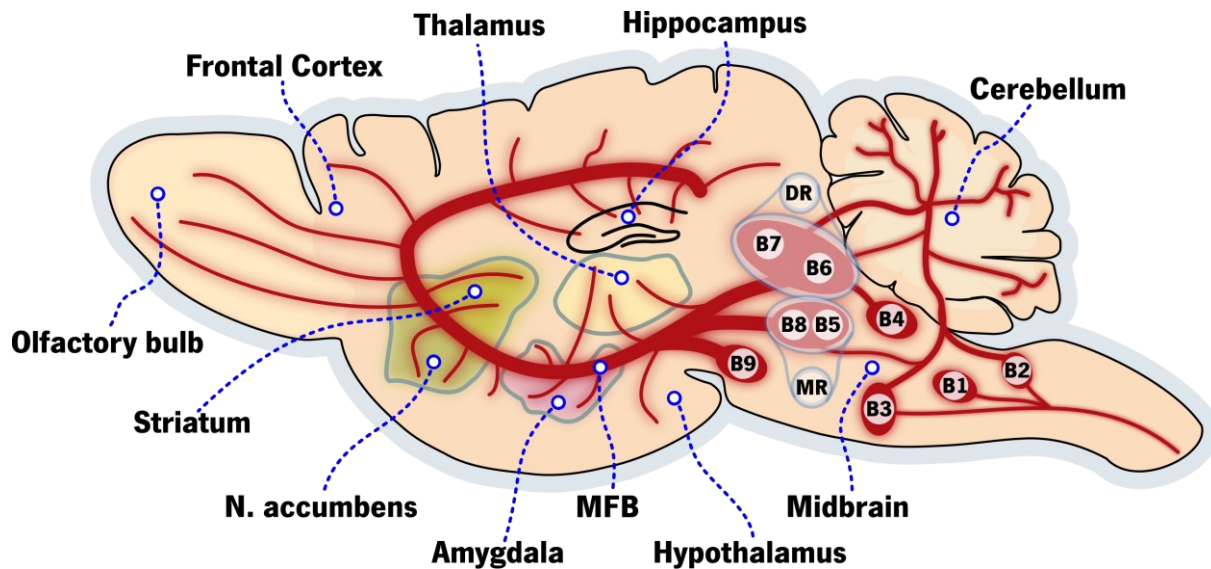


**Figure 1.7 Serotonergic system of the mouse brain.** Serotonergic neuronal projections arise from nine raphe nuclei (B1-B9) in the brainstem, that enervate all the regions of the brain. The caudal nuclei (B1-B3) primarily send projections to the spinal cord and cerebellum, while the more rostral nuclei, including the median raphe (MR: B5 and B8) and the dorsal raphe (DR: B6 and B7) nuclei, send projections to the forebrain, enervating all and overlapping regions. MFB - medial frontal bundle. Figure design based on [409, 420].

### 1.4.1 Serotonergic signaling

The multitude of physiological functions of 5-HT results from its wide distribution in the CNS and from the existence of seven 5-HT receptor classes (5-HT<sub>1</sub>, 5-HT<sub>2</sub>, 5-HT<sub>3</sub>, 5-HT<sub>4</sub>, 5-HT<sub>5</sub>, 5-HT<sub>6</sub>, 5-HT<sub>7</sub>), further divided in at least 14 different subclasses, according to the current accepted classification system [421, 422], as summarized in Table 1.5. All those receptors belong to the superfamily of the seven-transmembrane-domain G protein-coupled receptors (GPCRs), except for the 5-HT<sub>3</sub> family, which are ligand-gated ionic channels and permeable to sodium (Na<sup>+</sup>), potassium (K<sup>+</sup>) and Ca<sup>2+</sup> [422]. Six of the seven classes belong to the GPCRs, implicating that their signaling pathways are dependent on the connection to heterotrimeric GTP-binding proteins (G proteins), which undergo cycles of activation and inactivation, allowing reversible and specific signal transduction. The binding of serotonin to its GPCRs subsequently activates G proteins that, within the cell, are coupled to the intracellular loops and



C-terminus of those receptors. Then, G proteins dissociate from the receptor and their interaction with intracellular effectors is promoted [423]. G proteins are referred to by their subunits ( $\alpha$ ,  $\beta$  and  $\gamma$ ). The  $\alpha$  subunit is in charge of guanosine triphosphate (GTP) and guanosine diphosphate (GDP) binding, including GTP hydrolysis, while the other subunits ( $\beta$  and  $\gamma$ ) are associated in a complex [424]. As a result of G protein variety (16  $\alpha$ , 5  $\beta$  and 12  $\gamma$ ), the downstream-activated signaling might differ for each receptor.

**Table 1.5 Overview of serotonin receptors.** Based on [425, 426].

Receptor Class	Subclasses	Type	Main signaling pathway	Function	Main expression in the CNS
5-HT <sub>1</sub>	5-HT <sub>1A</sub>	G <sub>i/o</sub>	AC i	Inhibitory auto- and heteroreceptor	Widespread in the brain (mainly raphe nuclei, hippocampus, and cortex).
	5-HT <sub>1B</sub>	G <sub>i/o</sub>	AC i		Widespread in brain (mainly basal ganglia and cortex).
	5-HT <sub>1D</sub>	G <sub>i/o</sub>	AC i		Basal ganglia, hippocampus, cortex.
	5-HT <sub>1E</sub>	G <sub>i/o</sub>	AC i		Cortex, caudate putamen, and claustrum.
	5-HT <sub>1F</sub>	G <sub>i/o</sub>	AC i		Dorsal raphe nucleus, hippocampus, claustrum, caudate nucleus, brainstem, and cortex.
5-HT <sub>2</sub>	5-HT <sub>2A</sub>	G <sub>q/11</sub>	PLC s	Excitatory heteroreceptor	Cortex, claustrum, hippocampus, and basal ganglia.
	5-HT <sub>2B</sub>	G <sub>q/11</sub>	PLC s		Cerebellum, septum, hypothalamus, and amygdala.
	5-HT <sub>2C</sub>	G <sub>q/11</sub>	PLC s		Striatum, substantia nigra, amygdala, hippocampus, cortex, and choroid plexus.
5-HT <sub>3</sub>	Pentamer of 5-HT <sub>3A</sub> with 5-HT <sub>3B, C, D, E</sub> subunits	Ion channel		Excitatory heteroreceptor	Widespread in the brain (mainly area postrema, nucleus tractus solitarius, dorsal vagal complex, and limbic regions).
5-HT <sub>4</sub>		G <sub>s</sub>	AC s	Excitatory heteroreceptor	Cortex, basal ganglia, septum, and hippocampus.
5-HT <sub>5</sub>	5-HT <sub>5A</sub>	G <sub>i/o</sub>	AC i	Inhibitory	Olfactory bulb, hippocampus, hypothalamus, thalamus, cortex, striatum, and pons.
	* 5-HT <sub>5B</sub>	?	?		In rodents: habenula, raphe nuclei and hippocampus. In humans: pseudogene.
5-HT <sub>6</sub>		G <sub>s</sub>	AC s	Excitatory	Widespread in brain (mainly cortex, hippocampus, striatum, and amygdala).
5-HT <sub>7</sub>		G <sub>s</sub>	AC s	Excitatory	Thalamus, amygdala, cortex, hippocampus, and suprachiasmatic nucleus.

\* Not expressed in human. CNS - central nervous system; AC - adenylate cyclase; PLC - phospholipase C; i - inhibition; s - stimulation.

There are four distinct  $\alpha$ -subunit subfamilies:  $G_s$  proteins that stimulate adenylyl cyclase (AC);  $G_i$  that inhibit AC and activate G protein-coupled inwardly rectifying potassium (GIRK) channels [427];  $G_q$  proteins responsible for the activation of phospholipase C (PLC) [428]; and  $G_{12}$  proteins that activate Rho guanine-nucleotide exchange factors (GEFs) [429]. Additionally, signaling through  $\beta$  and  $\gamma$  subunits is known to have several effectors. Those include AC [430], PLC $\beta$ 2 [431], phosphoinositide 3-kinase (PI3K) [432], components of the mitogen activated protein kinase (MAPK) cascade family [433],  $Ca^{2+}$  [434] and  $K^+$  [435] channels. As evidenced in Table 1.5, the different 5-HT receptors are coupled to different G protein types, thus able to signal through different pathways.

### 5-HT<sub>1</sub> receptor family

In this family, five different subclasses of receptors can be found: 5-HT<sub>1A</sub>, 5-HT<sub>1B</sub>, 5HT<sub>1D</sub>, 5-HT<sub>1E</sub>, and 5-HT<sub>1F</sub>. They couple primarily through  $G_{i/o}$  proteins, not only inhibiting AC (and decreasing cyclic adenosine monophosphate (cAMP) levels), but also affecting numerous other effectors and signaling pathways.

**The special case of 5-HT<sub>1A</sub> receptor (5-HT<sub>1A</sub>R).** Those receptors are associated with  $G_{i/o}$  proteins, suggesting a negative coupling to AC and to ion channels in membranes. In fact, 5-HT<sub>1A</sub>R has been demonstrated to act through the cAMP pathway. The inhibitory action of this receptor on AC was evidenced by suppression of cAMP levels or by its ability to inhibit forskolin-stimulated AC activity [436, 437]. Surprisingly, it does not inhibit AC in a universal manner. This receptor has been shown not to inhibit AC in rat dorsal raphe neurons, a region where it is highly expressed. However, this might be species specific, since Palego and collaborators demonstrated that this was not the case in human dorsal raphe [438, 439]. Controversially, 5-HT<sub>1A</sub>R has been shown to stimulate AC in rat hippocampus [440]. This is perplexing since this receptor was not reported to couple to  $G_s$  [441] and most of the evidence gathered point to the opposite effect, but one cannot disregard the fact that this might happen in a very specific cellular context.

There is also evidence for 5-HT<sub>1A</sub>R activation to stimulate PLC and the hydrolysis of phosphatidylinositol biphosphate, however with a much lower efficacy than AC inhibition [442]. Perhaps this effect is highly cell-specific, since native 5-HT<sub>1A</sub>Rs in a human T-cell-like line also activate PLC [443], but transfected ones do not stimulate PLC in CHO cells [444], for instance.

Studies have demonstrated a 5-HT<sub>1A</sub>R role in ionic current pathways. The control of  $K^+$  channels by these receptors in neurons has been observed [445], in addition to the regulation of GIRK channels [446]. 5-HT<sub>1A</sub>R activation was also reported to influence  $Ca^{2+}$  currents in neurons [447].

Another 5-HT<sub>1A</sub>R-regulated transduction pathway is the MAPK signaling pathway, which includes several kinases [448, 449]. Of these, extracellular signal-regulated kinase (ERK) is particularly affected by 5-HT<sub>1A</sub>Rs. They were first reported to activate ERK by phosphorylation in (CHO-K1) non-neuronal cells expressing 5-HT<sub>1A</sub>Rs [450]. Phosphorylation of proteins by ERK in neurons led to ion channel activation, gene expression and neuroplasticity [451]. One example is the activation of the CREB transcription factor, by the serine/threonine protein kinase RSK, an ERK substrate [452]. Also, in CHO cells activation of the transfected 5-HT<sub>1A</sub>Rs induced another type of signaling, mediated by another serine/threonine protein kinase, Akt (also known as protein kinase B (PKB)), leading to the inactivation of GSK3 $\beta$  [453]. The coupling of this receptor to ERK1/2 and Akt was also observed in the hippocampus [454, 455]. Comprehensive reviews on the 5-HT<sub>1A</sub>R-dependent and complex signaling have been elaborated [456, 457].

A particular feature of the 5-HT<sub>1A</sub>R is its ability to function as an auto- and heteroreceptor [458]. A higher level of complexity in signaling derives from its inhibitory role as autoreceptor in serotonergic neurons against its inhibitory function as heteroreceptor on terminal targets of these 5HT-producing neurons. In support of this, numerous studies have evidenced regional differences in the functional characteristics of this receptor in the brain [459]. 5-HT<sub>1A</sub>Rs are found on serotonergic neuron cell bodies and dendrites, mainly in the midbrain raphe nucleus region, as presynaptic autoreceptors; and on terminal targets of 5-HT delivery as postsynaptic heteroreceptors, mostly in the limbic brain and cortical areas [458, 460, 461]. Presynaptically, this receptor acts as a stop signal, to inhibit the activity of the entire serotonergic system [462, 463]. Moreover, it has been demonstrated that in the raphe nucleus, the autoreceptor preferentially couples to G<sub>3</sub> in contrast to hippocampal heteroreceptors that preferentially couple to G<sub>2</sub> or G<sub>o</sub> [459, 464]. The negative regulation of neuronal 5-HT activity, by 5-HT<sub>1A</sub> autoreceptors, is in part dependent on the inhibition of AC [464] but, interestingly, this pathway seems to depend on the 5-HT<sub>1A</sub>R agonist used. 5-HT<sub>1A</sub>R mediated inhibition of AC in the dorsal raphe was ineffective using flibanserin (a 5-HT<sub>1A</sub>R agonist), while 5-HT and buspirone (a 5-HT<sub>1A</sub>R partial agonist) were effective, flibanserin being only effective in the pre-frontal cortex [465]. Differences in 5-HT<sub>1A</sub> auto- and heteroreceptor coupling to ERK1/2 activation have been documented. In rat raphe RN64A cells, endogenous 5-HT<sub>1A</sub>Rs couple to inhibit AC and ERK1/2 phosphorylation [466]. In contrast, 5-HT<sub>1A</sub>R in hippocampal-derived cells increased ERK1/2 phosphorylation [454]. Overall, 5-HT<sub>1A</sub> auto- and heteroreceptors can therefore signal to diverse and sometimes contrary signaling pathways.

### 5-HT<sub>2</sub> receptor family

There are three members of this subclass (5-HT<sub>2A</sub>, 5-HT<sub>2B</sub> and 5-HT<sub>2C</sub>) and in general coupled to G<sub>q/11</sub> proteins. Those receptors consistently couple to the PLC $\beta$  pathway, activating it and hydrolyzing phosphatidylinositol bisphosphate (PIP<sub>2</sub>) into inositol 1,4,5-trisphosphate (IP<sub>3</sub>) and diacylglycerol (DAG) [467, 468]. IP<sub>3</sub> serves as a second intracellular messenger to stimulate the release of Ca<sup>2+</sup> from the ER, while DAG activates protein kinase C (PKC) [469, 470]. This family of receptors also activates phospholipase A<sub>2</sub> (PLA<sub>2</sub>), leading to the release of arachidonic acid or to the stimulation of ERK1 and ERK2 of the MAPK pathway [471].

### 5-HT<sub>3</sub> receptor

Within 5-HT receptors, the 5-HT<sub>3</sub> receptor (5-HT<sub>3</sub>R) is the only member of the ligand-gated ionic channels superfamily [472]. They are present both post- and presynaptically on neuronal cell bodies and dendrites and trigger fast neuronal responses [473, 474]. These receptors are lowly expressed in the limbic system, such as the amygdala and the hippocampus, and in the frontal, piriform and entorhinal cortices. Higher levels of 5-HT<sub>3</sub>Rs were found in the brainstem, in areas such as the nucleus tractus solitarius and the nucleus of the spinal tract of the trigeminal nerve, and also in the spinal cord [473]. Structurally, 5-HT<sub>3</sub>R is composed by a pentameric structure surrounding a central ion channel, formed by five  $\alpha$ -helical M2 domains, which is permeable to cationic ions like K<sup>+</sup>, Na<sup>+</sup>, and Ca<sup>2+</sup> [475]. Two genes encoding 5-HT<sub>3</sub>R subunits (5-HT<sub>3A</sub> and 5-HT<sub>3B</sub>) exist in rodents, while five subunits (5-HT<sub>3A</sub>, 5-HT<sub>3B</sub>, 5-HT<sub>3C</sub>, 5-HT<sub>3D</sub>, 5-HT<sub>3E</sub>) have been cloned in human [476-478]. Functional receptors can be formed by the assembly of 5-HT<sub>3A</sub> subunits only, whereas receptors composed only by 5-HT<sub>3B/C/D/E</sub> subunits are not functional [479]. Native 5-HT<sub>3</sub>R are likely an assembly of 5-HT<sub>3A</sub> and 5-HT<sub>3B</sub> subunits and also possibly some 5-HT<sub>3C/D/E</sub> subunits [480], although the stoichiometry of the different subunits that compose a native pentameric receptor has not been totally elucidated [481]. Functionally, this receptor leads to the stimulation of nitric oxide (NO) synthase, which is followed by the induction of cyclic guanosine monophosphate (cGMP) that elicits chloride (Cl<sup>-</sup>) efflux [482].

### 5-HT<sub>4</sub> receptor

The 5-HT<sub>4</sub> receptor (5-HT<sub>4</sub>R) was first described by Dumuis and collaborators, in 1988, in colliculi and hippocampal neurons, and shown to be positively coupled to AC [483]. This subclass of receptor is principally present in limbic areas, namely in the hippocampus, nucleus accumbens, amygdala, hypothalamus, and septum. It is also found in the islands of Calleja, olfactory tubercle, striatum, globus

pallidus and substantia nigra [484]. Indirect evidence suggests that most 5-HT<sub>4</sub>Rs are localized postsynaptically, although lesions and electrophysiological studies also pointed towards a presynaptic localization in different neurons [485, 486]. 5-HT<sub>4</sub>Rs activate AC, thus raising intracellular cAMP levels [483, 487], albeit to a different extent upon agonist stimulation in HEK 293 cell lines transfected with different isoforms [488]. This could be explained by the different coupling to G proteins of the different isoforms of this receptor, which could account for functional differences between them. While human isoform 5-HT<sub>4</sub>(a) was found to couple only to G<sub>s</sub> proteins, isoform 5-HT<sub>4</sub>(b) coupled to G<sub>i/o</sub> in addition to G<sub>s</sub> coupling [488]. This type of receptor has also been found to regulate a variety of channels and consequently to modulate ionic current-mediated pathways. For instance, they activate L-type Ca<sup>2+</sup> channels [489], but can also have an inhibitory effect on other ionic currents [490].

### 5-HT<sub>5</sub> receptors

In this family, two different receptor subclasses have been identified: 5-HT<sub>5A</sub> and 5-HT<sub>5B</sub> [491]. In the brain, 5-HT<sub>5</sub>Rs are found in the cerebral cortex, hippocampus, cerebellum, hypothalamus, pons and striatum, among others, the distribution of 5-HT<sub>5B</sub>Rs being more limited in the brain [491, 492]. 5-HT<sub>5A</sub>R is expressed and functional in the human brain, but 5-HT<sub>5B</sub>R does not encode a functional protein [493]. So far, 5-HT<sub>5</sub>Rs have not been convincingly connected to a specific physiological effect or signal transduction pathway in mammalian cells. 5-HT<sub>5A</sub>R expression was predominantly observed in astrocytes, in the rat central nervous system. When transfected into glioma cells it decreased cAMP levels by 20 %, suggesting that it is negatively coupled to AC in astrocytes [494]. When expressed in C6 glioma cells, human 5-HT<sub>5A</sub>R activation led to (i) an inhibition of cAMP accumulation, and (ii) to an inhibition of ADP-ribosyl cyclase activity, indicating a decrease in cyclic ADP ribose, which constitutes a possible intracellular second messenger mediating ryanodine-sensitive Ca<sup>2+</sup> mobilization. Besides that, this receptor also regulated Ca<sup>2+</sup> level by IP3-sensitive Ca<sup>2+</sup> stores mobilization, consequently triggering K<sup>+</sup> outward currents [495]. In HEK cells, the 5-HT<sub>5A</sub>R couples to G<sub>i</sub> protein, inhibiting AC and PKA accumulation [496]. On the other hand, 5-HT<sub>5B</sub>R was shown to couple to a G protein in COS cells, but without altering cAMP accumulation or phosphoinositide turnover in fibroblast cell lines [497]. Hence, the specific G proteins to which these receptors couple, their downstream signaling, and physiological effects remain vaguely defined.

### 5-HT<sub>6</sub> receptor

In 1993, the rat 5-HT<sub>6</sub> receptor (5-HT<sub>6</sub>R) was cloned [498, 499] and later it was cloned in humans [500]. This receptor can predominantly be found in the caudate nucleus, olfactory tubercle, hippocampus, striatum, and nucleus accumbens [499, 501]. 5-HT<sub>6</sub>R activation stimulates AC activity through the interaction with G<sub>s</sub> proteins, therefore also activating the downstream PKA pathway in transfected cell lines [499, 500], striatal cultured neurons [502] and pig caudate membranes [503]. The activation of endogenously expressed 5-HT<sub>6</sub>Rs induces a reduction of inward currents involving K<sup>+</sup> channels, in striatal cholinergic neurons [504]. Moreover, in transfected cell lines, stimulation of this serotonin receptor activates ERK by a mechanism dependent on the phosphorylation of Fyn, a member of the Src family of non-receptor protein-tyrosine kinases. This ultimately activates ERK1/2 via Ras- and MEK-dependent pathways [505]. Signaling pathways associated with phosphorylated ERK1/2 expression in the hippocampus appear to be connected to the cognition-enhancing features of 5-HT<sub>6</sub>R modulators [506].

### 5-HT<sub>7</sub> receptor

The 5-HT<sub>7</sub> receptor (5-HT<sub>7</sub>R) is the third 5-HT class shown to couple to G<sub>s</sub> [507, 508]. It is expressed in the CNS, particularly in the hippocampus, hypothalamus, and neocortex, and has been thought to play a role in the circadian rhythm regulation [508, 509]. 5-HT<sub>7</sub>Rs are coupled to G<sub>s</sub> and their stimulation translates into a strong activation of AC and cAMP accumulation [507, 510]. In transfected HEK cells, the 5-HT<sub>7</sub>R besides stimulating AC5, depending on G<sub>s</sub> stimulation, also stimulated AC1 and AC8, which are insensitive to G<sub>s</sub> but sensitive to Ca<sup>2+</sup>/calmodulin [510]. This receptor was also shown to activate G<sub>12</sub> and to induce a serum response element-mediated gene transcription, in NIH3T3 cells, through small GTPases in a PKA- and pertussis-toxin-independent manner [511]. Stimulation of the MAPK pathway, through ERK1/2 was also reported for 5-HT<sub>7</sub>R in rat hippocampal neurons [512]. In HEK cells, cAMP and Ca<sup>2+</sup> both contributed to the Ras-dependent ERK1/2 activation in response to the stimulation of this class of 5-HT receptors [513].

Extensive reviews on 5-HT receptors' specific characteristics and signaling have been published [421, 514, 515]. The existence of such 5-HT receptor diversity largely contributes to the complex serotonin receptor mediated signaling network and could explain the vast and diverse range of serotonin-controlled functions in the organism. In 2018, a consolidative pathway map of serotonin has been constructed, and its schematic representation truly reveals the complexity associated to this neurotransmitter [516].

### 1.4.2 Serotonin signaling in the treatment of depression

Serotonin (5-HT) and its signaling are important for a wide range of neuropsychological processes, as represented in Figure 1.6, and drugs that target 5-HT receptors are extensively used in neurology and psychiatry. Mood is one of the aspects that is regulated by this neurotransmitter and therefore, it is not surprising that depression (also known as major depressive disorder - MDD), a persistent recurring mood condition [517], has been associated to 5-HT. The discovery that substances, such as reserpine, an antihypertensive, reduced monoamine levels and that some patients developed MDD upon drug treatment contributed to this association [518]. Moreover, the serendipitous finding of the action of antidepressant drugs, such as monoamine oxidase inhibitors (MAOIs) and tricyclic antidepressants (TCAs) suggested that depression was related to low concentrations of serotonin [519]. This led to the *serotonin hypothesis of clinical depression* which proposed, in simple terms, that a decreased activity of serotonin pathways played a role in the pathophysiology of this disorder. This 5-HT deficit would be reversed by antidepressants (MAOIs and TCAs), which would restore normal function in depressed patients [519].

Several 5-HT-related deficits have been linked to aspects of the pathophysiology of MDD. Interestingly, it has been shown that high-risk family members of MDD patients are more sensitive to challenges directed toward 5-HT processes, such as tryptophan/5-HT depletion [520, 521]. Also, depressed patients displayed low levels of 5-HT in blood platelets [522]. Moreover, depletion of dietary tryptophan induced a recurrence of depressive symptoms [523].

The strongest evidence for the role of 5-HT in MDD comes from the efficacy of increasing 5-HT extracellular levels in the treatment of depression. MAOIs act by inhibition of MAO enzyme, which catalyzes the oxidative deamination of a range of monoamines including 5-HT, histamine and catecholamines (dopamine, adrenaline, and noradrenaline). Therefore, MAOIs prevent the breakdown of monoamines, enhancing the availability of releasable neurotransmitters [524]. Besides increasing 5-HT levels in many regions of the CNS [525], MAOIs have been shown to modulate other aspects of 5-HT transmission, such as the desensitization of 5-HT<sub>1A</sub> autoreceptors and postsynaptic 5-HT<sub>2C</sub>Rs [526, 527]. On the other hand, TCAs block the reuptake of monoamines in the presynaptic neuron, leading to an increase in monoamine concentration [528]. Additionally, they act as competitive agonists on post-synaptic alpha cholinergic, muscarinic and histaminergic receptors [529]. For some TCA agents (nortriptyline and amitriptyline), a significant affinity for 5-HT<sub>2C</sub> and 5-HT<sub>2A</sub> receptors has been reported, which might contribute to their antidepressant properties [530].

Although MAOIs and TCAs do not differ in terms of efficacy in the treatment of MDD, both classes of drugs showed compelling antidepressant efficacy in comparison to placebo. Nevertheless, their side

effect profiles are wider than for other antidepressant classes, probably due to their activity in a large range of monoamine receptors [531]. Therefore, with the emergence of new compounds with fewer dangerous side effects and limited risks in overdose and comparable antidepressant effects, such as selective serotonin and norepinephrine reuptake inhibitors (SSRIs and SNRIs, respectively), they became less prescribed and are usually used only when there is intolerance or lack of response to the newer drugs.

### **1.4.3 Selective Serotonin Reuptake Inhibitors (SSRIs): mode of action**

Selective Serotonin Reuptake Inhibitors (SSRIs) represent an important advance in the pharmacotherapy, as they were a rationally designed medication. Nowadays, they are among the most prescribed drugs in medicine. There are six main SSRIs, including citalopram (Celexa®), escitalopram (Lexapro®), fluoxetine (Prozac®), fluvoxamine (Luvox®), paroxetine (Paxil®) and sertraline (Zoloft®) [532]. This class of drugs is used for the treatment of many psychiatric illnesses, such as major depressive disorder, panic disorder, obsessive-compulsive disorder (OCD) and even eating disorders [533].

SSRIs were all developed to have a similar mechanism of action that consists in 5-HT potentiation through the inhibition of its neuronal uptake pump, the serotonin transporter SERT. The advantage of this type of antidepressant, in comparison to other classes, is that they have a good side-effect profile, they are well tolerated and are safer in overdose. Although SSRIs are very similar in terms of efficacy and adverse effect profiles, these drugs have considerable differences in their pharmacokinetics and their effect on drug metabolizing enzymes, namely on cytochrome P450 [532]. Of those, citalopram seems to be the most selective inhibitor of 5-HT reuptake [534].

#### **1.4.3.1 The specific case of citalopram**

Citalopram hydrobromide (MW 405.35 Da) was developed by Lundbeck, a pharmaceutical company from Denmark. Citalopram is usually a therapeutic approach used for the treatment of depression, preventing relapses [535], and for other psychiatric conditions such as anxiety [536], panic perturbations (with or without agoraphobia) [537], or even OCD [538]. This compound is a (1:1) racemic mixture that comprises an S(+)-enantiomer (escitalopram) and an R(-)-enantiomer (R-citalopram). The S(+)-enantiomer has been shown to underlie essentially all the 5-HT reuptake inhibition [539]. As the other SSRIs, it exerts its effects by strongly inhibiting the reuptake of 5-HT from the synaptic cleft. It is the most selective of them, having minimal effects on noradrenaline and dopamine transporters, as well as



little or absent affinity for neurotransmitters such as acetylcholine, GABA, histamine, muscarinic, benzodiazepine and opioid receptors. It also has a low affinity for a range of serotonin receptors, including 5-HT<sub>1A</sub>, 5HT<sub>1B</sub>, 5-HT<sub>2A</sub>, 5-HT<sub>2C</sub> receptors [540]. In general, antidepressant therapy must be administered for two to four weeks before improvements become apparent. This has been attributed to the sequential occurrence of events: (i) the increased extracellular serotonin levels, that activates somatodendritic 5-HT<sub>1A</sub> autoreceptors in short term treatment; (ii) the resulting feedback inhibition of the raphe nucleus; and (iii) downregulation/desensitization of the autoreceptors and increase in serotonergic neurotransmission [541]. However, this desensitization hypothesis view has been challenged, since there is evidence that feedback inhibition, mediated by remaining receptors, persists, even though 5-HT<sub>1A</sub>Rs may desensitize. Thus, serotonin firing rates return to baseline, not because of 5-HT<sub>1A</sub> autoreceptor desensitization, but despite ongoing feedback inhibition. Also, it was suggested that slow-adaptative alterations prompted by antidepressants, such an adaptation in glutamatergic synaptic plasticity, might contribute to therapeutic effects [542]. Despite that, the general mechanism of action of SSRIs includes SERT inhibition that triggers an acute increase of 5-HT within the synapse and, ultimately, 5-HT binding to several receptors, which trigger subsequent intracellular signaling events mediated by G proteins [543].

The precise intracellular mechanisms of SSRI action, namely of citalopram, are not fully understood. Nevertheless, there are several reports in the literature acknowledging alterations prompted by citalopram administration. For instance, chronic administration of citalopram had an impact on glutamate N-methyl-D-aspartate (NMDA) receptor subunit mRNAs [544]. It was also demonstrated that chronic administration of citalopram increased the activation of CREB in the hippocampus [545], and increased the (mRNA) expression of brain-derived neurotrophic factor (BDNF) [546].

#### **1.4.4 Serotonergic signaling in the context of neurodegenerative disorders**

As serotonergic signaling is widespread throughout the brain and known to be involved in a multitude of cellular and organism functions (Figure 1.6), it is possible that its signaling dysregulation could impact and even contribute to neurodegenerative disorders, including polyQ diseases. Interestingly, drugs that directly target the serotonergic system, such as antidepressants, are often prescribed to patients with neurodegenerative diseases, to treat depression and anxiety symptoms [547]. Besides having a positive impact on mood, those could be positively impacting on other type of symptomatology associated to movement, and even act on the mechanism underlying each disease.

A building amount of preclinical and clinical reports are starting to emerge, in the literature, not only reporting 5-HT-related deficits in neurodegenerative disorders but also a neuroprotective effect of

antidepressants in this context [548-550]. In the post-mortem frontal cortex of AD patients, it has been shown that decreased 5-HT levels and increased 5-HT<sub>1A</sub>R density were associated to a faster rate of cognitive decline [551, 552]. A decrease in 5-HT<sub>2A</sub> and 5-HT<sub>6</sub> receptors was also observed in AD patients [553]. Interestingly, chronic administration of SSRIs was demonstrated to improve memory function in those patients [554, 555]. Moreover, serotonin signaling has been associated to the lowering of pathological hallmarks (amyloid- $\beta$  levels and plaques) in transgenic mice but also in humans [548].

The serotonergic system also seems to be affected in PD. In fact, there are several reports describing neuronal loss and dystrophic neurites in 5-HT producing neurons of the raphe nuclei of PD patients [556, 557]. Lewy bodies were also observed in 5-HT raphe neurons [557, 558]. Moreover, according to the Braak staging of PD, the raphe nuclei become affected in stage 2, becoming completely involved by stage 3 [559, 560]. Modulation of the 5-HT system in PD has potential therapeutic effect to improve symptomatology (as reviewed in [561]).

In the case of polyQ disorders, namely in HD, the antidepressant citalopram was tested, aiming at enhancing cognition in patients. In this study, the authors verified no effects on motor rating or executive functions or psychiatric symptoms, although an improvement was noticed in the depression symptoms, upon 16 weeks (short) treatment with citalopram [562]. As previously mentioned, compounds that target the serotonergic system have been tested in MJD clinical trials (see Table 1.3), namely due to the role of the serotonergic system in the cerebellum in regulating motor outputs such as locomotion [563], or based on previous observations. For instance, buspirone and tandospirone led to improvements in ataxia and eased other motor and non-motor symptoms [385, 387, 389]. Furthermore, an SSRI, fluoxetine was also tested in an open-label study. A short period of treatment was assessed (6 weeks) in a limited number of patients, revealing no improvements in motor abilities [388].

However, studies conducted in invertebrates and vertebrates suggest that SSRIs could have a beneficial impact in MJD. By screening of a library of USA Food and Drug Administration (FDA)-approved compounds, using a *C. elegans* model for MJD with expression of mutant ATXN3 in the nervous system, Teixeira-Castro and colleagues found that the SSRI citalopram could be an interesting new therapeutic strategy for this disease. It was able to significantly reduce ATXN3-dependent aggregation and ATXN3-induced neurotoxicity in worms, possibly through increasing mutant ATXN3 solubility. It was also demonstrated that MOD-5 (the *C. elegans* ortholog of the serotonin transporter and citalopram's target) and two other serotonin receptors, SER-1 and SER-4 (orthologs of the 5-HT<sub>2</sub> and 5-HT<sub>1</sub> receptors families, respectively), were necessary for therapeutic efficacy [303]. Moreover, the same was reproduced in a preclinical trial using the CMVMJD135 mouse model, treated pre-symptomatically with citalopram.

Chronic citalopram treatment improved motor symptoms and rescued body weight. It also drastically reduced ATXN3 aggregation in several regions of the brain, such as the pontine nuclei, the reticulotegmental nuclei of pons and the facial motor nuclei, areas affected in the disease. Astrogliosis was mitigated in the brainstem and neuroprotective effects were observed by (i) the rescue of motor neurons in the facial motor nuclei, and a decrease in the loss of ChAT+ neurons in the spinal cord upon treatment; and (ii) mitigation of calbindin D28-K-positive cells reduction observed in the cerebellar cortex of CMVMJD135 mice [303]. The beneficial effect of citalopram chronic treatment was further validated in an independent YAC transgenic MJD mouse model (YACMJD84.2). Interestingly, transgenic-treated mice revealed a 50 % decrease in the percentage of cells containing ATXN3-positive inclusions, in the substantia nigra, pontine nuclei, vestibular nuclei and facial nuclei. In this model, a decrease in soluble and insoluble forms of ATXN3 protein were also observed in some brain areas when comparing transgenic vehicle- and citalopram-treated mice. In this study, citalopram also led to alterations in the levels of specific chaperones (Hsp90 and Hsp40) and autophagy-related proteins (p62 and beclin-1), further suggesting that this drug could enhance the refolding and/or degradation of mutant ATXN3 [380].

These preclinical studies offered a strong base for a future attempt to perform a human clinical trial for MJD. In the meantime, continuing to understand how citalopram mediated its effects is the next step to find new possible therapeutic targets to be used in the treatment of this harshly damaging disease.

## 1.5 Aims of the thesis

Having in mind (i) the increasing impact of neurodegenerative disorders in the society (ii) the urgent need to find new therapies for these diseases and (iii) the therapeutic potential demonstrated by the SSRI citalopram in preclinical trials using different *C. elegans* and mouse models of MJD, here we specifically aimed to:

- Study citalopram's therapeutic effect in a preclinical setting, mimicking the most frequent clinical situation of symptom-driven diagnosis and treatment initiation of MJD patients, i.e., testing citalopram's therapeutic effect in a post-symptomatic chronic treatment modality (chapter 2);
- Uncover the molecular changes associated with citalopram action through a global transcriptomic analysis of transgenic vehicle-treated and transgenic citalopram-treated mice (chapter 3.1);
- Explore specific alterations in protein homeostasis, at the transcriptional level, triggered by SSRI chronic treatment (chapter 3.2);
- Decipher the molecular determinants underlying serotonergic signaling-mediated suppression of proteotoxicity, by performing a transcriptomic analysis of a genetic *C. elegans* model of increased

serotonergic neurotransmission, mimicking citalopram's action, by ablation of the serotonin transporter *mod-5*/SERT in animals expressing mutant ATXN3 proteins (chapter 4).

## References

1. Beard, J.R., Officer, A., de Carvalho, I.A., Sadana, R., *et al.*, The World report on ageing and health: a policy framework for healthy ageing. *Lancet*, 2016. **387**(10033): p. 2145-2154.[https://doi.org/10.1016/S0140-6736\(15\)00516-4](https://doi.org/10.1016/S0140-6736(15)00516-4).
2. Erkkinen, M.G., Kim, M.-O., and Geschwind, M.D., Clinical Neurology and Epidemiology of the Major Neurodegenerative Diseases. *Cold Spring Harbor Perspectives in Biology*, 2018. **10**(4).<https://doi.org/10.1101/cshperspect.a033118>.
3. Heemels, M.-T., Neurodegenerative diseases. *Nature*, 2016. **539**(7628): p. 179-179.<https://doi.org/10.1038/539179a>.
4. Dugger, B.N. and Dickson, D.W., Pathology of Neurodegenerative Diseases. *Cold Spring Harbor Perspectives in Biology*, 2017. **9**(7).<https://doi.org/10.1101/cshperspect.a028035>.
5. Taylor, J.P., Hardy, J., and Fischbeck, K.H., Toxic Proteins in Neurodegenerative Disease. *Science*, 2002. **296**(5575): p. 1991-1995.<https://doi.org/10.1126/science.1067122>.
6. Gitler, A.D., Dhillon, P., and Shorter, J., Neurodegenerative disease: models, mechanisms, and a new hope. *Disease Models & Mechanisms*, 2017. **10**(5): p. 499-502.<https://doi.org/10.1242/dmm.030205>.
7. Bertram, L. and Tanzi, R.E., The genetic epidemiology of neurodegenerative disease. *The Journal of Clinical Investigation*, 2005. **115**(6): p. 1449-1457.<https://doi.org/10.1172/JCI24761>.
8. Gan, L., Cookson, M.R., Petrucelli, L., and La Spada, A.R., Converging pathways in neurodegeneration, from genetics to mechanisms. *Nature Neuroscience*, 2018. **21**(10): p. 1300-1309.<https://doi.org/10.1038/s41593-018-0237-7>.
9. Margolis, R.L. and Ross, C.A., Expansion explosion: new clues to the pathogenesis of repeat expansion neurodegenerative diseases. *Trends in Molecular Medicine*, 2001. **7**(11): p. 479-482.[https://doi.org/10.1016/S1471-4914\(01\)02179-7](https://doi.org/10.1016/S1471-4914(01)02179-7).
10. Spada, A.R.L., Wilson, E.M., Lubahn, D.B., Harding, A.E., *et al.*, Androgen receptor gene mutations in X-linked spinal and bulbar muscular atrophy. *Nature*, 1991. **352**(6330): p. 77-79.<https://doi.org/10.1038/352077a0>.
11. MacDonald, M.E., Ambrose, C.M., Duyao, M.P., Myers, R.H., *et al.*, A novel gene containing a trinucleotide repeat that is expanded and unstable on Huntington's disease chromosomes. *Cell*, 1993. **72**(6): p. 971-983.[https://doi.org/10.1016/0092-8674\(93\)90585-E](https://doi.org/10.1016/0092-8674(93)90585-E).
12. Koide, R., Ikeuchi, T., Onodera, O., Tanaka, H., *et al.*, Unstable expansion of CAG repeat in hereditary dentatorubral-pallidolusian atrophy (DRPLA). *Nature Genetics*, 1994. **6**(1): p. 9-13.<https://doi.org/10.1038/ng0194-9>.
13. Nagafuchi, S., Yanagisawa, H., Sato, K., Shirayama, T., *et al.*, Dentatorubral and pallidolusian atrophy expansion of an unstable CAG trinucleotide on chromosome 12p. *Nature Genetics*, 1994. **6**(1): p. 14-18.<https://doi.org/10.1038/ng0194-14>.

14. Orr, H.T., Chung, M.-y., Banfi, S., Kwiatkowski, T.J., *et al.*, Expansion of an unstable trinucleotide CAG repeat in spinocerebellar ataxia type 1. *Nature Genetics*, 1993. **4**(3): p. 221-226.<https://doi.org/10.1038/ng0793-221>.
15. Pulst, S.-M., Nechiporuk, A., Nechiporuk, T., Gispert, S., *et al.*, Moderate expansion of a normally biallelic trinucleotide repeat in spinocerebellar ataxia type 2. *Nature Genetics*, 1996. **14**(3): p. 269-276.<https://doi.org/10.1038/ng1196-269>.
16. Sanpei, K., Takano, H., Igarashi, S., Sato, T., *et al.*, Identification of the spinocerebellar ataxia type 2 gene using a direct identification of repeat expansion and cloning technique, DIRECT. *Nature Genetics*, 1996. **14**(3): p. 277-284.<https://doi.org/10.1038/ng1196-277>.
17. Kawaguchi, Y., Okamoto, T., Taniwaki, M., Aizawa, M., *et al.*, CAG expansions in a novel gene for Machado-Joseph disease at chromosome 14q32.1. *Nature Genetics*, 1994. **8**(3): p. 221-228.<https://doi.org/10.1038/ng1194-221>.
18. Zhuchenko, O., Bailey, J., Bonnen, P., Ashizawa, T., *et al.*, Autosomal dominant cerebellar ataxia (SCA6) associated with small polyglutamine expansions in the  $\alpha$ 1A-voltage-dependent calcium channel. *Nature Genetics*, 1997. **15**(1): p. 62-69.<https://doi.org/10.1038/ng0197-62>.
19. David, G., Abbas, N., Stevanin, G., Dürr, A., *et al.*, Cloning of the SCA7 gene reveals a highly unstable CAG repeat expansion. *Nature Genetics*, 1997. **17**(1): p. 65-70.<https://doi.org/10.1038/ng0997-65>.
20. Nakamura, K., Jeong, S.-Y., Uchihara, T., Anno, M., *et al.*, SCA17, a novel autosomal dominant cerebellar ataxia caused by an expanded polyglutamine in TATA-binding protein. *Human Molecular Genetics*, 2001. **10**(14): p. 1441-1448.<https://doi.org/10.1093/hmg/10.14.1441>.
21. Margulis, B.A., Vigont, V., Lazarev, V.F., Kaznacheyeva, E.V., *et al.*, Pharmacological protein targets in polyglutamine diseases: Mutant polypeptides and their interactors. *FEBS Letters*, 2013. **587**(13): p. 1997-2007.<https://doi.org/10.1016/j.febslet.2013.05.022>.
22. McColgan, P. and Tabrizi, S.J., Huntington's disease: a clinical review. *European Journal of Neurology*, 2018. **25**(1): p. 24-34.<https://doi.org/10.1111/ene.13413>.
23. Ruano, L., Melo, C., Silva, M.C., and Coutinho, P., The Global Epidemiology of Hereditary Ataxia and Spastic Paraplegia: A Systematic Review of Prevalence Studies. *Neuroepidemiology*, 2014. **42**(3): p. 174-183.<https://doi.org/10.1159/000358801>.
24. van de Warrenburg, B.P.C., Sinke, R.J., Verschuuren-Bemelmans, C.C., Scheffer, H., *et al.*, Spinocerebellar ataxias in the Netherlands: prevalence and age at onset variance analysis. *Neurology*, 2002. **58**(5): p. 702-708.<https://doi.org/10.1212/WNL.58.5.702>.
25. Bird, T.D., Hereditary Ataxia Overview. GeneReviews®, ed. A.H. Adam MP, Pagon RA, *et al.*, editors. 1998 Oct 28 [Updated 2019 Jul 25], University of Washington, Seattle; 1993-2020.<https://www.ncbi.nlm.nih.gov/books/NBK1138/>.
26. Schöls, L., Bauer, P., Schmidt, T., Schulte, T., *et al.*, Autosomal dominant cerebellar ataxias: clinical features, genetics, and pathogenesis. *The Lancet Neurology*, 2004. **3**(5): p. 291-304.[https://doi.org/10.1016/S1474-4422\(04\)00737-9](https://doi.org/10.1016/S1474-4422(04)00737-9).

27. Takahashi, T., Katada, S., and Onodera, O., Polyglutamine Diseases: Where does Toxicity Come from? What is Toxicity? Where are We Going? *Journal of Molecular Cell Biology*, 2010. **2**(4): p. 180-191.<https://doi.org/10.1093/jmcb/mjq005>.
28. Lieberman, A.P., Shakkottai, V.G., and Albin, R.L., Polyglutamine Repeats in Neurodegenerative Diseases. *Annual Review of Pathology: Mechanisms of Disease*, 2019. **14**(1): p. 1-27.<https://doi.org/10.1146/annurev-pathmechdis-012418-012857>.
29. Banno, H., Katsuno, M., Suzuki, K., Tanaka, F., *et al.*, Neuropathology and Therapeutic Intervention in Spinal and Bulbar Muscular Atrophy. *International Journal of Molecular Sciences*, 2009. **10**(3): p. 1000-1012.<https://doi.org/10.3390/ijms10031000>.
30. Zoghbi, H.Y. and Orr, H.T., Glutamine Repeats and Neurodegeneration. *Annual Review of Neuroscience*, 2000. **23**(1): p. 217-247.<https://doi.org/10.1146/annurev.neuro.23.1.217>.
31. Williams, A.J. and Paulson, H.L., Polyglutamine neurodegeneration: protein misfolding revisited. *Trends in Neurosciences*, 2008. **31**(10): p. 521-528.<https://doi.org/10.1016/j.tins.2008.07.004>.
32. McMurray, C.T., Mechanisms of trinucleotide repeat instability during human development. *Nature Reviews Genetics*, 2010. **11**(11): p. 786-799.<https://doi.org/10.1038/nrg2828>.
33. R. La Spada, A., Trinucleotide Repeat Instability: Genetic Features and Molecular Mechanisms. *Brain Pathology*, 1997. **7**(3): p. 943-963.<https://doi.org/10.1111/j.1750-3639.1997.tb00895.x>.
34. Duyao, M., Ambrose, C., Myers, R., Novelletto, A., *et al.*, Trinucleotide repeat length instability and age of onset in Huntington's disease. *Nature Genetics*, 1993. **4**(4): p. 387-392.<https://doi.org/10.1038/ng0893-387>.
35. Maciel, P., Gaspar, C., DeStefano, A.L., Silveira, I., *et al.*, Correlation between CAG repeat length and clinical features in Machado-Joseph disease. *American Journal of Human Genetics*, 1995. **57**(1): p. 54-61.<https://www.ncbi.nlm.nih.gov/pmc/articles/PMC1801255/>.
36. Ranen, N.G., Stine, O.C., Abbott, M.H., Sherr, M., *et al.*, Anticipation and instability of IT-15 (CAG)<sub>n</sub> repeats in parent-offspring pairs with Huntington disease. *American journal of human genetics*, 1995. **57**(3): p. 593-602.<https://www.ncbi.nlm.nih.gov/pmc/articles/PMC1801258/>.
37. Gusella, J.F. and MacDonald, M.E., Molecular genetics: Unmasking polyglutamine triggers in neurodegenerative disease. *Nature Reviews Neuroscience*, 2000. **1**(2): p. 109-115.<https://doi.org/10.1038/35039051>.
38. Lee, J.-M., Correia, K., Loupe, J., Kim, K.-H., *et al.*, CAG Repeat Not Polyglutamine Length Determines Timing of Huntington's Disease Onset. *Cell*, 2019. **178**(4): p. 887-900.e14.<https://doi.org/10.1016/j.cell.2019.06.036>.
39. Alonso, I., Barros, J., Tuna, A., Coelho, J., *et al.*, Phenotypes of Spinocerebellar Ataxia Type 6 and Familial Hemiplegic Migraine Caused by a Unique CACNA1A Missense Mutation in Patients

- From a Large Family. *Archives of Neurology*, 2003. **60**(4): p. 610-614.<https://doi.org/10.1001/archneur.60.4.610>.
40. Nasir, J., Floresco, S.B., O'Kusky, J.R., Diewert, V.M., *et al.*, Targeted disruption of the Huntington's disease gene results in embryonic lethality and behavioral and morphological changes in heterozygotes. *Cell*, 1995. **81**(5): p. 811-823.[https://doi.org/10.1016/0092-8674\(95\)90542-1](https://doi.org/10.1016/0092-8674(95)90542-1).
  41. Schmitt, I., Linden, M., Khazneh, H., Evert, B.O., *et al.*, Inactivation of the mouse Atxn3 (ataxin-3) gene increases protein ubiquitination. *Biochemical and Biophysical Research Communications*, 2007. **362**(3): p. 734-739.<https://doi.org/10.1016/j.bbrc.2007.08.062>.
  42. Duyao, M.P., Auerbach, A.B., Ryan, A., Persichetti, F., *et al.*, Inactivation of the Mouse Huntingtons-Disease Gene Homolog *Hdh*. *Science*, 1995. **269**(5222): p. 407-410.<https://doi.org/10.1126/science.7618107>.
  43. Nakano, K.K., Dawson, D.M., and Spence, A., Machado disease. A hereditary ataxia in Portuguese emigrants to Massachusetts. *Neurology*, 1972. **22**(1): p. 49-49.<https://doi.org/10.1212/WNL.22.1.49>.
  44. Woods, B.T. and Schaumburg, H.H., Nigro-spino-dentatal degeneration with nuclear ophthalmoplegia: A unique and partially treatable clinico-pathological entity. *Journal of the Neurological Sciences*, 1972. **17**(2): p. 149-166.[https://doi.org/10.1016/0022-510X\(72\)90137-2](https://doi.org/10.1016/0022-510X(72)90137-2).
  45. Rosenberg, R.N., Nyhan, W.I., Bay, C., and Shore, P., Autosomal dominant striatonigral degeneration. A clinical, pathologic, and biochemical study of a new genetic disorder. *Neurology*, 1976. **26**(8): p. 703-703.<https://doi.org/10.1212/WNL.26.8.703>.
  46. Coutinho, P. and Andrade, C., Autosomal dominant system degeneration in Portuguese families of the Azores Islands. A new genetic disorder involving cerebellar, pyramidal, extrapyramidal and spinal cord motor functions. *Neurology*, 1978. **28**(7): p. 703-709.<https://doi.org/10.1212/WNL.28.7.703>.
  47. Lima, L. and Coutinho, P., Clinical criteria for diagnosis of Machado-Joseph disease: report of a non-Azorean Portuguese family. *Neurology*, 1980. **30**(3): p. 319-322.<https://doi.org/10.1212/WNL.30.3.319>.
  48. Rosenberg, R.N., Dominant ataxias. *Research publications-Association for Research in Nervous Mental Disease*, 1983. **60**: p. 195-213.<https://pubmed.ncbi.nlm.nih.gov/6823525/>.
  49. Barbeau, A., Roy, M., Cunha, L., Vincente, A.N.d., *et al.*, The natural history of Machado-Joseph disease: An analysis of 138 personally examined cases. *Canadian Journal of Neurological Sciences / Journal Canadien des Sciences Neurologiques*, 1984. **11**(S4): p. 510-525.<https://doi.org/10.1017/S0317167100034983>.
  50. Silveira, I., Miranda, C., Guimarães, L., Moreira, M.-C., *et al.*, Trinucleotide Repeats in 202 Families With Ataxia: A Small Expanded (CAG)<sub>n</sub> Allele at the SCA17 Locus. *Archives of Neurology*, 2002. **59**(4): p. 623-629.<https://doi.org/10.1001/archneur.59.4.623>.



51. Schöls, L., Amoiridis, G., Büttner, T., Przuntek, H., *et al.*, Autosomal dominant cerebellar ataxia: Phenotypic differences in genetically defined subtypes? *Annals of Neurology*, 1997. **42**(6): p. 924-932.<https://doi.org/10.1002/ana.410420615>.
52. Schöls, L., Amoiridis, G., Langkafel, M., Büttner, T., *et al.*, Machado-Joseph disease mutations as the genetic basis of most spinocerebellar ataxias in Germany. *Journal of Neurology, Neurosurgery & Psychiatry*, 1995. **59**(4): p. 449-450.<https://doi.org/10.1136/jnnp.59.4.449>.
53. Lopes-Cendes, I., Teive, H.G., Calcagnotto, M.E., Da Costa, J.C., *et al.*, Frequency of the different mutations causing spinocerebellar ataxia (SCA1, SCA2, MJD/SCA3 and DRPLA) in a large group of Brazilian patients. *Arquivos de Neuro-psiquiatria*, 1997. **55**(3b): p. 519-29.<https://doi.org/10.1590/s0004-282x1997000400001>.
54. Jardim, L.B., Silveira, I., Pereira, M.L., Ferro, A., *et al.*, A survey of spinocerebellar ataxia in South Brazil – 66 new cases with Machado-Joseph disease, SCA7, SCA8, or unidentified disease-causing mutations. *Journal of Neurology*, 2001. **248**(10): p. 870-876.<https://doi.org/10.1007/s004150170072>.
55. Jiang, H., Tang, B.S., Xu, B., Zhao, G.H., *et al.*, Frequency analysis of autosomal dominant spinocerebellar ataxias in mainland Chinese patients and clinical and molecular characterization of spinocerebellar ataxia type 6. *Chinese Medical Journal*, 2005. **118**(10): p. 837-43.<https://pubmed.ncbi.nlm.nih.gov/15989765/>.
56. Takano, H., Cancel, G., Ikeuchi, T., Lorenzetti, D., *et al.*, Close Associations between Prevalences of Dominantly Inherited Spinocerebellar Ataxias with CAG-Repeat Expansions and Frequencies of Large Normal CAG Alleles in Japanese and Caucasian Populations. *The American Journal of Human Genetics*, 1998. **63**(4): p. 1060-1066.<https://doi.org/10.1086/302067>.
57. Stevanin, G., Dürr, A., David, G., Didierjean, O., *et al.*, Clinical and molecular features of spinocerebellar ataxia type 6. *Neurology*, 1997. **49**(5): p. 1243-1246.<https://doi.org/10.1212/WNL.49.5.1243>.
58. Giunti, P., Sabbadini, G., Sweeney, M.G., Davis, M.B., *et al.*, The role of the SCA2 trinucleotide repeat expansion in 89 autosomal dominant cerebellar ataxia families. Frequency, clinical and genetic correlates. *Brain*, 1998. **121**(3): p. 459-467.<https://doi.org/10.1093/brain/121.3.459>.
59. Storey, E., du Sart, D., Shaw, J.H., Lorentzos, P., *et al.*, Frequency of spinocerebellar ataxia types 1, 2, 3, 6, and 7 in Australian patients with spinocerebellar ataxia. *American Journal of Medical Genetics*, 2000. **95**(4): p. 351-358.[https://doi.org/10.1002/1096-8628\(20001211\)95:4<351::AID-AJMG10>3.0.CO;2-R](https://doi.org/10.1002/1096-8628(20001211)95:4<351::AID-AJMG10>3.0.CO;2-R).
60. Moseley, M.L., Benzow, K.A., Schut, L.J., Bird, T.D., *et al.*, Incidence of dominant spinocerebellar and Friedreich triplet repeats among 361 ataxia families. *Neurology*, 1998. **51**(6): p. 1666-1671.<https://doi.org/10.1212/WNL.51.6.1666>.
61. Brusco, A., Gellera, C., Cagnoli, C., Saluto, A., *et al.*, Molecular Genetics of Hereditary Spinocerebellar Ataxia: Mutation Analysis of Spinocerebellar Ataxia Genes and CAG/CTG Repeat Expansion Detection in 225 Italian Families. *Archives of Neurology*, 2004. **61**(5): p. 727-733.<https://doi.org/10.1001/archneur.61.5.727>.

62. Mittal, U., Srivastava, A.K., Jain, S., Jain, S., *et al.*, Founder Haplotype for Machado-Joseph Disease in the Indian Population: Novel Insights From History and Polymorphism Studies. *Archives of Neurology*, 2005. **62**(4): p. 637-640.<https://doi.org/10.1001/archneur.62.4.637>.
63. Coutinho, M.P.M.d.A., Doença de Machado-Joseph: tentativa de definição, in Instituto de Ciências Biomédicas Abel Salazar, Porto. 1992.<https://hdl.handle.net/10216/10229>.
64. Maciel, P., Costa, M.d.C., Ferro, A., Rousseau, M., *et al.*, Improvement in the Molecular Diagnosis of Machado-Joseph Disease. *Archives of Neurology*, 2001. **58**(11): p. 1821-1827.<https://doi.org/10.1001/archneur.58.11.1821>.
65. Bettencourt, C., Santos, C., Kay, T., Vasconcelos, J., *et al.*, Analysis of segregation patterns in Machado–Joseph disease pedigrees. *Journal of Human Genetics*, 2008. **53**(10): p. 920-923.<https://doi.org/10.1007/s10038-008-0330-y>.
66. Klockgether, T., Lüdtke, R., Kramer, B., Abele, M., *et al.*, The natural history of degenerative ataxia: a retrospective study in 466 patients. *Brain*, 1998. **121**(4): p. 589-600.<https://doi.org/10.1093/brain/121.4.589>.
67. Paulson, H., Chapter 27 - Machado–Joseph disease/spinocerebellar ataxia type 3, in *Handbook of Clinical Neurology*, S.H. Subramony and A. Dürr, Editors. 2012, Elsevier. p. 437-449.<https://doi.org/10.1016/B978-0-444-51892-7.00027-9>.
68. Margolis, R.L., The spinocerebellar ataxias: order emerges from chaos. *Current Neurology Neuroscience Reports*, 2002. **2**(5): p. 447-456.<https://doi.org/10.1007/s11910-002-0072-8>.
69. Sakai, T. and Kawakami, H., Machado-Joseph disease: A proposal of spastic paraplegic subtype. *Neurology*, 1996. **46**(3): p. 846-7.<https://pubmed.ncbi.nlm.nih.gov/8618704/>.
70. Schöls, L., Haan, J., Riess, O., Amoiridis, G., *et al.*, Sleep disturbance in spinocerebellar ataxias: is the SCA3 mutation a cause of restless legs syndrome? *Neurology*, 1998. **51**(6): p. 1603-1607.<https://doi.org/10.1212/WNL.51.6.1603>.
71. Pedroso, J.L., Braga-Neto, P., Felício, A.C., Dutra, L.A., *et al.*, Sleep disorders in machado–joseph disease: Frequency, discriminative thresholds, predictive values, and correlation with ataxia-related motor and non-motor features. *The Cerebellum*, 2011. **10**(2): p. 291-295.<https://doi.org/10.1007/s12311-011-0252-7>.
72. Saute, J.A.M., da Silva, A.C.F., Donis, K.C., Vedolin, L., *et al.*, Depressive mood is associated with ataxic and non-ataxic neurological dysfunction in SCA3 patients. *The Cerebellum*, 2010. **9**(4): p. 603-605.<https://doi.org/10.1007/s12311-010-0205-6>.
73. Schmitz-Hübsch, T., Coudert, M., Tezenas du Montcel, S., Giunti, P., *et al.*, Depression comorbidity in spinocerebellar ataxia. *Movement Disorders*, 2011. **26**(5): p. 870-876.<https://doi.org/10.1002/mds.23698>.
74. Braga-Neto, P., Felício, A.C., Hoexter, M.Q., Pedroso, J.L., *et al.*, Cognitive and olfactory deficits in Machado–Joseph disease: A dopamine transporter study. *Parkinsonism & Related Disorders*, 2012. **18**(7): p. 854-858.<https://doi.org/10.1016/j.parkreldis.2012.04.015>.

75. França, M.C., Jr, D'Abreu, A., Friedman, J.H., Nucci, A., *et al.*, Chronic Pain in Machado-Joseph Disease: A Frequent and Disabling Symptom. *Archives of Neurology*, 2007. **64**(12): p. 1767-1770.<https://doi.org/10.1001/archneur.64.12.1767>.
76. França, M.C., Jr, D'Abreu, A., Nucci, A., and Lopes-Cendes, I., Muscle Excitability Abnormalities in Machado-Joseph Disease. *Archives of Neurology*, 2008. **65**(4): p. 525-529.<https://doi.org/10.1001/archneur.65.4.525>.
77. Kanai, K., Kuwabara, S., Arai, K., Sung, J.Y., *et al.*, Muscle cramp in Machado–Joseph disease: Altered motor axonal excitability properties and mexiletine treatment. *Brain*, 2003. **126**(4): p. 965-973.<https://doi.org/10.1093/brain/awg073>.
78. Brusse, E., Brusse-Keizer, M.G.J., Duivenvoorden, H.J., and van Swieten, J.C., Fatigue in spinocerebellar ataxia: patient self-assessment of an early and disabling symptom. *Neurology*, 2011. **76**(11): p. 953-959.<https://doi.org/10.1212/WNL.0b013e31821043a4>.
79. Saute, J.A.M., da Silva, A.C.F., Souza, G.N., Russo, A.D., *et al.*, Body Mass Index is Inversely Correlated with the Expanded CAG Repeat Length in SCA3/MJD Patients. *The Cerebellum*, 2012. **11**(3): p. 771-774.<https://doi.org/10.1007/s12311-011-0326-6>.
80. Saute, J.A.M., da Silva, A.C.F., Muller, A.P., Hansel, G., *et al.*, Serum insulin-like system alterations in patients with spinocerebellar ataxia type 3. *Movement Disorders*, 2011. **26**(4): p. 731-735.<https://doi.org/10.1002/mds.23428>.
81. Mendonça, N., França, M.C., Goncalves, A.F., and Januario, C., Clinical features of Machado-Joseph disease, in *Polyglutamine Disorders*. 2018, Springer. p. 255-273.[https://doi.org/10.1007/978-3-319-71779-1\\_13](https://doi.org/10.1007/978-3-319-71779-1_13).
82. Robitaille, Y., Lopes-Cendes, I., Becher, M., Rouleau, G., *et al.*, The Neuropathology of CAG Repeat Diseases: Review and Update of Genetic and Molecular Features. *Brain Pathology*, 1997. **7**(3): p. 901-926.<https://doi.org/10.1111/j.1750-3639.1997.tb00893.x>.
83. Gilman, S., The Spinocerebellar Ataxias. *Clinical Neuropharmacology*, 2000. **23**(6): p. 296-303.<https://doi.org/10.1097/00002826-200011000-00002>.
84. Rüb, U., Brunt, E.R., and Deller, T., New insights into the pathoanatomy of spinocerebellar ataxia type 3 (Machado–Joseph disease). *Current Opinion in Neurology*, 2008. **21**(2): p. 111-116.<https://doi.org/10.1097/WCO.0b013e3282f7673d>.
85. Durr, A., Stevanin, G., Cancel, G., Duyckaerts, C., *et al.*, Spinocerebellar ataxia 3 and machado-joseph disease: Clinical, molecular, and neuropathological features. *Annals of Neurology*, 1996. **39**(4): p. 490-499.<https://doi.org/10.1002/ana.410390411>.
86. Yamada, M., Tan, C.-F., Inenaga, C., Tsuji, S., *et al.*, Sharing of polyglutamine localization by the neuronal nucleus and cytoplasm in CAG-repeat diseases. *Neuropathology and Applied Neurobiology*, 2004. **30**(6): p. 665-675.<https://doi.org/10.1111/j.1365-2990.2004.00583.x>.
87. Takiyama, Y., Oyanagi, S., Kawashima, S., Sakamoto, H., *et al.*, A clinical and pathologic study of a large Japanese family with Machado- Joseph disease tightly linked to the DNA markers on

- chromosome 14q. *Neurology*, 1994. **44**(7): p. 1302-1302.<https://doi.org/10.1212/WNL.44.7.1302>
88. Kanda, T., Isozaki, E., Kato, S., Tanabe, H., *et al.*, Type III Machado-Joseph disease in a Japanese family: a clinicopathological study with special reference to the peripheral nervous system. *Clinical neuropathology*, 1989. **8**(3): p. 134-41.<https://pubmed.ncbi.nlm.nih.gov/2743650/>.
89. Koeppen, A.H., The pathogenesis of spinocerebellar ataxia. *The Cerebellum*, 2005. **4**(1): p. 62.<https://doi.org/10.1080/14734220510007950>.
90. Rosenberg, R.N., Machado-Joseph disease: An autosomal dominant motor system degeneration. *Movement Disorders*, 1992. **7**(3): p. 193-203.<https://doi.org/10.1002/mds.870070302>.
91. Rüb, U., Brunt, E.R., Del Turco, D., De Vos, R.A.I., *et al.*, Guidelines for the pathoanatomical examination of the lower brain stem in ingestive and swallowing disorders and its application to a dysphagic spinocerebellar ataxia type 3 patient. *Neuropathology and Applied Neurobiology*, 2003. **29**(1): p. 1-13.<https://doi.org/10.1046/j.1365-2990.2003.00437.x>.
92. Rüb, U., Brunt, E.R., Gierga, K., Schultz, C., *et al.*, The nucleus raphe interpositus in spinocerebellar ataxia type 3 (Machado-Joseph disease). *Journal of Chemical Neuroanatomy*, 2003. **25**(2): p. 115-127.[https://doi.org/10.1016/S0891-0618\(02\)00099-6](https://doi.org/10.1016/S0891-0618(02)00099-6).
93. Rüb, U., Del Turco, D., Del Tredici, K., de Vos, R.A.I., *et al.*, Thalamic involvement in a spinocerebellar ataxia type 2 (SCA2) and a spinocerebellar ataxia type 3 (SCA3) patient, and its clinical relevance. *Brain*, 2003. **126**(10): p. 2257-2272.<https://doi.org/10.1093/brain/awg234>.
94. Rüb, U., Brunt, E.R., De Vos, R.A.I., Del Turco, D., *et al.*, Degeneration of the central vestibular system in spinocerebellar ataxia type 3 (SCA3) patients and its possible clinical significance. *Neuropathology and Applied Neurobiology*, 2004. **30**(4): p. 402-414.<https://doi.org/10.1111/j.1365-2990.2004.00554.x>.
95. Rüb, U., Gierga, K., Brunt, E.R., de Vos, R.A.I., *et al.*, Spinocerebellar ataxias types 2 and 3: degeneration of the precerebellar nuclei isolates the three phylogenetically defined regions of the cerebellum. *Journal of Neural Transmission*, 2005. **112**(11): p. 1523-1545.<https://doi.org/10.1007/s00702-005-0287-3>.
96. Rüb, U., De Vos, R.A.I., Brunt, E.R., Sebestény, T., *et al.*, Spinocerebellar Ataxia Type 3 (SCA3): Thalamic Neurodegeneration Occurs Independently from Thalamic Ataxin-3 Immunopositive Neuronal Intranuclear Inclusions. *Brain Pathology*, 2006. **16**(3): p. 218-227.<https://doi.org/10.1111/j.1750-3639.2006.00022.x>.
97. Rüb, U., Brunt, E.R., Petrasch-Parwez, E., Schöls, L., *et al.*, Degeneration of ingestion-related brainstem nuclei in spinocerebellar ataxia type 2, 3, 6 and 7. *Neuropathology and Applied Neurobiology*, 2006. **32**(6): p. 635-649.<https://doi.org/10.1111/j.1365-2990.2006.00772.x>.
98. Rüb, U., Seidel, K., Özerden, I., Gierga, K., *et al.*, Consistent affection of the central somatosensory system in spinocerebellar ataxia type 2 and type 3 and its significance for clinical symptoms and rehabilitative therapy. *Brain Research Reviews*, 2007. **53**(2): p. 235-249.<https://doi.org/10.1016/j.brainresrev.2006.08.003>.

99. Iwabuchi, K., Tsuchiya, K., Uchihara, T., and Yagishita, S., Autosomal dominant spinocerebellar degenerations. Clinical, pathological, and genetic correlations. *Revue Neurologique (Paris)*, 1999. **155**(4): p. 255-70.<https://pubmed.ncbi.nlm.nih.gov/10367323/>.
100. Klockgether, T., Skalej, M., Wedekind, D., Luft, A.R., *et al.*, Autosomal dominant cerebellar ataxia type I. MRI-based volumetry of posterior fossa structures and basal ganglia in spinocerebellar ataxia types 1, 2 and 3. *Brain*, 1998. **121**(9): p. 1687-1693.<https://doi.org/10.1093/brain/121.9.1687>.
101. Etchebehere, E.C.S.C., Cendes, F., Lopes-Cendes, I., Pereira, J.A., *et al.*, Brain Single-Photon Emission Computed Tomography and Magnetic Resonance Imaging in Machado-Joseph Disease. *Archives of Neurology*, 2001. **58**(8): p. 1257-1263.<https://doi.org/10.1001/archneur.58.8.1257>.
102. Fahl, C.N., Branco, L.M.T., Bergo, F.P., D'Abreu, A., *et al.*, Spinal cord damage in Machado-Joseph disease. *The Cerebellum*, 2015. **14**(2): p. 128-132.<https://doi.org/10.1007/s12311-014-0619-7>.
103. Rezende, T.J.R., de Paiva, J.L.R., Martinez, A.R.M., Lopes-Cendes, I., *et al.*, Structural signature of SCA3: From presymptomatic to late disease stages. *Annals of Neurology*, 2018. **84**(3): p. 401-408.<https://doi.org/10.1002/ana.25297>.
104. Piccinin, C.C., Rezende, T.J.R., de Paiva, J.L.R., Moysés, P.C., *et al.*, A 5-Year Longitudinal Clinical and Magnetic Resonance Imaging Study in Spinocerebellar Ataxia Type 3. *Movement Disorders*, 2020. **35**(9): p. 1679-1684.<https://doi.org/10.1002/mds.28113>.
105. Taniwaki, T., Sakai, T., Kobayashi, T., Kuwabara, Y., *et al.*, Positron emission tomography (PET) in Machado-Joseph disease. *Journal of the Neurological Sciences*, 1997. **145**(1): p. 63-67.[https://doi.org/10.1016/S0022-510X\(96\)00242-0](https://doi.org/10.1016/S0022-510X(96)00242-0).
106. Soong, B.-w. and Liu, R.-s., Positron emission tomography in asymptomatic gene carriers of Machado-Joseph disease. *Journal of Neurology, Neurosurgery & Psychiatry*, 1998. **64**(4): p. 499-504.<https://doi.org/10.1136/jnnp.64.4.499>.
107. Soon, B.-w., Cheng, C.-H., Liu, R.-S., and Shan, D.-E., Machado-joseph disease: Clinical, molecular, and metabolic characterization in chinese kindreds. *Annals of Neurology*, 1997. **41**(4): p. 446-452.<https://doi.org/10.1002/ana.410410407>.
108. Wüllner, U., Reimold, M., Abele, M., Bürk, K., *et al.*, Dopamine Transporter Positron Emission Tomography in Spinocerebellar Ataxias Type 1, 2, 3, and 6. *Archives of Neurology*, 2005. **62**(8): p. 1280-1285.<https://doi.org/10.1001/archneur.62.8.1280>.
109. D'Abreu, A., França Jr, M., Appenzeller, S., Lopes-Cendes, I., *et al.*, Axonal Dysfunction in the Deep White Matter in Machado-Joseph Disease. *Journal of Neuroimaging*, 2009. **19**(1): p. 9-12.<https://doi.org/10.1111/j.1552-6569.2008.00260.x>.
110. Ross, C.A., When more is less: Pathogenesis of glutamine repeat neurodegenerative diseases. *Neuron*, 1995. **15**(3): p. 493-496.[https://doi.org/10.1016/0896-6273\(95\)90138-8](https://doi.org/10.1016/0896-6273(95)90138-8).

111. Paulson, H.L., Perez, M.K., Trotter, Y., Trojanowski, J.Q., *et al.*, Intranuclear Inclusions of Expanded Polyglutamine Protein in Spinocerebellar Ataxia Type 3. *Neuron*, 1997. **19**(2): p. 333-344.[https://doi.org/10.1016/S0896-6273\(00\)80943-5](https://doi.org/10.1016/S0896-6273(00)80943-5).
112. Seidel, K., den Dunnen, W.F.A., Schultz, C., Paulson, H., *et al.*, Axonal inclusions in spinocerebellar ataxia type 3. *Acta Neuropathologica*, 2010. **120**(4): p. 449-460.<https://doi.org/10.1007/s00401-010-0717-7>.
113. Paulson, H.L., Das, S.S., Crino, P.B., Perez, M.K., *et al.*, Machado-Joseph disease gene product is a cytoplasmic protein widely expressed in brain. *Annals of Neurology*, 1997. **41**(4): p. 453-462.<https://doi.org/10.1002/ana.410410408>.
114. Perez, M.K., Paulson, H.L., Pendse, S.J., Saionz, S.J., *et al.*, Recruitment and the Role of Nuclear Localization in Polyglutamine-mediated Aggregation. *Journal of Cell Biology*, 1998. **143**(6): p. 1457-1470.<https://doi.org/10.1083/jcb.143.6.1457>.
115. Chai, Y., Koppenhafer, S.L., Bonini, N.M., and Paulson, H.L., Analysis of the Role of Heat Shock Protein (Hsp) Molecular Chaperones in Polyglutamine Disease. *Journal of Neuroscience*, 1999. **19**(23): p. 10338-10347.<https://doi.org/10.1523/JNEUROSCI.19-23-10338.1999>.
116. Alves, S., Régulier, E., Nascimento-Ferreira, I., Hassig, R., *et al.*, Striatal and nigral pathology in a lentiviral rat model of Machado-Joseph disease. *Human Molecular Genetics*, 2008. **17**(14): p. 2071-2083.<https://doi.org/10.1093/hmg/ddn106>.
117. Cemal, C.K., Carroll, C.J., Lawrence, L., Lowrie, M.B., *et al.*, YAC transgenic mice carrying pathological alleles of the *MJD1* locus exhibit a mild and slowly progressive cerebellar deficit. *Human Molecular Genetics*, 2002. **11**(9): p. 1075-1094.<https://doi.org/10.1093/hmg/11.9.1075>.
118. Silva-Fernandes, A., Duarte-Silva, S., Neves-Carvalho, A., Amorim, M., *et al.*, Chronic Treatment with 17-DMAG Improves Balance and Coordination in A New Mouse Model of Machado-Joseph Disease. *Neurotherapeutics*, 2014. **11**(2): p. 433-449.<https://doi.org/10.1007/s13311-013-0255-9>.
119. Seidel, K., Siswanto, S., Fredrich, M., Bouzrou, M., *et al.*, On the distribution of intranuclear and cytoplasmic aggregates in the brainstem of patients with spinocerebellar ataxia type 2 and 3. *Brain Pathology*, 2017. **27**(3): p. 345-355.<https://doi.org/10.1111/bpa.12412>.
120. Takiyama, Y., Nishizawa, M., Tanaka, H., Kawashima, S., *et al.*, The gene for Machado-Joseph disease maps to human chromosome 14q. *Nature Genetics*, 1993. **4**(3): p. 300-304.<https://doi.org/10.1038/ng0793-300>.
121. Ichikawa, Y., Goto, J., Hattori, M., Toyoda, A., *et al.*, The genomic structure and expression of MJD, the Machado-Joseph disease gene. *Journal of Human Genetics*, 2001. **46**(7): p. 413-422.<https://doi.org/10.1007/s100380170060>.
122. Bettencourt, C., Santos, C., Montiel, R., do Carmo Costa, M., *et al.*, Increased transcript diversity: novel splicing variants of Machado-Joseph Disease gene (ATXN3). *Neurogenetics*, 2010. **11**(2): p. 193-202.<https://doi.org/10.1007/s10048-009-0216-y>.



123. Higgins, J.J., Nee, L.E., Vasconcelos, O., Ide, S.E., *et al.*, Mutations in American families with spinocerebellar ataxia (SCA) type 3: SCA3 is allelic to Machado-Joseph disease. *Neurology*, 1996. **46**(1): p. 208-213.<https://doi.org/10.1212/WNL.46.1.208>.
124. Cummings, C.J. and Zoghbi, H.Y., Fourteen and counting: unraveling trinucleotide repeat diseases. *Human Molecular Genetics*, 2000. **9**(6): p. 909-916.<https://doi.org/10.1093/hmg/9.6.909>.
125. Padiath, Q.S., Srivastava, A.K., Roy, S., Jain, S., *et al.*, Identification of a novel 45 repeat unstable allele associated with a disease phenotype at the MJD1/SCA3 locus. *American Journal of Medical Genetics*, 2005. **133B**(1): p. 124-126.<https://doi.org/10.1002/ajmg.b.30088>.
126. Gu, W., Ma, H., Wang, K., Jin, M., *et al.*, The Shortest Expanded Allele of the MJD1 Gene in a Chinese MJD Kindred with Autonomic Dysfunction. *European Neurology*, 2004. **52**(2): p. 107-111.<https://doi.org/10.1159/000080221>.
127. Goto, J., Watanabe, M., Ichikawa, Y., Yee, S.-B., *et al.*, Machado–Joseph disease gene products carrying different carboxyl termini. *Neuroscience Research*, 1997. **28**(4): p. 373-377.[https://doi.org/10.1016/S0168-0102\(97\)00056-4](https://doi.org/10.1016/S0168-0102(97)00056-4).
128. Weishäupl, D., Schneider, J., Peixoto Pinheiro, B., Ruess, C., *et al.*, Physiological and pathophysiological characteristics of ataxin-3 isoforms. *Journal of Biological Chemistry*, 2019. **294**(2): p. 644-661.<https://doi.org/10.1074/jbc.RA118.005801>.
129. Harris, G.M., Dodelzon, K., Gong, L., Gonzalez-Alegre, P., *et al.*, Splice Isoforms of the Polyglutamine Disease Protein Ataxin-3 Exhibit Similar Enzymatic yet Different Aggregation Properties. *PLOS ONE*, 2010. **5**(10): p. e13695.<https://doi.org/10.1371/journal.pone.0013695>.
130. Masino, L., Musi, V., Menon, R.P., Fusi, P., *et al.*, Domain architecture of the polyglutamine protein ataxin-3: a globular domain followed by a flexible tail. *FEBS Letters*, 2003. **549**(1-3): p. 21-25.[https://doi.org/10.1016/S0014-5793\(03\)00748-8](https://doi.org/10.1016/S0014-5793(03)00748-8).
131. Albrecht, M., Golatta, M., Wüllner, U., and Lengauer, T., Structural and functional analysis of ataxin-2 and ataxin-3. *European Journal of Biochemistry*, 2004. **271**(15): p. 3155-3170.<https://doi.org/10.1111/j.1432-1033.2004.04245.x>.
132. Burnett, B., Li, F., and Pittman, R.N., The polyglutamine neurodegenerative protein ataxin-3 binds polyubiquitylated proteins and has ubiquitin protease activity. *Human Molecular Genetics*, 2003. **12**(23): p. 3195-3205.<https://doi.org/10.1093/hmg/ddg344>.
133. Tait, D., Riccio, M., Sittler, A., Scherzinger, E., *et al.*, Ataxin-3 is Transported Into the Nucleus and Associates with the Nuclear Matrix. *Human Molecular Genetics*, 1998. **7**(6): p. 991-997.<https://doi.org/10.1093/hmg/7.6.991>.
134. Antony, P.M.A., Mäntele, S., Mollenkopf, P., Boy, J., *et al.*, Identification and functional dissection of localization signals within ataxin-3. *Neurobiology of Disease*, 2009. **36**(2): p. 280-292.<https://doi.org/10.1016/j.nbd.2009.07.020>.

135. Matos, C.A., de Almeida, L.P., and Nóbrega, C., Machado–Joseph disease/spinocerebellar ataxia type 3: lessons from disease pathogenesis and clues into therapy. *Journal of Neurochemistry*, 2019. **148**(1): p. 8-28.<https://doi.org/10.1111/jnc.14541>.
136. do Carmo Costa, M., Gomes-da-Silva, J., Miranda, C.J., Sequeiros, J., *et al.*, Genomic structure, promoter activity, and developmental expression of the mouse homologue of the Machado–Joseph disease (MJD) gene. *Genomics*, 2004. **84**(2): p. 361-373.<https://doi.org/10.1016/j.ygeno.2004.02.012>.
137. Schmitt, I., Brattig, T., Gossen, M., and Riess, O., Characterization of the rat spinocerebellar ataxia type 3 gene. *Neurogenetics*, 1997. **1**(2): p. 103-112.<https://doi.org/10.1007/s100480050015>.
138. Linhartová, I., Repitz, M., Dráber, P., Nemeč, M., *et al.*, Conserved domains and lack of evidence for polyglutamine length polymorphism in the chicken homolog of the Machado-Joseph disease gene product ataxin-3. *Biochimica et Biophysica Acta (BBA) - Gene Structure and Expression*, 1999. **1444**(2): p. 299-305.[https://doi.org/10.1016/S0167-4781\(99\)00004-4](https://doi.org/10.1016/S0167-4781(99)00004-4).
139. Rodrigues, A.-J., Coppola, G., Santos, C., Costa, M.d.C., *et al.*, Functional genomics and biochemical characterization of the *C. elegans* orthologue of the Machado-Joseph disease protein ataxin-3. *FASEB Journal*, 2007. **21**(4): p. 1126-1136.<https://doi.org/10.1096/fj.06-7002com>.
140. Albrecht, M., Hoffmann, D., Evert, B.O., Schmitt, I., *et al.*, Structural modeling of ataxin-3 reveals distant homology to adaptins. *Proteins*, 2003. **50**(2): p. 355-370.<https://doi.org/10.1002/prot.10280>.
141. Schmidt, T., Landwehrmeyer, G.B., Schmitt, I., Trottier, Y., *et al.*, An Isoform of Ataxin-3 Accumulates in the Nucleus of Neuronal Cells in Affected Brain Regions of SCA3 Patients. *Brain Pathology*, 1998. **8**(4): p. 669-679.<https://doi.org/10.1111/j.1750-3639.1998.tb00193.x>.
142. Trottier, Y., Cancel, G., An-Gourfinkel, I., Lutz, Y., *et al.*, Heterogeneous Intracellular Localization and Expression of Ataxin-3. *Neurobiology of Disease*, 1998. **5**(5): p. 335-347.<https://doi.org/10.1006/nbdi.1998.0208>.
143. Fujigasaki, H., Uchihara, T., Koyano, S., Iwabuchi, K., *et al.*, Ataxin-3 is translocated into the nucleus for the formation of intranuclear inclusions in normal and Machado–Joseph disease brains. *Experimental Neurology*, 2000. **165**(2): p. 248-256.<https://doi.org/10.1006/exnr.2000.7479>.
144. Wang, G., Ide, K., Nukina, N., Goto, J., *et al.*, Machado–Joseph Disease Gene Product Identified in Lymphocytes and Brain. *Biochemical and Biophysical Research Communications*, 1997. **233**(2): p. 476-479.<https://doi.org/10.1006/bbrc.1997.6484>.
145. Doss-Pepe, E.W., Stenroos, E.S., Johnson, W.G., and Madura, K., Ataxin-3 interactions with rad23 and valosin-containing protein and its associations with ubiquitin chains and the proteasome are consistent with a role in ubiquitin-mediated proteolysis. *Molecular and Cellular Biology*, 2003. **23**(18): p. 6469-83.<https://doi.org/10.1128/mcb.23.18.6469-6483.2003>.
146. Mao, Y., Senic-Matuglia, F., Di Fiore, P.P., Polo, S., *et al.*, Deubiquitinating function of ataxin-3: Insights from the solution structure of the Josephin domain. *Proceedings of the National Academy*



- of Sciences of the United States of America*, 2005. **102**(36): p. 12700-12705.<https://doi.org/10.1073/pnas.0506344102>.
147. Scheel, H., Tomiuk, S., and Hofmann, K., Elucidation of ataxin-3 and ataxin-7 function by integrative bioinformatics. *Human Molecular Genetics*, 2003. **12**(21): p. 2845-2852.<https://doi.org/10.1093/hmg/ddg297>.
148. Nijman, S.M.B., Luna-Vargas, M.P.A., Velds, A., Brummelkamp, T.R., *et al.*, A Genomic and Functional Inventory of Deubiquitinating Enzymes. *Cell*, 2005. **123**(5): p. 773-786.<https://doi.org/10.1016/j.cell.2005.11.007>.
149. Lam, Y.A., Xu, W., DeMartino, G.N., and Cohen, R.E., Editing of ubiquitin conjugates by an isopeptidase in the 26S proteasome. *Nature*, 1997. **385**(6618): p. 737-740.<https://doi.org/10.1038/385737a0>.
150. Amerik, A.Y. and Hochstrasser, M., Mechanism and function of deubiquitinating enzymes. *Biochimica et Biophysica Acta (BBA) - Molecular Cell Research*, 2004. **1695**(1): p. 189-207.<https://doi.org/10.1016/j.bbamcr.2004.10.003>.
151. Reyes-Turcu, F.E., Ventii, K.H., and Wilkinson, K.D., Regulation and Cellular Roles of Ubiquitin-Specific Deubiquitinating Enzymes. *Annual Review of Biochemistry*, 2009. **78**(1): p. 363-397.<https://doi.org/10.1146/annurev.biochem.78.082307.091526>.
152. Chai, Y., Berke, S.S., Cohen, R.E., and Paulson, H.L., Poly-ubiquitin Binding by the Polyglutamine Disease Protein Ataxin-3 Links Its Normal Function to Protein Surveillance Pathways. *Journal of Biological Chemistry*, 2004. **279**(5): p. 3605-3611.<https://doi.org/10.1074/jbc.M310939200>.
153. Berke, S.J.S., Chai, Y., Marrs, G.L., Wen, H., *et al.*, Defining the Role of Ubiquitin-interacting Motifs in the Polyglutamine Disease Protein, Ataxin-3. *Journal of Biological Chemistry*, 2005. **280**(36): p. 32026-32034.<https://doi.org/10.1074/jbc.M506084200>.
154. Zhong, X. and Pittman, R.N., Ataxin-3 binds VCP/p97 and regulates retrotranslocation of ERAD substrates. *Human Molecular Genetics*, 2006. **15**(16): p. 2409-2420.<https://doi.org/10.1093/hmg/ddl164>.
155. Wang, G.-h., Sawai, N., Kotliarova, S., Kanazawa, I., *et al.*, Ataxin-3, the MJD1 gene product, interacts with the two human homologs of yeast DNA repair protein RAD23, HHR23A and HHR23B. *Human Molecular Genetics*, 2000. **9**(12): p. 1795-1803.<https://doi.org/10.1093/hmg/9.12.1795>.
156. Nicastro, G., Menon, R.P., Masino, L., Knowles, P.P., *et al.*, The solution structure of the Josephin domain of ataxin-3: Structural determinants for molecular recognition. *Proceedings of the National Academy of Sciences of the United States of America*, 2005. **102**(30): p. 10493-10498.<https://doi.org/10.1073/pnas.0501732102>.
157. Nicastro, G., Masino, L., Esposito, V., Menon, R.P., *et al.*, Josephin domain of ataxin-3 contains two distinct ubiquitin-binding sites. *Biopolymers*, 2009. **91**(12): p. 1203-1214.<https://doi.org/10.1002/bip.21210>.

158. Boeddrich, A., Gaumer, S., Haacke, A., Tzvetkov, N., *et al.*, An arginine/lysine-rich motif is crucial for VCP/p97-mediated modulation of ataxin-3 fibrillogenesis. *The EMBO Journal*, 2006. **25**(7): p. 1547-1558.<https://doi.org/10.1038/sj.emboj.7601043>.
159. Matsumoto, M., Yada, M., Hatakeyama, S., Ishimoto, H., *et al.*, Molecular clearance of ataxin-3 is regulated by a mammalian E4. *The EMBO Journal*, 2004. **23**(3): p. 659-669.<https://doi.org/10.1038/sj.emboj.7600081>.
160. Costa, M.d.C., Bajanca, F., Rodrigues, A.-J., Tomé, R.J., *et al.*, Ataxin-3 Plays a Role in Mouse Myogenic Differentiation through Regulation of Integrin Subunit Levels. *PLOS ONE*, 2010. **5**(7): p. e11728.<https://doi.org/10.1371/journal.pone.0011728>.
161. Durcan, T.M., Kontogianna, M., Thorarinsdottir, T., Fallon, L., *et al.*, The Machado–Joseph disease-associated mutant form of ataxin-3 regulates parkin ubiquitination and stability. *Human Molecular Genetics*, 2011. **20**(1): p. 141-154.<https://doi.org/10.1093/hmg/ddq452>.
162. Durcan, T.M. and Fon, E.A., Mutant ataxin-3 promotes the autophagic degradation of parkin. *Autophagy*, 2011. **7**(2): p. 233-234.<https://doi.org/10.4161/auto.7.2.14224>.
163. Pfeiffer, A., Luijsterburg, M.S., Acs, K., Wiegant, W.W., *et al.*, Ataxin-3 consolidates the MDC1-dependent DNA double-strand break response by counteracting the SUMO-targeted ubiquitin ligase RNF4. *The EMBO Journal*, 2017. **36**(8): p. 1066-1083.<https://doi.org/10.15252/emj.201695151>.
164. Ashkenazi, A., Bento, C.F., Ricketts, T., Vicinanza, M., *et al.*, Polyglutamine tracts regulate beclin 1-dependent autophagy. *Nature*, 2017. **545**(7652): p. 108-111.<https://doi.org/10.1038/nature22078>.
165. Herzog, L.K., Kevei, É., Marchante, R., Böttcher, C., *et al.*, The Machado–Joseph disease deubiquitylase ataxin-3 interacts with LC3C/GABARAP and promotes autophagy. *Aging Cell*, 2020. **19**(1): p. e13051.<https://doi.org/10.1111/acer.13051>.
166. Mazzucchelli, S., De Palma, A., Riva, M., D'Urzo, A., *et al.*, Proteomic and biochemical analyses unveil tight interaction of ataxin-3 with tubulin. *The International Journal of Biochemistry & Cell Biology*, 2009. **41**(12): p. 2485-2492.<https://doi.org/10.1016/j.biocel.2009.08.003>.
167. Toulis, V., García-Monclús, S., de la Peña-Ramírez, C., Arenas-Galnares, R., *et al.*, The Deubiquitinating Enzyme Ataxin-3 Regulates Ciliogenesis and Phagocytosis in the Retina. *Cell Reports*, 2020. **33**(6): p. 108360.<https://doi.org/10.1016/j.celrep.2020.108360>.
168. Rosselli-Murai, L.K., Joseph, J.G., Lopes-Cendes, I., Liu, A.P., *et al.*, The Machado–Joseph disease-associated form of ataxin-3 impacts dynamics of clathrin-coated pits. *Cell Biology International*, 2020. **44**(5): p. 1252-1259.<https://doi.org/10.1002/cbin.11312>.
169. Yu, A., Shibata, Y., Shah, B., Calamini, B., *et al.*, Protein aggregation can inhibit clathrin-mediated endocytosis by chaperone competition. *Proceedings of the National Academy of Sciences*, 2014. **111**(15): p. E1481-E1490.<https://doi.org/10.1073/pnas.1321811111>.
170. Evert, B.O., Vogt, I.R., Vieira-Saecker, A.M., Ozimek, L., *et al.*, Gene Expression Profiling in Ataxin-3 Expressing Cell Lines Reveals Distinct Effects of Normal and Mutant Ataxin-3. *Journal of*

- Neuropathology & Experimental Neurology*, 2003. **62**(10): p. 1006-1018.<https://doi.org/10.1093/jnen/62.10.1006>.
171. Li, F., Macfarlan, T., Pittman, R.N., and Chakravarti, D., Ataxin-3 Is a Histone-binding Protein with Two Independent Transcriptional Corepressor Activities. *Journal of Biological Chemistry*, 2002. **277**(47): p. 45004-45012.<https://doi.org/10.1074/jbc.M205259200>.
172. Evert, B.O., Araujo, J., Vieira-Saecker, A.M., de Vos, R.A.I., *et al.*, Ataxin-3 Represses Transcription via Chromatin Binding, Interaction with Histone Deacetylase 3, and Histone Deacetylation. *The Journal of Neuroscience*, 2006. **26**(44): p. 11474-11486.<https://doi.org/10.1523/JNEUROSCI.2053-06.2006>.
173. Bichelmeier, U., Schmidt, T., Hübener, J., Boy, J., *et al.*, Nuclear Localization of Ataxin-3 Is Required for the Manifestation of Symptoms in SCA3: *In Vivo* Evidence. *The Journal of Neuroscience*, 2007. **27**(28): p. 7418-7428.<https://doi.org/10.1523/JNEUROSCI.4540-06.2007>.
174. Macedo-Ribeiro, S., Cortes, L., Maciel, P., and Carvalho, A.L., Nucleocytoplasmic Shuttling Activity of Ataxin-3. *PLOS ONE*, 2009. **4**(6): p. e5834.<https://doi.org/10.1371/journal.pone.0005834>.
175. Wei, F., Xiao, H., Hu, Z., Zhang, H., *et al.*, Subcellular localization of ataxin-3 and its effect on the morphology of cytoplasmic organoids. *Zhonghua yi xue yi chuan xue za zhi = Chinese Journal of Medical Genetics*, 2015. **32**(3): p. 353-7.<https://doi.org/10.3760/cma.j.issn.1003-9406.2015.03.011>.
176. Bevivino, A.E. and Loll, P.J., An expanded glutamine repeat destabilizes native ataxin-3 structure and mediates formation of parallel  $\beta$ -fibrils. *Proceedings of the National Academy of Sciences*, 2001. **98**(21): p. 11955-11960.<https://doi.org/10.1073/pnas.211305198>.
177. Carvalho, A.L., Silva, A., and Macedo-Ribeiro, S., Polyglutamine-Independent Features in Ataxin-3 Aggregation and Pathogenesis of Machado-Joseph Disease, in *Advances in Experimental Medicine and Biology*, C. Springer, Editor. 2018. p. 275-288.[https://doi.org/10.1007/978-3-319-71779-1\\_14](https://doi.org/10.1007/978-3-319-71779-1_14).
178. Ellisdon, A.M., Thomas, B., and Bottomley, S.P., The Two-stage Pathway of Ataxin-3 Fibrillogenesis Involves a Polyglutamine-independent Step. *Journal of Biological Chemistry*, 2006. **281**(25): p. 16888-16896.<https://doi.org/10.1074/jbc.M601470200>.
179. Gales, L., Cortes, L., Almeida, C., Melo, C.V., *et al.*, Towards a Structural Understanding of the Fibrillization Pathway in Machado-Joseph's Disease: Trapping Early Oligomers of Non-expanded Ataxin-3. *Journal of Molecular Biology*, 2005. **353**(3): p. 642-654.<https://doi.org/10.1016/j.jmb.2005.08.061>.
180. Kaye, R., Head, E., Thompson, J.L., McIntire, T.M., *et al.*, Common Structure of Soluble Amyloid Oligomers Implies Common Mechanism of Pathogenesis. *Science*, 2003. **300**(5618): p. 486-489.<https://doi.org/10.1126/science.1079469>.

181. McCampbell, A., Taylor, J.P., Taye, A.A., Robitschek, J., *et al.*, CREB-binding protein sequestration by expanded polyglutamine. *Human Molecular Genetics*, 2000. **9**(14): p. 2197-2202.<https://doi.org/10.1093/hmg/9.14.2197>.
182. Chai, Y., Koppenhafer, S.L., Shoesmith, S.J., Perez, M.K., *et al.*, Evidence for Proteasome Involvement in Polyglutamine Disease: Localization to Nuclear Inclusions in SCA3/MJD and Suppression of Polyglutamine Aggregation *in vitro*. *Human Molecular Genetics*, 1999. **8**(4): p. 673-682.<https://doi.org/10.1093/hmg/8.4.673>.
183. Schmidt, T., Lindenberg, K.S., Krebs, A., Schöls, L., *et al.*, Protein surveillance machinery in brains with spinocerebellar ataxia type 3: Redistribution and differential recruitment of 26S proteasome subunits and chaperones to neuronal intranuclear inclusions. *Annals of Neurology*, 2002. **51**(3): p. 302-310.<https://doi.org/10.1002/ana.10101>.
184. Donaldson, K.M., Li, W., Ching, K.A., Batalov, S., *et al.*, Ubiquitin-mediated sequestration of normal cellular proteins into polyglutamine aggregates. *Proceedings of the National Academy of Sciences*, 2003. **100**(15): p. 8892-8897.<https://doi.org/10.1073/pnas.1530212100>.
185. Gunawardena, S., Her, L.-S., Brusch, R.G., Laymon, R.A., *et al.*, Disruption of Axonal Transport by Loss of Huntingtin or Expression of Pathogenic PolyQ Proteins in *Drosophila*. *Neuron*, 2003. **40**(1): p. 25-40.[https://doi.org/10.1016/S0896-6273\(03\)00594-4](https://doi.org/10.1016/S0896-6273(03)00594-4).
186. Arrasate, M., Mitra, S., Schweitzer, E.S., Segal, M.R., *et al.*, Inclusion body formation reduces levels of mutant huntingtin and the risk of neuronal death. *Nature*, 2004. **431**(7010): p. 805-810.<https://doi.org/10.1038/nature02998>.
187. Tsvetkov, A.S., Arrasate, M., Barmada, S., Ando, D.M., *et al.*, Proteostasis of polyglutamine varies among neurons and predicts neurodegeneration. *Nature Chemical Biology*, 2013. **9**(9): p. 586-592.<https://doi.org/10.1038/nchembio.1308>.
188. Tarlac, V. and Storey, E., Role of proteolysis in polyglutamine disorders. *Journal of Neuroscience Research*, 2003. **74**(3): p. 406-416.<https://doi.org/10.1002/jnr.10746>.
189. Yang, W., Dunlap, J.R., Andrews, R.B., and Wetzel, R., Aggregated polyglutamine peptides delivered to nuclei are toxic to mammalian cells. *Human Molecular Genetics*, 2002. **11**(23): p. 2905-2917.<https://doi.org/10.1093/hmg/11.23.2905>.
190. Goti, D., Katzen, S.M., Mez, J., Kurtis, N., *et al.*, A Mutant Ataxin-3 Putative-Cleavage Fragment in Brains of Machado-Joseph Disease Patients and Transgenic Mice Is Cytotoxic above a Critical Concentration. *The Journal of Neuroscience*, 2004. **24**(45): p. 10266-10279.<https://doi.org/10.1523/JNEUROSCI.2734-04.2004>.
191. Haacke, A., Broadley, S.A., Boteva, R., Tsvetkov, N., *et al.*, Proteolytic cleavage of polyglutamine-expanded ataxin-3 is critical for aggregation and sequestration of non-expanded ataxin-3. *Human Molecular Genetics*, 2006. **15**(4): p. 555-568.<https://doi.org/10.1093/hmg/ddi472>.
192. Haacke, A., Hartl, F.U., and Breuer, P., Calpain Inhibition Is Sufficient to Suppress Aggregation of Polyglutamine-expanded Ataxin-3. *Journal of Biological Chemistry*, 2007. **282**(26): p. 18851-18856.<https://doi.org/10.1074/jbc.M611914200>.

193. Jung, J., Xu, K., Lessing, D., and Bonini, N.M., Preventing Ataxin-3 protein cleavage mitigates degeneration in a *Drosophila* model of SCA3. *Human Molecular Genetics*, 2009. **18**(24): p. 4843-4852.<https://doi.org/10.1093/hmg/ddp456>.
194. Colomer Gould, V.F., Goti, D., Pearce, D., Gonzalez, G.A., *et al.*, A Mutant ataxin-3 fragment results from processing at a site N-terminal to amino acid 190 in brain of Machado–Joseph disease-like transgenic mice. *Neurobiology of Disease*, 2007. **27**(3): p. 362-369.<https://doi.org/10.1016/j.nbd.2007.06.005>.
195. Ikeda, H., Yamaguchi, M., Sugai, S., Aze, Y., *et al.*, Expanded polyglutamine in the Machado–Joseph disease protein induces cell death *in vitro* and *in vivo*. *Nature Genetics*, 1996. **13**(2): p. 196-202.<https://doi.org/10.1038/ng0696-196>.
196. Breuer, P., Haacke, A., Evert, B.O., and Wüllner, U., Nuclear Aggregation of Polyglutamine-expanded Ataxin-3: Fragments escape the cytoplasmic quality control. *Journal of Biological Chemistry*, 2010. **285**(9): p. 6532-6537.<https://doi.org/10.1074/jbc.M109.036335>.
197. Wellington, C.L., Ellerby, L.M., Hackam, A.S., Margolis, R.L., *et al.*, Caspase Cleavage of Gene Products Associated with Triplet Expansion Disorders Generates Truncated Fragments Containing the Polyglutamine Tract. *Journal of Biological Chemistry*, 1998. **273**(15): p. 9158-9167.<https://doi.org/10.1074/jbc.273.15.9158>.
198. Berke, S.J.S., Schmied, F.A.F., Brunt, E.R., Ellerby, L.M., *et al.*, Caspase-mediated proteolysis of the polyglutamine disease protein ataxin-3. *Journal of Neurochemistry*, 2004. **89**(4): p. 908-918.<https://doi.org/10.1111/j.1471-4159.2004.02369.x>.
199. William C. Earnshaw, Luis M. Martins, and Kaufmann, S.H., Mammalian Caspases: Structure, Activation, Substrates, and Functions During Apoptosis. *Annual Review of Biochemistry*, 1999. **68**(1): p. 383-424.<https://doi.org/10.1146/annurev.biochem.68.1.383>.
200. Goll, D.E., Thompson, V.F., Li, H., Wei, W., *et al.*, The Calpain System. *Physiological Reviews*, 2003. **83**(3): p. 731-801.<https://doi.org/10.1152/physrev.00029.2002>.
201. Hübener, J., Weber, J.J., Richter, C., Honold, L., *et al.*, Calpain-mediated ataxin-3 cleavage in the molecular pathogenesis of spinocerebellar ataxia type 3 (SCA3). *Human Molecular Genetics*, 2012. **22**(3): p. 508-518.<https://doi.org/10.1093/hmg/dds449>.
202. Koch, P., Breuer, P., Peitz, M., Jungverdorben, J., *et al.*, Excitation-induced ataxin-3 aggregation in neurons from patients with Machado–Joseph disease. *Nature*, 2011. **480**(7378): p. 543-546.<https://doi.org/10.1038/nature10671>.
203. Fei, E., Jia, N., Zhang, T., Ma, X., *et al.*, Phosphorylation of ataxin-3 by glycogen synthase kinase 3 $\beta$  at serine 256 regulates the aggregation of ataxin-3. *Biochemical and Biophysical Research Communications*, 2007. **357**(2): p. 487-492.<https://doi.org/10.1016/j.bbrc.2007.03.160>.
204. Matos, C.A., Nóbrega, C., Louros, S.R., Almeida, B., *et al.*, Ataxin-3 phosphorylation decreases neuronal defects in spinocerebellar ataxia type 3 models. *Journal of Cell Biology*, 2016. **212**(4): p. 465-480.<https://doi.org/10.1083/jcb.201506025>.

205. Mueller, T., Breuer, P., Schmitt, I., Walter, J., *et al.*, CK2-dependent phosphorylation determines cellular localization and stability of ataxin-3. *Human Molecular Genetics*, 2009. **18**(17): p. 3334-3343.<https://doi.org/10.1093/hmg/ddp274>.
206. Todi, S.V., Winborn, B.J., Scaglione, K.M., Blount, J.R., *et al.*, Ubiquitination directly enhances activity of the deubiquitinating enzyme ataxin-3. *The EMBO Journal*, 2009. **28**(4): p. 372-382.<https://doi.org/10.1038/emboj.2008.289>.
207. Todi, S.V., Scaglione, K.M., Blount, J.R., Basrur, V., *et al.*, Activity and Cellular Functions of the Deubiquitinating Enzyme and Polyglutamine Disease Protein Ataxin-3 Are Regulated by Ubiquitination at Lysine 117. *Journal of Biological Chemistry*, 2010. **285**(50): p. 39303-39313.<https://doi.org/10.1074/jbc.M110.181610>.
208. Warrick, J.M., Morabito, L.M., Bilen, J., Gordesky-Gold, B., *et al.*, Ataxin-3 Suppresses Polyglutamine Neurodegeneration in *Drosophila* by a Ubiquitin-Associated Mechanism. *Molecular Cell*, 2005. **18**(1): p. 37-48.<https://doi.org/10.1016/j.molcel.2005.02.030>.
209. Tsou, W.-L., Burr, A.A., Ouyang, M., Blount, J.R., *et al.*, Ubiquitination Regulates the Neuroprotective Function of the Deubiquitinase Ataxin-3 *in Vivo*. *Journal of Biological Chemistry*, 2013. **288**(48): p. 34460-34469.<https://doi.org/10.1074/jbc.M113.513903>.
210. Hübener, J. and Riess, O., Polyglutamine-induced neurodegeneration in SCA3 is not mitigated by non-expanded ataxin-3: Conclusions from double-transgenic mouse models. *Neurobiology of Disease*, 2010. **38**(1): p. 116-124.<https://doi.org/10.1016/j.nbd.2010.01.005>.
211. Alves, S., Nascimento-Ferreira, I., Dufour, N., Hassig, R., *et al.*, Silencing ataxin-3 mitigates degeneration in a rat model of Machado–Joseph disease: no role for wild-type ataxin-3? *Human Molecular Genetics*, 2010. **19**(12): p. 2380-2394.<https://doi.org/10.1093/hmg/ddq111>.
212. Geiss-Friedlander, R. and Melchior, F., Concepts in sumoylation: a decade on. *Nature Reviews Molecular Cell Biology*, 2007. **8**(12): p. 947-956.<https://doi.org/10.1038/nrm2293>.
213. Zhou, Y.-F., Liao, S.-S., Luo, Y.-Y., Tang, J.-G., *et al.*, SUMO-1 Modification on K166 of PolyQ-Expanded aTaxin-3 Strengthens Its Stability and Increases Its Cytotoxicity. *PLOS ONE*, 2013. **8**(1): p. e54214.<https://doi.org/10.1371/journal.pone.0054214>.
214. Almeida, B., Abreu, I.A., Matos, C.A., Fraga, J.S., *et al.*, SUMOylation of the brain-predominant Ataxin-3 isoform modulates its interaction with p97. *Biochimica et Biophysica Acta (BBA) - Molecular Basis of Disease*, 2015. **1852**(9): p. 1950-1959.<https://doi.org/10.1016/j.bbadis.2015.06.010>.
215. Jeitner, T.M., Pinto, J.T., Krasnikov, B.F., Horswill, M., *et al.*, Transglutaminases and neurodegeneration. *Journal of Neurochemistry*, 2009. **109**(s1): p. 160-166.<https://doi.org/10.1111/j.1471-4159.2009.05843.x>.
216. Lin, Y., He, H., Luo, Y., Zhu, T., *et al.*, Inhibition of Transglutaminase Exacerbates Polyglutamine-Induced Neurotoxicity by Increasing the Aggregation of Mutant Ataxin-3 in an SCA3 *Drosophila* Model. *Neurotoxicity Research*, 2015. **27**(3): p. 259-267.<https://doi.org/10.1007/s12640-014-9506-8>.



217. Mastroberardino, P.G., Iannicola, C., Nardacci, R., Bernassola, F., *et al.*, 'Tissue' transglutaminase ablation reduces neuronal death and prolongs survival in a mouse model of Huntington's disease. *Cell Death & Differentiation*, 2002. **9**(9): p. 873-880.<https://doi.org/10.1038/sj.cdd.4401093>.
218. Pennuto, M., Palazzolo, I., and Poletti, A., Post-translational modifications of expanded polyglutamine proteins: impact on neurotoxicity. *Human Molecular Genetics*, 2009. **18**(R1): p. R40-R47.<https://doi.org/10.1093/hmg/ddn412>.
219. Muma, N.A. and Mi, Z., Serotonylation and Transamidation of Other Monoamines. *ACS Chemical Neuroscience*, 2015. **6**(7): p. 961-969.<https://doi.org/10.1021/cn500329r>.
220. Lepack, A.E., Werner, C.T., Stewart, A.F., Fulton, S.L., *et al.*, Dopaminylation of histone H3 in ventral tegmental area regulates cocaine seeking. *Science*, 2020. **368**(6487): p. 197-201.<https://doi.org/10.1126/science.aaw8806>.
221. Holmberg, C.I., Staniszewski, K.E., Mensah, K.N., Matouschek, A., *et al.*, Inefficient degradation of truncated polyglutamine proteins by the proteasome. *The EMBO Journal*, 2004. **23**(21): p. 4307-4318.<https://doi.org/10.1038/sj.emboj.7600426>.
222. de Pril, R., Fischer, D.F., Maat-Schieman, M.L.C., Hobo, B., *et al.*, Accumulation of aberrant ubiquitin induces aggregate formation and cell death in polyglutamine diseases. *Human Molecular Genetics*, 2004. **13**(16): p. 1803-1813.<https://doi.org/10.1093/hmg/ddh188>.
223. Bence, N.F., Sampat, R.M., and Kopito, R.R., Impairment of the Ubiquitin-Proteasome System by Protein Aggregation. *Science*, 2001. **292**(5521): p. 1552-1555.<https://doi.org/10.1126/science.292.5521.1552>.
224. Qiu, J.H., Asai, A., Chi, S., Saito, N., *et al.*, Proteasome Inhibitors Induce Cytochrome c-Caspase-3-Like Protease-Mediated Apoptosis in Cultured Cortical Neurons. *The Journal of Neuroscience*, 2000. **20**(1): p. 259-265.<https://doi.org/10.1523/JNEUROSCI.20-01-00259.2000>.
225. Keller, J.N. and Markesbery, W.R., Proteasome inhibition results in increased poly-ADP-ribosylation: Implications for neuron death. *Journal of Neuroscience Research*, 2000. **61**(4): p. 436-442.[https://doi.org/10.1002/1097-4547\(20000815\)61:4<436::AID-JNR10>3.0.CO;2-Z](https://doi.org/10.1002/1097-4547(20000815)61:4<436::AID-JNR10>3.0.CO;2-Z).
226. Ding, Q., Dimayuga, E., Markesbery, W.R., and Keller, J.N., Proteasome inhibition increases DNA and RNA oxidation in astrocyte and neuron cultures. *Journal of Neurochemistry*, 2004. **91**(5): p. 1211-1218.<https://doi.org/10.1111/j.1471-4159.2004.02802.x>.
227. Cummings, C.J., Mancini, M.A., Antalffy, B., DeFranco, D.B., *et al.*, Chaperone suppression of aggregation and altered subcellular proteasome localization imply protein misfolding in SCA1. *Nature Genetics*, 1998. **19**(2): p. 148-154.<https://doi.org/10.1038/502>.
228. Warrick, J.M., Chan, H.Y.E., Gray-Board, G.L., Chai, Y., *et al.*, Suppression of polyglutamine-mediated neurodegeneration in *Drosophila* by the molecular chaperone HSP70. *Nature Genetics*, 1999. **23**(4): p. 425-428.<https://doi.org/10.1038/70532>.
229. Chan, H.Y.E., Warrick, J.M., Gray-Board, G.L., Paulson, H.L., *et al.*, Mechanisms of chaperone suppression of polyglutamine disease: selectivity, synergy and modulation of protein solubility in

- Drosophila*. *Human Molecular Genetics*, 2000. **9**(19): p. 2811-2820.<https://doi.org/10.1093/hmg/9.19.2811>.
230. Fujikake, N., Nagai, Y., Popiel, H.A., Okamoto, Y., *et al.*, Heat Shock Transcription Factor 1-activating Compounds Suppress Polyglutamine-induced Neurodegeneration through Induction of Multiple Molecular Chaperones. *Journal of Biological Chemistry*, 2008. **283**(38): p. 26188-26197.<https://doi.org/10.1074/jbc.M710521200>.
231. Teixeira-Castro, A., Ailion, M., Jalles, A., Brignull, H.R., *et al.*, Neuron-specific proteotoxicity of mutant ataxin-3 in *C. elegans*: rescue by the DAF-16 and HSF-1 pathways. *Human Molecular Genetics*, 2011. **20**(15): p. 2996-3009.<https://doi.org/10.1093/hmg/ddr203>.
232. Kim, S., Nollen, E.A.A., Kitagawa, K., Bindokas, V.P., *et al.*, Polyglutamine protein aggregates are dynamic. *Nature Cell Biology*, 2002. **4**(10): p. 826-831.<https://doi.org/10.1038/ncb863>.
233. Menzies, F.M., Fleming, A., and Rubinsztein, D.C., Compromised autophagy and neurodegenerative diseases. *Nature Reviews Neuroscience*, 2015. **16**(6): p. 345-357.<https://doi.org/10.1038/nrn3961>.
234. Menzies, F.M., Huebener, J., Renna, M., Bonin, M., *et al.*, Autophagy induction reduces mutant ataxin-3 levels and toxicity in a mouse model of spinocerebellar ataxia type 3. *Brain*, 2010. **133**(1): p. 93-104.<https://doi.org/10.1093/brain/awp292>
235. Nascimento-Ferreira, I., Santos-Ferreira, T., Sousa-Ferreira, L., Auregan, G., *et al.*, Overexpression of the autophagic beclin-1 protein clears mutant ataxin-3 and alleviates Machado–Joseph disease. *Brain*, 2011. **134**(5): p. 1400-1415.<https://doi.org/10.1093/brain/awr047>.
236. Lin, M.T. and Beal, M.F., Mitochondrial dysfunction and oxidative stress in neurodegenerative diseases. *Nature*, 2006. **443**(7113): p. 787-795.<https://doi.org/10.1038/nature05292>.
237. Chou, A.-H., Yeh, T.-H., Kuo, Y.-L., Kao, Y.-C., *et al.*, Polyglutamine-expanded ataxin-3 activates mitochondrial apoptotic pathway by upregulating Bax and downregulating Bcl-xL. *Neurobiology of Disease*, 2006. **21**(2): p. 333-345.<https://doi.org/10.1016/j.nbd.2005.07.011>.
238. Tsai, H.-F., Tsai, H.-J., and Hsieh, M., Full-length expanded ataxin-3 enhances mitochondrial-mediated cell death and decreases Bcl-2 expression in human neuroblastoma cells. *Biochemical and Biophysical Research Communications*, 2004. **324**(4): p. 1274-1282.<https://doi.org/10.1016/j.bbrc.2004.09.192>.
239. Yu, Y.-C., Kuo, C.-L., Cheng, W.-L., Liu, C.-S., *et al.*, Decreased antioxidant enzyme activity and increased mitochondrial DNA damage in cellular models of Machado-Joseph disease. *Journal of Neuroscience Research*, 2009. **87**(8): p. 1884-1891.<https://doi.org/10.1002/jnr.22011>.
240. Kazachkova, N., Raposo, M., Montiel, R., Cymbron, T., *et al.*, Patterns of Mitochondrial DNA Damage in Blood and Brain Tissues of a Transgenic Mouse Model of Machado-Joseph Disease. *Neurodegenerative Diseases*, 2013. **11**(4): p. 206-214.<https://doi.org/10.1159/000339207>.



241. Ramos, A., Kazachkova, N., Silva, F., Maciel, P., *et al.*, Differential mtDNA Damage Patterns in a Transgenic Mouse Model of Machado–Joseph Disease (MJD/SCA3). *Journal of Molecular Neuroscience*, 2015. **55**(2): p. 449-453.<https://doi.org/10.1007/s12031-014-0360-1>.
242. Raposo, M., Ramos, A., Santos, C., Kazachkova, N., *et al.*, Accumulation of Mitochondrial DNA Common Deletion Since The Preataxic Stage of Machado-Joseph Disease. *Molecular Neurobiology*, 2019. **56**(1): p. 119-124.<https://doi.org/10.1007/s12035-018-1069-x>.
243. Pozzi, C., Valtorta, M., Tedeschi, G., Galbusera, E., *et al.*, Study of subcellular localization and proteolysis of ataxin-3. *Neurobiology of Disease*, 2008. **30**(2): p. 190-200.<https://doi.org/10.1016/j.nbd.2008.01.011>.
244. Hsu, J.-Y., Jhang, Y.-L., Cheng, P.-H., Chang, Y.-F., *et al.*, The Truncated C-terminal Fragment of Mutant ATXN3 Disrupts Mitochondria Dynamics in Spinocerebellar Ataxia Type 3 Models. *Frontiers in Molecular Neuroscience*, 2017. **10**(196).<https://doi.org/10.3389/fnmol.2017.00196>.
245. Harmuth, T., Prell-Schicker, C., Weber, J.J., Gellerich, F., *et al.*, Mitochondrial Morphology, Function and Homeostasis Are Impaired by Expression of an N-terminal Calpain Cleavage Fragment of Ataxin-3. *Frontiers in Molecular Neuroscience*, 2018. **11**(368).<https://doi.org/10.3389/fnmol.2018.00368>.
246. Laço, M.N., Oliveira, C.R., Paulson, H.L., and Rego, A.C., Compromised mitochondrial complex II in models of Machado–Joseph disease. *Biochimica et Biophysica Acta (BBA) - Molecular Basis of Disease*, 2012. **1822**(2): p. 139-149.<https://doi.org/10.1016/j.bbadis.2011.10.010>.
247. Araujo, J., Breuer, P., Dieringer, S., Krauss, S., *et al.*, FOXO4-dependent upregulation of superoxide dismutase-2 in response to oxidative stress is impaired in spinocerebellar ataxia type 3. *Human Molecular Genetics*, 2011. **20**(15): p. 2928-2941.<https://doi.org/10.1093/hmg/ddr197>.
248. Pacheco, L.S., da Silveira, A.F., Trott, A., Houenou, L.J., *et al.*, Association between Machado–Joseph disease and oxidative stress biomarkers. *Mutation Research/Genetic Toxicology and Environmental Mutagenesis*, 2013. **757**(2): p. 99-103.<https://doi.org/10.1016/j.mrgentox.2013.06.023>.
249. de Assis, A.M., Saute, J.A.M., Longoni, A., Haas, C.B., *et al.*, Peripheral Oxidative Stress Biomarkers in Spinocerebellar Ataxia Type 3/Machado–Joseph Disease. *Frontiers in Neurology*, 2017. **8**(485).<https://doi.org/10.3389/fneur.2017.00485>.
250. Gunawardena, S. and Goldstein, L.S.B., Polyglutamine Diseases and Transport Problems: Deadly Traffic Jams on Neuronal Highways. *Archives of Neurology*, 2005. **62**(1): p. 46-51.<https://doi.org/10.1001/archneur.62.1.46>.
251. Millicamps, S. and Julien, J.-P., Axonal transport deficits and neurodegenerative diseases. *Nature Reviews Neuroscience*, 2013. **14**(3): p. 161-176.<https://doi.org/10.1038/nrn3380>.
252. Guo, W., Stoklund Dittlau, K., and Van Den Bosch, L., Axonal transport defects and neurodegeneration: Molecular mechanisms and therapeutic implications. *Seminars in Cell &*

- Developmental Biology*, 2020. **99**: p. 133-150.<https://doi.org/10.1016/j.semcdb.2019.07.010>.
253. Lee, W.-C.M., Yoshihara, M., and Littleton, J.T., Cytoplasmic aggregates trap polyglutamine-containing proteins and block axonal transport in a *Drosophila* model of Huntington's disease. *Proceedings of the National Academy of Sciences of the United States of America*, 2004. **101**(9): p. 3224-3229.<https://doi.org/10.1073/pnas.0400243101>.
254. Burnett, B.G. and Pittman, R.N., The polyglutamine neurodegenerative protein ataxin 3 regulates aggresome formation. *Proceedings of the National Academy of Sciences of the United States of America*, 2005. **102**(12): p. 4330-4335.<https://doi.org/10.1073/pnas.0407252102>.
255. Rodrigues, A.-J., do Carmo Costa, M., Silva, T.-L., Ferreira, D., *et al.*, Absence of ataxin-3 leads to cytoskeletal disorganization and increased cell death. *Biochimica et Biophysica Acta (BBA) - Molecular Cell Research*, 2010. **1803**(10): p. 1154-1163.<https://doi.org/10.1016/j.bbamcr.2010.07.004>.
256. Neves-Carvalho, A., Logarinho, E., Freitas, A., Duarte-Silva, S., *et al.*, Dominant negative effect of polyglutamine expansion perturbs normal function of ataxin-3 in neuronal cells. *Human Molecular Genetics*, 2015. **24**(1): p. 100-117.<https://doi.org/10.1093/hmg/ddu422>.
257. Wiatr, K., Marczak, Ł., Pérot, J.-B., Brouillet, E., *et al.*, Broad Influence of Mutant Ataxin-3 on the Proteome of the Adult Brain, Young Neurons, and Axons Reveals Central Molecular Processes and Biomarkers in SCA3/MJD Using Knock-In Mouse Model. *Frontiers in Molecular Neuroscience*, 2021. **14**(74).<https://doi.org/10.3389/fnmol.2021.658339>.
258. Brini, M., Cali, T., Ottolini, D., and Carafoli, E., Neuronal calcium signaling: function and dysfunction. *Cellular and Molecular Life Sciences*, 2014. **71**(15): p. 2787-2814.<https://doi.org/10.1007/s00018-013-1550-7>.
259. Pchitskaya, E., Popugaeva, E., and Bezprozvanny, I., Calcium signaling and molecular mechanisms underlying neurodegenerative diseases. *Cell Calcium*, 2018. **70**: p. 87-94.<https://doi.org/10.1016/j.ceca.2017.06.008>.
260. Schrank, S., Barrington, N., and Stutzmann, G.E., Calcium-Handling Defects and Neurodegenerative Disease. *Cold Spring Harbor Perspectives in Biology*, 2020. **12**(7).<https://doi.org/10.1101/cshperspect.a035212>.
261. Chen, X., Tang, T.-S., Tu, H., Nelson, O., *et al.*, Deranged Calcium Signaling and Neurodegeneration in Spinocerebellar Ataxia Type 3. *The Journal of Neuroscience*, 2008. **28**(48): p. 12713-12724.<https://doi.org/10.1523/JNEUROSCI.3909-08.2008>.
262. Pellistri, F., Bucciantini, M., Invernizzi, G., Gatta, E., *et al.*, Different ataxin-3 amyloid aggregates induce intracellular Ca<sup>2+</sup> deregulation by different mechanisms in cerebellar granule cells. *Biochimica et Biophysica Acta (BBA) - Molecular Cell Research*, 2013. **1833**(12): p. 3155-3165.<https://doi.org/10.1016/j.bbamcr.2013.08.019>.
263. Zhivotovsky, B. and Orrenius, S., Calcium and cell death mechanisms: A perspective from the cell death community. *Cell Calcium*, 2011. **50**(3): p. 211-221.<https://doi.org/10.1016/j.ceca.2011.03.003>.

264. Okazawa, H., Polyglutamine diseases: a transcription disorder? *Cellular and Molecular Life Sciences CMLS*, 2003. **60**(7): p. 1427-1439.<https://doi.org/10.1007/s00018-003-3013-z>.
265. Riley, B.E. and Orr, H.T., Polyglutamine neurodegenerative diseases and regulation of transcription: assembling the puzzle. *Genes & Development*, 2006. **20**(16): p. 2183-2192.<https://doi.org/10.1101/gad.1436506>.
266. Kazantsev, A., Preisinger, E., Dranovsky, A., Goldgaber, D., *et al.*, Insoluble detergent-resistant aggregates form between pathological and nonpathological lengths of polyglutamine in mammalian cells. *Proceedings of the National Academy of Sciences*, 1999. **96**(20): p. 11404-11409.<https://doi.org/10.1073/pnas.96.20.11404>.
267. Chou, A.-H., Yeh, T.-H., Ouyang, P., Chen, Y.-L., *et al.*, Polyglutamine-expanded ataxin-3 causes cerebellar dysfunction of SCA3 transgenic mice by inducing transcriptional dysregulation. *Neurobiology of Disease*, 2008. **31**(1): p. 89-101.<https://doi.org/10.1016/j.nbd.2008.03.011>.
268. Evert, B.O., Vogt, I.R., Kindermann, C., Ozimek, L., *et al.*, Inflammatory Genes Are Upregulated in Expanded Ataxin-3-Expressing Cell Lines and Spinocerebellar Ataxia Type 3 Brains. *The Journal of Neuroscience*, 2001. **21**(15): p. 5389-5396.<https://doi.org/10.1523/JNEUROSCI.21-15-05389.2001>.
269. Wiatr, K., Piasecki, P., Marczak, Ł., Wojciechowski, P., *et al.*, Altered Levels of Proteins and Phosphoproteins, in the Absence of Early Causative Transcriptional Changes, Shape the Molecular Pathogenesis in the Brain of Young Presymptomatic Ki91 SCA3/MJD Mouse. *Molecular Neurobiology*, 2019. **56**(12): p. 8168-8202.<https://doi.org/10.1007/s12035-019-01643-4>.
270. Zeng, L., Zhang, D., McLoughlin, H.S., Zalon, A.J., *et al.*, Loss of the Spinocerebellar Ataxia type 3 disease protein ATXN3 alters transcription of multiple signal transduction pathways. *PLOS ONE*, 2018. **13**(9): p. e0204438.<https://doi.org/10.1371/journal.pone.0204438>.
271. Toonen, L.J.A., Overzier, M., Evers, M.M., Leon, L.G., *et al.*, Transcriptional profiling and biomarker identification reveal tissue specific effects of expanded ataxin-3 in a spinocerebellar ataxia type 3 mouse model. *Molecular Neurodegeneration*, 2018. **13**(1): p. 31.<https://doi.org/10.1186/s13024-018-0261-9>.
272. Carmona, V., Cunha-Santos, J., Onofre, I., Simões, A.T., *et al.*, Unravelling Endogenous MicroRNA System Dysfunction as a New Pathophysiological Mechanism in Machado-Joseph Disease. *Molecular Therapy*, 2017. **25**(4): p. 1038-1055.<https://doi.org/10.1016/j.ymthe.2017.01.021>.
273. Wang, Z.-J., Hanet, A., Weishäupl, D., Martins, I.M., *et al.*, Divalproex sodium modulates nuclear localization of ataxin-3 and prevents cellular toxicity caused by expanded ataxin-3. *CNS Neuroscience & Therapeutics*, 2018. **24**(5): p. 404-411.<https://doi.org/10.1111/cns.12795>.
274. Sowa, A.S., Martin, E., Martins, I.M., Schmidt, J., *et al.*, Karyopherin  $\alpha$ -3 is a key protein in the pathogenesis of spinocerebellar ataxia type 3 controlling the nuclear localization of ataxin-3. *Proceedings of the National Academy of Sciences*, 2018. **115**(11): p. E2624-E2633.<https://doi.org/10.1073/pnas.1716071115>.

275. Hou, Y., Dan, X., Babbar, M., Wei, Y., *et al.*, Ageing as a risk factor for neurodegenerative disease. *Nature Reviews Neurology*, 2019. **15**(10): p. 565-581.<https://doi.org/10.1038/s41582-019-0244-7>.
276. López-Otín, C., Blasco, M.A., Partridge, L., Serrano, M., *et al.*, The Hallmarks of Aging. *Cell*, 2013. **153**(6): p. 1194-1217.<https://doi.org/10.1016/j.cell.2013.05.039>.
277. Löw, P., The role of ubiquitin–proteasome system in ageing. *General and Comparative Endocrinology*, 2011. **172**(1): p. 39-43.<https://doi.org/10.1016/j.ygcen.2011.02.005>.
278. Saez, I. and Vilchez, D., The Mechanistic Links Between Proteasome Activity, Aging and Agerelated Diseases. *Current Genomics*, 2014. **15**(1): p. 38-51.<https://doi.org/10.2174/138920291501140306113344>.
279. Morimoto, R.I., Proteotoxic stress and inducible chaperone networks in neurodegenerative disease and aging. *Genes & Development*, 2008. **22**(11): p. 1427-1438.<https://doi.org/10.1101/gad.1657108>.
280. Cuervo, A.M. and Wong, E., Chaperone-mediated autophagy: roles in disease and aging. *Cell Research*, 2014. **24**(1): p. 92-104.<https://doi.org/10.1038/cr.2013.153>.
281. Tan, C.-C., Yu, J.-T., Tan, M.-S., Jiang, T., *et al.*, Autophagy in aging and neurodegenerative diseases: implications for pathogenesis and therapy. *Neurobiology of Aging*, 2014. **35**(5): p. 941-957.<https://doi.org/10.1016/j.neurobiolaging.2013.11.019>.
282. Morley, J.F., Brignull, H.R., Weyers, J.J., and Morimoto, R.I., The threshold for polyglutamine-expansion protein aggregation and cellular toxicity is dynamic and influenced by aging in *Caenorhabditis elegans*. *Proceedings of the National Academy of Sciences*, 2002. **99**(16): p. 10417-10422.<https://doi.org/10.1073/pnas.152161099>.
283. Ben-Zvi, A., Miller, E.A., and Morimoto, R.I., Collapse of proteostasis represents an early molecular event in *Caenorhabditis elegans* aging. *Proceedings of the National Academy of Sciences*, 2009. **106**(35): p. 14914-14919.<https://doi.org/10.1073/pnas.0902882106>.
284. de Magalhães, J.P., Curado, J., and Church, G.M., Meta-analysis of age-related gene expression profiles identifies common signatures of aging. *Bioinformatics*, 2009. **25**(7): p. 875-881.<https://doi.org/10.1093/bioinformatics/btp073>.
285. Kenyon, C.J., The genetics of ageing. *Nature*, 2010. **464**(7288): p. 504-512.<https://doi.org/10.1038/nature08980>.
286. Bishop, N.A., Lu, T., and Yankner, B.A., Neural mechanisms of ageing and cognitive decline. *Nature*, 2010. **464**(7288): p. 529-535.<https://doi.org/10.1038/nature08983>.
287. Arpa, J., Sanz-Gallego, I., Medina-Báez, J., Portela, L.V.C., *et al.*, Subcutaneous insulin-like growth factor-1 treatment in spinocerebellar ataxias: An open label clinical trial. *Movement Disorders*, 2011. **26**(2): p. 358-359.<https://doi.org/10.1002/mds.23423>.

288. Rincon, M., Muzumdar, R., Atzmon, G., and Barzilai, N., The paradox of the insulin/IGF-1 signaling pathway in longevity. *Mechanisms of Ageing and Development*, 2004. **125**(6): p. 397-403.<https://doi.org/10.1016/j.mad.2004.03.006>.
289. Nakae, J., Kido, Y., and Accili, D., Distinct and Overlapping Functions of Insulin and IGF-1 Receptors. *Endocrine Reviews*, 2001. **22**(6): p. 818-835.<https://doi.org/10.1210/edrv.22.6.0452>.
290. Boulianne, G.L., Neuronal regulation of lifespan: clues from flies and worms. *Mechanisms of Ageing and Development*, 2001. **122**(9): p. 883-894.[https://doi.org/10.1016/S0047-6374\(01\)00245-7](https://doi.org/10.1016/S0047-6374(01)00245-7).
291. Sittler, A., Muriel, M.P., Marinello, M., Brice, A., *et al.*, Deregulation of autophagy in postmortem brains of Machado-Joseph disease patients. *Neuropathology*, 2018. **38**(2): p. 113-124.<https://doi.org/10.1111/neup.12433>.
292. Duarte-Silva, S., Neves-Carvalho, A., Soares-Cunha, C., Silva, J.M., *et al.*, Neuroprotective Effects of Creatine in the CMVMJD135 Mouse Model of Spinocerebellar Ataxia Type 3. *Movement Disorders*, 2018. **33**(5): p. 815-826.<https://doi.org/10.1002/mds.27292>.
293. Cunha-Santos, J., Duarte-Neves, J., Carmona, V., Guarente, L., *et al.*, Caloric restriction blocks neuropathology and motor deficits in Machado–Joseph disease mouse models through SIRT1 pathway. *Nature Communications*, 2016. **7**(1): p. 11445.<https://doi.org/10.1038/ncomms11445>.
294. Sulston, J.E. and Horvitz, H.R., Post-embryonic cell lineages of the nematode, *Caenorhabditis elegans*. *Developmental Biology*, 1977. **56**(1): p. 110-156.[https://doi.org/10.1016/0012-1606\(77\)90158-0](https://doi.org/10.1016/0012-1606(77)90158-0).
295. Sulston, J.E., Schierenberg, E., White, J.G., and Thomson, J.N., The embryonic cell lineage of the nematode *Caenorhabditis elegans*. *Developmental Biology*, 1983. **100**(1): p. 64-119.[https://doi.org/10.1016/0012-1606\(83\)90201-4](https://doi.org/10.1016/0012-1606(83)90201-4).
296. Sulston, J.E., Neuronal Cell Lineages in the Nematode *Caenorhabditis elegans*. *Cold Spring Harbor Symposia on Quantitative Biology*, 1983. **48**: p. 443-452.<https://doi.org/10.1101/sqb.1983.048.01.049>.
297. Bargmann, C.I. and Kaplan, J.M., Signal Transduction In The *Caenorhabditis elegans* Nervous System. *Annual Review of Neuroscience*, 1998. **21**(1): p. 279-308.<https://doi.org/10.1146/annurev.neuro.21.1.279>.
298. Bono, M.d. and Maricq, A.V., Neuronal substrates of complex behaviors in *C. elegans*. *Annual Review of Neuroscience*, 2005. **28**(1): p. 451-501.<https://doi.org/10.1146/annurev.neuro.27.070203.144259>.
299. Oikonomou, G. and Shaham, S., The Glia of *Caenorhabditis elegans*. *Glia*, 2011. **59**(9): p. 1253-1263.<https://doi.org/10.1002/glia.21084>.
300. Rankin, C.H., From gene to identified neuron to behaviour in *Caenorhabditis elegans*. *Nature Reviews Genetics*, 2002. **3**(8): p. 622-630.<https://doi.org/10.1038/nrg864>.

301. Nollen, E.A.A., Garcia, S.M., van Haften, G., Kim, S., *et al.*, Genome-wide RNA interference screen identifies previously undescribed regulators of polyglutamine aggregation. *Proceedings of the National Academy of Sciences of the United States of America*, 2004. **101**(17): p. 6403-6408.<https://doi.org/10.1073/pnas.0307697101>.
302. Brignull, H.R., Moore, F.E., Tang, S.J., and Morimoto, R.I., Polyglutamine Proteins at the Pathogenic Threshold Display Neuron-Specific Aggregation in a Pan-Neuronal *Caenorhabditis elegans* Model. *The Journal of Neuroscience*, 2006. **26**(29): p. 7597-7606.<https://doi.org/10.1523/JNEUROSCI.0990-06.2006>.
303. Teixeira-Castro, A., Jalles, A., Esteves, S., Kang, S., *et al.*, Serotonergic signalling suppresses ataxin 3 aggregation and neurotoxicity in animal models of Machado-Joseph disease. *Brain*, 2015. **138**(11): p. 3221-3237.<https://doi.org/10.1093/brain/aww262>.
304. Pereira-Sousa, J., Ferreira-Lomba, B., Bellver-Sanchis, A., Vilasboas-Campos, D., *et al.*, Identification of the 5-HT<sub>1A</sub> serotonin receptor as a novel therapeutic target in a *C. elegans* model of Machado-Joseph disease. *Neurobiology of Disease*, 2021. **152**: p. 105278.<https://doi.org/10.1016/j.nbd.2021.105278>.
305. Ahringer, J., Turn to the worm! *Current Opinion in Genetics & Development*, 1997. **7**(3): p. 410-415.[https://doi.org/10.1016/S0959-437X\(97\)80157-8](https://doi.org/10.1016/S0959-437X(97)80157-8).
306. Khan, L.A., Bauer, P.O., Miyazaki, H., Lindenberg, K.S., *et al.*, Expanded polyglutamines impair synaptic transmission and ubiquitin-proteasome system in *Caenorhabditis elegans*. *Journal of Neurochemistry*, 2006. **98**(2): p. 576-587.<https://doi.org/10.1111/j.1471-4159.2006.03895.x>.
307. Christie, N.T.M., Lee, A.L., Fay, H.G., Gray, A.A., *et al.*, Novel Polyglutamine Model Uncouples Proteotoxicity from Aging. *PLOS ONE*, 2014. **9**(5): p. e96835.<https://doi.org/10.1371/journal.pone.0096835>.
308. Boy, J., Schmidt, T., Schumann, U., Grasshoff, U., *et al.*, A transgenic mouse model of spinocerebellar ataxia type 3 resembling late disease onset and gender-specific instability of CAG repeats. *Neurobiology of Disease*, 2010. **37**(2): p. 284-293.<https://doi.org/10.1016/j.nbd.2009.08.002>.
309. Boy, J., Schmidt, T., Wolburg, H., Mack, A., *et al.*, Reversibility of symptoms in a conditional mouse model of spinocerebellar ataxia type 3. *Human Molecular Genetics*, 2009. **18**(22): p. 4282-4295.<https://doi.org/10.1093/hmg/ddp381>.
310. Hübener, J., Vauti, F., Funke, C., Wolburg, H., *et al.*, N-terminal ataxin-3 causes neurological symptoms with inclusions, endoplasmic reticulum stress and ribosomal dislocation. *Brain*, 2011. **134**(7): p. 1925-1942.<https://doi.org/10.1093/brain/awr118>.
311. Silva-Fernandes, A., Costa, M.d.C., Duarte-Silva, S., Oliveira, P., *et al.*, Motor uncoordination and neuropathology in a transgenic mouse model of Machado-Joseph disease lacking intranuclear inclusions and ataxin-3 cleavage products. *Neurobiology of Disease*, 2010. **40**(1): p. 163-176.<https://doi.org/10.1016/j.nbd.2010.05.021>.



312. Torashima, T., Koyama, C., Iizuka, A., Mitsumura, K., *et al.*, Lentivector-mediated rescue from cerebellar ataxia in a mouse model of spinocerebellar ataxia. *EMBO Reports*, 2008. **9**(4): p. 393-399.<https://doi.org/10.1038/embor.2008.31>.
313. Schmidt, J., Mayer, A.K., Bakula, D., Freude, J., *et al.*, Vulnerability of frontal brain neurons for the toxicity of expanded ataxin-3. *Human Molecular Genetics*, 2019. **28**(9): p. 1463-1473.<https://doi.org/10.1093/hmg/ddy437>.
314. Switonski, P.M., Szlachcic, W.J., Krzyzosiak, W.J., and Figiel, M., A new humanized ataxin-3 knock-in mouse model combines the genetic features, pathogenesis of neurons and glia and late disease onset of SCA3/MJD. *Neurobiology of Disease*, 2015. **73**: p. 174-188.<https://doi.org/10.1016/j.nbd.2014.09.020>.
315. Ramani, B., Harris, G.M., Huang, R., Seki, T., *et al.*, A knockin mouse model of spinocerebellar ataxia type 3 exhibits prominent aggregate pathology and aberrant splicing of the disease gene transcript. *Human Molecular Genetics*, 2015. **24**(5): p. 1211-1224.<https://doi.org/10.1093/hmg/ddu532>
316. Ramani, B., Panwar, B., Moore, L.R., Wang, B., *et al.*, Comparison of spinocerebellar ataxia type 3 mouse models identifies early gain-of-function, cell-autonomous transcriptional changes in oligodendrocytes. *Human Molecular Genetics*, 2017. **26**(17): p. 3362-3374.<https://doi.org/10.1093/hmg/ddx224>.
317. Haas, E., Incebacak, R.D., Hentrich, T., Huridou, C., *et al.*, A Novel SCA3 Knock-in Mouse Model Mimics the Human SCA3 Disease Phenotype Including Neuropathological, Behavioral, and Transcriptional Abnormalities Especially in Oligodendrocytes. *Molecular Neurobiology*, 2021.<https://doi.org/10.1007/s12035-021-02610-8>.
318. Switonski, P.M., Fiszer, A., Kazmierska, K., Kurpisz, M., *et al.*, Mouse Ataxin-3 Functional Knock-Out Model. *NeuroMolecular Medicine*, 2011. **13**(1): p. 54-65.<https://doi.org/10.1007/s12017-010-8137-3>.
319. Esteves, S., Duarte-Silva, S., Naia, L., Neves-Carvalho, A., *et al.*, Limited Effect of Chronic Valproic Acid Treatment in a Mouse Model of Machado-Joseph Disease. *PLOS ONE*, 2015. **10**(10): p. e0141610.<https://doi.org/10.1371/journal.pone.0141610>.
320. Tomioka, I., Ishibashi, H., Minakawa, E.N., Motohashi, H.H., *et al.*, Transgenic Monkey Model of the Polyglutamine Diseases Recapitulating Progressive Neurological Symptoms. *eNeuro*, 2017. **4**(2): p. ENEURO.0250-16.2017.<https://doi.org/10.1523/ENEURO.0250-16.2017>.
321. Dawson, T.M., Golde, T.E., and Lagier-Tourenne, C., Animal models of neurodegenerative diseases. *Nature Neuroscience*, 2018. **21**(10): p. 1370-1379.<https://doi.org/10.1038/s41593-018-0236-8>.
322. Jucker, M., The benefits and limitations of animal models for translational research in neurodegenerative diseases. *Nature Medicine*, 2010. **16**(11): p. 1210-1214.<https://doi.org/10.1038/nm.2224>.

323. Warrick, J.M., Paulson, H.L., Gray-Board, G.L., Bui, Q.T., *et al.*, Expanded Polyglutamine Protein Forms Nuclear Inclusions and Causes Neural Degeneration in *Drosophila*. *Cell*, 1998. **93**(6): p. 939-949.[https://doi.org/10.1016/S0092-8674\(00\)81200-3](https://doi.org/10.1016/S0092-8674(00)81200-3).
324. Kretzschmar, D., Tschäpe, J., Bettencourt Da Cruz, A., Asan, E., *et al.*, Glial and neuronal expression of polyglutamine proteins induce behavioral changes and aggregate formation in *Drosophila*. *Glia*, 2005. **49**(1): p. 59-72.<https://doi.org/10.1002/glia.20098>.
325. Watchon, M., Yuan, K.C., Mackovski, N., Svahn, A.J., *et al.*, Calpain Inhibition Is Protective in Machado–Joseph Disease Zebrafish Due to Induction of Autophagy. *The Journal of Neuroscience*, 2017. **37**(32): p. 7782-7794.<https://doi.org/10.1523/JNEUROSCI.1142-17.2017>.
326. Ouyang, S., Xie, Y., Xiong, Z., Yang, Y., *et al.*, CRISPR/Cas9-Targeted Deletion of Polyglutamine in Spinocerebellar Ataxia Type 3-Derived Induced Pluripotent Stem Cells. *Stem Cells and Development* 2018. **27**(11): p. 756-770.<https://doi.org/10.1089/scd.2017.0209>.
327. Nakamori, M., Panigrahi, G.B., Lanni, S., Gall-Duncan, T., *et al.*, A slipped-CAG DNA-binding small molecule induces trinucleotide-repeat contractions *in vivo*. *Nature Genetics*, 2020. **52**(2): p. 146-159.<https://doi.org/10.1038/s41588-019-0575-8>.
328. Alves, S., Nascimento-Ferreira, I., Auregan, G., Hassig, R., *et al.*, Allele-Specific RNA Silencing of Mutant Ataxin-3 Mediates Neuroprotection in a Rat Model of Machado-Joseph Disease. *PLOS ONE*, 2008. **3**(10): p. e3341.<https://doi.org/10.1371/journal.pone.0003341>.
329. Nóbrega, C., Nascimento-Ferreira, I., Onofre, I., Albuquerque, D., *et al.*, Silencing Mutant Ataxin-3 Rescues Motor Deficits and Neuropathology in Machado-Joseph Disease Transgenic Mice. *PLOS ONE*, 2013. **8**(1): p. e52396.<https://doi.org/10.1371/journal.pone.0052396>.
330. Kotowska-Zimmer, A., Ostrovska, Y., and Olejniczak, M., Universal RNAi Triggers for the Specific Inhibition of Mutant Huntingtin, Atrophin-1, Ataxin-3, and Ataxin-7 Expression. *Molecular Therapy - Nucleic Acids*, 2020. **19**: p. 562-571.<https://doi.org/10.1016/j.omtn.2019.12.012>.
331. Nóbrega, C., Codêso, J.M., Mendonça, L., and Pereira de Almeida, L., RNA Interference Therapy for Machado–Joseph Disease: Long-Term Safety Profile of Lentiviral Vectors Encoding Short Hairpin RNAs Targeting Mutant Ataxin-3. *Human Gene Therapy*, 2019. **30**(7): p. 841-854.<https://doi.org/10.1089/hum.2018.157>.
332. Conceição, M., Mendonça, L., Nóbrega, C., Gomes, C., *et al.*, Intravenous administration of brain-targeted stable nucleic acid lipid particles alleviates Machado-Joseph disease neurological phenotype. *Biomaterials*, 2016. **82**: p. 124-137.<https://doi.org/10.1016/j.biomaterials.2015.12.021>.
333. do Carmo Costa, M., Luna-Cancelon, K., Fischer, S., Ashraf, N.S., *et al.*, Toward RNAi Therapy for the Polyglutamine Disease Machado–Joseph Disease. *Molecular Therapy*, 2013. **21**(10): p. 1898-1908.<https://doi.org/10.1038/mt.2013.144>.
334. Martier, R., Sogorb-Gonzalez, M., Stricker-Shaver, J., Hübener-Schmid, J., *et al.*, Development of an AAV-Based MicroRNA Gene Therapy to Treat Machado-Joseph Disease. *Molecular Therapy - Methods & Clinical Development*, 2019. **15**: p. 343-358.<https://doi.org/10.1016/j.omtm.2019.10.008>.



335. Rodríguez-Lebrón, E., Costa, M.d., Luna-Cancelon, K., Peron, T.M., *et al.*, Silencing Mutant ATXN3 Expression Resolves Molecular Phenotypes in SCA3 Transgenic Mice. *Molecular Therapy*, 2013. **21**(10): p. 1909-1918.<https://doi.org/10.1038/mt.2013.152>.
336. Evers, M.M., Tran, H.-D., Zalachoras, I., Pepers, B.A., *et al.*, Ataxin-3 protein modification as a treatment strategy for spinocerebellar ataxia type 3: Removal of the CAG containing exon. *Neurobiology of Disease*, 2013. **58**: p. 49-56.<https://doi.org/10.1016/j.nbd.2013.04.019>.
337. Kourkouta, E., Weij, R., González-Barriga, A., Mulder, M., *et al.*, Suppression of Mutant Protein Expression in SCA3 and SCA1 Mice Using a CAG Repeat-Targeting Antisense Oligonucleotide. *Molecular Therapy - Nucleic Acids*, 2019. **17**: p. 601-614.<https://doi.org/10.1016/j.omtn.2019.07.004>.
338. McLoughlin, H.S., Moore, L.R., Chopra, R., Komlo, R., *et al.*, Oligonucleotide therapy mitigates disease in spinocerebellar ataxia type 3 mice. *Annals of Neurology*, 2018. **84**(1): p. 64-77.<https://doi.org/10.1002/ana.25264>.
339. Moore, L.R., Rajpal, G., Dillingham, I.T., Qutob, M., *et al.*, Evaluation of Antisense Oligonucleotides Targeting ATXN3 in SCA3 Mouse Models. *Molecular Therapy - Nucleic Acids*, 2017. **7**: p. 200-210.<https://doi.org/10.1016/j.omtn.2017.04.005>.
340. Toonen, L.J.A., Rigo, F., van Attikum, H., and van Roon-Mom, W.M.C., Antisense Oligonucleotide-Mediated Removal of the Polyglutamine Repeat in Spinocerebellar Ataxia Type 3 Mice. *Molecular Therapy - Nucleic Acids*, 2017. **8**: p. 232-242.<https://doi.org/10.1016/j.omtn.2017.06.019>.
341. Simões, A.T., Gonçalves, N., Koeppen, A., Déglon, N., *et al.*, Calpastatin-mediated inhibition of calpains in the mouse brain prevents mutant ataxin 3 proteolysis, nuclear localization and aggregation, relieving Machado–Joseph disease. *Brain*, 2012. **135**(8): p. 2428-2439.<https://doi.org/10.1093/brain/aws177>.
342. Simões, A.T., Gonçalves, N., Nobre, R.J., Duarte, C.B., *et al.*, Calpain inhibition reduces ataxin-3 cleavage alleviating neuropathology and motor impairments in mouse models of Machado–Joseph disease. *Human Molecular Genetics*, 2014. **23**(18): p. 4932-4944.<https://doi.org/10.1093/hmg/ddu209>.
343. Hansen, S.K., Stummann, T.C., Borland, H., Hasholt, L.F., *et al.*, Induced pluripotent stem cell-derived neurons for the study of spinocerebellar ataxia type 3. *Stem Cell Research*, 2016. **17**(2): p. 306-317.<https://doi.org/10.1016/j.scr.2016.07.004>.
344. Ito, N., Kamiguchi, K., Nakanishi, K., Sokolovskya, A., *et al.*, A novel nuclear DnaJ protein, DNAJC8, can suppress the formation of spinocerebellar ataxia 3 polyglutamine aggregation in a J-domain independent manner. *Biochemical and Biophysical Research Communications*, 2016. **474**(4): p. 626-633.<https://doi.org/10.1016/j.bbrc.2016.03.152>.
345. Robertson, A.L., Headey, S.J., Saunders, H.M., Ecroyd, H., *et al.*, Small heat-shock proteins interact with a flanking domain to suppress polyglutamine aggregation. *Proceedings of the National Academy of Sciences*, 2010. **107**(23): p. 10424-10429.<https://doi.org/10.1073/pnas.0914773107>.

346. Yoshida, H., Yoshizawa, T., Shibasaki, F., Shoji, S.i., *et al.*, Chemical Chaperones Reduce Aggregate Formation and Cell Death Caused by the Truncated Machado–Joseph Disease Gene Product with an Expanded Polyglutamine Stretch. *Neurobiology of Disease*, 2002. **10**(2): p. 88-99.<https://doi.org/10.1006/nbdi.2002.0502>.
347. Santana, M.M., Paixão, S., Cunha-Santos, J., Silva, T.P., *et al.*, Trehalose alleviates the phenotype of Machado–Joseph disease mouse models. *Journal of Translational Medicine*, 2020. **18**(1): p. 161.<https://doi.org/10.1186/s12967-020-02302-2>.
348. Todi, S.V., Laco, M.N., Winborn, B.J., Travis, S.M., *et al.*, Cellular Turnover of the Polyglutamine Disease Protein Ataxin-3 Is Regulated by Its Catalytic Activity \*. *Journal of Biological Chemistry*, 2007. **282**(40): p. 29348-29358.<https://doi.org/10.1074/jbc.M704126200>.
349. Blount, J.R., Tsou, W.-L., Ristic, G., Burr, A.A., *et al.*, Ubiquitin-binding site 2 of ataxin-3 prevents its proteasomal degradation by interacting with Rad23. *Nature Communications*, 2014. **5**(1): p. 4638.<https://doi.org/10.1038/ncomms5638>.
350. Jana, N.R., Dikshit, P., Goswami, A., Kotliarova, S., *et al.*, Co-chaperone CHIP Associates with Expanded Polyglutamine Protein and Promotes Their Degradation by Proteasomes \*. *Journal of Biological Chemistry*, 2005. **280**(12): p. 11635-11640.<https://doi.org/10.1074/jbc.M412042200>.
351. Williams, A.J., Knutson, T.M., Colomer Gould, V.F., and Paulson, H.L., *In vivo* suppression of polyglutamine neurotoxicity by C-terminus of Hsp70-interacting protein (CHIP) supports an aggregation model of pathogenesis. *Neurobiology of Disease*, 2009. **33**(3): p. 342-353.<https://doi.org/10.1016/j.nbd.2008.10.016>.
352. Wang, H., Jia, N., Fei, E., Wang, Z., *et al.*, p45, an ATPase subunit of the 19S proteasome, targets the polyglutamine disease protein ataxin-3 to the proteasome. *Journal of Neurochemistry*, 2007. **101**(6): p. 1651-1661.<https://doi.org/10.1111/j.1471-4159.2007.04460.x>.
353. Sutton, J.R., Blount, J.R., Libohova, K., Tsou, W.-L., *et al.*, Interaction of the polyglutamine protein ataxin-3 with Rad23 regulates toxicity in *Drosophila* models of Spinocerebellar Ataxia Type 3. *Human Molecular Genetics*, 2017. **26**(8): p. 1419-1431.<https://doi.org/10.1093/hmg/ddx039>.
354. Ravikumar, B., Duden, R., and Rubinsztein, D.C., Aggregate-prone proteins with polyglutamine and polyalanine expansions are degraded by autophagy. *Human Molecular Genetics*, 2002. **11**(9): p. 1107-1117.<https://doi.org/10.1093/hmg/11.9.1107>.
355. Duarte-Silva, S., Neves-Carvalho, A., Soares-Cunha, C., Teixeira-Castro, A., *et al.*, Lithium Chloride Therapy Fails to Improve Motor Function in a Transgenic Mouse Model of Machado-Joseph Disease. *The Cerebellum*, 2014. **13**(6): p. 713-727.<https://doi.org/10.1007/s12311-014-0589-9>.
356. Duarte-Silva, S., Silva-Fernandes, A., Neves-Carvalho, A., Soares-Cunha, C., *et al.*, Combined therapy with m-TOR-dependent and -independent autophagy inducers causes neurotoxicity in a mouse model of Machado–Joseph disease. *Neuroscience*, 2016. **313**: p. 162-173.<https://doi.org/10.1016/j.neuroscience.2015.11.030>.

357. Nascimento-Ferreira, I., Nóbrega, C., Vasconcelos-Ferreira, A., Onofre, I., *et al.*, Beclin 1 mitigates motor and neuropathological deficits in genetic mouse models of Machado–Joseph disease. *Brain*, 2013. **136**(7): p. 2173-2188.<https://doi.org/10.1093/brain/awt144>.
358. Li, Z., Wang, C., Wang, Z., Zhu, C., *et al.*, Allele-selective lowering of mutant HTT protein by HTT–LC3 linker compounds. *Nature*, 2019. **575**(7781): p. 203-209.<https://doi.org/10.1038/s41586-019-1722-1>.
359. Jung, J. and Bonini, N., CREB-Binding Protein Modulates Repeat Instability in a *Drosophila* Model for PolyQ Disease. *Science*, 2007. **315**(5820): p. 1857-1859.<https://doi.org/10.1126/science.1139517>
360. Chou, A.-H., Chen, S.-Y., Yeh, T.-H., Weng, Y.-H., *et al.*, HDAC inhibitor sodium butyrate reverses transcriptional downregulation and ameliorates ataxic symptoms in a transgenic mouse model of SCA3. *Neurobiology of Disease*, 2011. **41**(2): p. 481-488.<https://doi.org/10.1016/j.nbd.2010.10.019>.
361. Chou, A.-H., Chen, Y.-L., Hu, S.-H., Chang, Y.-M., *et al.*, Polyglutamine-expanded ataxin-3 impairs long-term depression in Purkinje neurons of SCA3 transgenic mouse by inhibiting HAT and impairing histone acetylation. *Brain Research*, 2014. **1583**: p. 220-229.<https://doi.org/10.1016/j.brainres.2014.08.019>.
362. Yi, J., Zhang, L., Tang, B., Han, W., *et al.*, Sodium Valproate Alleviates Neurodegeneration in SCA3/MJD via Suppressing Apoptosis and Rescuing the Hypoacetylation Levels of Histone H3 and H4. *PLOS ONE*, 2013. **8**(1): p. e54792.<https://doi.org/10.1371/journal.pone.0054792>.
363. Lopes-Ramos, C.M., Pereira, T.C., Dogini, D.B., Gilioli, R., *et al.*, Lithium carbonate and coenzyme Q10 reduce cell death in a cell model of Machado-Joseph disease. *Brazilian Journal of Medical and Biological Research*, 2016. **49**.<https://doi.org/10.1590/1414-431x20165805>
364. Silva, S.C.D., Searching for therapeutic strategies in a mouse model of Machado-Joseph disease: targeting proteostases, in School of Medicine. 2015, University of Minho.<http://hdl.handle.net/1822/40642>.
365. Wu, Y.-L., Chang, J.-C., Lin, W.-Y., Li, C.-C., *et al.*, Caffeic acid and resveratrol ameliorate cellular damage in cell and *Drosophila* models of spinocerebellar ataxia type 3 through upregulation of Nrf2 pathway. *Free Radical Biology and Medicine*, 2018. **115**: p. 309-317.<https://doi.org/10.1016/j.freeradbiomed.2017.12.011>.
366. Pohl, F., Teixeira-Castro, A., Costa, M.D., Lindsay, V., *et al.*, GST-4-Dependent Suppression of Neurodegeneration in *C. elegans* Models of Parkinson's and Machado-Joseph Disease by Rapeseed Pomace Extract Supplementation. *Frontiers in Aging Neuroscience*, 2019. **13**(1091).<https://doi.org/10.3389/fnins.2019.01091>.
367. Vilasboas-Campos, D., Costa, M.D., Teixeira-Castro, A., Rios, R., *et al.*, Neurotherapeutic effect of *Hyptis* spp. leaf extracts in *Caenorhabditis elegans* models of tauopathy and polyglutamine disease: Role of the glutathione redox cycle. *Free Radical Biology and Medicine*, 2020.<https://doi.org/10.1016/j.freeradbiomed.2020.10.018>.

368. Krause, T., Gerbershagen, M.U., Fiege, M., Weißhorn, R., *et al.*, Dantrolene – A review of its pharmacology, therapeutic use and new developments. *Anaesthesia*, 2004. **59**(4): p. 364-373.<https://doi.org/10.1111/j.1365-2044.2004.03658.x>.
369. Jeub, M., Herbst, M., Spauschus, A., Fleischer, H., *et al.*, Potassium channel dysfunction and depolarized resting membrane potential in a cell model of SCA3. *Experimental Neurology*, 2006. **201**(1): p. 182-192.<https://doi.org/10.1016/j.expneurol.2006.03.029>.
370. Shakkottai, V.G., do Carmo Costa, M., Dell'Orco, J.M., Sankaranarayanan, A., *et al.*, Early Changes in Cerebellar Physiology Accompany Motor Dysfunction in the Polyglutamine Disease Spinocerebellar Ataxia Type 3. *The Journal of Neuroscience*, 2011. **31**(36): p. 13002-13014.<https://doi.org/10.1523/JNEUROSCI.2789-11.2011>.
371. Chuang, C.-Y., Yang, C.-C., Soong, B.-W., Yu, C.-Y., *et al.*, Modeling spinocerebellar ataxias 2 and 3 with iPSCs reveals a role for glutamate in disease pathology. *Scientific Reports*, 2019. **9**(1): p. 1166.<https://doi.org/10.1038/s41598-018-37774-2>.
372. Schmidt, J., Schmidt, T., Golla, M., Lehmann, L., *et al.*, *In vivo* assessment of riluzole as a potential therapeutic drug for spinocerebellar ataxia type 3. *Journal of Neurochemistry*, 2016. **138**(1): p. 150-162.<https://doi.org/10.1111/jnc.13606>.
373. Mendonça, L.S., Nóbrega, C., Hirai, H., Kaspar, B.K., *et al.*, Transplantation of cerebellar neural stem cells improves motor coordination and neuropathology in Machado-Joseph disease mice. *Brain*, 2014. **138**(2): p. 320-335.<https://doi.org/10.1093/brain/awu352>.
374. Duarte-Neves, J., Gonçalves, N., Cunha-Santos, J., Simões, A.T., *et al.*, Neuropeptide Y mitigates neuropathology and motor deficits in mouse models of Machado–Joseph disease. *Human Molecular Genetics*, 2015. **24**(19): p. 5451-5463.<https://doi.org/10.1093/hmg/ddv271>.
375. Nóbrega, C., Carmo-Silva, S., Albuquerque, D., Vasconcelos-Ferreira, A., *et al.*, Re-establishing ataxin-2 downregulates translation of mutant ataxin-3 and alleviates Machado–Joseph disease. *Brain*, 2015. **138**(12): p. 3537-3554.<https://doi.org/10.1093/brain/awv298>.
376. Nóbrega, C., Mendonça, L., Marcelo, A., Lamazière, A., *et al.*, Restoring brain cholesterol turnover improves autophagy and has therapeutic potential in mouse models of spinocerebellar ataxia. *Acta Neuropathologica*, 2019. **138**(5): p. 837-858.<https://doi.org/10.1007/s00401-019-02019-7>.
377. Gonçalves, N., Simões, A.T., Cunha, R.A., and de Almeida, L.P., Caffeine and adenosine A2A receptor inactivation decrease striatal neuropathology in a lentiviral-based model of Machado–Joseph disease. *Annals of Neurology*, 2013. **73**(5): p. 655-666.<https://doi.org/10.1002/ana.23866>.
378. Chou, A.-H., Chen, Y.-L., Chiu, C.-C., Yuan, S.-J., *et al.*, T1-11 and JMF1907 ameliorate polyglutamine-expanded ataxin-3-induced neurodegeneration, transcriptional dysregulation and ataxic symptom in the SCA3 transgenic mouse. *Neuropharmacology*, 2015. **99**: p. 308-317.<https://doi.org/10.1016/j.neuropharm.2015.08.009>.

379. Gonçalves, N., Simões, A.T., Prediger, R.D., Hirai, H., *et al.*, Caffeine alleviates progressive motor deficits in a transgenic mouse model of spinocerebellar ataxia. *Annals of Neurology*, 2017. **81**(3): p. 407-418.<https://doi.org/10.1002/ana.24867>.
380. Ashraf, N.S., Duarte-Silva, S., Shaw, E.D., Maciel, P., *et al.*, Citalopram Reduces Aggregation of ATXN3 in a YAC Transgenic Mouse Model of Machado-Joseph Disease. *Molecular Neurobiology*, 2019. **56**(5): p. 3690-3701.<https://doi.org/10.1007/s12035-018-1331-2>.
381. Costa, M.d.C., Ashraf, N.S., Fischer, S., Yang, Y., *et al.*, Unbiased screen identifies aripiprazole as a modulator of abundance of the polyglutamine disease protein, ataxin-3. *Brain*, 2016. **139**(11): p. 2891-2908.<https://doi.org/10.1093/brain/aww228>.
382. Mendonça, L.S., Nóbrega, C., Tavino, S., Brinkhaus, M., *et al.*, Ibuprofen enhances synaptic function and neural progenitors proliferation markers and improves neuropathology and motor coordination in Machado–Joseph disease models. *Human Molecular Genetics*, 2019. **28**(22): p. 3691-3703.<https://doi.org/10.1093/hmg/ddz097>.
383. Uchihara, T., Fujigasaki, H., Koyano, S., Nakamura, A., *et al.*, Non-expanded polyglutamine proteins in intranuclear inclusions of hereditary ataxias – triple-labeling immunofluorescence study. *Acta Neuropathologica*, 2001. **102**(2): p. 149-152.<https://doi.org/10.1007/s004010100364>.
384. Da Silva, J.D., Teixeira-Castro, A., and Maciel, P., From Pathogenesis to Novel Therapeutics for Spinocerebellar Ataxia Type 3: Evading Potholes on the Way to Translation. *Neurotherapeutics*, 2019. **16**(4): p. 1009-1031.<https://doi.org/10.1007/s13311-019-00798-1>.
385. Friedman, J.H., Machado-Joseph disease/spinocerebellar ataxia 3 responsive to buspirone. *Movement Disorders*, 1997. **12**(4): p. 613-614.<https://doi.org/10.1002/mds.870120426>.
386. Schulte, T., Mattern, R., Berger, K., Szymanski, S., *et al.*, Double-blind Crossover Trial of Trimethoprim-Sulfamethoxazole in Spinocerebellar Ataxia Type 3/Machado-Joseph Disease. *Archives of Neurology*, 2001. **58**(9): p. 1451-1457.<https://doi.org/10.1001/archneur.58.9.1451>.
387. Takei, A., Honma, S., Kawashima, A., Yabe, I., *et al.*, Beneficial effects of tandospirone on ataxia of a patient with Machado-Joseph disease. *Psychiatry and Clinical Neurosciences*, 2002. **56**(2): p. 181-185.<https://doi.org/10.1046/j.1440-1819.2002.00952.x>.
388. Monte, T.L., Rieder, C.R.M., Tort, A.B., Rockenback, I., *et al.*, Use of fluoxetine for treatment of Machado-Joseph disease: an open-label study. *Acta Neurologica Scandinavica*, 2003. **107**(3): p. 207-210.<https://doi.org/10.1034/j.1600-0404.2003.02132.x>.
389. Takei, A., Fukazawa, T., Hamada, T., Sohma, H., *et al.*, Effects of Tandospirone on “5-HT1A Receptor-Associated Symptoms” in Patients with Machado-Joseph Disease: An Open-Label Study. *Clinical Neuropharmacology*, 2004. **27**(1): p. 9-13.<https://doi.org/10.1097/00002826-200401000-00005>.
390. Liu, C.-S., Hsu, H.-M., Cheng, W.-L., and Hsieh, M., Clinical and molecular events in patients with Machado–Joseph disease under lamotrigine therapy. *Acta Neurologica Scandinavica*, 2005. **111**(6): p. 385-390.<https://doi.org/10.1111/j.1600-0404.2005.00405.x>.

391. Zesiewicz, T.A., Greenstein, P.E., Sullivan, K.L., Wecker, L., *et al.*, A randomized trial of varenicline (Chantix) for the treatment of spinocerebellar ataxia type 3. *Neurology*, 2012. **78**(8): p. 545-550.<https://doi.org/10.1212/WNL.0b013e318247cc7a>.
392. Lei, L.-F., Yang, G.-P., Wang, J.-L., Chuang, D.-M., *et al.*, Safety and efficacy of valproic acid treatment in SCA3/MJD patients. *Parkinsonism & Related Disorders*, 2016. **26**: p. 55-61.<https://doi.org/10.1016/j.parkreldis.2016.03.005>.
393. Saute, J.A.M., de Castilhos, R.M., Monte, T.L., Schumacher-Schuh, A.F., *et al.*, A randomized, phase 2 clinical trial of lithium carbonate in Machado-Joseph disease. *Movement Disorders*, 2014. **29**(4): p. 568-573.<https://doi.org/10.1002/mds.25803>.
394. Romano, S., Coarelli, G., Marcotulli, C., Leonardi, L., *et al.*, Riluzole in patients with hereditary cerebellar ataxia: a randomised, double-blind, placebo-controlled trial. *The Lancet Neurology*, 2015. **14**(10): p. 985-991.[https://doi.org/10.1016/S1474-4422\(15\)00201-X](https://doi.org/10.1016/S1474-4422(15)00201-X).
395. Tsai, Y.-A., Liu, R.-S., Lirng, J.-F., Yang, B.-H., *et al.*, Treatment of Spinocerebellar Ataxia with Mesenchymal Stem Cells: A Phase I/IIa Clinical Study. *Cell Transplantation*, 2017. **26**(3): p. 503-512.<https://doi.org/10.3727/096368916X694373>.
396. Zaltzman, R., Elyoseph, Z., Lev, N., and Gordon, C.R., Trehalose in Machado-Joseph Disease: Safety, Tolerability, and Efficacy. *The Cerebellum*, 2020. **19**(5): p. 672-679.<https://doi.org/10.1007/s12311-020-01150-6>.
397. Benussi, A., Dell'Era, V., Cantoni, V., Bonetta, E., *et al.*, Cerebello-spinal tDCS in ataxia. A randomized, double-blind, sham-controlled, crossover trial. *Neurology*, 2018. **91**(12): p. e1090-e1101.<https://doi.org/10.1212/WNL.0000000000006210>.
398. Lee, W.-J., Moon, J., Kim, T.-J., Jun, J.-S., *et al.*, The c-Abl inhibitor, nilotinib, as a potential therapeutic agent for chronic cerebellar ataxia. *Journal of Neuroimmunology*, 2017. **309**: p. 82-87.<https://doi.org/10.1016/j.jneuroim.2017.05.015>.
399. Duarte-Silva, S. and Maciel, P., Pharmacological Therapies for Machado-Joseph Disease, in *Polyglutamine Disorders*, C. Nóbrega and L. Pereira de Almeida, Editors. 2018, Springer, Cham.: Advances in Experimental Medicine and Biology. p. 369-394.[https://doi.org/10.1007/978-3-319-71779-1\\_19](https://doi.org/10.1007/978-3-319-71779-1_19).
400. Dahlström, A. and Fuxe, K., Localization of monoamines in the lower brain stem. *Experientia*, 1964. **20**(7): p. 398-399.<https://doi.org/10.1007/BF02147990>.
401. Steinbusch, H.W.M., Distribution of serotonin-immunoreactivity in the central nervous system of the rat—Cell bodies and terminals. *Neuroscience*, 1981. **6**(4): p. 557-618.[https://doi.org/10.1016/0306-4522\(81\)90146-9](https://doi.org/10.1016/0306-4522(81)90146-9).
402. Varnäs, K., Halldin, C., and Hall, H., Autoradiographic distribution of serotonin transporters and receptor subtypes in human brain. *Human Brain Mapping*, 2004. **22**(3): p. 246-260.<https://doi.org/10.1002/hbm.20035>.



403. Erspamer, V., Occurrence of indolealkylamines in nature, in *5-Hydroxytryptamine and related indolealkylamines*. 1966, Springer, Berlin, Heidelberg. p. 132-181.[https://doi.org/10.1007/978-3-642-85467-5\\_4](https://doi.org/10.1007/978-3-642-85467-5_4).
404. Gershon, M.D. and Tack, J., The Serotonin Signaling System: From Basic Understanding To Drug Development for Functional GI Disorders. *Gastroenterology*, 2007. **132**(1): p. 397-414.<https://doi.org/10.1053/j.gastro.2006.11.002>.
405. Berger, M., Gray, J.A., and Roth, B.L., The Expanded Biology of Serotonin. *Annual Review of Medicine*, 2009. **60**(1): p. 355-366.<https://doi.org/10.1146/annurev.med.60.042307.110802>.
406. Dayan, P. and Huys, Q.J.M., Serotonin in Affective Control. *Annual Review of Neuroscience*, 2009. **32**(1): p. 95-126.<https://doi.org/10.1146/annurev.neuro.051508.135607>.
407. Jacobs, B.L. and Azmitia, E.C., Structure and function of the brain serotonin system. *Physiological Reviews*, 1992. **72**(1): p. 165-229.<https://doi.org/10.1152/physrev.1992.72.1.165>.
408. Lesch, K.-P., Linking emotion to the social brain. *EMBO Reports*, 2007. **8**(S1): p. S24-S29.<https://doi.org/10.1038/sj.embor.7401008>.
409. Soiza-Reilly, M. and Gaspar, P., Chapter 2 - From B1 to B9: a guide through hindbrain serotonin neurons with additional views from multidimensional characterization, in *Handbook of Behavioral Neuroscience*, C.P. Müller and K.A. Cunningham, Editors. 2020, Elsevier. p. 23-40.<https://doi.org/10.1016/B978-0-444-64125-0.00002-5>.
410. Hornung, J.-P., CHAPTER 1.3 - The Neuroanatomy of the Serotonergic System, in *Handbook of Behavioral Neuroscience*, C.P. Müller and B.L. Jacobs, Editors. 2010, Elsevier. p. 51-64.[https://doi.org/10.1016/S1569-7339\(10\)70071-0](https://doi.org/10.1016/S1569-7339(10)70071-0).
411. Lovenberg, W., Jequier, E., and Sjoerdsma, A., Tryptophan Hydroxylation in Mammalian Systems, in *Advances in Pharmacology*, S. Garattini and P.A. Shore, Editors. 1968, Academic Press. p. 21-36.[https://doi.org/10.1016/S1054-3589\(08\)61153-9](https://doi.org/10.1016/S1054-3589(08)61153-9).
412. Yu, P.-L., Fujimura, M., Okumiya, K., Kinoshita, M., *et al.*, Immunohistochemical localization of tryptophan hydroxylase in the human and rat gastrointestinal tracts. *The Journal of Comparative Neurology* 1999. **411**(4): p. 654-665.[https://doi.org/10.1002/\(SICI\)1096-9861\(19990906\)411:4<654::AID-CNE9>3.0.CO;2-H](https://doi.org/10.1002/(SICI)1096-9861(19990906)411:4<654::AID-CNE9>3.0.CO;2-H).
413. Walther, D.J., Peter, J.-U., Bashammakh, S., Hortnagl, H., *et al.*, Synthesis of serotonin by a second tryptophan hydroxylase isoform. *Science*, 2003. **299**(5603): p. 76-76.<https://doi.org/10.1126/science.1078197>.
414. Lovenberg, W., Weissbach, H., and Udenfriend, S., Aromatic L-Amino Acid Decarboxylase. *Journal of Biological Chemistry*, 1962. **237**(1): p. 89-93.[https://doi.org/10.1016/S0021-9258\(18\)81366-7](https://doi.org/10.1016/S0021-9258(18)81366-7).
415. Erickson, J.D., Schafer, M.K., Bonner, T.I., Eiden, L.E., *et al.*, Distinct pharmacological properties and distribution in neurons and endocrine cells of two isoforms of the human vesicular

- monoamine transporter. *Proceedings of the National Academy of Sciences*, 1996. **93**(10): p. 5166-5171.<https://doi.org/10.1073/pnas.93.10.5166>
416. Lesch, K.-P., Balling, U., Gross, J., Strauss, K., *et al.*, Organization of the human serotonin transporter gene. *Journal of Neural Transmission/General Section JNT*, 1994. **95**(2): p. 157-162.<https://doi.org/10.1007/BF01276434>.
417. Murphy, D.L., Lerner, A., Rudnick, G., and Lesch, K.-P., Serotonin transporter: gene, genetic disorders, and pharmacogenetics. *Molecular interventions*, 2004. **4**(2): p. 109-123.<https://doi.org/10.1124/mi.4.2.8>.
418. Bortolato, M., Chen, K., and Shih, J.C., CHAPTER 2.4 - The Degradation of Serotonin: Role of MAO, in *Handbook of Behavioral Neuroscience*, C.P. Müller and B.L. Jacobs, Editors. 2010, Elsevier. p. 203-218.[https://doi.org/10.1016/S1569-7339\(10\)70079-5](https://doi.org/10.1016/S1569-7339(10)70079-5).
419. Nieuwenhuys, R., Survey of Chemically Defined Cell Groups and Pathways, in *Chemoarchitecture of the Brain*, R. Nieuwenhuys, Editor. 1985, Springer Berlin Heidelberg: Berlin, Heidelberg. p. 7-113.[https://doi.org/10.1007/978-3-642-70426-0\\_3](https://doi.org/10.1007/978-3-642-70426-0_3).
420. Lesch, K.P. and Waider, J., Serotonin in the modulation of neural plasticity and networks: implications for neurodevelopmental disorders. *Neuron*, 2012. **76**(1): p. 175-91.<https://doi.org/10.1016/j.neuron.2012.09.013>.
421. Nichols, D.E. and Nichols, C.D., Serotonin Receptors. *Chemical Reviews*, 2008. **108**(5): p. 1614-1641.<https://doi.org/10.1021/cr078224o>.
422. Marin, P., Bécamel, C., Chaumont-Dubel, S., Vandermoere, F., *et al.*, Chapter 5 - Classification and signaling characteristics of 5-HT receptors: toward the concept of 5-HT receptosomes, in *Handbook of Behavioral Neuroscience*, C.P. Müller and K.A. Cunningham, Editors. 2020, Elsevier. p. 91-120.<https://doi.org/10.1016/B978-0-444-64125-0.00005-0>.
423. Rajagopal, S. and Ponnusamy, M., Overview of G-Protein Coupled Receptor, in *Metabotropic GPCRs: TGR5 and P2Y Receptors in Health and Diseases*. 2018, Springer. p. 1-18.[https://doi.org/10.1007/978-981-13-1571-8\\_1](https://doi.org/10.1007/978-981-13-1571-8_1).
424. Gilman, A.G., G Proteins: Transducers of Receptor-Generated Signals. *Annual Review of Biochemistry*, 1987. **56**(1): p. 615-649.<https://doi.org/10.1146/annurev.bi.56.070187.003151>.
425. Filip, M. and Bader, M., Overview on 5-HT receptors and their role in physiology and pathology of the central nervous system. *Pharmacological Reports*, 2009. **61**(5): p. 761-777.[https://doi.org/10.1016/S1734-1140\(09\)70132-X](https://doi.org/10.1016/S1734-1140(09)70132-X).
426. Deen, M., Christensen, C.E., Hougaard, A., Hansen, H.D., *et al.*, Serotonergic mechanisms in the migraine brain – a systematic review. *Cephalgia*, 2016. **37**(3): p. 251-264.<https://doi.org/10.1177/0333102416640501>.
427. Pierce, K.L., Premont, R.T., and Lefkowitz, R.J., Seven-transmembrane receptors. *Nature Reviews Molecular Cell Biology*, 2002. **3**(9): p. 639-650.<https://doi.org/10.1038/nrm908>.



428. Smrcka, A., Hepler, Brown, K., and Sternweis, P., Regulation of polyphosphoinositide-specific phospholipase C activity by purified Gq. *Science*, 1991. **251**(4995): p. 804-807. <https://doi.org/10.1126/science.1846707>.
429. Kranenburg, O., Poland, M., Horck, F.P.G.v., Drechsel, D., *et al.*, Activation of RhoA by Lysophosphatidic Acid and  $G\alpha_{12/13}$  Subunits in Neuronal Cells: Induction of Neurite Retraction. *Molecular Biology of the Cell*, 1999. **10**(6): p. 1851-1857. <https://doi.org/10.1091/mbc.10.6.1851>.
430. Tang, W. and Gilman, A., Type-specific regulation of adenylyl cyclase by G protein beta gamma subunits. *Science*, 1991. **254**(5037): p. 1500-1503. <https://doi.org/10.1126/science.1962211>.
431. Katz, A., Wu, D., and Simon, M.I., Subunits  $\beta\gamma$  of heterotrimeric G protein activate  $\beta 2$  isoform of phospholipase C. *Nature*, 1992. **360**(6405): p. 686-689. <https://doi.org/10.1038/360686a0>.
432. Stephens, L., Smrcka, A., Cooke, F.T., Jackson, T.R., *et al.*, A novel phosphoinositide 3 kinase activity in myeloid-derived cells is activated by G protein  $\beta\gamma$  subunits. *Cell*, 1994. **77**(1): p. 83-93. [https://doi.org/10.1016/0092-8674\(94\)90237-2](https://doi.org/10.1016/0092-8674(94)90237-2).
433. Inglese, J., Koch, W.J., Touhara, K., and Lefkowitz, R.J.,  $G_{\beta\gamma}$  interactions with PH domains and Ras-MAPK signaling pathways. *Trends in Biochemical Sciences*, 1995. **20**(4): p. 151-156. [https://doi.org/10.1016/S0968-0004\(00\)88992-6](https://doi.org/10.1016/S0968-0004(00)88992-6).
434. Ikeda, S.R., Voltage-dependent modulation of N-type calcium channels by G-protein  $\beta\gamma$  subunits. *Nature*, 1996. **380**(6571): p. 255-258. <https://doi.org/10.1038/380255a0>.
435. Logothetis, D.E., Kurachi, Y., Galper, J., Neer, E.J., *et al.*, The  $\beta\gamma$  subunits of GTP-binding proteins activate the muscarinic  $K^+$  channel in heart. *Nature*, 1987. **325**(6102): p. 321-326. <https://doi.org/10.1038/325321a0>.
436. De Vivo, M. and Maayani, S., Characterization of the 5-hydroxytryptamine<sub>1A</sub> receptor-mediated inhibition of forskolin-stimulated adenylyl cyclase activity in guinea pig and rat hippocampal membranes. *Journal of Pharmacology and Experimental Therapeutics*, 1986. **238**(1): p. 248-253. <https://jpet.aspetjournals.org/content/238/1/248.long>.
437. Weiss, S., Sebben, M., Kemp, D.E., and Bockaert, J., Serotonin 5-HT<sub>1</sub> receptors mediate inhibition of cyclic AMP production in neurons. *European Journal of Pharmacology*, 1986. **120**(2): p. 227-230. [https://doi.org/10.1016/0014-2999\(86\)90544-3](https://doi.org/10.1016/0014-2999(86)90544-3).
438. Palego, L., Giromella, A., Marazziti, D., Borsini, F., *et al.*, Effects of postmortem delay on serotonin and (+)8-OH-DPAT-mediated inhibition of adenylyl cyclase activity in rat and human brain tissues. *Brain Research*, 1999. **816**(1): p. 165-174. [https://doi.org/10.1016/S0006-8993\(98\)01156-1](https://doi.org/10.1016/S0006-8993(98)01156-1).
439. Palego, L., Giromella, A., Marazziti, D., Giannaccini, G., *et al.*, Lack of stereoselectivity of 8-hydroxy-2(di-N-propylamino)tetralin-mediated inhibition of forskolin-stimulated adenylyl cyclase activity in human pre- and post-synaptic brain regions. *Neurochemistry International*, 2000. **36**(3): p. 225-232. [https://doi.org/10.1016/S0197-0186\(99\)00123-0](https://doi.org/10.1016/S0197-0186(99)00123-0).

440. Cadogan, A.K., Kendall, D.A., and Marsden, C.A., Serotonin 5-HT<sub>1A</sub> Receptor Activation Increases Cyclic AMP Formation in the Rat Hippocampus *In Vivo*. *Journal of Neurochemistry*, 1994. **62**(5): p. 1816-1821.<https://doi.org/10.1046/j.1471-4159.1994.62051816.x>.
441. Raymond, J.R., Olsen, C.L., and Gettys, T.W., Cell-specific physical and functional coupling of human 5-HT<sub>1A</sub> receptors to inhibitory G protein  $\alpha$ -subunits and lack of coupling to Gs. $\alpha$ . *Biochemistry*, 1993. **32**(41): p. 11064-11073.<https://doi.org/10.1021/bi00092a016>.
442. Raymond, J.R., Albers, F.J., Middleton, J.P., Lefkowitz, R.J., *et al.*, 5-HT<sub>1A</sub> and histamine H1 receptors in HeLa cells stimulate phosphoinositide hydrolysis and phosphate uptake via distinct G protein pools. *Journal of Biological Chemistry*, 1991. **266**(1): p. 372-379.[https://doi.org/10.1016/S0021-9258\(18\)52444-3](https://doi.org/10.1016/S0021-9258(18)52444-3).
443. Aune, T.M., McGrath, K.M., Sarr, T., Bombara, M.P., *et al.*, Expression of 5HT1a receptors on activated human T cells. Regulation of cyclic AMP levels and T cell proliferation by 5-hydroxytryptamine. *The Journal of Immunology*, 1993. **151**(3): p. 1175-1183.<https://www.jimmunol.org/content/jimmunol/151/3/1175.full.pdf>.
444. Newman-Tancredi, A., Wootton, R., and Strange, P.G., High-level stable expression of recombinant 5-HT<sub>1A</sub> 5-hydroxytryptamine receptors in Chinese hamster ovary cells. *Biochemical Journal*, 1992. **285**(3): p. 933-938.<https://doi.org/10.1042/bj2850933>.
445. Hamon, M., Gozlan, H., El Mestikawy, S., Emerit, M.B., *et al.*, The Central 5-HT<sub>1A</sub> Receptors: Pharmacological, Biochemical, Functional, and Regulatory Properties<sup>a</sup>. *Annals of the New York Academy of Sciences*, 1990. **600**(1): p. 114-129.<https://doi.org/10.1111/j.1749-6632.1990.tb16877.x>.
446. Penington, N.J., Kelly, J.S., and Fox, A.P., Whole-cell recordings of inwardly rectifying K<sup>+</sup> currents activated by 5-HT<sub>1A</sub> receptors on dorsal raphe neurones of the adult rat. *The Journal of Physiology*, 1993. **469**(1): p. 387-405.<https://doi.org/10.1113/jphysiol.1993.sp019819>.
447. Penington, N.J. and Kelly, J.S., Serotonin receptor activation reduces calcium current in an acutely dissociated adult central neuron. *Neuron*, 1990. **4**(5): p. 751-758.[https://doi.org/10.1016/0896-6273\(90\)90201-P](https://doi.org/10.1016/0896-6273(90)90201-P).
448. Peyssonnaud, C. and Eychène, A., The Raf/MEK/ERK pathway: new concepts of activation. *Biology of the Cell*, 2001. **93**(1-2): p. 53-62.[https://doi.org/10.1016/S0248-4900\(01\)01125-X](https://doi.org/10.1016/S0248-4900(01)01125-X).
449. Morrison, D.K., MAP Kinase Pathways. *Cold Spring Harbor Perspectives in Biology*, 2012. **4**(11).<https://doi.org/10.1101/cshperspect.a011254>.
450. Garnovskaya, M.N., van Biesen, T., Hawes, B., Casañas Ramos, S., *et al.*, Ras-Dependent Activation of Fibroblast Mitogen-Activated Protein Kinase by 5-HT<sub>1A</sub> Receptor *via* a G Protein  $\beta\gamma$ -Subunit-Initiated Pathway. *Biochemistry*, 1996. **35**(43): p. 13716-13722.<https://doi.org/10.1021/bi961764n>.
451. Sweatt, J.D., Mitogen-activated protein kinases in synaptic plasticity and memory. *Current Opinion in Neurobiology*, 2004. **14**(3): p. 311-317.<https://doi.org/10.1016/j.conb.2004.04.001>.

452. Xing, J., Ginty, D.D., and Greenberg, M.E., Coupling of the RAS-MAPK Pathway to Gene Activation by RSK2, a Growth Factor-Regulated CREB Kinase. *Science*, 1996. **273**(5277): p. 959-963.<https://doi.org/10.1126/science.273.5277.959>.
453. Hsiung, S.-c., Tamir, H., Franke, T.F., and Liu, K.-p., Roles of extracellular signal-regulated kinase and Akt signaling in coordinating nuclear transcription factor- $\kappa$ B-dependent cell survival after serotonin 1A receptor activation. *Journal of Neurochemistry*, 2005. **95**(6): p. 1653-1666.<https://doi.org/10.1111/j.1471-4159.2005.03496.x>.
454. Adayev, T., El-Sherif, Y., Barua, M., Penington, N.J., *et al.*, Agonist Stimulation of the Serotonin<sub>1A</sub> Receptor Causes Suppression of Anoxia-Induced Apoptosis via Mitogen-Activated Protein Kinase in Neuronal HN2-5 Cells. *Journal of Neurochemistry*, 1999. **72**(4): p. 1489-1496.<https://doi.org/10.1046/j.1471-4159.1999.721489.x>.
455. Polter, A.M., Yang, S., Jope, R.S., and Li, X., Functional significance of glycogen synthase kinase-3 regulation by serotonin. *Cellular Signalling*, 2012. **24**(1): p. 265-271.<https://doi.org/10.1016/j.cellsig.2011.09.009>.
456. Polter, A.M. and Li, X., 5-HT<sub>1A</sub> receptor-regulated signal transduction pathways in brain. *Cellular Signalling*, 2010. **22**(10): p. 1406-1412.<https://doi.org/10.1016/j.cellsig.2010.03.019>.
457. Albert, P.R. and Vahid-Ansari, F., The 5-HT<sub>1A</sub> receptor: Signaling to behavior. *Biochimie*, 2019. **161**: p. 34-45.<https://doi.org/10.1016/j.biochi.2018.10.015>.
458. Sotelo, C., Cholley, B., El Mestikawy, S., Gozlan, H., *et al.*, Direct Immunohistochemical Evidence of the Existence of 5-HT<sub>1A</sub> Autoreceptors on Serotonergic Neurons in the Midbrain Raphe Nuclei. *European Journal of Neuroscience*, 1990. **2**(12): p. 1144-1154.<https://doi.org/10.1111/j.1460-9568.1990.tb00026.x>.
459. la Cour, C.M., El Mestikawy, S., Hanoun, N., Hamon, M., *et al.*, Regional Differences in the Coupling of 5-Hydroxytryptamine-1A Receptors to G Proteins in the Rat Brain. *Molecular Pharmacology*, 2006. **70**(3): p. 1013-1021.<https://doi.org/10.1124/mol.106.022756>.
460. Riad, M., Garcia, S., Watkins, K.C., Jodoin, N., *et al.*, Somatodendritic localization of 5-HT<sub>1A</sub> and preterminal axonal localization of 5-HT<sub>1B</sub> serotonin receptors in adult rat brain. *The Journal of Comparative Neurology*, 2000. **417**(2): p. 181-194.[https://doi.org/10.1002/\(SICI\)1096-9861\(20000207\)417:2<181::AID-CNE4>3.0.CO;2-A](https://doi.org/10.1002/(SICI)1096-9861(20000207)417:2<181::AID-CNE4>3.0.CO;2-A).
461. Verge, D., Daval, G., Patey, A., Gozlan, H., *et al.*, Presynaptic 5-HT autoreceptors on serotonergic cell bodies and/or dendrites but not terminals are of the 5-HT<sub>1A</sub> subtype. *European Journal of Pharmacology*, 1985. **113**(3): p. 463-464.[https://doi.org/10.1016/0014-2999\(85\)90099-8](https://doi.org/10.1016/0014-2999(85)90099-8).
462. Hjorth, S. and Auerbach, S.B., Further evidence for the importance of 5-HT<sub>1A</sub> autoreceptors in the action of selective serotonin reuptake inhibitors. *European Journal of Pharmacology*, 1994. **260**(2): p. 251-255.[https://doi.org/10.1016/0014-2999\(94\)90346-8](https://doi.org/10.1016/0014-2999(94)90346-8).
463. Richer, M., Hen, R., and Blier, P., Modification of serotonin neuron properties in mice lacking 5-HT<sub>1A</sub> receptors. *European Journal of Pharmacology*, 2002. **435**(2): p. 195-203.[https://doi.org/10.1016/S0014-2999\(01\)01607-7](https://doi.org/10.1016/S0014-2999(01)01607-7).

464. Valdizán, E.M., Castro, E., and Pazos, A., Agonist-dependent modulation of G-protein coupling and transduction of 5-HT<sub>1A</sub> receptors in rat dorsal raphe nucleus. *International Journal of Neuropsychopharmacology*, 2010. **13**(7): p. 835-843.<https://doi.org/10.1017/S1461145709990940>.
465. Marazziti, D., Palego, L., Giromella, A., Rosa Mazzoni, M., *et al.*, Region-dependent effects of flibanserin and buspirone on adenylyl cyclase activity in the human brain. *International Journal of Neuropsychopharmacology*, 2002. **5**(2): p. 131-140.<https://doi.org/10.1017/S1461145702002869>.
466. Kushwaha, N. and Albert, P.R., Coupling of 5-HT<sub>1A</sub> autoreceptors to inhibition of mitogen-activated protein kinase activation via G $\beta\gamma$  subunit signaling. *European Journal of Neuroscience*, 2005. **21**(3): p. 721-732.<https://doi.org/10.1111/j.1460-9568.2005.03904.x>.
467. Conn, P.J. and Sanders-Bush, E., Selective 5HT-2 antagonists inhibit serotonin stimulated phosphatidylinositol metabolism in cerebral cortex. *Neuropharmacology*, 1984. **23**(8): p. 993-996.[https://doi.org/10.1016/0028-3908\(84\)90017-0](https://doi.org/10.1016/0028-3908(84)90017-0).
468. Pritchett, D.B., Bach, A.W., Wozny, M., Taleb, O., *et al.*, Structure and functional expression of cloned rat serotonin 5HT-2 receptor. *The EMBO Journal*, 1988. **7**(13): p. 4135-4140.<https://doi.org/10.1002/j.1460-2075.1988.tb03308.x>.
469. Berridge, M.J., Inositol trisphosphate and diacylglycerol as second messengers. *Biochemical Journal*, 1984. **220**(2): p. 345-360.<https://doi.org/10.1042/bj2200345>.
470. Brose, N., Betz, A., and Wegmeyer, H., Divergent and convergent signaling by the diacylglycerol second messenger pathway in mammals. *Current Opinion in Neurobiology*, 2004. **14**(3): p. 328-340.<https://doi.org/10.1016/j.conb.2004.05.006>.
471. Leysen, J.E., 5-HT<sub>2</sub> Receptors. *Current Drug Targets - CNS & Neurological Disorders*, 2004. **3**(1): p. 11-26.<https://doi.org/10.2174/1568007043482598>.
472. Derkach, V., Surprenant, A., and North, R.A., 5-HT<sub>3</sub> receptors are membrane ion channels. *Nature*, 1989. **339**(6227): p. 706-709.<https://doi.org/10.1038/339706a0>.
473. Miquel, M.-C., Emerit, M.B., Nosjean, A., Simon, A., *et al.*, Differential subcellular localization of the 5-HT<sub>3A</sub> receptor subunit in the rat central nervous system. *European Journal of Neuroscience*, 2002. **15**(3): p. 449-457.<https://doi.org/10.1046/j.0953-816x.2001.01872.x>.
474. Sugita, S., Shen, K.Z., and North, R.A., 5-hydroxytryptamine is a fast excitatory transmitter at 5-HT<sub>3</sub> receptors in rat amygdala. *Neuron*, 1992. **8**(1): p. 199-203.[https://doi.org/10.1016/0896-6273\(92\)90121-S](https://doi.org/10.1016/0896-6273(92)90121-S).
475. Barnes, N.M., Hales, T.G., Lummis, S.C.R., and Peters, J.A., The 5-HT<sub>3</sub> receptor – the relationship between structure and function. *Neuropharmacology*, 2009. **56**(1): p. 273-284.<https://doi.org/10.1016/j.neuropharm.2008.08.003>.
476. Maricq, A., Peterson, A., Brake, A., Myers, R., *et al.*, Primary structure and functional expression of the 5HT<sub>3</sub> receptor, a serotonin-gated ion channel. *Science*, 1991. **254**(5030): p. 432-437.<https://doi.org/10.1126/science.1718042>

477. Davies, P.A., Pistis, M., Hanna, M.C., Peters, J.A., *et al.*, The 5-HT<sub>3B</sub> subunit is a major determinant of serotonin-receptor function. *Nature*, 1999. **397**(6717): p. 359-363.<https://doi.org/10.1038/16941>.
478. Niesler, B., Frank, B., Kapeller, J., and Rappold, G.A., Cloning, physical mapping and expression analysis of the human 5-HT<sub>3</sub> serotonin receptor-like genes HTR3C, HTR3D and HTR3E. *Gene*, 2003. **310**: p. 101-111.[https://doi.org/10.1016/S0378-1119\(03\)00503-1](https://doi.org/10.1016/S0378-1119(03)00503-1).
479. Boyd, G.W., Low, P., Dunlop, J.I., Robertson, L.A., *et al.*, Assembly and Cell Surface Expression of Homomeric and Heteromeric 5-HT<sub>3</sub> Receptors: The Role of Oligomerization and Chaperone Proteins. *Molecular and Cellular Neuroscience*, 2002. **21**(1): p. 38-50.<https://doi.org/10.1006/mcne.2002.1160>.
480. Niesler, B., Walstab, J., Combrink, S., Möller, D., *et al.*, Characterization of the Novel Human Serotonin Receptor Subunits 5-HT<sub>3C</sub>, 5-HT<sub>3D</sub>, and 5-HT<sub>3E</sub>. *Molecular Pharmacology*, 2007. **72**(1): p. 8-17.<https://doi.org/10.1124/mol.106.032144>.
481. Niesler, B., Kapeller, J., Hammer, C., and Rappold, G., Serotonin type 3 receptor genes: HTR3A, B, C, D, E. *Pharmacogenomics*, 2008. **9**(5): p. 501-504.<https://doi.org/10.2217/14622416.9.5.501>.
482. King, B.N., Stoner, M.C., Haque, S.M., and Kellum, J.M., A Nitroergic Secretomotor Neurotransmitter in the Chloride Secretory Response to Serotonin. *Digestive Diseases and Sciences*, 2004. **49**(2): p. 196-201.<https://doi.org/10.1023/B:DDAS.0000017438.30998.08>.
483. Dumuis, A., Bouhelal, R., Sebben, M., Cory, R., *et al.*, A nonclassical 5-hydroxytryptamine receptor positively coupled with adenylate cyclase in the central nervous system. *Molecular Pharmacology*, 1988. **34**(6): p. 880-887.<https://molpharm.aspetjournals.org/content/molpharm/34/6/880.full.pdf>.
484. Bockaert, J., Claeysen, S., Compan, V., and Dumuis, A., 5-HT<sub>4</sub> Receptors. *Current Drug Targets - CNS & Neurological Disorders*, 2004. **3**(1): p. 39-51.<https://doi.org/10.2174/1568007043482615>.
485. Bijak, M. and Misgeld, U., Effects of serotonin through serotonin<sub>1A</sub> and serotonin<sub>4</sub> receptors on inhibition in the guinea-pig dentate gyrus *in vitro*. *Neuroscience*, 1997. **78**(4): p. 1017-1026.[https://doi.org/10.1016/S0306-4522\(96\)00666-5](https://doi.org/10.1016/S0306-4522(96)00666-5).
486. Liu, M., Geddis, M.S., Wen, Y., Setlik, W., *et al.*, Expression and function of 5-HT<sub>4</sub> receptors in the mouse enteric nervous system. *American Journal of Physiology-Gastrointestinal and Liver Physiology*, 2005. **289**(6): p. G1148-G1163.<https://doi.org/10.1152/ajpgi.00245.2005>.
487. Bockaert, J., Claeysen, S., Sebben, M., and Dumuis, A., 5-HT<sub>4</sub> Receptors: Gene, Transduction and Effects on Olfactory Memory. *Annals of the New York Academy of Sciences*, 1998. **861**(1): p. 1-15.<https://doi.org/10.1111/j.1749-6632.1998.tb10167.x>.
488. Pindon, A., van Hecke, G., van Gompel, P., Lesage, A.S., *et al.*, Differences in Signal Transduction of Two 5-HT<sub>4</sub> Receptor Splice Variants: Compound Specificity and Dual Coupling with G $\alpha$ s- and G $\alpha$ i/o-Proteins. *Molecular Pharmacology*, 2002. **61**(1): p. 85-96.<https://doi.org/10.1124/mol.61.1.85>.

489. Ouadid, H., Seguin, J., Dumuis, A., Bockaert, J., *et al.*, Serotonin increases calcium current in human atrial myocytes via the newly described 5-hydroxytryptamine<sub>4</sub> receptors. *Molecular Pharmacology*, 1992. **41**(2): p. 346-351.<https://molpharm.aspetjournals.org/content/molpharm/41/2/346.full.pdf>.
490. Fagni, L., Dumuis, A., Sebben, M., and Bockaert, J., The 5-HT<sub>4</sub> receptor subtype inhibits K<sup>+</sup> current in colliculi neurones via activation of a cyclic AMP-dependent protein kinase. *British Journal of Pharmacology*, 1992. **105**(4): p. 973-979.<https://doi.org/10.1111/j.1476-5381.1992.tb09087.x>.
491. Matthes, H., Boschert, U., Amlaiky, N., Grailhe, R., *et al.*, Mouse 5-hydroxytryptamine<sub>5A</sub> and 5-hydroxytryptamine<sub>5B</sub> receptors define a new family of serotonin receptors: cloning, functional expression, and chromosomal localization. *Molecular Pharmacology*, 1993. **43**(3): p. 313-9.<https://molpharm.aspetjournals.org/content/43/3/313.short>.
492. Nelson, D.L., 5-HT<sub>5</sub> Receptors. *Current Drug Targets - CNS & Neurological Disorders*, 2004. **3**(1): p. 53-58.<https://doi.org/10.2174/1568007043482606>.
493. Grailhe, R., Grabtree, G.W., and Hen, R., Human 5-HT<sub>5</sub> receptors: the 5-HT<sub>5A</sub> receptor is functional but the 5-HT<sub>5B</sub> receptor was lost during mammalian evolution. *European Journal of Pharmacology*, 2001. **418**(3): p. 157-167.[https://doi.org/10.1016/S0014-2999\(01\)00933-5](https://doi.org/10.1016/S0014-2999(01)00933-5).
494. Carson, M.J., Thomas, E.A., Danielson, P.E., and Sutcliffe, J.G., The 5-HT<sub>5A</sub> serotonin receptor is expressed predominantly by astrocytes in which it inhibits cAMP accumulation: A mechanism for neuronal suppression of reactive astrocytes. *Glia*, 1996. **17**(4): p. 317-326.[https://doi.org/10.1002/\(SICI\)1098-1136\(199608\)17:4<317::AID-GLIA6>3.0.CO;2-W](https://doi.org/10.1002/(SICI)1098-1136(199608)17:4<317::AID-GLIA6>3.0.CO;2-W).
495. Noda, M., Yasuda, S., Okada, M., Higashida, H., *et al.*, Recombinant human serotonin 5A receptors stably expressed in C6 glioma cells couple to multiple signal transduction pathways. *Journal of Neurochemistry*, 2003. **84**(2): p. 222-232.<https://doi.org/10.1046/j.1471-4159.2003.01518.x>.
496. Francken, B.J.B., Jurzak, M., Vanhauwe, J.F.M., Luyten, W.H.M.L., *et al.*, The human 5-HT<sub>5A</sub> receptor couples to G<sub>i</sub>/G<sub>o</sub> proteins and inhibits adenylate cyclase in HEK 293 cells. *European Journal of Pharmacology*, 1998. **361**(2): p. 299-309.[https://doi.org/10.1016/S0014-2999\(98\)00744-4](https://doi.org/10.1016/S0014-2999(98)00744-4).
497. Wisden, W., Parker, E.M., Mahle, C.D., Grisel, D.A., *et al.*, Cloning and characterization of the rat 5-HT<sub>5B</sub> receptor. *FEBS Letters*, 1993. **333**(1-2): p. 25-31.[https://doi.org/10.1016/0014-5793\(93\)80368-5](https://doi.org/10.1016/0014-5793(93)80368-5).
498. Monsma, F.J., Shen, Y., Ward, R.P., Hamblin, M.W., *et al.*, Cloning and expression of a novel serotonin receptor with high affinity for tricyclic psychotropic drugs. *Molecular Pharmacology*, 1993. **43**(3): p. 320-327.<https://molpharm.aspetjournals.org/content/molpharm/43/3/320.full.pdf>.
499. Ruat, M., Traiffort, E., Arrang, J.M., Tardivellacombe, J., *et al.*, A Novel Rat Serotonin (5-HT<sub>6</sub>) Receptor: Molecular Cloning, Localization and Stimulation of cAMP Accumulation. *Biochemical and Biophysical Research Communications*, 1993. **193**(1): p. 268-276.<https://doi.org/10.1006/bbrc.1993.1619>.



500. Kohen, R., Metcalf, M.A., Khan, N., Druck, T., *et al.*, Cloning, Characterization, and Chromosomal Localization of a Human 5-HT<sub>6</sub> Serotonin Receptor. *Journal of Neurochemistry*, 1996. **66**(1): p. 47-56.<https://doi.org/10.1046/j.1471-4159.1996.66010047.x>.
501. Gérard, C., Mestikawy, S.E., Lebrand, C., Adrien, J., *et al.*, Quantitative RT-PCR distribution of serotonin 5-HT<sub>6</sub> receptor mRNA in the central nervous system of control or 5,7-dihydroxytryptamine-treated rats. *Synapse*, 1996. **23**(3): p. 164-173.[https://doi.org/10.1002/\(SICI\)1098-2396\(199607\)23:3<164::AID-SYN5>3.0.CO;2-6](https://doi.org/10.1002/(SICI)1098-2396(199607)23:3<164::AID-SYN5>3.0.CO;2-6).
502. Sebben, M., Ansanay, H., Bockaert, J., and Dumuis, A., 5-HT<sub>6</sub> receptors positively coupled to adenylyl cyclase in striatal neurones in culture. *Neuroreport*, 1994. **5**(18): p. 2553-2557.<https://doi.org/10.1097/00001756-199412000-00037>.
503. Schoeffter, P. and Waeber, C., 5-Hydroxytryptamine receptors with a 5-HT<sub>6</sub> receptor-like profile stimulating adenylyl cyclase activity in pig caudate membranes. *Naunyn-Schmiedeberg's Archives of Pharmacology*, 1994. **350**(4): p. 356-360.<https://doi.org/10.1007/BF00178951>.
504. Bonsi, P., Cuomo, D., Ding, J., Sciamanna, G., *et al.*, Endogenous Serotonin Excites Striatal Cholinergic Interneurons via the Activation of 5-HT<sub>2c</sub>, 5-HT<sub>6</sub>, and 5-HT<sub>7</sub> Serotonin Receptors: Implications for Extrapyramidal Side Effects of Serotonin Reuptake Inhibitors. *Neuropsychopharmacology*, 2007. **32**(8): p. 1840-1854.<https://doi.org/10.1038/sj.npp.1301294>.
505. Yun, H.-M., Kim, S., Kim, H.-J., Kostenis, E., *et al.*, The Novel Cellular Mechanism of Human 5-HT<sub>6</sub> Receptor through an Interaction with Fyn\*. *Journal of Biological Chemistry*, 2007. **282**(8): p. 5496-5505.<https://doi.org/10.1074/jbc.M606215200>.
506. Marcos, B., Cabero, M., Solas, M., Aisa, B., *et al.*, Signalling pathways associated with 5-HT<sub>6</sub> receptors: relevance for cognitive effects. *International Journal of Neuropsychopharmacology*, 2010. **13**(6): p. 775-784.<https://doi.org/10.1017/S146114570999054X>.
507. Bard, J.A., Zgombick, J., Adham, N., Vaysse, P., *et al.*, Cloning of a novel human serotonin receptor (5-HT<sub>7</sub>) positively linked to adenylyl cyclase. *Journal of Biological Chemistry*, 1993. **268**(31): p. 23422-23426.[https://doi.org/10.1016/S0021-9258\(19\)49479-9](https://doi.org/10.1016/S0021-9258(19)49479-9).
508. Lovenberg, T.W., Baron, B.M., de Lecea, L., Miller, J.D., *et al.*, A novel adenylyl cyclase-activating serotonin receptor (5-HT<sub>7</sub>) implicated in the regulation of mammalian circadian rhythms. *Neuron*, 1993. **11**(3): p. 449-458.[https://doi.org/10.1016/0896-6273\(93\)90149-L](https://doi.org/10.1016/0896-6273(93)90149-L).
509. Stowe, R.L. and Barnes, N.M., Selective labelling of 5-HT<sub>7</sub> receptor recognition sites in rat brain using [<sup>3</sup>H]5-carboxamidotryptamine. *Neuropharmacology*, 1998. **37**(12): p. 1611-1619.[https://doi.org/10.1016/S0028-3908\(98\)00117-8](https://doi.org/10.1016/S0028-3908(98)00117-8).
510. Baker, L.P., Nielsen, M.D., Impey, S., Metcalf, M.A., *et al.*, Stimulation of Type 1 and Type 8 Ca<sup>2+</sup>/Calmodulin-sensitive Adenylyl Cyclases by the G<sub>s</sub>-coupled 5-Hydroxytryptamine Subtype 5-HT<sub>7A</sub> Receptor\*. *Journal of Biological Chemistry*, 1998. **273**(28): p. 17469-17476.<https://doi.org/10.1074/jbc.273.28.17469>.
511. Kvachnina, E., Liu, G., Dityatev, A., Renner, U., *et al.*, 5-HT<sub>7</sub> Receptor Is Coupled to G $\alpha$  Subunits of Heterotrimeric G12-Protein to Regulate Gene Transcription and Neuronal Morphology. *The*

- Journal of Neuroscience*, 2005. **25**(34): p. 7821-7830.<https://doi.org/10.1523/JNEUROSCI.1790-05.2005>
512. Errico, M., Crozier, R.A., Plummer, M.R., and Cowen, D.S., 5-HT<sub>7</sub> receptors activate the mitogen activated protein kinase extracellular signal related kinase in cultured rat hippocampal neurons. *Neuroscience*, 2001. **102**(2): p. 361-367.[https://doi.org/10.1016/S0306-4522\(00\)00460-7](https://doi.org/10.1016/S0306-4522(00)00460-7).
513. Norum, J.H., Hart, K., and Levy, F.O., Ras-dependent ERK Activation by the Human G<sub>s</sub>-coupled Serotonin Receptors 5-HT<sub>4(b)</sub> and 5-HT<sub>7(a)</sub>\*. *Journal of Biological Chemistry*, 2003. **278**(5): p. 3098-3104.<https://doi.org/10.1074/jbc.M206237200>.
514. Raymond, J.R., Mukhin, Y.V., Gelasco, A., Turner, J., *et al.*, Multiplicity of mechanisms of serotonin receptor signal transduction. *Pharmacology & Therapeutics*, 2001. **92**(2): p. 179-212.[https://doi.org/10.1016/S0163-7258\(01\)00169-3](https://doi.org/10.1016/S0163-7258(01)00169-3).
515. Masson, J., Emerit, M.B., Hamon, M., and Darmon, M., Serotonergic signaling: multiple effectors and pleiotropic effects. *Wiley Interdisciplinary Reviews: Membrane Transport and Signaling*, 2012. **1**(6): p. 685-713.<https://doi.org/10.1002/wmts.50>.
516. Sahu, A., Gopalakrishnan, L., Gaur, N., Chatterjee, O., *et al.*, The 5-Hydroxytryptamine signaling map: an overview of serotonin-serotonin receptor mediated signaling network. *Journal of Cell Communication and Signaling*, 2018. **12**(4): p. 731-735.<https://doi.org/10.1007/s12079-018-0482-2>.
517. Otte, C., Gold, S.M., Penninx, B.W., Pariante, C.M., *et al.*, Major depressive disorder. *Nature Reviews Disease Primers*, 2016. **2**(1): p. 16065.<https://doi.org/10.1038/nrdp.2016.65>.
518. Joseph J. Schildkraut, The Catecholamine Hypothesis Of Affective Disorders: A Review Of Supporting Evidence. *American Journal of Psychiatry*, 1965. **122**(5): p. 509-522.<https://doi.org/10.1176/ajp.122.5.509>.
519. Coppen, A., The Biochemistry of Affective Disorders. *British Journal of Psychiatry*, 1967. **113**(504): p. 1237-1264.<https://doi.org/10.1192/bjp.113.504.1237>.
520. Benkelfat, C., Ellenbogen, M.A., Dean, P., Palmour, R.M., *et al.*, Mood-Lowering Effect of Tryptophan Depletion: Enhanced Susceptibility in Young Men at Genetic Risk for Major Affective Disorders. *Archives of General Psychiatry*, 1994. **51**(9): p. 687-697.<https://doi.org/10.1001/archpsyc.1994.03950090019003>.
521. van der Veen, F.M., Evers, E.A.T., Deutz, N.E.P., and Schmitt, J.A.J., Effects of Acute Tryptophan Depletion on Mood and Facial Emotion Perception Related Brain Activation and Performance in Healthy Women with and without a Family History of Depression. *Neuropsychopharmacology*, 2007. **32**(1): p. 216-224.<https://doi.org/10.1038/sj.npp.1301212>.
522. Maurer-Spurej, E., Pittendreigh, C., and Misri, S., Platelet serotonin levels support depression scores for women with postpartum depression. *Journal of Psychiatry & Neuroscience*, 2007. **32**(1): p. 23-29.<https://www.ncbi.nlm.nih.gov/pmc/articles/PMC1764545/>.



523. Booi, L., Van der Does, W., Benkelfat, C., Bremner, J.D., *et al.*, Predictors of Mood Response to Acute Tryptophan Depletion: A Reanalysis. *Neuropsychopharmacology*, 2002. **27**(5): p. 852-861.[https://doi.org/10.1016/S0893-133X\(02\)00361-5](https://doi.org/10.1016/S0893-133X(02)00361-5).
524. Tipton, K.F., Boyce, S., O'Sullivan, J., Davey, G.P., *et al.*, Monoamine Oxidases: Certainties and Uncertainties. *Current Medicinal Chemistry*, 2004. **11**(15): p. 1965-1982.<https://doi.org/10.2174/0929867043364810>.
525. Udenfriend, S., Weissbach, H., and Bogdanski, D.F., Effect Of Iproniazid On Serotonin Metabolism *In Vivo*. *Journal of Pharmacology and Experimental Therapeutics*, 1957. **120**(2): p. 255-260.<https://jpet.aspetjournals.org/content/120/2/255>.
526. Blier, P. and de Montigny, C., Possible serotonergic mechanisms underlying the antidepressant and anti-obsessive-compulsive disorder responses. *Biological Psychiatry*, 1998. **44**(5): p. 313-323.[https://doi.org/10.1016/S0006-3223\(98\)00114-0](https://doi.org/10.1016/S0006-3223(98)00114-0).
527. Bonhomme, N. and Esposito, E., Involvement of Serotonin and Dopamine in the Mechanism of Action of Novel Antidepressant Drugs: A Review. *Journal of Clinical Psychopharmacology*, 1998. **18**(6): p. 447-454.<https://doi.org/10.1097/00004714-199812000-00005>.
528. Nelson, J.C., Tricyclic and tetracyclic drugs, in *The American Psychiatric Association Publishing Textbook of Psychopharmacology. 5th ed.* Arlington, VA: American Psychiatric Association Publishing. 2017. p. 305-334.<https://doi.org/10.1176/appi.books.9781615371624.as09>.
529. Raisman, R., Briley, M., and Langer, S.Z., Specific tricyclic antidepressant binding sites in rat brain. *Nature*, 1979. **281**(5727): p. 148-150.<https://doi.org/10.1038/281148a0>.
530. Sánchez, C. and Hyttel, J., Comparison of the Effects of Antidepressants and Their Metabolites on Reuptake of Biogenic Amines and on Receptor Binding. *Cellular and Molecular Neurobiology*, 1999. **19**(4): p. 467-489.<https://doi.org/10.1023/A:1006986824213>.
531. Chockalingam, R., Gott, B.M., and Conway, C.R., Tricyclic Antidepressants and Monoamine Oxidase Inhibitors: Are They Too Old for a New Look?, in *Antidepressants: From Biogenic Amines to New Mechanisms of Action*, M. Macaluso and S.H. Preskorn, Editors. 2019, Springer International Publishing: Cham. p. 37-48.[https://doi.org/10.1007/164\\_2018\\_133](https://doi.org/10.1007/164_2018_133).
532. Preskorn, S.H., Ross, R., and Stanga, C., Selective serotonin reuptake inhibitors, in *Antidepressants: Past, present and future*, S.H. Preskorn, *et al.*, Editors. 2004, Springer: Berlin, Heidelberg. p. 241-262.[https://doi.org/10.1007/978-3-642-18500-7\\_9](https://doi.org/10.1007/978-3-642-18500-7_9).
533. Vaswani, M., Linda, F.K., and Ramesh, S., Role of selective serotonin reuptake inhibitors in psychiatric disorders: a comprehensive review. *Progress in Neuro-Psychopharmacology and Biological Psychiatry*, 2003. **27**(1): p. 85-102.[https://doi.org/10.1016/S0278-5846\(02\)00338-X](https://doi.org/10.1016/S0278-5846(02)00338-X).
534. Hyttel, J., Pharmacological characterization of selective serotonin reuptake inhibitors (SSRIs). *International Clinical Psychopharmacology*, 1994. **9**: p. 19-26.<https://doi.org/10.1097/00004850-199403001-00004>.

535. Tan, J.Y. and Levin, G.M., Citalopram in the Treatment of Depression and Other Potential Uses in Psychiatry. *Pharmacotherapy*, 1999. **19**(6): p. 675-689.<https://doi.org/10.1592/phco.19.9.675.31538>.
536. Varia, I. and Rauscher, F., Treatment of generalized anxiety disorder with citalopram. *International Clinical Psychopharmacology*, 2002. **17**(3).<https://doi.org/10.1097/00004850-200205000-00002>.
537. Humble, M. and Wistedt, B., Serotonin, Panic Disorder and Agoraphobia: Short-term and Long-term Efficacy of Citalopram in Panic Disorders. *International Clinical Psychopharmacology*, 1992. **6**: p. 21-40.<https://doi.org/10.1097/00004850-199206005-00003>.
538. Montgomery, S.A., Kasper, S., Stein, D.J., Hedegaard, K.B., *et al.*, Citalopram 20 mg, 40 mg and 60 mg are all effective and well tolerated compared with placebo in obsessive-compulsive disorder. *International Clinical Psychopharmacology*, 2001. **16**(2).<https://doi.org/10.1097/00004850-200103000-00002>.
539. Hyttel, J., Bøgesø, K.P., Perregaard, J., and Sánchez, C., The pharmacological effect of citalopram residues in the (S)-(+)-enantiomer. *Journal of neural transmission. General section*, 1992. **88**(2): p. 157-60.<https://doi.org/10.1007/bf01244820>.
540. Noble, S. and Benfield, P., Citalopram. *CNS Drugs*, 1997. **8**(5): p. 410-431.<https://doi.org/10.2165/00023210-199708050-00009>.
541. Chaput, Y., de Montigny, C., and Blier, P., Effects of a selective 5-HT reuptake blocker, citalopram, on the sensitivity of 5-HT autoreceptors: Electrophysiological studies in the rat brain. *Naunyn-Schmiedeberg's Archives of Pharmacology*, 1986. **333**(4): p. 342-348.<https://doi.org/10.1007/BF00500007>.
542. Commons, K.G. and Linnros, S.E., Delayed Antidepressant Efficacy and the Desensitization Hypothesis. *ACS Chemical Neuroscience*, 2019. **10**(7): p. 3048-3052.<https://doi.org/10.1021/acschemneuro.8b00698>.
543. Shelton, R.C., Intracellular Mechanisms of Antidepressant Drug Action. *Harvard Review of Psychiatry*, 2000. **8**(4): p. 161-174.<https://doi.org/10.1080/hrp.8.4.161>.
544. Boyer, P.-A., Skolnick, P., and Fossom, L.H., Chronic administration of imipramine and citalopram alters the expression of NMDA receptor subunit mRNAs in mouse brain. *Journal of Molecular Neuroscience*, 1998. **10**(3): p. 219-233.<https://doi.org/10.1007/BF02761776>.
545. Mombereau, C., Gur, T.L., Onksen, J., and Blendy, J.A., Differential effects of acute and repeated citalopram in mouse models of anxiety and depression. *International Journal of Neuropsychopharmacology*, 2010. **13**(3): p. 321-334.<https://doi.org/10.1017/S1461145709990630>.
546. Russo-Neustadt, A.A., Alexandre, H., Garcia, C., Ivy, A.S., *et al.*, Hippocampal Brain-Derived Neurotrophic Factor Expression Following Treatment with Reboxetine, Citalopram, and Physical Exercise. *Neuropsychopharmacology*, 2004. **29**(12): p. 2189-2199.<https://doi.org/10.1038/sj.npp.1300514>.

547. Baquero, M. and Martín, N., Depressive symptoms in neurodegenerative diseases. *World Journal of Clinical Cases*, 2015. **3**(8): p. 682-693.<https://doi.org/10.12998/wjcc.v3.i8.682>.
548. Cirrito, J.R., Disabato, B.M., Restivo, J.L., Verges, D.K., *et al.*, Serotonin signaling is associated with lower amyloid- $\beta$  levels and plaques in transgenic mice and humans. *Proceedings of the National Academy of Sciences*, 2011. **108**(36): p. 14968-14973.<https://doi.org/10.1073/pnas.1107411108>.
549. Sheline, Y.I., West, T., Yarasheski, K., Swarm, R., *et al.*, An Antidepressant Decreases CSF A $\beta$  Production in Healthy Individuals and in Transgenic AD Mice. *Science Translational Medicine*, 2014. **6**(236): p. 236re4-236re4.<https://doi.org/10.1126/scitranslmed.3008169>.
550. Jamwal, S. and Kumar, P., Antidepressants for neuroprotection in Huntington's disease: A review. *European Journal of Pharmacology*, 2015. **769**: p. 33-42.<https://doi.org/10.1016/j.ejphar.2015.10.033>.
551. Lai, M.K.P., Tsang, S.W.Y., Francis, P.T., Keene, J., *et al.*, Postmortem serotonergic correlates of cognitive decline in Alzheimer's disease. *NeuroReport*, 2002. **13**(9): p. 1175-1178.<https://doi.org/10.1097/00001756-200207020-00021>.
552. Nazarali, A.J. and Reynolds, G.P., Monoamine neurotransmitters and their metabolites in brain regions in Alzheimer's disease: a postmortem study. *Cellular and Molecular Neurobiology* 1992. **12**(6): p. 581-7.<https://doi.org/10.1007/bf00711237>.
553. Lorke, D.E., Lu, G., Cho, E., and Yew, D.T., Serotonin 5-HT<sub>2A</sub> and 5-HT<sub>6</sub> receptors in the prefrontal cortex of Alzheimer and normal aging patients. *BMC Neuroscience*, 2006. **7**(1): p. 36.<https://doi.org/10.1186/1471-2202-7-36>.
554. Mowla, A., Mosavinasab, M., Haghshenas, H., and Haghghi, A.B., Does Serotonin Augmentation Have Any Effect on Cognition and Activities of Daily Living in Alzheimer's Dementia? A Double-Blind, Placebo-Controlled Clinical Trial. *Journal of Clinical Psychopharmacology*, 2007. **27**(5): p. 484-7.<https://doi.org/10.1097/jcp.0b013e31814b98c1>.
555. Mossello, E., Boncinelli, M., Caleri, V., Cavallini, M.C., *et al.*, Is Antidepressant Treatment Associated with Reduced Cognitive Decline in Alzheimer's Disease? *Dementia and Geriatric Cognitive Disorders*, 2008. **25**(4): p. 372-379.<https://doi.org/10.1159/000121334>.
556. Halliday, G.M., Blumbergs, P.C., Cotton, R.G.H., Blessing, W.W., *et al.*, Loss of brainstem serotonin- and substance P-containing neurons in Parkinson's disease. *Brain Research*, 1990. **510**(1): p. 104-107.[https://doi.org/10.1016/0006-8993\(90\)90733-R](https://doi.org/10.1016/0006-8993(90)90733-R).
557. Halliday, G.M., Li, Y.W., Blumbergs, P.C., Joh, T.H., *et al.*, Neuropathology of immunohistochemically identified brainstem neurons in Parkinson's disease. *Annals of Neurology*, 1990. **27**(4): p. 373-385.<https://doi.org/10.1002/ana.410270405>.
558. Mann, D.M.A. and Yates, P.O., Pathological Basis For Neurotransmitter Changes In Parkinson's Disease. *Neuropathology and Applied Neurobiology*, 1983. **9**(1): p. 3-19.<https://doi.org/10.1111/j.1365-2990.1983.tb00320.x>.

559. Braak, H., Tredici, K.D., Rüb, U., de Vos, R.A.I., *et al.*, Staging of brain pathology related to sporadic Parkinson's disease. *Neurobiology of Aging*, 2003. **24**(2): p. 197-211.[https://doi.org/10.1016/S0197-4580\(02\)00065-9](https://doi.org/10.1016/S0197-4580(02)00065-9).
560. Braak, H., Ghebremedhin, E., Rüb, U., Bratzke, H., *et al.*, Stages in the development of Parkinson's disease-related pathology. *Cell and Tissue Research*, 2004. **318**(1): p. 121-134.<https://doi.org/10.1007/s00441-004-0956-9>.
561. Ohno, Y., Shimizu, S., Tokudome, K., Kunisawa, N., *et al.*, New insight into the therapeutic role of the serotonergic system in Parkinson's disease. *Progress in Neurobiology*, 2015. **134**: p. 104-121.<https://doi.org/10.1016/j.pneurobio.2015.09.005>.
562. Beglinger, L.J., Adams, W.H., Langbehn, D., Fiedorowicz, J.G., *et al.*, Results of the citalopram to enhance cognition in Huntington disease trial. *Movement Disorders*, 2014. **29**(3): p. 401-405.<https://doi.org/10.1002/mds.25750>.
563. Jacobs, B.L. and Fornal, C.A., 5-HT and motor control: a hypothesis. *Trends in Neurosciences*, 1993. **16**(9): p. 346-352.[https://doi.org/10.1016/0166-2236\(93\)90090-9](https://doi.org/10.1016/0166-2236(93)90090-9).

---

**Preclinical evidence supporting early initiation of  
citalopram treatment in Machado-Joseph disease**

---

## Preclinical evidence supporting early initiation of citalopram treatment in Machado-Joseph disease

Sofia Esteves<sup>1,2,\*</sup>, Stéphanie Oliveira<sup>1,2,\*</sup>, Sara Duarte-Silva<sup>1,2</sup>, Daniela Cunha-Garcia<sup>1,2</sup>, Andreia Teixeira-Castro<sup>1,2,3,#</sup> and Patrícia Maciel<sup>1,2,#</sup>

\* These authors contributed equally to this work.

# These authors share co-senior authorship.

<sup>1</sup> Life and Health Sciences Research Institute (ICVS), School of Medicine, University of Minho, Braga, Portugal.

<sup>2</sup> ICVS/3B's - PT Government Associate Laboratory, Braga/Guimarães, Portugal.

<sup>3</sup> Department of Molecular Biosciences, Northwestern University, Evanston, Illinois 60208, USA.

Contribution of the author Stéphanie Oliveira:

This article has two first co-authors and Stéphanie Oliveira performed the analyses, figures, and interpretation of the animal behavior (Figure 1, 2 and 3). The data presented in the remaining figures (Figure 4, 5 and supplementary) were prepared, collected, analyzed, and interpreted by Stéphanie Oliveira. The article presented is original having not been and will not be included in any other thesis.

Manuscript published in *Molecular Neurobiology* (*Mol Neurobiol* **56**, 3626–3637 (2019)).

<https://doi.org/10.1007/s12035-018-1332-1>

---



## Preclinical Evidence Supporting Early Initiation of Citalopram Treatment in Machado-Joseph Disease

Sofia Esteves<sup>1,2</sup> · Stéphanie Oliveira<sup>1,2</sup> · Sara Duarte-Silva<sup>1,2</sup> · Daniela Cunha-Garcia<sup>1,2</sup> · Andreia Teixeira-Castro<sup>1,2,3</sup> · Patrícia Maciel<sup>1,2</sup>

Received: 8 June 2018 / Accepted: 23 August 2018 / Published online: 1 September 2018  
© Springer Science+Business Media, LLC, part of Springer Nature 2018

### Abstract

Spinocerebellar ataxias are dominantly inherited neurodegenerative disorders with no disease-modifying treatment. We previously identified the selective serotonin reuptake inhibitor citalopram as a safe and effective drug to be repurposed for Machado-Joseph disease. Pre-symptomatic treatment of transgenic (CMVMJD135) mice strikingly ameliorated mutant ataxin-3 (ATXN3) pathogenesis. Here, we asked whether citalopram treatment initiated at a post-symptomatic age would still show efficacy. We used a cohort of CMVMJD135 mice that shows increased phenotypic severity and faster disease progression (CMVMJD135hi) compared to the mice used in the first trial. Groups of hemizygous CMVMJD135hi mice were orally treated with citalopram. Behavior, protein analysis, and pathology assessment were performed blindly to treatment. Our results show that even when initiated after symptom onset, treatment of CMVMJD135hi mice with citalopram ameliorated motor coordination and balance, attenuating disease progression, albeit to a lesser extent than that seen with pre-symptomatic treatment initiation. There was no impact on ATXN3 aggregation, which contrasts with the robust reduction in ATXN3-positive inclusions observed in CMVMJD135 mice, when treated pre-symptomatically. Post-symptomatic treatment of CMVMJD135hi mice revealed, however, a limited neuroprotective effect by showing a tendency to repair cerebellar calbindin staining, and to increase the number of motor neurons and of NeuN-positive cells in certain brain regions. While supporting that early initiation of treatment with citalopram leads to a marked increase in efficacy, these results strengthen our previous observation that modulation of serotonergic signaling by citalopram is a promising therapeutic approach for Machado-Joseph disease even after symptom onset.

**Keywords** Spinocerebellar ataxia type 3 · Selective serotonin reuptake inhibitor · Citalopram · Post-symptomatic treatment · Transgenic model

---

Sofia Esteves and Stéphanie Oliveira contributed equally to the work.

Andreia Teixeira-Castro and Patrícia Maciel share co-senior authorship.

**Electronic supplementary material** The online version of this article (<https://doi.org/10.1007/s12035-018-1332-1>) contains supplementary material, which is available to authorized users.

✉ Andreia Teixeira-Castro  
accastro@med.uminho.pt

✉ Patrícia Maciel  
pmaciel@med.uminho.pt

<sup>1</sup> Life and Health Sciences Research Institute (ICVS), School of Medicine, University of Minho, Campus of Gualtar, 4710-057 Braga, Portugal

<sup>2</sup> ICVS/3B's - PT Government Associate Laboratory, Braga/Guimarães, Portugal

<sup>3</sup> Department of Molecular Biosciences, Northwestern University, Evanston, IL 60208, USA

### Abbreviations

5-HT Serotonin  
MJD Machado-Joseph disease  
SSRI Selective serotonin reuptake inhibitor.

### Introduction

Machado-Joseph disease (MJD) or spinocerebellar ataxia type 3 is a clinically heterogeneous neurodegenerative disease [1, 2], caused by an expansion of a cytosine-adenine-guanine (CAG) repeat tract in the *ATXN3* gene, which encodes for an abnormally long polyglutamine (polyQ) segment in the ataxin-3 protein (ATXN3) [3]. The symptoms of MJD reflect the involvement of multiple neurological systems, which include ataxia, diplopia, dysphagia,



dysarthria, and ophthalmoplegia, as well as fasciculations, amyotrophy, dystonia, and/or spasticity [4, 5]. This disorder is characterized by a widespread neuronal degeneration affecting several regions of the central nervous system, such as the cerebellum, brainstem, basal ganglia, and spinal cord [6]. No effective disease-modifying treatment is currently available for MJD.

Citalopram is a safe, well-tolerated antidepressant that belongs to the group of the selective serotonin reuptake inhibitors (SSRIs) [7, 8]. These compounds share the same cellular target, the serotonin (5-HT) transporter (SERT), which is responsible for 5-HT uptake into serotonergic neurons [9]. While the exact mechanism of action of SSRIs has yet to be elucidated, these compounds may exert their antidepressant activity by inhibiting SERT and increasing extracellular levels of 5-HT [10].

Antidepressants are often prescribed to patients with neurodegenerative diseases to treat depression and anxiety symptoms [11]. Interestingly, several antidepressants have also shown neuroprotective effects in vitro, as well as in animal models of Alzheimer's disease, Parkinson's disease, Huntington's disease, or spinal and bulbar muscular atrophy [12–19].

We previously described an in vivo repurposing screen of 1200 FDA-approved small molecules and identified chemical suppressors of mutant ATXN3-induced neurotoxicity in *Caenorhabditis elegans* [20]. Through this unbiased approach, we found that citalopram and other SSRIs reduced mutant ATXN3 aggregation in *C. elegans* and restored its motor capacity. In this simple animal model, early initiation and prolonged treatment with citalopram resulted in increased therapeutic efficacy. Chronic citalopram treatment of CMVMJD135 mice [22], a vertebrate model of MJD, when initiated at a pre-symptomatic age, strikingly ameliorated their motor coordination impairments, reducing mutant ATXN3 aggregation and neuronal loss [20]. These results suggest that small-molecule modulation of serotonergic signaling in pre-symptomatic stages may represent a promising therapeutic approach for MJD.

To mimic the most frequent clinical situation of symptom-driven diagnosis and treatment of MJD patients, here, we asked whether citalopram treatment would still be effective to ameliorate mutant ATXN3-mediated pathogenesis if initiated after motor symptom installation in MJD mice.

Our results showed that, indeed, post-symptomatic citalopram treatment ameliorated loss of balance and motor coordination, attenuating disease progression in a cohort of MJD mice of increased disease severity (CMVMJD135hi). These results suggest that 5-HT recapture inhibition can be used as a disease-modifying therapy for MJD and perhaps other conformational disorders, even when initiated after symptom onset, but also support increased efficacy of early treatment initiation.

## Materials and Methods

### Ethics Statement

All animal procedures were conducted in accordance with European regulations (European Union Directive 2010/63/EU). Animal facilities and the persons directly involved in animal experimentation (SE, SD-S, SO, AT-C) were certified by the Portuguese regulatory entity—Direcção Geral de Alimentação e Veterinária. All the protocols were approved by the Animal Ethics Committee of the Life and Health Sciences Research Institute, University of Minho. All experiments were designed with commitment to the principles of refinement, reduction, and replacement and performed according to FELASA guidelines to minimize discomfort, stress, and pain to the animals, with defined humane endpoints (20% reduction of the body weight, inability to reach food and water, presence of wounds in the body, and dehydration) [23]. The status of specified pathogens of sentinel animals, maintained in the same animal room, was monitored throughout the study.

### Transgenic Mouse Model and Drug Administration

CMVMJD135hi mice (background C57BL/6) were generated as previously described [22], but by selecting progenitor animals with a mean CAG repeat size of  $138 \pm 5$  [ $\pm$  standard deviation (SD)]. Animals were housed in a conventional animal facility at weaning, in groups of five animals, in filter-topped polysulfone cages  $267 \times 207 \times 140$  mm ( $370$  cm<sup>2</sup> floor area) (Tecniplast, Buguggiate, Italy), using corncob bedding (Scobis Due, Mucedola SRL, Settimo Milanese, Italy). All animals were maintained under standard laboratory conditions: an artificial 12-h light/dark cycle (lights on from 8 am to 8 pm), with  $21 \pm 1$  °C of room temperature and a relative humidity of 50–60%. Mice were fed with a standard diet (4RF25 during the gestation and postnatal periods, and 4RF21 after weaning; Mucedola SRL, Settimo Milanese, Italy) and water ad libitum. DNA extraction, animal genotyping, and CAG repeat size analyses were performed as previously described [24]. The mean CAG repeat size [ $\pm$  SD] for all transgenic mice used in this study, the CMVMJD135hi animals, was of  $138 \pm 5$ , distributed evenly among treatments (CMVMJD135hi  $138 \pm 6$  and CMVMJD135hi cit  $137 \pm 5$ ). Age-matched WT littermate animals were used as controls. Male mice were used in this study. The first symptom that appears in CMVMJD135 mice is loss of motor strength in the hanging wire test using an inverted grid, which is already installed at 6 weeks of age, followed by the appearance of motor uncoordination deficits [22]. To verify installation of motor symptoms in CMVMJD135hi mice, we evaluated balance and motor coordination of the mice on the balance beam walk and motor swimming paradigms [25]. Transgenic



animals showed increased latency time to reach the safe platforms in both behavioral tests when compared to WT animals at 10 weeks of age. Therefore, treatment was initiated at 11 weeks of age. We administrated citalopram hydrobromide (CAS 59729-32-7, kindly provided by H. Lundbeck A/S, Denmark) in the drinking water at a dosage of 8 mg/kg. Citalopram-supplemented water was changed three times per week throughout the entire duration of the trial to ensure drug activity. The trial was terminated at 28 weeks of age, when most of the vehicle-treated transgenic animals could not complete any of the motor tests (e.g., balance beam walk test, motor swimming test, and footprints).

### Experimental Design

ARRIVE guidelines were followed throughout the study [26]. Experimental design was based on power analyses for optimization of sample size, as described previously [20]. Mouse sample size calculations were previously performed for each behavioral test and pathological analyses, assuming a power of 0.95 and 0.8, respectively, and a significance level of  $p < 0.05$  [20]. Transgenic and non-transgenic drug- and placebo-treated animals were alternately housed and assigned to treatment. All behavioral experiments and neuropathological analyses were conducted by researchers who were blind to genotype and treatment. We used groups of 13–16 animals per genotype/treatment for behavioral tests and groups of four to six animals for quantification of ATXN3 intranuclear inclusions, assessment of astrogliosis, cell counts, and Western blot analyses. Regarding genotype-phenotype correlations, data obtained in the previous preclinical trial using vehicle-treated CMVMJD135 mice [20] was used for correlation analyses in conjugation with data from the CMVMJD135hi mice (present study). Motor performance in the balance beam walk and motor swimming tests were analyzed at 26 weeks of age for all animals ( $n = 27$ ) and correlated to their CAG repeat number.

### Behavioral Assessment

Behavioral assessment was performed during the diurnal period, with five males per cage, including CMVMJD135hi hemizygous transgenic mice and WT littermates ( $n = 15–16$  per genotype) treated with citalopram or with vehicle (water). Body weight was registered throughout the study. All behavioral tests started in a symptomatic stage (10 weeks) and were conducted until 26 or 28 weeks of age. Neurological testing included (1) a selection of tests from the SHIRPA protocol, namely assessment of tremors, gait quality, and limb clasping [27, 28]; (2) footprinting analysis and stride length quantification; (3) balance beam walk (12-mm and 27-mm square beams); and (4) motor swimming tests. All behavioral tests were performed as previously described [20, 22, 24]. Briefly,

tremors assessment was performed while the animals were in a viewing jar and scored (as *absent*, *mild* (discontinuous tremor), or *severe* (continuous tremor)) while animals were immobile. *Gait quality* was assessed by the experimenter in an open arena (55 × 33 × 18 cm). Freely moving animals were scored as *normal*, *abnormal* (incorrect posture of the body and tail, with decreased distance over the ground), and *limited* (very limited movement). To determine *limb clasping*, animals were picked up by the tail and slowly descending towards a horizontal surface. Mice were observed and scored as *absent* (extension of the hindlimbs), *mild* (contraction observed in one of the limbs), or *severe* (contraction observed in both limbs). To register *footprint* patterns, the fore and hind paws of the animals were coated with non-toxic red and black inks, respectively. Animals were allowed to walk along a 100 cm long × 4.2 cm width × 10 cm height inclined runway (a clean paper sheet was used for each mouse) in the direction of an enclosed safe black box. *Stride length* was obtained by measuring the distance between two paw prints. Three values were obtained in six consecutive steps and the mean of the three values was used. The same consecutive steps were used to evaluate the severity of *foot dragging*. Mice were scored as *absent/mild* = 0 (up to three steps), *mild* = 1 (more than three steps out of six), and *severe* = 2 (all steps out of six). *Balance beam walk test* comprised 3 days of training (three trials per animal) in the 12-mm square beam, and, in the fourth day, animals were tested in the 12-mm and/or in the 27-mm square beam (two trials per animal were recorded). If the animal turned around or fell from the beam, the trial was considered invalid. Each animal is allowed to fail twice. The time the animals took to cross the beams was recorded, and if animals stopped, this time was discounted. The percentage of therapeutic efficacy was calculated taking the mean latency time to reach the safe platform in the beam walk test of transgenic mice and subtracting the mean latency time of WT mice in each preclinical trial, to obtain a reference value. This value corresponded to 100% of therapeutic efficacy in that trial (i.e., assuming that the best possible drug will make the transgenic animals behave like WT). The difference between latency time of vehicle-treated transgenic mice and latency time of cit-treated mouse of the same trial, relative to the value of 100% efficacy, corresponded to the percentage of therapeutic effect. This was calculated at 26 weeks of age both in the pre-[20] and post-symptomatic trials (this study). In the motor swimming test, mice were trained for two consecutive days (animals were allowed three trials) to cross a transparent acrylic water tank (100 cm long) to a safe (black acrylic-made) platform at the end. The latency to cross this tank was registered from a 60-cm distance (the initiation position was marked with a blue line). The water temperature was maintained at 23 °C using a thermostat. Animals were tested for three consecutive days (two trials per animal) and the latency to cross the tank assessed by the experimenter.

## Immunohistochemistry and Quantification of Neuronal Inclusions

Twenty-eight-week-old WT and CMVMJD135hi littermate mice, vehicle- and citalopram-treated ( $n = 4–6$  per group), were deeply anesthetized [a mixture of ketamine hydrochloride (150 mg/kg) plus medetomidine (0.3 mg/kg)] and transcardially perfused with phosphate-buffered saline (PBS) followed by 4% paraformaldehyde (PFA) (Panreac, USA). Brains were removed and postfixed overnight in PFA and either embedded in paraffin or transferred to a 30% sucrose solution for vibratome processing. Spinal cord tissues were postfixed overnight in PFA and transferred to a 30% sucrose solution for vibratome processing. Brain slices (4- $\mu$ m-thick paraffin sections or 40- $\mu$ m-thick vibratome sections) and spinal cord vibratome sections (50- $\mu$ m-thick) were subjected to antigen retrieval and then incubated with mouse anti-ATXN3 (1H9) (1:750 for paraffin and 1:500 for vibratome sections, MAB5360, Millipore), rabbit anti-GFAP (1:500, Dako Corporation), goat anti-choline acetyltransferase (ChAT, 1:500, AB144P, Millipore), mouse anti-neuronal nuclei (NeuN, 1:100, MAB377, Millipore), and rabbit anti-calbindin D-28K (1:1000, AB1778, Millipore) antibodies, which were detected by incubation with a biotinylated anti-polyvalent antibody, followed by detection through biotin-streptavidin coupled to horseradish peroxidase and reaction with the DAB (3,3'-diaminobenzidine) substrate (Lab Vision™ Ultra-Vision™ Detection kit, Thermo Scientific or VECTASTAIN® Elite® ABC-HRP Kit, Vector Laboratories). Brain and spinal cord sections were counterstained with hematoxylin 25% following standard procedures. Quantification of ATXN3-positive inclusions was performed in the pontine nuclei (PN), reticulotegmental nucleus of the pons (RtTg), facial motor nuclei (7N), lateral reticular nuclei (LRt), vestibular nuclei (VN), deep cerebellar nuclei (DCN), and lumbar spinal cord (LSC). Number of GFAP-positive cells was determined in the substantia nigra (SN) and of calbindin-positive cells in the Purkinje cells of the cerebellar cortex (PjC CBX). Counts of ChAT-positive cells were conducted in the LSC, 7N, and dorsal striatum (DS). Quantification of NeuN-positive neurons was performed in the PN, DCN, and VN. All quantifications were carried out in either vehicle- or citalopram-treated animals ( $n = 4$  for each condition, 4 slices per animal) and normalized to total area and to WT- or transgenic-vehicle controls using an Olympus BX51 stereological microscope (Olympus, Japan) and the Visiopharm integrator system software (Visiopharm, Denmark) as previously described [24].

## Immunoblotting Analysis

Protein isolation from mouse brainstem, cerebellum, and spinal cord tissue and Western blotting were performed as

previously described [24]. Briefly, the blots were incubated overnight at 4 °C with the primary antibodies mouse anti-ATXN3 (1H9) (1:2000, MAB5360, Millipore) and mouse anti-tubulin (1:5000, T5168, Sigma). Mouse ATXN3 and tubulin were used as loading controls. Antibody affinity was detected by chemiluminescence, and Western blot quantifications were performed using Chemidoc XRS Software with ImageLab Software (Bio-Rad), following the manufacturer's instructions.

## Statistical Analysis

Normality of variance assumptions was evaluated with Kolmogorov-Smirnov (K-S) or Shapiro-Wilk (S-W) test (chosen according to  $n$  value of each experiment), absolute value of skewness, kurtosis, and Z-score. Substantial departure from normality was considered when K-S or S-W test showed  $P < 0.05$ , absolute value of skewness  $> 2$ , absolute value of kurtosis  $> 7$  and Z-score  $> 1.9$  [29]. Continuous variables with normal distributions and with homogeneity of variance (evaluated by Levene's test) were analyzed with repeated-measures two-way ANOVA for longitudinal multiple comparisons, using genotype and treatment as factors. One-way ANOVA was used for paired comparisons, using Tukey test for post hoc comparisons. Variables lacking homogeneity of variances were analyzed with parametric tests using Welch's correction (and Games-Howell was used for post hoc comparisons). Other variables were analyzed through non-parametric Mann-Whitney  $U$  test or Kruskal-Wallis  $H$  test for two or more groups, respectively. Genotype-phenotype correlations were analyzed using Pearson correlation coefficient (GraphPad). All statistical analyses were performed using SPSS 22.0 (SPSS Inc., Chicago, IL) and G-Power 3.1.9.2 (University Kiel, Germany). A critical value for significance of  $P < 0.05$  was used throughout the study. Crosses ( $\times$ ) represent CMVMJD135 and CMVMJD135hi comparisons, asterisks (\*) represent WT and CMVMJD135hi comparisons, ampersands (&) represent WT versus WT cit comparisons, and number signs (#) represent CMVMJD135hi and CMVMJD135hi cit comparisons.

## Results

### Establishment of a Cohort of CMVMJD135 Mice with a More Severe Phenotype

To determine the efficacy of post-symptomatic citalopram treatment in an animal model of disease with increased pathogenicity, we used a transgenic mouse model of MJD, the CMVMJD135, replicating patients' symptomatology by displaying progressive motor dysfunction and selective neuropathology [22]. As seen in MJD patients [30], the mean CAG



repeat number in the CMVMJD135 mice correlates inversely with the age at onset of symptoms and directly with symptom severity and disease progression. This feature can be used to generate subsets of animals with distinct degrees of disease severity and progression rates. In this study, we chose to increase the mean CAG repeat length of the original CMVMJD135 mice, used in our previous study with citalopram [20], by 10 repeats (CMVMJD135hi). The increase in mean CAG repeat size from 128 in CMVMJD135 mice (CMVMJD135 vehicle group of our previous study) to 138 in CMVMJD135hi mice caused a significant aggravation of the motor uncoordination and loss of balance, as measured by the motor swimming and balance beam walk behavior paradigms (Fig. 1b, c). CMVMJD135hi mice also showed an accelerated rate of disease progression (ANOVA repeated measures,  $P=0.042$  for motor swimming and  $P<0.0001$  for balance beam tests). Latency time in both behavioral tasks significantly correlated with the CAG repeat length of the two groups (Pearson

correlation coefficient  $r^2=0.4037$  ( $n=27$ ) and  $r^2=0.6315$  ( $n=22$ ), respectively;  $P<0.001$ ) at 26 weeks of age (Fig. 1d, e). Age at onset of symptoms was significantly anticipated in CMVMJD135hi mice, by four or more weeks to a maximum of 16 weeks for stride length evaluation (Supplementary Table 1).

### Symptomatic Citalopram Treatment of CMVMJD135hi Mice Ameliorated Gait Quality

At 10 weeks of age, CMVMJD135hi mice showed significant impairments in motor coordination and balance compared to WT animals (Supplementary Fig. 1). Oral chronic administration of citalopram (8 mg/kg) or drinking water to CMVMJD135hi mice and to WT non-transgenic littermate controls was initiated at 11 weeks of age (study design shown in Fig. 2a). Assessment of mouse body weight throughout the duration of the trial (until 28 weeks of age; Fig. 2b) revealed no changes caused by citalopram treatment. Whereas some

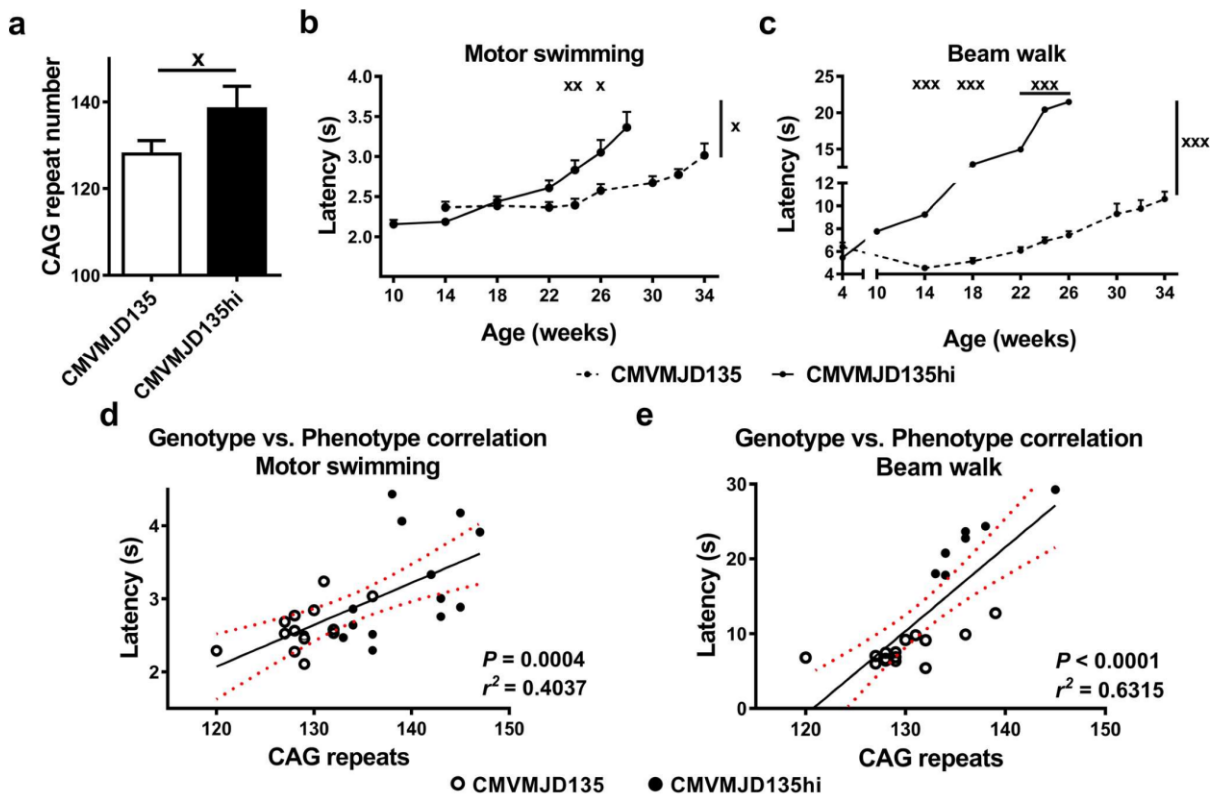


**Fig. 1** CMVMJD135hi mice present increased phenotype severity related to higher (CAG) $n$  repeat length. **a** CAG repeat number comparison between two independent mouse groups, the one used previously in the pre-symptomatic citalopram preclinical trial (CMVMJD135) and CMVMJD135hi mice (present study) ( $n=27$ ). Significant differences were observed between CMVMJD135 and CMVMJD135hi mouse groups (treated with vehicle) in preclinical trials regarding their performance in the **b** motor swimming test and in the **c** balance beam walk test (12-mm square). Genotype versus phenotype

correlation for the **d** motor swimming test (CMVMJD135 + CMVMJD135hi,  $n=27$ ) and **e** 12-mm square balance beam walk (CMVMJD135 + CMVMJD135hi,  $n=22$ ) at 26 weeks of age. Open circles refer to CMVMJD135 group and closed circles refer to CMVMJD135hi group. Data are presented as mean  $\pm$  SD (a) or mean  $\pm$  SEM (b, c), \* $P<0.05$ , \*\* $P<0.01$ , and \*\*\* $P<0.001$  (Student's  $t$  test, repeated-measures two-way ANOVA, Tukey correction, and Pearson correlation coefficient).  $r^2$  square of the Pearson correlation coefficient

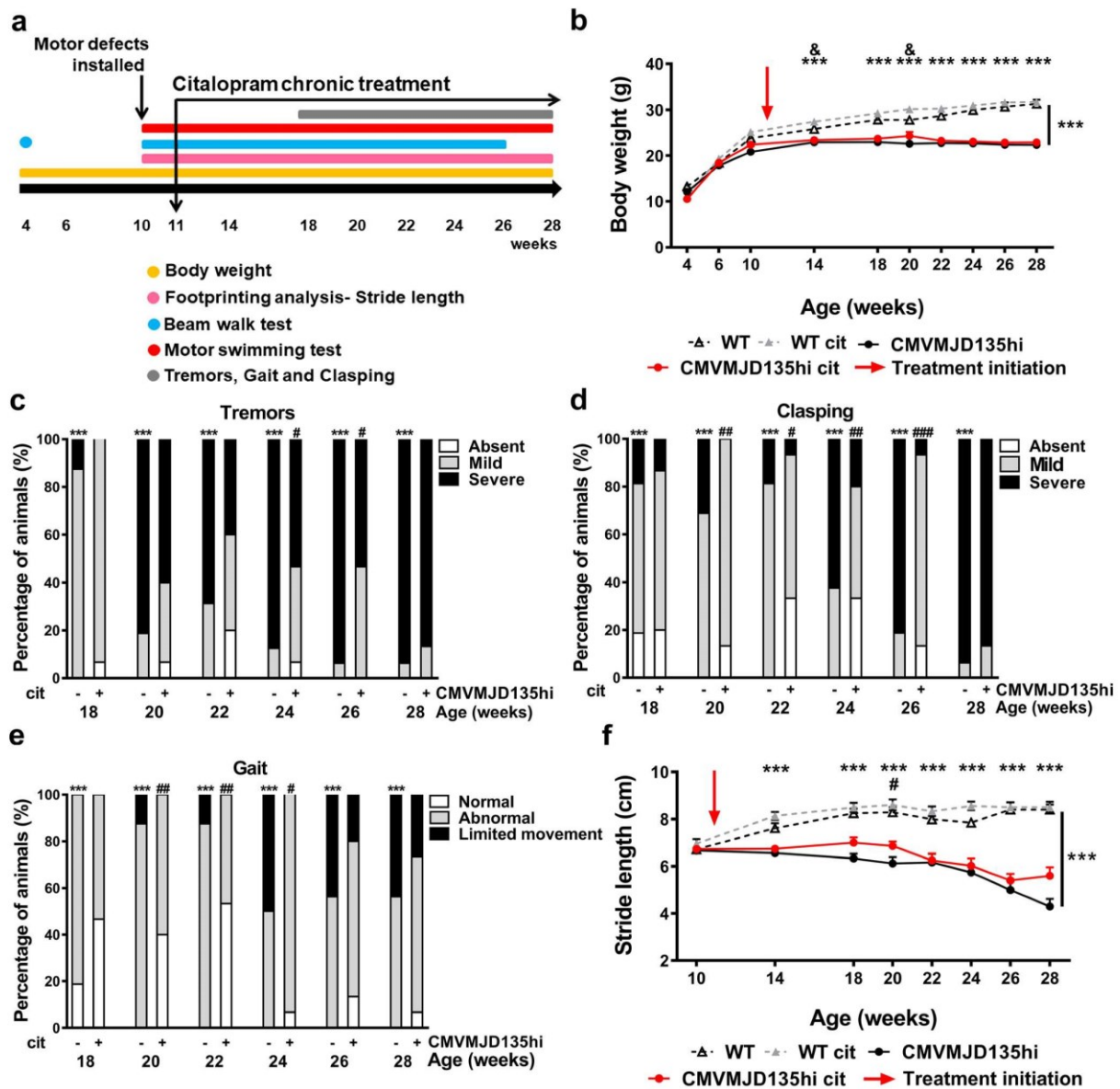


**Fig. 2** Chronic post-symptomatic citalopram treatment ameliorated gait quality of CMVMJD135hi mice. **a** Schematic representation of the preclinical therapeutic trial design. **b** Body weight, **c** tremors, **d** limb claspings, **e** gait quality, and **f** footprint stride length were evaluated until 28 weeks of age in WT and CMVMJD135hi vehicle- and citalopram-treated mice (WT,  $n = 13$ ; WT cit,  $n = 17$ ; CMVMJD135hi,  $n = 16$ ; CMVMJD135hi cit,  $n = 15$ ). Mild improvements were observed for tremors, claspings, gait quality, and stride length, while no effect was observed in body weight upon treatment. Data are presented as mean  $\pm$  SEM; \* $P < 0.05$ , \*\* $P < 0.01$ , and \*\*\* $P < 0.001$ . Asterisks (\*) indicate

statistical significance between WT and CMVMJD135hi mice; the ampersands and number signs indicate statistical significance between WT and WT cit and between CMVMJD135hi and CMVMJD135hi cit mice, respectively. WT mice show no signs of tremors, altered limb claspings, or gait quality and are not represented in **c**, **d**, and **e** for simplicity (repeated-measures two-way ANOVA, one-way ANOVA, Tukey correction, and Mann Whitney  $U$  test for non-continuous variables). The red arrow indicates age of treatment initiation at 11 weeks. cit citalopram

neurological symptoms of CMVMJD135hi mice, like body tremors, showed only marginal improvements upon citalopram treatment (Fig. 2c), limb claspings and gait quality scores were restored until 26 weeks of age (Fig. 2d, e). In agreement with what was observed when citalopram was administered before

the onset of motor symptoms, treated CMVMJD135hi mice still displayed dragging of the paws (Supplementary Fig. 2); however, the stride length was significantly ameliorated at 20 weeks of age (Fig. 2f) in this trial, even though no changes were observed beyond this time point.

### Post-symptomatic Treatment with Citalopram Improves Motor Coordination and Balance in CMVMJD135hi Mice

Vehicle-treated CMVMJD135hi mice showed severe motor coordination and balance defects, which precluded testing of citalopram's beneficial effects at advanced stages of disease progression, as by 26 weeks, 40% of the animals were unable to cross the balance beam. Nevertheless, upon citalopram treatment, we observed a significant amelioration in motor performance in the different beam sizes analyzed, until 26 weeks of age (Fig. 3a, b). The animals that did not perform the test (40%) at 26 weeks had a mean CAG repeat size of  $140 \pm 6$  [ $\pm$  standard deviation (SD)] whereas the animals that were able to cross the beam (60%) had a mean CAG repeat size of  $136 \pm 4$ , being this difference statistically significant (Student's *t* test,  $P=0.04$ ). However, among the mice that completed the task, citalopram-treated mice with a higher CAG repeat length did not take more time to traverse the beam, which suggests a disease-modifying effect for citalopram, being the slope of the correlation curve between CAG repeat length and latency to fall lower (Supplementary Fig. 3). In the motor swimming test, citalopram-treated CMVMJD135hi mice took less time to reach the safe platform (Fig. 3c), although not reaching statistical significance.

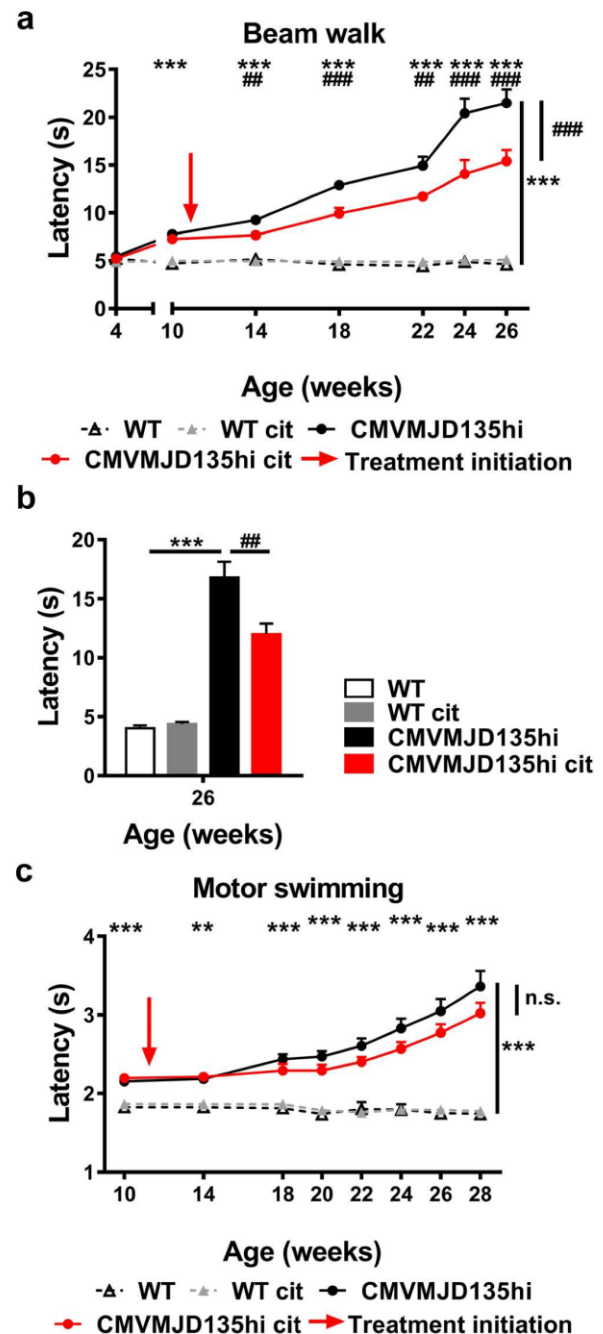
Overall, these results demonstrate that post-symptomatic citalopram treatment can still reduce the impairment in motor coordination and delay disease progression of MJD transgenic mice, although to a lesser extent than when the treatment is initiated before the onset of motor symptoms.

### Post-symptomatic Treatment with Citalopram Confers a Limited Neuroprotective Effect to CMVMJD135hi Mice

The analysis of brain tissue of post-symptomatic citalopram-treated CMVMJD135hi mice suggested that the positive impact on animals' behavior may be accounted by the limited

neuroprotective effects exerted by the SSRI, even when administered after symptom installation. Concerning mutant protein aggregation, and in contrast with pre-symptomatic treatment, the number of ATXN3 intranuclear inclusions in several areas of the brainstem and in the ventral horn of the lumbar spinal cord did not change when treatment was initiated at symptomatic ages (Fig. 4a and Supplementary Fig. 4a).

**Fig. 3** Citalopram post-symptomatic treatment improves balance and coordination of CMVMJD135hi mice. **a** Significant differences were observed in the 12-mm square balance beam walk (curve comparison over time  $P<0.001$ , 14–26 weeks) and in the **b** 27-mm square beam ( $P<0.01$ , 26 weeks). At 26 weeks, data is shown for only 60% of the CMVMJD135hi vehicle-treated animals, since the other 40% were unable to complete this test. **c** In the motor swimming test, transgenic treated mice (CMVMJD135hi cit,  $n=15$ ) took slightly less time to cross the swimming pool than vehicle-treated mice (CMVMJD135hi,  $n=16$ ) (curve comparison over time  $P>0.05$ , 10–28 weeks). Data are presented as mean  $\pm$  SEM,  $*P<0.05$ ,  $**P<0.01$ , and  $***P<0.001$ . The asterisks (\*) indicate statistical significance between WT and CMVMJD135hi mice; the number signs indicate statistical significance between CMVMJD135hi and CMVMJD135hi cit mice (repeated-measures two-way ANOVA and one-way ANOVA, Tukey correction). The red arrow indicates age of treatment initiation at 11 weeks





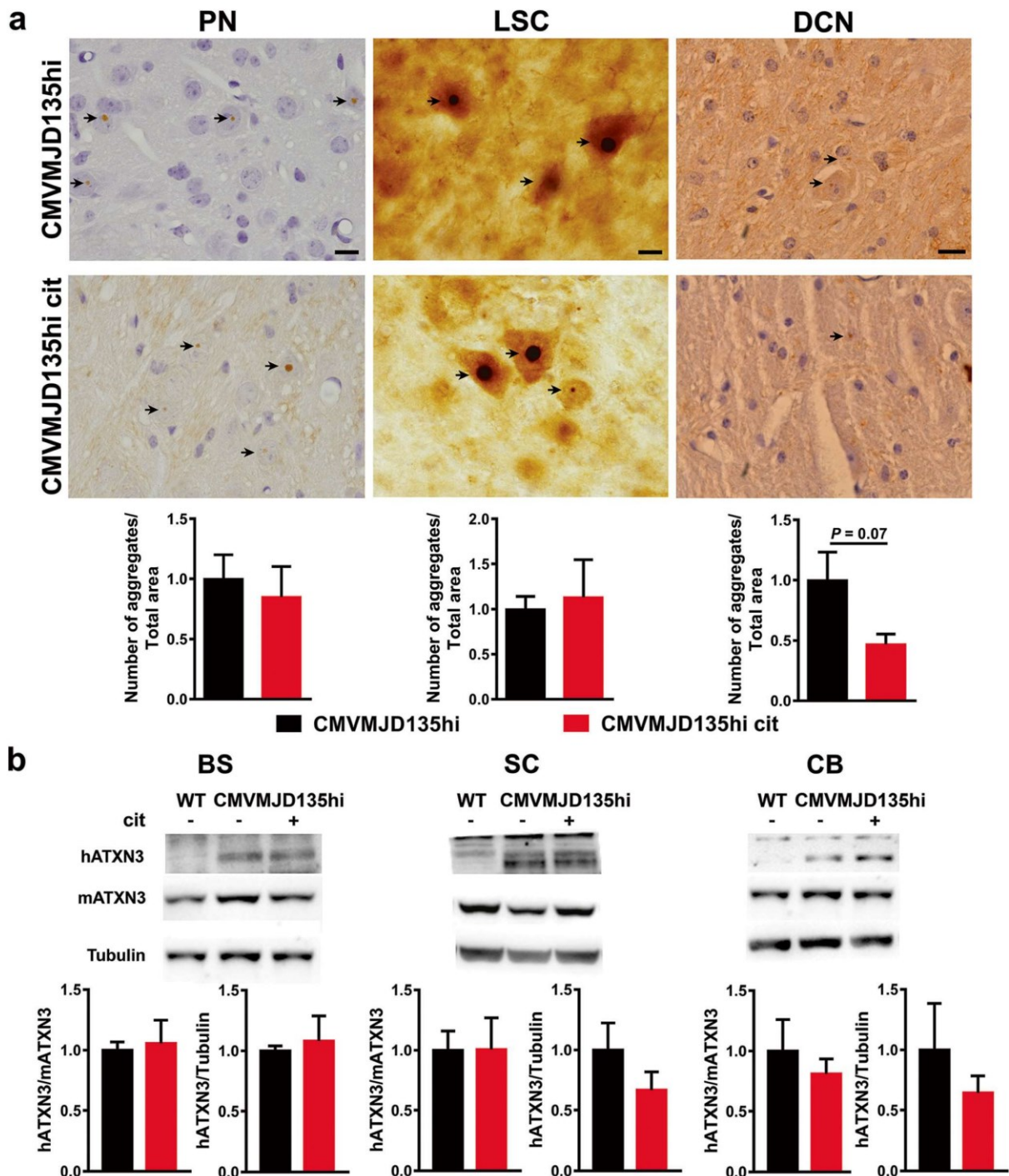


**Fig. 4** Impact of post-symptomatic citalopram treatment of CMVMJD135hi mice on brain ATXN3 intranuclear inclusions and protein levels. **a** ATXN3-positive inclusions in the pontine nuclei (PN), lumbar spinal cord (LSC), and deep cerebellar nuclei (DCN) of vehicle- and citalopram-treated CMVMJD135hi mice ( $n = 4$ , 28 weeks). **b** Brainstem (BS), spinal cord (SC), and cerebellum (CB) immunoblots and quantification of total human ATXN3 protein from vehicle- and

citalopram-treated CMVMJD135hi mice ( $n = 4$ , 28 weeks). Data are presented as mean  $\pm$  SEM, normalized to WT,  $P > 0.05$ , Student's  $t$  test, Levene correction for SC data. Scale bars = 10  $\mu$ m (PN and LSC) and 20  $\mu$ m (DCN). cit citalopram, WT wild-type, PN pontine nuclei, LSC lumbar spinal cord, DCN deep cerebellar nuclei, BS brainstem, SC spinal cord, CB cerebellum

There was, however, a tendency towards reduction of ATXN3 aggregation in the deep cerebellar nuclei (DCN) of CMVMJD135hi mice ( $P=0.071$ ) (Fig. 4a). As seen for pre-symptomatic treatment of CMVMJD135 mice [20], total levels of ATXN3 protein did not change significantly upon post-symptomatic treatment of CMVMJD135hi mice in the brainstem (BS), spinal cord (SC), and cerebellum (CB) (Fig. 4b and Supplementary Fig. 5).

Post-symptomatic treatment of CMVMJD135hi mice with citalopram failed to attenuate reactive astrogliosis in the substantia nigra (SN) (Fig. 5a). Moreover, citalopram treatment exerted limited neuroprotective effects. In brain regions like the pontine nuclei (PN) of the brainstem and in the DCN, in which at 28 weeks of age there is only a scarce neuronal loss, SSRI treatment led to a tendency of an increase in the number of NeuN-positive neurons in transgenic mice. At this age, there is also a trend towards a reduction of ChAT-positive motor neurons in the spinal cord of transgenic animals, and citalopram treatment circumvented this neuronal loss to some extent. The reduction in calbindin D-28K-positive cells seen in the Purkinje cells of the cerebellar cortex of CMVMJD135hi mice was also partially prevented by post-symptomatic citalopram treatment (Fig. 5b and Supplementary Fig. 4b). These results suggest that, unlike in early treatment, in which there was a robust suppression in mutant ATXN3 aggregation, post-symptomatic citalopram treatment promotes neuronal survival in certain regions of the mouse brain, in agreement with the observed phenotypic effects, but has a weak to absent impact on mutant protein aggregation.

## Discussion

In this study, we observed that post-symptomatic treatment of MJD transgenic mice with the SSRI citalopram attenuated their loss of balance and motor dysfunction, highlighting the importance of the use of antidepressants in neurodegenerative diseases beyond the treatment of depressive symptoms.

The therapeutic capacity of citalopram in CMVMJD135hi mice that show increased symptom severity and faster progression rates compared to CMVMJD135 mice [20] further supports the advancement of this drug to clinical trials in MJD patients. As the disease progresses, however, the ability of citalopram to prevent aggregation and neuronal loss may not be sufficient to cope with the already installed neurodegenerative process; hence, an early initiation of treatment may be required. Importantly, the safety profile of SSRIs [31] allows preventive treatment of mutation carriers as well as its administration after symptom installation, with

treatment efficacy being reported in two rodent models of MJD [20, 21]. Our previous results showed that pre-symptomatic citalopram treatment [20] exerted its effects mostly in the CNS-related symptoms rather than on the periphery (e.g., muscular strength). Here, treatment was initiated after the manifestation of core motor coordination symptoms, resulting in a percentage of therapeutic efficacy of 36%, as measured at 26 weeks of age in the balance beam walk test, in contrast with the 66% obtained when treatment was initiated before the installation of motor defects. This may be due to the combination of late treatment initiation (at 11 versus 5 weeks), reduced treatment duration (17 versus 29 weeks), and increased severity of the symptoms of CMVMJD135hi mice. Both pre- and post-symptomatic citalopram preclinical trials resulted in preservation and/or an increase in the number of neuronal cells in affected brain regions of transgenic mice, corresponding to those affected in MJD patients but not typically assessed when studying the mechanism of action of SSRIs in major depressive disorder models [32].

While citalopram treatment presented a striking effect in protein aggregation suppression, when initiated before the appearance of ATXN3 inclusions [20], this was not so evident when the treatment was initiated post-symptomatically, at an age in which inclusions are already present. The timing of citalopram treatment initiation appears therefore to have a differential impact on ATXN3 folding/aggregation suggesting that this drug may modulate specific proteostasis subnetwork(s) acting preferentially on the prevention of formation of new aggregates and/or on the generation of new seeds, and less so by disaggregating the inclusion bodies already formed. Interestingly, and regarding the possible mechanism of action of citalopram in the context of protein aggregation diseases such as MJD, neurosensory release of 5-HT has been shown to activate cell non-autonomously the heat shock factor 1 and downstream molecular chaperones and to suppress protein misfolding in non-neuronal tissues of *C. elegans* [33]. On the other hand, neuronal mitochondrial proteotoxic stress induces 5-HT release from serotonergic neurons and activates the unfolded protein response of the mitochondria in *C. elegans* intestine cells [34]. If a similar mechanism is occurring in vertebrates, this would be consistent with an aggregation preventive rather than disruptive mechanism, which is in accordance with our data. Importantly, pre-symptomatic treatment of a second MJD transgenic mouse model (YACMJDQ84.2) [35] with citalopram also resulted in a reduction in ATXN3 inclusions and abundance, and in the modulation of certain components of cellular proteostasis, including restoration of Hsp90beta levels in brains of mice treated with this drug [21].



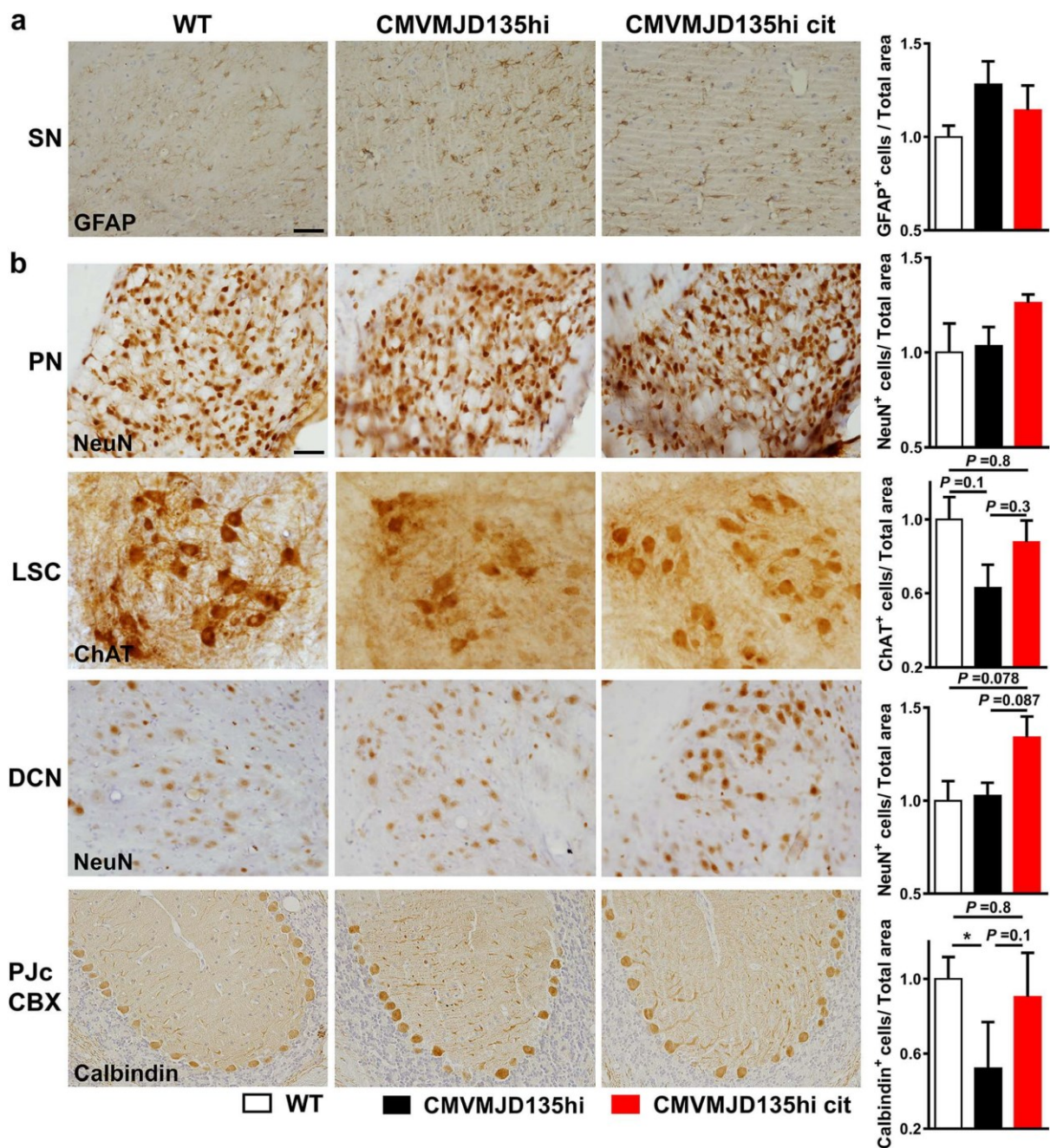


**Fig. 5** Assessment of the neuroprotective effects of citalopram post-symptomatic treatment in CMVMJD135hi mice. **a** Immunohistochemistry and quantification of GFAP-positive cells per area in substantia nigra (SN) from WT, vehicle- and citalopram-treated CMVMJD135hi mice ( $n = 5$  per group, 28 weeks). **b** Immunohistochemistry and quantification of NeuN-positive cells per total area in the pontine (PN) and deep cerebellar nuclei (DCN), ChAT-positive cells per total area in the lumbar spinal cord (LSC), and calbindin D-28K-positive Purkinje cells per total area in the cerebellar cortex (PJc CBX) from WT, vehicle- and citalopram-treated CMVMJD135hi mice

( $n = 4$  per group, 28 weeks). At least 992 GFAP-positive cells were counted in the SN; 4973 and 3622 NeuN-positive cells were counted in the PN and DCN, respectively; 344 ChAT-positive cells were counted in the LSC, and 4052 calbindin D-28K-positive Purkinje cells were counted in the PJc CBX, per condition. Data are presented as mean  $\pm$  SEM, normalized to WT values,  $P < 0.05$  (one-way ANOVA). Scale bar = 50  $\mu$ m. cit citalopram, WT wild-type, SN substantia nigra, PN pontine nuclei, LSC lumbar spinal cord, DCN deep cerebellar nuclei, PJc CBX Purkinje cells of the cerebellar cortex



The differential impact of citalopram treatment on ATXN3 proteotoxicity in the cerebellum, brainstem, and spinal cord seen in this work and in the study by Ashraf et al. may reflect the distinct expression pattern/activation of 5-HT receptors [36–38]; therefore, it would be important to identify the specific 5-HT receptors required for citalopram's effect on toxicity and aggregation of mutant ATXN3. Previous studies in *C. elegans* implicated the homologs of 5HT1 and 5HT2 receptor families in this response [20]. Consistently, the antipsychotic aripiprazole was recently identified in an unbiased screen as a modulator of ATXN3 abundance. Agonism of 5HT1A and antagonism of 5HT2A receptors by aripiprazole may contribute to its therapeutic effect in Machado-Joseph disease cell and animal models [39].

Our results support a novel use for citalopram in the treatment of MJD patients. However, the therapeutic effect found after the installation of core motor symptoms in mice indicates that early initiation of treatment is preferable, bringing new insight into the design of prospective clinical trials for this and perhaps other neurodegenerative diseases.

**Acknowledgments** We are grateful to the members of the Maciel laboratory for sharing reagents and for critical analysis of the data and discussions on the manuscript. We thank members of the Morimoto lab for critical analysis of the results and figures. We also thank H. Lundbeck A/S for providing citalopram hydrobromide and Dr. Karina Fog for scientific discussions. We are grateful to Maria do Carmo Costa for critical review of the manuscript.

**Author Contributions** SE, SO, AT-C, and PM contributed to the research project conception and organization. SE, SO, SD-S, DG-C, and AT-C performed the experiments. SE, SO, SD-S, and AT-C contributed to the statistical analysis design. SE, SO, and SD-S performed the statistical analysis. SE and AT-C wrote the first draft of the article. SO, SD-S, DG-C, AT-C, and PM reviewed and criticized the manuscript. All authors read and approved the final manuscript.

**Funding** This work has been funded by the European Regional Development Funds (FEDER), through the Competitiveness Factors Operational Programme (COMPETE), and by National funds, through the Foundation for Science and Technology (FCT), under the scope of the project POCI-01-0145-FEDER-007038. This article has been developed under the scope of the project NORTE-01-0145-FEDER-000013, supported by the Northern Portugal Regional Operational Programme (NORTE 2020), under the Portugal 2020 Partnership Agreement, through the FEDER. This work was also supported by FCT and COMPETE through the projects [PTDC/SAU-GMG/112617/2009] (to PM) and [EXPL/BIM-MEC/0239/2012] (to AT-C), by FCT through the project [POCI-01-0145-FEDER-016818 (PTDC/NEU-NMC/3648/2014)] (to PM), by National Ataxia foundation (to PM and to AT-C), and by Ataxia UK (to PM). SE, SD-S, SO, and AT-C were supported by the FCT individual fellowships, SFRH/BD/78554/2011, SFRH/BD/78388/2011, PD/BD/127818/2016, and SFRH/BPD/102317/2014, respectively. FCT fellowships are co-financed by POPH, QREN, Governo da República Portuguesa, and EU/FSE.

## Compliance with Ethical Standards

**Conflict of Interest** The authors declare that they have no conflict of interest.

## References

- Coutinho P, Andrade C (1978) Autosomal dominant system degeneration in Portuguese families of the Azores Islands. A new genetic disorder involving cerebellar, pyramidal, extrapyramidal and spinal cord motor functions. *Neurology* 28(7):703–709
- Lima L, Coutinho P (1980) Clinical criteria for diagnosis of Machado-Joseph disease: report of a non-Azorena Portuguese family. *Neurology* 30(3):319–322
- Kawaguchi Y, Okamoto T, Taniwaki M, Aizawa M, Inoue M, Katayama S, Kawakami H, Nakamura S et al (1994) CAG expansions in a novel gene for Machado-Joseph disease at chromosome 14q32.1. *Nat Genet* 8(3):221–228. <https://doi.org/10.1038/ng1194-221>
- Coutinho P, Sequeiros J (1981) Clinical, genetic and pathological aspects of Machado-Joseph disease. *J Genet Hum* 29(3):203–209
- Sequeiros J, Coutinho P (1993) Epidemiology and clinical aspects of Machado-Joseph disease. *Adv Neurol* 61:139–153
- Rub U, Brunt ER, Deller T (2008) New insights into the pathoanatomy of spinocerebellar ataxia type 3 (Machado-Joseph disease). *Curr Opin Neurol* 21(2):111–116. <https://doi.org/10.1097/WCO.0b013e3282f7673d>
- Cipriani A, Purgato M, Furukawa TA, Trespici C, Imperadore G, Signoretti A, Churchill R, Watanabe N et al (2012) Citalopram versus other anti-depressive agents for depression. *Cochrane Database Syst Rev* 7:CD006534. <https://doi.org/10.1002/14651858.CD006534.pub2>
- Aboukhatwa M, Dosanjh L, Luo Y (2010) Antidepressants are a rational complementary therapy for the treatment of Alzheimer's disease. *Mol Neurodegener* 5:10. <https://doi.org/10.1186/1750-1326-5-10>
- Blakely RD, Berson HE, Fremeau RT Jr, Caron MG, Peek MM, Prince HK, Bradley CC (1991) Cloning and expression of a functional serotonin transporter from rat brain. *Nature* 354(6348):66–70. <https://doi.org/10.1038/354066a0>
- Pittenger C, Duman RS (2008) Stress, depression, and neuroplasticity: a convergence of mechanisms. *Neuropsychopharmacology* 33(1):88–109. <https://doi.org/10.1038/sj.npp.1301574>
- Baquero M, Martin N (2015) Depressive symptoms in neurodegenerative diseases. *World J Clin Cases* 3(8):682–693. <https://doi.org/10.12998/wjcc.v3.i8.682>
- Lauterbach EC, Victoroff J, Coburn KL, Shillcutt SD, Doonan SM, Mendez MF (2010) Psychopharmacological neuroprotection in neurodegenerative disease: assessing the preclinical data. *J Neuropsychiatry Clin Neurosci* 22(1):8–18. <https://doi.org/10.1176/appi.neuropsych.22.1.8>
- Minamiyama M, Katsuno M, Adachi H, Doi H, Kondo N, Iida M, Ishigaki S, Fujioka Y et al (2012) Naratriptan mitigates CGRP1-associated motor neuron degeneration caused by an expanded polyglutamine repeat tract. *Nat Med* 18(10):1531–1538. <https://doi.org/10.1038/nm.2932>
- Cirrito JR, Disabato BM, Restivo JL, Verges DK, Goebel WD, Sathyan A, Hayreh D, D'Angelo G et al (2011) Serotonin signaling is associated with lower amyloid-beta levels and plaques in transgenic mice and humans. *Proc Natl Acad Sci U S A* 108(36):14968–14973. <https://doi.org/10.1073/pnas.1107411108>
- Sheline YI, West T, Yarasheski K, Swarm R, Jasielec MS, Fisher JR, Ficker WD, Yan P et al (2014) An antidepressant decreases CSF

- Abeta production in healthy individuals and in transgenic AD mice. *Sci Transl Med* 6(236):236re234. <https://doi.org/10.1126/scitranslmed.3008169>
16. Ubhi K, Inglis C, Mante M, Patrick C, Adame A, Spencer B, Rockenstein E, May V et al (2012) Fluoxetine ameliorates behavioral and neuropathological deficits in a transgenic model mouse of alpha-synucleinopathy. *Exp Neurol* 234(2):405–416. <https://doi.org/10.1016/j.expneurol.2012.01.008>
  17. Duan W, Peng Q, Masuda N, Ford E, Tryggestad E, Ladenheim B, Zhao M, Cadet JL et al (2008) Sertraline slows disease progression and increases neurogenesis in N171-82Q mouse model of Huntington's disease. *Neurobiol Dis* 30(3):312–322. <https://doi.org/10.1016/j.nbd.2008.01.015>
  18. Pakaski M, Bjelik A, Hugyecz M, Kasa P, Janka Z, Kalman J (2005) Imipramine and citalopram facilitate amyloid precursor protein secretion in vitro. *Neurochem Int* 47(3):190–195. <https://doi.org/10.1016/j.neuint.2005.03.004>
  19. Chung YC, Kim SR, Jin BK (2010) Paroxetine prevents loss of nigrostriatal dopaminergic neurons by inhibiting brain inflammation and oxidative stress in an experimental model of Parkinson's disease. *J Immunol* 185(2):1230–1237. <https://doi.org/10.4049/jimmunol.1000208>
  20. Teixeira-Castro A, Jalles A, Esteves S, Kang S, da Silva Santos L, Silva-Fernandes A, Neto MF, Briellmann RM et al (2015) Serotonergic signalling suppresses ataxin 3 aggregation and neurotoxicity in animal models of Machado-Joseph disease. *Brain* 138(11):3221–3237. <https://doi.org/10.1093/brain/awv262>
  21. Ashraf NS, Duarte-Silva S, Shaw ED, Maciel P, Paulson HL, Teixeira-Castro A, do Carmo Costa M (2018) Citalopram reduces aggregation of ATXN3 in a YAC transgenic mouse model of Machado-Joseph disease. *Mol Neurobiol*. <https://doi.org/10.1007/s12035-018-1331-2>
  22. Silva-Fernandes A, Duarte-Silva S, Neves-Carvalho A, Amorim M, Soares-Cunha C, Oliveira P, Thirstrup K, Teixeira-Castro A et al (2014) Chronic treatment with 17-DMAG improves balance and coordination in a new mouse model of Machado-Joseph disease. *Neurotherapeutics* 11:433–449. <https://doi.org/10.1007/s13311-013-0255-9>
  23. Nicklas W, Baneux P, Boot R, Decelle T, Deeny AA, Fumanelli M, Illgen-Wilcke B (2002) Recommendations for the health monitoring of rodent and rabbit colonies in breeding and experimental units. *Lab Anim* 36(1):20–42
  24. Silva-Fernandes A, Costa Mdo C, Duarte-Silva S, Oliveira P, Botelho CM, Martins L, Mariz JA, Ferreira T et al (2010) Motor uncoordination and neuropathology in a transgenic mouse model of Machado-Joseph disease lacking intranuclear inclusions and ataxin-3 cleavage products. *Neurobiol Dis* 40(1):163–176. <https://doi.org/10.1016/j.nbd.2010.05.021>
  25. Carter RJ, Lione LA, Humby T, Mangiarini L, Mahal A, Bates GP, Dunnett SB, Morton AJ (1999) Characterization of progressive motor deficits in mice transgenic for the human Huntington's disease mutation. *J Neurosci* 19(8):3248–3257
  26. Kilkenny C, Browne WJ, Cuthill IC, Emerson M, Altman DG (2010) Improving bioscience research reporting: the ARRIVE guidelines for reporting animal research. *PLoS Biol* 8(6):e1000412. <https://doi.org/10.1371/journal.pbio.1000412>
  27. Rogers DC, Fisher EM, Brown SD, Peters J, Hunter AJ, Martin JE (1997) Behavioral and functional analysis of mouse phenotype: SHIRPA, a proposed protocol for comprehensive phenotype assessment. *Mamm Genome* 8(10):711–713
  28. Rafael JA, Nitta Y, Peters J, Davies KE (2000) Testing of SHIRPA, a mouse phenotypic assessment protocol, on Dmd(mdx) and Dmd(mdx3cv) dystrophin-deficient mice. *Mamm Genome* 11(9):725–728
  29. Kim HY (2013) Statistical notes for clinical researchers: assessing normal distribution (2) using skewness and kurtosis. *Restor Dent Endod* 38(1):52–54. <https://doi.org/10.5395/rde.2013.38.1.52>
  30. Maciel P, Gaspar C, DeStefano AL, Silveira I, Coutinho P, Radvany J, Dawson DM, Sudarsky L et al (1995) Correlation between CAG repeat length and clinical features in Machado-Joseph disease. *Am J Hum Genet* 57(1):54–61
  31. Nemeroff CB (2003) Overview of the safety of citalopram. *Psychopharmacol Bull* 37(1):96–121
  32. Krishnan V, Nestler EJ (2008) The molecular neurobiology of depression. *Nature* 455(7215):894–902. <https://doi.org/10.1038/nature07455>
  33. Tatum MC, Ooi FK, Chikka MR, Chauve L, Martinez-Velazquez LA, Steinbusch HW, Morimoto RI, Prahlad V (2015) Neuronal serotonin release triggers the heat shock response in *C. elegans* in the absence of temperature increase. *Curr Biol* 25(2):163–174. <https://doi.org/10.1016/j.cub.2014.11.040>
  34. Berendzen KM, Durieux J, Shao LW, Tian Y, Kim HE, Wolff S, Liu Y, Dillin A (2016) Neuroendocrine coordination of mitochondrial stress signaling and proteostasis. *Cell* 166(6):1553–1563. <https://doi.org/10.1016/j.cell.2016.08.042>
  35. Cernal CK, Carroll CJ, Lawrence L, Lowrie MB, Ruddle P, Al-Mahdawi S, King RH, Pook MA et al (2002) YAC transgenic mice carrying pathological alleles of the MJD1 locus exhibit a mild and slowly progressive cerebellar deficit. *Hum Mol Genet* 11(9):1075–1094
  36. Lesch KP, Waider J (2012) Serotonin in the modulation of neural plasticity and networks: implications for neurodevelopmental disorders. *Neuron* 76(1):175–191. <https://doi.org/10.1016/j.neuron.2012.09.013>
  37. Oostland M, van Hooft JA (2013) The role of serotonin in cerebellar development. *Neuroscience* 248:201–212. <https://doi.org/10.1016/j.neuroscience.2013.05.029>
  38. Perrier JF, Cotel F (2015) Serotonergic modulation of spinal motor control. *Curr Opin Neurobiol* 33:1–7. <https://doi.org/10.1016/j.conb.2014.12.008>
  39. Costa MDC, Ashraf NS, Fischer S, Yang Y, Schapka E, Joshi G, McQuade TJ, Dharia RM et al (2016) Unbiased screen identifies aripiprazole as a modulator of abundance of the polyglutamine disease protein, ataxin-3. *Brain* 139(11):2891–2908. <https://doi.org/10.1093/brain/aww228>

---

## **Supplementary data**

**Supplementary material to:**

**Molecular Neurobiology**

**Preclinical evidence supporting early initiation of citalopram treatment in Machado-Joseph disease**

Sofia Esteves<sup>1,2,\*</sup>, Stéphanie Oliveira<sup>1,2,\*</sup>, Sara Duarte-Silva<sup>1,2</sup>, Daniela Garcia-Cunha<sup>1,2</sup>, Andreia Teixeira-Castro<sup>1,2,3,#</sup> and Patrícia Maciel<sup>1,2,#</sup>

\* These authors contributed equally to this work.

# These authors share co-senior authorship.

<sup>1</sup>Life and Health Sciences Research Institute (ICVS), School of Medicine, University of Minho, Braga, Portugal; <sup>2</sup>ICVS/3B's - PT Government Associate Laboratory, Braga/Guimarães, Portugal; <sup>3</sup>Department of Molecular Biosciences, Northwestern University, Evanston, Illinois 60208, USA.

**Corresponding authors:**

Patrícia Maciel, PhD

Life and Health Sciences Research Institute (ICVS);

School of Medicine; University of Minho;

Campus of Gualtar, 4710-057 Braga, Portugal.

[Tel:+351253604824](tel:+351253604824); Fax: +351253604820; E-mail: [pmaciel@med.uminho.pt](mailto:pmaciel@med.uminho.pt)

Andreia Teixeira-Castro, PhD

Life and Health Sciences Research Institute (ICVS);

School of Medicine; University of Minho;

Campus of Gualtar, 4710-057 Braga, Portugal.

[Tel:+351253604871](tel:+351253604871); Fax: +351253604820; E-mail: [accastro@med.uminho.pt](mailto:accastro@med.uminho.pt)

**Table S2.1 Age at which phenotypic differences are first detected in CMVMJD135 and CMVMJD135hi mice.**

Phenotypic manifestation	Age at symptom onset, weeks		
	CMVMJD135	CMVMJD135hi	Anticipation
Stride length shortening	30	14	16
Beam walk increased latency	20	10	10
Reduced body weight gain	20	14	6
Decreased gait quality score	22	(18) #	≥4

#Numbers within ( ) represent the age (in weeks) at which the phenotype was first detected, however in this case the animals were not tested in previous ages, meaning that the anticipation value can be higher.

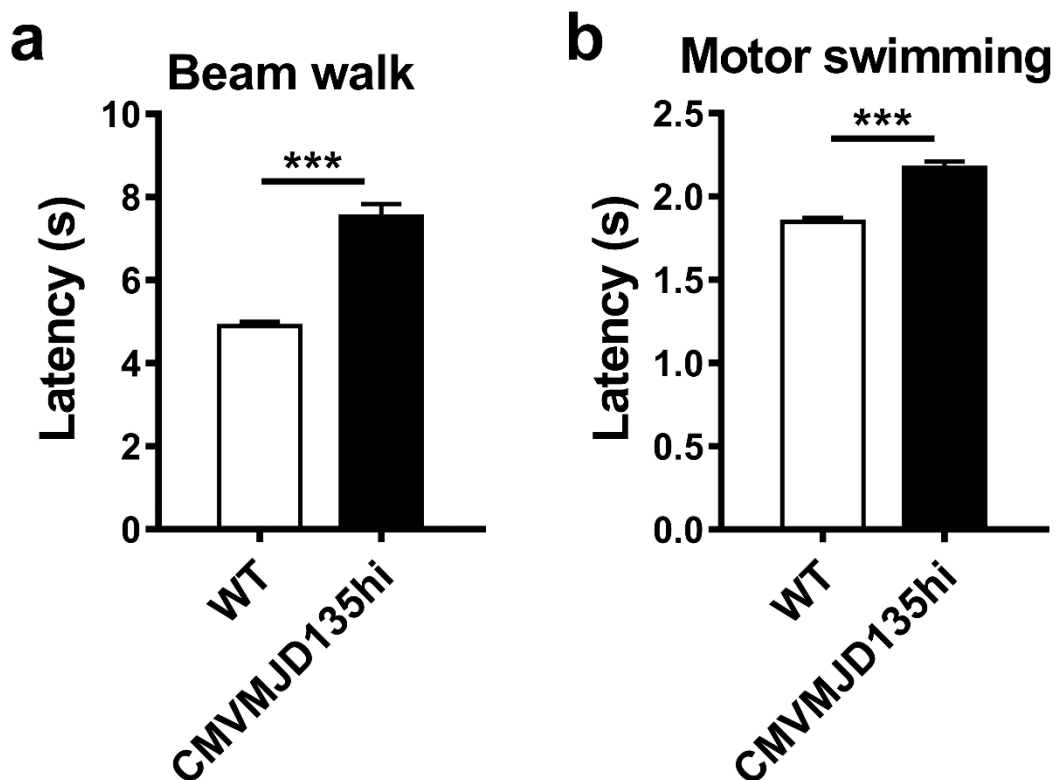


**Figure S2.1 CMVMJD135hi transgenic mice show defects in motor coordination and balance at 10 weeks of age.** **a** Significant differences were observed in the square balance beam walk ( $P < 0.0001$ , 10 weeks), and in **b** the motor swimming tests ( $P < 0.0001$ , 10 weeks) between WT (WT,  $n = 30$ ) and transgenic mice (CMVMJD135hi,  $n = 31$ ). Data are presented as mean  $\pm$  SEM, \*\*\*  $P < 0.001$ . (Student's  $t$ -test). Citalopram treatment was initiated at 11 weeks of age.

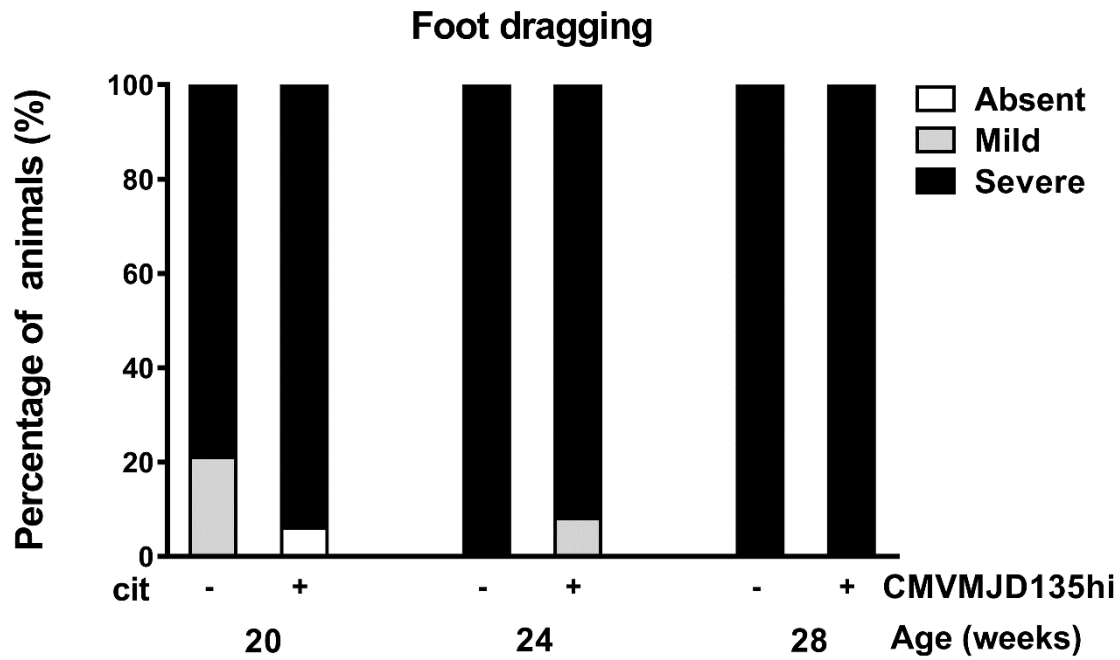


**Figure S2.2 No effect of chronic post-symptomatic citalopram treatment in CMVMJD135hi mice foot dragging.** Quantitative analysis performed at 20 (CMVMJD135hi,  $n = 14$ , CMVMJD135hi cit,  $n = 17$ ), 24 (CMVMJD135hi,  $n = 14$ , CMVMJD135hi cit,  $n = 13$ ) and at 28 weeks (CMVMJD135hi,  $n = 13$ , CMVMJD135hi cit,  $n = 14$ ). (Kruskal-Wallis test was used to compare ranks and no statistical differences were found).

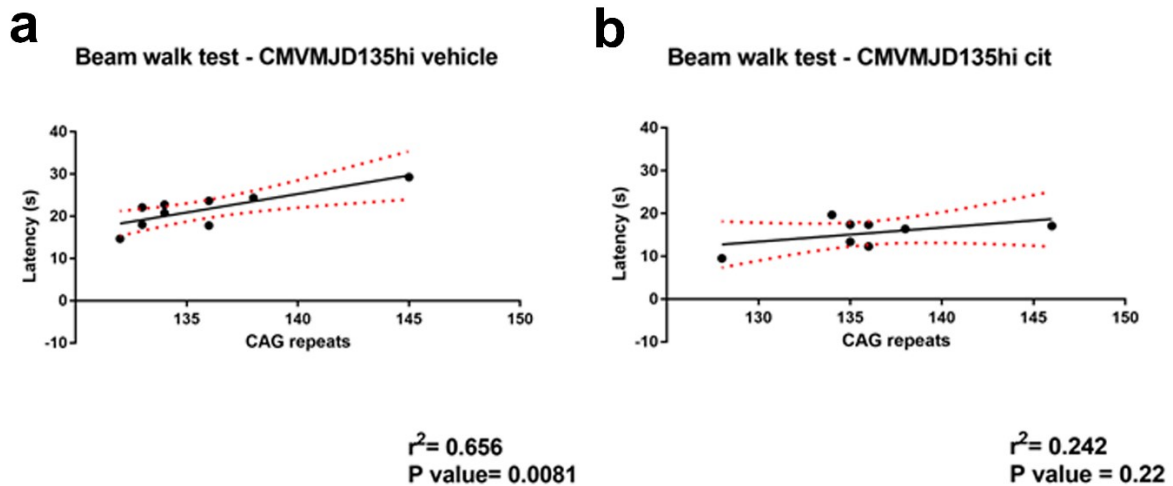


**Figure S2.3 Vehicle-treated and not citalopram-treated CMVMJD135hi mice present increased phenotype severity related to higher (CAG)<sub>n</sub> repeat length.** Genotype versus phenotype correlation for the 12 mm square balance beam walk of **a** vehicle-treated CMVMJD135hi mice ( $n = 9$ ) and of **b** CMVMJD135hi treated with citalopram ( $n = 7$ ) at 26 weeks of age. (Pearson correlation coefficient).  $r^2$  = Square of the Pearson correlation coefficient.



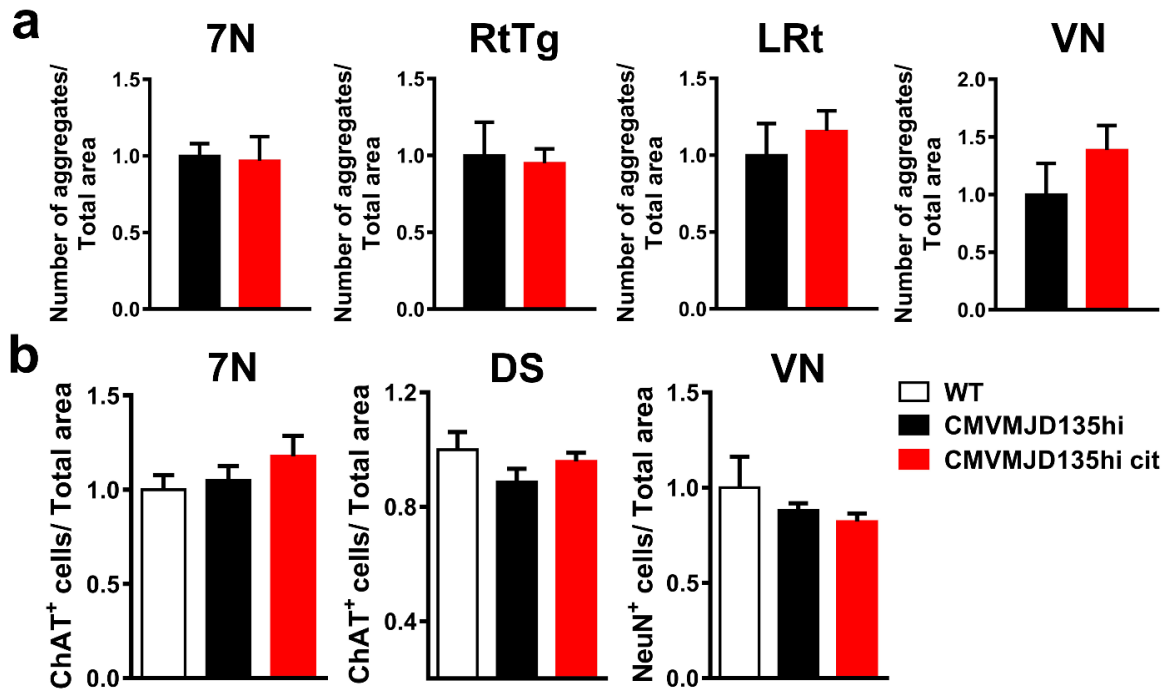


**Figure S2.4 Impact of citalopram post-symptomatic treatment on ATXN3 aggregation and ChAT- and NeuN-positive cells in CMVMJD135hi mice.** **a** Neuronal inclusions in the facial nuclei (7N), in the reticulotegmental nuclei of pons (RtTg), in the lateral reticular nuclei (LRt), and in the vestibular nuclei (VN) of vehicle- and citalopram-treated CMVMJD135hi mice ( $n = 4$ , 28 weeks). **b** Quantification of ChAT-positive cells per total area in the facial nuclei (7N) and dorsal striatum (DS); and of NeuN-positive cells per total area in the vestibular nuclei (VN) from WT, vehicle- and citalopram-treated CMVMJD135hi mice ( $n = 4$  per group, 28 weeks). Data are presented as mean  $\pm$  SEM, normalized to WT,  $P < 0.05$  (one-way ANOVA). cit - citalopram; WT - wild-type; 7N - facial nuclei, RtTg - reticulotegmental nuclei of pons; LRt - lateral reticular nuclei; VN - vestibular nuclei; DS - dorsal striatum.

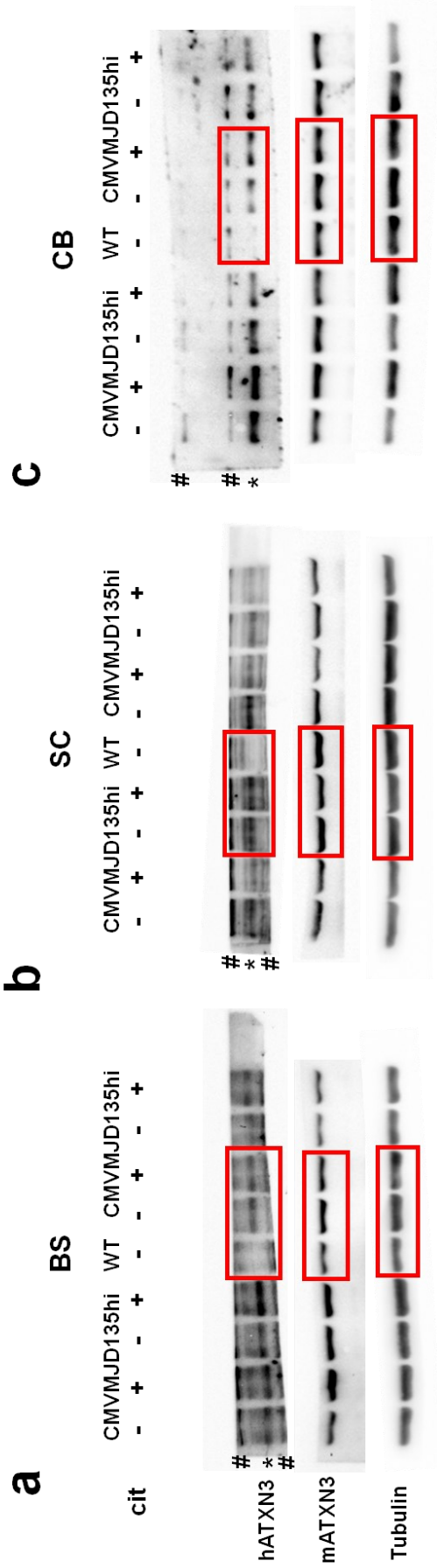


**Figure S2.5 Impact of post-symptomatic citalopram treatment of CMVMJD135hi mice on brain ATXN3 protein levels. a** Brainstem (BS), **b** spinal cord (SC), and **c** cerebellum (CB) immunoblots of total human ATXN3 (hATXN3) protein from vehicle- and citalopram-treated CMVMJD135hi mice ( $n = 4$ , 28 weeks). The hATXN3 protein band does not appear in WT animals, as expected. The red rectangles represent the bands presented in Figure 2.4. cit - citalopram; WT - wild-type; BS - brainstem; SC - spinal cord; CB - cerebellum; \* = hATXN3 specific band, which was quantified; mATXN3 - mouse ATXN3; # - unspecific binding.



---

**Finding the molecular determinants of serotonergic  
signaling modulation in a mouse model of MJD**

---

This chapter is composed by two sub-chapters (3.1 and 3.2). Chapter 3.1 *“Possible role of the dysregulation of the serotonin 1A receptor signaling in MJD pathogenesis and its reestablishment by citalopram treatment”* describes a transcriptomic analysis, using RNA-sequencing, performed in a mouse model of MJD pre-symptomatically treated with vehicle or citalopram, and the possible important role of serotonin 1A receptor in MJD. Chapter 3.2 *“Exploring the modulation of the protein homeostasis by citalopram chronic treatment in a MJD mouse model”* is an extension of the RNA-seq data analysis conducted in chapter 3.1 and is focused on proteostasis alterations triggered by the chronic administration of citalopram in this mouse model.

---

## Chapter 3.1

---

### **Possible role of the dysregulation of the serotonin 1A receptor signaling in MJD pathogenesis and its reestablishment by citalopram treatment**

---

---

**Possible role of the dysregulation of the serotonin 1A receptor signaling in MJD pathogenesis and its reestablishment by citalopram treatment**

Stéphanie Oliveira<sup>1,2</sup>, Sara Duarte-Silva<sup>1,2</sup>, Bruna Ferreira-Lomba<sup>1,2</sup>, Joana Pereira-Sousa<sup>1,2</sup>, Olaf Riess<sup>3,4</sup>, Jeannette Hübener-Schmid<sup>3,4</sup>, Patrícia Maciel<sup>1,2</sup>, Andreia Teixeira-Castro<sup>1,2,3</sup>

<sup>1</sup> Life and Health Sciences Research Institute (ICVS), School of Medicine, University of Minho, Campus of Gualtar, 4710-057 Braga, Portugal.

<sup>2</sup> ICVS/3B's - PT Government Associate Laboratory, Braga/Guimarães, Portugal.

<sup>3</sup> Institute of Medical Genetics and Applied Genomics, University of Tübingen, Tübingen, Germany.

<sup>4</sup> Centre for Rare Diseases, Tübingen, Germany.

(Manuscript *in preparation*)

---

---

## Abstract

Machado-Joseph disease (MJD) is a dominantly inherited and late-onset neurodegenerative disorder currently lacking effective treatment. Previously, we identified the selective serotonin reuptake inhibitor (SSRI) antidepressant citalopram as a reliable and effective drug with the potential to be repurposed for this disorder. Chronic pre-symptomatic treatment of transgenic MJD (CMVMJD135) mice markedly ameliorated mutant ataxin-3 (ATXN3)-mediated pathogenesis. Recently, we demonstrated that chronic post-symptomatic treatment also improved motor coordination and balance, attenuating disease progression, although to a lesser extent than previously seen with pre-symptomatic treatment initiation. Here, we intend to uncover the molecular features underlying the mechanism of action (MOA) of citalopram in the suppression of MJD pathogenesis. Therefore, we performed a transcriptomic analysis (RNA-seq) of the striatum of citalopram-treated and non-treated mice, to get further clues on the molecular alterations generated by this treatment.

Interestingly, transcriptomic analysis results suggested that serotonergic receptor signaling is altered at baseline in the striatum of CMVMJD135 mice, and that citalopram chronic treatment had the capacity to restore the expression of a subset of genes downregulated in transgenic mice to wild-type levels; including the serotonin receptor 5-HT<sub>1A</sub> (5-HT<sub>1A</sub>R), that could be relevant to the human disorder too. The expression of some downstream targets of this G protein-coupled receptor was altered upon treatment, indicative of a role of 5-HT<sub>1A</sub>R-mediated signaling pathways in the MOA of citalopram in MJD, possibly involving the regulation of the CREB transcription factor program. In fact, we demonstrated that CREB is necessary for the effect of citalopram in ATXN3 pathogenesis context, since in its absence the treatment effect is mostly lost in a *C. elegans* MJD model.

While unveiling some of the key features of citalopram's MOA in the context of MJD, these results further support the use of this antidepressant as a disease-modifying therapeutic approach for MJD and maybe for other similar neurodegenerative disorders.

## 1. Introduction

The expansion of the cytosine-adenosine-guanine (CAG) triplet repeat within the coding region of specific genes is at the root of several neurodegenerative diseases, such as the spinal and bulbar muscular atrophy (SBMA), Huntington's disease (HD), dentatorubral-pallidoluysian atrophy (DRPLA) and several dominantly inherited spinocerebellar ataxias (SCAs) [1]. Among the latter, spinocerebellar ataxia type 3 (SCA3) or Machado-Joseph disease (MJD) is the most common dominantly inherited worldwide [2]. The symptomatology associated to MJD includes ataxia, diplopia, ophthalmoplegia, dysphagia, dysarthria, fasciculations, dystonia, amyotrophy and/or spasticity, reflecting the involvement of various neurological systems [3, 4]. Pathologically, there is a prevalent neuronal degeneration affecting several parts of the central nervous system, including the brainstem, cerebellum, basal ganglia and the spinal cord [5]. Some symptoms are not entirely justified by cerebellar neuropathology, such as dystonia and chorea, and striatal pathology could contribute for it [6]. Until now, there is no effective disease-modifying treatment available for this disorder.

Citalopram, a selective serotonin reuptake inhibitor (SSRI), is a well-tolerated antidepressant belonging to a class of safe drugs that enhances serotonergic neurotransmission through efficient and selective inhibition of serotonin (5-HT) reuptake [7]. SSRIs share a principal target, the cell surface-located 5-HT transporter, SERT, which promotes 5-HT reuptake into serotonergic neurons [8, 9]. The mechanism by which SSRIs exert their function is not fully understood yet, but SERT inhibition and the consequent rising of 5-HT extracellular levels might constitute the initial steps of this process [10]. The desensitization of presynaptic receptors accounting for the increased 5-HT synaptic levels is one of the hypotheses of how SSRIs mediate their therapeutic effects [11-13], but SSRIs may also modify postsynaptic serotonergic receptors signaling [14, 15].

Interestingly, antidepressants have shown to have neuroprotective properties [16, 17] in the context of neurodegenerative disorders [18, 19]. Beneficial effects have been reported for Alzheimer's disease [20-22], Parkinson's disease [23-25] and Huntington's disease [26-28], for instance. This is relevant since patients with neurodegenerative pathologies or chronic conditions are often treated for depressive symptoms [29].

In line with these reports is our previous description of an *in vivo* screen of FDA-approved small molecules that identified compounds able to suppress mutant ataxin-3 (ATXN3)-induced neurotoxicity in an invertebrate model - *Caenorhabditis elegans* (*C. elegans*)- of MJD [30]. By making use of this unbiased strategy, citalopram and other SSRIs were found to restore the motor capacity and to reduce ATXN3 aggregation in this model. Early initiation and chronic administration of citalopram in the invertebrate

model resulted in increased efficacy. Furthermore, in a subsequent experiment, citalopram chronic treatment in a MJD mouse model (CMVMJD135 [31]) at an age where symptoms were negligible, led to a marked amelioration in locomotor behavior as well as a drastic reduction in ATXN3 aggregation and neuronal loss [30], thus confirming the reports of SSRIs' beneficial effects on the pathogenesis of neurodegenerative disorders and representing a promising therapeutic strategy for MJD. To understand if citalopram treatment would still be effective in a clinical condition of symptom-driven diagnosis, MJD mice, displaying increased phenotypic severity and faster disease progression, were treated post-symptomatically after presenting motor symptoms [32]. Improvements in motor coordination and balance were observed, attenuating disease progression, although to a lesser extent than previously seen upon pre-symptomatic treatment, with mild impact on neuroprotection and no alterations in ATXN3 aggregation.

Altogether, these observations suggest that 5-HT reuptake and resultant 5-HT signaling modulation can be used as a disease-modifying therapy for, not only MJD, but for other conformational disorders. However, the full mechanism of action (MOA) of SSRIs is not completely understood, much less in the context of a polyglutamine disease. Here, we aimed at uncovering the molecular features underlying the MOA of citalopram in the suppression of MJD pathogenesis. To achieve this, we performed a transcriptomic analysis (RNA-seq) of the striatum of citalopram-treated and non-treated mice. Our results indicate that although there is no major transcriptomic dysregulation in the striatum of CMVMJD135 transgenic mice, there is an imbalance in serotonergic receptor signaling that is restored upon citalopram treatment. Accordingly, we found that 5-HT<sub>1A</sub> receptor (5-HT<sub>1A</sub>R) expression is diminished in CMVMJD135 mice and restored in transgenic-treated mice, suggesting that this receptor could play a preponderant role in the disease and constitute a potential new therapeutic target.

## **2. Materials and methods**

### *2.1 Animal research: ethics statement*

The present work required the use of vertebrate animals (mouse - *Mus musculus*) samples. Each animal procedure was performed in accordance with applicable European regulations on animal care and experimentation (European Union Directive 2010/63/EU). The experimental design was constructed with commitment to the 3R's (Replacement, Reduction and Refinement) principle and performed ensuring the Federation of European Laboratory Animal Science Associations (FELASA) guidelines were followed [33]. The minimum of animals required to avoid unnecessary experimental repetitions or the use of additional animals, allowing a careful statistical analysis, was considered (based on power analyses of the behavior

and pathological phenotypes of CMVMJD135 mice, reported in Teixeira-Castro, A. *et al*, 2015 [30] supplementary Table 2). Since genetically modified (transgenic) animals used develop motor problems, human endpoints were defined to minimize stress, discomfort and/or pain (20 % reduction of the body weight, incapacity to feed by not being able to reach food and/or water, presence of visible wounds in the body). However, those endpoints did not need to be applied in practice, since the experiments were conceived to not include ages at which animals attain this stage of disease severity. All the projects and protocols were approved by the Animal Ethics Committee of the Life and Health Sciences Research Institute (ICVS) at the University of Minho. ICVS is a certified laboratory by the Portuguese regulatory entity - Direção Geral de Alimentação e Veterinária (DGAV), and all persons directly involved in animal experimentation are highly trained and individually certified by DGAV. ARRIVE guidelines [34, 35], developed by the UK National Centre for the Replacement, Refinement and Reduction of Animals in Research (NC3Rs), were followed to improve reporting of animal research. General health monitoring was performed throughout the study, with special attention to the pathogen status of sentinel animals residing in the same room in the animal facility.

## 2.2 Mouse samples: transgenic mouse model maintenance and drug administration

Striatum samples used in this study were obtained from 34-week-old CMVMJD135 male mice treated chronically with citalopram hydrobromide CAS 59729-32-7 (Lundbeck, Copenhagen, Denmark), in the drinking water at 8 mg/kg/day, in a pre-symptomatic form (treatment initiation at 5 weeks of age with a duration of 29 weeks), as previously described [30]. Briefly, animals were generated and genotyped as formerly reported ([31] and [36], respectively). At weaning animals were housed in groups of five and maintained in filter-topped polysulfone cages (268 × 215 × 141 mm; floor area: 370 cm<sup>2</sup>, Tecniplast, Buguggiate, Italy). A bedding composed of corncob (Scobis Due, Mucedola SRL, Settimo Milanese, Italy) was used. Mice were maintained in standard conditions (21 ± 1 °C and a relative humidity of 50 to 60 %) under an artificial 12 h light/dark cycle, corresponding to light on from 8 am to 8 pm. Animals were fed with 4RF21 diet after weaning, while 4RF25 diet was used during gestation and post-natal phases (Mucedola SRL, Settimo Milanese, Italy), and had access to water *ad libitum*. Mice were handled and performed motor behavior analysis as previously reported [30]. To collect samples, occision of 34-week-old CMVMJD135 and WT littermates was performed by decapitation, followed by a quick removal of the brain that was snap frozen in liquid nitrogen and dissected. Brain regions were stored in -80 °C deep freezers until further use. Samples from age and genetic background-matched transgenic and



wild-type (WT) littermate mice were used. The mean  $\pm$  standard deviation (SD) of the CAG repeat size for the MJD mice used in this study was  $128 \pm 5$ .

### 2.3 RNA sequencing (RNA-seq) of mouse striatum

Striatum tissue stored at  $-80\text{ }^{\circ}\text{C}$ , from 34-week-old CMVMJD135 male mice, was sent to the c.ATG facility in Tübingen, Germany, for RNA extraction and sequencing ( $n = 5$  per group: WT, transgenic (Tg), and Tg treated with citalopram (cit)). Total DNA, RNA, and microRNA was extracted simultaneously using the AllPrep DNA/RNA/miRNA Universal Kit (Cat. No. 80224, Qiagen, Hilden, Germany). Extraction was performed according to the manufacturer's handbook (version from February 2016), more specifically the protocol for "Simultaneous Purification of Genomic DNA and Total RNA, including miRNA, from Tissues" was used. Modifications to the referred protocol are described in the following paragraph.

The disruption of the striatum tissue was performed in 600  $\mu\text{L}$  of Buffer RLT Plus without supplementation with  $\beta$ -mercaptoethanol. All the lysate was used and further processed. In steps that included the addition of ethanol (step 9 and 11), the same was added very slowly by meticulously increasing pipetting up and down to avoid the formation of precipitates. The optional centrifugation was performed (step 21) at full speed for 3-4 min. For elution (step 22), 30  $\mu\text{L}$  of RNase-free water was used, directly pipetted on the top of the membrane, and incubated for 1-2 min before centrifugation. The elution step was repeated with the eluate to increase RNA concentration.

After RNA quality assessment, performed using a 2100 Bioanalyzer system (G2939BA, Agilent, Santa Clara, CA, USA), samples with best RNA integrity number ( $\text{RIN} > 7$ ) were selected for library construction. The amount of 100 ng of total RNA was enriched for polyA-containing molecules and the construction of cDNA libraries was achieved using the resulting mRNA and the TruSeq Stranded mRNA (Cat. No. 20020595, Illumina®, San Diego, CA, USA). Library molarity was assessed by measuring library size (approximately 350-400 bp) using the 2100 Bioanalyzer system (G2939BA, Agilent, Santa Clara, CA, USA). Library concentration (approximately 1 ng/ $\mu\text{L}$ ) was determined using the Quant-iT™ dsDNA Assay Kit, high sensitivity (HS) (Invitrogen™, Cat. No. Q33120, Waltham, MA, USA). Sequencing data was produced on an Illumina® NovaSeq 6000 (Illumina®, San Diego, CA, USA) in paired-end sequencing mode (50 bp reads), with a sequencing depth of 13 to 40 million cluster counts per sample. The preparation of the library and of the sequencing procedures were performed by the same person and the design chosen to minimize technical batch effects.

## 2.4 RNA-seq analysis

Read quality assessment of the RNA-seq data was performed using *ngs-bits* (<https://github.com/imgag/ngs-bits>) to identify low average quality sequencing cycles, repetitive sequences from PCR amplification or adaptor contamination. Reads were then aligned with *STAR* (version 2.5.2b) [37] against a custom-built genome composed by the *Ensembl M. musculus* genome GRCm38, allowing gapped alignments to account for splicing. *Samtools* (version 1.1) was used to verify alignment quality [38]. Read counting was performed using *Subread* (version 1.5.1) [39]. Normalized read counts for all genes were obtained through *edgeR* (version 3.18.1) and the weighted trimmed mean of M-values [40]. Transcripts covered with less than 1 cpm (counts per million) in more than four samples were excluded from following analysis, leaving 15145 genes to subsequent determination of differential expression in each of the pair-wise comparisons between experimental groups. A statistical model integrating the pair relationship and the group property of samples was tested by fitting a negative binomial distribution through a generalized linear model (GLM) approach. Gene expression fold changes ( $\log_2$  Fold Change,  $\log_2$  FC) were obtained, as well as respective raw p-value and adjusted p-value (FDR), this last one being obtained by Benjamini-Hochberg procedure. Differentially expressed genes (DEGs) were considered based on the following filters: absolute  $\log_2$  FC of at least 1 (i.e., double or half the expression strength) and p-value  $\leq 0.05$ .

Canonical pathway analysis was carried out using Ingenuity Pathway Analysis (IPA, Qiagen, Redwood City, CA, USA) software [41]. Heatmaps were created using Morpheus: versatile matrix visualization and analysis software (Broad Institute, Cambridge, MA, USA) [42].

## 2.5 Quantitative Reverse Transcriptase PCR (qRT-PCR)

**Mouse samples.** Total RNA from the striatum of 34-week-old WT and CMVMJD135 littermate male mice, vehicle- and citalopram-treated ( $n = 4$  WT vehicle, 3 Tg vehicle, 3 Tg cit) was extracted using the Qiagen AllPrep DNA/RNA/miRNA Universal Kit, as described in section 2.3. RNA concentration and quality were determined by spectrophotometry and electrophoresis, respectively, and/or assessed using Experion™ RNA StdSens kit (#7007103, Bio-Rad, Hercules, CA, USA). First-strand complementary DNA (cDNA) was synthesized using iScript™ cDNA Synthesis Kit (#1708891, Bio-Rad, Hercules, CA, USA) and amplified by quantitative reverse-transcriptase polymerase chain reaction (qRT-PCR) in an Applied Biosystems™ 7500 Real Time PCR System (Applied Biosystems™ by Thermo Fisher Scientific, Waltham, MA, USA), using 5× HIT FIREPol® EvaGreen® qPCR Mix plus (Cat. No. 08-24-00020, Solis BioDyne, Tartu, Estonia), according to the manufacturer's instructions (equal amounts of RNA were initially used

for each sample). Primers were designed using the *Primer-Blast tool* from the National Center for Biotechnology Information (NCBI) [43], on the basis of the respective GenBank mRNA sequences (Table 3.1.1). Primer efficiencies were then tested before conducting qRT-PCR. Raw data was extracted using 7500 software version 2.0.6 (Applied Biosystems™, Waltham, MA, USA). Gene expression data were normalized to the housekeeping gene beta-2-microglobulin (*B2m*). Statistical analysis was run using  $2^{-\Delta ct}$  values and graphical representation was constructed using normalized  $2^{-\Delta ct}$  values to the control sample average ( $2^{-\Delta\Delta ct}$ ) [44].

**Human samples.** *Post-mortem* striatum and cerebellum tissues were kindly provided by the Michigan Brain Bank (P30 AG053760 University of Michigan Alzheimer’s Disease Core Center). Total RNA extraction was performed using Qiagen AllPrep DNA/RNA/miRNA Universal Kit, as described in section 2.3. RNA quality assessment was performed using Experion™ RNA StdSens kit (#7007103, Bio-Rad, Hercules, CA, USA). First-strand cDNA synthesis, primers design (Table 3.1.1) and qRT-PCR were performed as described for mouse samples. Gene expression data were normalized to the housekeeping gene *B2M*.

**Table 3.1.1 List of primers used for the determination of gene expression by qRT-PCR.**

Species	Gene (NCBI Reference Sequence)	Forward primer (5'- 3')	Reverse primer (5'- 3')
<i>Mus musculus</i>	<b>Htr1a</b> (NM_008308.4)	CTCGGCGATTCAAGGAAGAA	TTCTAGAGCAAGAGGGAGGG
	<b>B2m</b> (NM_009735.3)	CCTTCAGCAAGGACTGGTCT	TCTCAGTCCCAGTAGACGGT
<i>Homo sapiens</i>	<b>5-HT<sub>1a</sub></b> (NM_000524.3)	GGTAACCTGCGACCTGTTCA	GGCGTCCTCTTGTTCACGTA
	<b>B2M</b> (NM_004048.3)	AGCAGCATCATGGAGGTTTGA	TCAAACATGGAGACAGCACTCA

## 2.6 Nematode strains and general methods

*Caenorhabditis elegans* (*C. elegans*) Bristol strain N2 (WT) and *Escherichia coli* (*E. coli*, OP50) food source were obtained from the *Caenorhabditis* genetics center (CGC, University of Minnesota, USA). AT3q130, the *C. elegans* model of MJD and AT3q75 strain (displaying a pathological sub-threshold of CAG repeats) were previously generated by our research group [45]. Standard methods were used for culturing and observing *C. elegans*, unless otherwise noted [46]. Briefly, nematodes were grown at 20 °C, on Nematode Growth Medium (NGM) plates seeded with OP50, grown overnight (≈ 16 h) at 37 °C and at 180 revolutions per minute (rpm), in Luria Broth (LB) media. Populations were synchronized using two approaches: either by collecting eggs laid by adult worms within a 2-3 h period, or by treating young

adult animals with an alkaline hypochlorite solution (composed by 0.25 M NaOH, 20 % household bleach containing  $\approx$  2.5 % NaClO, and H<sub>2</sub>O), for 7 min.

## 2.7 Generation of *C. elegans* mutant and double mutant strains

**Generation of the *crh-1* strain by CRISPR/Cas9.** To create the strain harboring a point mutation in the *crh-1* gene, clustered regularly interspaced short palindromic repeats (CRISPR) and CRISPR-associated protein 9 (Cas9) - CRISPR/Cas9 - technology was used [47], and the Custom Alt-R® CRISPR/Cas9 guide RNA tool (Integrated DNA Technologies, Coralville, IA, USA) to generate *crh1(mnh4)* CRISPR RNAs (crRNAs). crRNAs with high on-target efficiency and low off-target prediction scores, closest to target site, were chosen. To create a point mutation in the *crh-1* gene, introducing a premature stop codon just before the bZIP (DNA binding) domain of this protein, one crRNA was designed (GAUUCAUCUUCACCGUGCA). A single-stranded oligodeoxynucleotide (ssODN) comprising flanking regions of the target site was used as a repair template (CAATGACGGCGGCTCAATGCGAATGGGCGGT**TGAT**CGCTGCACGGTGAAGATGAATCGAATCGAAAGCG). This template aimed at introducing a premature stop codon (p.P35X) by point mutating g.9618G>**T** in exon 5 of *crh-1* gene (Y41C4A.4g.1, unspliced + UTR form = 10921 bp, was used to design the templates). An alteration in the PAM sequence was also introduced (g.9621C>**T**), which eliminates a restriction site of MspA1I enzyme in the WT, being useful for screening purposes. The injection was performed in WT worms, consisting of crRNA and ssODN *crh-1* specific oligos and crRNA and ssODN repair template for *dpy-10*, used as a marker for the efficiency of Cas9 protein activity. crRNAs, ssODNs and EnGen® Cas9 NLS, *S. pyogenes* enzyme (New England BioLabs, Ipswich, MA, USA) composed the mixture injected in worms. First, the injection mixture was incubated for 15 min at 37 °C and injections of WT young adult worms were performed as previously described [48]. After the injection, animals were maintained at 25 °C and the progeny screened, 72 h later, for the roller phenotype. Non-roller animals were isolated, thus avoiding the *dpy-10* mutation, and PCR was used to detect the *crh-1* mutation in the following F2 generation. After Sanger sequencing verification, the *crh-1* mutant strain generated harbored the following alterations: p.H37R and p.G38X, and an additional forty more nucleotides after the stop codon, followed by a substitution at g.9627C>G. Therefore, the stop codon was successfully introduced before the bZIP domain, although instead of a proline (P35) substitution, a glycine (P38) was substituted (p.P38X), predictably not impacting on the intended outcome - the expression of a truncated CRH-1 protein without the DNA binding (bZIP) domain.

**PCR assay for *crh-1* mutation detection.** Worm lysis was achieved by placing 20 worms in 20  $\mu$ L of lysis buffer (50 mM KCl, 10 mM Tris-base pH = 8.3, 2.5 mM MgCl<sub>2</sub>, 0.45 % Nonidet P-40 (IGEPAL), 0.45 % Tween 20, 0.01 % (w/v) gelatin) supplemented with 0.1 mg/mL of Proteinase K (20 mg/mL) before use. Worms were then placed at -80 °C for at least 30 min. After that, worms were heated at 65 °C for 1 h, followed by an inactivation of the Proteinase K at 95 °C for 15 min. For PCR, 2  $\mu$ L of the worm lysates were used with the Supreme NZYtaq II 2 $\times$  Green Master Mix (Cat. No. MB36003, NZYTech - Genes & Enzymes, Lisbon, Portugal) and specific primers at a final concentration of 0.2  $\mu$ M, according to the manufacturer's guidelines (see Table 3.1.2 for primers description). Cycling parameters were adjusted in the following manner: initial denaturation at 98 °C for 2 min (1 cycle); denaturation at 98 °C, annealing at 52 °C and extension at 72 °C for 30 s during 35 cycles, and a final extension for 5 min at 72 °C. To confirm the presence of PCR products, 10  $\mu$ L were run in a 1.5 % agarose electrophoresis gel. Then 10  $\mu$ L of PCR product were digested, for 2 h at 37 °C, with 0.1  $\mu$ L of MspA1I restriction enzyme (#R05775, New England BioLabs, Ipswich, MA, USA) in 2  $\mu$ L of CutSmart® Buffer (#B72045, New England BioLabs, Ipswich, MA, USA), per reaction. Then the digestion product was run in an agarose electrophoresis gel, in the same conditions as above described, to allow the distinction between WT (two PCR bands of 256 and 198 bp), heterozygous (three PCR bands of 480, 256 and 198 bp) and homozygous (one PCR band of 480 bp) *crh-1* mutant animals. Additional confirmation of the genotype was done by Sanger sequencing.

**Table 3.1.2 Primers used for *crh-1* mutation screening.**

Species	Gene (Sequence)	Forward primer (5'- 3')	Reverse primer (5'- 3')
<i>C. elegans</i>	<i>crh-1</i> (Y41C4A.4)	TCGAAACCATTGTTTTTCCAA	CCAAAAATTCCTTTTTCTTCCA

**Double mutant generation.** To create a *crh-1* mutant in the mutant ATXN3 background, *crh-1* male worms were generated by heat shock treatment. For that, five NGM plates with five *crh-1* L4 stage worms were incubated at 30 °C for 8 h, then returned at 20 °C. Three to four days after, the plates were screened for the presence of males. To generate the double mutant strain, thirteen *crh-1* males and three L4 hermaphrodites of mutant ATXN3 strain (AT3q130) were placed in a seeded NGM plate, for two days at 15 °C. Then, hermaphrodite animals were isolated and placed back at 20 °C. From the progeny, three days later, three to five hermaphrodite fluorescent worms (indicative of the presence of YFP-labelled ATXN3 of AT3q130 animals) were isolated and left 72 h at 20 °C. After this period, twenty-four to thirty-two fluorescent worms were single-out and screened, by PCR, to evaluate the presence of *crh-1*

mutation. From the cross, WT animals for *chr-1* mutation and the double mutants (harboring the *crh-1* mutation in mutant ATXN3 background) were obtained. All the strains used are described in Table 3.1.3.

**Table 3.1.3 *C. elegans* strains used in this study.** \*Strains specifically generated for the present work.

ID number	Strain name	Genotype	Observations
N2 (Bristol)	WT	WT	Obtained from CGC
MAC037/ AM519	ATXN3 WT (AT3q75)	<i>rmls237[P<sub>gef-1</sub>::AT3v1-1q75::yfp]</i>	
MAC001/ AM685	ATXN3 mutant (AT3q130)	<i>rmls263[P<sub>gef-1</sub>::AT3v1-1q130::yfp] II</i>	
MAC389*	<i>chr-1</i> mutant ( <i>crh-1</i> )	<i>crh-1(mnh4) III</i>	Alterations in <i>crh-1</i> gene: p.H37R, p.G38X, by CRISPR/Cas9 (aa numbers in isoform g)
MAC391*	AT3Q130; <i>crh-1</i>	<i>rmls263[P<sub>gef-1</sub>::AT3v1-1q130::yfp] II</i> ; <i>crh-1(mnh4) III</i>	Resulting from the cross between MAC001 and MAC389
MAC392*	ATXN3 mutant (AT3Q130 <i>crh-1</i> WT)	<i>rmls263[P<sub>gef-1</sub>::AT3v1-1q130::yfp] II</i>	Resulting from the cross between MAC001 and MAC389

## 2.8 Chronic treatment of the nematodes with citalopram (drug assay)

The chronic treatment of *C. elegans* strains with citalopram was performed in liquid culture, in a 96-well plate, as previously described [49]. Each well, with a final volume of 60 µL, contained an average of twenty-five N2 (WT), WT ATXN3 (AT3Q75), and *chr-1* animals, and an average of forty mutant ATXN3 (AT3q130) or double mutant (AT3q130;*chr-1*) animals, in egg stage, representing 15 µL of the final volume. The number of eggs used for the AT3q130 and AT3q130;*chr-1* animals was higher because a lower number of eggs hatch after the hypochlorite treatment in these strains. Drugs were added (25 µL) at the appropriate concentration: 5 or 25 µM citalopram hydrobromide (CAS. No. 59729-32-7, Kemprotec, Cumbria, UK), all prepared in dimethyl sulfoxide (DMSO, D8418, Sigma-Aldrich, St. Louis, MO, USA) - drug vehicle. *E. coli* OP50 bacteria was added (20 µL) to a final OD<sub>595</sub> of 0.9, measured in a microplate reader (NanoQuant Infinite M200 Microplate Reader, Tecan, Männedorf, Switzerland).

To obtain a population of synchronized worms, the alkaline hypochlorite solution method was used as described in section 2.6. Animals were washed in M9 buffer then resuspended in S-medium (S-Basal, 10 mM potassium citrate pH = 6, 10X trace metal solution, 3 mM CaCl<sub>2</sub>, 3 mM MgSO<sub>4</sub>), to

the appropriate egg number and transferred to the 96-well plate. The OP50 bacteria was grown in the conditions referred in section 2.6, pelleted by centrifugation ( $4000 \times g$ , at  $4\text{ }^{\circ}\text{C}$ , for 30 min) and finally inactivated by three cycles of freeze/thawing (in liquid nitrogen), and frozen at  $-80\text{ }^{\circ}\text{C}$  until further use. Before the drug assay, the OP50 pellets were resuspended in S-medium supplemented with 0.004 mg/mL cholesterol (C8667, Sigma-Aldrich, St. Louis, MO, USA), 0.5X penicillin-streptomycin (P4333, Sigma-Aldrich, St. Louis, MO, USA) and nystatin (N6261, Sigma-Aldrich, St. Louis, MO, USA). Worms were grown under continuous shaking at 180 rpm and at  $20\text{ }^{\circ}\text{C}$  (in a Shel Lab SI9R Orbital Shaking Incubator, Cornelius, OR, USA) for four days.

### 2.9 *C. elegans* motility assay

Four-day-old animals coming from the drug assay were transferred onto unseeded NGM plates (equilibrated at  $20\text{ }^{\circ}\text{C}$ ) and allowed to dry for 45 min before starting the assays. Motility assays were conducted at  $20\text{ }^{\circ}\text{C}$  as formerly reported [45, 50]. Simultaneously, about ten animals were placed in the center of a 1 cm diameter circle drawn in a seeded 35 mm NGM plate, equilibrated at  $20\text{ }^{\circ}\text{C}$ . Animals remaining inside the circle after 1 min were scored as locomotion defective. In each assay, a minimum of 50 animals were tested per condition. Since these behavior assays were run in triplicates or quadruplicates ( $n = 3$  or  $4$ ) a total of at least 150 worms were assayed. The percentage of locomotion defective animals per condition was calculated by dividing the number of worms inside the circle after 1 min by the total number of worms analyzed.

### 2.10 *Statistical analysis*

The statistical analysis was performed using the IBM© SPSS® software, version 26 (IBM, Armonk, NY, USA) and graphical imaging developed using GraphPad Prism 8 software, version 8.0.1 (GraphPad Software, San Diego, CA, USA). Normal distribution of continuous variables was evaluated with Kolmogorov-Smirnov or Shapiro-Wilk's test (chosen according to the  $n$  value of the experiment analyzed). Homogeneity of variances between groups was confirmed by performing Levene's test. Deviation from normality and homogeneity of variances was assumed when one of the above-mentioned tests showed a  $p \leq 0.05$ . As previous assumptions were not met, non-parametric tests were performed: independent sample Kruskal-Wallis  $H$  test (Figure 3.1.4C) and independent sample Mann-Whitney  $U$  test (Figure 3.1.4D and E). Also, a bootstrap sampling with bias correction (BCa) was performed when previous assumptions were not verified, followed by a robust ANOVA (using R batch for SPSS) with Brown-Forsythe correction, due to sample size lower than 6 (Figure 3.1.7).

### 3. Results

#### 3.1 Transcriptomic analysis of mouse MJD model reveals alterations in serotonergic signaling

After gathering observations that citalopram treatment has a beneficial effect on MJD animal models at behavior and neuropathological levels (as evidenced in chapter 2 of this thesis [32] and in previous reports [30, 51]), we wanted to further understand the MOA of citalopram and its impact in brain cells by determining which genes or cellular pathways were altered upon treatment. In this way, we performed a transcriptomic analysis in RNA extracted from the striatum of 34-week-old citalopram-treated and non-treated transgenic MJD mice (CMVMJD135). Although the striatum is not a major affected brain region in MJD, there are several pathological elements, including intranuclear inclusions, in MJD patients described in this area [52]. Furthermore, the striatum is involved in the control of movement and is composed by the caudate and putamen nuclei, described to be atrophic in MJD [53]. Importantly, this region communicates with other relevant brain areas, including the substantia nigra and global pallidus, also known to be affected in this disease [54]. Animals were treated chronically with citalopram or vehicle, and treatment was initiated at a pre-symptomatic age (5 weeks) lasting for 29 weeks. The overall gene expression profile among the groups analyzed in this experiment, WT vehicle (WT), CMVMJD135 vehicle (Tg) and CMVMJD135 citalopram-treated (Tg cit) is distinct (Figure 3.1.1).

Different comparisons were studied, namely: WT *versus* transgenic MJD mice, to evaluate changes caused by the expression of mutant ATXN3 proteins; transgenic *versus* transgenic-treated mice, to determine the changes triggered by citalopram chronic treatment; and the comparison between WT and transgenic treated mice, to determine if any of the changes in gene expression were restored to WT levels by citalopram treatment. The differential gene expression analysis was based on fold changes (absolute  $\log_2$  FC of at least 1) and p-value  $\leq 0.05$ . Only 69 genes (45 up- and 24 downregulated) were found to be differentially expressed when comparing WT to transgenic mice, while this number was substantially larger upon citalopram chronic treatment, for which 489 up- and 682 downregulated genes were observed (Figure 3.1.2), revealing that citalopram treatment is producing considerable changes in gene expression of MJD animals.



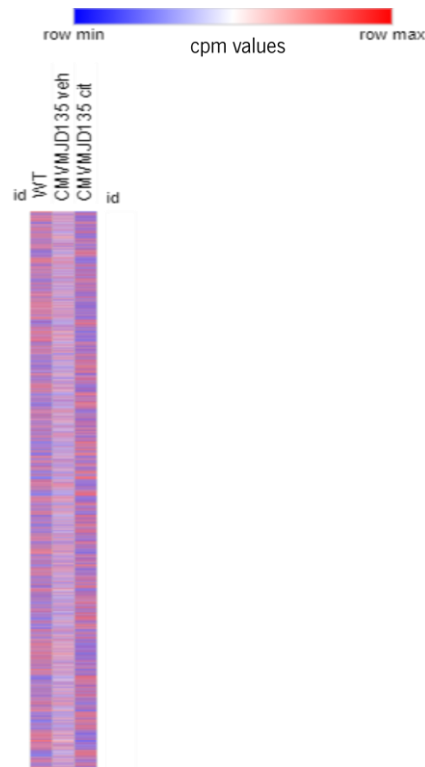


**Figure 3.1.1 Different mRNA expression profile between groups in the striatum of MJD mice.** Each row represents the mean of count per millions (cpm) values, for a gene, in each group ( $n = 5$  WT, 4 Tg and 3 Tg cit). The total of genes identified in the RNA-seq (15145) are represented (one row corresponds to one gene) and a relative color scheme is used in which the row minimum and maximum values are converted to colors. Heatmap generated from CLUE MORPHEUS [42].

Using Ingenuity Pathway Analysis (IPA) software [41] several canonical pathways were found to be altered (Figure 3.1.3). In transgenic animals, transcriptomic alterations were observed in pathways related to hormones, the immune system, iron homeostasis, neuroprotection, responses to stress-related signals and serotonergic signaling (Figure 3.1.3A). Upon citalopram treatment a higher number of pathways were found to be altered. Among those, pathways related to DNA repair, G protein-coupled receptors, growth factors, mitochondria/cell death and vital signal transduction pathways were identified (Figure 3.1.3B).

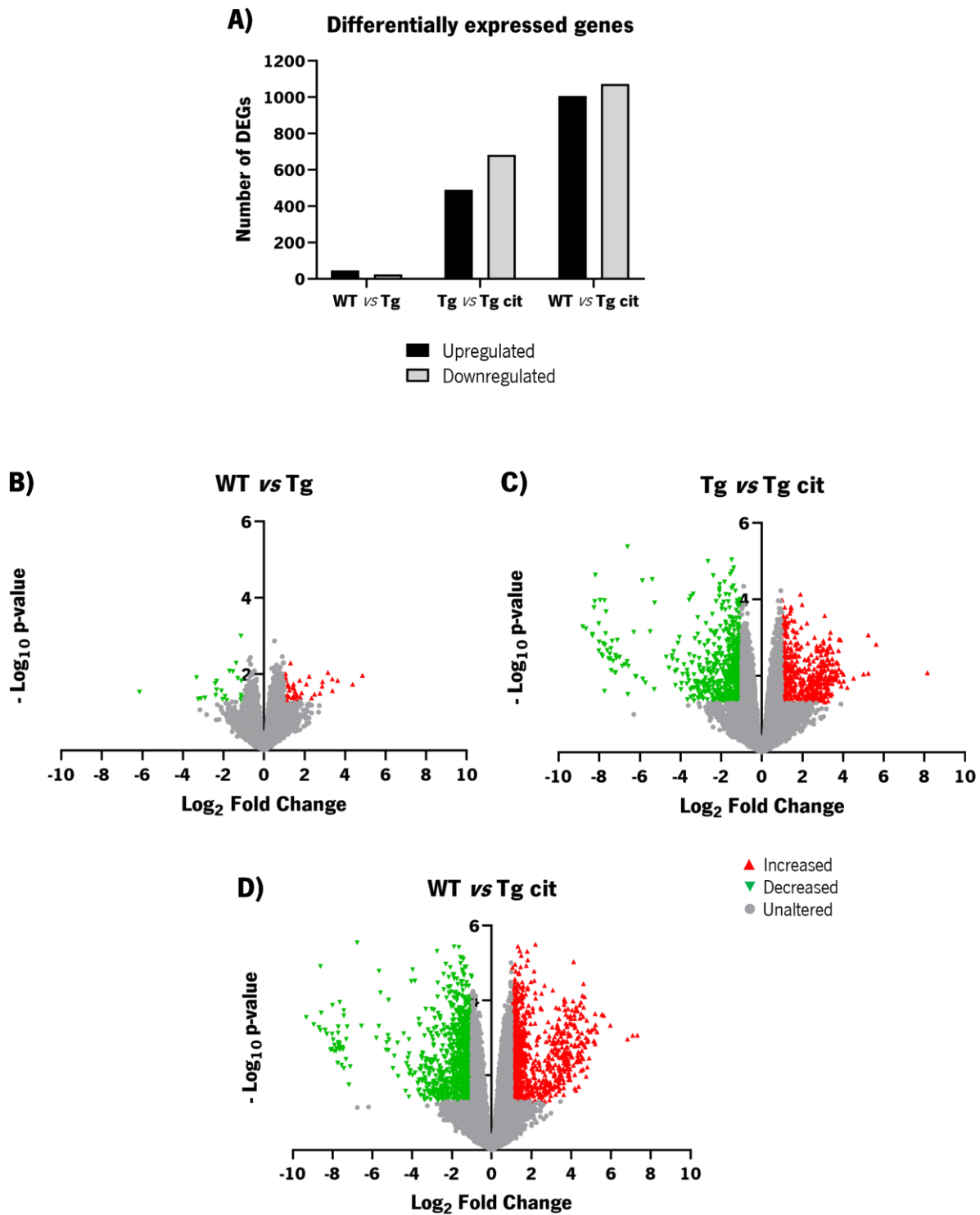


**Figure 3.1.2 Expression profile of CMVMJD135 transgenic (Tg) mice is altered upon citalopram treatment.**

**A)** Number of differentially expressed genes - DEGs (up- and downregulated) in each comparison group. An increase in these genes is observed upon citalopram treatment. **B)** WT vs Tg, **C)** Tg vs Tg cit, **and D)** WT vs Tg cit volcano plots of all genes identified in the RNA-seq, evidencing the altered expression of significant genes (decreased in green and increased in red).

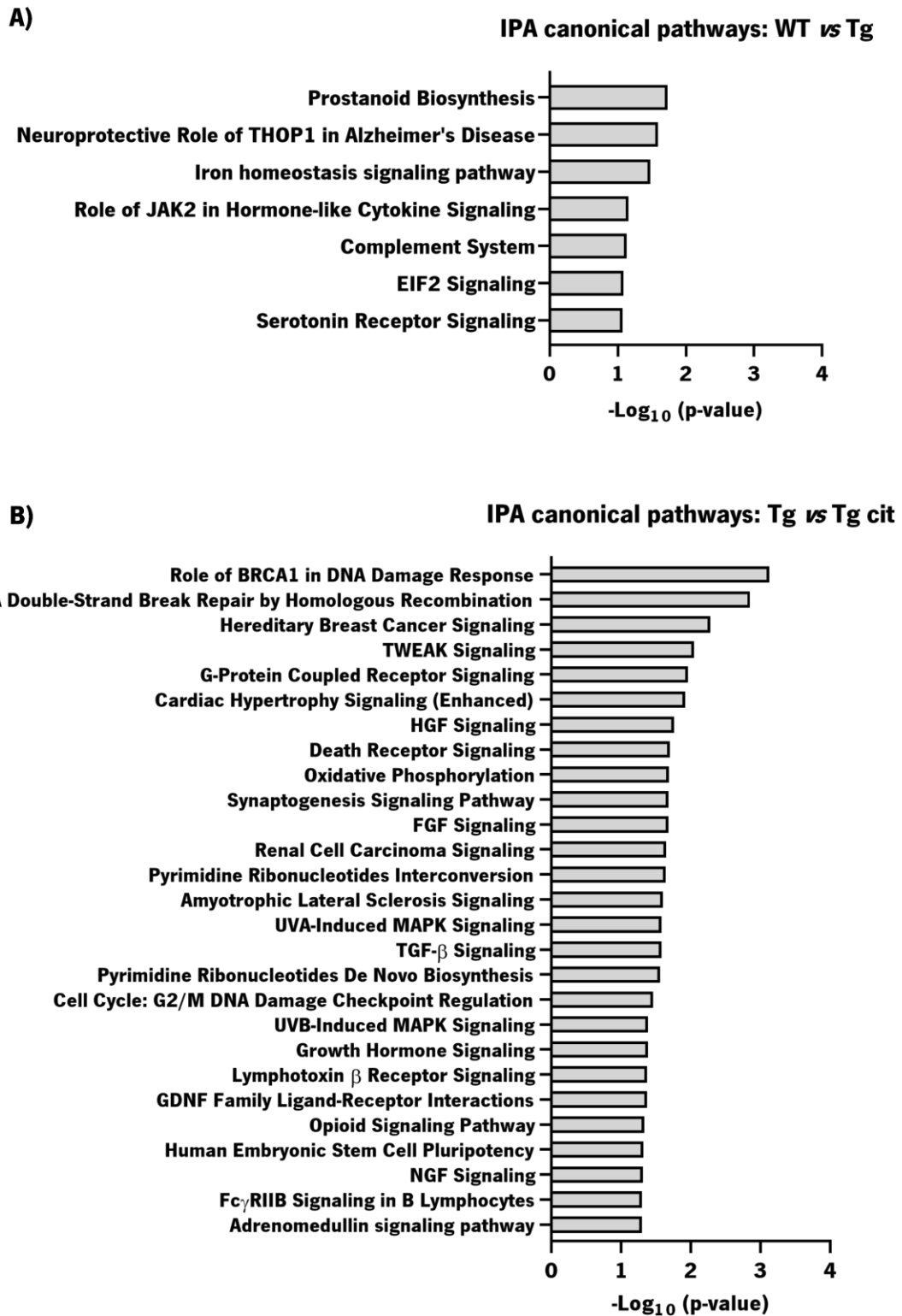


**Figure 3.1.3 Serotonergic signaling and other pathways alterations in transgenic mice and upon citalopram chronic treatment. A)** Canonical pathways altered in WT *versus* transgenic CMVMJD135 mice (WT *vs* Tg) comparison. **B)** Canonical pathways altered in transgenic CMVMJD135 vehicle- and citalopram-treated mice (Tg *vs* Tg cit). Analysis conducted on IPA software [41].

As an SSRI, citalopram acts directly on serotonin neurotransmission and, notably, pathways related to this process were found altered in MJD and upon treatment: the serotonin receptor signaling and the G protein-coupled receptor signaling, respectively (Figure 3.1.3). Interestingly, a subset of genes (represented by the 10 common genes between WT *vs* Tg and Tg *vs* Tg cit comparisons, Figure 3.1.4A) altered in the disease and whose expression was restored to WT levels by citalopram upon chronic treatment (Figure 3.1.4B), included a serotonin receptor gene, the *Htr1a* (or *5-HT<sub>1A</sub>R*, in human). Moreover, a decreased expression of the *5-HT<sub>2A</sub>* receptor (*5-HT<sub>2A</sub>R*) was observed, but only upon citalopram treatment, contributing to the idea that this drug could trigger adaptive changes in serotonin brain signaling through modulation of specific 5-HT receptors. This is in accordance with the findings from the canonical pathway analysis, unveiling a possible citalopram-induced adaptation of this signaling in the brain at the molecular level.

Validation of RNA-seq results for *5-HT<sub>1A</sub>R* was also attempted in mouse samples by qRT-PCR, and our preliminary findings reproduced the results obtained in the transcriptomic analysis, although only to a certain extent (Figure 3.1.4C). We are currently validating these results in an independent group of MJD mice upon chronic citalopram treatment.

To further investigate the clinical relevance of this receptor in the human disease, we determined expression levels of this receptor in the *post-mortem* brain tissue of healthy individuals and MJD patients. Although no statistical significance was observed, *5-HT<sub>1A</sub>R* expression levels were found to be tendentially reduced in the striatum and cerebellum of MJD patients (Figure 3.1.4D and E, respectively). The reduced number of post-mortem brain tissue samples available and difficulties in RNA extraction due to tissue preservation conditions may have contributed to this.

### **3.2 Alterations in genes associated to *5-HT<sub>1A</sub>R* transduction pathways upon citalopram chronic treatment**

Associated to the *5-HT<sub>1A</sub>R*, some signal transduction pathways have been described, which can impact on several cellular responses [55]. Some early studies indicated that *5-HT<sub>1A</sub>R*s were coupled to the inhibitory G proteins ( $G_{\alpha/o}$ ) to inhibit adenylyl cyclase (AC) leading to the reduction in cAMP levels [56]. Other studies have shown a role for this G protein-coupled receptor in the regulation not only of the mitogen-activated protein kinases (MAPK), but also of the phosphoinositide 3-kinase (PI3K)-PKB/Akt pathway [57]. Although these signaling pathways typically induce post-translational modifications, it is possible that downstream changes in gene expression may also occur. To further explore the involvement

of downstream pathways of 5-HT<sub>1A</sub>R in citalopram's MOA, we searched for genes encoding proteins belonging to those pathways, that were differentially expressed in our RNA-seq data.

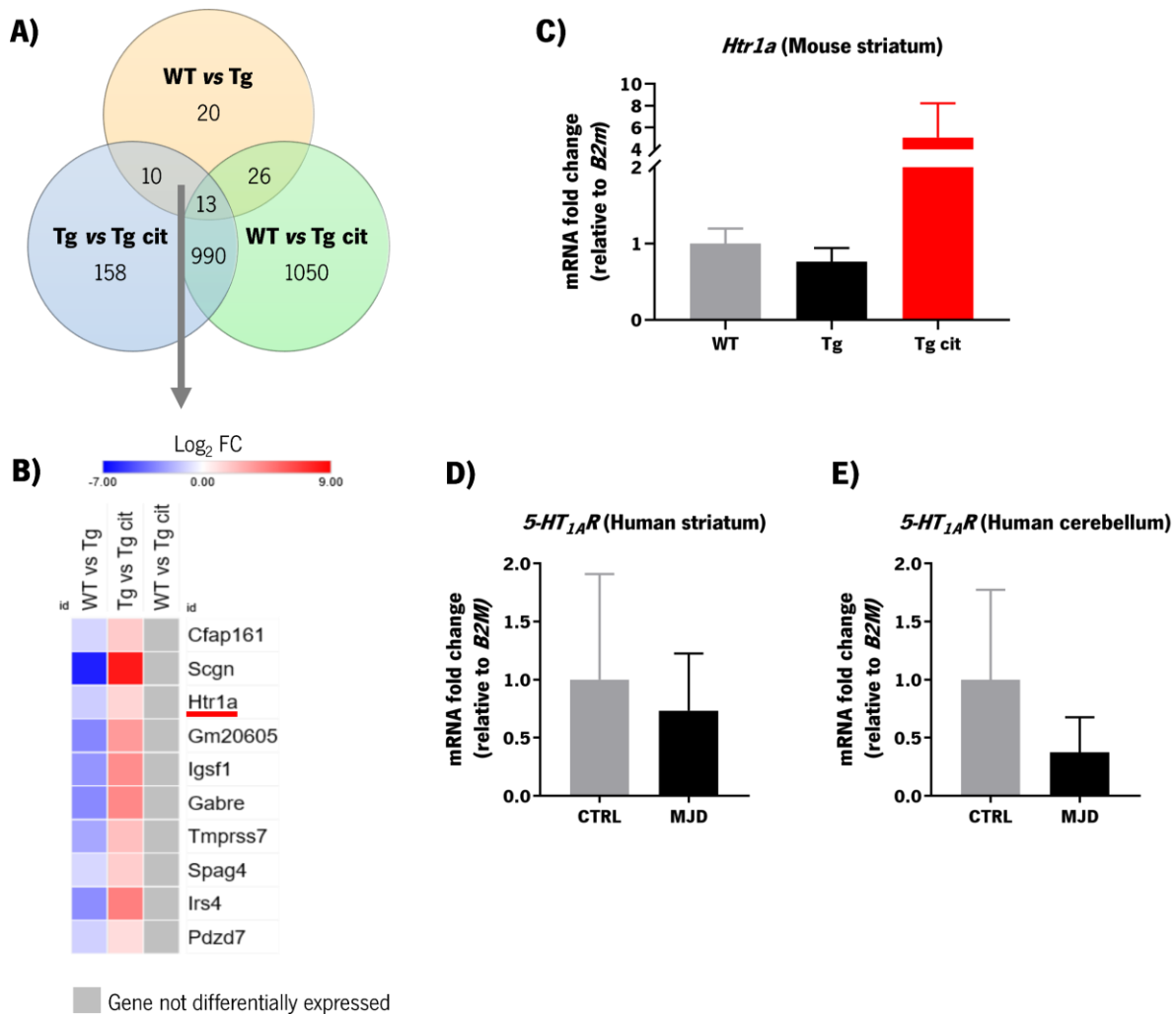
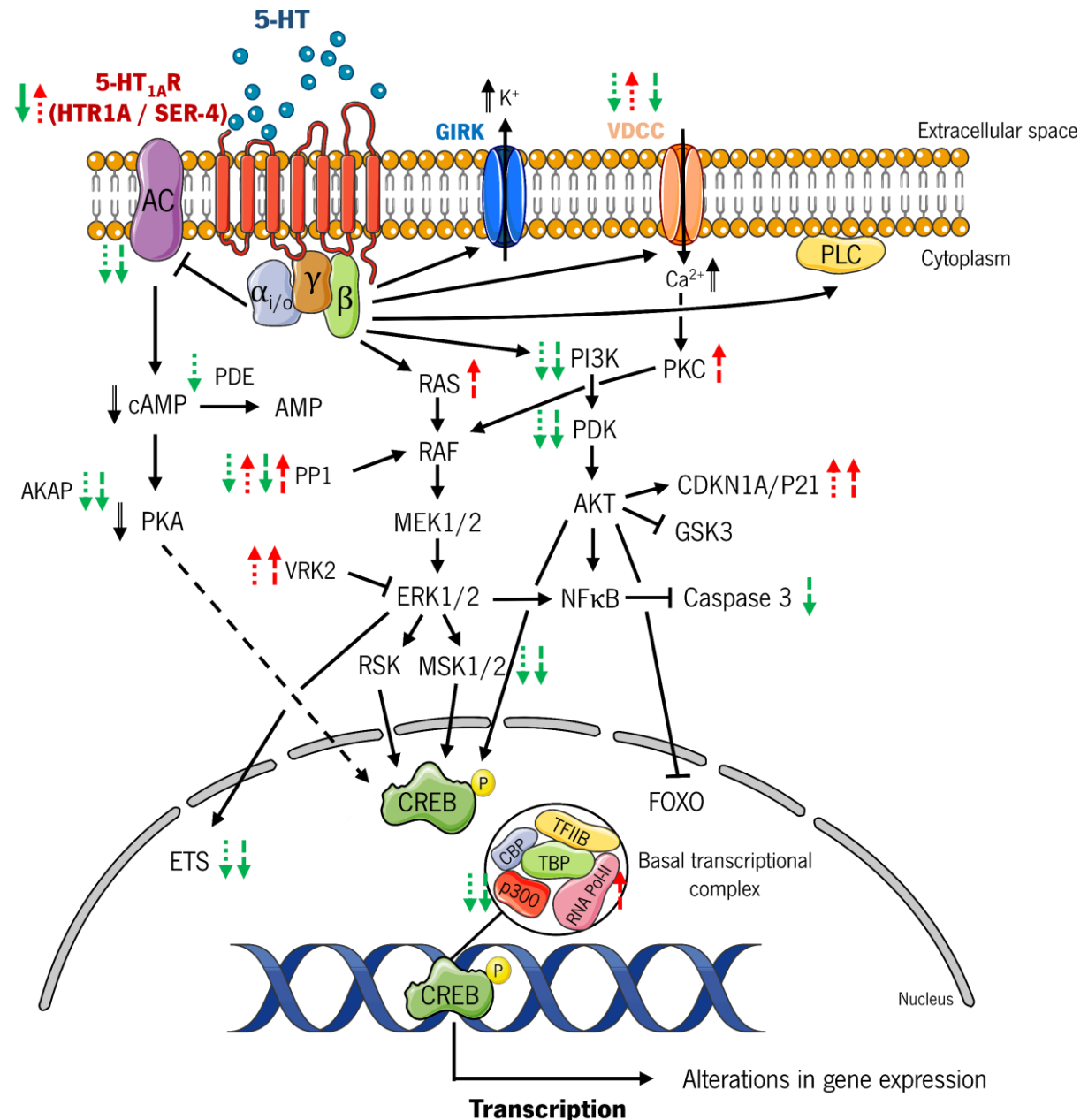


**Figure 3.1.4 Serotonin receptor *Htr1a*/5-HT<sub>1A</sub>R gene expression is altered in CMVMJD135 mice and restored upon citalopram treatment. A)** Venn diagram of the differentially expressed genes (DEGs) distribution across the different groups. **B)** Heatmap [42] showing the ten common genes between WT vs Tg and Tg vs Tg cit comparisons. All genes are downregulated (blue) in transgenic mice and upregulated (red) upon citalopram treatment, being restored to WT levels, since there are no alterations in the expression of those genes (grey) when WT is compared to transgenic treated animals (WT vs Tg cit). **C)** Validation of the *Htr1a*/5-HT<sub>1A</sub>R gene expression in the striatum of 34-week-old mice ( $n = 4$  WT, 3 Tg, 3 Tg cit), by qRT-PCR. Data presented as mean  $\pm$  SEM, \* $p \leq 0.05$ , \*\* $p \leq 0.01$ , \*\*\* $p < 0.001$  (Kruskal-Wallis  $H$  test:  $H(2) = 5.185$ ,  $p = 0.075$ ;  $\eta^2 = 0.454$ ). mRNA expression of the *Htr1a*/5-HT<sub>1A</sub>R gene, determined by qRT-PCR, in the **D)** striatum ( $n = 4$  CTRL, 3 MJD; mean  $\pm$  SEM), Mann-Whitney  $U$  Test:  $U = 8.000$ ,  $n_1 = 4$ ,  $n_2 = 3$ ,  $p = 0.629$ ;  $\eta^2 = 0.071$  and **E)** cerebellum ( $n = 5$  CTRL, 3 MJD, mean  $\pm$  SEM), Mann-Whitney  $U$  Test:  $U = 8.000$ ,  $n_1 = 5$ ,  $n_2 = 3$ ,  $p = 1.000$ ;  $\eta^2 = 0.003$ ), of controls (CTRL) and MJD patients (MJD). Bar graphs represent fold changes of mRNA levels relatively to *B2m*/*B2M* gene used as an internal control.

A simplified representative scheme of 5-HT<sub>1A</sub>R transduction pathways (Figure 3.1.5) was made, highlighting the DEGs found in our analysis. Remarkably, changes in genes involved in all the 5-HT<sub>1A</sub>R transduction pathways were observed namely in the cAMP, the MAPK/extracellular-signal activated kinase (ERK), and the PI3K-PKB/Akt pathways. Within the cAMP signaling pathway, a decrease in AC, cyclic nucleotide phosphodiesterase (PDE) and PKA-anchoring proteins (AKAPs) expression upon citalopram treatment was verified. In the MAPK/ERK pathway, an increase in small guanosine triphosphate-(GTP)ase RAF was observed in WT *vs* Tg citalopram-treated comparison. Increased expression of vaccinia-related kinase 2 (VRK2) and differential expression of protein phosphatases 1 (PP1)-related molecules was also observed in our dataset, upon treatment. A decrease in ribosomal protein S6 kinase A5 (RPS6KA5/MSK1) and in ETS Proto-Oncogene 1 (ETS1) transcription factor was also seen. In the PI3K-PKB/Akt pathway, a decreased expression of PI3K and 3'-phosphoinositide-dependent kinase (PDK) was found. Also, possibly linked to this pathway as side target of the PI3K-PKB/Akt pathway, cyclin dependent kinase inhibitor 1A (CDKN1A) and caspase 3 (this last one only in WT *vs* Tg cit) were found to have increased and decreased expression upon treatment, respectively. Besides that, some voltage-dependent calcium channels (VDCCs) were found to be altered upon treatment and an increase in protein kinase c (PKC) was also observed, but this last one only between WT *vs* Tg cit (Figure 3.1.5). With the exception of the 5-HT<sub>1A</sub>R, which was found to be downregulated in Tg mice, most of the changes observed corresponded to the effect of citalopram chronic treatment, since the DEGs are found in the Tg *vs* Tg cit and WT *vs* Tg cit comparisons; this last comparison being suggestive of putative alterations caused by citalopram treatment, independently of the pathology, in the cases where differential expression is not observed in the WT *vs* Tg and Tg *vs* Tg cit comparisons (perhaps due to high variability in gene counts of Tg animals). This will require additional validation. These observations may not be sufficient to conclude on the relevance of one pathway over the other, as there is a strong interplay/crosstalk between them, however our analysis suggested possible downstream transcription factors of relevance for this mechanism. Of note, there is convergence of these transduction signal pathways towards the cAMP-response element binding protein (CREB), the expression of some genes encoding proteins of its basal transcriptional complex being altered (namely E1A binding protein p300 (p300) and RNA Polymerase II (RNA Pol-II)), supporting a possible role of this transcription factor in this process. Additionally, alterations in RPS6KA5/MSK1 expression could also point to the involvement of CREB, since this transcription factor is an RPS6KA5/MSK1 substrate [58]. Overall, the observed molecular changes, suggest that the 5-HT<sub>1A</sub>R and its downstream signaling cascades could indeed be important for the neuroprotective role of citalopram in MJD.



**Legend:**

- |  |  |
|--|--|
| <u>Black arrows</u>                    | <u>Other arrows : mRNA increase (up/red) / decrease (down/green)</u> |
| → Direct interaction                   | → WT vs Tg   |
| - - → Indirect interaction             | .... → Tg vs Tg cit  |
| ⇒ Described effect (increase/decrease) | - - - - → WT vs Tg cit   |
| ⊥ Inhibition                           |  |

**Figure 3.1.5 Citalopram-induced molecular alterations in the 5-HT<sub>1A</sub>R transduction signaling pathways in MJD transgenic mice.** Schematic representation of the serotonin 5-HT<sub>1A</sub> receptor (5-HT<sub>1A</sub>R/HTR1A and SER-4 in *C. elegans*)-dependent signaling in cells, with the altered expression of some genes based on mouse RNA-seq data. 5-HT<sub>1A</sub>R primarily couples to heterotrimeric guanosine triphosphate (GTP)-binding protein (G protein) G<sub>i/o</sub> and its activation function to inhibit adenylyl cyclase (AC), consequently altering signaling through the cyclic adenosine 3',5'-monophosphate (cAMP)

pathway. Two other main pathways are described to be 5-HT<sub>1A</sub>R signaling pathways: the mitogen-activated protein kinase (MAPK)/extracellular-signal activated kinase (ERK), and the phosphoinositide 3-kinase (PI3K)-PKB/Akt pathways. As depicted, the mRNA expression of several molecules of those signaling pathways were found to be differentially expressed. A convergence of these main pathways towards transcription factors (TFs) is noted, namely the cAMP pathway binding protein (CREB), for which changes within its basal transcriptional machinery components, such as in E1A binding protein p300 (p300) and RNA Polymerase II (RNA Pol-II), are observed. In addition, 5-HT<sub>1A</sub>R can also influence G protein-coupled inwardly rectifying potassium (GIRK) channels, increasing potassium (K<sup>+</sup>) extracellularly. Alterations in voltage-dependent calcium channels (VDCCs) were also found, and 5-HT<sub>1A</sub>R activation is known to lead to increased calcium (Ca<sup>2+</sup>) levels. Activation of phospholipase C (PLC) is also mediated by 5-HT<sub>1A</sub>Rs. 5HT - serotonin; PDE - cyclic nucleotide phosphodiesterase; AMP - adenosine monophosphate; PKA - protein kinase A; AKAP - PKA-anchoring protein; RAS - family of small GTP binding proteins; RAF - serine/threonine kinase; MEK1/2 - mitogen-activated protein kinase 1/2; ERK1/2 - extracellular signal-regulated kinase 1/2; RSK - ribosomal s6 kinase; MSK1/2 - mitogen- and stress-activated kinases 1/2; ETS - ETS-domain family of transcription factor; PKC - protein kinase C; PDK - 3'-phosphoinositide-dependent kinase; AKT - protein kinase B; CDKN1A - cyclin dependent kinase inhibitor 1A; GSK3 - glycogen synthase kinase 3; NF-κB - nuclear factor kappa B; FOXO - forkhead box O transcription factors. Image constructed using the free Smart SERVIER medical art database [59].

### **3.3 Possible role of CREB transcriptional program in citalopram-mediated suppression of ATXN3-mediated pathogenesis**

The 5-HT<sub>1A</sub>R transduction pathways are multiple and a lot of players are known to be involved. One example is the activation of the of the transcription factor CREB. This widely studied transcription factor has been known for its role in depression, stress and anxiety [60]. Interestingly, CREB is a substrate for a wide range of cellular kinases including PKA [61], protein kinase RSK [62], AKT [63] and MSK1[64], which are effectors of 5-HT<sub>1A</sub>R-mediated downstream signaling (Figure 3.1.5). Moreover, CREB is essential for a multitude of cellular processes, impacting on several tissues, including the nervous system [65], by regulating transcription of its target genes. Therefore, we hypothesized that if citalopram was regulating the 5-HT<sub>1A</sub>R and somehow activating its downstream pathways, CREB could also be an important player in the suppression of mutant ATXN3-mediated proteotoxicity in MJD animal models upon citalopram treatment.

In order to test this, we first determined if CREB targets previously described in the literature were represented in our transcriptomic analysis. Several reports used different strategies to identify possible CREB targets: some more based on genome-wide/bioinformatic approaches [66, 67], others based on stimulating cells with compounds known to induce this transcription factor [68, 69], and also the combination of both approaches [70]. By merging the data retrieved from these studies, we identified 4522 genes as possible CREB targets. From this list, 85 % were identified in our RNA-seq data,



representing  $\approx 26\%$  of the total of genes detected in our transcriptomic analysis (Figure 3.1.6A). Regarding the total number of DEGs detected in our study, approximately 20% were CREB targets (Figure 3.1.6B), suggesting no enrichment in this category of genes. Moreover, when looking further into the different comparisons, 10% of the genes with altered expression in transgenic mice compared to WT were putative target genes of this transcription factor, a number that increases up to 18% upon citalopram treatment (Figure 3.1.6C and D, respectively), suggesting that citalopram could be modulating the action of this factor by activating a subset of its target genes. Nevertheless, we must be careful in this interpretation since the total number of genes in each comparison analyzed is very different.

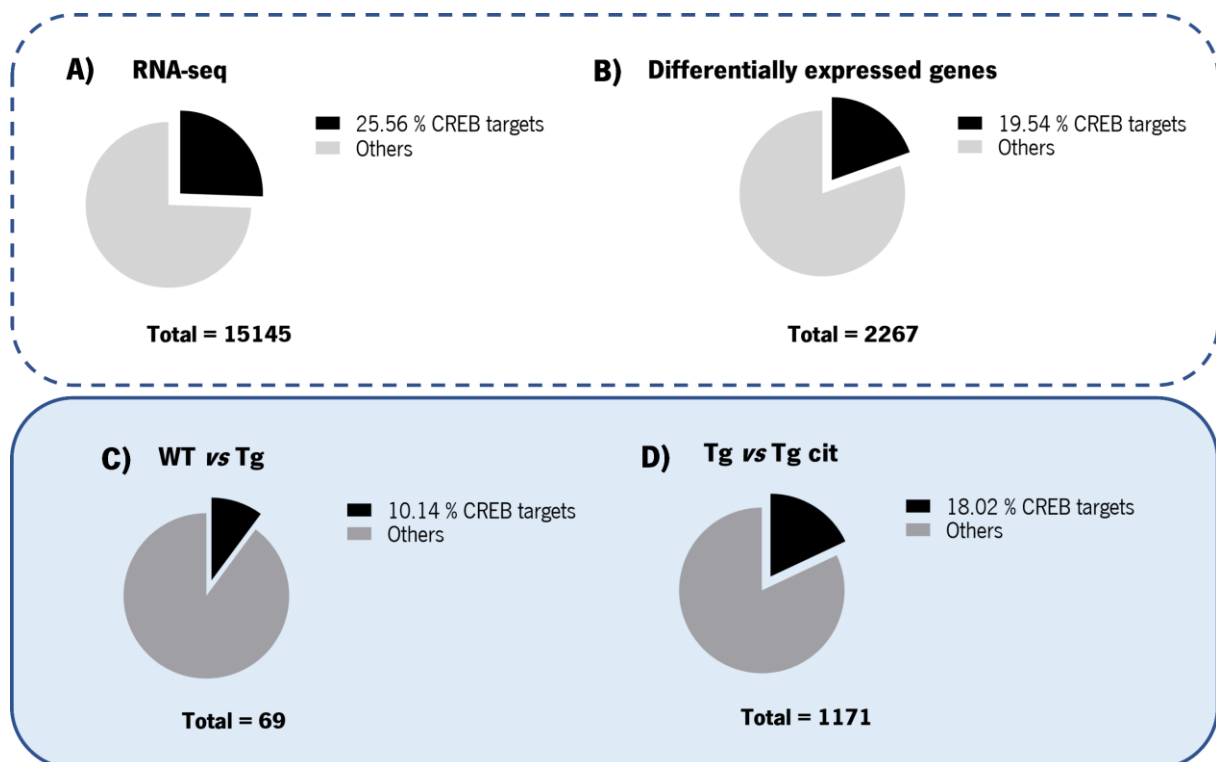


**Figure 3.1.6 Presence of CREB target genes in the mouse striatum transcriptomic analysis.** Percentage of possible CREB target genes found in **A)** the RNA-seq total data, **B)** the differentially expressed genes (DEGs), **C)** altered in the transgenic mice (WT vs Tg) and **D)** altered upon citalopram treatment (WT vs Tg cit).

The function of the genes whose transcription is CREB-dependent can be diverse. Table 3.1.4 lists the ten top up- and downregulated genes with higher fold changes, in the comparisons of interest, classified as possible CREB targets based on our literature search. Note that only seven CREB target genes were found in the WT vs Tg comparison, while 211 were found in transgenic treated animals (Tg vs Tg cit comparison). In the literature, the existent view is that CREB functions as an effector of 5-HT<sub>1A</sub>R-mediated signaling. For instance, it has been shown that 5-HT<sub>1A</sub>R activation in the hippocampus

**Table 3.1.4 List of a subset of CREB target genes found in the transcriptomic analysis.** Based on the most altered expression in each comparison of interest ( $\text{Log}_2$  fold change (FC)).

Comparison	Effect	Gene symbol	Description	$\text{Log}_2$ FC
WT vs Tg	Up	<i>A430005L14Rik</i>	RIKEN cDNA A430005L14 gene	1.31
		<i>Csrp2</i>	Cysteine and glycine-rich protein 2	1.21
		<i>Pth1</i>	Peptidyl-tRNA hydrolase 1 homolog	1.06
	Down	<i>Htr1a</i>	5-hydroxytryptamine (serotonin) receptor 1A	-1.37
		<i>Pdzd7</i>	PDZ domain containing 7	-1.30
		<i>Spag4</i>	Sperm associated antigen 4	-1.11
		<i>Cfap161</i>	Cilia and flagella associated protein 161	-1.14
Tg vs Tg cit	Up	<i>Wdr86</i>	WD repeat domain 86	3.44
		<i>Ngb</i>	Neuroglobin	2.91
		<i>Amd2</i>	S-adenosylmethionine decarboxylase 2	2.90
		<i>Greb1</i>	Gene regulated by estrogen in breast cancer protein	2.78
		<i>Cebpd</i>	CCAAT/enhancer binding protein (C/EBP), delta	2.76
		<i>Cartpt</i>	CART prepropeptide	2.70
		<i>Nr2f2</i>	Nuclear receptor subfamily 2, group F, member 2	2.47
		<i>Cck</i>	Cholecystokinin	2.35
		<i>Rbm47</i>	RNA binding motif protein 47	2.32
		<i>Tomm6</i>	Translocase of outer mitochondrial membrane 6 homolog (yeast)	2.25
	Down	<i>Ttc29</i>	Tetratricopeptide repeat domain 29	-8.26
		<i>Slc39a5</i>	Solute carrier family 39 (metal ion transporter), member 5	-7.42
		<i>Atrip</i>	ATR interacting protein	-7.20
		<i>Ankfn1</i>	Ankyrin-repeat and fibronectin type III domain containing 1	-4.57
		<i>Oprm1</i>	Opioid receptor, mu 1	-3.59
		<i>Exo1</i>	Exonuclease 1	-3.16
		<i>Fzd3</i>	Frizzled class receptor 3	-3.07
		<i>Inhba</i>	Inhibin beta-A	-2.78
		<i>Dbf4</i>	DBF4 zinc finger	-2.69
<i>Gucy1a2</i>	Guanylate cyclase 1, soluble, alpha 2	-2.58		

upregulates levels of phosphorylated CREB [71]. Interestingly, the *5-HT<sub>1A</sub>R/Htr1a* gene itself is among the potential CREB targets found in our analysis (being referred in only one study, which reports a

“comprehensive definition of transcription factor binding sites in a metazoan species” based on forskolin-treated PC12 cells and CREB binding sites near or within annotated genes [70]). This raises the possibility that CREB could also regulate *5-HT<sub>1A</sub>R* transcription in specific conditions, although, from our knowledge, this has not been demonstrated yet.

Among the DEGs, the *Csrp2* gene, altered in transgenic animals, is a member of the cysteine-rich protein (CSRP) family, encoding a group of LIM domain proteins, and it was described as important for development and cellular growth and differentiation. In addition, it has been shown that CSRP2 is regulated by heat shock factor 1 (HSF1) and could hypothetically play a role in the modulation of protein aggregation [72]. Other CREB target genes in this list could have relevant functions in the context of MJD. The *Ttc29* gene, encoding a conserved axonemal dynein protein [73], belongs to a family of proteins harboring a tetratricopeptide repeat (TPR) domain, which are crucial for the function of the molecular chaperone heat shock protein 90 (Hsp90) [74]. *Tomm6* encoding a translocase of the outer mitochondrial membrane and part of the TOM complex, could play a role in stress situations and could be implicated in the activation of responses such as the unfolded protein response of the mitochondria (UPR<sup>mt</sup>) [75]. Although it seems that we did not find an effective enrichment of CREB targets in the DEGs in comparison to the total CREB targets detected in our RNA-seq experiment, a subset of genes activated by CREB could be crucial for the therapeutic efficacy of citalopram in animal models of MJD.

To test whether CREB transcription is essential for the MOA of citalopram *in vivo*, a *C. elegans* strain bearing a null mutation in the CREB gene, *crh-1(mnh4)*, was generated using the CRISPR/Cas9 technology, and then crossed with animals expressing mutant ATXN3 proteins in the *C. elegans* nervous system (the AT3q130 model). By combining compound treatment with genetic ablation of *CREB/crh-1*, results showed that although *crh-1* mutation *per se* does not affect the phenotype of the transgenic worms, citalopram loses its effect on locomotor behavior when *crh-1* is mutated in ATXN3 worms (Figure 3.1.7), suggesting that this drug is, at least partially, dependent on CREB to improve the locomotion of ATXN3 animals. Further experiments will be needed to confirm these preliminary results.

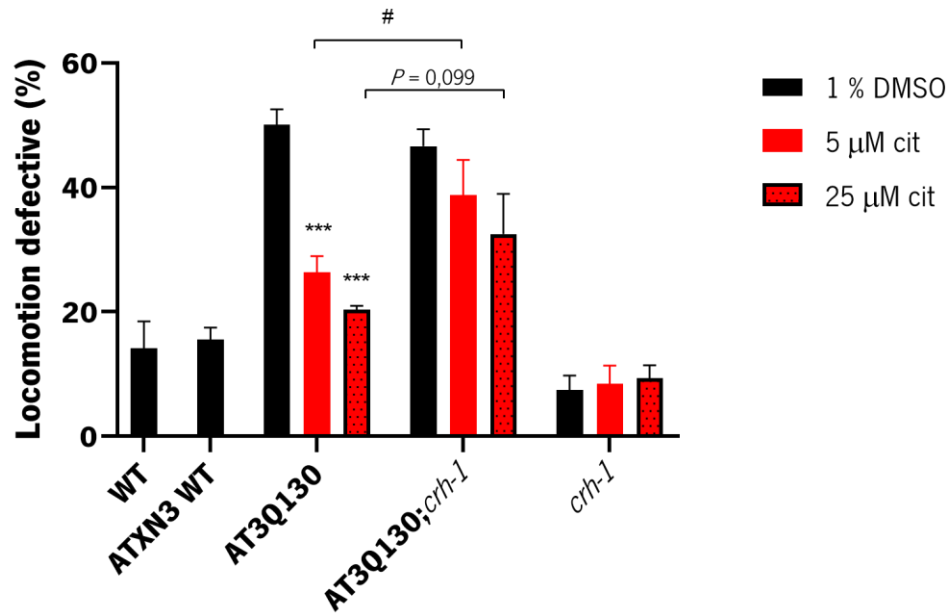


**Figure 3.1.7 Citalopram is dependent on CREB/CRH-1 transcription factor to improve motility on ATXN3 animals.** Citalopram (5 and 25 μM) is able to improve to locomotor behavior of AT3Q130 worms but this effect is lost when *crh-1* is mutated in ATXN3 worms (AT3Q130;*crh-1*). Represented is mean ± SEM ( $n = 4$ ), \* $P \leq 0.05$ , \*\* $P \leq 0.01$ , \*\*\* $P < 0.001$  comparing drug treatment with vehicle, and # $P \leq 0.05$ , ## $P \leq 0.01$ , ### $P \leq 0.001$  comparing strain effect within the same drug treatment (Factorial ANOVA with Brown-Forsythe correction):  $F(13, 22.527) = 18.018$ ,  $P < 0.001$ ,  $\omega^2 p = 0.858$ . cit - citalopram; DMSO - dimethyl sulfoxide.

#### 4. Discussion

In this study, we aimed at understanding the MOA of citalopram in the context of ATXN3 pathogenesis, going beyond the already described inhibition of the SERT transporter and the consequently increased levels of 5-HT at the synaptic cleft, induced by SSRI antidepressants. We took advantage of MJD animal models developed in our lab, the CMVMJD135 mouse model and the AT3q130 *C. elegans* model, to perform transcriptomic analysis, and validate candidate target genes, respectively. This work has contributed to uncover novel actors in the pathology of MJD, one of several polyglutamine disorders, contributing to a better understanding of the disease and possibly paving the way to the modification in the actual treatment for this group of pathologies.

The need for treatments for neurodegenerative disorders is at its pinnacle, since those impose an enormous medical and social burden as the number of patients with these diagnoses constantly increases worldwide [76]. In this panorama, the repurposing of drugs has become an attractive strategy for finding new medicines, that benefited from previous investments while making the transition into clinical activities less risky and in a shorter timeline [77]. Citalopram is used for the treatment of depression, to prevent

relapses [78], but also used to treat other psychiatric conditions such as, anxiety [79], panic perturbations (with or without agoraphobia) [80] or even obsessive-compulsive disorder (OCD) [81]. Patients with neurodegenerative diseases are often prescribed antidepressants for their depressive state [29], so it is important to clarify how antidepressants exert the neuroprotective effects that have been associated to their administration [16-28]. The canonical mechanism of action of SSRIs is based on SERT transporter blockade in pre-synaptic neurons, which impairs the reuptake of 5-HT from the synaptic cleft, thus increasing its concentration in this local. So, how does a single mode of action explain the clinical improvements in distinct pathologies? First, we must take into account that 5-HT is the most widely distributed neurotransmitter in the brain [82, 83] and that the serotonergic system arises from nine raphe nuclei (B1-B9) that cluster 5-HT producing neurons. Some of those neurons, from the rostral (medial and dorsal) raphe, project axons primarily to the forebrain innervating virtually all regions (hypothalamus, amygdala, thalamus, striatum, frontal cortex, hippocampus) and others, from the caudal raphe nuclei, project mainly to the spinal cord and cerebellum [84]. Consequently, it is easy to think that acting on the serotonergic system will impact on a variety of organismal functions. In addition, there are seven 5-HT receptor classes (5-HT<sub>1</sub>, 5-HT<sub>2</sub>, 5-HT<sub>3</sub>, 5-HT<sub>4</sub>, 5-HT<sub>5</sub>, 5-HT<sub>6</sub>, 5-HT<sub>7</sub>), further divided in at least 14 different 5-HT receptors [85]. While all 5-HT receptor subtypes display a post-synaptic location on 5-HT target cells, others are also found in 5-HT neurons: 5-HT<sub>1A</sub> [86] and 5-HT<sub>1B/D</sub> [87]. In MJD, some studies have been conducted involving SSRIs and/or the modulation of the 5-HT<sub>1A</sub>R. A unique study using the SSRI fluoxetine was conducted in MJD patients, as an open-label study. No significant improvement was observed in motor function, after 6 weeks of treatment. Note that only 13 patients were used (current natural history of disease studies suggesting much larger numbers are required to detect effects), and the study was quite short, whereas we previously reported that a prolonged chronic treatment with SSRIs (in different animal models) was essential to improve neurological dysfunction with increased efficacy [30, 32]. Buspirone, a 5-HT<sub>1A</sub>R partial agonist, was also tested in patients with cerebellar ataxia (including MJD), in an open-label study, showing significant improvements in clinical self-assessment scores, but with no improvements in motor performance [88]. The same compound was used for the treatment of the same type of patients, this time in a double-blind drug placebo study, confirming that buspirone is active in patients with cerebellar atrophy, the effect being partial and not clinically major [89]. A case report describing buspirone treatment in MJD was published in 1997, highlighting a significant improvement in gait after treatment [90]. Tandospirone, another 5-HT<sub>1A</sub>R partial agonist, was also described to improve cerebellar ataxia in MJD patients [91, 92]. Moreover, recent work from our lab revealed that a highly specific and potent 5-HT<sub>1A</sub>R agonist, befiradol, can rescue neuronal dysfunction and reduce ATXN3

aggregation in the AT3q130 *C. elegans* model [93]. Here, we show that the expression of the 5-HT<sub>1A</sub>R is decreased and reverted upon citalopram treatment in the striatum of the CMVMJD135 mouse model, in accordance with a possible imbalance of the serotonergic system in ataxia. These observations are aligned with the “serotonergic hypothesis” for cerebellar ataxia, evidenced by Trouillas [94], stating that serotonergic deficits might be involved in the etiology of some cases of cerebellar ataxia. To our knowledge, this is the first description of a decreased expression of this receptor in MJD, needing therefore independent validation. Moreover, the effect of citalopram in MJD could be the result of the activation of post-synaptic 5-HT<sub>1A</sub>R and of its associated-transduction pathways in target neurons, possibly leading to the modulation of CREB, as suggested by our results.

Different signaling pathways have been described for 5-HT<sub>1A</sub> receptors, evidence also pointing to differences in signaling between 5-HT<sub>1A</sub> auto- and hetero-receptors. In the serotonergic raphe nucleus, 5-HT<sub>1A</sub> autoreceptors are preferentially coupled to G<sub>β3</sub> proteins, while heteroreceptors in the hippocampus are preferentially coupled to G<sub>αi</sub> or G<sub>αo</sub> [95, 96]. The agonist binding to the heteroreceptor primarily functions to inhibit adenylyl cyclase (AC), through G<sub>αi</sub> or G<sub>αo</sub>, decreasing cAMP levels and PKA activity [97]. In fact, we observed a decrease in AC mRNA expression in the striatum of MJD mice treated with citalopram, supporting the hypothesis that the effects that we detected are heteroreceptor dependent. However, no alterations were observed regarding cAMP or PKA mRNA levels, just a downregulation in the mRNA levels of one of the phosphodiesterase (PDE) proteins, responsible for the hydrolysis of cAMP (Figure 3.1.5). The 5-HT<sub>1A</sub>R also affects the MAPK/ERK pathway, particularly ERK, whose phosphorylation in neurons activates receptors and ion channels, altering gene expression and neuroplasticity [98]. The 5-HT<sub>1A</sub>R was first reported to activate this pathway in non-neuronal cells expressing this receptor [99]. Our results also indicated an alteration in the expression of some players in this pathway according to what was previously described (Figure 3.1.5). Another pathway that is known to be activated by 5-HT<sub>1A</sub>R is the PI3K-PKB/Akt pathway. The heterologous expression of 5-HT<sub>1A</sub>Rs increased Akt phosphorylation, being sensitive to G<sub>βγ</sub> and mediated by PI3K [100]. Once more, components of this pathway showed altered expression in our data set. As previously mentioned, several kinases belonging to each one of these pathways can phosphorylate CREB and thus activate it (reviewed in [101]), therefore citalopram modulation of serotonergic signaling might, through 5-HT<sub>1A</sub>R, regulate this transcription factor. Indeed, there is a broad understanding that antidepressant chronic treatment stimulates CREB function [102-104], despite some conflicting results that have been published [105]. In the nervous system, CREB is a transcription factor that has a complex role in diverse processes ranging from neurodevelopment, learning, memory and synaptic plasticity to neuroprotection (reviewed in [65, 106]). It was first identified

as a target of the cAMP signaling pathway, although other studies pointed that it can be targeted by other signaling pathways, activated by a wide range of stimuli (about 300, reviewed in [107]). Activation of CREB is dependent of phosphorylation at serine 133 (ser-133) residue, allowing the recruitment of the transcriptional coactivators CREB-binding protein (CBP) and its paralogue p300, thus enhancing its activity. This enrollment of CBP is proposed to mediate the activation of target genes through histone acetyltransferase activity and by association with RNA polymerase II (RNA-pol-II) complexes [108, 109]. Interestingly, these proteins (p300 and RNA-pol-II) showed altered mRNA expression in our data upon citalopram treatment, adding evidence towards a possible CREB involvement in citalopram-mediated action. Even though phosphorylation of ser-133 is generally accepted to be a decisive event in the regulation of CREB-mediated transcription, several other modifications can influence this process. Phosphorylation at different residues [110, 111], ubiquitylation [112], acetylation [113], glycosylation [114] have been reported to produce such CREB regulation. Also, the newly discovered serotonylation mechanism [115], could possibly play a role in CREB activity modulation, in this context, although nothing has been described in that way yet. Having this in mind, we found a relevant number of CREB targets in our analysis (Figure 3.1.6), and this could be reflecting the complex regulation of this transcription factor triggered by citalopram. Furthermore, supporting the role of CREB in citalopram action, we found that its proper function was necessary for the therapeutic effects of this drug in mutant ATXN3 worms (Figure 3.1.7).

On the other hand, if we think about polyQ diseases as a whole, transcription dysregulation has been proposed as a potential mechanism for their pathology. In fact, the interaction between expanded polyQ stretches with a coactivator of CREB - TAF<sub>II</sub>130, was observed and suppressed CREB-dependent transcriptional activation [116], representing a possible pathogenic process. Additionally, in MJD, the interaction of normal and expanded ATXN3 with p300 and PCAF (Kat2b) was observed, leading to the inhibition of the transcription mediated by these coactivators [117]. Moreover, a transcriptional dysregulation was also described in SCA3 mice expressing polyQ-expanded ATXN3, decreasing mRNA expression levels of proteins involved in the MAPK pathway, heat shock proteins and transcription factors involved in neuronal survival and differentiation, among others [118]. Therefore, it is possible that a transcriptional dysregulation mediated by a deficient 5-HT signaling, in MJD, could contribute to pathology. In this way, the beneficial impact of citalopram on locomotor behavior and neuropathology of MJD animal models could be the result, at least in part, of reverting CREB-mediated abnormal transcription by enhancing 5-HT signaling.

## 5. Conclusion

Although the serotonin system has been shown to be relevant in ataxia disorders, the precise mechanism(s) associated to this involvement remains elusive. Here we propose, for the first time, that a dysregulation of the serotonergic signaling through the 5-HT<sub>1A</sub>R could be a determinant feature in MJD and that antidepressant treatment with citalopram could help restoring this imbalance. This could be achieved through the modulation of 5-HT<sub>1A</sub>R downstream signaling pathways, culminating in the regulation of transcription factors such as CREB, as suggested by our results. This study further supports citalopram as a disease-modifying therapeutic approach for MJD and perhaps for related neurodegenerative disorders.

## Final considerations

To complete the initial observations presented in this chapter, more experiments are necessary to support our hypothesis, namely to:

- Quantify the mRNA expression of the *5-HT<sub>1A</sub>R* in an independent cohort of animals (male and/or female mice, in the striatum and other brain regions relevant for the disease);
- Evaluate the activation state (phosphorylation, augmented expression) of key factors in each of the *5-HT<sub>1A</sub>R* transduction signaling pathways to clarify their importance for the MOA of citalopram;
- Determine CREB activation (phosphorylation state) in treated and non-treated transgenic MJD mice;
- Verify the impact of CREB mutation on ATXN3 aggregation and survival of the *C. elegans* AT3Q130;*crh-1* double mutant.

## Acknowledgments

We are greatly thankful to the members of the Maciel laboratory for sharing reagents, for critical analysis of the data and discussion on the manuscript. We kindly acknowledge Dr. Luísa Pinto from Bn'ML - Behavioral & Molecular Lab, for assisting in the logistic processes for shipment of samples. We are thankful to Dr. Maria do Carmo Costa for helping in the RNA-seq data analyses. We are grateful for some strains that were provided by the CGC, which is funded by NIH Office of Research Infrastructure Programs (P40 OD010440). We also kindly thank the Michigan Brain Bank (P30 AG053760 University of Michigan Alzheimer's Disease Core Center) for providing human brain tissue for analysis.



## **Funding**

This work was funded by National funds, through the Foundation for Science and Technology (FCT) - project UIDB/50026/2020 and UIDP/50026/2020; and by FEDER, through the Competitiveness Internationalization Operational Programme (POCI) under the scope of the projects: POCI-01-0145-FEDER-031987, NORTE-01-0145-FEDER-000013 and NORTE-01-0145-FEDER-000023, supported by North Portugal Regional Operational Programme (NORTE 2020), under the PORTUGAL 2020 Partnership Agreement, through the European Regional Development Fund (ERDF). This work was also funded through the National Ataxia Foundation (NAF), USA, and by the U.S. Department of Defense (DoD) - grant award number: W81XWH-19-1-0638. Stéphanie Oliveira was supported by a doctoral programme fellowship: Inter-University Doctoral Programme in Ageing and Chronic Disease from FCT - PD/BD/127818/2016.

## References

1. Gusella, J.F. and MacDonald, M.E., Molecular genetics: Unmasking polyglutamine triggers in neurodegenerative disease. *Nature Reviews Neuroscience*, 2000. **1**(2): p. 109-115.<https://doi.org/10.1038/35039051>.
2. Schöls, L., Bauer, P., Schmidt, T., Schulte, T., *et al.*, Autosomal dominant cerebellar ataxias: clinical features, genetics, and pathogenesis. *The Lancet Neurology*, 2004. **3**(5): p. 291-304.[https://doi.org/10.1016/S1474-4422\(04\)00737-9](https://doi.org/10.1016/S1474-4422(04)00737-9).
3. Bettencourt, C. and Lima, M., Machado-Joseph Disease: from first descriptions to new perspectives. *Orphanet Journal of Rare Diseases*, 2011. **6**(1): p. 35.<https://doi.org/10.1186/1750-1172-6-35>.
4. Coutinho, P. and Andrade, C., Autosomal dominant system degeneration in Portuguese families of the Azores Islands. A new genetic disorder involving cerebellar, pyramidal, extrapyramidal and spinal cord motor functions. *Neurology*, 1978. **28**(7): p. 703-709.<https://doi.org/10.1212/WNL.28.7.703>.
5. Rüb, U., Brunt, E.R., and Deller, T., New insights into the pathoanatomy of spinocerebellar ataxia type 3 (Machado–Joseph disease). *Current Opinion in Neurology*, 2008. **21**(2): p. 111-116.<https://doi.org/10.1097/WCO.0b013e3282f7673d>.
6. Lee, W.Y., Jin, D.K., Oh, M.R., Lee, J.E., *et al.*, Frequency Analysis and Clinical Characterization of Spinocerebellar Ataxia Types 1, 2, 3, 6, and 7 in Korean Patients. *Archives of Neurology*, 2003. **60**(6): p. 858-863.<https://doi.org/10.1001/archneur.60.6.858>.
7. Milne, R.J. and Goa, K.L., Citalopram. *Drugs*, 1991. **41**(3): p. 450-477.<https://doi.org/10.2165/00003495-199141030-00008>.
8. Morrissette, D.A. and Stahl, S.M., Modulating the serotonin system in the treatment of major depressive disorder. *CNS Spectrums*, 2014. **19**(S1): p. 54-68.<https://doi.org/10.1017/S1092852914000613>.
9. Blakely, R.D., Berson, H.E., Freneau, R.T., Caron, M.G., *et al.*, Cloning and expression of a functional serotonin transporter from rat brain. *Nature*, 1991. **354**(6348): p. 66-70.<https://doi.org/10.1038/354066a0>.
10. Nutt, D.J., Forshall, S., Bell, C., Rich, A., *et al.*, Mechanisms of action of selective serotonin reuptake inhibitors in the treatment of psychiatric disorders. *European Neuropsychopharmacology*, 1999. **9**: p. S81-S86.[https://doi.org/10.1016/S0924-977X\(99\)00030-9](https://doi.org/10.1016/S0924-977X(99)00030-9).
11. Blier, P. and de Montigny, C., Current advances and trends in the treatment of depression. *Trends in Pharmacological Sciences*, 1994. **15**(7): p. 220-226.[https://doi.org/10.1016/0165-6147\(94\)90315-8](https://doi.org/10.1016/0165-6147(94)90315-8).
12. Hervás, I., Vilaró, M.T., Romero, L., Scorza, M.C., *et al.*, Desensitization of 5-HT<sub>1A</sub> Autoreceptors by a Low Chronic Fluoxetine Dose Effect of the Concurrent Administration of WAY-100635.

- Neuropsychopharmacology*, 2001. **24**(1): p. 11-20.[https://doi.org/10.1016/S0893-133X\(00\)00175-5](https://doi.org/10.1016/S0893-133X(00)00175-5).
13. El Mansari, M., Sánchez, C., Chouvet, G., Renaud, B., *et al.*, Effects of Acute and Long-Term Administration of Escitalopram and Citalopram on Serotonin Neurotransmission: an *In Vivo* Electrophysiological Study in Rat Brain. *Neuropsychopharmacology*, 2005. **30**(7): p. 1269-1277.<https://doi.org/10.1038/sj.npp.1300686>.
  14. Fillion, G. and Fillion, M.P., Modulation of affinity of postsynaptic serotonin receptors by antidepressant drugs. *Nature*, 1981. **292**(5821): p. 349-351.<https://doi.org/10.1038/292349a0>.
  15. Blier, P., Bergeron, R., and Montigny, C.d., Selective activation of postsynaptic 5-HT<sub>1A</sub> receptors induces rapid antidepressant response. *Neuropsychopharmacology*, 1997. **16**(5): p. 333-338.[https://doi.org/10.1016/S0893-133X\(96\)00242-4](https://doi.org/10.1016/S0893-133X(96)00242-4).
  16. Chilmonczyk, Z., Bojarski, A.J., Pilc, A., and Sylte, I., Serotonin transporter and receptor ligands with antidepressant activity as neuroprotective and proapoptotic agents. *Pharmacological Reports*, 2017. **69**(3): p. 469-478.<https://doi.org/10.1016/j.pharep.2017.01.011>.
  17. Taler, M., Miron, O., Gil-Ad, I., and Weizman, A., Neuroprotective and procognitive effects of sertraline: *In vitro* and *in vivo* studies. *Neuroscience Letters*, 2013. **550**: p. 93-97.<https://doi.org/10.1016/j.neulet.2013.06.033>.
  18. Kim, H.-J., Kim, W., and Kong, S.-Y., Antidepressants for neuro-regeneration: from depression to Alzheimer's disease. *Archives of Pharmacal Research*, 2013. **36**(11): p. 1279-1290.<https://doi.org/10.1007/s12272-013-0238-8>.
  19. Jamwal, S. and Kumar, P., Antidepressants for neuroprotection in Huntington's disease: A review. *European Journal of Pharmacology*, 2015. **769**: p. 33-42.<https://doi.org/10.1016/j.ejphar.2015.10.033>.
  20. Cirrito, J.R., Disabato, B.M., Restivo, J.L., Verges, D.K., *et al.*, Serotonin signaling is associated with lower amyloid- $\beta$  levels and plaques in transgenic mice and humans. *Proceedings of the National Academy of Sciences*, 2011. **108**(36): p. 14968-14973.<https://doi.org/10.1073/pnas.1107411108>.
  21. Sheline, Y.I., West, T., Yarasheski, K., Swarm, R., *et al.*, An Antidepressant Decreases CSF A $\beta$  Production in Healthy Individuals and in Transgenic AD Mice. *Science Translational Medicine*, 2014. **6**(236): p. 236re4-236re4.<https://doi.org/10.1126/scitranslmed.3008169>.
  22. Pákási, M., Bjelik, A., Hugyecz, M., Kása, P., *et al.*, Imipramine and citalopram facilitate amyloid precursor protein secretion *in vitro*. *Neurochemistry International*, 2005. **47**(3): p. 190-195.<https://doi.org/10.1016/j.neuint.2005.03.004>.
  23. Rampello, L., Chiechio, S., Raffaele, R., Vecchio, I., *et al.*, The SSRI, Citalopram, Improves Bradykinesia in Patients With Parkinson's Disease Treated with L-Dopa. *Clinical Neuropharmacology*, 2002. **25**(1).<https://doi.org/10.1097/00002826-200201000-00004>.

24. Ubhi, K., Inglis, C., Mante, M., Patrick, C., *et al.*, Fluoxetine ameliorates behavioral and neuropathological deficits in a transgenic model mouse of  $\alpha$ -synucleinopathy. *Experimental Neurology*, 2012. **234**(2): p. 405-416.<https://doi.org/10.1016/j.expneurol.2012.01.008>.
25. Chung, Y.C., Kim, S.R., and Jin, B.K., Paroxetine Prevents Loss of Nigrostriatal Dopaminergic Neurons by Inhibiting Brain Inflammation and Oxidative Stress in an Experimental Model of Parkinson's Disease. *The Journal of Immunology*, 2010. **185**(2): p. 1230-1237.<https://doi.org/10.4049/jimmunol.1000208>.
26. Duan, W., Peng, Q., Masuda, N., Ford, E., *et al.*, Sertraline slows disease progression and increases neurogenesis in N171-82Q mouse model of Huntington's disease. *Neurobiology of Disease*, 2008. **30**(3): p. 312-322.<https://doi.org/10.1016/j.nbd.2008.01.015>.
27. Duan, W., Guo, Z., Jiang, H., Ladenheim, B., *et al.*, Paroxetine retards disease onset and progression in Huntingtin mutant mice. *Annals of Neurology*, 2004. **55**(4): p. 590-594.<https://doi.org/10.1002/ana.20075>.
28. Peng, Q., Masuda, N., Jiang, M., Li, Q., *et al.*, The antidepressant sertraline improves the phenotype, promotes neurogenesis and increases BDNF levels in the R6/2 Huntington's disease mouse model. *Experimental Neurology*, 2008. **210**(1): p. 154-163.<https://doi.org/10.1016/j.expneurol.2007.10.015>.
29. Baquero, M. and Martín, N., Depressive symptoms in neurodegenerative diseases. *World Journal of Clinical Cases*, 2015. **3**(8): p. 682-693.<https://doi.org/10.12998/wjcc.v3.i8.682>.
30. Teixeira-Castro, A., Jalles, A., Esteves, S., Kang, S., *et al.*, Serotonergic signalling suppresses ataxin 3 aggregation and neurotoxicity in animal models of Machado-Joseph disease. *Brain*, 2015. **138**(11): p. 3221-3237.<https://doi.org/10.1093/brain/awv262>.
31. Silva-Fernandes, A., Duarte-Silva, S., Neves-Carvalho, A., Amorim, M., *et al.*, Chronic Treatment with 17-DMAG Improves Balance and Coordination in A New Mouse Model of Machado-Joseph Disease. *Neurotherapeutics*, 2014. **11**(2): p. 433-449.<https://doi.org/10.1007/s13311-013-0255-9>.
32. Esteves, S., Oliveira, S., Duarte-Silva, S., Cunha-Garcia, D., *et al.*, Preclinical Evidence Supporting Early Initiation of Citalopram Treatment in Machado-Joseph Disease. *Molecular Neurobiology*, 2019. **56**(5): p. 3626-3637.<https://doi.org/10.1007/s12035-018-1332-1>.
33. Nicklas, W., Baneux, P., Boot, R., Decelle, T., *et al.*, Recommendations for the health monitoring of rodent and rabbit colonies in breeding and experimental units. *Laboratory Animals*, 2002. **36**(1): p. 20-42.<https://doi.org/10.1258/0023677021911740>.
34. Kilkeny, C., Browne, W.J., Cuthill, I.C., Emerson, M., *et al.*, Improving Bioscience Research Reporting: The ARRIVE Guidelines for Reporting Animal Research. *PLOS Biology*, 2010. **8**(6): p. e1000412.<https://doi.org/10.1371/journal.pbio.1000412>.
35. Percie du Sert, N., Hurst, V., Ahluwalia, A., Alam, S., *et al.*, The ARRIVE guidelines 2.0: Updated guidelines for reporting animal research. *PLOS Biology*, 2020. **18**(7): p. e3000410.<https://doi.org/10.1371/journal.pbio.3000410>.

36. Silva-Fernandes, A., Costa, M.d.C., Duarte-Silva, S., Oliveira, P., *et al.*, Motor uncoordination and neuropathology in a transgenic mouse model of Machado–Joseph disease lacking intranuclear inclusions and ataxin-3 cleavage products. *Neurobiology of Disease*, 2010. **40**(1): p. 163-176.<https://doi.org/10.1016/j.nbd.2010.05.021>.
37. Dobin, A., Davis, C.A., Schlesinger, F., Drenkow, J., *et al.*, STAR: ultrafast universal RNA-seq aligner. *Bioinformatics*, 2013. **29**(1): p. 15-21.<https://doi.org/10.1093/bioinformatics/bts635>.
38. Li, H., Handsaker, B., Wysoker, A., Fennell, T., *et al.*, The Sequence Alignment/Map format and SAMtools. *Bioinformatics*, 2009. **25**(16): p. 2078-2079.<https://doi.org/10.1093/bioinformatics/btp352>.
39. Liao, Y., Smyth, G.K., and Shi, W., The Subread aligner: fast, accurate and scalable read mapping by seed-and-vote. *Nucleic Acids Research*, 2013. **41**(10): p. e108-e108.<https://doi.org/10.1093/nar/gkt214>.
40. Robinson, M.D. and Oshlack, A., A scaling normalization method for differential expression analysis of RNA-seq data. *Genome Biology*, 2010. **11**(3): p. R25.<https://doi.org/10.1186/gb-2010-11-3-r25>.
41. QIAGEN. QIAGEN Ingenuity Pathway Analysis (IPA). 2020 [Last accessed 2020 July]; Available from: <https://digitalinsights.qiagen.com/products-overview/discovery-insights-portfolio/analysis-and-visualization/qiagen-ipa/>.
42. Broad Institute. CLUE MORPHEUS. 2020 [Last accessed 2020 November]; Morpheus: versatile matrix visualization and analysis software ]. Available from: <https://clue.io/morpheus>.
43. National Center for Biotechnology Information (NCBI). Primer-Blast. 2020 [Last accessed 2020 October]; Primer-BLAST: A tool for finding specific primers]. Available from: <https://www.ncbi.nlm.nih.gov/tools/primer-blast/>.
44. Livak, K.J. and Schmittgen, T.D., Analysis of Relative Gene Expression Data Using Real-Time Quantitative PCR and the  $2^{-\Delta\Delta Ct}$  Method. *Methods*, 2001. **25**(4): p. 402-408.<https://doi.org/10.1006/meth.2001.1262>.
45. Teixeira-Castro, A., Ailion, M., Jalles, A., Brignull, H.R., *et al.*, Neuron-specific proteotoxicity of mutant ataxin-3 in *C. elegans*: rescue by the DAF-16 and HSF-1 pathways. *Human Molecular Genetics*, 2011. **20**(15): p. 2996-3009.<https://doi.org/10.1093/hmg/ddr203>.
46. Brenner, S., The Genetics of *Caenorhabditis elegans*. *Genetics*, 1974. **77**(1): p. 71-94.<https://www.genetics.org/content/77/1/71.short>.
47. Paix, A., Folkmann, A., Rasoloson, D., and Seydoux, G., High Efficiency, Homology-Directed Genome Editing in *Caenorhabditis elegans* Using CRISPR-Cas9 Ribonucleoprotein Complexes. *Genetics*, 2015. **201**(1): p. 47-54.<https://doi.org/10.1534/genetics.115.179382>
48. Mello, C.C., Kramer, J.M., Stinchcomb, D., and Ambros, V., Efficient gene transfer in *C.elegans*: extrachromosomal maintenance and integration of transforming sequences. *The EMBO Journal*, 1991. **10**(12): p. 3959-3970.<https://doi.org/10.1002/j.1460-2075.1991.tb04966.x>.

49. Voisine, C., Varma, H., Walker, N., Bates, E.A., *et al.*, Identification of Potential Therapeutic Drugs for Huntington's Disease using *Caenorhabditis elegans*. *PLOS ONE*, 2007. **2**(6): p. e504.<https://doi.org/10.1371/journal.pone.0000504>.
50. Gidalevitz, T., Ben-Zvi, A., Ho, K.H., Brignull, H.R., *et al.*, Progressive Disruption of Cellular Protein Folding in Models of Polyglutamine Diseases. *Science*, 2006. **311**(5766): p. 1471-1474.<https://doi.org/10.1126/science.1124514>.
51. Ashraf, N.S., Duarte-Silva, S., Shaw, E.D., Maciel, P., *et al.*, Citalopram Reduces Aggregation of ATXN3 in a YAC Transgenic Mouse Model of Machado-Joseph Disease. *Molecular Neurobiology*, 2019. **56**(5): p. 3690-3701.<https://doi.org/10.1007/s12035-018-1331-2>.
52. Yamada, M., Tan, C.-F., Inenaga, C., Tsuji, S., *et al.*, Sharing of polyglutamine localization by the neuronal nucleus and cytoplasm in CAG-repeat diseases. *Neuropathology and Applied Neurobiology*, 2004. **30**(6): p. 665-675.<https://doi.org/10.1111/j.1365-2990.2004.00583.x>.
53. Klockgether, T., Skalej, M., Wedekind, D., Luft, A.R., *et al.*, Autosomal dominant cerebellar ataxia type I. MRI-based volumetry of posterior fossa structures and basal ganglia in spinocerebellar ataxia types 1, 2 and 3. *Brain*, 1998. **121**(9): p. 1687-1693.<https://doi.org/10.1093/brain/121.9.1687>.
54. Telford, R. and Vattoth, S., MR Anatomy of Deep Brain Nuclei with Special Reference to Specific Diseases and Deep Brain Stimulation Localization. *The Neuroradiology Journal*, 2014. **27**(1): p. 29-43.<https://doi.org/10.15274/NRJ-2014-10004>.
55. Polter, A.M. and Li, X., 5-HT<sub>1A</sub> receptor-regulated signal transduction pathways in brain. *Cellular Signalling*, 2010. **22**(10): p. 1406-1412.<https://doi.org/10.1016/j.cellsig.2010.03.019>.
56. De Vivo, M. and Maayani, S., Characterization of the 5-hydroxytryptamine<sub>1A</sub> receptor-mediated inhibition of forskolin-stimulated adenylate cyclase activity in guinea pig and rat hippocampal membranes. *Journal of Pharmacology and Experimental Therapeutics*, 1986. **238**(1): p. 248-253.<https://jpet.aspetjournals.org/content/238/1/248.long>.
57. Rojas, P.S. and Fiedler, J.L., What Do We Really Know About 5-HT<sub>1A</sub> Receptor Signaling in Neuronal Cells? *Frontiers in Cellular Neurosciences*, 2016. **10**(272).<https://doi.org/10.3389/fncel.2016.00272>.
58. Wiggin, G.R., Soloaga, A., Foster, J.M., Murray-Tait, V., *et al.*, MSK1 and MSK2 Are Required for the Mitogen- and Stress-Induced Phosphorylation of CREB and ATF1 in Fibroblasts. *Molecular and Cellular Biology*, 2002. **22**(8): p. 2871-2881.<https://doi.org/10.1128/MCB.22.8.2871-2881.2002>.
59. Smart SERVIER Medical Art. SERVIER 2020 [Last accessed 2021 February]; Available from: <https://smart.servier.com/>.
60. Blendy, J.A., The role of CREB in depression and antidepressant treatment. *Biological Psychiatry*, 2006. **59**(12): p. 1144-50.<https://doi.org/10.1016/j.biopsych.2005.11.003>.

61. Gonzalez, G.A. and Montminy, M.R., Cyclic AMP stimulates somatostatin gene transcription by phosphorylation of CREB at serine 133. *Cell*, 1989. **59**(4): p. 675-680.[https://doi.org/10.1016/0092-8674\(89\)90013-5](https://doi.org/10.1016/0092-8674(89)90013-5).
62. Xing, J., Ginty, D.D., and Greenberg, M.E., Coupling of the RAS-MAPK Pathway to Gene Activation by RSK2, a Growth Factor-Regulated CREB Kinase. *Science*, 1996. **273**(5277): p. 959-963.<https://doi.org/10.1126/science.273.5277.959>.
63. Du, K. and Montminy, M., CREB Is a Regulatory Target for the Protein Kinase Akt/PKB. *Journal of Biological Chemistry*, 1998. **273**(49): p. 32377-32379.<https://doi.org/10.1074/jbc.273.49.32377>.
64. Deak, M., Clifton, A.D., Lucocq, J.M., and Alessi, D.R., Mitogen- and stress-activated protein kinase-1 (MSK1) is directly activated by MAPK and SAPK2/p38, and may mediate activation of CREB. *The EMBO Journal*, 1998. **17**(15): p. 4426-4441.<https://doi.org/10.1093/emboj/17.15.4426>.
65. Lonze, B.E. and Ginty, D.D., Function and Regulation of CREB Family Transcription Factors in the Nervous System. *Neuron*, 2002. **35**(4): p. 605-623.[https://doi.org/10.1016/S0896-6273\(02\)00828-0](https://doi.org/10.1016/S0896-6273(02)00828-0).
66. Zhang, X., Odom, D.T., Koo, S.-H., Conkright, M.D., *et al.*, Genome-wide analysis of cAMP-response element binding protein occupancy, phosphorylation, and target gene activation in human tissues. *Proceedings of the National Academy of Sciences of the United States of America*, 2005. **102**(12): p. 4459-4464.<https://doi.org/10.1073/pnas.0501076102>.
67. Conkright, M.D., Guzmán, E., Flechner, L., Su, A.I., *et al.*, Genome-Wide Analysis of CREB Target Genes Reveals A Core Promoter Requirement for cAMP Responsiveness. *Molecular Cell*, 2003. **11**(4): p. 1101-1108.[https://doi.org/10.1016/S1097-2765\(03\)00134-5](https://doi.org/10.1016/S1097-2765(03)00134-5).
68. Benito, E., Valor, L.M., Jimenez-Minchan, M., Huber, W., *et al.*, cAMP Response Element-Binding Protein Is a Primary Hub of Activity-Driven Neuronal Gene Expression. *The Journal of Neuroscience*, 2011. **31**(50): p. 18237-18250.<https://doi.org/10.1523/JNEUROSCI.4554-11.2011>.
69. Pardo, L., Valor, L.M., Eraso-Pichot, A., Barco, A., *et al.*, CREB Regulates Distinct Adaptive Transcriptional Programs in Astrocytes and Neurons. *Scientific Reports*, 2017. **7**(1): p. 6390.<https://doi.org/10.1038/s41598-017-06231-x>.
70. Impey, S., McCorkle, S.R., Cha-Molstad, H., Dwyer, J.M., *et al.*, Defining the CREB Regulon: A Genome-Wide Analysis of Transcription Factor Regulatory Regions. *Cell*, 2004. **119**(7): p. 1041-1054.<https://doi.org/10.1016/j.cell.2004.10.032>.
71. Zhang, J., Huang, X.-Y., Ye, M.-L., Luo, C.-X., *et al.*, Neuronal Nitric Oxide Synthase Alteration Accounts for the Role of 5-HT<sub>1A</sub> Receptor in Modulating Anxiety-Related Behaviors. *The Journal of Neuroscience*, 2010. **30**(7): p. 2433-2441.<https://doi.org/10.1523/JNEUROSCI.5880-09.2010>.



72. Hayashida, N., Fujimoto, M., Tan, K., Prakasam, R., *et al.*, Heat shock factor 1 ameliorates proteotoxicity in cooperation with the transcription factor NFAT. *The EMBO Journal*, 2010. **29**(20): p. 3459-3469.<https://doi.org/10.1038/emboj.2010.225>.
73. Lorès, P., Dacheux, D., Kherraf, Z.-E., Nsota Mbango, J.-F., *et al.*, Mutations in TTC29, Encoding an Evolutionarily Conserved Axonemal Protein, Result in Asthenozoospermia and Male Infertility. *The American Journal of Human Genetics*, 2019. **105**(6): p. 1148-1167.<https://doi.org/10.1016/j.ajhg.2019.10.007>.
74. Russell, L.C., Whitt, S.R., Chen, M.-S., and Chinkers, M., Identification of Conserved Residues Required for the Binding of a Tetratricopeptide Repeat Domain to Heat Shock Protein 90. *Journal of Biological Chemistry*, 1999. **274**(29): p. 20060-20063.<https://doi.org/10.1074/jbc.274.29.20060>.
75. Harbauer, Angelika B., Zahedi, René P., Sickmann, A., Pfanner, N., *et al.*, The Protein Import Machinery of Mitochondria—A Regulatory Hub in Metabolism, Stress, and Disease. *Cell Metabolism*, 2014. **19**(3): p. 357-372.<https://doi.org/10.1016/j.cmet.2014.01.010>.
76. Heemels, M.-T., Neurodegenerative diseases. *Nature*, 2016. **539**(7628): p. 179-179.<https://doi.org/10.1038/539179a>.
77. Ashburn, T.T. and Thor, K.B., Drug repositioning: identifying and developing new uses for existing drugs. *Nature Reviews Drug Discovery*, 2004. **3**(8): p. 673-683.<https://doi.org/10.1038/nrd1468>.
78. Tan, J.Y. and Levin, G.M., Citalopram in the Treatment of Depression and Other Potential Uses in Psychiatry. *Pharmacotherapy*, 1999. **19**(6): p. 675-689.<https://doi.org/10.1592/phco.19.9.675.31538>.
79. Varia, I. and Rauscher, F., Treatment of generalized anxiety disorder with citalopram. *International Clinical Psychopharmacology*, 2002. **17**(3).<https://doi.org/10.1097/00004850-200205000-00002>.
80. Humble, M. and Wistedt, B., Serotonin, Panic Disorder and Agoraphobia: Short-term and Long-term Efficacy of Citalopram in Panic Disorders. *International Clinical Psychopharmacology*, 1992. **6**: p. 21-40.<https://doi.org/10.1097/00004850-199206005-00003>.
81. Montgomery, S.A., Kasper, S., Stein, D.J., Hedegaard, K.B., *et al.*, Citalopram 20 mg, 40 mg and 60 mg are all effective and well tolerated compared with placebo in obsessive-compulsive disorder. *International Clinical Psychopharmacology*, 2001. **16**(2).<https://doi.org/10.1097/00004850-200103000-00002>.
82. Steinbusch, H.W.M., Distribution of serotonin-immunoreactivity in the central nervous system of the rat—Cell bodies and terminals. *Neuroscience*, 1981. **6**(4): p. 557-618.[https://doi.org/10.1016/0306-4522\(81\)90146-9](https://doi.org/10.1016/0306-4522(81)90146-9).
83. Dahlström, A. and Fuxe, K., Localization of monoamines in the lower brain stem. *Experientia*, 1964. **20**(7): p. 398-399.<https://doi.org/10.1007/BF02147990>.



84. Jacobs, B.L. and Azmitia, E.C., Structure and function of the brain serotonin system. *Physiological Reviews*, 1992. **72**(1): p. 165-229.<https://doi.org/10.1152/physrev.1992.72.1.165>.
85. Nichols, D.E. and Nichols, C.D., Serotonin Receptors. *Chemical Reviews*, 2008. **108**(5): p. 1614-1641.<https://doi.org/10.1021/cr078224o>.
86. Sotelo, C., Cholley, B., El Mestikawy, S., Gozlan, H., *et al.*, Direct Immunohistochemical Evidence of the Existence of 5-HT<sub>1A</sub> Autoreceptors on Serotonergic Neurons in the Midbrain Raphe Nuclei. *European Journal of Neuroscience*, 1990. **2**(12): p. 1144-1154.<https://doi.org/10.1111/j.1460-9568.1990.tb00026.x>.
87. Limberger, N., Deicher, R., and Starke, K., Species differences in presynaptic serotonin autoreceptors: mainly 5-HT<sub>1B</sub> but possibly in addition 5-HT<sub>1D</sub> in the rat, 5-HT<sub>1D</sub> in the rabbit and guinea-pig brain cortex. *Naunyn-Schmiedeberg's Archives of Pharmacology*, 1991. **343**(4): p. 353-364.<https://doi.org/10.1007/BF00179039>.
88. Lou, J.-S., Goldfarb, L., McShane, L., Gatev, P., *et al.*, Use of Buspirone for Treatment of Cerebellar Ataxia: An Open-Label Study. *Archives of Neurology*, 1995. **52**(10): p. 982-988.<https://doi.org/10.1001/archneur.1995.00540340074015>.
89. Trouillas, P., Xie, J., Adeleine, P., Michel, D., *et al.*, Buspirone, a 5-Hydroxytryptamine<sub>1A</sub> Agonist, Is Active in Cerebellar Ataxia: Results of a Double-blind Drug Placebo Study in Patients With Cerebellar Cortical Atrophy. *Archives of Neurology*, 1997. **54**(6): p. 749-752.<https://doi.org/10.1001/archneur.1997.00550180059013>.
90. Friedman, J.H., Machado-Joseph disease/spinocerebellar ataxia 3 responsive to buspirone. *Movement Disorders*, 1997. **12**(4): p. 613-614.<https://doi.org/10.1002/mds.870120426>.
91. Takei, A., Honma, S., Kawashima, A., Yabe, I., *et al.*, Beneficial effects of tandospirone on ataxia of a patient with Machado-Joseph disease. *Psychiatry and Clinical Neurosciences*, 2002. **56**(2): p. 181-185.<https://doi.org/10.1046/j.1440-1819.2002.00952.x>.
92. Takei, A., Fukazawa, T., Hamada, T., Sohma, H., *et al.*, Effects of Tandospirone on "5-HT<sub>1A</sub> Receptor-Associated Symptoms" in Patients with Machado-Joseph Disease: An Open-Label Study. *Clinical Neuropharmacology*, 2004. **27**(1): p. 9-13.<https://doi.org/10.1097/00002826-200401000-00005>.
93. Pereira-Sousa, J., Ferreira-Lomba, B., Bellver-Sanchis, A., Vilasboas-Campos, D., *et al.*, Identification of the 5-HT<sub>1A</sub> serotonin receptor as a novel therapeutic target in a *C. elegans* model of Machado-Joseph disease. *Neurobiology of Disease*, 2021. **152**: p. 105278.<https://doi.org/10.1016/j.nbd.2021.105278>.
94. Trouillas, P., The Cerebellar Serotonergic System and its Possible Involvement in Cerebellar Ataxia. *Canadian Journal of Neurological Sciences / Journal Canadien des Sciences Neurologiques*, 1993. **20**(S3): p. S78-S82.<https://doi.org/10.1017/S0317167100048575>.
95. la Cour, C.M., El Mestikawy, S., Hanoun, N., Hamon, M., *et al.*, Regional Differences in the Coupling of 5-Hydroxytryptamine-1A Receptors to G Proteins in the Rat Brain. *Molecular Pharmacology*, 2006. **70**(3): p. 1013-1021.<https://doi.org/10.1124/mol.106.022756>.

96. Valdizán, E.M., Castro, E., and Pazos, A., Agonist-dependent modulation of G-protein coupling and transduction of 5-HT<sub>1A</sub> receptors in rat dorsal raphe nucleus. *International Journal of Neuropsychopharmacology*, 2010. **13**(7): p. 835-843.<https://doi.org/10.1017/S1461145709990940>.
97. Taskén, K. and Aandahl, E.M., Localized Effects of cAMP Mediated by Distinct Routes of Protein Kinase A. *Physiological Reviews*, 2004. **84**(1): p. 137-167.<https://doi.org/10.1152/physrev.00021.2003>.
98. Sweatt, J.D., Mitogen-activated protein kinases in synaptic plasticity and memory. *Current Opinion in Neurobiology*, 2004. **14**(3): p. 311-317.<https://doi.org/10.1016/j.conb.2004.04.001>.
99. Garnovskaya, M.N., van Biesen, T., Hawes, B., Casañas Ramos, S., *et al.*, Ras-Dependent Activation of Fibroblast Mitogen-Activated Protein Kinase by 5-HT<sub>1A</sub> Receptor *via* a G Protein  $\beta\gamma$ -Subunit-Initiated Pathway. *Biochemistry*, 1996. **35**(43): p. 13716-13722.<https://doi.org/10.1021/bi961764n>.
100. Hsiung, S.-c., Tamir, H., Franke, T.F., and Liu, K.-p., Roles of extracellular signal-regulated kinase and Akt signaling in coordinating nuclear transcription factor- $\kappa$ B-dependent cell survival after serotonin 1A receptor activation. *Journal of Neurochemistry*, 2005. **95**(6): p. 1653-1666.<https://doi.org/10.1111/j.1471-4159.2005.03496.x>.
101. Mayr, B. and Montminy, M., Transcriptional regulation by the phosphorylation-dependent factor CREB. *Nature Reviews Molecular Cell Biology*, 2001. **2**(8): p. 599-609.<https://doi.org/10.1038/35085068>.
102. Carlezon, W.A., Duman, R.S., and Nestler, E.J., The many faces of CREB. *Trends in Neurosciences*, 2005. **28**(8): p. 436-445.<https://doi.org/10.1016/j.tins.2005.06.005>.
103. Tardito, D., Musazzi, L., Tiraboschi, E., Mallei, A., *et al.*, Early induction of CREB activation and CREB-regulating signalling by antidepressants. *International Journal of Neuropsychopharmacology*, 2009. **12**(10): p. 1367-1381.<https://doi.org/10.1017/S1461145709000376>.
104. Nibuya, M., Nestler, E., and Duman, R., Chronic antidepressant administration increases the expression of cAMP response element binding protein (CREB) in rat hippocampus. *The Journal of Neuroscience*, 1996. **16**(7): p. 2365-2372.<https://doi.org/10.1523/JNEUROSCI.16-07-02365.1996>
105. Kuipers, S.D., Trentani, A., Westenbroek, C., Bramham, C.R., *et al.*, Unique patterns of FOS, phospho-CREB and BrdU immunoreactivity in the female rat brain following chronic stress and citalopram treatment. *Neuropharmacology*, 2006. **50**(4): p. 428-440.<https://doi.org/10.1016/j.neuropharm.2005.10.006>.
106. Sakamoto, K., Karelina, K., and Obrietan, K., CREB: a multifaceted regulator of neuronal plasticity and protection. *Journal of Neurochemistry*, 2011. **116**(1): p. 1-9.<https://doi.org/10.1111/j.1471-4159.2010.07080.x>.

107. Johannessen, M., Delghandi, M.P., and Moens, U., What turns CREB on? *Cellular Signalling*, 2004. **16**(11): p. 1211-1227.<https://doi.org/10.1016/j.cellsig.2004.05.001>.
108. Nakajima, T., Uchida, C., Anderson, S.F., Parvin, J.D., *et al.*, Analysis of a cAMP-responsive activator reveals a two-component mechanism for transcriptional induction via signal-dependent factors. *Genes & Development*, 1997. **11**(6): p. 738-747.<https://doi.org/10.1101/gad.11.6.738>.
109. Kee, B.L., Arias, J., and Montminy, M.R., Adaptor-mediated Recruitment of RNA Polymerase II to a Signal-dependent Activator. *Journal of Biological Chemistry*, 1996. **271**(5): p. 2373-2375.<https://doi.org/10.1074/jbc.271.5.2373>.
110. Wu, X. and McMurray, C.T., Calmodulin Kinase II Attenuation of Gene Transcription by Preventing cAMP Response Element-binding Protein (CREB) Dimerization and Binding of the CREB-binding Protein. *Journal of Biological Chemistry*, 2001. **276**(3): p. 1735-1741.<https://doi.org/10.1074/jbc.M006727200>.
111. Sun, P. and Maurer, R.A., An Inactivating Point Mutation Demonstrates That Interaction of cAMP Response Element Binding Protein (CREB) with the CREB Binding Protein Is Not Sufficient for Transcriptional Activation. *Journal of Biological Chemistry*, 1995. **270**(13): p. 7041-7044.<https://doi.org/10.1074/jbc.270.13.7041>.
112. Taylor, C.T., Furuta, G.T., Synnestvedt, K., and Colgan, S.P., Phosphorylation-dependent targeting of cAMP response element binding protein to the ubiquitin/proteasome pathway in hypoxia. *Proceedings of the National Academy of Sciences*, 2000. **97**(22): p. 12091-12096.<https://doi.org/10.1073/pnas.220211797>.
113. Lu, Q., Hutchins, A.E., Doyle, C.M., Lundblad, J.R., *et al.*, Acetylation of cAMP-responsive Element-binding Protein (CREB) by CREB-binding Protein Enhances CREB-dependent Transcription. *Journal of Biological Chemistry*, 2003. **278**(18): p. 15727-15734.<https://doi.org/10.1074/jbc.M300546200>.
114. Lamarre-Vincent, N. and Hsieh-Wilson, L.C., Dynamic Glycosylation of the Transcription Factor CREB: A Potential Role in Gene Regulation. *Journal of the American Chemical Society*, 2003. **125**(22): p. 6612-6613.<https://doi.org/10.1021/ja028200t>.
115. Farrelly, L.A., Thompson, R.E., Zhao, S., Lepack, A.E., *et al.*, Histone serotonylation is a permissive modification that enhances TFIID binding to H3K4me3. *Nature*, 2019. **567**(7749): p. 535-539.<https://doi.org/10.1038/s41586-019-1024-7>.
116. Shimohata, T., Nakajima, T., Yamada, M., Uchida, C., *et al.*, Expanded polyglutamine stretches interact with TAFII130, interfering with CREB-dependent transcription. *Nature Genetics*, 2000. **26**(1): p. 29-36.<https://doi.org/10.1038/79139>.
117. Li, F., Macfarlan, T., Pittman, R.N., and Chakravarti, D., Ataxin-3 Is a Histone-binding Protein with Two Independent Transcriptional Corepressor Activities. *Journal of Biological Chemistry*, 2002. **277**(47): p. 45004-45012.<https://doi.org/10.1074/jbc.M205259200>.

118. Chou, A.-H., Yeh, T.-H., Ouyang, P., Chen, Y.-L., *et al.*, Polyglutamine-expanded ataxin-3 causes cerebellar dysfunction of SCA3 transgenic mice by inducing transcriptional dysregulation. *Neurobiology of Disease*, 2008. **31**(1): p. 89-101. <https://doi.org/10.1016/j.nbd.2008.03.011>.

## Chapter 3.2

---

### **Exploring the modulation of protein homeostasis by citalopram chronic treatment in a MJD mouse model**

---

**Exploring the modulation of protein homeostasis by citalopram chronic treatment in a MJD mouse model**

Stéphanie Oliveira<sup>1,2</sup>, Sara Duarte-Silva<sup>1,2</sup>, Olaf Riess<sup>3,4</sup>, Jeannette Hübener-Schmid<sup>3,4</sup>, Patricia Maciel<sup>1,2</sup>, Andreia Teixeira-Castro<sup>1,2,3</sup>

<sup>1</sup> Life and Health Sciences Research Institute (ICVS), School of Medicine, University of Minho, Campus of Gualtar, 4710-057 Braga, Portugal

<sup>2</sup> ICVS/3B's - PT Government Associate Laboratory, Braga/Guimarães, Portugal

<sup>3</sup> Institute of Medical Genetics and Applied Genomics, University of Tübingen, Tübingen, Germany

<sup>4</sup> Centre for Rare Diseases, Tübingen, Germany

(Manuscript *in preparation*)

---

## **Abstract**

The operational health of the proteome is ensured by a complex set of molecular players and integrated responses that constitute the protein quality control (PQC) network. The PQC network is a flexible system that participates in development, aging and responds to several environmental and cellular stresses.

Misfolding and protein function alterations triggered by genetic causes is at the base of polyglutamine disorders, that include spinocerebellar ataxia type 3 (SCA3) or Machado-Joseph disease (MJD), for which there is no disease-modifying treatment. Previously, we reported that citalopram, a selective serotonin reuptake inhibitor (SSRI), could be effectively repurposed for this disorder. Chronic pre-symptomatic treatment of MJD transgenic mice improved mutant ataxin-3 (ATXN3)-mediated pathogenesis, involving a drastic reduction in ATXN3 protein aggregation.

Here, we postulate that the improved motor coordination/balance and the suppression of ATXN3 proteotoxicity observed in MJD animal models, upon modulation of the serotonergic signaling by citalopram, is obtained through an enhancement and/or adaptation of the proteostasis capacity. Thus, by making use of transcriptomic analysis (RNA-sequencing) data, previously collected from the striatum of citalopram-treated and non-treated mice, and by constructing a database of described components of the PQC network, we searched for mutant ATXN3 and citalopram-mediated alterations in the expression of genes belonging to PQC mechanisms.

Our results showed no striking alterations in the PQC machinery in MJD transgenic mice at baseline. In contrast, citalopram treatment elicited several changes in the expression of PQC genes, mostly related to folding and conformational maintenance, and to the degradation modules of the PQC network. Interestingly, citalopram also led to an increase in players of the antioxidant response. Moreover, some of the changes observed in proteostasis might be triggered by the transcription factor cAMP-response element binding protein (CREB), an effector of the serotonin receptor 5-HT<sub>1A</sub> (5-HT<sub>1A</sub>R) transduction pathways, since several of the observed changes in the components of the PQC in cells are CREB targets.

Altogether, these results support the idea that the mechanism of action of citalopram could involve the modulation of the PQC machinery, boosting neuronal proteostasis capacity and, through this, be effective in counteracting MJD.

## 1. Introduction

Polyglutamine (polyQ) diseases are a group of nine inherited, late-onset and fatal neurodegenerative disorders caused by the expansion of the cytosine-adenosine-guanine (CAG) repeat, which is then translated into an atypically extended glutamine tract in the disease-associated protein [1].

Machado-Joseph disease (MJD) or spinocerebellar ataxia type 3 (SCA3) is a dominantly inherited polyQ disorder and the most common form of dominant spinocerebellar ataxia worldwide [2, 3]. Although all polyQ conditions have specific clinical symptomatology and pathology, the genes responsible for these diseases have no homology except for the polyQ domain itself, suggesting a possible shared pathological mechanism. It is believed that this particular domain highly promotes the toxic properties of the proteins [4]. The fact that functionally unrelated genes harbor polyQ expansions is a convincing indicator of a toxic gain-of-function of these proteins. A common assumed toxic gain-of-function mechanism involves disease-associated protein misfolding, the formation of toxic intermediate oligomeric species and deposition into aggregates, that may contribute to neuronal dysfunction and eventually cell death [5]. The aggregation process of these proteins causes an impairment in the cellular protein homeostasis, which also declines with aging further exacerbating cellular damage. Besides misfolding of the protein and consequent altered function, other hypotheses have been postulated to explain polyQ disease pathogenesis, such as (i) the abnormal protein interactions induced by the mutant protein; (ii) altered mitochondrial function; (iii) deregulated calcium homeostasis; (iv) defective DNA repair; and (v) defective axonal transport [6, 7].

In 2008, Balch and collaborators introduced the term *proteostasis* referring to the dynamic regulation of protein biogenesis, folding/conformation, trafficking and degradation, which constitutes the protein quality control (PQC) network, leading to a balanced and functional proteome [8]. Dysregulation of protein maintenance/stability seems to be a central process in polyQ disorders, including MJD. The expansion of the polyQ tract in proteins provokes a change in their conformation and increases aggregation propensity [9]. Additionally, the toxicity inherent to polyQ expansions is thought to be linked to the aberrant association of PQC components and other metastable proteins with these aggregates. For instance, in MJD, molecular chaperones, components of the ubiquitin-proteasome system (UPS) and transcription regulators are found sequestered into these aggregates, forming big neuronal inclusions [10-13]. This could strongly influence the proteostasis state of cells with this type of deposits. Beyond that, ATXN3 misfolding can directly have an impact on one of the PQC branches - degradation - because of its role, in the UPS, as a deubiquitylating enzyme [14-16]. Studies have proposed that ATXN3 helps in the proteasomal degradation of ubiquitylated proteins, by processing polyubiquitin chains of certain



substrates preceding digestion [17] and, in opposition, also protects others from degradation [18-20]. It is not surprising at all that clinical trials, for treating MJD, have been carried by intervention on mechanisms related to the PQC. Trehalose, which has been initially described as a chemical chaperone [21], with the ability to inhibit aggregation [22], alleviating motor symptoms and aggregation in MJD mouse models [23], but then shown to be implicated in autophagy mechanism [24], is being tested in MJD patients [25]. Also, nilotinib, another autophagy enhancer showed promising results in patients with chronic cerebellar ataxia [26].

Interestingly, serotonergic signaling appears to play an important role in cellular processes aiming at fixing protein damage and keeping homeostasis. Studies conducted in *Caenorhabditis elegans* (*C. elegans*) demonstrated that the simple activation of serotonergic neurons, with resulting serotonin (5-HT) release, is sufficient to lead to the activation of different responses in the worm peripheral tissues. This included the activation of the heat shock factor 1 (HSF1), which upregulates heat shock proteins (HSPs) - molecular chaperones - suppressing protein misfolding and aggregation [27]. Another study has reported that aggregation-prone proteins, in *C. elegans* neurons, are able to bind to mitochondria, triggering the unfolded protein response of the mitochondria (UPR<sup>mt</sup>), in intestine cells, and that 5-HT release from neurons is essential for this response, allowing signal propagation [28].

Undeniably, the modulation of serotonergic signaling could be beneficial for protein conformation disorders. In previous work, we described citalopram, an antidepressant belonging to the selective serotonin reuptake inhibitor (SSRI) category, that enhances serotonin signaling, as a potential therapeutic approach for MJD [29, 30]. Improvements were observed in motor behavior and suppression of mutant ataxin-3 (ATXN3) aggregation was achieved in MJD animal models, indicating that 5-HT recapture inhibition modulates proteotoxicity. Still, the exact downstream process by which this occurs remains to be clarified. Several lines of evidence suggest that antidepressants have neuroprotective effects associated to protein homeostasis responses. Zschocke and colleagues demonstrated that antidepressants, including citalopram, induce autophagy in astrocytes and neurons [31]. Moreover, SSRIs have been shown to alter the expression of HSPs [32], to induce the expression of the anti-oxidative enzyme heme oxygenase-1 (HO-1) [33] and to lessen endoplasmic reticulum (ER) stress via induction of the molecular chaperone sigma-1 receptor (Sig-1R) [34]. Unpublished results from our lab also pointed towards a citalopram-mediated induction of proteostasis-associated responses in *C. elegans*. Citalopram treatment of green fluorescent protein (GFP)-based reporter strains of the UPR<sup>mt</sup> and of the antioxidant response (strains harboring *hsp-60p::gfp* [35] and *gcs-1p::gfp* [36] transgenes, respectively), induced these responses, although in a mild way, at least for the antioxidant response (Teixeira-Castro, A. *et al.*,

*in preparation*). Furthermore, when citalopram chronic treatment was applied to a dynamin-1 temperature sensitive mutant (*dyn-1(ts)*) [37], that displays normal protein conformation and locomotion at 20 °C and becomes unfolded, leading to a paralysis phenotype, when animals are shifted to a 28 °C environment, led to a suppression of the paralysis phenotype. Altogether, these observations suggest that citalopram could be acting through an overall promotion of cellular protein homeostasis by maintaining and/or restoring normal protein conformation and triggering responses that promote cell optimal function and survival.

In this study, we hypothesized that the suppression of proteotoxicity, by modulation of the 5-HT signaling, could be achieved through an improvement of the proteostasis capacity, by eliciting specific proteostasis subnetworks. We made use of a transcriptomic analysis performed in the striatum of CMVMJD135 mice, treated and non-treated with citalopram, to search for potential changes in the PQC mechanisms upon treatment with this drug. Some alterations in the expression of genes belonging to the core PQC mechanisms and accessory pathways were found upon citalopram treatment. A substantial increase in the expression of protein degradation pathway-encoding genes, followed by lesser alterations in genes of folding/conformational maintenance were observed upon citalopram chronic treatment. Differentially expressed degradation genes included ubiquitin-specific proteins, voltage-gated channels, and cell death-related proteins. In the folding/conformational maintenance category, chaperones were present, including tetratricopeptide repeat (TPR) domain proteins that were highly represented. When auxiliary PQC signaling and stress pathways were assessed, the antioxidant response was the one with most differentially expressed genes upon SSRI treatment. These results further contribute to unveil citalopram-dependent molecular alterations that might underlie its efficacy in improving mutant ATXN3-mediated phenotypes.

## **2. Materials and methods**

### *2.1 Transcriptomic data*

The transcriptomic data used in the study was obtained by RNA-sequencing (RNA-seq) of the striatum of the CMVMJD135 mouse model, as previously described (see chapter 3.1 of the present thesis, section 2.1 to 2.2, for detailed information and protocols used for mice generation, maintenance, treatment administration, and retrieving of tissues). In brief, total RNA extracted from the striatum of 34-week-old male mice, with a mean  $\pm$  standard deviation (SD) of the CAG repeat size of  $128 \pm 5$ , treated pre-symptomatically and chronically with citalopram hydrobromide CAS 59729-32-7 (Lundbeck, Copenhagen, Denmark), at 8 mg/kg/day in drinking water, was used. The treatment was initiated at 5

weeks of age and administered for 29 weeks. RNA-seq was performed in wild-type (WT), transgenic (Tg) and transgenic-citalopram treated (Tg cit) littermate mice ( $n = 5$  per group). The RNA-seq protocol and analysis details are given in chapter 3.1, section 2.3 and 2.4. Gene expression was obtained for each group ( $n = 5$  WT,  $n = 4$  Tg and  $n = 3$  Tg cit) and differential expression in all possible different comparisons was analyzed: WT *versus* (*vs*) Tg; Tg *vs* Tg cit and WT *vs* Tg cit. Absolute log<sub>2</sub> fold change (FC) of at least 1 (i.e., double or half the expression strength) and  $p$ -value  $\leq 0.05$  were considered for differentially expressed genes (DEGs).

## 2.2 Transcriptomic data analysis: protein quality control (PQC) network

To determine alterations in the expression of genes belonging to the PQC machinery in our data, we first gathered a list of genes which were previously described to be part of this network. The list was organized into three core modules: protein synthesis, folding/conformational maintenance, and degradation.

The construction of the PQC core module gene list was based on the review work of Klaips, Javaraj and Hartl, where several data sources are cited for each module of the PQC network (synthesis, folding and degradation), including the number of components they found in each one [38]. To retrieve genes belonging to the synthesis part of the PQC they described the use of the *Harmonizome* database, which is an online “collection of processed datasets gathered aiming at serve and mine knowledge about genes and proteins” [39]. This database was used to obtain a list of synthesis-associated genes. Since no description was made in Klaips *et al.* article on how the search was conducted in the database, we opted to use the keywords “ribosome” and “eukaryotic translation” to obtain a list of synthesis-associated genes. A total of 310 genes were obtained compared to the 279 referred in Klaips *et al.*, 2017. The folding/conformational maintenance genes were based on the reports of Brehme *et al.* [40], representing the human chaperome, and Tebbenkamp and colleagues [41], who performed an analysis of the chaperome in the adult mouse brain, in 2014 and 2010, respectively. Only Brehme *et al.* was referred in the article by Klaips *et al.* A list of 414 folding/conformational maintenance-related genes was obtained, compared to the 322 mentioned in Klaips *et al.* work. The genes in the protein degradation category were based on the combined analysis of the following articles: García-Prat *et al.*, 2016 [42], Li *et al.*, 2008 [43], Nijman *et al.*, 2005 [44] and Sowa *et al.*, 2009 [45] (all listed in Klaips *et al.*). A list of 1407 degradation-relevant genes was obtained, compared to the 1383 total genes reported in Klaips *et al.* Genes belonging to cellular compartment-specific stress responses accessory to the PQC, such as the unfolded protein response (UPR), the heat shock response (HSR) and the antioxidant response, were

based on García-Prat *et al.*, 2016 report [42]. Eighty-four genes composed each of the UPR and HSR lists, while 113 genes composed the antioxidant response gene list.

Whenever the gene identification (ID) reported in the source articles used was not from mouse, it was converted into *Mus musculus* species gene symbol and *Ensembl* ID to allow comparison with the RNA-seq dataset, using either the *Database for Annotation, Visualization and Integrated Discovery (DAVID)* version 6.8 [46, 47], more specifically the *Gene ID conversion* tool, or *BioMart* [48] from *Ensembl* database [49]. Next, mouse ID converted lists obtained were manually curated for the presence of unconverted genes and, if so, a manual search in *Ensembl* database was carried to find any existing homologue for this specific gene, since automatic conversion tools might not be updated so often. After this revision, final PQC components lists were obtained: 94, 414 and 1407 genes composed the list of the synthesis, the folding/conformational maintenance, and the degradation PQC modules, respectively. Final gene lists of the PQC network were then compared with each one of the RNA-seq lists of DEGs.

### 3. Results

#### 3.1 Gene expression changes of components of the core of the PQC network in MJD mice and upon citalopram treatment

Our previous (published and unpublished) experimental work suggested that citalopram treatment, as an SSRI, could mediate its positive effects on protein conformational disorders, namely in MJD, through its action on protein and cellular homeostasis. Reduction of ATXN3 aggregation and induction of transcriptional responses, such as the UPR<sup>mit</sup>, upon citalopram chronic treatment, supported this hypothesis.

The objective of this study was to investigate if changes in the mRNA expression of PQC players could be associated to the therapeutic effects of citalopram chronic administration in transgenic mice. For that, we constructed a list of PQC components based on literature reports. A total of 1875 genes were found in the literature search. These were further divided into three major core categories: protein synthesis (94 genes), folding and conformational maintenance (414 genes) and degradation (1407 genes). In comparison to what is described on Klaipe *et al.* [38], the principal source used for the elaboration of the core PQC lists, 94 *vs* 279 genes were found in the synthesis module, while 414 *vs* 332 were found in the folding/conformational maintenance module, and 1407 *vs* 1388 in the degradation module. Aside from the synthesis module, the numbers are relatively equivalent to what is generally referred in the literature (consisting in a total of  $\approx$  2000 components that act to maintain cellular proteostasis). The smaller number of genes gathered in the synthesis list can be explained by the absence

of an exact methodology description used in Klaips *et al.* to be followed in the present work, that might be reflected by different keywords used in the *Harmonizome* database, for instance. Also, the fact that all the genes retrieved were then converted into *Mus musculus* orthologs for RNA-seq comparison purposes might introduce slight variations in the number of genes listed. From the total list of PQC core pathway genes, 10.7 % were detected in our RNA-seq analysis (Figure 3.2.1A) and 8.1 % had altered expression (Figure 3.2.1B). From these differentially expressed genes (DEGs), the majority belonged to the degradation (6.4 %), and also to the folding/conformational maintenance (1.76 %) branches of the PQC network (Figure 3.2.1B). Specifically, in CMVMJD135 transgenic mice compared to WT, 4.35 % of the genes with altered expression encoded PQC components (Figure 3.2.1C), a number that doubled up to 8.28 % when transgenic treated and non-treated animals were analyzed (Figure 3.2.1D). As observed for the global analysis, a higher number of components of the degradation pathways, followed by the folding/conformational maintenance category, were found in the transgenic *versus* transgenic-treated mice.

Focusing on the synthesis part of the PQC network, no genes were found to be altered in the transgenic mice at baseline, and only two genes were downregulated upon citalopram treatment: *Urb1*, URB1 ribosome biogenesis 1 homolog, and *Eif2ak2*, eukaryotic translation initiation factor 2-alpha kinase 2 (Table 3.2.1).

In the folding and conformational maintenance module of the PQC network, one gene was altered in the transgenic mice (*Ptgds*, prostaglandin D2 synthase) when compared to WT animals, while nineteen were differentially expressed upon citalopram treatment (Table 3.2.1). Interestingly, this gene encodes a protein (also known as L-PGDS or  $\beta$ -trace protein) proposed to be a major amyloid  $\beta$ -chaperone in the CSF [50], as well as playing a role as a disaggregase of A $\beta$  pre-formed fibrils [51]. Some of the genes found to be altered upon treatment, in this category, are well known molecular chaperones and cochaperones, generally associated with the folding of proteins, with potential impact on important cellular processes [52]. Interestingly, several proteins harboring a tetratricopeptide repeat (TPR) domain [53] were also differentially expressed, up- or downregulated upon treatment. TPR domain-containing proteins are described to bind to the heat shock proteins Hsp90 and Hsp70, allowing them to function as chaperones [54]. Some of the TPR domain-containing genes found showed high expression changes, such as *Ttc29*, indicating that these might be tightly influenced by treatment administration. Although not much has been reported about these TPR domain-containing genes, displayed in Table 3.2.1, TTC29 has been proposed to play a role as a dynein-associated protein, important for cellular transport, namely along

axonemes [55]. This suggest that a set of functions accomplished by TPR proteins could be triggered and/or enhanced by citalopram, in the context of MJD.

In the last category of the PQC network analyzed - degradation - a total of two genes showed altered expression (downregulation) in transgenic mice at baseline, while treatment with citalopram induced alterations in 76 genes within this category (some of these genes are listed in Table 3.2.1). Remarkably, the serotonin receptor *Htr1a/5-HT<sub>1A</sub>R* is categorized as a degradation gene of the PQC machinery, which is in line with the description of its role as an autophagy inducer in retinal pigment epithelium [56] and in lung adenocarcinomas cell lines [57]. The protein degradation-relevant genes altered upon citalopram treatment in transgenic mice are various and include genes encoding for ubiquitin-specific proteins, voltage-gated channels, transmembrane proteins, and Bcl-2-related proteins (see Table 3.2.1). This is indicative that citalopram treatment could perhaps shape the cellular environment by activating several genes implicated in degradation and alleviating protein aggregation burden. Further studies are required to conclude more about this matter.

Overall, a modest percentage of PQC genes had altered expression in the transcriptomic data and the results suggest that, perhaps counter-intuitively, no major changes in cellular proteostasis mechanisms are contributing/associated to ATXN3 pathogenesis. Instead, a consistently higher number of these genes are found to be differentially expressed upon citalopram administration, supporting the idea that the mode of action of citalopram may include modulation of proteostasis.

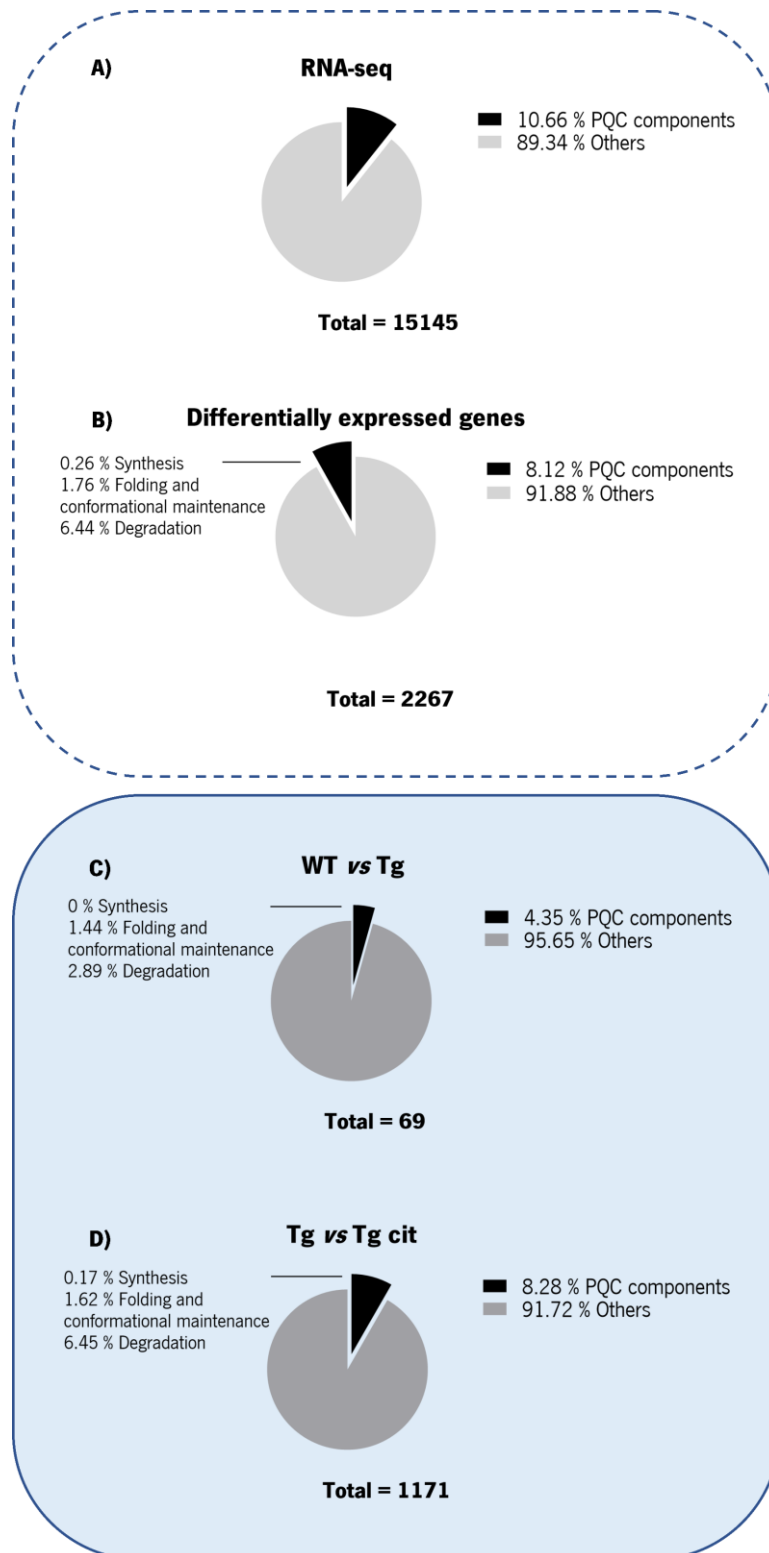


**Figure 3.2.1 Components of the degradation branch of the protein quality control (PQC) network show altered expression in the striatum of MJD transgenic mice, mostly upon citalopram treatment.** Percentage (%) of PQC components in **A)** the total RNA-seq data, **B)** the total of differentially expressed genes (DEGs) and the DEGs of **C)** Wild-type (WT) *vs* Transgenic (Tg) and **D)** Tg *vs* Tg-citalopram (cit)-treated mice, with information for each PQC core categories (synthesis, folding/conformational maintenance, and degradation).

**Table 3.2.1 List of a subset of the DEGs found in the different PQC core categories, according to each comparison analyzed.** Only the ten most up- or downregulated genes (in red and green, respectively) are shown in each comparison, listed in decreasing order of fold change (Log<sub>2</sub> FC). DEGs - differentially expressed genes; PQC - protein quality control.

PQC branch	Comparison	Gene	Description	Log <sub>2</sub> FC	CREB target?
<b>Synthesis</b>	Tg vs Tg cit	<i>Eif2ak2</i>	Eukaryotic translation initiation factor 2-alpha kinase 2	-1.73	No
		<i>Urb1</i>	URB1 ribosome biogenesis 1 homolog ( <i>S. Cerevisiae</i> )	-1.04	No
<b>Folding and conformational maintenance</b>	WT vs Tg	<i>Ptgds</i>	Prostaglandin D2 synthase (brain)	1.00	No
	Tg vs Tg cit	<i>Txnrd3</i>	Thioredoxin reductase 3	1.78	Yes
		<i>Ttc9b</i>	Tetratricopeptide repeat domain 9B	1.26	No
		<i>Hsf4</i>	Heat shock transcription factor 4	1.09	Yes
		<i>Hspbp1</i>	HSPA (heat shock 70kda) binding protein, cytoplasmic cochaperone 1	1.08	Yes
		<i>Rapsn</i>	Receptor-associated protein of the synapse	1.08	No
		<i>Ttc29</i>	Tetratricopeptide repeat domain 29	-8.26	Yes
		<i>Crybg3</i>	Beta-gamma crystallin domain containing 3	-5.50	No
		<i>Ttc21a</i>	Tetratricopeptide repeat domain 21A	-2.18	No
		<i>Lrp2bp</i>	Lrp2 binding protein	-1.95	No
		<i>Dnajc25</i>	Dnaj heat shock protein family (Hsp40) member C25	-1.54	No
		<i>Ttc12</i>	Tetratricopeptide repeat domain 12	-1.45	No
		<i>Atad2</i>	Atpase family, AAA domain containing 2	-1.39	Yes
		<i>Atad5</i>	Atpase family, AAA domain containing 5	-1.31	No
		<i>Uty</i>	Ubiquitously transcribed tetratricopeptide repeat gene, Y chromosome	-1.26	No
		<i>Kdm6a</i>	Lysine (K)-specific demethylase 6A	-1.20	Yes
<b>Degradation</b>	WT vs Tg	<i>Daw1</i>	Dynein assembly factor with WDR repeat domains 1	-2.33	No



<b>Degradation</b>		<i>Htr1a</i>	5-hydroxytryptamine (serotonin) receptor 1A	-1.37	Yes
	Tg vs Tg cit	<i>Usp50</i>	Ubiquitin specific peptidase 50	3.39	No
		<i>Kcns3</i>	Potassium voltage-gated channel, delayed-rectifier, subfamily S, member 3	3.23	No
		<i>Ubc</i>	Ubiquitin C	1.95	Yes
		<i>Kcnc4</i>	Potassium voltage gated channel, Shaw-related subfamily, member 4	1.90	No
		<i>Cebpb</i>	CCAAT/enhancer binding protein (C/EBP), beta	1.76	Yes
		<i>Bok</i>	BCL2-related ovarian killer	1.63	Yes
		<i>Trim47</i>	Tripartite motif-containing 47	1.54	Yes
		<i>Htr1a</i>	5-hydroxytryptamine (serotonin) receptor 1A	1.49	Yes
		<i>Fbxo36</i>	F-box protein 36	1.23	Yes
		<i>Anapc11</i>	Anaphase promoting complex subunit 11	1.17	Yes
		<i>Kcna3</i>	Potassium voltage-gated channel, shaker-related subfamily, member 3	-8.82	No
		<i>Tmem74</i>	Transmembrane protein 74	-8.23	No
		<i>Rad51</i>	RAD51 recombinase	-3.45	No
		<i>Kctd16</i>	Potassium channel tetramerisation domain containing 16	-2.39	No
		<i>Vps13c</i>	Vacuolar protein sorting 13C	-2.35	No
		<i>Btbd7</i>	BTB (POZ) domain containing 7	-2.17	No
		<i>Sntb2</i>	Syntrophin, basic 2	-2.09	Yes
		<i>Klhl3</i>	Kelch-like 3	-2.00	No
		<i>Muc1</i>	Mucin 1, transmembrane	-1.88	No
<i>Klhl11</i>	Kelch-like 11	-1.73	No		

### 3.2 Gene expression changes of stress responses auxiliary to the PQC network in MJD mice and upon citalopram treatment

PQC is an integrated system also consisting of accessory signaling and stress pathways, including the UPR [58], the heat shock response (HSR) [59] and the oxidative stress pathway [60], among others. Based on the data provided by García-Prat and colleagues, in 2016 [42], we analyzed citalopram impact in the expression of genes related to the UPR, the HSR and the antioxidant response in the CMVMJD135 mouse model treated chronically with citalopram.

The HSR and UPR gene lists were composed by 84 genes each and the antioxidant response list contained 113 genes. From these lists, six UPR, five HSR and 24 antioxidant response genes were found among the total of the RNA-seq DEGs, independently of the comparison (supplementary Table S3.2.1). Thus, the antioxidant response pathway is the most represented pathway in the transcriptomic data.

Regarding the HSR, no genes were altered in the transgenic mice at baseline, but one gene, *Hsf4* (heat shock transcription factor 4), that was upregulated upon treatment (Table 3.2.2).

Although no alterations were found in the transgenic mice regarding the UPR, two genes had altered expression after citalopram treatment: *Cebpb* (CCAAT/enhancer binding protein (C/EBP), beta) gene was upregulated and a downregulation of *Edem3* (ER degradation enhancer, mannosidase alpha-like 3) gene was observed (Table 3.2.2).

The antioxidant response had one gene expression alteration in the transgenic mice at baseline: *Krt1* (keratin 1). Keratins are also found in the brain [61, 62] and increased expression of *Krt1* was found in tissues of *Keap1* KO mice (an inhibitor of the Nrf2 activity, which regulates the expression of antioxidant proteins) and during keratinocyte differentiation, so this gene might be activated by Nrf2 transcription factor as part of its-mediated signaling pathways [63, 64]. Six genes were differentially expressed upon citalopram chronic treatment: *Sod3* (superoxide dismutase 3), *Sesn3* (sestrin 3), *Mt1* (metallothionein 1), *Ngb* (neuroglobin), *Gpx3* (glutathione peroxidase 3) and *Txnrd3* (thioredoxin reductase 3) as displayed in Table 3.2.2.

**Table 3.2.2 List of the DEGs found in the different PQC accessory pathways, according to each comparison analyzed.** Up- or downregulated genes (in red and green, respectively) are shown in each comparison, listed in decreasing order of fold change (Log<sub>2</sub> FC). DEGs - differentially expressed genes; PQC - protein quality control; HSR - heat shock response. UPR - unfolded protein response.

PQC pathway	Comparison	Gene	Description	Fold Change (Log <sub>2</sub> FC)	CREB target?
<b>HSR</b>	Tg vs Tg cit	<i>Hsf4</i>	Heat shock transcription factor 4	1.09	Yes
<b>UPR</b>	Tg vs Tg cit	<i>Cebpb</i>	CCAAT/enhancer binding protein (C/EBP), beta	1.76	Yes
		<i>Edem3</i>	ER degradation enhancer, mannosidase alpha-like 3	-1.00	No
<b>Antioxidant response</b>	WT vs Tg	<i>Krt1</i>	Keratin 1	1.15	No
	Tg vs Tg cit	<i>Gpx3</i>	Glutathione peroxidase 3	3.38	No
		<i>Ngb</i>	Neuroglobin	2.91	Yes
		<i>Txnrd3</i>	Thioredoxin reductase 3	1.78	Yes
		<i>Mt1</i>	Metallothionein 1	1.02	Yes
		<i>Sod3</i>	Superoxide dismutase 3, extracellular	1.00	No
		<i>Sesn3</i>	Sestrin 3	-1.61	No

Even though only slight changes were observed in PQC accessory stress response pathways in our CMVMJD135 mice transcriptomic data, these could be a window to understanding the type of responses induced by citalopram chronic treatment. In this way, some of the beneficial effects observed after this SSRI chronic treatment, in MJD animal models, could be explained by the modulation of pathways like these, that act in response to certain cellular triggers (temperature, misfolded proteins, aggregation, for instance). Alterations in the antioxidant response, namely in glutathione peroxidase *Gpx3*, which displays a high fold change, could be linked to modifications observed in MJD patients, whose antioxidant capacity is decreased [65, 66]. This diminished antioxidant capacity in patients is reflected by decreased levels of glutathione peroxidase and superoxide dismutase enzymes [65, 66], expression of which was found to be upregulated upon citalopram treatment in our RNA-seq dataset (*Gpx3* and *Sod3*, Table 3.2.2). Hence, citalopram seems to be acting in one of the described toxicity-mediating mechanisms of MJD which is mitochondrial impairment and oxidative stress. Regarding the HSR, the upregulated expression of *Hsf4* in treated MJD mice, could be indicative of a response normally triggered by exposure of cells and tissues to extreme conditions that cause acute and/or chronic stress. Expression of *Hsf4* is primarily related to eye tissues, but it is also expressed in the brain, skeletal muscle and pancreas [67],

and associated to the expression of small heat shock proteins named crystallins, which maintain protein stability [68]. Finally, UPR-related mechanisms might also contribute to citalopram mechanism of action, since upon treatment a couple of genes within this pathway had altered expression (*Cebpb* and *Edem*, Table 3.2.2). *Cebpb* encodes a transcription factor which activation is induced upon ER stress, fitting with the description that ATXN3 interacts with players of the ER-associated degradation (ERAD) system (like valosin-containing protein - VCP/P97 [69]), and that, consequently, mutant ATXN3 leads to deficient ER function, promoting ER stress. Regarding *Edem3*, the protein it encodes was reported to accelerate the degradation, through ERAD, of misfolded glycoproteins [70]. Although this gene is downregulated upon treatment (Table 3.2.2), our observation suggests that citalopram can modulate this type of PQC auxiliary responses.

### **3.3 Involvement of CREB transcription program in citalopram-induced alterations of the PQC machinery**

Serotonergic signaling modulation by citalopram, in the context of MJD, could require the cAMP response element-binding protein - CREB - transcription factor to mediate its protective effects (as explored in the chapter 3.1 of this thesis). As CREB is involved in the transcription of target genes with a multitude of functions, we asked whether a subset of the PQC altered genes, found in the transcriptomic analysis, were putative targets of this transcription factor. For this, we compared PQC genes with altered expression with the list of CREB target genes described in chapter 3.1.

When analyzing the synthesis module of the PQC network, none of the genes in this category were CREB targets (see Table 3.2.1). In the folding/conformational maintenance category, six genes were found to be CREB targets, all of them with differences in expression upon citalopram treatment. Regarding degradation, one gene differentially expressed in the transgenic mice (*Htr1a/5-HT<sub>1A</sub>R*) was found to be a CREB target. The 5-HT<sub>1A</sub>R has been described as a CREB target only in one of the research article used in the elaboration of our CREB target list, possibly due to the comprehensive methodology used in this work [71]. From our knowledge, no descriptions of CREB being able to directly alter the transcription of this receptor were reported and further research is therefore needed to clarify this point. Twenty-eight genes, among the 76 protein degradation-related genes altered upon citalopram treatment, were classified as targets of CREB. Additionally, when auxiliary stress responses of the PQC were analyzed, some CREB targets were also found. In the HSR, *Hsf4* was described as a target of CREB. In the UPR, the *Cebpb* gene and, involved in the antioxidant response, the *Mt1*, *Ngb* and *Txnrd3* genes were

categorized as targets of the CREB transcription factor. A summary of these observations is shown in Table 3.2.3.

Considering the results presented, it seems that CREB might not be a decisive factor in ATXN3-mediated pathogenesis, but could play a role, at least partially, in citalopram-mediated changes in proteostasis. No changes in CREB targets belonging to the different PQC mechanisms were observed in transgenic mice at baseline, except for the degradation branch, in which one of the two genes with altered expression is targeted by this transcription factor. On the other hand, in treated transgenic mice at least 30 % of the DEGs in each PQC category and/or pathway, except for synthesis, were CREB targets. Folding and conformational maintenance as well as degradation might therefore assume a higher relevance in the MOA of this drug, since a greater number of genes are changed in those categories (32 and 37 %, respectively, as displayed in Table 3.2.3). Moreover, this suggests that CREB could be implicated in the modulation of protein homeostasis responses and further supports its role as an agent in the mechanism of action of citalopram.

**Table 3.2.3 Proportion of PQC components that are also CREB targets in the mouse transcriptomic analysis.**

PQC - protein quality control. DEGs - differentially expressed genes.

Comparison PN branch	WT vs Tg			Tg vs Tg cit		
	DEGs	CREB targets	CREB targets (%)	DEGs	CEB targets	CREB targets (%)
Synthesis	0	0	<b>0</b>	2	0	<b>0</b>
Folding and conformational maintenance	1	0	<b>0</b>	19	6	<b>32</b>
Degradation	2	1	<b>50</b>	76	28	<b>37</b>
HSR	0	0	<b>0</b>	1	1	<b>100</b>
UPR	0	0	<b>0</b>	2	1	<b>50</b>
Antioxidant response	1	0	<b>0</b>	6	3	<b>50</b>

## 4. Discussion

Little is known about how antidepressant activity impacts on cellular proteostasis. In this study, we aimed at unveiling citalopram's effect on the PQC machinery, in the context of the neurodegenerative disorder MJD. Although this study is mostly exploratory, since the analyses described were only based on transcriptomic data and not further validated at the mRNA or protein level, it strengthened previous observations on the modulation of the PQC network by this SSRI and perhaps on its contribution to the offsetting of MJD animal models' phenotypes. Additionally, it gave us some clues about specific PQC mechanisms that could be triggered by treatment.

Many inherited neurodegenerative disorders, as MJD, are caused by mutations in the sequence of a polypeptide chain. Mutations like these contribute to protein instability, misfolding and ultimately to disease. In this context, PQC system assumes a critical role assuring proteome equilibrium. Notably, PQC machinery is dynamically regulated by multiple signaling pathways [72], and in response to a wide range of signals, such as genetic changes, environmental stress and aging [73-75].

In this study, although, unexpectedly, no major alterations were observed in the disease context alone, it is possible that the modulation of specific players can be important. Also, we must not forget that the starting point for the analysis is one specific time point and a very particular region of the brain, which perhaps could display a different protein state than other brain regions, namely in terms of misfolding and aggregation. Indeed, CMVMJD135 animals do not show big mutant ATXN3 aggregation in the striatum, at least the ones detected by immunohistochemistry analysis. The presence of smaller oligomeric species still needs further investigation. This point should be clarified in future analysis to better interpret the present results.

Previously, it was shown that although modulating PQC responses, like the HSR, had a beneficial effect on aggregation and motor phenotype of a HD mouse model, this effect was transient and decreased along with disease progression, despite an increase in aggregate load over time [76]. So, the simple presence of polyQ protein aggregates apparently fails to constitutively activate stress responses. This was explained by a change in chromatin structure (hypoacetylation of tetra-acetylated histone H4) which reduced heat shock factor 1 (HSF1) binding [76]. In MJD, ATXN3 is known to modulate histone acetylation and deacetylation at specific promoters. Indeed, normal and pathological forms of ATXN3 were described to bind to histone H4 [77]. Moreover, mutant ATXN3 was shown to cause hypoacetylation of histones H3 and H4 [78], which suggest that HSR and other similar responses might be activated with increasing difficulty as the disease progresses. Still, some expression changes were observed in transgenic mice and the alteration in one or few specific players of core PQC mechanisms could be important in the

context of the disease. An alteration in the folding/conformational maintenance category was observed with a prostaglandin D2 synthase gene, *Ptgds*. This gene has been proposed as a potential biomarker for Parkinson's disease (PD) due to its upregulation in patients [79]. It catalyzes the conversion of prostaglandin H2 (PGH2) to prostaglandin D2 (PGD2), which is known to play a role in sleep [80], smooth muscle contraction/relaxation [81] and to inhibit platelet aggregation [82]. Very interestingly, PTGDS, also known as L-PGDS or  $\beta$ -trace protein, is proposed to be a major amyloid  $\beta$ -chaperone in human cerebrospinal fluid (CSF) [50]. Moreover, recently, a role as disaggregase of A $\beta$  pre-formed fibrils has been proposed for this protein [51]. The upregulation of the gene in our data might be consistent with this disaggregase role.

In the degradation module, two genes were altered in the transgenic mice: *Daw1* and *Htr1a*. The first, a dynein assembly factor, has been shown to support normal ciliary movement by favoring delivery of dynein complexes to axonemal microtubules [83, 84]. Curiously, dynein motor machinery plays a role in autophagy and aggregation, since microtubule disruption inhibits autophagosome-lysosome fusion [85], and dynein mutations harm autophagic clearance of aggregation-prone proteins [86]. Somehow, a subtle dysfunction in the degradation process, more specifically in autophagy could exist in our CMVMJD135 model as it has been proposed by others [87], even though our observations with the autophagy inducing drugs lithium and CCI-779 suggest that the ability to activate this process is preserved in this model [88, 89]. Regarding *Htr1a*/5-HT<sub>1A</sub>R, it has been demonstrated that the activation of this receptor can lead to autophagy in tumor cells [57]. Therefore, it is possible that the *Htr1a*/5-HT<sub>1A</sub>R downregulation observed in our mice model could contribute for a dysfunction of this degradation process.

Interestingly, when we addressed the effect of citalopram on the PQC core machinery in MJD, we observed that the expression of a high number of genes was driven (Table 3.2.1), particularly in the folding/conformational maintenance and degradation modules of the PQC network. Nonetheless, two genes in the synthesis branch are downregulated in the transgenic mice upon citalopram treatment: *Eif2ak2* and *Urb1*. The Eukaryotic Translation Initiation Factor 2 Alpha Kinase 2 (*Eif2ak2* or *PKR*) phosphorylates eIF2 $\alpha$  and decreases translation activity in mammals [90]. In Alzheimer's (AD), Parkinson's (PD) and Huntington's diseases (HD), it has been implicated in mediating an ER stress-induced process of cell death [91, 92], so the downregulation of this gene by citalopram treatment could be protective. To the best of our knowledge, nothing has been described about the *Urb1* gene, which encodes a ribosome assembly factor, in the context of neurodegenerative diseases, but its action is reported to occur downstream of mTOR complex 1, to regulate ribosome biogenesis and protein synthesis [93], and it has been described to contribute to cancer cell proliferation [94, 95].

In the folding/conformational maintenance module, several groups of genes were altered. Noticeable was the presence of molecular chaperones, defined as any protein that interacts with and helps in the folding/assembly of another without remaining in its final structure [96]. Interestingly, citalopram seems to upregulate the *Hspbp1* gene, encoding a co-chaperone that regulates protein degradation by inhibiting the ubiquitin ligase activity of the C-terminus of Hsp70-interacting protein (CHIP) and so abolishes chaperone-assisted protein degradation [97]. Also, it has been reported that *Hspbp1* regulates the formation of stress granules [98]. A possible modulation of the heat shock response is suggested by the increased expression of *Hsf4* observed, a gene that is highly cell-type specific and associated with the expression of crystallins [68, 99]. Highly represented are proteins with a tetratricopeptide repeat (TPR) domain [53], some up- and others downregulated. For instance, this domain is essential for the binding to the heat shock proteins Hsp90 and Hsp70 for them to function as molecular chaperones [54, 100, 101]. Therefore, we could suspect a role in this way for TPR proteins found in our analysis. However, not much is described about the TPR proteins listed in Table 3.2.1, so future experiments should be performed to address this. Some studies reported that they might play a role as dynein chaperones to help in the stabilization of microfilaments [55, 102], be important in ciliary pathologies [103] and also play a role in cancer [104] or even psychiatric disorders [105]. Intriguingly, ATXN3 is known to be required for cytoskeletal organization of neuronal cells [19] and, very recently, also proved to be important for regulation of ciliogenesis and ciliary retrograde transport in the retina [106]. So, we might envisage that citalopram modulation of genes related to these processes might contribute to restore some cellular equilibrium due to ATXN3 impaired function and consequent accumulation into aggregates.

Among, the degradation genes altered upon treatment, we found genes related to ubiquitin, as *Usp50* or *Ubc*, which were upregulated. The protein quality control and clearance systems, such as the UPS or the ER-associated protein degradation (ERAD), are essential in the context of conformational disorders [107]. Enhancement of degradation by citalopram could be possible by a hypothetical improvement of polyubiquitylation (upregulation of *Ubc*) or activation of *Usp50* (a deubiquitylating enzyme) that could potentially counteract ERAD deficiency by ATXN3 dysfunction [69, 108], although the function of *Usp50* has not been extensively characterized yet. Several potassium voltage-gated channels also seem to be modulated by citalopram treatment. Indeed, studies have indicated that there is a potassium channel dysfunction in models of MJD [109, 110], so citalopram might act in favor of the regulation of these channels to restore existing defects in the disease. The presence of *Bok* (Bcl-2 related ovarian killer), a pro-apoptotic factor, among the genes differentially expressed upon citalopram chronic



treatment, might indicate a role for this compound in the induction of apoptosis, as it has already been demonstrated [111].

The effect of SSRI treatment on PQC auxiliary pathways is also interesting (Table 3.2.2). A significant regulation in the antioxidant response seems to happen following citalopram treatment, since a higher number of genes were found to be altered. This is not at all indicative of a minor relevance of the other pathways, since we were looking at a specific point in time, after a long chronic treatment. The responses elicited in the beginning of the drug administration might differ a little from the ones prevailing at the end.

The antioxidant response provides organisms with an effective line of defense against environmental insults and stressors, namely oxidative stress [112]. It has been suggested that mutant ATXN3 contributes to a decrease in antioxidant capacity and increased oxidative stress susceptibility, ultimately leading to neuronal cell death in MJD. This occurs through ATXN3 regulation of FOXO4 pathway *via* the superoxide dismutase 2 (SOD2), which is disturbed upon expression of the mutant protein [113]. Additionally, other studies have reported an increase in mitochondrial DNA damage, activation of apoptotic pathways, as well as a reduction in antioxidant enzyme activity [114-116]. In fact, a decreased antioxidant capacity was observed in MJD patients, resultant of increased ROS generation and decreased levels of superoxide dismutase and glutathione peroxidase [65], along with a reduction in thiol levels (glutathione and thioredoxins) and higher levels of DNA damage [66]. Citalopram treatment seemed to be able to revert this reduction in antioxidant activity by increasing the expression of some of these enzymes (superoxide dismutase, glutathione peroxidase and thioredoxin reductase - see Table 3.2.2). Undeniably, therapeutic strategies that were shown to modulate the antioxidant response, in animal models of MJD, have had a positive effect on motor function [117, 118]. In this way, the modulation of the serotonergic signaling by this SSRI and its positive effects on the motor function and pathology of MJD models, previously observed in our lab, could be, in part, a result of its capacity to act on the antioxidant response.

Modulation of the UPR by citalopram in MJD context happens, although to a lesser extent than for other PQC accessory responses. ATXN3 protein may also contribute for an impaired UPR [119] and ERAD mechanism. Interestingly, citalopram altered the expression of *Edem3*, a gene described as being able to accelerate the degradation of misfolded glycoproteins, through ERAD [70]. Although this particular gene was downregulated, upregulation of *Cebpb* gene might indicate an activation of the UPR [120]. On the other hand, a very specific type of HSR could possibly be modulated through citalopram chronic treatment by upregulation of *Hsf4* gene. As above mentioned, its expression is usually cell-type specific,

but it was also found in the brain, and could be both an activator or repressor of heat shock genes by alternative splicing, although more often associated to the repression of heat shock genes expression [67, 121]. Transcriptomic analysis alone is not sufficient to infer on the exact status of the HSR but is a strong indication it is being modulated by citalopram. About these results, we must not disregard that uncontrolled activation of the HSR might be detrimental since it could elicit cellular dysfunction in certain neurodegenerative conditions [122].

As evidenced in chapter 3.1 of this thesis, we hypothesized that citalopram action, in MJD, might involve the restoration of the expression of the 5-HT<sub>1A</sub> serotonin receptor, its downstream transduction pathways and a final effector of those, the CREB transcription factor. We thought that if this were to be true, and CREB was to be playing a significant role in the mechanism of action of citalopram in MJD, some molecules involved in responses triggered by citalopram, as the ones associated to the PQC network, would be CREB targets. Effectively, some genes involved in the PQC machinery are CREB targets, as evidenced in the results (Table 3.2.3), which gives some support to our hypothesis. Furthermore, CREB involvement in proteostasis processes have already been described [123, 124]. However, more experimental evidence needs to be gathered to assure the veracity of our assumptions.

## **5. Conclusions**

The disruption of protein cellular dynamics is a well-established feature in polyQ disorders, namely MJD. In this study we show that serotonergic signaling modulation, through the SSRI citalopram, can alter the expression of several genes related to the PQC network, with higher impact on a subset related to protein degradation pathways and, to a lesser extent, on protein folding/conformational maintenance-related genes. Citalopram chronic treatment also seems to regulate the antioxidant response in the CMVMJD135 (MJD) mouse model. Likewise, the results point towards a possible role of the CREB transcription factor in the gene expression changes brought by citalopram. Although more research is needed to confirm these findings, essential clues on how this antidepressant offsets MJD animal models' phenotypes have been revealed.

## **Final considerations**

Observations made in this chapter could be completed by performing additional experiments, to test our hypothesis. Some assays are listed below:

- Confirm the changes in mRNA expression of PQC components, by qRT-PCR, in an independent cohort of animals (male and/or female mice striatum and other brain regions relevant for the disease);

- Confirm the impact of these changes at the protein level by Western blot;
- Explore the function of TPR domain-containing proteins in MJD models;
- Verify the dependence of the effect of citalopram treatment upon key regulators of the antioxidant response, using, for example, *C. elegans* mutant strains or by performing RNAi assays in citalopram-treated transgenic worms.

### **Acknowledgments**

We acknowledge the members of the Maciel laboratory for sharing reagents, for critical analysis of the data and discussion on the manuscript.

### **Funding**

This work was funded by National funds, through the Foundation for Science and Technology (FCT) - project UIDB/50026/2020 and UIDP/50026/2020; and by FEDER, through the Competitiveness Internationalization Operational Programme (POCI) under the scope of the projects: POCI-01-0145-FEDER-031987, NORTE-01-0145-FEDER-000013 and NORTE-01-0145-FEDER-000023, supported by North Portugal Regional Operational Programme (NORTE 2020), under the PORTUGAL 2020 Partnership Agreement, through the European Regional Development Fund (ERDF). This work has also been funded through the National Ataxia Foundation (NAF), USA, and by the U.S. Department of Defense (DoD) - grant award number: W81XWH-19-1-0638. Stéphanie Oliveira was also supported by a doctoral programme fellowship: Inter-University Doctoral Programme in Ageing and Chronic Disease from FCT - PD/BD/127818/2016.

## References

1. Margolis, R.L. and Ross, C.A., Expansion explosion: new clues to the pathogenesis of repeat expansion neurodegenerative diseases. *Trends in Molecular Medicine*, 2001. **7**(11): p. 479-482.[https://doi.org/10.1016/S1471-4914\(01\)02179-7](https://doi.org/10.1016/S1471-4914(01)02179-7).
2. Bird, T.D., Hereditary Ataxia Overview. GeneReviews®, ed. A.H. Adam MP, Pagon RA, *et al.*, editors. 1998 Oct 28 [Updated 2019 Jul 25], University of Washington, Seattle; 1993-2020.<https://www.ncbi.nlm.nih.gov/books/NBK1138/>.
3. Schöls, L., Bauer, P., Schmidt, T., Schulte, T., *et al.*, Autosomal dominant cerebellar ataxias: clinical features, genetics, and pathogenesis. *The Lancet Neurology*, 2004. **3**(5): p. 291-304.[https://doi.org/10.1016/S1474-4422\(04\)00737-9](https://doi.org/10.1016/S1474-4422(04)00737-9).
4. Zoghbi, H.Y. and Orr, H.T., Glutamine Repeats and Neurodegeneration. *Annual Review of Neuroscience*, 2000. **23**(1): p. 217-247.<https://doi.org/10.1146/annurev.neuro.23.1.217>.
5. Ross, C.A., Intranuclear Neuronal Inclusions: A Common Pathogenic Mechanism for Glutamine-Repeat Neurodegenerative Diseases? *Neuron*, 1997. **19**(6): p. 1147-1150.[https://doi.org/10.1016/S0896-6273\(00\)80405-5](https://doi.org/10.1016/S0896-6273(00)80405-5).
6. Gatchel, J.R. and Zoghbi, H.Y., Diseases of Unstable Repeat Expansion: Mechanisms and Common Principles. *Nature Reviews Genetics*, 2005. **6**(10): p. 743-755.<https://doi.org/10.1038/nrg1691>.
7. Massey, T.H. and Jones, L., The central role of DNA damage and repair in CAG repeat diseases. *Disease Models & Mechanisms*, 2018. **11**(1): p. dmm031930.<https://doi.org/10.1242/dmm.031930>.
8. Balch, W.E., Morimoto, R.I., Dillin, A., and Kelly, J.W., Adapting Proteostasis for Disease Intervention. *Science*, 2008. **319**(5865): p. 916-919.<https://doi.org/10.1126/science.1141448>.
9. Khare, S.D., Ding, F., Gwanmesia, K.N., and Dokholyan, N.V., Molecular Origin of Polyglutamine Aggregation in Neurodegenerative Diseases. *PLOS Computational Biology*, 2005. **1**(3): p. e30.<https://doi.org/10.1371/journal.pcbi.0010030>.
10. Chai, Y., Koppenhafer, S.L., Bonini, N.M., and Paulson, H.L., Analysis of the Role of Heat Shock Protein (Hsp) Molecular Chaperones in Polyglutamine Disease. *Journal of Neuroscience*, 1999. **19**(23): p. 10338-10347.<https://doi.org/10.1523/JNEUROSCI.19-23-10338.1999>.
11. Chai, Y., Koppenhafer, S.L., Shoesmith, S.J., Perez, M.K., *et al.*, Evidence for Proteasome Involvement in Polyglutamine Disease: Localization to Nuclear Inclusions in SCA3/MJD and Suppression of Polyglutamine Aggregation *in vitro*. *Human Molecular Genetics*, 1999. **8**(4): p. 673-682.<https://doi.org/10.1093/hmg/8.4.673>.
12. Chai, Y., Wu, L., Griffin, J.D., and Paulson, H.L., The Role of Protein Composition in Specifying Nuclear Inclusion Formation in Polyglutamine Disease. *Journal of Biological Chemistry*, 2001. **276**(48): p. 44889-44897.<https://doi.org/10.1074/jbc.M106575200>.

13. Schmidt, T., Lindenberg, K.S., Krebs, A., Schöls, L., *et al.*, Protein surveillance machinery in brains with spinocerebellar ataxia type 3: Redistribution and differential recruitment of 26S proteasome subunits and chaperones to neuronal intranuclear inclusions. *Annals of Neurology*, 2002. **51**(3): p. 302-310.<https://doi.org/10.1002/ana.10101>.
14. Donaldson, K.M., Li, W., Ching, K.A., Batalov, S., *et al.*, Ubiquitin-mediated sequestration of normal cellular proteins into polyglutamine aggregates. *Proceedings of the National Academy of Sciences*, 2003. **100**(15): p. 8892-8897.<https://doi.org/10.1073/pnas.1530212100>.
15. Doss-Pepe, E.W., Stenroos, E.S., Johnson, W.G., and Madura, K., Ataxin-3 interactions with rad23 and valosin-containing protein and its associations with ubiquitin chains and the proteasome are consistent with a role in ubiquitin-mediated proteolysis. *Molecular and Cellular Biology*, 2003. **23**(18): p. 6469-83.<https://doi.org/10.1128/mcb.23.18.6469-6483.2003>.
16. Burnett, B., Li, F., and Pittman, R.N., The polyglutamine neurodegenerative protein ataxin-3 binds polyubiquitylated proteins and has ubiquitin protease activity. *Human Molecular Genetics*, 2003. **12**(23): p. 3195-3205.<https://doi.org/10.1093/hmg/ddg344>.
17. Wang, H., Ying, Z., and Wang, G., Ataxin-3 Regulates Aggresome Formation of Copper-Zinc Superoxide Dismutase (SOD1) by Editing K63-linked Polyubiquitin Chains. *Journal of Biological Chemistry*, 2012. **287**(34): p. 28576-28585.<https://doi.org/10.1074/jbc.M111.299990>.
18. Costa, M.d.C., Bajanca, F., Rodrigues, A.-J., Tomé, R.J., *et al.*, Ataxin-3 Plays a Role in Mouse Myogenic Differentiation through Regulation of Integrin Subunit Levels. *PLOS ONE*, 2010. **5**(7): p. e11728.<https://doi.org/10.1371/journal.pone.0011728>.
19. Neves-Carvalho, A., Logarinho, E., Freitas, A., Duarte-Silva, S., *et al.*, Dominant negative effect of polyglutamine expansion perturbs normal function of ataxin-3 in neuronal cells. *Human Molecular Genetics*, 2015. **24**(1): p. 100-117.<https://doi.org/10.1093/hmg/ddu422>.
20. Liu, H., Li, X., Ning, G., Zhu, S., *et al.*, The Machado–Joseph Disease Deubiquitinase Ataxin-3 Regulates the Stability and Apoptotic Function of p53. *PLOS Biology*, 2016. **14**(11): p. e2000733.<https://doi.org/10.1371/journal.pbio.2000733>.
21. Tapia, H. and Koshland, Douglas E., Trehalose Is a Versatile and Long-Lived Chaperone for Desiccation Tolerance. *Current Biology*, 2014. **24**(23): p. 2758-2766.<https://doi.org/10.1016/j.cub.2014.10.005>.
22. Liu, R., Barkhordarian, H., Emadi, S., Park, C.B., *et al.*, Trehalose differentially inhibits aggregation and neurotoxicity of beta-amyloid 40 and 42. *Neurobiology of Disease*, 2005. **20**(1): p. 74-81.<https://doi.org/10.1016/j.nbd.2005.02.003>.
23. Santana, M.M., Paixão, S., Cunha-Santos, J., Silva, T.P., *et al.*, Trehalose alleviates the phenotype of Machado–Joseph disease mouse models. *Journal of Translational Medicine*, 2020. **18**(1): p. 161.<https://doi.org/10.1186/s12967-020-02302-2>.
24. Sarkar, S., Davies, J.E., Huang, Z., Tunnacliffe, A., *et al.*, Trehalose, a Novel mTOR-independent Autophagy Enhancer, Accelerates the Clearance of Mutant Huntingtin and  $\alpha$ -Synuclein. *Journal of Biological Chemistry*, 2007. **282**(8): p. 5641-5652.<https://doi.org/10.1074/jbc.M609532200>.

25. Zaltzman, R., Elyoseph, Z., Lev, N., and Gordon, C.R., Trehalose in Machado-Joseph Disease: Safety, Tolerability, and Efficacy. *The Cerebellum*, 2020. **19**(5): p. 672-679.<https://doi.org/10.1007/s12311-020-01150-6>.
26. Lee, W.-J., Moon, J., Kim, T.-J., Jun, J.-S., *et al.*, The c-Abl inhibitor, nilotinib, as a potential therapeutic agent for chronic cerebellar ataxia. *Journal of Neuroimmunology*, 2017. **309**: p. 82-87.<https://doi.org/10.1016/j.jneuroim.2017.05.015>.
27. Tatum, Marcus C., Ooi, Felicia K., Chikka, Madhusudana R., Chauve, L., *et al.*, Neuronal Serotonin Release Triggers the Heat Shock Response in *C. elegans* in the Absence of Temperature Increase. *Current Biology*, 2015. **25**(2): p. 163-174.<https://doi.org/10.1016/j.cub.2014.11.040>.
28. Berendzen, K.M., Durieux, J., Shao, L.-W., Tian, Y., *et al.*, Neuroendocrine Coordination of Mitochondrial Stress Signaling and Proteostasis. *Cell*, 2016. **166**(6): p. 1553-1563.e10.<https://doi.org/10.1016/j.cell.2016.08.042>.
29. Teixeira-Castro, A., Jalles, A., Esteves, S., Kang, S., *et al.*, Serotonergic signalling suppresses ataxin 3 aggregation and neurotoxicity in animal models of Machado-Joseph disease. *Brain*, 2015. **138**(11): p. 3221-3237.<https://doi.org/10.1093/brain/awv262>.
30. Esteves, S., Oliveira, S., Duarte-Silva, S., Cunha-Garcia, D., *et al.*, Preclinical Evidence Supporting Early Initiation of Citalopram Treatment in Machado-Joseph Disease. *Molecular Neurobiology*, 2019. **56**(5): p. 3626-3637.<https://doi.org/10.1007/s12035-018-1332-1>.
31. Zschocke, J., Zimmermann, N., Berning, B., Ganal, V., *et al.*, Antidepressant Drugs Diversely Affect Autophagy Pathways in Astrocytes and Neurons—Dissociation from Cholesterol Homeostasis. *Neuropsychopharmacology*, 2011. **36**(8): p. 1754-1768.<https://doi.org/10.1038/npp.2011.57>.
32. Guest, P.C., Knowles, M.R., Molon-Noblot, S., Salim, K., *et al.*, Mechanisms of action of the antidepressants fluoxetine and the substance P antagonist L-000760735 are associated with altered neurofilaments and synaptic remodeling. *Brain Research*, 2004. **1002**(1): p. 1-10.<https://doi.org/10.1016/j.brainres.2003.11.064>.
33. Lin, H.-Y., Yeh, W.-L., Huang, B.-R., Lin, C., *et al.*, Desipramine Protects Neuronal Cell Death and Induces Heme Oxygenase-1 Expression in Mes23.5 Dopaminergic Neurons. *PLOS ONE*, 2012. **7**(11): p. e50138.<https://doi.org/10.1371/journal.pone.0050138>.
34. Omi, T., Tanimukai, H., Kanayama, D., Sakagami, Y., *et al.*, Fluvoxamine alleviates ER stress via induction of Sigma-1 receptor. *Cell Death & Disease*, 2014. **5**(7): p. e1332-e1332.<https://doi.org/10.1038/cddis.2014.301>.
35. Yoneda, T., Benedetti, C., Urano, F., Clark, S.G., *et al.*, Compartment-specific perturbation of protein handling activates genes encoding mitochondrial chaperones. *Journal of Cell Science*, 2004. **117**(18): p. 4055-4066.<https://doi.org/10.1242/jcs.01275>.
36. An, J.H. and Blackwell, T.K., SKN-1 links *C. elegans* mesendodermal specification to a conserved oxidative stress response. *Genes & Development*, 2003. **17**(15): p. 1882-1893.<https://doi.org/10.1101/gad.1107803>.

37. Clark, S.G., Shurland, D.-L., Meyerowitz, E.M., Bargmann, C.I., *et al.*, A dynamin GTPase mutation causes a rapid and reversible temperature-inducible locomotion defect in *C. elegans*. *Proceedings of the National Academy of Sciences*, 1997. **94**(19): p. 10438-10443.<https://doi.org/10.1073/pnas.94.19.10438>.
38. Klaips, C.L., Jayaraj, G.G., and Hartl, F.U., Pathways of cellular proteostasis in aging and disease. *Journal of Cell Biology*, 2017. **217**(1): p. 51-63.<https://doi.org/10.1083/jcb.201709072>.
39. Rouillard, A.D., Gundersen, G.W., Fernandez, N.F., Wang, Z., *et al.*, The harmonizome: a collection of processed datasets gathered to serve and mine knowledge about genes and proteins. *Database*, 2016. **2016**.<https://doi.org/10.1093/database/baw100>.
40. Brehme, M., Voisine, C., Rolland, T., Wachi, S., *et al.*, A Chaperome Subnetwork Safeguards Proteostasis in Aging and Neurodegenerative Disease. *Cell Reports*, 2014. **9**(3): p. 1135-1150.<https://doi.org/10.1016/j.celrep.2014.09.042>.
41. Tebbenkamp, A.T.N. and Borchelt, D.R., Analysis of Chaperone mRNA Expression in the Adult Mouse Brain by Meta Analysis of the Allen Brain Atlas. *PLOS ONE*, 2010. **5**(10): p. e13675.<https://doi.org/10.1371/journal.pone.0013675>.
42. Garcia-Prat, L., Martinez-Vicente, M., Perdiguero, E., Ortet, L., *et al.*, Autophagy maintains stemness by preventing senescence. *Nature*, 2016. **529**(7584): p. 37-42.<https://doi.org/10.1038/nature16187>.
43. Li, W., Bengtson, M.H., Ulbrich, A., Matsuda, A., *et al.*, Genome-Wide and Functional Annotation of Human E3 Ubiquitin Ligases Identifies MULAN, a Mitochondrial E3 that Regulates the Organelle's Dynamics and Signaling. *PLOS ONE*, 2008. **3**(1): p. e1487.<https://doi.org/10.1371/journal.pone.0001487>.
44. Nijman, S.M.B., Luna-Vargas, M.P.A., Velds, A., Brummelkamp, T.R., *et al.*, A Genomic and Functional Inventory of Deubiquitinating Enzymes. *Cell*, 2005. **123**(5): p. 773-786.<https://doi.org/10.1016/j.cell.2005.11.007>.
45. Sowa, M.E., Bennett, E.J., Gygi, S.P., and Harper, J.W., Defining the Human Deubiquitinating Enzyme Interaction Landscape. *Cell*, 2009. **138**(2): p. 389-403.<https://doi.org/10.1016/j.cell.2009.04.042>.
46. Huang da, W., Sherman, B.T., and Lempicki, R.A., Systematic and integrative analysis of large gene lists using DAVID bioinformatics resources. *Nature Protocols*, 2009. **4**(1): p. 44-57.<https://doi.org/10.1038/nprot.2008.211>.
47. Huang, D.W., Sherman, B.T., and Lempicki, R.A., Bioinformatics enrichment tools: paths toward the comprehensive functional analysis of large gene lists. *Nucleic Acids Research*, 2008. **37**(1): p. 1-13.<https://doi.org/10.1093/nar/gkn923>.
48. Smedley, D., Haider, S., Ballester, B., Holland, R., *et al.*, BioMart – biological queries made easy. *BMC Genomics*, 2009. **10**(1): p. 22.<https://doi.org/10.1186/1471-2164-10-22>.
49. Yates, A.D., Achuthan, P., Akanni, W., Allen, J., *et al.*, Ensembl 2020. *Nucleic Acids Research*, 2019. **48**(D1): p. D682-D688.<https://doi.org/10.1093/nar/gkz966>.

50. Kanekiyo, T., Ban, T., Aritake, K., Huang, Z.-L., *et al.*, Lipocalin-type prostaglandin D synthase/ $\beta$ -trace is a major amyloid  $\beta$ -chaperone in human cerebrospinal fluid. *Proceedings of the National Academy of Sciences*, 2007. **104**(15): p. 6412-6417.<https://doi.org/10.1073/pnas.0701585104>.
51. Kannaian, B., Sharma, B., Phillips, M., Chowdhury, A., *et al.*, Abundant neuroprotective chaperone Lipocalin-type prostaglandin D synthase (L-PGDS) disassembles the Amyloid- $\beta$  fibrils. *Scientific Reports*, 2019. **9**(1): p. 12579.<https://doi.org/10.1038/s41598-019-48819-5>.
52. Young, J.C., Barral, J.M., and Ulrich Hartl, F., More than folding: localized functions of cytosolic chaperones. *Trends in Biochemical Sciences*, 2003. **28**(10): p. 541-547.<https://doi.org/10.1016/j.tibs.2003.08.009>.
53. Blatch, G.L. and Lässle, M., The tetratricopeptide repeat: a structural motif mediating protein-protein interactions. *BioEssays*, 1999. **21**(11): p. 932-939.[https://doi.org/10.1002/\(SICI\)1521-1878\(199911\)21:11<932::AID-BIES5>3.0.CO;2-N](https://doi.org/10.1002/(SICI)1521-1878(199911)21:11<932::AID-BIES5>3.0.CO;2-N).
54. Assimon, V.A., Southworth, D.R., and Gestwicki, J.E., Specific Binding of Tetratricopeptide Repeat Proteins to Heat Shock Protein 70 (Hsp70) and Heat Shock Protein 90 (Hsp90) Is Regulated by Affinity and Phosphorylation. *Biochemistry*, 2015. **54**(48): p. 7120-7131.<https://doi.org/10.1021/acs.biochem.5b00801>.
55. Brooks, E.R., Control of intraflagellar transport: studies of the planar cell polarity effector Fuz, the small GTPase Rsg1, and the novel protein TTC29. 2014.<http://hdl.handle.net/2152/24703>.
56. Thampi, P., Rao, H.V., Mitter, S.K., Cai, J., *et al.*, The 5HT<sub>1a</sub> Receptor Agonist 8-Oh DPAT Induces Protection from Lipofuscin Accumulation and Oxidative Stress in the Retinal Pigment Epithelium. *PLOS ONE*, 2012. **7**(4): p. e34468.<https://doi.org/10.1371/journal.pone.0034468>.
57. Liu, Y., Zhang, H., Wang, Z., Wu, P., *et al.*, 5-Hydroxytryptamine<sub>1a</sub> receptors on tumour cells induce immune evasion in lung adenocarcinoma patients with depression via autophagy/pSTAT3. *European Journal of Cancer*, 2019. **114**: p. 8-24.<https://doi.org/10.1016/j.ejca.2019.03.017>.
58. Bernales, S., Morales Soto, M., and McCullagh, E., Unfolded protein stress in the endoplasmic reticulum and mitochondria: a role in neurodegeneration. *Frontiers in Aging Neuroscience*, 2012. **4**(5).<https://doi.org/10.3389/fnagi.2012.00005>.
59. Morimoto, R.I., The Heat Shock Response: Systems Biology of Proteotoxic Stress in Aging and Disease. *Cold Spring Harbor Symposia on Quantitative Biology*, 2011. **76**: p. 91-99.<https://doi.org/10.1101/sqb.2012.76.010637>.
60. Zhang, H., Davies, K.J.A., and Forman, H.J., Oxidative stress response and Nrf2 signaling in aging. *Free Radical Biology and Medicine*, 2015. **88**: p. 314-336.<https://doi.org/10.1016/j.freeradbiomed.2015.05.036>.
61. Franko, M.C., Gibbs, C.J., Rhoades, D.A., and Gajdusek, D.C., Monoclonal antibody analysis of keratin expression in the central nervous system. *Proceedings of the National Academy of Sciences*, 1987. **84**(10): p. 3482-3485.<https://doi.org/10.1073/pnas.84.10.3482>.



62. Zhang, D., Dong, X., Liu, X., Ye, L., *et al.*, Proteomic Analysis of Brain Regions Reveals Brain Regional Differences and the Involvement of Multiple Keratins in Chronic Alcohol Neurotoxicity. *Alcohol and Alcoholism*, 2020. **55**(2): p. 147-156.<https://doi.org/10.1093/alcalc/aaa007>.
63. Wakabayashi, N., Itoh, K., Wakabayashi, J., Motohashi, H., *et al.*, *Keap1*-null mutation leads to postnatal lethality due to constitutive Nrf2 activation. *Nature Genetics*, 2003. **35**(3): p. 238-245.<https://doi.org/10.1038/ng1248>.
64. Piao, M.S., Park, J.-J., Choi, J.-Y., Lee, D.-H., *et al.*, Nrf2-dependent and Nrf2-independent induction of phase 2 detoxifying and antioxidant enzymes during keratinocyte differentiation. *Archives of Dermatological Research*, 2012. **304**(5): p. 387-395.<https://doi.org/10.1007/s00403-012-1215-7>.
65. de Assis, A.M., Saute, J.A.M., Longoni, A., Haas, C.B., *et al.*, Peripheral Oxidative Stress Biomarkers in Spinocerebellar Ataxia Type 3/Machado–Joseph Disease. *Frontiers in Neurology*, 2017. **8**(485).<https://doi.org/10.3389/fneur.2017.00485>.
66. Pacheco, L.S., da Silveira, A.F., Trott, A., Houenou, L.J., *et al.*, Association between Machado–Joseph disease and oxidative stress biomarkers. *Mutation Research/Genetic Toxicology and Environmental Mutagenesis*, 2013. **757**(2): p. 99-103.<https://doi.org/10.1016/j.mrgentox.2013.06.023>.
67. Nakai, A., Tanabe, M., Kawazoe, Y., Inazawa, J., *et al.*, HSF4, a new member of the human heat shock factor family which lacks properties of a transcriptional activator. *Molecular and Cellular Biology*, 1997. **17**(1): p. 469-481.<https://doi.org/10.1128/MCB.17.1.469>.
68. Fujimoto, M., Izu, H., Seki, K., Fukuda, K., *et al.*, HSF4 is required for normal cell growth and differentiation during mouse lens development. *The EMBO Journal*, 2004. **23**(21): p. 4297-4306.<https://doi.org/10.1038/sj.emboj.7600435>.
69. Zhong, X. and Pittman, R.N., Ataxin-3 binds VCP/p97 and regulates retrotranslocation of ERAD substrates. *Human Molecular Genetics*, 2006. **15**(16): p. 2409-2420.<https://doi.org/10.1093/hmg/ddl164>.
70. Hirao, K., Natsuka, Y., Tamura, T., Wada, I., *et al.*, EDEM3, a Soluble EDEM Homolog, Enhances Glycoprotein Endoplasmic Reticulum-associated Degradation and Mannose Trimming. *Journal of Biological Chemistry*, 2006. **281**(14): p. 9650-9658.<https://doi.org/10.1074/jbc.M512191200>.
71. Impey, S., McCorkle, S.R., Cha-Molstad, H., Dwyer, J.M., *et al.*, Defining the CREB Regulon: A Genome-Wide Analysis of Transcription Factor Regulatory Regions. *Cell*, 2004. **119**(7): p. 1041-1054.<https://doi.org/10.1016/j.cell.2004.10.032>.
72. Morimoto, R.I., Proteotoxic stress and inducible chaperone networks in neurodegenerative disease and aging. *Genes & Development*, 2008. **22**(11): p. 1427-1438.<https://doi.org/10.1101/gad.1657108>.
73. Douglas, P.M. and Dillin, A., Protein homeostasis and aging in neurodegeneration. *Journal of Cell Biology*, 2010. **190**(5): p. 719-729.<https://doi.org/10.1083/jcb.201005144>.

74. Prahlad, V. and Morimoto, R.I., Integrating the stress response: lessons for neurodegenerative diseases from *C. elegans*. *Trends in Cell Biology*, 2009. **19**(2): p. 52-61.<https://doi.org/10.1016/j.tcb.2008.11.002>.
75. Prahlad, V., Cornelius, T., and Morimoto, R.I., Regulation of the Cellular Heat Shock Response in *Caenorhabditis elegans* by Thermosensory Neurons. *Science*, 2008. **320**(5877): p. 811-814.<https://doi.org/10.1126/science.1156093>.
76. Labbadia, J., Cunliffe, H., Weiss, A., Katsyuba, E., *et al.*, Altered chromatin architecture underlies progressive impairment of the heat shock response in mouse models of Huntington disease. *The Journal of Clinical Investigation*, 2011. **121**(8): p. 3306-3319.<https://doi.org/10.1172/JCI57413>.
77. Li, F., Macfarlan, T., Pittman, R.N., and Chakravarti, D., Ataxin-3 Is a Histone-binding Protein with Two Independent Transcriptional Corepressor Activities. *Journal of Biological Chemistry*, 2002. **277**(47): p. 45004-45012.<https://doi.org/10.1074/jbc.M205259200>.
78. Chou, A.-H., Chen, Y.-L., Hu, S.-H., Chang, Y.-M., *et al.*, Polyglutamine-expanded ataxin-3 impairs long-term depression in Purkinje neurons of SCA3 transgenic mouse by inhibiting HAT and impairing histone acetylation. *Brain Research*, 2014. **1583**: p. 220-229.<https://doi.org/10.1016/j.brainres.2014.08.019>.
79. Jiang, F., Wu, Q., Sun, S., Bi, G., *et al.*, Identification of potential diagnostic biomarkers for Parkinson's disease. *FEBS Open Bio*, 2019. **9**(8): p. 1460-1468.<https://doi.org/10.1002/2211-5463.12687>.
80. Hayaishi, O. and Urade, Y., Prostaglandin D2 in Sleep-Wake Regulation: Recent Progress and Perspectives. *The Neuroscientist*, 2002. **8**(1): p. 12-15.<https://doi.org/10.1177/107385840200800105>.
81. Chiba, Y., Suto, W., and Sakai, H., Augmented Pla2g4c/Ptgs2/Hpgds axis in bronchial smooth muscle tissues of experimental asthma. *PLOS ONE*, 2018. **13**(8): p. e0202623.<https://doi.org/10.1371/journal.pone.0202623>.
82. Watanabe, T., Narumiya, S., Shimizu, T., and Hayaishi, O., Characterization of the biosynthetic pathway of prostaglandin D2 in human platelet-rich plasma. *Journal of Biological Chemistry*, 1982. **257**(24): p. 14847-53.[https://doi.org/10.1016/S0021-9258\(18\)33360-X](https://doi.org/10.1016/S0021-9258(18)33360-X).
83. Ahmed, N.T., Gao, C., Lucker, B.F., Cole, D.G., *et al.*, ODA16 aids axonemal outer row dynein assembly through an interaction with the intraflagellar transport machinery. *Journal of Cell Biology*, 2008. **183**(2): p. 313-322.<https://doi.org/10.1083/jcb.200802025>.
84. Gao, C., Wang, G., Amack, J.D., and Mitchell, D.R., Oda16/Wdr69 is essential for axonemal dynein assembly and ciliary motility during zebrafish embryogenesis. *Developmental Dynamics* 2010. **239**(8): p. 2190-2197.<https://doi.org/10.1002/dvdy.22355>.
85. Webb, J.L., Ravikumar, B., and Rubinsztein, D.C., Microtubule disruption inhibits autophagosome-lysosome fusion: implications for studying the roles of aggresomes in polyglutamine diseases. *The International Journal of Biochemistry & Cell Biology*, 2004. **36**(12): p. 2541-2550.<https://doi.org/10.1016/j.biocel.2004.02.003>.

86. Ravikumar, B., Acevedo-Arozena, A., Imarisio, S., Berger, Z., *et al.*, Dynein mutations impair autophagic clearance of aggregate-prone proteins. *Nature Genetics*, 2005. **37**(7): p. 771-776.<https://doi.org/10.1038/ng1591>.
87. Sittler, A., Muriel, M.P., Marinello, M., Brice, A., *et al.*, Dereglulation of autophagy in postmortem brains of Machado-Joseph disease patients. *Neuropathology*, 2018. **38**(2): p. 113-124.<https://doi.org/10.1111/neup.12433>.
88. Duarte-Silva, S., Neves-Carvalho, A., Soares-Cunha, C., Teixeira-Castro, A., *et al.*, Lithium Chloride Therapy Fails to Improve Motor Function in a Transgenic Mouse Model of Machado-Joseph Disease. *The Cerebellum*, 2014. **13**(6): p. 713-727.<https://doi.org/10.1007/s12311-014-0589-9>.
89. Duarte-Silva, S., Silva-Fernandes, A., Neves-Carvalho, A., Soares-Cunha, C., *et al.*, Combined therapy with m-TOR-dependent and -independent autophagy inducers causes neurotoxicity in a mouse model of Machado–Joseph disease. *Neuroscience*, 2016. **313**: p. 162-173.<https://doi.org/10.1016/j.neuroscience.2015.11.030>.
90. Clemens, M.J., Regulation of eukaryotic protein synthesis by protein kinases that phosphorylate initiation factor eIF-2. *Molecular Biology Reports*, 1994. **19**(3): p. 201-210.<https://doi.org/10.1007/BF00986962>.
91. Bando, Y., Onuki, R., Katayama, T., Manabe, T., *et al.*, Double-strand RNA dependent protein kinase (PKR) is involved in the extrastriatal degeneration in Parkinson's disease and Huntington's disease. *Neurochemistry International*, 2005. **46**(1): p. 11-18.<https://doi.org/10.1016/j.neuint.2004.07.005>.
92. Peel, A.L., Rao, R.V., Cottrell, B.A., Hayden, M.R., *et al.*, Double-stranded RNA-dependent protein kinase, PKR, binds preferentially to Huntington's disease (HD) transcripts and is activated in HD tissue. *Human Molecular Genetics*, 2001. **10**(15): p. 1531-1538.<https://doi.org/10.1093/hmg/10.15.1531>.
93. He, J., Yang, Y., Zhang, J., Chen, J., *et al.*, Ribosome biogenesis protein Urb1 acts downstream of mTOR complex 1 to modulate digestive organ development in zebrafish. *Journal of Genetics and Genomics*, 2017. **44**(12): p. 567-576.<https://doi.org/10.1016/j.jgg.2017.09.013>.
94. Wang, T., Zhang, W.-S., Wang, Z.-X., Wu, Z.-W., *et al.*, RAPTOR promotes colorectal cancer proliferation by inducing mTORC1 and upregulating ribosome assembly factor URB1. *Cancer Medicine*, 2020. **9**(4): p. 1529-1543.<https://doi.org/10.1002/cam4.2810>.
95. Wang, T., Li, L.-Y., Chen, Y.-F., Fu, S.-W., *et al.*, Ribosome Assembly Factor URB1 Contributes to Colorectal Cancer Proliferation via Transcriptional Activation of ATF4. *Cancer Science*, 2020. **00**(n/a): p. 1-16.<https://doi.org/10.1111/cas.14643>.
96. Ellis, J., Proteins as molecular chaperones. *Nature*, 1987. **328**(6129): p. 378-379.<https://doi.org/10.1038/328378a0>.
97. Alberti, S., Böhse, K., Arndt, V., Schmitz, A., *et al.*, The Cochaperone HspBP1 Inhibits the CHIP Ubiquitin Ligase and Stimulates the Maturation of the Cystic Fibrosis Transmembrane

- Conductance Regulator. *Molecular Biology of the Cell*, 2004. **15**(9): p. 4003-4010.<https://doi.org/10.1091/mbc.e04-04-0293>.
98. Mahboubi, H., Moujaber, O., Kodiha, M., and Stochaj, U., The Co-Chaperone HspBP1 Is a Novel Component of Stress Granules that Regulates Their Formation. *Cells*, 2020. **9**(4): p. 825.<https://doi.org/10.3390/cells9040825>.
99. Bu, L., Jin, Y., Shi, Y., Chu, R., *et al.*, Mutant DNA-binding domain of HSF4 is associated with autosomal dominant lamellar and Marner cataract. *Nature Genetics*, 2002. **31**(3): p. 276-278.<https://doi.org/10.1038/ng921>.
100. Russell, L.C., Whitt, S.R., Chen, M.-S., and Chinkers, M., Identification of Conserved Residues Required for the Binding of a Tetratricopeptide Repeat Domain to Heat Shock Protein 90. *Journal of Biological Chemistry*, 1999. **274**(29): p. 20060-20063.<https://doi.org/10.1074/jbc.274.29.20060>.
101. Prodromou, C., Siligardi, G., O'Brien, R., Woolfson, D.N., *et al.*, Regulation of Hsp90 ATPase activity by tetratricopeptide repeat (TPR)-domain co-chaperones. *The EMBO Journal*, 1999. **18**(3): p. 754-762.<https://doi.org/10.1093/emboj/18.3.754>.
102. Cao, S., Ho, G.H., and Lin, V.C.L., Tetratricopeptide repeat domain 9A is an interacting protein for tropomyosin Tm5NM-1. *BMC Cancer*, 2008. **8**(1): p. 231.<https://doi.org/10.1186/1471-2407-8-231>.
103. Thomas, L., Bouhouche, K., Whitfield, M., Thouvenin, G., *et al.*, TTC12 Loss-of-Function Mutations Cause Primary Ciliary Dyskinesia and Unveil Distinct Dynein Assembly Mechanisms in Motile Cilia Versus Flagella. *The American Journal of Human Genetics*, 2020. **106**(2): p. 153-169.<https://doi.org/10.1016/j.ajhg.2019.12.010>.
104. Wang, W., Ren, S., Wang, Z., Zhang, C., *et al.*, Increased expression of TTC21A in lung adenocarcinoma infers favorable prognosis and high immune infiltrating level. *International Immunopharmacology*, 2020. **78**: p. 106077.<https://doi.org/10.1016/j.intimp.2019.106077>.
105. Gelernter, J., Yu, Y., Weiss, R., Brady, K., *et al.*, Haplotype spanning TTC12 and ANKK1, flanked by the DRD2 and NCAM1 loci, is strongly associated to nicotine dependence in two distinct American populations. *Human Molecular Genetics*, 2006. **15**(24): p. 3498-3507.<https://doi.org/10.1093/hmg/ddl426>.
106. Toulis, V., García-Monclús, S., de la Peña-Ramírez, C., Arenas-Galnares, R., *et al.*, The Deubiquitinating Enzyme Ataxin-3 Regulates Ciliogenesis and Phagocytosis in the Retina. *Cell Reports*, 2020. **33**(6): p. 108360.<https://doi.org/10.1016/j.celrep.2020.108360>.
107. Tai, H.-C. and Schuman, E.M., Ubiquitin, the proteasome and protein degradation in neuronal function and dysfunction. *Nature Reviews Neuroscience*, 2008. **9**(11): p. 826-838.<https://doi.org/10.1038/nrn2499>.
108. Lemus, L. and Goder, V., Regulation of Endoplasmic Reticulum-Associated Protein Degradation (ERAD) by Ubiquitin. *Cells*, 2014. **3**(3): p. 824-847.<https://doi.org/10.3390/cells3030824>.

109. Jeub, M., Herbst, M., Spauschus, A., Fleischer, H., *et al.*, Potassium channel dysfunction and depolarized resting membrane potential in a cell model of SCA3. *Experimental Neurology*, 2006. **201**(1): p. 182-192. <https://doi.org/10.1016/j.expneurol.2006.03.029>.
110. Bushart, D.D., Zalon, A.J., Zhang, H., Morrison, L.M., *et al.*, Antisense Oligonucleotide Therapy Targeted Against ATXN3 Improves Potassium Channel–Mediated Purkinje Neuron Dysfunction in Spinocerebellar Ataxia Type 3. *The Cerebellum*, 2020. <https://doi.org/10.1007/s12311-020-01179-7>.
111. Xia, Z., Bergstrand, A., DePierre, J.W., and Nässberger, L., The antidepressants imipramine, clomipramine, and citalopram induce apoptosis in human acute myeloid leukemia HL-60 cells via caspase-3 activation. *Journal of Biochemical and Molecular Toxicology*, 1999. **13**(6): p. 338-347. [https://doi.org/10.1002/\(SICI\)1099-0461\(1999\)13:6<338::AID-JBT8>3.0.CO;2-7](https://doi.org/10.1002/(SICI)1099-0461(1999)13:6<338::AID-JBT8>3.0.CO;2-7).
112. Raghunath, A., Sundarraj, K., Nagarajan, R., Arfuso, F., *et al.*, Antioxidant response elements: Discovery, classes, regulation and potential applications. *Redox Biology*, 2018. **17**: p. 297-314. <https://doi.org/10.1016/j.redox.2018.05.002>.
113. Araujo, J., Breuer, P., Dieringer, S., Krauss, S., *et al.*, FOXO4-dependent upregulation of superoxide dismutase-2 in response to oxidative stress is impaired in spinocerebellar ataxia type 3. *Human Molecular Genetics*, 2011. **20**(15): p. 2928-2941. <https://doi.org/10.1093/hmg/ddr197>.
114. Chou, A.-H., Yeh, T.-H., Kuo, Y.-L., Kao, Y.-C., *et al.*, Polyglutamine-expanded ataxin-3 activates mitochondrial apoptotic pathway by upregulating Bax and downregulating Bcl-xL. *Neurobiology of Disease*, 2006. **21**(2): p. 333-345. <https://doi.org/10.1016/j.nbd.2005.07.011>.
115. Yu, Y.-C., Kuo, C.-L., Cheng, W.-L., Liu, C.-S., *et al.*, Decreased antioxidant enzyme activity and increased mitochondrial DNA damage in cellular models of Machado-Joseph disease. *Journal of Neuroscience Research*, 2009. **87**(8): p. 1884-1891. <https://doi.org/10.1002/jnr.22011>.
116. Laço, M.N., Oliveira, C.R., Paulson, H.L., and Rego, A.C., Compromised mitochondrial complex II in models of Machado–Joseph disease. *Biochimica et Biophysica Acta (BBA) - Molecular Basis of Disease*, 2012. **1822**(2): p. 139-149. <https://doi.org/10.1016/j.bbadis.2011.10.010>.
117. Pohl, F., Teixeira-Castro, A., Costa, M.D., Lindsay, V., *et al.*, GST-4-Dependent Suppression of Neurodegeneration in *C. elegans* Models of Parkinson's and Machado-Joseph Disease by Rapeseed Pomace Extract Supplementation. *Frontiers in Aging Neuroscience*, 2019. **13**(1091). <https://doi.org/10.3389/fnins.2019.01091>.
118. Vilasboas-Campos, D., Costa, M.D., Teixeira-Castro, A., Rios, R., *et al.*, Neurotherapeutic effect of *Hyptis* spp. leaf extracts in *Caenorhabditis elegans* models of tauopathy and polyglutamine disease: Role of the glutathione redox cycle. *Free Radical Biology and Medicine*, 2020. <https://doi.org/10.1016/j.freeradbiomed.2020.10.018>.
119. Hübener, J., Vauti, F., Funke, C., Wolburg, H., *et al.*, N-terminal ataxin-3 causes neurological symptoms with inclusions, endoplasmic reticulum stress and ribosomal dislocation. *Brain*, 2011. **134**(7): p. 1925-1942. <https://doi.org/10.1093/brain/awr118>.

120. Chen, C., Dudenhausen, E.E., Pan, Y.-X., Zhong, C., *et al.*, Human CCAAT/Enhancer-binding Protein  $\beta$  Gene Expression Is Activated by Endoplasmic Reticulum Stress through an Unfolded Protein Response Element Downstream of the Protein Coding Sequence. *Journal of Biological Chemistry*, 2004. **279**(27): p. 27948-27956.<https://doi.org/10.1074/jbc.M313920200>.
121. Tanabe, M., Sasai, N., Nagata, K., Liu, X.-D., *et al.*, The Mammalian HSF4 Gene Generates Both an Activator and a Repressor of Heat Shock Genes by Alternative Splicing. *Journal of Biological Chemistry*, 1999. **274**(39): p. 27845-27856.<https://doi.org/10.1074/jbc.274.39.27845>.
122. Hoozemans, J.J.M., Veerhuis, R., Van Haastert, E.S., Rozemuller, J.M., *et al.*, The unfolded protein response is activated in Alzheimer's disease. *Acta Neuropathologica*, 2005. **110**(2): p. 165-172.<https://doi.org/10.1007/s00401-005-1038-0>.
123. Kikuchi, D., Tanimoto, K., and Nakayama, K., CREB is activated by ER stress and modulates the unfolded protein response by regulating the expression of IRE1 $\alpha$  and PERK. *Biochemical and Biophysical Research Communications*, 2016. **469**(2): p. 243-250.<https://doi.org/10.1016/j.bbrc.2015.11.113>.
124. Liu, B., Wu, N., and Shen, Y., Cyclic AMP response element binding protein (CREB) participates in the heat-inducible expression of human *hsp90 $\beta$*  gene. *Chinese Science Bulletin*, 2001. **46**(19): p. 1645.<https://doi.org/10.1007/BF02900627>.

---

## **Supplementary data**

**Table S3.2.1 List of the DEGs found among all RNA-seq comparison analyzed belonging to the different PQC accessory pathways.** Up- or downregulated genes (in red and green, respectively) are shown in each comparison, listed in decreasing order of fold change (Log<sub>2</sub> FC). DEGs - differentially expressed genes; RNA-seq - RNA-sequencing; PQC - protein quality control; HSR - heat shock response; UPR - unfolded protein response.

PQC pathway	Comparison	Gene	Description	Fold Change (Log <sub>2</sub> FC)	CREB target?	
<b>HSR</b>	Tg vs Tg cit	<i>Hsf4</i>	Heat shock transcription factor 4	1.09	Yes	
	WT vs Tg cit	<i>Pfdn2</i>	Prefoldin 2	1.27	Yes	
		<i>Bag1</i>	BCL2-associated athanogene 1	1.23	No	
		<i>Cryab</i>	Crystallin, alpha B	1.02	No	
		<i>Bag4</i>	BCL2-associated athanogene 4	-1.01	Yes	
<b>UPR</b>	Tg vs Tg cit	<i>Cebpb</i>	CCAAT/enhancer binding protein (C/EBP), beta	1.76	Yes	
		<i>Edem3</i>	ER degradation enhancer, mannosidase alpha-like 3	-1.00	No	
	WT vs Tg cit	<i>Cebpb</i>	CCAAT/enhancer binding protein (C/EBP), beta	1.94	Yes	
		<i>Pfdn2</i>	Prefoldin 2	1.27	Yes	
		<i>Atf4</i>	Activating transcription factor 4	1.15	Yes	
		<i>Edem3</i>	ER degradation enhancer, mannosidase alpha-like 3	-1.25	No	
		<i>Uggt2</i>	UDP-glucose glycoprotein glucosyltransferase 2	-1.08	No	
		<i>Ddit3</i>	DNA-damage inducible transcript 3	1.02	Yes	
	<b>Antioxidant response</b>	WT vs Tg	<i>Krt1</i>	Keratin 1	1.15	No
		Tg vs Tg cit	<i>Gpx3</i>	Glutathione peroxidase 3	3.38	No
<i>Ngb</i>			Neuroglobin	2.91	Yes	
<i>Txnrd3</i>			Thioredoxin reductase 3	1.78	Yes	
<i>Mt1</i>			Metallothionein 1	1.02	Yes	
<i>Sod3</i>			Superoxide dismutase 3, extracellular	1.00	No	
<i>Sesn3</i>			Sestrin 3	-1.61	No	
WT vs Tg cit		<i>Gpx3</i>	Glutathione peroxidase 3	2.38	No	
		<i>Mt1</i>	Metallothionein 1	1.62	Yes	
		<i>Glx5</i>	Glutaredoxin 5	1.52	No	
		<i>Mt2</i>	Metallothionein 2	1.48	No	
	<i>Krt1</i>	Keratin 1	1.28	No		



	<i>Ucp2</i>	Uncoupling protein 2 (mitochondrial, proton carrier)	1.26	No
	<i>Fth1</i>	Ferritin heavy polypeptide 1	1.19	Yes
	<i>Sod3</i>	Superoxide dismutase 3, extracellular	1.18	No
	<i>Ehd2</i>	EH-domain containing 2	1.17	No
	<i>Gpx8</i>	Glutathione peroxidase 8 (putative)	1.17	Yes
	<i>Gpx1</i>	Glutathione peroxidase 1	1.14	No
	<i>Cyba</i>	Cytochrome b-245, alpha polypeptide	1.10	No
	<i>Prdx5</i>	Peroxiredoxin 5	1.06	No
	<i>Txn14a</i>	Thioredoxin-like 4A	1.04	Yes
	<i>Txndc17</i>	Thioredoxin domain containing 17	1.04	No
	<i>Gpx4</i>	Glutathione peroxidase 4	1.03	Yes
	<i>Sesn3</i>	Sestrin 3	-1.98	No
	<i>Ercc6</i>	Excision repair cross-complementing rodent repair deficiency, complementation group 6	-1.14	No
	<i>Apc</i>	Adenomatosis polyposis coli	-1.11	No
	<i>Aox1</i>	Aldehyde oxidase 1	-1.06	No
	<i>Als2</i>	Amyotrophic lateral sclerosis 2 (juvenile)	-1.02	Yes
	<i>Atr</i>	Ataxia telangiectasia and Rad3 related	-1.01	No

**Serotonin transporter ablation restores the transcriptomic profile and induces protective responses in a *C. elegans* MJD model**

---

**Serotonin transporter ablation restores the transcriptomic profile and induces protective responses in a *C. elegans* MJD model**

Stéphanie Oliveira<sup>1,2</sup>, Joana Pereira-Sousa<sup>1,2</sup>, Jian Li<sup>3</sup>, Patrícia Maciel<sup>1,2</sup>, Andreia Teixeira-Castro<sup>1,2</sup>

<sup>1</sup> Life and Health Sciences Research Institute (ICVS), School of Medicine, University of Minho, Campus of Gualtar, 4710-057 Braga, Portugal

<sup>2</sup> ICVS/3B's – PT Government Associate Laboratory, Braga/Guimarães, Portugal

<sup>3</sup> Department of Molecular Biosciences, Northwestern University, Evanston, IL 60208, USA

(Manuscript *in preparation*)

---

## Abstract

There is an increased need to find effective therapies for neurodegenerative disorders. Machado-Joseph disease (MJD), a dominantly inherited neurodegenerative disorder, is one example of those lacking a disease-modifying treatment.

Our previous work demonstrated that acting on serotonergic signaling could be a new therapeutic approach for MJD. By using a repurposing strategy, we found that treatment with the antidepressant citalopram, a selective serotonin reuptake inhibitor (SSRI), rescued neuronal dysfunction and drastically improved ataxin-3 (ATXN3) aggregation in *C. elegans* and mouse models of MJD. Similar to the pharmacological inhibition, genetic ablation of the serotonin transporter SERT/MOD-5 in the MJD *C. elegans* model restored locomotor behavior and strikingly decreased mutant ATXN3 aggregation.

Here, to further uncover the molecular determinants underlying serotonergic signaling-mediated suppression of proteotoxicity, we took a genetic approach and performed a transcriptomic analysis of a genetic *C. elegans* model mimicking citalopram action, by *mod-5* (SERT) transporter ablation in mutant ATXN3 animals.

Transcriptomic analysis showed that AT3q130 (Q130) mutant ATXN3 animals have a completely altered transcriptomic profile that becomes strikingly similar to WT animals, upon *mod-5* ablation. Indeed, *mod-5* deletion can revert the transcriptomic changes of Q130 animals, since alterations in gene expression (up- or downregulation) in those animals assumed the exact opposite direction in the absence of the serotonin transporter, which suggests that *mod-5* acts as a genetic modifier of this abnormal gene expression in Q130 animals. Enrichment analyses revealed that this could be the result of the activation of general defense responses, such as those prompted by biotic stress, also involving protein quality control (PQC) mechanisms, namely autophagy and lysosomal pathways, among others. The response profile obtained with serotonin modulation shares similarities with those existing in long-lived *C. elegans* mutant strains, such as an increased gene expression of PQC genes (namely lysosomal- and autophagy-related components and heat shock proteins). The results also pointed towards a possible participation of the CREB transcription factor in some of these responses, although more studies are needed to confirm this preliminary observation.

Overall, our results demonstrate that serotonergic signaling modulation induce a rebalance of mutant ATXN3-induced transcriptomic changes and generates protective responses, supporting the use of drugs targeting this signaling as a promising therapeutic approach for MJD.

## 1. Introduction

Machado-Joseph disease (MJD) or spinocerebellar ataxia type 3 (SCA3) is a dominantly inherited, late-onset, progressive and fatal neurodegenerative disorder [1, 2]. It is considered the most common form of spinocerebellar ataxia worldwide [3, 4] and its etiology is based on the expansion of the cytosine-adenosine-guanine (CAG) repeat within the coding region of the ataxin-3 (*ATXN3*) gene product [5]. The expanded CAG tract in *ATXN3* makes the protein more prone to misfold and to aggregate into neuronal inclusions that are mostly observed in affected areas of the brain [6, 7]. Presently, there is no disease-modifying treatment available for this pathology.

By performing an *in vivo* screen of FDA-approved small molecules, we previously identified the antidepressant citalopram, a serotonin selective reuptake inhibitor (SSRI), as a compound able to rescue mutant *ATXN3*-mediated neuronal dysfunction in both a *Caenorhabditis elegans* (*C. elegans*) and a mouse model of MJD [8]. SSRIs are known to enhance serotonergic transmission, by targeting the serotonin transporter (SERT/MOD-5), present in the pre-synaptic neurons, thus blocking the reuptake of serotonin (5-HT) from the extracellular space, making it more available in the synaptic cleft [9]. In line with this, we also demonstrated that genetic ablation of MOD-5 by itself rescued *ATXN3*-mediated motor dysfunction and aggregation in *C. elegans*, confirming the beneficial effect of pharmacological inhibition of 5-HT recapture [8]. These results evidenced that the modulation of the serotonergic signaling, through serotonin recapture inhibition, modifies proteotoxicity and constitutes a promising therapeutic approach for MJD. Studies from others also revealed that antidepressants, namely SSRIs, show neuroprotective properties [10, 11], including in the context of neurodegenerative disorders [12, 13]. Interestingly, Tatum and colleagues demonstrated that the stimulation of serotonin release from one *C. elegans* neuron is able to suppress protein misfolding in peripheral tissues, through the transient induction of molecular chaperones [14]. Another report showed that aggregation-prone proteins (polyglutamine, polyQ) bind to mitochondria in *C. elegans* neurons triggering a generalized unfolded-protein response of the mitochondria (UPR<sup>mt</sup>) in the worms' intestine [15]. Noticeable is that serotonin release is necessary for this signal propagation to restore protein homeostasis (a.k.a. proteostasis) [15]. In line with these reports, we verified that the absence of MOD-5, and consequent increase in extracellular serotonin, in MJD worms was able to markedly decrease aggregation [8], but how this is achieved at the molecular level remains to be elucidated.

In MJD models, modifiers of mutant *ATXN3*-mediated pathogenesis have been described. For instance, knockout of calpain-1, a calcium-dependent cysteine protease, in YACMJD84.2 mice partially rescued disease-associated features, such as body weight loss and decreased survival, but did not impact

on aggregation [16]. Interestingly, a genome-wide screening for modifiers of ATXN3 neurodegeneration in *Drosophila* revealed that a significant proportion of the modifiers affected protein misfolding, and included two major classes: chaperones and ubiquitin pathway components [17]. Other modifier genes found had molecular functions related to: (i) nuclear export; (ii) protein transcription and translation regulation; (iii) polyA binding protein; (iv) insulin signaling; and (v) fatty acid oxidation [17]. Citalopram also impacts on those pathways, as explored in chapters 3.1 and 3.2. Since *mod-5* ablation mimics citalopram/SSRI treatment (inhibition of the 5-HT recapture), proving to be even superior at rescuing the mutant ATXN3-mediated phenotypes, it is possible to use this genetic approach to understand the molecular details of the mode of action of this group of drugs as modifiers of ATXN3 pathogenesis.

The objective of this work is centered on understanding if the enhancement of serotonergic transmission by SERT/MOD-5 ablation can trigger similar transcriptional changes and cellular responses as observed upon serotonin reuptake inhibition by citalopram, and to gain further insight into the molecular mechanisms underlying this using a simpler organism. To achieve this goal, we made use of a previously generated *C. elegans* model of ATXN3 pathogenesis (Q130) [18] in which we ablated the SERT transporter - MOD-5, and performed transcriptomic analysis by RNA-sequencing (RNA-seq). The results showed that MOD-5 absence strikingly restores the transcriptomic profile of mutant ATXN3 worms to resemble WT animals, likely by triggering specific defense responses that also contribute to the maintenance of proteostasis. Several responses related to biotic stress, the autophagic mechanism, the lysosome, among others, were found differentially expressed upon *mod-5* knockout in Q130 animals. Expression changes in known polyQ aggregation regulators were also observed and our preliminary results show that cAMP response element-binding protein (CREB) transcription factor could play a role in mediating the observed *mod-5*-dependent changes in Q130 worms.

This study unveils *mod-5* as a modifier of mutant ATXN3-induced transcriptional changes, revealing genes and mechanisms that may constitute the framework of this beneficial therapeutic modulation of serotonergic signaling.

## **2. Materials and methods**

### *2.1 C. elegans strains and generation of double mutants*

Nematode Bristol N2 (wild-type, WT), MT9772 (*mod-5*) [19] strains and *Escherichia coli* (OP50) food source were obtained from the *Caenorhabditis* genetics center (CGC, University of Minnesota, USA). The *C. elegans* model of MJD, AT3q130 or Q130 (MAC001/AM685), was generated by our research group as previously described [18]. All the strains used in this work are listed in Table 4.1.

Standard methods were used for culturing and monitoring nematodes, unless otherwise noted [20]. Worms were grown on nematode growth medium (NGM) plates seeded with OP50, at 20 °C. OP50 was grown overnight (for approximately 16 h), at 37 °C and at 180 revolutions per minute (rpm), in Luria Broth (LB) media. Synchronized populations were obtained either by collecting eggs laid by adult hermaphrodite worms within a 2-3 h period, or by subjecting a young adult population to an alkaline hypochlorite solution (containing 0.25 M NaOH, 20 % household bleach (with  $\approx$  2.5 % NaClO), completed with H<sub>2</sub>O) for 7 min.

The double mutant strain *mod-5*; AT3q130 (*mod-5*; Q130) was previously generated by crossing the two independent strains AT3q130 and *mod-5* (Table 4.1). Briefly, *mod-5* male worms were obtained through heat shock treatment consisting in the incubation of five L4 stage *mod-5* worms, at 30 °C for 8 h, then maintained at 20 °C for three to four days, and plates were screened for male presence. Then, thirteen *mod-5* males and three L4 hermaphrodites Q130 worms were placed in a 60 mm NGM seeded plate, at 15 °C for two days. Each hermaphrodite worm was isolated in a NGM seeded plate and maintained at 20 °C. Three days later, from their progeny, three to five hermaphrodite fluorescent worms (ATXN3 is expressed in fusion with the YFP in the Q130 strain) were isolated and placed back at 20 °C for 72 h. Next, from the progeny of isolated fluorescent worms, twenty-four to thirty-two fluorescent worms were isolated and screened by PCR to verify the presence of *mod-5* mutation.

**Table 4.1** *C. elegans* strains used in this study.

ID number	Strain name	Genotype	Observations
N2 (Bristol)	WT	WT	Obtained from CGC
MAC001/ AM685	AT3q130 or Q130	<i>rmls263[P<sub>igef1</sub>::AT3v1-1q130::yfp] II</i>	
MT9772	<i>mod-5</i>	<i>mod-5(n3314) I</i>	Obtained from CGC
MAC074	<i>mod-5</i> ; AT3q130 ( <i>mod-5</i> ; Q130)	<i>mod-5(n3314) I; rmls263[P<sub>igef1</sub>::AT3v1-1q130::yfp] II</i>	Resulting from the cross between MAC001 and MT9772

The presence of the mutation was confirmed by PCR (see primers used in Table 4.2). In summary, worm lysis was carried by placing 20 worms in 20  $\mu$ L of lysis buffer (50 mM KCl, 10 mM Tris-base pH = 8.3, 2.5 mM MgCl<sub>2</sub>, 0.45 % Nonidet P-40 (IGEPAL), 0.45 % Tween 20, 0.01 % (w/v) gelatin), supplemented with 0.1 mg/mL of Proteinase K (20 mg/mL) before use, and by maintaining them at -80 °C, for at least 30 min. In a thermocycler, worms were then heated at 65 °C for 1 h, and lysis was completed by an inactivation of Proteinase K at 95 °C for 15 min. From the lysis, 1.5  $\mu$ L were

used and added to the mix containing Promega PCR Master Mix (Cat. No. M7505, Promega, Madison, WI, USA) and primers with a final concentration of 0.2  $\mu$ M, according to the manufacturer's guidelines (primers used are described in Table 4.2). The following cycling parameters were used: denaturation at 95 °C for 5 min (1 cycle); denaturation at 95 °C (1 min), annealing at 60.4 °C (1 min) and extension at 72 °C for 2 min and 30 s during 35 cycles, and a final extension for 10 min at 72 °C. Following PCR amplification, total PCR product was run in a 1.5 % agarose electrophoresis gel. The PCR was designed with three primers (Table 4.2) allowing distinction between the PCR products of WT (one band of 332 bp), heterozygous (two bands: 332 and 416 bp) and homozygous *mod-5* worms (one band of 416 bp).

**Table 4.2 Primers used for *mod-5* mutation screening.**

Gene (Sequence)	Forward primer (5'- 3')	Reverse primer (5'- 3') 1	Reverse primer (5'- 3') 2
<i>mod-5</i> (Y54E10BR.7)	GTTCAAATTCGGCGAATC	CACAAGGCAGGCTAATTTCA	CAACTCGGCCTTCTTTTGTC

## 2.2 Worm preparation for RNA extraction

*C. elegans* strains were grown in NGM plates, seeded with inactivated OP50. Briefly, bacteria suspended in LB medium was centrifuged at 4000  $\times g$ , for 30 min at 4 °C, in 50 mL centrifuge tubes. Then, supernatants were discarded, and the pellets were submitted to three cycles of freeze (in liquid nitrogen) - thaw (in a water bath at 37 °C). Bacteria pellets were immersed in liquid nitrogen one last time and stored at -80 °C until further use. To seed the plates, an inactivated pellet of OP50 was resuspended in 5 mL of S-Basal solution, supplemented with 1 % penicillin-streptomycin (P4333, Sigma-Aldrich, St. Louis, MO, USA) and 1 % nystatin (N6261, Sigma-Aldrich, St. Louis, MO, USA), to avoid pellet contaminations. Dimethyl sulfoxide (DMSO, D8418, Sigma-Aldrich, St. Louis, MO, USA), at a final concentration of 1 %, was also added at the time, since it was the vehicle of drugs tested at the same time, but not analyzed in this chapter. Previous experiments demonstrated that 1 % DMSO is not toxic for nematodes [18, 21] and does not affect animal's development [8]. Ninety mm NGM plates were seeded with 750  $\mu$ L of inactivated bacterial mixture and left to dry in an airflow chamber for 1 h.

Eggs from each strain, retrieved by bleaching of adult worms by hypochlorite treatment (see section 2.1), were resuspended in S-Basal medium and the number of eggs/ $\mu$ L were counted. A volume containing approximately 750 eggs of N2 and *mod-5*, and 1000 eggs of Q130 and *mod-5*; Q130 animals was pipetted into each plate. Three plates per condition were prepared for each biological replicate.



Plates were maintained at 20 °C, for 4 days. After that, day 2 adult worms were washed with M9 solution and transferred to 15 mL centrifuge tubes. After having settled down by gravity at the bottom of the tube, worms were washed at least three times more in M9, to remove all the bacteria. Worms were then transferred to 1.5 mL centrifuge tubes and after settling down, the excess of M9 buffer was removed. TRIzol™ reagent (Cat. No. 15596018, Invitrogen™, Waltham, MA, USA) was added to each sample (500 µL). The samples were immediately flash frozen in liquid nitrogen and stored at -80 °C.

### 2.3 RNA extraction

The tubes containing worm pellets were placed in dry ice to allow slow thawing. New tubes with caps were prepared and the thawed TRIzol™ worm solution transferred to them. Glass beads (acid-washed, G8772, Sigma-Aldrich, St. Louis, MO, USA) were added to disrupt the animals in a 1:1 proportion relatively to the worm pellet. The disruption was achieved by placing the tubes with worms and beads in a FastPrep-24™ classic bead beating grinder and lysis system (116004500, MP Biomedicals™, Irvine, CA, USA) and performing 6 cycles of 30 s agitation plus 1 min on ice. The worms' body wall disruption was determined by using a stereo microscope. After letting the beads deposit at the bottom of the tubes, the supernatant was removed to a new 1.5 mL centrifuge tube. Chloroform (C2432, Sigma-Aldrich, St. Louis, MO, USA) was added to the samples (150 µL) and those were homogenized in a vortex mixer during 15 s, at 4 °C, and let be seated at room temperature (RT) for 3 min. Samples were then centrifuged at 12000 rpm for 15 min, at 4 °C. The aqueous (superior transparent) phase was retrieved and transferred to a gDNA Eliminator spin column, from the Qiagen RNeasy® Plus Mini kit (Cat. No. 74136, Qiagen, Hilden, Germany). From this step, the Qiagen RNeasy® Plus Mini kit was used according to the manufacturer's instruction. The protocol for "Purification of Total RNA from Animal Tissues", from page 25, step n.º 4, of the Qiagen RNeasy® Plus Mini Handbook (September 2020), available online ([RNeasy Plus Mini Handbook - QIAGEN](#)), was followed. In step n.º 5, 350 µL of 70 % ethanol were used. The optional step n.º 10 of the protocol was performed.

### 2.4 Transcriptomic analysis by RNA-sequencing

Total RNA extracted from N2 (WT), *mod-5*, Q130 and the double mutant *mod-5*; Q130 strains was assessed for quality using Experion™ RNA StdSens kit (#7007103, Bio-Rad, Hercules, CA, USA), in accordance with manufacturer's instructions. Only samples with an RNA quality indicator (RQI) above 8.7 were used for further analyses. RNA samples were sent to the Clinical Genomics Center of the Oklahoma

Medical Research Foundation (OMRF), in Oklahoma City (Oklahoma 73104), USA, for RNA-sequencing (RNA-seq).

From total RNA, mRNA was enriched using polyT beads and libraries were constructed using NEBnext® Ultra™ II Directional RNA library Prep kit for Illumina® (E7760, New England BioLabs, Ipswich, MA, USA), as suggested by the facility. Sequencing data was produced on NextSeq 500 (Illumina®, San Diego, CA, USA) in a 75-bp single-read sequencing mode (SR75) with at least 20 million reads per sample. All RNA-seq experiments were performed in biological triplicates.

RNA-seq results were mapped to WS220 using *RNA STAR* [22] and differential expression analyses were done using *EdgeR*. Gene expression fold changes ( $\log_2$  Fold Change,  $\log_2$  FC) were obtained, and raw p-value and adjusted p-value (FDR) determined, this last one through Benjamini-Hochberg procedure. Differentially expressed genes (DEGs) were acquired considering the following filters: raw p-value  $\leq 0.001$  and adjusted p-value (FDR)  $\leq 0.05$ .

A list of DEGs was obtained for the following comparisons: WT (N2) *versus (vs)* Q130, Q130 *vs mod-5*; Q130, WT *vs mod-5* and WT *vs mod-5*; Q130.

## 2.5 Transcriptomic data: gene, phenotype and tissue enrichment analyses

Gene Enrichment Analysis (GEA), Phenotype Enrichment Analysis (PEA) and Tissue Enrichment Analysis (TEA) were performed using DEGs in the Gene Set Enrichment analysis tool [23, 24] of *WormBase* (version: WS278) [25], using standard settings. A list of *WormBase* gene IDs were introduced into the platform and a q value threshold of 0.1 used (default setting). These enrichment analyses allow a unified approach to enrichment testing in *C. elegans*, facilitating the biological interpretation of genome-wide experiments.

Other platforms and software to perform enrichment analyses were tried, but we were stopped by the fact that the majority of those did not allow the direct input of nematode data (namely *WormBase* accession numbers and official *C. elegans* gene symbols) or could only recognize a small number of genes of the total dataset. In fact, some needed to be first converted to mouse and/or human homologues. First, when we tried this approach, the conversion rate was almost always under 30 %. Second, the conversion among species is not linear, so one *C. elegans* gene can have several mouse/human ortholog genes and the other way around is also true. We thought this could be misleading and decided to use *WormBase* Enrichment Suite to conduct our analysis.

Before performing enrichment and other analyses, DEGs were screened for cuticle and development (vitellogenins) genes using the *Database for Annotation, Visualization and Integrated*

*Discovery (DAVID)* version 6.8 [26, 27] (data not shown), and 49 genes in total were removed from DEGs lists. The expression of these genes is extremely variable during development [28, 29] and as ATXN3 expression can provoke a slight developmental delay, genes from those categories are always present in transcriptomic analyses, so they were removed to avoid misleading interpretation of the results.

Heatmaps were created using Morpheus: versatile matrix visualization and analysis software (Broad Institute, Cambridge, MA, USA) [30].

### 2.6 Transcriptomic data analysis: protein quality control (PQC); suppressors and enhancers of polyQ aggregation and CREB targets

To evaluate the presence of gene alterations in the transcriptomic data related to the PQC network, aggregation modulators, and cAMP response element-binding protein (CREB) targets, lists of genes described to belong to these categories were constructed based on literature reports.

The general PQC list was based on the report of Walther and collaborators in 2015 [31]. This list was divided into three core branches of the PQC: synthesis, folding and conformational maintenance, and degradation. A list of genes whose silencing suppress polyQ aggregation was elaborated based on the study of Silva *et. al.* in 2011 [32] and a list of genes that lead to increased polyQ aggregation (upon silencing) was based in the report of Nollen and co-workers [33]. Finally, data described by Lakhina and colleagues, in 2015, was used to construct a list of CREB targets, conjugating basal and CREB-dependent targets [34].

Whenever the gene identification (ID) was not contemplating *WormBase* IDs, the gene symbols were converted in those using the *Database for Annotation, Visualization and Integrated Discovery (DAVID)* version 6.8 [26, 27]. Final lists of each one of the categories described were then matched against our transcriptomic *C. elegans* data.

## 3. Results

### 3.1 *C. elegans* serotonin transporter ablation restores the transcriptomic profile of mutant ATXN3-expressing worms resembling WT animals

In previous work, we observed that the ablation of the serotonin transporter *mod-5* was able to markedly improve locomotion and decrease aggregation in a MJD *C. elegans* model [8]. Here, we wanted to understand what type of alterations and cellular responses, at the transcriptomic level, would be triggered by this modulation of the serotonergic system in the MJD context. For that, we performed RNA-seq in adult nematodes (day 2 of adulthood) in a *C. elegans* model of MJD proteotoxicity - AT3q130

strain (Q130) - harboring a deletion of the serotonin transporter *mod-5* [19] (*mod-5*; Q130). Different comparisons were studied: (i) WT *versus* mutant ATXN3 (WT *vs* Q130), to assess alterations caused by mutant ATXN3 expression; (ii) mutant ATXN3 *versus* double mutant ATXN3 worms with deletion of *mod-5* transporter (Q130 *vs mod-5*; Q130) to determine changes triggered by *mod-5*-dependent serotonergic modulation in MJD background; (iii) WT *vs mod-5* mutant worms (WT *vs mod-5*), to assess the magnitude of transcriptomic changes upon serotonergic modulation in a WT background; and (iv) WT *versus* double mutant worms (WT *vs mod-5*; Q130) to understand how different are double mutants from control.

First, we observed that the transcriptome profile of the Q130 strain is unmistakably different from the others, that are clustered more closely to each other in a multidimensional scaling analysis (MDS) (Figure 4.1). Interestingly, the deletion of *mod-5* in mutant ATXN3 background reverts this profile making it more similar to WT, where the *mod-5*; Q130 strain appears closer to the WT strain in the plot (Figure 4.1).

When analyzing the expression changes in each comparison, clearly a higher number of altered transcripts were observed in WT *vs* Q130 and Q130 *vs mod-5*; Q130 comparisons (Figure 4.2A and B), than when the WT strain is compared to either *mod-5* or the double mutant strains (Figure 4.2C and D, respectively). The distribution of DEGs is also represented in Figure 4.2E, evidencing the number of specific genes for each individual comparison and shared genes among comparisons. The highest number of shared DEGs among comparisons was observed between WT *vs* Q130 and Q130 *vs mod-5*; Q130 comparisons, where 409 genes were found (Figure 4.2E). This was further confirmed by the number of up- and downregulated DEGs found in each comparison (Figure 4.2F), which was higher in the above referred comparisons.

In WT *vs* Q130, 239 and 423 genes were found to be up- and downregulated, respectively. While in the double mutant comparison (Q130 *vs mod-5*; Q130) 435 and 325 genes were up- and downregulated, respectively. A lot less genes were found to be altered when comparing WT *vs mod-5* and WT *vs mod-5*; Q130: 31 and 41, and 54 and 77 genes were up- and downregulated in each one of these comparisons, respectively (Figure 4.2F). This was a striking indication that the transcriptome of mutant ATXN3 worms was strongly different from WT and from the double mutant *mod-5*; Q130 animals, while *mod-5* and *mod-5*; Q130 strains were not that different from control animals. Moreover, it seemed that Q130 *vs mod-5*; Q130 double mutant was almost mirroring the results from WT compared to mutant ATXN3 worms, i.e., the genes that were downregulated in the ATXN3 mutant *vs* WT comparison were upregulated in the double mutant *vs* Q130 comparison and *vice-versa* (Figure 4.2). In fact, after

verification, all the 409 genes, which were common only to these two comparisons, were in opposite directions (Figure 4.2E and F; Supplementary Figure S4.1).

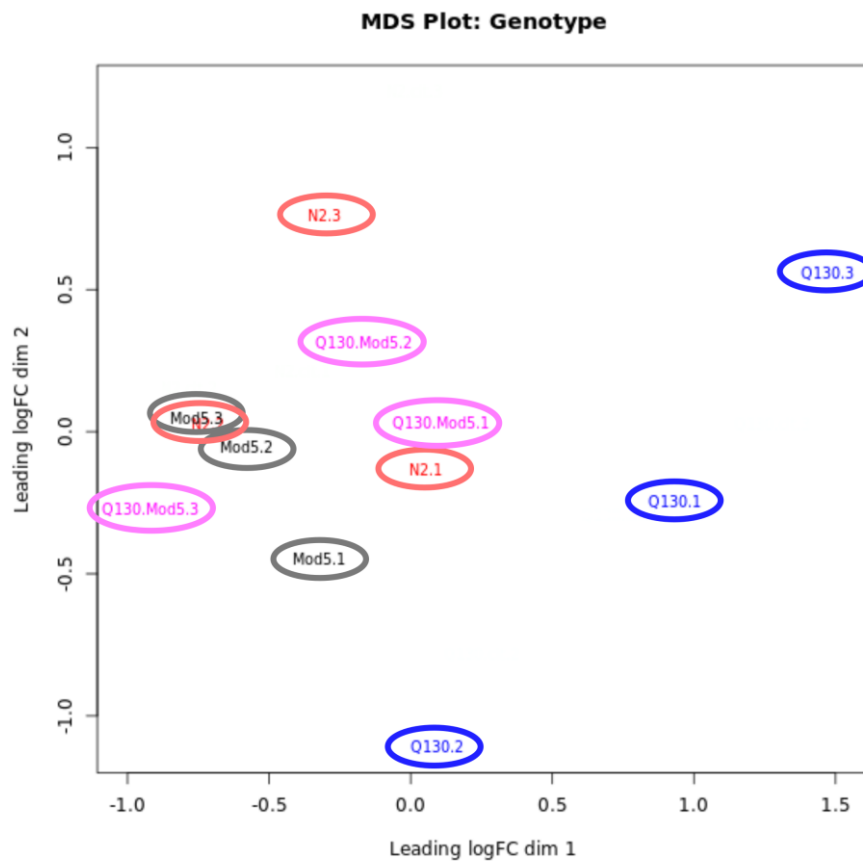


**Figure 4.1 Deletion of *mod-5* in Q130 worms alters their transcriptome to become more similar to WT.**

Multidimensional scaling (MDS) plot, where proximity between samples indicates similarity. Wild-type (WT) corresponds to N2 strain; mutant ATXN3 strain corresponds to Q130; double mutant harboring *mod-5* deletion in ATXN3 background corresponds to *mod-5*; Q130 strain and serotonin transporter deletion corresponds to *mod-5* strain.  $n = 3$  for each strain.

Taken together, these results besides demonstrating that Q130 worms had an altered transcriptome profile, revealed that *mod-5*-dependent serotonergic signaling modulation was impacting on Q130 worms, reverting their transcriptome to closely resemble WT (since only a small number of genes have altered expression between WT and *mod-5*; Q130). Furthermore, when taking into consideration the locomotor and aggregation positive effects previously observed in *mod-5*; Q130 strain [8] together with those on transcriptomic profile presented in this thesis, it highly suggests that *mod-5* transporter ablation alters the expression of a considerable set of genes that will translate in a remarkable improvement of the phenotype of ATXN3 mutant worms and establishes *mod-5* as a genetic modifier of MJD pathogenesis in *C. elegans*.

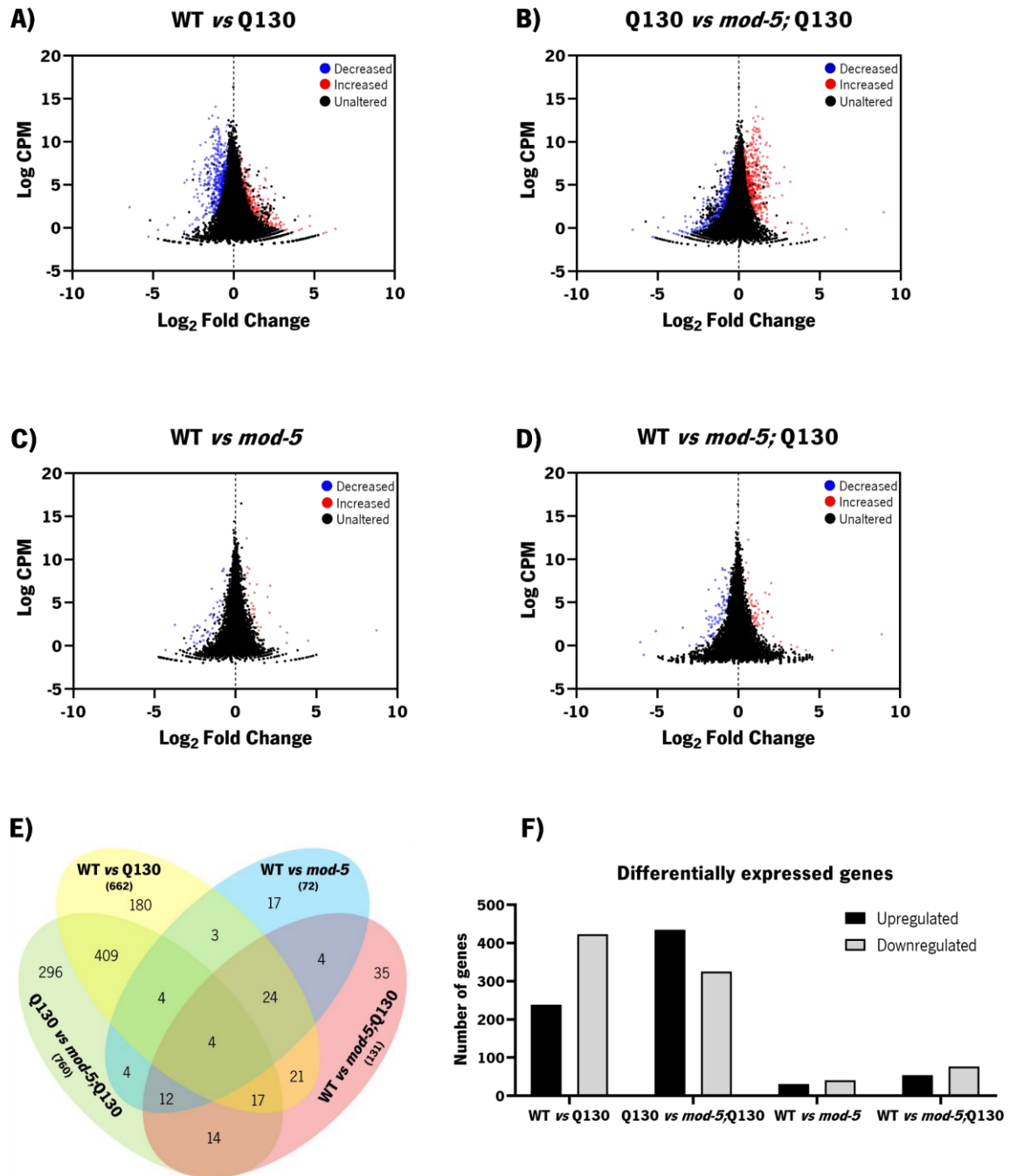


**Figure 4.2 Substantial and contrasting changes in transcript expression are observed in WT vs Q130 and Q130 vs *mod-5*; Q130 comparisons. A) - D)** Representation of the relationship between average expression (Log CPM, counts per million) and fold change (Log<sub>2</sub> fold change). Red dots indicate upregulated and blue dots indicate downregulated genes, called as differentially expressed at p-value ≤ 0.001 and FDR ≤ 0.05, in each comparison: **A)** WT vs Q130, **B)** Q130 vs *mod-5*; Q130, **C)** WT vs *mod-5* and **D)** WT vs *mod-5*; Q130. **E)** Venn diagram representing the distribution of the differentially expressed genes (DEGs) in each comparison; the total number of DEGs in each comparison is listed between brackets (). **F)** Number of up- (black bars) and downregulated (grey bars) genes found in each comparison.

### 3.2 Serotonin signaling modulation triggers protective responses in ATXN3 mutant animals

The transcriptome analysis of mutant Q130 and double mutant *mod-5*; Q130 animals revealed that the serotonin transporter *mod-5* ablation is changing the gene expression profile of ATXN3 mutant worms. To elucidate which pathways and/or biological processes underlie these profound changes in the transcriptome profile, enrichment analyses were performed using the *WormBase* Gene Set Enrichment analysis tool [23, 24].

As depicted in Figure 4.3, which represents the Gene Enrichment Analysis (GEA) performed, the most altered gene ontology (GO) terms of Q130 worms (*vs* WT) were related to defense responses (involving the response to biotic stimulus and immune system). Also, alterations in genes related to the lytic vacuole were observed, which could be linked to the autophagy mechanism, and to alterations in enzymatic activity, namely of peptidases and hydrolases (Figure 4.3A). These could be underlying ATXN3-mediated pathogenesis. On the other hand, the ablation of the *mod-5* transporter seemed to also alter the same kind of responses, besides triggering more specific responses (which did not appear in the WT *vs* Q130 comparison) such as the response to topologically incorrect proteins, among others (Figure 4.3B). When WT animals were compared to double mutant *mod-5*; Q130 animals, defense responses were most represented, followed by the immune response, and responses relative to folding of the proteins (Figure 4.3C), although, overall, those changes were not as significant as in the other comparisons studied (Figure 4.3A, B). The lower significance might further indicate that in *mod-5*; Q130 animals transcriptome alterations were reverted to a great extent and that this strain resembled more WT worms. Moreover, when analyzing WT *vs mod-5* comparison (Fig. 4.3D), identical responses were obtained with the same significance range (only missing extracellular space and peptidase activity), which suggests that such responses might be specifically modulated by *mod-5* ablation and consequent impact on serotonergic signaling, independently of mutant ATXN3 expression.

Interestingly, *mod-5* ablation completely reverted the direction of gene expression in defense responses that are downregulated in Q130 strain (Figure 4.4A). Moreover, it increased the expression of genes related to the lytic vacuole (Figure 4.4B), modulated responses directly related to protein conformation/misfolding and auxiliary pathways to protein quality control (PQC) machinery, as the unfolded protein response - UPR (Figure 4.4C), and increased the expression of genes belonging to the autophagic mechanism (Figure 4.4D). Lytic vacuole and autophagy processes are important for proteostasis and protein clearance in the context of ATXN3-mediated pathogenesis. Additionally, the modulation of responses directly related to protein conformation/misfolding could help explain the improvements in aggregation and neuronal dysfunction previously observed in *mod-5*; Q130 strain [8].

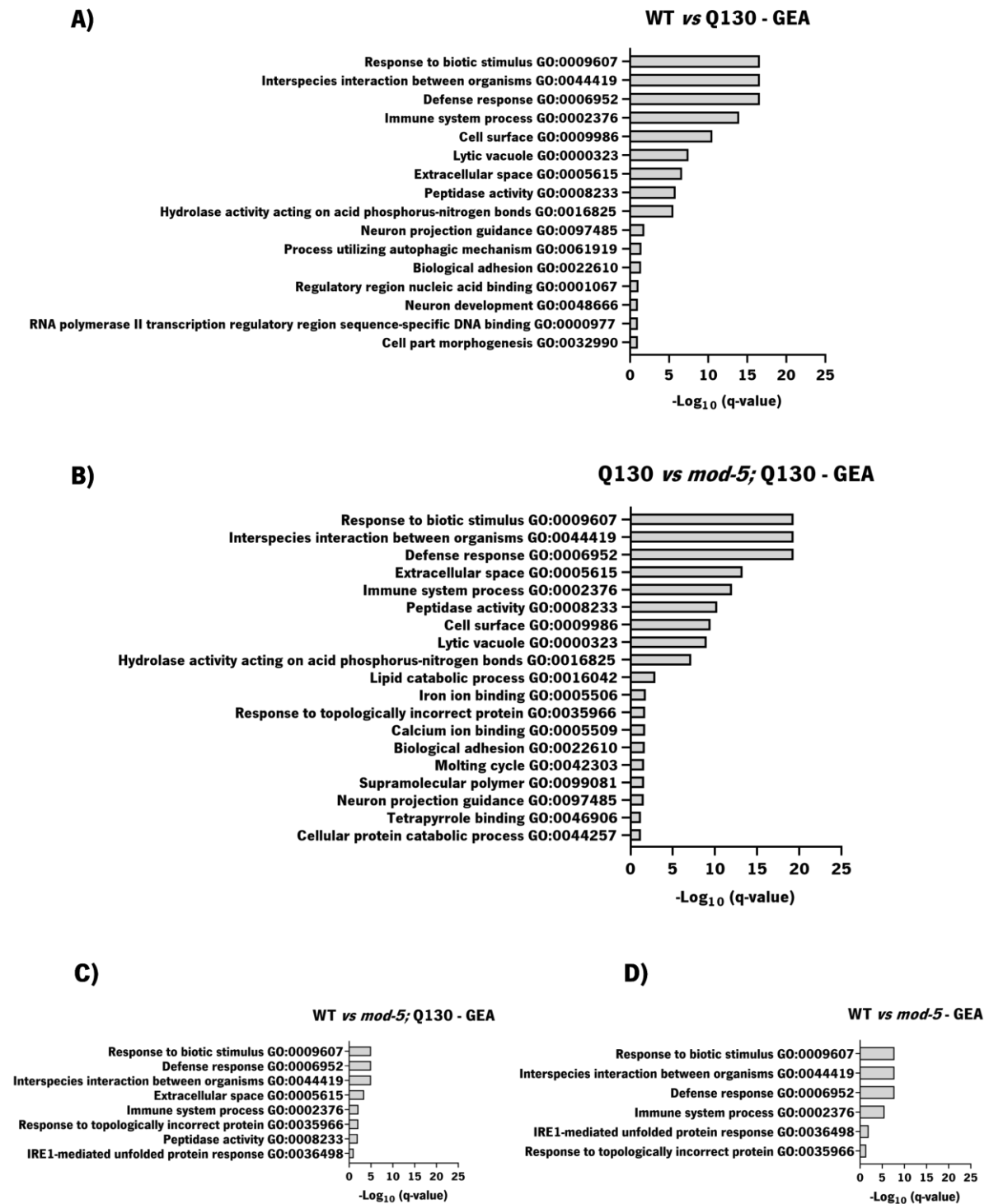


**Figure 4.3 Organism defense responses are altered in ATXN3 animals and upon serotonin transporter ablation.** Gene Enrichment Analysis (GEA) of the differentially expressed genes (DEGs) in each comparison. **A)** WT vs Q130, **B)** Q130 vs *mod-5*; Q130, **C)** WT vs *mod-5*; Q130, and **D)** WT vs *mod-5*, using Enrichment Analysis tool from *WormBase* [23, 24].



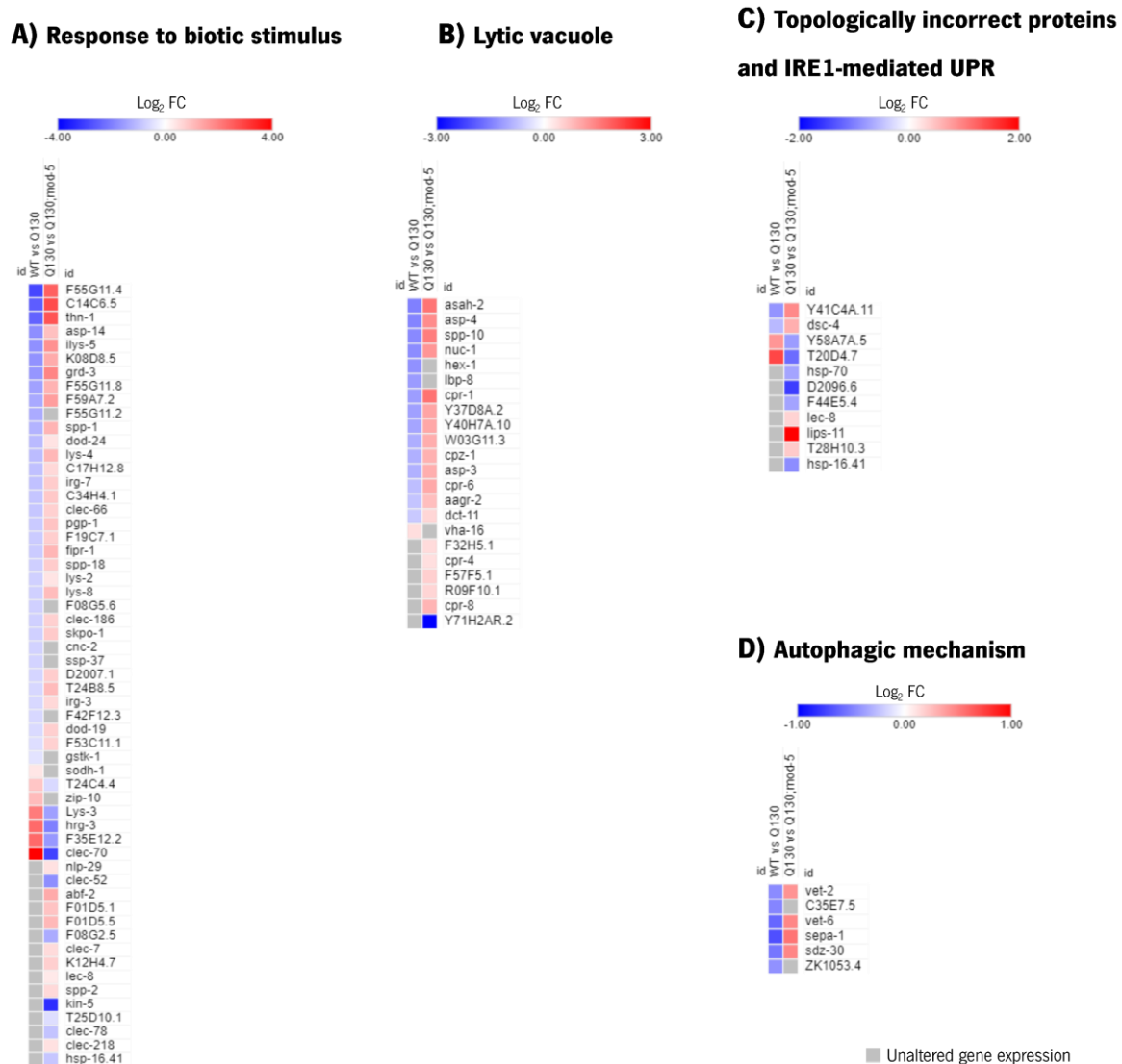


**Figure 4.4 Modulation of different responses by serotonin transporter *mod-5* ablation.** Heatmaps showing the gene expression alterations (Log<sub>2</sub> FC - fold change) between WT vs Q130 and Q130 vs *mod-5*; Q130 comparisons. Serotonin transporter ablation seems to activate or, at least, modulate some responses that are altered in Q130 MJD model: **A)** Response to biotic stimulus, **B)** Lytic vacuole; other responses seem to be triggered by *mod-5* alone such as: **C)** Response to topologically incorrect protein and inositol-requiring enzyme 1 (IRE1)-mediated unfolded protein response (UPR) (this last category corresponding to genes *hsp-70* and *hsp16.41*); and **D)** Process utilizing autophagic mechanism. Heatmaps were created using Morpheus online tool [30].

The Worm Phenotype Ontology is a hierarchically structured and controlled set of terms to classify and organize phenotype descriptions associated with *C. elegans* genes [35], that is at the base of Phenotype Enrichment Analysis (PEA) of *WormBase* Gene Set Enrichment analysis tool [23, 24].

Performing this analysis would tell us if DEGs in the different comparisons studied are associated to specific phenotypes. Relatively to this analysis, as expected, the Q130 strain displayed a wide range of alterations compared to WT (Figure 4.5A). Those ranged from development to several neuron-associated alterations, including axon trajectory and fasciculation, cord commissures and neurite morphology. Curiously, it seems that gene expression changes related to those seen when *C. elegans* larvae enter dauer arrest is associated to Q130 animals, under conditions that usually do not favor this transition (dauer constitutive phenotypes). Relatively to the double mutant *mod-5*; Q130, the MJD model transcriptome was altered by serotonergic signaling modulation in terms of molting (associated to animals exhibiting variations in timing and/or ability to molt), larval physiology, accumulation of vacuoles in the intestine, hypersensitivity to cadmium and dauer metabolism (Figure 4.5B). When comparing WT to *mod-5*; Q130, some variations were exhibited by worms compared to a given control (nematode phenotype) and the only specific difference obtained was related to cadmium hypersensitivity (Figure 4.5C). Within this category are five genes: *hsp-16.41*, *F44E5.4* (a cytoplasmic hsp-70), *B0024.4* (uncharacterized protein), *hsp16.2*, and *pud-4* (*pud* stands for protein up-regulated in *daf-2(loss-of-function)*). These have been described to be cadmium-responsive genes and to have strong, medium and/or weak (only *B0024.4* gene) protective effect against cadmium toxicity and their inhibition resulted in an increased sensitivity to this metal toxicity [36].

The last analysis performed using *WormBase* Gene Set Enrichment analysis tool [23, 24] consisted in Tissue Enrichment Analysis (TEA), which relies on *C. elegans* cell and anatomy ontology that considers five major aspects: cell lineage, position, cell type, organ and function [37]. This analysis allowed to perceive possible differences in *C. elegans* tissues, based on the DEGs of the comparisons tested. Results revealed that ATXN3 proteotoxicity impacted on accessory cells, which refers to cells that extend long processes around sensory neuron endings and have a support role very similar to “glia-like” cells. The main alterations were related to neuronal support cells, including sheath, socked and even GLR cells [38] (Figure 4.6A). On the other hand, *mod-5* deletion in the mutant ATXN3 background, besides having an impact on accessory cells, also led to alterations in the intestine and muscular system. Of note, the PVD neuron was also influenced by this modulation of the serotonin signaling pathway (Figure 4.6B). It is classified as a sensory neuron that responds to harsh touch (mechanosensation) [39] and to cold temperatures (thermosensation) [40]. No results were obtained for WT *vs mod-5*; Q130 and WT *vs mod-5* comparisons, indicating that the double mutant *mod-5*; Q130 is not different from WT at the tissue level, i.e., that *mod-5* ablation rescued ATXN3-mediated phenotype of Q130 worms, and that *mod-5* mutant has no major differences, at this level, when compared to control.

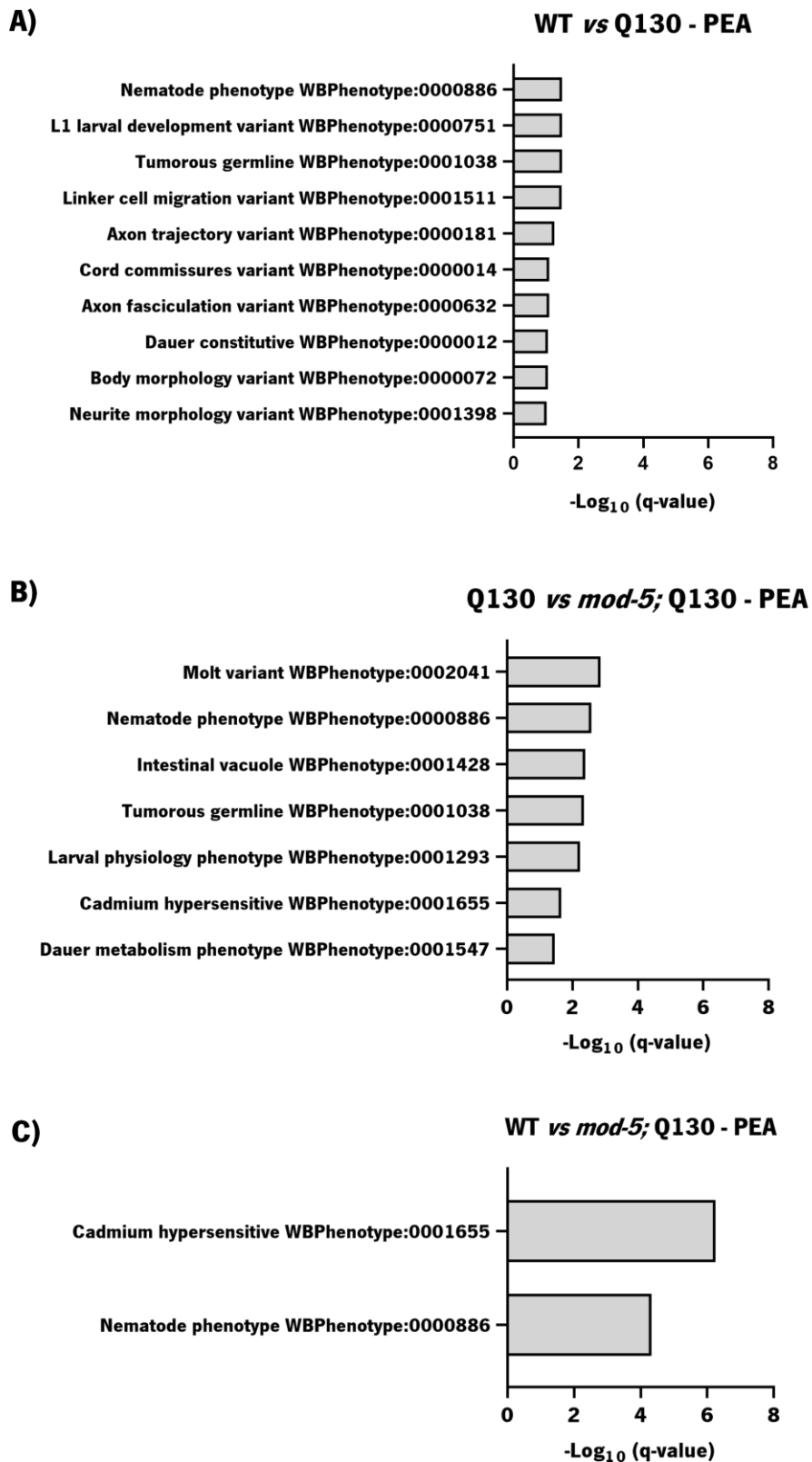


**Figure 4.5 Alterations in worm phenotype triggered by ATXN3-mediated proteotoxicity and serotonin signaling modulation.** Phenotype Enrichment Analysis (PEA) of the differentially expressed genes (DEGs) in each comparison. **A)** WT vs Q130, **B)** Q130 vs *mod-5*; Q130, and **C)** WT vs *mod-5*; Q130, using Enrichment Analysis tool from *WormBase* [23, 24].

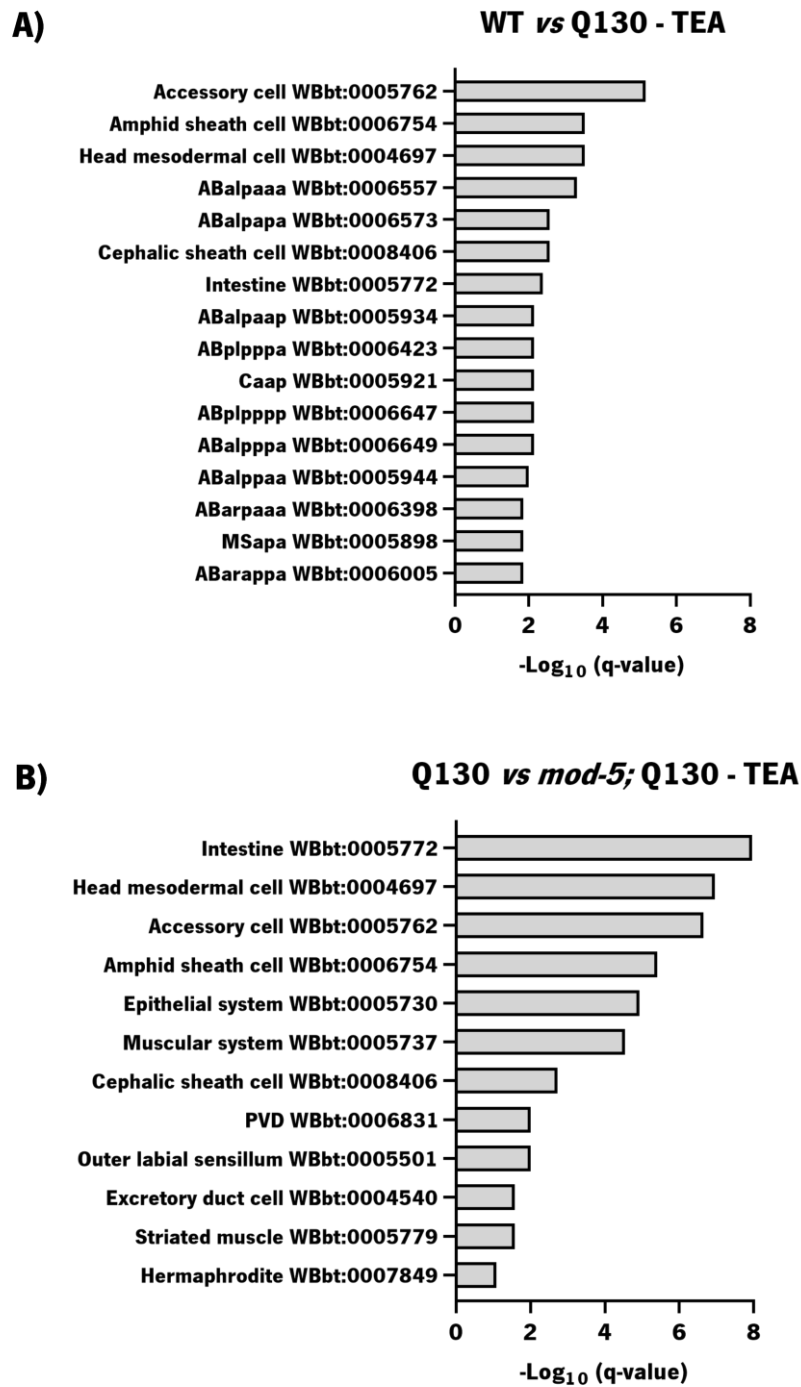


**Figure 4.6 Alterations in worm tissues triggered by ATXN3-mediated proteotoxicity and serotonin signaling modulation.** Tissue Enrichment Analysis (TEA) of the differentially expressed genes (DEGs) in each comparison. **A)** WT vs Q130, and **B)** Q130 vs *mod-5*; Q130, using Enrichment Analysis tool from *WormBase* [23, 24].

### 3.3 Alterations in proteome homeostasis-related genes are induced by *mod-5* serotonin transporter ablation in a *C. elegans* model of MJD

Following the observation that mechanisms related to proteostasis, namely autophagy, lytic vacuole, protein misfolding and auxiliary responses of PQC machinery (namely the UPR) could be underlying the improvements observed, we conducted an analysis to evaluate more specifically which branches and players of the PQC network could be altered. Based on the literature (see section 2.6 from materials and methods of this chapter), we elaborated a list of PQC genes that we compared with our data.

A total of 660 genes reported to participate in the PQC were found, in the literature, and further divided into the three main PQC modules: protein synthesis (209 genes), folding and conformational maintenance (233 genes) and degradation (218 genes). From this gene list, we found in our data a total of 31 that were differentially expressed, corresponding to 3.10 % of the total of DEGs (Figure 4.7A). In spite of the low number of DEGs within this class, the highest percentage (2 %) of them belonged to the folding and conformational maintenance module of the PQC.

Relatively to the comparisons studied, 2.38 % of the genes found to be differentially expressed in the WT *vs* Q130 comparison encode for PQC components, most of them acting in pathways related to protein degradation (Figure 4.7B). Deletion of *mod-5* resulted in 2.82 % of DEGs involved in the maintenance of protein homeostasis. However, we observed a shift in the most represented PQC category, which in this case was the folding and conformational maintenance module with 2.3 % (Figure 4.7C). This change in the most represented PQC module between comparisons suggests a role of serotonergic signaling modulation in the maintenance of the correct protein folding state in the ATXN3 background, potentially associated with the reduced protein aggregation seen in this strain.

In the ATXN3 strain, a major part of the PQC components was found to be downregulated, independently of the category they belong to, as listed in Table 4.3. The opposite was observed in the double mutant strain, in which a higher number of upregulated genes was found. In the folding and maintenance part of the PQC, several genes displayed increased expression (abnormal gut esterase - *ges-1*, cysteine protease related - *cpr-1*, ShK domain and peroxidase domain containing protein - *skpo-1*, and glutathione peroxidase - *gpx-3*) and could be possibly related to the lysosome and other stress triggered responses in the *mod-5*; Q130 strain. Intriguingly, heat shock proteins were downregulated. This is consistent with an adaptation to the decreased aggregation observed in the double mutant at this stage but does not explain how this decreased aggregation arose. In the degradation part of the PQC, genes encoding ubiquitin ligase components were the major category found. These were

mostly downregulated in WT *vs* Q130 comparison, and some of them were then found to be upregulated when the Q130 strain was compared to the double mutant *mod-5*; Q130 (Table 4.3).

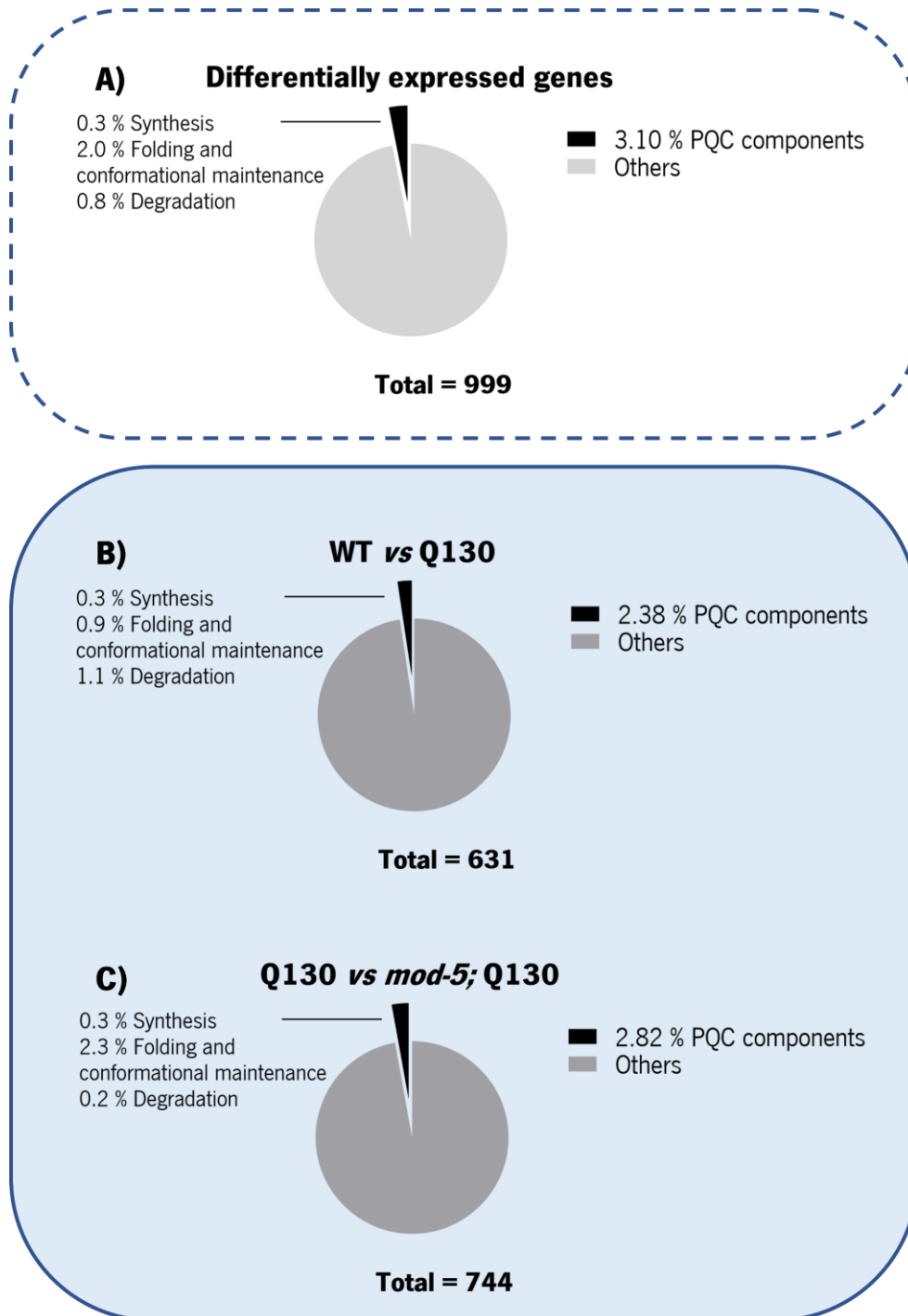


**Figure 4.7 Representativity of the protein quality control (PQC) machinery in the *C. elegans* transcriptomic analysis.** Percentage (%) of PQC components in **A)** the total of differentially expressed genes (DEGs) and the DEGs of **B)** Wild-type (WT) *vs* Q130 strain, and **C)** Q130 *vs* the double mutant *mod-5*; Q130, with information for each PQC module (synthesis, folding/conformational maintenance, and degradation).

**Table 4.3 List of the DEGs found in the different PQC categories, according to the main comparisons performed.** DEGs - differentially expressed genes; PQC - proteostasis quality control; FC - fold change.

PQC branch	Gene	Description	Log <sub>2</sub> FC		CREB target?
			WT vs Q130	Q130 vs <i>mod-5</i> ; Q130	
<b>Synthesis</b>	<i>Y65B4A.6</i>	Hypothetical protein	-0.66	0.55	No
	<i>ceh-58</i>	<i>C. elegans</i> Homeobox	-0.56		No
	<i>ceh-91</i>	<i>C. elegans</i> Homeobox		-0.50	No
<b>Folding and conformational maintenance</b>	<i>ges-1</i>	Abnormal Gut Esterase	-1.49	1.39	No
	<i>hex-1</i>	HEXosaminidase	-1.29		Yes
	<i>F41C3.5</i>	Uncharacterized serine carboxypeptidase F41C3.5	-1.28	1.66	No
	<i>cpr-1</i>	Gut-specific cysteine proteinase	-1.16	1.66	No
	<i>skpo-1</i>	Peroxidase skpo-1	-0.74	0.84	No
	<i>vha-16</i>	Vacuolar H ATPase	0.39		No
	<i>tatn-1</i>	Tyrosine AminoTraNsferase		0.46	No
	<i>hsp-70</i>	Heat Shock Protein		-0.71	Yes
	<i>hsp-16.41</i>	Heat shock protein		-0.89	Yes
	<i>hsp-16.2</i>	Heat Shock Protein		-0.92	Yes
	<i>gst-1</i>	Glutathione transferase omega-1		-0.75	No
	<i>gpx-3</i>	Glutathione peroxidase 3		0.68	No
	<i>fkf-4</i>	Peptidyl-prolyl cis-trans isomerase		-1.27	Yes
	<i>F57F5.1</i>	Hypothetical protein		0.56	No
	<i>F44E5.5</i>	Hypothetical protein		-0.58	No
	<i>F44E5.4</i>	Hypothetical protein		-0.72	Yes
	<i>F32H5.1</i>	Hypothetical protein		0.42	No
	<i>cpr-8</i>	Cysteine PRotease related		0.89	No
	<i>cpr-4</i>	Cathepsin B-like cysteine proteinase 4		0.37	No

<b>Degradation</b>	<i>skr-8</i>	SKp1 Related (ubiquitin ligase complex component)	-0.74		Yes
	<i>skr-9</i>	SKp1 Related (ubiquitin ligase complex component)	-0.58		Yes
	<i>skr-7</i>	SKp1 Related (ubiquitin ligase complex component)	-0.57	0.45	Yes
	<i>skr-13</i>	SKp1 Related (ubiquitin ligase complex component)	-0.57		Yes
	<i>skr-10</i>	SKp1 Related (ubiquitin ligase complex component)	-0.53		Yes
	<i>skr-14</i>	SKp1 Related (ubiquitin ligase complex component)	-0.44	0.39	No
	<i>rfp-1</i>	E3 ubiquitin-protein ligase	0.64		No

### 3.4 Serotonin transporter *mod-5* ablation in ATXN3 background alters the expression level of polyQ aggregation regulators

To verify the impact of serotonergic signaling modulation in the expression of regulators of polyQ aggregation, we determined if genes, previously described to modify the aggregation of polyQ-containing proteins were altered in our transcriptomic data. Behind this assumption is the reduction in ATXN3 aggregation previously observed in the *mod-5*; Q130 double mutant [8].

We found that four genes described to suppress polyQ aggregation when silenced by RNAi, and downregulation of which enhanced the functional characteristics of the PQC [32] were differentially expressed in our analysis. Two of them (*Y37D8A.16* and *ttr-14*) were upregulated in the Q130 strain and downregulated when *mod-5* mutation is present in this strain (Table 4.4). This is in accordance with the aggregation phenotype observed in Q130 animals, which is reversed in the double-mutant.

On the other hand, genes that when suppressed caused a premature appearance of polyQ aggregation were also found within the DEGs list, five in total (Table 4.4) [33]. Only one gene (*act-4*) encoding an actin isoform was upregulated in the Q130 strain. This observation suggest that some



mechanisms might still be triggered in Q130 animals in an attempt to surpass aggregation. However, the downregulation of *act-4* and the other four genes in *mod-5*; Q130 double mutant is counterintuitive.

These results further support the idea that serotonergic modulation in ATXN3 animals is able to modulate polyQ aggregation, by still unknown mechanisms including the modulation of the expression levels of proteostasis regulators.

**Table 4.4 List of known regulators of polyQ aggregation showing differential expression in our dataset.**

FC – fold change.

Impact on aggregation after silencing	Gene	Description	Log <sub>2</sub> FC		CREB target?
			WT vs Q130	Q130 vs <i>mod-5</i> ; Q130	
Suppression	<i>Y37D8A.16</i>	Hypothetical protein	0.60	-0.50	Yes
	<i>ttr-14</i>	TransThyretin-Related family domain	1.51	-1.27	Yes
	<i>tps-2</i>	Trehalose 6-Phosphate Synthase		-0.38	No
	<i>fbxb-11</i>	F-box B protein	-0.63		No
Increase	<i>noah-2</i>	NOmpA Homolog ( <i>Drosophila</i> nompA: no mechanoreceptor potential A)		-0.88	Yes
	<i>let-4</i>	Leucine-rich repeat-containing protein let-4		-0.82	Yes
	<i>gei-13</i>	Gex-3-interacting protein 13		-0.80	Yes
	<i>bus-8</i>	Hypothetical protein		-1.23	Yes
	<i>act-4</i>	Actin-4	0.39	-0.40	Yes

### 3.5 CREB role in *mod-5* ablation-induced proteostasis in ATXN3 mutant animals

As evidenced in chapter 3.1 of this thesis, the inhibition of serotonin transporter SERT/*mod-5*, by citalopram, led to serotonin signaling modulation that could possibly culminate in cAMP response element-binding protein (CREB) transcription program induction. Indeed, the reversion of ATXN3-mediated locomotor defects in the Q130 strain prompted by serotonin reuptake inhibition was attenuated when CREB was mutated, which indicated at least a partial dependence on this transcription factor for 5-HT modulation to have an effect. Moreover, CREB induction could be implicated in the proteostasis state of cells, in this context, as explored in chapter 3.2. To determine if the genetic ablation of *mod-5* could also require CREB to generate the improvements observed in the MJD *C. elegans* model, we determined the number of DEG-targets of this transcription factor.

Based on the work of Lakhina and colleagues [34], we gathered a list of potential CREB basal and CREB memory-induced target genes in *C. elegans*. Then, we compared this list against our transcriptomic data. More than a quarter of the altered genes in the transcriptomic analysis are CREB targets (Figure 4.8A). About the same percentage of the CREB targets were observed in WT *vs* Q130 (Figure 4.8B) and Q130 *vs mod-5*; Q130 comparisons (Figure 4.8C), suggesting that CREB might play a role in the mechanism behind the recovery triggered by serotonin transporter ablation.

Additionally, we observed that some PQC genes are indeed CREB targets, namely heat shock proteins and ubiquitin-related components (see Table 4.3). Interestingly, half of the RNA-seq overlapping genes, whose silencing caused suppression of polyQ aggregation, and all genes whose silencing caused enhancement of polyQ aggregation that were found to be altered in our data are CREB targets (Table 4.4).

Although more experiments are necessary to confirm the involvement of CREB in *mod-5* ablation-dependent serotonergic signaling, the results are compatible with the hypothesis that this transcription factor could be intervening in the reversal of MJD animal models' phenotypes, though yet to determine mechanisms.

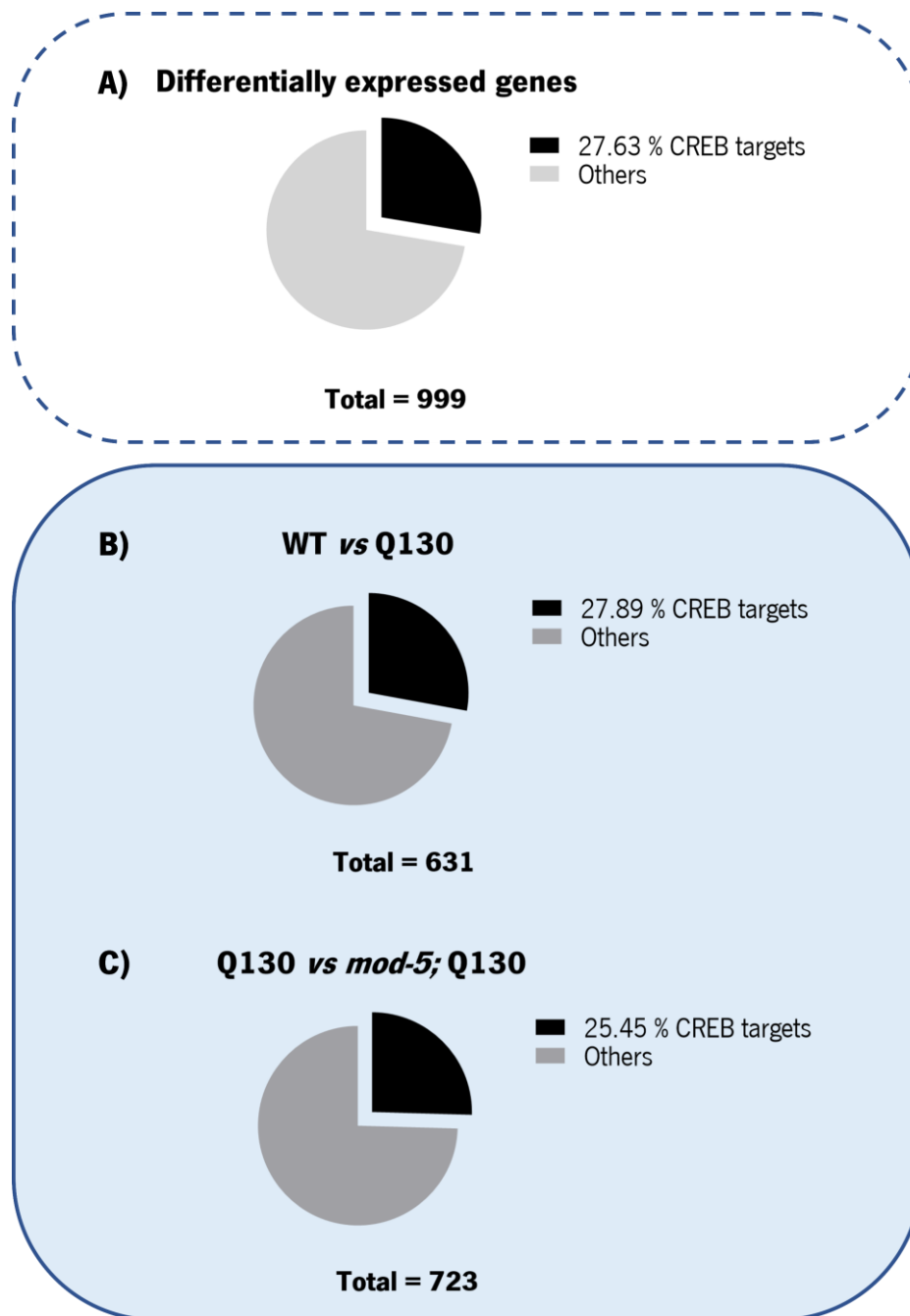


**Figure 4.8 Representativity of the CREB targets in the transcriptomic analysis.** Percentage (%) of CREB targets in **A)** the total of differentially expressed genes (DEGs) and the DEGs of **B)** Wild-type (WT) vs Q130 strain and **C)** Q130 vs the double mutant *mod-5*; Q130 strain.

## 4. Discussion

In this study we describe the effects of serotonergic signaling modulation, through serotonin reuptake inhibition by ablation of *mod-5/SERT* transporter, on the transcriptome of a *C. elegans* MJD model. We observed that serotonin modulation strikingly reverted the transcriptomic profile of Q130 animals, making them more WT alike. Our results showed that these transcriptomic alterations involved protective- and proteome homeostasis-related responses in *mod-5*; Q130 worms, for a subset of which the CREB transcription factor might play a role.

The first impressive finding is that *mod-5* deletion could drastically alter the transcriptomic profile of the Q130 *C. elegans* MJD model making it molecularly more similar to WT. In this way, all the genes that were altered in the Q130 strain, common to the *mod-5*; Q130 double mutant, were perfectly mirroring each other, i.e., if one gene was increased in Q130 strain it would be decreased in the *mod-5*; Q130 animals and *vice-versa*. This complete shift in the Q130 transcriptome is interesting since expanded ATXN3 has been shown to lead to transcriptional dysregulation [41, 42], and here, we found that the transcriptional alterations induced by mutant ATXN3 were counteracted by modulation of the serotonin signaling pathway. However, this was not observed in mice (chapter 3), perhaps due to an increase in organism complexity.

Overall, the transcriptomic data analysis showed that several protective and proteostasis-related responses, including several genes belonging to folding and conformational maintenance and degradation modules of the PQC machinery, had decreased expression in Q130 worms, but were upregulated in *mod-5*; Q130 animals. This suggests that proteome dyshomeostasis is accompanied by ATXN3 proteotoxicity and that the enhancement of the serotonin signaling is beneficial in the reversion of this state. One of the things that seemed to be mediated by *mod-5* serotonin transporter ablation was the upregulation of genes playing a role in defense responses, namely responses associated to biotic stresses. ATXN3 proteotoxicity led to a decrease in the expression of genes encoding proteins belonging to these types of responses, which was increased upon *mod-5* deletion in mutant ATXN3 animals. In fact, it has been shown that *C. elegans* that grow in contact with pathogens display increased resistance to posterior exposure to pathogens, along with an increase in lifespan and augmented resistance to heat shock [43]; so, if the biotic stress responses were increased in our double mutant animals, a possible increase in the heat shock response, for instance, could also be triggered. In the case of *mod-5*; Q130 double mutants, the heat shock response failed to be activated, since heat shock proteins were downregulated, but this could be instead indicative of a reversion of the proteotoxic stress and that the activation of this response is no longer needed. In fact, we cannot disregard that this kind of responses could have been triggered

at a different time point in life, and that gene expression data should be complemented with verification of protein level.

Lysosome function and autophagy could also play a role in *mod-5*-mediated effects on ATXN3 worms, since several genes involved in these processes were altered (mostly upregulated) upon *mod-5* ablation. For instance, *cpr-1* and other genes encoding cysteine proteases (orthologs of the human cathepsins) are a class of intracellular enzymes important for protein turnover within the lysosome [44], and were shown to be involved in the degradation of polyQ proteins and to regulate amyloid beta levels and neuronal deficits in models of Alzheimer's disease [45-47]. Lytic vacuoles or lysosomes are crucial for cellular degradation, helping to maintain cell homeostasis. Recently, a study showed that in worms the expression of lysosome genes was increased in long-lived mutant strains and that the functions of *daf-16*/FOXO and *skn-1*/NRF2 transcription factors were crucial for this upregulation to take place. Moreover, an altered lysosome function affected clearance of aggregation-prone proteins and lifespan in those mutants [48]. Autophagy also plays a role in the degradation of protein aggregates (aggrephagy) [49], being important for a decreased toxicity of those in *C. elegans* models of MJD [50], and also relevant in human context, since dysregulated autophagy has been observed in postmortem brain of MJD patients [51]. In line with this, hormetic stressors and heat shock factor 1 (HSF-1) overexpression have been shown to lead to autophagy activation contributing to stress resistance and hormesis [52]. Indeed, HSF-1 activation has proven to be effective in the suppression of ATXN3 phenotypes in *C. elegans* [18]. Those mechanisms seem to be modulated and important in response to serotonin signaling modulation in MJD. Additional responses seem to be regulated upon *mod-5* serotonin transporter ablation. Although not much altered in the Q130 strain, responses to misfolded proteins were modulated in the *mod-5*; Q130 double mutants (response to topologically incorrect protein and IRE-1-mediated UPR). This is in accordance with previous published results that demonstrated that serotonin is an important mediator in the activation of generalized UPR in *C. elegans* [15]. Interestingly, in the work by Hetz and collaborators the inhibition of the IRE-1 axis led to cytoprotection and to an upregulation of autophagy, showing, for the first time, that the UPR can have a negative regulatory effect on autophagy [53]. Possibly, the same type of negative regulatory effect could have happened through *mod-5* modulation since genes in this category (Figure 4.4C) were downregulated. Other PQC auxiliary pathways might account for the *mod-5*-mediated positive impact on Q130 worms. A gene involved in the oxidative stress response, *tatn-1*, was also upregulated [54] in double mutants; this gene has been shown to regulate dauer decision and to be a modulator of the *daf-2* insulin/IGF-1-like (IGFR) signaling pathway [55]. Increased expression of antioxidant enzyme-encoding genes was also verified, such as glutathione peroxidase, reinforcing the importance of

the antioxidant response in the *mod-5* ablation-dependent mechanism. This further supports the relevance of serotonergic signaling modulation in MJD, since antioxidant capacity has been shown to be decreased in serum from MJD patients [56].

Interestingly, phenotype enrichment analysis also pointed that dauer constitutive phenotype could be triggered independently of the canonical cues (population density, food availability and high temperature), suggesting that the mechanisms that lead to dauer state are disconcerted in the presence of mutant ATXN3, or possibly partially induced to promote stress-resistance without properly shifting into a dauer state. Among the pathways that regulate dauer arrest are the guanylyl cyclase, the TGF $\beta$ -like, the insulin-like and the steroid hormone pathways [57]. Dauer formation has been associated with increased autophagy [58], which could provide an explanation for the dauer constitutive state attributed to the Q130 strain in the analysis performed. In addition, our results showed that a dauer-like metabolism phenotype was also promoted by *mod-5* mutation in ATXN3 background. In the dauer state, the larvae do not feed, and their metabolism depends on internal food reservoirs. Dauers do not undergo a shift toward aerobic respiration [59] and have high mRNA expression of the heat shock protein Hsp90 [60], elevated superoxide dismutase [61, 62] and catalase [62]. Expression profiles of *C. elegans* dauer larvae and *daf-2* (a long-lived inducing-mutation) adults have been studied and showed that a cohort of longevity genes have similar expression in both. These include HSP20/ $\alpha$ -crystallin gene family, detoxification genes (the cytochrome P450s - CYPs, the short chain dehydrogenase/reductases - SRDs, and UDP-glucuronosyltransferases - UGTs), transthyretin-related proteins (TRP), as well as metabolism, oxidoreductase activity and electron transport genes [63, 64]. Some changes in the expression of genes belonging to these categories are observed in our RNA-seq data (data not shown) and would require further studies.

Double mutants were also predicted to be hypersensitive to cadmium (a toxic environmental pollutant), meaning that they would respond to it at a lower concentration or shorter exposure. Interestingly, genes found in this category (*hsp-16.41*, *F44E5.4* (a cytoplasmic hsp-70), and *hsp16.2*) are associated to proteotoxic stress response and are important for the folding and stability of proteins. Besides the genes reported in the results, this response could be associated with alterations seen in genes associated with metal detoxification: metallothioneins (*mtl-1*, *mtl-2*), cadmium responsive *cdr-1* gene, toxin-regulated targets of MAPK *ttm-1* gene or even glutathione and phytochelatins (PCs) genes [36, 65]. This is in accordance with some of the changes that we see in our data. For instance, *ges-1* is also a cadmium-responsive gene, and glutathione genes were also differentially expressed, see Table 4.3. Interestingly, among the DEGs from our mouse RNA-seq we observed an increase in the metallothionein

1 (*Mt1*) gene and in glutathione *Gpx3* gene upon treatment, see chapter 3.2, Table 3.3.2. However, a proper confirmation of the presence of these phenotypes in the studied strains will be needed.

Still regarding the PQC network, some genes have been described as regulators of polyQ aggregation. We observed an upregulation of some of these genes described to suppress aggregation, when silenced, in the Q130 strain that were downregulated in *mod-5*; Q130 double mutant strain. This indicates that the modulation of these regulators upon *mod-5* deletion might contribute for the beneficial effects observed in MJD background. Additionally, when looking at genes whose reported silencing resulted in the premature appearance of aggregates, one was increased in Q130 strain (*act-4*) while those found in the double mutant were all decreased. While suggesting that some mechanisms might still be activated to surpass aggregation in Q130 animals, the downregulation of these genes in the double-mutant is counterintuitive but could reflect the decreased state of aggregation observed in those animals and therefore the uselessness of activating certain mechanisms in those conditions. Further assays would be necessary to further conclude if those specific genes are or not major contributors to aggregation in Q130 strain and involved in the reduction of aggregation in the *mod-5*; Q130 worms.

Interestingly, a significant number of CREB targets was found in the analyses performed which indicates that, at least in part, CREB could be an important factor downstream of serotonergic signaling enhancement by *mod-5* ablation. In support of this, gene enrichment analysis showed two terms possibly related to transcription in WT *vs* Q130: regulatory region nucleic acid and RNA polymerase II transcription regulatory region sequence-specific DNA binding, suggesting a possible contribution of transcriptional impairment in the Q130 strain. Transcription dysregulation in the presence of expanded ATXN3 has been described before [41]. Moreover, an interaction between ATXN3 and major acetyltransferases cAMP-response-element binding protein (CBP) and p300 (CREB cofactors) has been reported [66] and the incorporation of those factors in ATXN3 nuclear inclusions could account for these transcriptional alterations [67]. Still, more studies are needed to clarify the role of CREB downstream of serotonin signaling modulation of pathogenesis in MJD.

Phenotype enrichment analysis suggested that Q130 animals would likely present several neuronal abnormalities (in axon trajectory, cord commissures, axon fasciculation and neurite morphology), as expected, due to mutant ATXN3-induced proteotoxicity. Additionally, when analyzing tissue enrichment data, the MJD strain differed in the expression of genes mostly associated to accessory cells, namely in amphid and cephalic sheath cells. Amphid sheath cells are part of the specific sensory organ called sensilla in association with neuronal terminals, playing a role in mechanosensation, chemotaxis, osmotaxis and dauer pheromone sensation [68, 69]. Cephalic sheath cells are part of the

cephalic sensillum and play a role in isolating the nerve ring, as well as in its assembly and morphogenesis, providing important substrates for early axon guidance [70]. Regarding the *mod-5*;Q130 strain, phenotype enrichment revealed lack of neuronal defects that were present when comparing WT vs Q130 animals, suggesting a beneficial effect of serotonin modulation. Regarding tissue expression, alterations in the expression of genes associated with intestinal tissues were dominant, and might be related to upregulation of the autophagy and lysosome pathways, since it was reported that these processes in the intestine are essential for host defense [71], and our results evidenced that responses against biotic stimulus were enhanced in the double mutant strain. Accessory cells and other tissues (muscle, for instance) were altered upon serotonin modulation in the organism, which suggests that improvements in the conditions of those tissues/cells could be triggered. Specifically, alteration in the expression of genes associated with the PVD neuron were found, suggestive of changes in its function (mechano- and thermosensation) [39, 40]. Additional phenotype characterization studies will be needed to understand the full extension of the alterations triggered by *mod-5* serotonin transporter ablation regarding tissue and/or cell specificities.

## 5. Conclusions

MJD is a complex disorder in which many aspects need clarification to provide elevated chances of obtaining a disease-modifying therapy. In this study, we attempted to gain insight on how serotonergic signaling enhancement, through serotonin transporter ablation, is effective in offsetting MJD animal models' phenotypes, as it was observed, in previous work, with the antidepressant citalopram.

The enhancement of serotonergic signaling is a clear modifier of ATNX3 proteotoxicity by triggering a set of general defense responses, that might increase the capacity of the organism to better cope with polyQ expansion-derived complications. Such responses include responses activated upon biotic stimuli/stresses, lysosome and autophagy processes, as well as other PQC-related pathways. The response profile obtained with serotonin modulation seem to be very close to those existing in long-lived *C. elegans* mutant strains. As hypothesized in previous chapters, the CREB transcription factor could play a role in the activation of these diverse responses, although more studies are needed to support this idea.

## Acknowledgments

We would like to thank the members of the Maciel laboratory for critical analysis of the data and discussion on the manuscript, as well as for sharing reagents. We are thankful for the strains that were



provided by the *Caenorhabditis* genetics center (CGC), which is funded by NIH Office of Research Infrastructure Programs (P40 OD010440).

### **Funding**

This work was funded by National funds, through the Foundation for Science and Technology (FCT) - project UIDB/50026/2020 and UIDP/50026/2020; and by FEDER, through the Competitiveness Internationalization Operational Programme (POCI) under the scope of the projects: POCI-01-0145-FEDER-031987, NORTE-01-0145-FEDER-000013 and NORTE-01-0145-FEDER-000023, supported by North Portugal Regional Operational Programme (NORTE 2020), under the PORTUGAL 2020 Partnership Agreement, through the European Regional Development Fund (ERDF). This work was also funded through National Ataxia Foundation (NAF), USA. Stéphanie Oliveira was supported by a doctoral programme fellowship (Inter-University Doctoral Programme in Ageing and Chronic Disease from FCT - PD/BD/127818/2016).

## References

1. Coutinho, P. and Andrade, C., Autosomal dominant system degeneration in Portuguese families of the Azores Islands. A new genetic disorder involving cerebellar, pyramidal, extrapyramidal and spinal cord motor functions. *Neurology*, 1978. **28**(7): p. 703-709.<https://doi.org/10.1212/WNL.28.7.703>.
2. Bettencourt, C. and Lima, M., Machado-Joseph Disease: from first descriptions to new perspectives. *Orphanet Journal of Rare Diseases*, 2011. **6**(1): p. 35.<https://doi.org/10.1186/1750-1172-6-35>.
3. Bird, T.D., Hereditary Ataxia Overview. GeneReviews®, ed. A.H. Adam MP, Pagon RA, *et al.*, editors. 1998 Oct 28 [Updated 2019 Jul 25], University of Washington, Seattle; 1993-2020.<https://www.ncbi.nlm.nih.gov/books/NBK1138/>.
4. Schöls, L., Bauer, P., Schmidt, T., Schulte, T., *et al.*, Autosomal dominant cerebellar ataxias: clinical features, genetics, and pathogenesis. *The Lancet Neurology*, 2004. **3**(5): p. 291-304.[https://doi.org/10.1016/S1474-4422\(04\)00737-9](https://doi.org/10.1016/S1474-4422(04)00737-9).
5. Kawaguchi, Y., Okamoto, T., Taniwaki, M., Aizawa, M., *et al.*, CAG expansions in a novel gene for Machado-Joseph disease at chromosome 14q32.1. *Nature Genetics*, 1994. **8**(3): p. 221-228.<https://doi.org/10.1038/ng1194-221>.
6. Bevivino, A.E. and Loll, P.J., An expanded glutamine repeat destabilizes native ataxin-3 structure and mediates formation of parallel  $\beta$ -fibrils. *Proceedings of the National Academy of Sciences*, 2001. **98**(21): p. 11955-11960.<https://doi.org/10.1073/pnas.211305198>.
7. Paulson, H.L., Perez, M.K., Trotter, Y., Trojanowski, J.Q., *et al.*, Intranuclear Inclusions of Expanded Polyglutamine Protein in Spinocerebellar Ataxia Type 3. *Neuron*, 1997. **19**(2): p. 333-344.[https://doi.org/10.1016/S0896-6273\(00\)80943-5](https://doi.org/10.1016/S0896-6273(00)80943-5).
8. Teixeira-Castro, A., Jalles, A., Esteves, S., Kang, S., *et al.*, Serotonergic signalling suppresses ataxin 3 aggregation and neurotoxicity in animal models of Machado-Joseph disease. *Brain*, 2015. **138**(11): p. 3221-3237.<https://doi.org/10.1093/brain/aww262>.
9. Nutt, D.J., Forshall, S., Bell, C., Rich, A., *et al.*, Mechanisms of action of selective serotonin reuptake inhibitors in the treatment of psychiatric disorders. *European Neuropsychopharmacology*, 1999. **9**: p. S81-S86.[https://doi.org/10.1016/S0924-977X\(99\)00030-9](https://doi.org/10.1016/S0924-977X(99)00030-9).
10. Chilmonczyk, Z., Bojarski, A.J., Pilc, A., and Sylte, I., Serotonin transporter and receptor ligands with antidepressant activity as neuroprotective and proapoptotic agents. *Pharmacological Reports*, 2017. **69**(3): p. 469-478.<https://doi.org/10.1016/j.pharep.2017.01.011>.
11. Taler, M., Miron, O., Gil-Ad, I., and Weizman, A., Neuroprotective and procognitive effects of sertraline: *In vitro* and *in vivo* studies. *Neuroscience Letters*, 2013. **550**: p. 93-97.<https://doi.org/10.1016/j.neulet.2013.06.033>.

12. Kim, H.-J., Kim, W., and Kong, S.-Y., Antidepressants for neuro-regeneration: from depression to Alzheimer's disease. *Archives of Pharmacal Research*, 2013. **36**(11): p. 1279-1290.<https://doi.org/10.1007/s12272-013-0238-8>.
13. Jamwal, S. and Kumar, P., Antidepressants for neuroprotection in Huntington's disease: A review. *European Journal of Pharmacology*, 2015. **769**: p. 33-42.<https://doi.org/10.1016/j.ejphar.2015.10.033>.
14. Tatum, Marcus C., Ooi, Felicia K., Chikka, Madhusudana R., Chauve, L., *et al.*, Neuronal Serotonin Release Triggers the Heat Shock Response in *C. elegans* in the Absence of Temperature Increase. *Current Biology*, 2015. **25**(2): p. 163-174.<https://doi.org/10.1016/j.cub.2014.11.040>.
15. Berendzen, K.M., Durieux, J., Shao, L.-W., Tian, Y., *et al.*, Neuroendocrine Coordination of Mitochondrial Stress Signaling and Proteostasis. *Cell*, 2016. **166**(6): p. 1553-1563.e10.<https://doi.org/10.1016/j.cell.2016.08.042>.
16. Weber, J.J., Haas, E., Maringer, Y., Hauser, S., *et al.*, Calpain-1 ablation partially rescues disease-associated hallmarks in models of Machado-Joseph disease. *Human Molecular Genetics*, 2020. **29**(6): p. 892-906.<https://doi.org/10.1093/hmg/ddaa010>.
17. Bilen, J. and Bonini, N.M., Genome-Wide Screen for Modifiers of Ataxin-3 Neurodegeneration in *Drosophila*. *PLOS Genetics*, 2007. **3**(10): p. e177.<https://doi.org/10.1371/journal.pgen.0030177>.
18. Teixeira-Castro, A., Ailion, M., Jalles, A., Brignull, H.R., *et al.*, Neuron-specific proteotoxicity of mutant ataxin-3 in *C. elegans* : rescue by the DAF-16 and HSF-1 pathways. *Human Molecular Genetics*, 2011. **20**(15): p. 2996-3009.<https://doi.org/10.1093/hmg/ddr203>.
19. Ranganathan, R., Sawin, E.R., Trent, C., and Horvitz, H.R., Mutations in the *Caenorhabditis elegans* Serotonin Reuptake Transporter MOD-5 Reveal Serotonin-Dependent and -Independent Activities of Fluoxetine. *The Journal of Neuroscience*, 2001. **21**(16): p. 5871-5884.<https://doi.org/10.1523/JNEUROSCI.21-16-05871.2001>.
20. Brenner, S., The Genetics of *Caenorhabditis elegans*. *Genetics*, 1974. **77**(1): p. 71-94.<https://www.genetics.org/content/77/1/71.short>.
21. Voisine, C., Varma, H., Walker, N., Bates, E.A., *et al.*, Identification of Potential Therapeutic Drugs for Huntington's Disease using *Caenorhabditis elegans*. *PLOS ONE*, 2007. **2**(6): p. e504.<https://doi.org/10.1371/journal.pone.0000504>.
22. Dobin, A., Davis, C.A., Schlesinger, F., Drenkow, J., *et al.*, STAR: ultrafast universal RNA-seq aligner. *Bioinformatics*, 2013. **29**(1): p. 15-21.<https://doi.org/10.1093/bioinformatics/bts635>.
23. Angeles-Albores, D., N. Lee, R.Y., Chan, J., and Sternberg, P.W., Tissue enrichment analysis for *C. elegans* genomics. *BMC Bioinformatics*, 2016. **17**(1): p. 366.<https://doi.org/10.1186/s12859-016-1229-9>.

24. Angeles-Albores, D., Lee, R.Y.N., Chan, J., and Sternberg, P.W., Two new functions in the WormBase Enrichment Suite. *microPublication Biology*, 2018. <https://doi.org/10.17912/W25Q2N>.
25. Harris, T.W., Arnaboldi, V., Cain, S., Chan, J., *et al.*, WormBase: a modern Model Organism Information Resource. *Nucleic Acids Research*, 2019. **48**(D1): p. D762-D767. <https://doi.org/10.1093/nar/gkz920>.
26. Huang da, W., Sherman, B.T., and Lempicki, R.A., Systematic and integrative analysis of large gene lists using DAVID bioinformatics resources. *Nature Protocols*, 2009. **4**(1): p. 44-57. <https://doi.org/10.1038/nprot.2008.211>.
27. Huang, D.W., Sherman, B.T., and Lempicki, R.A., Bioinformatics enrichment tools: paths toward the comprehensive functional analysis of large gene lists. *Nucleic Acids Research*, 2008. **37**(1): p. 1-13. <https://doi.org/10.1093/nar/gkn923>.
28. Hill, A.A., Hunter, C.P., Tsung, B.T., Tucker-Kellogg, G., *et al.*, Genomic Analysis of Gene Expression in *C. elegans*. *Science*, 2000. **290**(5492): p. 809-812. <https://doi.org/10.1126/science.290.5492.809>.
29. Johnstone, I.L. and Barry, J.D., Temporal reiteration of a precise gene expression pattern during nematode development. *The EMBO Journal*, 1996. **15**(14): p. 3633-3639. <https://doi.org/10.1002/j.1460-2075.1996.tb00732.x>.
30. Broad Institute. CLUE MORPHEUS. 2020 [Last accessed 2020 November]; Morpheus: versatile matrix visualization and analysis software ]. Available from: <https://clue.io/morpheus>.
31. Walther, Dirk M., Kasturi, P., Zheng, M., Pinkert, S., *et al.*, Widespread Proteome Remodeling and Aggregation in Aging *C. elegans*. *Cell*, 2015. **161**(4): p. 919-932. <https://doi.org/10.1016/j.cell.2015.03.032>.
32. Silva, M.C., Fox, S., Beam, M., Thakkar, H., *et al.*, A Genetic Screening Strategy Identifies Novel Regulators of the Proteostasis Network. *PLOS Genetics*, 2011. **7**(12): p. e1002438. <https://doi.org/10.1371/journal.pgen.1002438>.
33. Nollen, E.A.A., Garcia, S.M., van Haften, G., Kim, S., *et al.*, Genome-wide RNA interference screen identifies previously undescribed regulators of polyglutamine aggregation. *Proceedings of the National Academy of Sciences of the United States of America*, 2004. **101**(17): p. 6403-6408. <https://doi.org/10.1073/pnas.0307697101>.
34. Lakhina, V., Arey, Rachel N., Kaletsky, R., Kauffman, A., *et al.*, Genome-wide Functional Analysis of CREB/Long-Term Memory-Dependent Transcription Reveals Distinct Basal and Memory Gene Expression Programs. *Neuron*, 2015. **85**(2): p. 330-345. <https://doi.org/10.1016/j.neuron.2014.12.029>.
35. Schindelman, G., Fernandes, J.S., Bastiani, C.A., Yook, K., *et al.*, Worm Phenotype Ontology: Integrating phenotype data within and beyond the *C. elegans* community. *BMC Bioinformatics*, 2011. **12**(1): p. 32. <https://doi.org/10.1186/1471-2105-12-32>.

36. Cui, Y., McBride, S.J., Boyd, W.A., Alper, S., *et al.*, Toxicogenomic analysis of *Caenorhabditis elegans* reveals novel genes and pathways involved in the resistance to cadmium toxicity. *Genome Biology*, 2007. **8**(6): p. R122.<https://doi.org/10.1186/gb-2007-8-6-r122>.
37. Lee, R.Y.N. and Sternberg, P.W., Building a Cell and Anatomy Ontology of *Caenorhabditis elegans*. *Comparative and Functional Genomics*, 2003. **4**: p. 482457.<https://doi.org/10.1002/cfg.248>.
38. Tang, Y., Illes, P., and Verkhatsky, A., Glial-neuronal Sensory Organs: Evolutionary Journey from *Caenorhabditis elegans* to Mammals. *Neuroscience Bulletin*, 2020: p. 1-4.<https://doi.org/10.1007/s12264-020-00464-z>.
39. Way, J.C. and Chalfie, M., The *mec-3* gene of *Caenorhabditis elegans* requires its own product for maintained expression and is expressed in three neuronal cell types. *Genes & Development*, 1989. **3**(12a): p. 1823-1833.<https://doi.org/10.1101/gad.3.12a.1823>.
40. Chatzigeorgiou, M., Yoo, S., Watson, J.D., Lee, W.-H., *et al.*, Specific roles for DEG/ENaC and TRP channels in touch and thermosensation in *C. elegans* nociceptors. *Nature Neuroscience*, 2010. **13**(7): p. 861-868.<https://doi.org/10.1038/nn.2581>.
41. Chou, A.-H., Yeh, T.-H., Ouyang, P., Chen, Y.-L., *et al.*, Polyglutamine-expanded ataxin-3 causes cerebellar dysfunction of SCA3 transgenic mice by inducing transcriptional dysregulation. *Neurobiology of Disease*, 2008. **31**(1): p. 89-101.<https://doi.org/10.1016/j.nbd.2008.03.011>.
42. Evert, B.O., Vogt, I.R., Vieira-Saecker, A.M., Ozimek, L., *et al.*, Gene Expression Profiling in Ataxin-3 Expressing Cell Lines Reveals Distinct Effects of Normal and Mutant Ataxin-3. *Journal of Neuropathology & Experimental Neurology*, 2003. **62**(10): p. 1006-1018.<https://doi.org/10.1093/jnen/62.10.1006>.
43. Leroy, M., Mosser, T., Manière, X., Alvarez, D.F., *et al.*, Pathogen-induced *Caenorhabditis elegans* developmental plasticity has a hormetic effect on the resistance to biotic and abiotic stresses. *BMC Evolutionary Biology*, 2012. **12**(1): p. 187.<https://doi.org/10.1186/1471-2148-12-187>.
44. Turk, V., Turk, B., and Turk, D., Lysosomal cysteine proteases: facts and opportunities. *The EMBO Journal*, 2001. **20**(17): p. 4629-4633.<https://doi.org/10.1093/emboj/20.17.4629>.
45. Bhutani, N., Piccirillo, R., Hourez, R., Venkatraman, P., *et al.*, Cathepsins L and Z Are Critical in Degrading Polyglutamine-containing Proteins within Lysosomes. *Journal of Biological Chemistry*, 2012. **287**(21): p. 17471-17482.<https://doi.org/10.1074/jbc.M112.352781>.
46. Mueller-Steiner, S., Zhou, Y., Arai, H., Roberson, E.D., *et al.*, Antiamyloidogenic and Neuroprotective Functions of Cathepsin B: Implications for Alzheimer's Disease. *Neuron*, 2006. **51**(6): p. 703-714.<https://doi.org/10.1016/j.neuron.2006.07.027>.
47. Sun, B., Zhou, Y., Halabisky, B., Lo, I., *et al.*, Cystatin C-Cathepsin B Axis Regulates Amyloid Beta Levels and Associated Neuronal Deficits in an Animal Model of Alzheimer's Disease. *Neuron*, 2008. **60**(2): p. 247-257.<https://doi.org/10.1016/j.neuron.2008.10.001>.

48. Sun, Y., Li, M., Zhao, D., Li, X., *et al.*, Lysosome activity is modulated by multiple longevity pathways and is important for lifespan extension in *C. elegans*. *eLife*, 2020. **9**: p. e55745.<https://doi.org/10.7554/eLife.55745>.
49. Rogov, V., Dötsch, V., Johansen, T., and Kirkin, V., Interactions between Autophagy Receptors and Ubiquitin-like Proteins Form the Molecular Basis for Selective Autophagy. *Molecular Cell*, 2014. **53**(2): p. 167-178.<https://doi.org/10.1016/j.molcel.2013.12.014>.
50. Khan, L.A., Yamanaka, T., and Nukina, N., Genetic impairment of autophagy intensifies expanded polyglutamine toxicity in *Caenorhabditis elegans*. *Biochemical and Biophysical Research Communications*, 2008. **368**(3): p. 729-735.<https://doi.org/10.1016/j.bbrc.2008.01.150>.
51. Sittler, A., Muriel, M.P., Marinello, M., Brice, A., *et al.*, Deregulation of autophagy in postmortem brains of Machado-Joseph disease patients. *Neuropathology*, 2018. **38**(2): p. 113-124.<https://doi.org/10.1111/neup.12433>.
52. Kumsta, C., Chang, J.T., Schmalz, J., and Hansen, M., Hormetic heat stress and HSF-1 induce autophagy to improve survival and proteostasis in *C. elegans*. *Nature Communications*, 2017. **8**(1): p. 14337.<https://doi.org/10.1038/ncomms14337>.
53. Hetz, C., Thielen, P., Matus, S., Nassif, M., *et al.*, XBP-1 deficiency in the nervous system protects against amyotrophic lateral sclerosis by increasing autophagy. *Genes & Development*, 2009. **23**(19): p. 2294-2306.<https://doi.org/10.1101/gad.1830709>.
54. Ipson, B.R., Green, R.A., Wilson, J.T., Watson, J.N., *et al.*, Tyrosine aminotransferase is involved in the oxidative stress response by metabolizing meta-tyrosine in *Caenorhabditis elegans*. *Journal of Biological Chemistry*, 2019. **294**(24): p. 9536-9554.<https://doi.org/10.1074/jbc.RA118.004426>.
55. Ferguson, A.A., Roy, S., Kormanik, K.N., Kim, Y., *et al.*, TATN-1 Mutations Reveal a Novel Role for Tyrosine as a Metabolic Signal That Influences Developmental Decisions and Longevity in *Caenorhabditis elegans*. *PLOS Genetics*, 2013. **9**(12): p. e1004020.<https://doi.org/10.1371/journal.pgen.1004020>.
56. de Assis, A.M., Saute, J.A.M., Longoni, A., Haas, C.B., *et al.*, Peripheral Oxidative Stress Biomarkers in Spinocerebellar Ataxia Type 3/Machado-Joseph Disease. *Frontiers in Neurology*, 2017. **8**(485).<https://doi.org/10.3389/fneur.2017.00485>.
57. Hu, P.J., Dauer, in *WormBook*. 2007, The *C. elegans* Research Community. p. 1-19.<https://doi.org/10.1895/wormbook.1.144.1>.
58. Meléndez, A., Tallóczy, Z., Seaman, M., Eskelinen, E.-L., *et al.*, Autophagy Genes Are Essential for Dauer Development and Life-Span Extension in *C. elegans*. *Science*, 2003. **301**(5638): p. 1387-1391.<https://doi.org/10.1126/science.1087782>.
59. Wadsworth, W.G. and Riddle, D.L., Developmental regulation of energy metabolism in *Caenorhabditis elegans*. *Developmental Biology*, 1989. **132**(1): p. 167-173.[https://doi.org/10.1016/0012-1606\(89\)90214-5](https://doi.org/10.1016/0012-1606(89)90214-5).

60. Dalley, B.K. and Golomb, M., Gene expression in the *Caenorhabditis elegans* dauer larva: Developmental regulation of Hsp90 and other genes. *Developmental Biology*, 1992. **151**(1): p. 80-90.[https://doi.org/10.1016/0012-1606\(92\)90215-3](https://doi.org/10.1016/0012-1606(92)90215-3).
61. Larsen, P.L., Aging and resistance to oxidative damage in *Caenorhabditis elegans*. *Proceedings of the National Academy of Sciences*, 1993. **90**(19): p. 8905-8909.<https://doi.org/10.1073/pnas.90.19.8905>.
62. Vanfleteren, J.R. and De Vreese, A., The gerontogenes *age-1* and *daf-2* determine metabolic rate potential in aging *Caenorhabditis elegans*. *The FASEB Journal*, 1995. **9**(13): p. 1355-1361.<https://doi.org/10.1096/fasebj.9.13.7557026>.
63. McElwee, J.J., Schuster, E., Blanc, E., Thomas, J.H., *et al.*, Shared Transcriptional Signature in *Caenorhabditis elegans* Dauer Larvae and Long-lived *daf-2* Mutants Implicates Detoxification System in Longevity Assurance. *Journal of Biological Chemistry*, 2004. **279**(43): p. 44533-44543.<https://doi.org/10.1074/jbc.M406207200>.
64. Murphy, C.T., McCarroll, S.A., Bargmann, C.I., Fraser, A., *et al.*, Genes that act downstream of DAF-16 to influence the lifespan of *Caenorhabditis elegans*. *Nature*, 2003. **424**(6946): p. 277-283.<https://doi.org/10.1038/nature01789>.
65. Vatamaniuk, O.K., Bucher, E.A., Ward, J.T., and Rea, P.A., A New Pathway for Heavy Metal Detoxification in Animals: Phytochelatin synthase is required for cadmium tolerance in *Caenorhabditis elegans*. *Journal of Biological Chemistry*, 2001. **276**(24): p. 20817-20820.<https://doi.org/10.1074/jbc.C100152200>.
66. Li, F., Macfarlan, T., Pittman, R.N., and Chakravarti, D., Ataxin-3 Is a Histone-binding Protein with Two Independent Transcriptional Corepressor Activities. *Journal of Biological Chemistry*, 2002. **277**(47): p. 45004-45012.<https://doi.org/10.1074/jbc.M205259200>.
67. McCampbell, A., Taylor, J.P., Taye, A.A., Robitschek, J., *et al.*, CREB-binding protein sequestration by expanded polyglutamine. *Human Molecular Genetics*, 2000. **9**(14): p. 2197-2202.<https://doi.org/10.1093/hmg/9.14.2197>.
68. Bargmann, C., Chemosensation in *C. elegans* (October 25, 2006), in *Wormbook*, The *C. elegans* Research Community, Editor. 2006.<https://doi.org/10.1895/wormbook.1.123.1>.
69. Altun, Z. and Hall, D., Nervous system, neuronal support cells, in *WormAtlas*. 2010.<https://doi.org/10.3908/wormatlas.1.19>.
70. Wadsworth, W.G., Bhatt, H., and Hedgecock, E.M., Neuroglia and Pioneer Neurons Express UNC-6 to Provide Global and Local Netrin Cues for Guiding Migrations in *C. elegans*. *Neuron*, 1996. **16**(1): p. 35-46.[https://doi.org/10.1016/S0896-6273\(00\)80021-5](https://doi.org/10.1016/S0896-6273(00)80021-5).
71. Curt, A., Zhang, J., Minnerly, J., and Jia, K., Intestinal autophagy activity is essential for host defense against *Salmonella typhimurium* infection in *Caenorhabditis elegans*. *Developmental & Comparative Immunology*, 2014. **45**(2): p. 214-218.<https://doi.org/10.1016/j.dci.2014.03.009>.

---

## **Supplementary data**



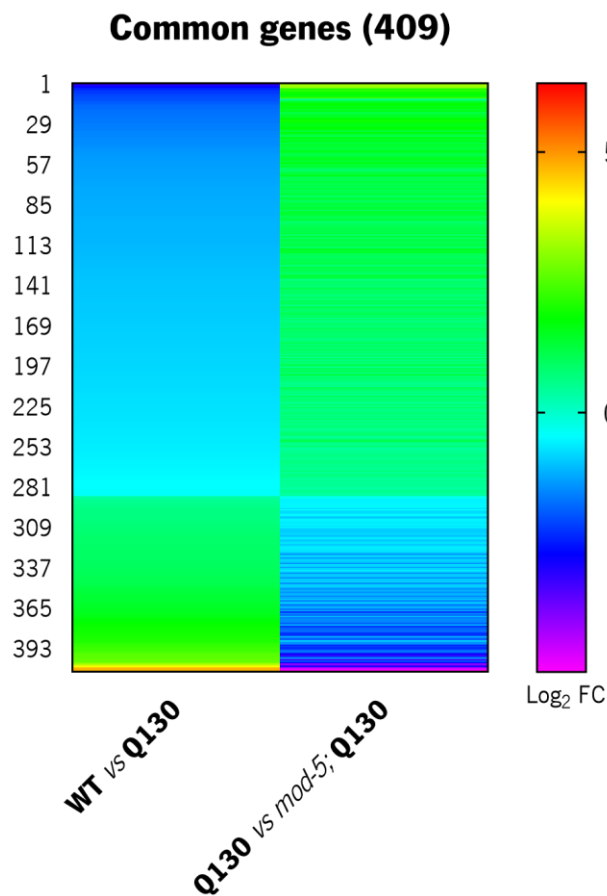


**Figure S4.1 Contrasting alterations in the expression of the common genes between WT vs Q130 and Q130 vs *mod-5*; Q130 comparisons.** Genes common only to the WT vs Q130 and the Q130 vs *mod-5*; Q130 comparisons are displayed in a heatmap. Fold changes (Log<sub>2</sub> FC) values were used. Each row represents a gene (some are numbered in the left side of the heatmap), in a total of 409 genes. Whenever a gene is downregulated (Log<sub>2</sub> FC < 0) in the WT vs Q130 comparison, the same gene is upregulated (Log<sub>2</sub> FC > 0) in the Q130 vs *mod-5*; Q130 one and *vice-versa* (Heatmap created using GraphPad Prism 8 software, version 8.0.1 (GraphPad Software, San Diego, CA, USA)).

## Chapter 5

---

### **General discussion and future perspectives**

Nowadays, neurological diseases, such as Machado-Joseph disease (MJD), are the primary cause of disability worldwide and researchers are eager to find effective therapeutic approaches to treat them [1]. There is an increased perception that pathologies affecting gait and balance are among the most determinant for an impaired quality of life and increased mortality [2, 3]. The need to find novel therapeutic strategies able to modify disease progression and to prevent its associated incapacity is urgent. Although MJD has a defined genetic cause, its heterogeneity in symptomatology, reflecting a brain multisystem dysfunction, and the complexity of the cellular mechanisms affected by the altered gene product represent a challenge to the development of disease-modifying treatments. In fact, besides the classic ataxia and motor signs, MJD patients present other symptoms such as sleep disorders, depression, anxiety, chronic pain, cramps, among others. The presence of neuronal ataxin-3 (ATXN3) protein aggregates and neuronal loss in several brain areas, such as the cerebellar dentate nucleus, substantia nigra, red and pontine nucleus and spinal cord, are also hallmarks of the disease [4]. The mutation of the *ATXN3* gene is thought to trigger an avalanche of cellular abnormalities, including impaired proteostasis, mitochondrial dysfunction and oxidative stress, defective calcium homeostasis, transcription alterations, and even defective axonal transport, underlying ATXN3-mediated neurodegeneration [5]. Currently, there is no specific treatment for MJD and only treatment of symptoms is targeted with available therapies, following recommendations that are mainly derived from studies in other neurodegenerative disorders. The challenge resides in finding a disease-modifying treatment that tackles all aspects of the pathology without having major side effects.

In this work, we strengthened previous observations that the use of citalopram and consequent modulation of the serotonergic system is a promising new therapeutic approach to be considered for the treatment of MJD. Importantly, the early initiation and chronic treatment duration seem to be key to obtain the best results (chapter 2). To better understand how citalopram is leading to the phenotypic and pathological ameliorations in MJD animal models, we performed a transcriptomic analysis in both mouse and *C. elegans* MJD models (chapter 3.1, 3.2 and 4).

In this chapter, the main findings, strengths, and limitations of the work developed throughout the years will be discussed. A special focus on the aims of the thesis will be made and suggestion for further research will be put forward.

## **5.1 Citalopram as a valid therapeutic approach: preclinical trials' design and lessons**

In chapter 2, we aimed at predicting the therapeutic potential of citalopram in the clinical context, that is, if the beneficial effects would still be relevant in a post-symptomatic phase of the disease. This

sometimes disregarded aspect in preclinical trials is important because, although genetic testing is available for MJD, most patients are only diagnosed after the appearance of the first symptoms. Preclinical trials are challenging; however, ensuring that those are adequately planned, have a correct design, are properly executed, and accurately reported potentiates their reproducibility and translation to the clinic.

**Animal model.** One crucial aspect in the planning of a preclinical trial is to ensure that we have the best animal model possible to answer our question. Having this in mind, there are three conditions commonly used to validate a mouse model: (i) *construct validity*, which is related to the biological features that cause the human disorder and should be present in the model; (ii) *face validity*, which refers to the analogy to the symptoms of the human disease, comprising the *endophenotypes* (behavioral symptoms, pathological, physiological, and chemical abnormalities) that can be modulated in animals; (iii) *predictive validity*, which refers to the specificity of treatment responses that should be similar between animal models and humans. This last one is, of course, limited by the intrinsic differences between other animal species and humans regarding disease mechanism(s) and drug pharmacokinetics (absorption, distribution, metabolism and excretion) [6]. Hence, it is essential to have a model of the disease that satisfies all these criteria, with a well characterized phenotype and pathological features. Measuring outcomes of clinical relevance, such as the identification of translatable biomarkers, is indispensable. Nevertheless, there is no perfect model. Different models of the same disorder may have different genetic backgrounds and therefore be variable in the manifestation of phenotypes and pathology, respond differently in terms of pharmacokinetics and pharmacodynamics to the same compound, and might also differ in responses among sexes (male *versus* female) due to their inherent differences in biology. Thus, preclinical testing in more than one mouse model and using two genders can contribute to an increase in the confidence that a protective therapy would be translatable.

The CMVMJD135 mouse model used in this thesis is among the most extensively characterized transgenic mouse models for this disorder, at the phenotypic and pathological levels. It expresses mutant human ATXN3 at near endogenous levels, exhibiting the aggregation pattern that is an MJD hallmark, and manifests MJD-like motor symptoms that appear in a gradual form and progress over time, which recapitulates what happens in the human disease [7]. Furthermore, some compounds tested in human clinical trials with MJD patients, such as lithium carbonate [8] and valproic acid [9], were tested in the CMVMJD135 mouse model being the results concordant with the clinical trials. Lithium had no overall impact in CMVMJD135 mouse phenotype [10], while valproic acid had some effects [11], as observed in MJD patients. Thus, it has a high construct, face, and predictive validity, making it a powerful model to address the questions raised in this thesis. Indeed, before conducting the experiments contained in

chapter 2, this model had already been tested in a slight different paradigm with citalopram [12] and in several preclinical trials in the lab maintaining the phenotype and characteristics as first described [7, 10-14].

**Experimental design.** Another critical aspect to assure the validity of the results obtained in a preclinical stage is the experimental design. Currently, for ethical (3Rs policy [15, 16] and European Union legislation (2010/63/EU) regulating animal use in life sciences) and logistical reasons, the number of animals used should be reduced as much as possible. To achieve that without compromising the validity of the results obtained, sample size should be estimated according to the anticipated magnitude of a specific biological effect, to the inherent variability of the target population and to the parameters being tested. The number of animals needs to be sufficient for a significant difference to be detected according to the parameters referred above and to the statistical power required to ensure robust results. The minimum number of animals needed for the CMVMJD135 model had previously been estimated [12] for the different measures tested in the present work. The use of littermate control animals, evaluation of both sexes, randomization and blinded assessment should also be considered when designing and conducting a preclinical assay. Littermate male and female mice should ideally be assessed in the same experiment, to exclude sex-specific drug effects and randomly assigned to each group (control and treatment). Controls needed should always be included into the study design, as a reference value, and researchers measuring the outcomes should be blinded to the genotype and treatment. In the work presented (chapter 2), only male mice were used due to logistic reasons in the animal housing, this constituting a limitation, but proper controls were used throughout the study. One of the strong points of the CMVMJD135 model is that the phenotype is highly comparable between males and females. Although not assessed in the same experiment, CMVMJD135 female mice were also tested with citalopram and a positive therapeutic effect was observed (Neves-Carvalho *et al.*, personal communication). Since then, several independent preclinical trials were conducted in this mouse model, in both sexes, by independent experimenters and the beneficial therapeutic effect of citalopram was robust and always observed. In the present work, drug (citalopram) and placebo treatments were alternately allocated to animals. Researchers were blind to treatment and whenever possible also to genotype, although as the animals age, MJD-like symptoms progress and the genotype becomes obvious to the experimenter.

**Defining the dosages.** One of the possible causes of clinical trial failure is the improper translation of drug dosage tested in preclinical trials to humans. Many times, a compound found to work well in mice is ineffective when it reaches the clinical stage. To address this issue, in 2007, Reagan-Show and collaborators proposed the body surface area (BSA) normalization method for dose translation from

animal to human studies. This method correlates well among several mammalian species and includes in the analysis several parameters of biology, such as basal metabolism, oxygen utilization, caloric expenditure, blood volume, circulating plasma proteins and renal function [17]. According to this method, the dosage of citalopram used in this study (8 mg/kg/day, already described as non-toxic and effective in mice with the same genetic background [18]) corresponds to a 38 mg/day dose in a 60 kg person. The most common dose of citalopram used in adults for treatment of depression is 20 mg/day, but it may start at a lower dose and be increased to a maximum dose of 40 mg/day. The citalopram dose defined in our studies is therefore within the recommended range, although some revision in dosing for older adults has been made [19]. More recently, the use of the BSA method has been questioned, and the inclusion of other parameters (physiologic, pharmacokinetic and toxicology data) for interspecies scaling has been suggested [20]. This is particularly relevant for new drugs and compounds for which there is no toxicity data available. As citalopram is already widely used in the clinic, its safety profile in humans is well established.

**Data handling and ARRIVE guidelines.** A preclinical assay should be carefully planned, the methodology used and data obtained comprehensively described. Readouts, time points of assessment and completion of the study should be defined in advance, according to the objective of the research. After readouts are defined, the method of statistical analysis should be chosen accordingly. Exclusion criteria should also be established prior to the study. Any data removed before the analysis should be acknowledged. Avoiding omission, insufficient and/or inadequate reporting of animal experimental data is essential as it may add to the reasons why preclinical experiments are not successfully reproduced or later fail when translated to clinic. To improve the reporting of animal experiments, the ARRIVE (Animals in Research: Reporting *In Vivo* Experiments) guidelines were created [21]. They consist in a checklist of information (updated recently) to include in publications aiming at describing *in vivo* experiments that would allow others not only to reproduce but also inspect the work satisfactorily, evaluating its methodological rigor [22]. For the studies described in this work, which are published or *in preparation*, complete details of assay methodologies used, assessments performed, information on the animal model used and specific characteristics (genetic background, CAG repeat length), exclusion criteria, and statistical analysis were provided according to the guidelines. An additional concern regarding reporting of experiments by researchers is the view that successful proven hypotheses are more likely to be published than the ones who fail to be proven, the so-called negative results. It is vital that negative results are also published in open-access journals. Underreporting negative results will introduce a significant

bias, which consequently can misinform researchers and more resources will be wasted on research that remain unpublished and not available to the scientific community [23].

**Reproducibility and validation.** A key aspect for science is that results obtained should be replicated by different researchers and, if possible, in independent laboratories thus corroborating the findings and increasing the confidence for potential translation. Regarding the CMVMJD135 model, it has a robust phenotype, replicated by different experimenters in our and in independent foreign laboratories [24-26]. Reproducibility and validation of treatments are also of major importance. The therapeutic effect of citalopram has been observed in the CMVMJD135 mouse model, by different experimenters in two different animal facilities, accounting for the robustness of the findings (Neves-Carvalho, A. *et al.*, personal communication; Oliveira, S. *et al.*, unpublished results). Furthermore, citalopram treatment was validated in an independent laboratory, in a different MJD model (YACMJD84.2), in which a reduction in ATXN3 aggregation was observed upon treatment [27], giving further strength to the idea that this therapeutic approach, validated in chapter 2, is a undeniable candidate for translation.

**Citalopram as a therapeutic approach.** In this work, we found that the post-symptomatic treatment of MJD mice with the SSRI citalopram still attenuated motor dysfunction and loss of balance, even in a cohort of mice with increased symptoms severity and faster disease progression. Although not having a strong impact in neuropathology, this is still relevant since, as previously referred, lack of gait and balance are determinant for an impaired quality of life. The use of this antidepressant beyond the treatment of depression could attenuate the progressive decline in motor abilities of MJD patients. Importantly, with this work, we found that citalopram could be relevant in a clinical context. Most of the preclinical trials reported in the literature, for MJD, do not evaluate the therapeutic potential of pre- and post-symptomatic pharmacological treatment initiation. Assessment of other therapeutic strategies using genetic approaches in MJD have been made in both conditions, but using different mouse models (lentiviral-based and transgenic mice) [28]. Even when looking at other neurodegenerative disorders, where both paradigms are also relevant, studies performing pre- and post-symptomatic treatment initiation are not generally found in the literature. Still, some examples exist regarding amyotrophic lateral sclerosis (ALS) [29, 30] or even SCA17 [31], with improvements observed in both pre- and post-symptomatic treatments, using valproic acid and arimocloamol for ALS, and using granulocyte-colony stimulating factor (G-CSF) for SCA17. To the best of our knowledge, citalopram is the first pharmacological approach tested in a preclinical setting in MJD, in both pre- and post-symptomatic paradigms in the same mouse model, with encouraging improvements. As citalopram has a safe profile it could be used as a prophylactic treatment for mutation carriers (as genetic testing is available) or after disease onset. Although it might not seem

always necessary to test therapeutic approaches pre-symptomatically in neurodegenerative disorders (especially in diseases in which diagnosis is only made after symptom onset), we cannot disregard that it might give us clues about the disease pathological mechanisms and/or responses triggered by the therapeutic intervention tested. In the case of citalopram, early initiation of treatment seems to be key to prevent aggregation and neuronal loss. A different timing in citalopram treatment initiation showed a differential impact on ATXN3 aggregation. The pre-symptomatic treatment led to a striking decrease in ATXN3 aggregation in several areas of the brain, while in the post-symptomatic treatment only tendencies towards a decrease were observed. This suggests that citalopram may act preferentially in the prevention and/or stalling of the aggregation formation process, and less so by disaggregation or degradation of ATXN3 inclusions already formed. Also, our RNA-seq results exploring proteostasis upon citalopram pre-symptomatic treatment in CMVMJD135 mouse model (chapter 3.1) showed that genes encoding proteins involved in protein degradation and conformational maintenance are differentially expressed upon treatment. The activation of these pathways might contribute to prevent aggregate formation along disease progression, making the cell more prone to cope with the upcoming burden. However, when treatment is initiated later and after symptom onset, it might not be sufficient to avoid aggregation formation at the same extent, due to shortcoming of proteostasis resources. It has been shown, for instance, that chaperones and other proteins (as proteasome subunits) can be recruited into the aggregates [32], disturbing the recuperation of misfolded protein and degradation of proteins. Another point that highly influences disease severity and progression is CAG repeat number. In this work, we also generated a CMVMJD135 cohort of mice with increased disease severity by increasing the mean CAG repeat number by 10 (CMVMJD135hi). As described in patients [33], the mean CAG repeat number is directly proportional to symptom severity and disease progression and inversely correlates with the age at onset of symptoms in this mouse model. Indeed, clinical anticipation was observed in this model by four to a maximum of sixteen weeks, as well as a significant aggravation of motor symptomatology. Despite citalopram treatment being started after symptom onset, improvements in locomotor behavior and a delay of the disease progression were observed. This type of study, closer to what happens in a clinical setting, is essential and means that in practice, even in more severe cases, patients would still benefit from citalopram treatment. Overall, the results support a novel use for citalopram in the context of MJD and brings a new perspective into the design of future clinical trials for this disorder.



## **5.2 RNA-sequencing as a tool to explore cellular mechanisms: general and technical considerations**

Finding new therapies is essential, however understanding how they modulate cellular responses is necessary to: (i) better understand the mechanism of disease-associated pathogenicity; (ii) find new possible targets and/or target pathways; and (iii) be able to finetune the therapeutic strategy to make it more directed and to increase efficacy. When the target of the therapeutic approach is known (as in citalopram's case, which is the serotonin (5-HT) transporter (SERT)), it is still essential to understand how the beneficial therapeutic effects are mediated i.e., what is the mode of action. What are the cellular changes triggered by the action on this target? How are the outcomes observed (e.g., improvement in motor behavior and pathology) triggered? Is it a group of downstream cellular effects or a specific one that is being relevant for the drug to be effective in disease context? Being able to answer to these questions is key to better understand the disease itself and to develop a more targeted and holistic therapeutic approach. With citalopram, we know that 5-HT reuptake is blocked and that the levels of this neurotransmitter increase at the synaptic cleft [34]. However, what happens downstream of these events is much less clear, even more in a pathological context such as in MJD. Gene profiling technologies, such as RNA-sequencing (RNA-seq) can be a good tool to provide insight on the cellular state in a specific condition and later associate the changes observed with a behavioral phenotype. In chapters 3.1, 3.2 and 4, we aimed at unraveling the cellular alterations prompted by citalopram in MJD by means of transcriptomic analysis, in two different MJD animal models.

RNA-seq is a relatively recent methodology that allows transcriptome profiling using deep-sequencing approach. It is a multi-step technique, which starts with RNA extraction and ends with bioinformatic analysis of the data generated. Basically, a sample of RNA (total or fractionated) is converted into a library of complementary DNA (cDNA) fragments with an adaptor to one or both ends of the strands. Each strand is then sequenced (with or without amplification) in a high-throughput fashion to obtain shorter sequences from one end or both ends (single and pair-end sequencing, respectively). After the sequencing step, the reads can be aligned to a reference genome or transcripts, or *de novo* assembled without the genomic sequence. Counts of reads are mapped to each gene. A genome-scale transcription map is then generated and consists of both the structure of the transcripts and/or the level of expression. Expression levels of different genes, for transcriptome sequencing, are defined by counting the number of reads mapped to a particular gene, then normalizing the read counts by the length of the gene model and the total number of mapped reads in the sample. After, the results can be analyzed using bioinformatical tools to further infer on the expression changes revealed by the technique [35, 36]. Several

parameters are important to assure that the technique is performed in the best conditions and trustable results are generated.

**RNA quality.** The quality of RNA used is very important for successful cDNA library preparation. Ensuring that RNA of high purity (with no contaminants) and high integrity (since it is easily degraded) is extracted from samples is crucial. RNA quality control is normally assessed with commercially available kits, based on microfluidic capillary electrophoresis, such as Bioanalyzer RNA assay (Agilent Technologies, USA) or Experion™ RNA kit (Bio-Rad, USA). In the RNA-seq analyses presented in chapter 3.1 and 4, RNA control quality was assessed. Although all the precautions in RNA sample extraction were taken, RNA quality from CMVMJD135 mouse samples was sufficient, but not optimal, to follow with RNA-seq experiments. This lower RNA quality might be explained by a less efficient conservation of the samples after tissue collection and/or degradation during tissue processing. To ensure data quality, we are currently validating RNA-seq findings in an independent set of animals for the genes of interest. In comparison, RNA quality from *C. elegans* samples was extremely high. One of the reasons for this, might be due to the immediate conservation of *C. elegans* in TRIzol™ reagent, right after worm collection and until the tissue homogenization step from RNA extraction was performed. This reagent maintains the integrity of the RNA through a high inhibition of RNase activity and helps in the disruption of cell components during the homogenization of the tissue. The nature of the two tissues and the immediate conservation of *C. elegans* in TRIzol™ are the main differences between the RNA extraction protocols performed in *C. elegans* and in mice. Future mice tissue collections for RNA will include tissue preservation in TRIzol™ and the RNA quality tested.

**RNA-seq methodological aspects.** RNA-seq comprises several steps in a complex data processing scheme. Inevitably, questions arise as to the most correct and cost-efficient way of performing this type of experiments. In the RNA-seq performed, strand-specific library preparation kits were used to generate accurate and reliable profiles of expression, allowing to know which strand (sense or antisense) corresponds to the original mRNA. Without this, a biased estimate of transcription can occur [37]. Different strategies were used to prepare libraries: paired-end (enabling sequencing of both ends of a cDNA fragment) was used for mouse RNA-seq, while single-end (only one end is sequenced) was used for *C. elegans* RNA-seq. Paired-end reads facilitate alignment to the reference genome, making it easier to detect genomic rearrangements, repetitive sequence elements, gene fusions and novel transcripts. However, being more expansive, it can impact in the number of samples sequenced. With a lower number of biological replicates, the power of the experiment to find differential expression will decrease. Moreover, it has been shown that increasing sample size is more potent to increase power than sequencing depth

(particularly when it reaches 20 million reads, which is the case in our *C. elegans* RNA-seq experiment) [38]. Although using paired-end reads can be more precise, using single-end reads with additional replicates may be more desirable than using paired-end reads with less replicates [39]. Based on this and in the fact that we had already performed mouse RNA-seq analysis with paired-end reads, we thought that increasing our replicates for the *C. elegans* analysis would be a better option.

**RNA-seq analysis challenges.** In this work, all the data obtained including gene differential expression analysis was acquired by specialized persons in facilities where the experiments were conducted. One limitation in our mouse RNA-seq was that false discovery rate (FDR), a correction for multiple comparison, was not considered for differential gene expression. When FDR was applied, no differentially expressed genes (DEGs) were retrieved in WT *vs* Tg comparison and a substantial decrease in these was observed in the remaining comparisons analyzed. For this reason, we decided to only consider p-value and fold change parameters to obtain DEGs and to add an independent validation of the hits by RT-qPCR. The following enrichment analysis was performed by us and consisted in the biological interpretation of the list of DEGs of a total of several hundred to several thousands of genes. This can be challenging as there are several tools to conduct those analyses [40], but generally, classification schemes such as the Gene Ontology (GO) consortium [41] and Ingenuity Pathway Analysis (IPA) [42] are often used to identify functional categories. The determination that the list of DEGs contains an overrepresentation for one or more biological functions/pathways can certainly help to find mechanisms underlying disease and/or drug-mediated therapeutic effect. Several databases and online tools were tested (for mouse data: *Panther* Classification System [43], ConsensusPath *DB* [44, 45], iRegulon [46], *DAVID* database [40, 47], and Ingenuity Pathway Analysis (IPA) [42]; for *C. elegans* data: g:Profiler [48], WormCat [49] and *WormBase* Enrichment suite [50, 51]) and results obtained were quite similar (data not shown). The Ingenuity Pathway Analysis (IPA) software was chosen to pursue with CVMMJD135 mouse data analysis, since more parameters were analyzed at the same time. With IPA, it was possible to perform at once a canonical pathway analysis, but also to obtain regulator effects, upstream regulators and generate mechanistic networks, among other analyses. However, when we attempted to analyze *C. elegans* data with IPA we noticed that only few genes (not more than 10 %) were mapped and recognized by it. This was probably due to the fact that IPA uses *HomoloGene*, a tool of the National Center for Biotechnology Information (NCBI) [52], for automated detection of homologs and it was not optimal for the *C. elegans* transcriptome. Other tools were used to convert *C. elegans* genes into orthologs, like *Biomart* tool, from *Ensembl* database [53], and *Ortholist 2* compendium of *C. elegans*- human orthologs [54]. Unfortunately, this only increased the mapping of the genes up to 30 %, which we thought to be insufficient and

potentially misleading. Consequently, we searched for *C. elegans* specific tools in the literature and opted to use the *WormBase* Enrichment suite. With this tool, we were able not only to perform a GO enrichment analysis (which recapitulated most of the analyses performed by g:Profiler (except the analysis for DNA regulatory motifs presence) and WormCat, having highly similar results), but also to obtain information about phenotype and tissue specificities which was not possible with the other tools. Still, some genes lack proper annotation, which is an inherent limitation in this kind of analyses. Also, of note, all DEGs were analyzed together and not split in up- or downregulated DEGs in the enrichment analyses performed. Although there is no consensus in the literature on “the most correct” manner to do it, a report suggested that a separate approach should be considered. This would ultimately increase the power of disease-associated pathway detection, leading to the identification of more pertinent pathways to explain phenotypic differences [55]. A separated analysis could be considered to verify if any significant differences are found using this method.

**General limitations.** When performing any kind of cellular measurement, we must be aware of the biological context that will be revealed by the results. For instance, when measuring steady-state levels of mRNA, we are unaware of mRNA stability or turnover rates and those eventually determine protein abundance. Therefore, the sole expression of genes can be a poor or misleading predictor of protein levels [56]. Another aspect to keep in mind is that gene expression is highly tissue specific [57], differing also within the same tissue [58], reflecting the expression of an heterogeneous cell population. In chapters 3.1 and 4, a mouse specific region of the brain (striatum) and a population of whole worms were analyzed by RNA-seq, respectively. Therefore, it is essential to consider the different kind of samples used, when analyzing and contextualizing the results.

**Advances.** Over the last decade, RNA-seq has become a widely used tool for transcriptome analysis. New RNA-seq technologies have been developed and allow to study different parts of RNA biology; from single-cell RNA-seq (scRNAseq), which allows to compare the transcriptome of individual cells, to spatial transcriptomics which has been in development and will allow to study the transcriptome along with its spatial information (reviewed in [59]). So, nowadays, RNA-seq methods provide experimenters with detailed data regarding tissues or specific cells, but without accounting for localization within the tissue, making difficult to relate cellular environment to gene expression. Within our project, the use of those advanced techniques would provide answers to specific questions. For instance, is the transcriptome of cells containing ataxin-3 aggregates different from those cells without aggregates? Or why are cells from one brain region more susceptible to neuronal loss while the adjacent region is spared? Are there transcriptomic differences that could help explain this? Are there differences in specific 5-HT receptors

and 5-HT signaling? These questions could be addressed using recent and in development RNA-seq technology and could bring new perspectives, not only for MJD but for other neurodegenerative disorders.

### **5.3 Serotonergic signaling in MJD: a new perspective**

Despite the greater understanding of the pathological mechanisms underlying polyQ diseases, including MJD, all aspects are not fully elucidated yet and new pieces have been added to this complex puzzle.

The idea that there could be some serotonergic dysfunction in the brain of patients with neurodegenerative disorders can be found in the literature. In Alzheimer's disease (AD), a reduction in 5-HT transporter binding (using PET radiotracers) in nondepressed AD patients was observed, suggesting that 5-HT defects could contribute to disease pathology and not only to emotional state of the patients [60]. In Parkinson's disease (PD), serotonergic transmission was found to be decreased in patients, by means of a 5-HT<sub>1A</sub>R binding decrease using PET radiotracers, correlating with the severity of tremors [61]. In Huntington's disease (HD), *postmortem* analyses found that there is a reduced number of serotonin-containing cells in the dorsal raphe nuclei, indicating that changes in the serotonergic system are also present in this polyQ disorder [62]. Several years ago, the serotonergic hypothesis of cerebellar ataxia was described by Trouillas, already indicating that the serotonergic system could be defective in patients with cerebellar ataxia, presenting low 5-hydroxyindoleacetic acid (5-HIAA) (5-HT metabolite) values, but also increased serotonergic turnover [63]. Alterations in the serotonergic system of patients with ataxia is not entirely surprising, since the serotonergic system modulates an array of diverse behavioral and physiological processes and it is known to be a modulator of motor function [64]. It regulates motor output mediated by central pattern generators that are important for locomotion [65]. Furthermore, serotonergic system projections are widespread across the brain and it is probable that they modulate motor action through simultaneous connections with multiple brain regions involved in motor control, namely the basal ganglia, the cerebellum and the spinal cord [66], which are affected in MJD. Clinical studies indicated behavioral effects of serotonergic modulation in the cerebellar system. In patients with cerebellar ataxia, as above referred, 5-HT metabolites were found to be decreased in the cerebellum and the administration of a 5-HT precursor partially reversed ataxia [63, 67]. While data from CMVMDJ135 symptomatic mice does not point to a 5-HT depletion nor a 5-HT turnover (5-HIAA/5-HT ratio) problem in the brain [12], in MJD symptomatic patients, the 5-HT precursor tryptophan was found to be reduced in serum samples, suggesting that 5-HT synthesis and/or release could somehow be altered [68]. Although these results might seem contradictory, we must acknowledge that tryptophan is

mostly obtained from the diet and that 95 % of the serotonin production happens in the intestine [69]. Therefore, tryptophan levels in patients' serum might not be the best indicator to infer about serotonin state in the brain. Supporting this is the fact that L-type amino acid transporter (that transport tryptophan and other amino acids from the blood across the blood-brain barrier - BBB) has higher affinity for amino acids and higher expression in the BBB than in peripheral tissues [70, 71]. Consequently, the use of methods to quantify 5-HT and its precursors directly in brain is needed to further add on this matter.

Although no alterations in serotonin levels were found in our studies, RNA-seq data points to an alteration in serotonin signaling in MJD (chapter 3.1). Interestingly, a decreased expression of the 5-HT<sub>1A</sub>R was found in the CMVMJD135 transgenic mouse, indicating a possible serotonin transmission dysfunction, that could ultimately be implicated in the motor deficits observed in this model. Theoretically, if this were the case, we could expect that 5-HT<sub>1A</sub>R receptor absence would lead to some motor impairment in WT mice. Curiously, 5-HT<sub>1A</sub>R knockout (KO) mice are generally described as models for anxiety-like phenotype and no gross motor alterations are observed. Still, a (not significant) tendency toward a decrease in cumulative locomotor activity was seen between one 5-HT<sub>1A</sub>R KO mouse model and its genotype-matched WT mice, suggestive of a possible contribution of this receptor to motor-related functions [72]. This could account for the hypothesis that 5-HT<sub>1A</sub>R is central for locomotor behavior in MJD, although no anxiety-like phenotype was observed in our CMVMJD135 mouse model (Correia, J. S. *et al.*, *in preparation*), anxiety also being difficult to assess due to motor dependency of the tests. At this point, we cannot exclude the fact that 5-HT<sub>1A</sub>R absence or decreased-mediated signaling could be compensated by other 5-HT receptors or mechanisms. Additionally, when the expression of this receptor was verified by RT-qPCR in *post-mortem* brain tissues of MJD patients, a tendency towards a decreased expression relative to control was observed in the striatum, but also in the cerebellum, important areas for motor behavior. From our knowledge, this is the first description of a decreased 5-HT<sub>1A</sub>R expression in the context of MJD and could account for a potential central role of this receptor in the disease. The decreased expression could alter 5-HT<sub>1A</sub>R-dependent activity and/or signaling in the brain. Supporting this is the observation that MJD patients are prone to manifest 5-HT<sub>1A</sub>R-associated symptoms, such as ataxia, insomnia, anorexia, depression, and pain, and that the use of agonists of this receptor has proven to be beneficial in clinical trials [73-75]. Therefore, 5-HT signaling seems to be altered in MJD and based on our findings, alterations in specific receptors, namely 5-HT<sub>1A</sub>R, could have a significant role in the disease. More studies are needed to further verify this hypothesis.

#### **5.4 Serotonergic signaling modulation by citalopram in MJD: mode of action**

Selective serotonin reuptake inhibitors (SSRIs) are a class of serotonergic modulators compounds widely used to treat psychiatric conditions, such as depression, panic disorders, obsessive-compulsive disorder, eating disorders, among others. They act by blocking 5-HT reuptake thus potentiating 5-HT signaling. Current research, including our work, suggests that the therapeutic potential of these compounds may go beyond psychiatric conditions and impact on conformational disorders, having a neuroprotective effect. Still, due to the often depressed state of patients with neurodegenerative conditions, one might argue that the beneficial effect of serotonergic acting compounds on neurodegenerative diseases might be secondary to the antidepressant effect and that motor ameliorations were a result of that. However, while studies show that antidepressant symptoms were ameliorated in MJD patients in response to those compounds, this effect was reported to happen posteriorly to the alleviation of ataxia symptoms, which happened 2 weeks before [75]. Additionally, despite depressive symptoms being quite common in MJD patients, depression seems to be of a reactive nature and not primarily related to the disease process itself. Depression correlated with age and physical incapacitation in the MJD carriers, while spouses had abnormally high depressive score compared to healthy individuals, furthermore, individuals at 50 % risk for MJD did not show any sign of a depressive state. Moreover, in order to test if the common prejudice is true, the same study also showed that in comparison to a multiple sclerosis (MS) group far less incapacitated than the MJD one, MS patients presented higher depressive scores, suggesting a different pattern of associated risk factors and different nature of depressive symptoms [76].

Already, preclinical trials have evidenced that the modulation of the serotonergic system with SSRIs could be beneficial in neurodegenerative disorders. In AD, fluoxetine has been shown to attenuate impairment of spatial learning ability and prevent neurodegeneration in double transgenic AD mice. Moreover, this was accompanied by a decrease in amyloid- $\beta$  deposition [77]. Citalopram was also reported to be effective in restoring short-term memory deficits, halting disease progression and inhibiting amyloid- $\beta$  deposition in a APP/PS1 AD mouse model [78]. The same compound was described to decrease amyloid- $\beta$  deposition in humans [18, 79]. In PD, it was also demonstrated that fluoxetine is able to prevent neurodegeneration, partially recovering motor function in a MPTP mouse model [80]. In polyQ disorders, such as Huntington's disease (HD), SSRIs have also been reported to ameliorate disease-associated features. For instance, paroxetine administration to HD mutant mice increased survival, attenuated motor dysfunction, improved energy metabolism and delayed disease onset [81]. Another, SSRI, sertraline, was found to attenuate behavioral abnormalities, increase survival, upregulate

brain derived neurotrophic factor (BDNF) levels, as well as to preserve chaperone protein HSP70 and BCL-2 levels, and increase neurogenesis in the brain. However, no impact on huntingtin inclusions was observed [82]. Previous work in our lab was pioneer in showing the potential of SSRI for MJD treatment, in a preclinical stage. We demonstrated that citalopram chronic treatment of the CMVMJD135 MJD mouse model was able to ameliorate motor symptoms and to reduce ATXN3 inclusions [12]. These results suggested that the modulation of the serotonergic signaling in MJD, as others had observed in other neurodegenerative disorders, could be a good therapeutic option. How citalopram mediates its effects in MJD is not well understood and was one of the points we attempted to clarify in this thesis.

The RNA-seq technique allowed us to further explore citalopram-mediated effects in the context of MJD. After the finding that 5-HT<sub>1A</sub>R was decreased in transgenic mice, we observed that expression levels of this receptor were restored to WT levels upon citalopram treatment. Additionally, 5-HT<sub>2A</sub>R expression was also altered (decreased) upon treatment, being the only other 5-HT receptor differentially expressed when comparing transgenic-vehicle and transgenic-treated animals. Therefore, specific modulation of these receptors could contribute to the offset of the pathological effects that we observed upon treatment. For instance, the differential impact observed on ATXN3 aggregation upon citalopram treatment in different brain regions observed in the CMVMJD135 ([12], chapter 2) and YACMJD84.2 [27] mouse models, might indicate a distinct expression and/or activation of 5-HT receptors. Interestingly, the brain regions of the brainstem analyzed in both models show a decrease in ATXN3 aggregation under citalopram treatment (e.g., pontine nuclei (PN), facial motor nuclei (7N), substantia nigra (SN), reticulotegmental nucleus of the pons (RtTg), vestibular nuclei (VN)), while no alterations or tendencies toward a decrease were observed in the cerebellum (deep cerebellar nuclei - DCN). From the transcriptomic analysis performed in the striatum of CMVMJD135 mice, alterations in the expression of the 5-HT<sub>1A</sub> and 5-HT<sub>2A</sub> receptors upon treatment were observed. Interestingly, those receptors are mostly expressed in limbic and brainstem regions and barely detectable in the cerebellum [83-86]. However, more recently, 5-HT<sub>1A</sub>Rs were found in calbindin-containing neurons, which includes the Purkinje cells in the cerebellum [86]. Moreover, some brainstem nuclei (as the facial nuclei) are enriched in 5-HT<sub>2A</sub>R [86]. This suggests not only a link between the expression of 5-HT receptors and citalopram's effect on ATXN3 aggregation, but that the presence of these two receptors maybe necessary to decrease aggregation in a certain brain region. Accordingly, previous *C. elegans* studies implicated homologs of the 5-HT<sub>1</sub> and 5-HT<sub>2</sub> receptor families in citalopram response [12]. In our previous work, we showed that ablation of *ser-1* (ortholog of human receptors from the 5-HT<sub>2</sub> family) compromised the beneficial action of citalopram. Also, ablation of *ser-4*, the 5-HT<sub>1A</sub>R *C. elegans* homolog, rescued motor neuron dysfunction and reduced



ATXN3 aggregation of MJD worms, in line with its role as an autoreceptor, which by negative feedback regulates 5-HT levels. Of note, neither *ser-4* nor *ser-1* were found to be differentially expressed in the worm transcriptomic data analyzed. However, preliminary results showed that the expression of *ser-4*, measured by RT-qPCR, in the *mod-5*; Q130 strain was no different from WT or Q130 animals; and, interestingly, mRNA expression levels of *ser-1* were found to be decreased in the *mod-5*; Q130 strain in comparison to mutant ATXN3 animals (Pereira-Sousa *et al.*, *unpublished results*). This is in accordance with the decreased mRNA expression of this receptor ortholog (5-HT<sub>2A</sub>) in the mouse RNA-seq analysis, upon citalopram treatment.

The alteration in 5-HT<sub>1A</sub>R and 5-HT<sub>2A</sub>R expression upon citalopram treatment in MJD mice reveals that serotonergic signaling modulation could possibly remodel 5-HT receptors' expression, certainly also altering their activity and downstream-associated pathways. As the mouse RNA-seq analysis was performed in the striatum, the effects observed on 5-HT<sub>1A</sub>R are consistent with a postsynaptic heteroreceptor role, since those are present in non-5-HT neurons, in 5-HT projecting areas. Elements of the 5-HT<sub>1A</sub>R-regulated signal transduction pathways were also found altered upon treatment, corresponding to players of the cyclic adenosine 3',5'-monophosphate (cAMP), the mitogen-activated protein kinases (MAPK)/extracellular-signal activated kinase (ERK), and the phosphoinositide 3-kinase (PI3K)-PKB/AKT pathways. Moreover, a common effector of these three main 5-HT<sub>1A</sub>R downstream pathways is the CREB transcription factor. This is one strong candidate to mediate the effects of citalopram, since neuroprotection has been associated to it [87], and several lines of investigation showed that CREB activity is altered by chronic antidepressant treatments [88, 89]. CREB target genes were also found to be altered in our transcriptomic data (both resulting from citalopram-treated MJD mice and *mod-5* ablation in *C. elegans*) although confirmation of its activation is needed, by verifying its phosphorylation levels in the striatum, but also in other affected brain areas in MJD. This is in accordance with a transcriptional profiling realized in a different MJD mouse model (YACMJD84.2), which revealed that the CREB pathway is among the most consistently altered in a combined analysis of four brain regions (brainstem, cerebellum, striatum, and cortex) [90]. The authors found that the higher number of differentially expressed genes were detected in the brainstem and the striatum and surprisingly to a lesser extent in the cerebellum. When analyzing these brain regions individually, axon guidance and synaptic transmission pathways were most significantly altered in the striatum and strongest changes were found in the PI3K cascade and cholesterol biosynthesis pathways in the brainstem. Interestingly, all those changes occurred before the onset of motor and coordination deficits in this model [90]. Thus, citalopram treatment could potentially act on that particular pathway and positively modify cellular signaling through

it. Additionally, agonism of 5-HT<sub>1A</sub> and antagonism of 5-HT<sub>2A</sub> receptors, conducted by aripiprazole, an atypical antipsychotic, was found to modulate ATXN3 abundance in animal models of the disease [91]. A downregulation of 5-HT<sub>2A</sub>R was also found in our RNA-seq data, only upon citalopram treatment. Therefore, it might be likely that citalopram exerts its beneficial effect also through other 5-HT receptors. Studies conducted within our research group showed that chronic and acute administration of a specific 5-HT<sub>1A</sub>R agonist - befiradol or NLX-112 - rescued motor function and suppressed mutant ATXN3 aggregation in the Q130 *C. elegans* model. The action of this drug was dependent on 5-HT<sub>1A</sub>/SER-4 receptor [92]. At this moment, preclinical experiments are being conducted with befiradol using the CMVMJD135 mouse model with positive impact on animals' motor behavior, to further assess the therapeutic potential of this 5-HT<sub>1A</sub>R agonist in MJD.

Summing up, at this point, our working hypothesis is that citalopram, upon chronic treatment, enhances serotonergic signaling by inhibition of 5-HT recapture, altering the expression of specific 5-HT receptors in specific brain regions, restoring 5-HT<sub>1A</sub>R levels and decreasing 5-HT<sub>2A</sub>R expression. This would determine possible changes in signal transduction pathways regulated by these receptors (which need to be further elucidated), ultimately enabling the motor and pathological improvements observed in MJD animal models (Figure 5.1).

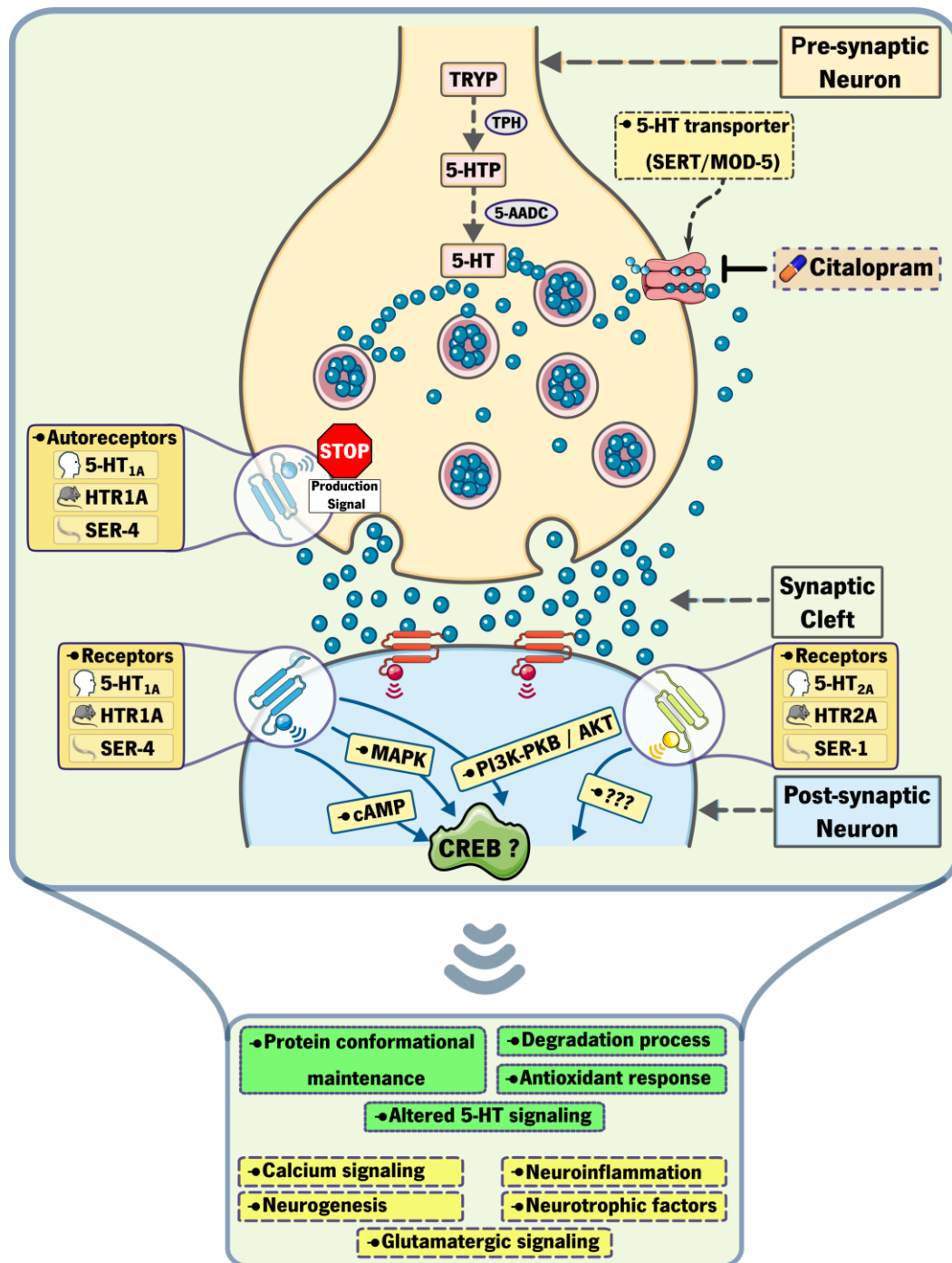


**Figure 5.1 Model for serotonergic-signaling modulation by citalopram in MJD models.** Citalopram enhances serotonin (5-HT) signaling by inhibition of serotonin recapture through the serotonin transporter SERT (SLC6A4 or MOD-5 in invertebrates). Upon chronic citalopram treatment of CMVMJD135 mice, 5-HT<sub>1A</sub> autoreceptors become desensitized, inactivating the negative feedback (STOP production signal) in presynaptic neurons, contributing to the increase in 5-HT availability at the synaptic cleft. An increase in 5-HT<sub>1A</sub>R (heteroreceptors) and a decrease in 5-HT<sub>2A</sub>R expression levels is observed and a subsequent alteration in signaling pathways associated with these receptors is likely. Changes in cyclic adenosine 3',5'-monophosphate (cAMP), the mitogen-activated protein kinases (MAPK)/extracellular-signal activated kinase (ERK), and the phosphoinositide 3-kinase (PI3K)-PKB/AKT signaling, in response to 5-HT<sub>1A</sub>R, might result in cAMP response

element-binding protein (CREB) transcription factor activation and ultimately lead to the cellular mechanisms' changes observed in MJD. Alterations in 5-HT<sub>2A</sub>R-dependent signaling might also contribute to the beneficial effects observed in MJD animal models upon citalopram treatment. In green upper boxes represented are responses found to be altered upon citalopram treatment in transcriptomic data related to proteostasis. In yellow are other possible mechanisms being reverted in MJD by SSRI action. TRYP - tryptophan; TPH - tryptophan 5-hydroxylase; 5-HTP - 5-hydroxy-L-tryptophan; 5-AADC - aromatic L-amino acid decarboxylase.

#### **5.4.1 Serotonergic signaling modulation by citalopram in MJD: protein homeostasis and neuroprotection**

The lack of impact of the post-symptomatic treatment on ataxin-3 aggregation contrasts with the drastic decrease in ATXN3 aggregation observed upon pre-symptomatic treatment. No alterations in ATXN3 protein levels were detected in the CMVMJD135 mouse model, both in pre- and post-symptomatic treatment, indicating that citalopram might not be primarily promoting the degradation of the mutant protein, but rather impacting on protein folding/aggregation. In contrast, citalopram treatment of the YACMJD84.2 mouse model showed a reduction in all soluble forms of ATXN3 and even a tendency toward reduction of insoluble forms in the brainstem and cervical spinal cord [27]. This could be model specific, since the YAC model carries the full-length *MJD1* gene with a polyQ tract expansion and all the enhancers and long-range regulatory elements thought to be necessary for cell-specific expression of this gene at physiological levels [93]. On the other hand, the CMVMJD135 model expresses expanded human ATXN3 under the control of the CMV promoter, which drives a strong general and constitutive expression of genes under its control [7]. The different regulatory regions driving *ATXN3* expression might explain a differential impact of citalopram treatment on ATXN3 levels in these two models.

The timing of citalopram treatment initiation (pre- or post-symptomatic) in CMVMJD135 mice also appears to have a differential impact on aggregation, suggesting that this SSRI may modulate specific protein quality control (PQC) responses, preferentially related to the prevention of aggregation formation. Interestingly, citalopram pre-symptomatic treatment in the YACMJDQ84.2 mice, besides inducing a reduction in ATXN3 aggregation, restored Hsp90 $\beta$  levels (a proteostasis component) in mouse brains [93]. Indeed, in the present work, alterations in the expression of chaperones were also observed in mice and, in the *C. elegans* results, a response to topologically incorrect proteins was found. Nevertheless, the transcriptomic analyses performed (which both represent a pre-symptomatic intervention) revealed that a high percentage of the genes differentially expressed belong, not only to the folding/conformational maintenance branch, but mostly to the degradation branches of the PQC network, in both mouse and *C. elegans* MJD models (chapters 3.2 and 4). Interestingly, in the transcriptomic data from *C. elegans*,

serotonin transporter *mod-5* ablation in our MJD model, mimicking the mode of action of citalopram, drastically shifted the transcriptomic profile of ATXN3 mutant worms. This shift, that enhances serotonergic signaling, triggered protective responses in ATXN3 mutant animals, which comprised responses to biotic stimuli, the lytic vacuole and autophagy, as part of the degradation process. Of note, as it happens in our MJD mouse model, ATXN3 expression in our *C. elegans* ATXN3 mutant animals is under the control of the *rgef-1* promoter that encodes for the *C. elegans* ortholog of the Ca<sup>2+</sup>-regulated Ras nucleotide exchange factor (RasGRP), widely expressed in the nervous system. This different control of *ATXN3* expression might justify the lack of changes in ATXN3 protein levels in mutant ATXN3 worms upon citalopram treatment [12]. Therefore, and although no alteration on ATXN3 protein levels are found, citalopram probably also mediated its effect through the modulation of the degradation processes of other proteins/cellular components, such as through autophagy, as already reported for citalopram in a neuronal context [94].

In invertebrates, it has been shown that polyQ-containing proteins bind to mitochondria in neurons, eliciting the unfolded protein response of the mitochondria (UPR<sup>mit</sup>) in the intestine of *C. elegans*, serotonin release being required for this signaling to occur [95]. In line with this, similar responses have been detected in our transcriptomic mouse data, including the UPR and the heat shock response (HSR), although not as expressive as the antioxidant response, which is known to be decreased in MJD patients [96]. When we compare the transcriptional analyses conducted in mice and worms, in terms of proteostasis, quite similar responses are found. The *C. elegans* transcriptomic data further points to the modulation of UPR and antioxidant responses. Consistently, citalopram was described to reduce oxidative stress in patients with major depression, normalizing levels of lipid peroxidation, superoxide dismutase, and ascorbic acid in the serum of these patients [97], strongly suggesting that the modulation of antioxidant defenses may be one of the mechanism underlying neuroprotective effects of citalopram in MJD. In support of this idea, we found alterations in players of the antioxidant response among the DEGs in mouse RNA-seq data, such as increased expression of superoxide dismutase (SOD3) and glutathione peroxidase (GPX3), this last one also increased after treatment among *C. elegans* RNA-seq DEGs. Data from MJD patients also strengthen this view, since levels of glutathione peroxidase were found to be decreased in symptomatic patients and were associated with disease severity, being proposed as a potential biomarker for the disease [96].

Citalopram neuroprotection in MJD could also involve other mechanisms, besides aggregation and proteostasis, that were not extensively addressed in the present thesis work (Figure 5.1). From the neuropathological analysis, a restoration of the cholinergic and calbindin positive neurons was observed

upon citalopram treatment. The astrogliosis observed in CMVMJD135 mice was also mitigated upon treatment. This is indicative that the modulation of serotonin signaling by citalopram could be impacting on the cholinergic system, although citalopram is the most specific of the SSRIs, having low affinity for cholinergic and other neurotransmitter receptors [98]. It seems more likely that citalopram is generally attenuating neuronal loss and or maybe promoting neurogenesis, as it has been observed, for instance, in the hippocampus [99]. Although still a matter of debate, neurogenesis has been described in other brain regions than the classically described loci - hippocampus and subventricular zone. In fact, novel neurogenic zones have been pointed such as the cortex, hypothalamus, amygdala, striatum and substantia nigra, these last two being affected in MJD (reviewed in [100]). Thus, a role for citalopram in promoting neurogenesis in these affected regions could be suggested, but studies need to be performed to assess this hypothesis. Another mechanism involves the decreased calbindin staining in the Purkinje cells of the CMVMJD135 mice and recovery upon SSRI treatment, that could be indicative of a disturbed calcium signaling ultimately leading to cerebellum dysfunction and ataxia. Lastly, citalopram could be modifying the inflammatory profile of the brain and besides astrogliosis, changes in inflammatory cytokines and microglia activity could be altered upon treatment.

Overall, chronic antidepressant treatment seems to be crucial for neuroprotection to happen at its fullest in MJD. This enables serotonergic signaling to be modulated (possibly through specific 5-HT receptors-dependent signaling pathways) and a set of general cellular defense responses to be triggered (as hypothesized in Figure 5.1), increasing the organism's capacity to cope with polyQ expansion-derived complications.

#### Main conclusions gathered throughout this work

- Post-symptomatic chronic administration of citalopram in CMVMJD135 mice was still effective in improving motor dysfunction and retained some neuroprotective effect.
- Serotonergic signaling was altered in MJD mice and patients, that display decreased levels of 5-HT<sub>1A</sub>R; these levels were restored in mice by citalopram pre-symptomatic administration.
- The effects of citalopram could be mediated through 5-HT<sub>1A</sub>R (and perhaps 5-HT<sub>2A</sub>R) and downstream transduction pathways, possibly involving the CREB transcription factor.
- In MJD models, serotonergic signaling modulation by citalopram triggered a protective response, namely by altering the expression of genes belonging to the PQC machinery (protein conformational maintenance, degradation processes and the antioxidant response).

Undoubtedly, some results from this hypothesis-generating work need further validation, which is ongoing, but also represent the starting point to unveil the mode of action of citalopram in MJD. In the process, uncovered and to be uncovered differences in the serotonergic system of MJD carriers might be more relevant than initially thought.

### **5.5 Serotonin signaling modulation in MJD: future perspectives**

At the molecular level, by studying the modulation of the serotonergic signaling by inhibition of 5-HT recapture, we found that 5-HT<sub>1A</sub>R could have a preponderant role, not only for citalopram action, but in the disease itself. To our knowledge no specific studies have been conducted to characterize the serotonergic system in MJD. Autoradiography experiments, using a specific set of 5-HT<sub>1A</sub>R radioligands, are being performed to understand if a general difference in the quantity and distribution of functionally active 5-HT<sub>1A</sub>R exists across the CMVMJD135 mouse brain, compared to control. For that, two specific radioligands are being used: [<sup>18</sup>F]MPPF, which is a 5-HT<sub>1A</sub>R antagonist, thought to bind to the receptor, independently of the functional state (i.e., active state, believed to mediate receptor activation (functional receptor/G protein coupling); and inactive state (non-functional/G protein uncoupled); and [<sup>18</sup>F]F15599 a 5-HT<sub>1A</sub>R agonist which binds selectively to functional receptors [101, 102]. In this line, using PET radioligands to study 5-HT<sub>1A</sub>R in several human brain areas would also be interesting, to further infer on a possible central role for this receptor in MJD. Following this, understanding which 5-HT<sub>1A</sub>R transduction pathways are important for the phenotypic ameliorations and principally, to further confirm if CREB transcription factor is indispensable for citalopram treatment to be effective in offsetting MJD phenotype, is necessary. In the MJD *C. elegans* model, citalopram seemed to be dependent on CREB to be effective. Verifying CREB activation (phosphorylation state), upon treatment, through Western blot analysis in MJD mice brain will help to confirm this aspect. Also, as the findings exposed in this work result mainly from citalopram chronic exposure (29 weeks), to determine if similar molecular changes in serotonergic signaling and proteostasis are triggered with a shorter treatment would be useful to better understand at which extent could this therapeutic approach be beneficial. Recently, experiments in CMVMJD135 mice were conducted to compare pathological and molecular changes associated to a smaller duration chronic treatment (4 weeks) in symptomatic animals (beginning treatment at 30-weeks of age). Our preliminary results from motor performance analysis in this cohort of mice show improvements in motor coordination after 2 weeks of treatment (Oliveira, S. *et al*, *in preparation*). Several additional parameters will be soon analyzed, regarding aggregation, neuronal loss, 5-HT receptor expression, CREB activation, as well as evaluation of the activation of PQC-related responses. This would give us further clues on which of the

effects of citalopram are essential to allow MJD burden alleviation, since the first adaptations triggered by the treatment might differ from those observed after a long-time exposure.

The fact that citalopram (pre- and post-symptomatic) administration led to good results in preclinical trials and in different MJD mouse models, make it a strong candidate to be tested in human clinical trials. If successful, it could be used as a preventive measure (since genetic testing is available) or as a symptomatic treatment after disease diagnosis and symptom installation. Of course, there is a still relatively long way to go before this could happen. Setting up a clinical trial in a rare disease has intrinsic difficulties, such as to find a significant number of participants willing to take part in such a journey. Moreover, the more studied is the compound in the context to be tested, the greater are the chances of it to be successfully translated into clinics. In that way, building up on the results exposed in this thesis work is crucial to reach that ultimate stage.

As evidenced in this work, SSRI action in the brain is multiple, and several dysfunctional aspects reported in MJD seem to be eased by this treatment. To further invest in deciphering the mechanisms associated to citalopram-mediated improvements in MJD phenotypes would augment the actual understanding of the disease and, more importantly, could pave the way for the scientific and medical community to finally have a disease-modifying therapy to offer for this disorder.



## References

1. Gammon, K., Neurodegenerative disease: Brain windfall. *Nature*, 2014. **515**(7526): p. 299-300.<https://doi.org/10.1038/nj7526-299a>.
2. Muslimović, D., Post, B., Speelman, J.D., Schmand, B., *et al.*, Determinants of disability and quality of life in mild to moderate Parkinson disease. *Neurology*, 2008. **70**(23): p. 2241-2247.<https://doi.org/10.1212/01.wnl.0000313835.33830.80>.
3. Verghese, J., LeValley, A., Hall, C.B., Katz, M.J., *et al.*, Epidemiology of Gait Disorders in Community-Residing Older Adults. *Journal of the American Geriatrics Society*, 2006. **54**(2): p. 255-261.<https://doi.org/10.1111/j.1532-5415.2005.00580.x>.
4. D'Abreu, A., França, M.C., Paulson, H.L., and Lopes-Cendes, I., Caring for Machado–Joseph disease: Current understanding and how to help patients. *Parkinsonism & Related Disorders*, 2010. **16**(1): p. 2-7.<https://doi.org/10.1016/j.parkreldis.2009.08.012>.
5. Nóbrega, C., Simões, A.T., Duarte-Neves, J., Duarte, S., *et al.*, Molecular Mechanisms and Cellular Pathways Implicated in Machado-Joseph Disease Pathogenesis, in *Advances in Experimental Medicine and Biology* C. Nóbrega and L. Pereira de Almeida, Editors. 2018, Springer, Cham. p. 349-367.[https://doi.org/10.1007/978-3-319-71779-1\\_18](https://doi.org/10.1007/978-3-319-71779-1_18).
6. Chadman, K.K., Yang, M., and Crawley, J.N., Criteria for validating mouse models of psychiatric diseases. *American Journal of Human genetics*, 2009. **150B**(1): p. 1-11.<https://doi.org/10.1002/ajmg.b.30777>.
7. Silva-Fernandes, A., Duarte-Silva, S., Neves-Carvalho, A., Amorim, M., *et al.*, Chronic Treatment with 17-DMAG Improves Balance and Coordination in A New Mouse Model of Machado-Joseph Disease. *Neurotherapeutics*, 2014. **11**(2): p. 433-449.<https://doi.org/10.1007/s13311-013-0255-9>.
8. Saute, J.A.M., de Castilhos, R.M., Monte, T.L., Schumacher-Schuh, A.F., *et al.*, A randomized, phase 2 clinical trial of lithium carbonate in Machado-Joseph disease. *Movement Disorders*, 2014. **29**(4): p. 568-573.<https://doi.org/10.1002/mds.25803>.
9. Lei, L.-F., Yang, G.-P., Wang, J.-L., Chuang, D.-M., *et al.*, Safety and efficacy of valproic acid treatment in SCA3/MJD patients. *Parkinsonism & Related Disorders*, 2016. **26**: p. 55-61.<https://doi.org/10.1016/j.parkreldis.2016.03.005>.
10. Duarte-Silva, S., Neves-Carvalho, A., Soares-Cunha, C., Teixeira-Castro, A., *et al.*, Lithium Chloride Therapy Fails to Improve Motor Function in a Transgenic Mouse Model of Machado-Joseph Disease. *The Cerebellum*, 2014. **13**(6): p. 713-727.<https://doi.org/10.1007/s12311-014-0589-9>.
11. Esteves, S., Duarte-Silva, S., Naia, L., Neves-Carvalho, A., *et al.*, Limited Effect of Chronic Valproic Acid Treatment in a Mouse Model of Machado-Joseph Disease. *PLOS ONE*, 2015. **10**(10): p. e0141610.<https://doi.org/10.1371/journal.pone.0141610>.

12. Teixeira-Castro, A., Jalles, A., Esteves, S., Kang, S., *et al.*, Serotonergic signalling suppresses ataxin 3 aggregation and neurotoxicity in animal models of Machado-Joseph disease. *Brain*, 2015. **138**(11): p. 3221-3237.<https://doi.org/10.1093/brain/awv262>.
13. Duarte-Silva, S., Silva-Fernandes, A., Neves-Carvalho, A., Soares-Cunha, C., *et al.*, Combined therapy with m-TOR-dependent and -independent autophagy inducers causes neurotoxicity in a mouse model of Machado–Joseph disease. *Neuroscience*, 2016. **313**: p. 162-173.<https://doi.org/10.1016/j.neuroscience.2015.11.030>.
14. Duarte-Silva, S., Neves-Carvalho, A., Soares-Cunha, C., Silva, J.M., *et al.*, Neuroprotective Effects of Creatine in the CMVMJD135 Mouse Model of Spinocerebellar Ataxia Type 3. *Movement Disorders*, 2018. **33**(5): p. 815-826.<https://doi.org/10.1002/mds.27292>.
15. Russell, W.M.S. and Burch, R.L., The principles of humane experimental technique. 1959, London, UK.: Methuen.<https://caat.ihsp.edu/principles/the-principles-of-humane-experimental-technique>.
16. Balls, M., It's Time to Reconsider The Principles of Humane Experimental Technique. *Alternatives to Laboratory Animals*, 2020. **48**(1): p. 40-46.<https://doi.org/10.1177/0261192920911339>.
17. Reagan-Shaw, S., Nihal, M., and Ahmad, N., Dose translation from animal to human studies revisited. *The FASEB Journal*, 2008. **22**(3): p. 659-661.<https://doi.org/10.1096/fj.07-9574LSF>.
18. Cirrito, J.R., Disabato, B.M., Restivo, J.L., Verges, D.K., *et al.*, Serotonin signaling is associated with lower amyloid- $\beta$  levels and plaques in transgenic mice and humans. *Proceedings of the National Academy of Sciences*, 2011. **108**(36): p. 14968-14973.<https://doi.org/10.1073/pnas.1107411108>.
19. McCarrell, J.L., Bailey, T.A., Duncan, N.A., Covington, L.P., *et al.*, A review of citalopram dose restrictions in the treatment of neuropsychiatric disorders in older adults. *Mental Health Clinician*, 2019. **9**(4): p. 280-286.<https://doi.org/10.9740/mhc.2019.07.280>
20. Blanchard, O.L. and Smoliga, J.M., Translating dosages from animal models to human clinical trials—revisiting body surface area scaling. *The FASEB Journal*, 2015. **29**(5): p. 1629-1634.<https://doi.org/10.1096/fj.14-269043>.
21. Kilkenny, C., Browne, W.J., Cuthill, I.C., Emerson, M., *et al.*, Improving Bioscience Research Reporting: The ARRIVE Guidelines for Reporting Animal Research. *PLOS Biology*, 2010. **8**(6): p. e1000412.<https://doi.org/10.1371/journal.pbio.1000412>.
22. Percie du Sert, N., Hurst, V., Ahluwalia, A., Alam, S., *et al.*, The ARRIVE guidelines 2.0: Updated guidelines for reporting animal research. *PLOS Biology*, 2020. **18**(7): p. e3000410.<https://doi.org/10.1371/journal.pbio.3000410>.
23. Mlinarić, A., Horvat, M., and Šupak Smolčić, V., Dealing with the positive publication bias: Why you should really publish your negative results. *Biochemia Medica*, 2017. **27**(3): p. 030201-030201.<https://doi.org/10.11613/BM.2017.030201>.

24. Gao, R., Liu, Y., Silva-Fernandes, A., Fang, X., *et al.*, Inactivation of PNKP by Mutant ATXN3 Triggers Apoptosis by Activating the DNA Damage-Response Pathway in SCA3. *PLOS Genetics*, 2015. **11**(1): p. e1004834.<https://doi.org/10.1371/journal.pgen.1004834>.
25. Rodríguez-Cueto, C., Hernández-Gálvez, M., Hillard, C.J., Maciel, P., *et al.*, Altered striatal endocannabinoid signaling in a transgenic mouse model of spinocerebellar ataxia type-3. *PLOS ONE*, 2017. **12**(4): p. e0176521.<https://doi.org/10.1371/journal.pone.0176521>.
26. Costa, M.d.C., Radzwion, M., McLoughlin, H.S., Ashraf, N.S., *et al.*, *In Vivo* Molecular Signatures of Cerebellar Pathology in Spinocerebellar Ataxia Type 3. *Movement Disorders*, 2020. **35**(10): p. 1774-1786.<https://doi.org/10.1002/mds.28140>.
27. Ashraf, N.S., Duarte-Silva, S., Shaw, E.D., Maciel, P., *et al.*, Citalopram Reduces Aggregation of ATXN3 in a YAC Transgenic Mouse Model of Machado-Joseph Disease. *Molecular Neurobiology*, 2019. **56**(5): p. 3690-3701.<https://doi.org/10.1007/s12035-018-1331-2>.
28. Nascimento-Ferreira, I., Nóbrega, C., Vasconcelos-Ferreira, A., Onofre, I., *et al.*, Beclin 1 mitigates motor and neuropathological deficits in genetic mouse models of Machado–Joseph disease. *Brain*, 2013. **136**(7): p. 2173-2188.<https://doi.org/10.1093/brain/awt144>.
29. Sugai, F., Yamamoto, Y., Miyaguchi, K., Zhou, Z., *et al.*, Benefit of valproic acid in suppressing disease progression of ALS model mice. *European Journal of Neuroscience*, 2004. **20**(11): p. 3179-3183.<https://doi.org/10.1111/j.1460-9568.2004.03765.x>.
30. Kalmar, B., Novoselov, S., Gray, A., Cheetham, M.E., *et al.*, Late stage treatment with arimoclomol delays disease progression and prevents protein aggregation in the SOD1<sup>G93A</sup> mouse model of ALS. *Journal of Neurochemistry*, 2008. **107**(2): p. 339-350.<https://doi.org/10.1111/j.1471-4159.2008.05595.x>.
31. Chang, Y.-C., Lin, C.-W., Hsu, C.-M., Lee-Chen, G.-J., *et al.*, Targeting the prodromal stage of spinocerebellar ataxia type 17 mice: G-CSF in the prevention of motor deficits via upregulating chaperone and autophagy levels. *Brain Research*, 2016. **1639**: p. 132-148.<https://doi.org/10.1016/j.brainres.2016.03.004>.
32. Schmidt, T., Lindenberg, K.S., Krebs, A., Schöls, L., *et al.*, Protein surveillance machinery in brains with spinocerebellar ataxia type 3: Redistribution and differential recruitment of 26S proteasome subunits and chaperones to neuronal intranuclear inclusions. *Annals of Neurology*, 2002. **51**(3): p. 302-310.<https://doi.org/10.1002/ana.10101>.
33. Maciel, P., Gaspar, C., DeStefano, A.L., Silveira, I., *et al.*, Correlation between CAG repeat length and clinical features in Machado-Joseph disease. *American Journal of Human Genetics*, 1995. **57**(1): p. 54-61.<https://www.ncbi.nlm.nih.gov/pmc/articles/PMC1801255/>.
34. Nutt, D.J., Forshall, S., Bell, C., Rich, A., *et al.*, Mechanisms of action of selective serotonin reuptake inhibitors in the treatment of psychiatric disorders. *European Neuropsychopharmacology*, 1999. **9**: p. S81-S86.[https://doi.org/10.1016/S0924-977X\(99\)00030-9](https://doi.org/10.1016/S0924-977X(99)00030-9).
35. Wang, Z., Gerstein, M., and Snyder, M., RNA-Seq: a revolutionary tool for transcriptomics. *Nature Reviews Genetics*, 2009. **10**(1): p. 57-63.<https://doi.org/10.1038/nrg2484>.

36. Li, B., Ruotti, V., Stewart, R.M., Thomson, J.A., *et al.*, RNA-Seq gene expression estimation with read mapping uncertainty. *Bioinformatics*, 2009. **26**(4): p. 493-500.<https://doi.org/10.1093/bioinformatics/btp692>.
37. Zhao, S., Zhang, Y., Gordon, W., Quan, J., *et al.*, Comparison of stranded and non-stranded RNA-seq transcriptome profiling and investigation of gene overlap. *BMC Genomics*, 2015. **16**(1): p. 675.<https://doi.org/10.1186/s12864-015-1876-7>.
38. Ching, T., Huang, S., and Garmire, L.X., Power analysis and sample size estimation for RNA-Seq differential expression. *RNA*, 2014. **20**(11): p. 1684-1696.<https://doi.org/10.1261/rna.046011.114>.
39. Corley, S.M., MacKenzie, K.L., Beverdam, A., Roddam, L.F., *et al.*, Differentially expressed genes from RNA-Seq and functional enrichment results are affected by the choice of single-end versus paired-end reads and stranded versus non-stranded protocols. *BMC Genomics*, 2017. **18**(1): p. 399.<https://doi.org/10.1186/s12864-017-3797-0>.
40. Huang, D.W., Sherman, B.T., and Lempicki, R.A., Bioinformatics enrichment tools: paths toward the comprehensive functional analysis of large gene lists. *Nucleic Acids Research*, 2008. **37**(1): p. 1-13.<https://doi.org/10.1093/nar/gkn923>.
41. Ashburner, M., Ball, C.A., Blake, J.A., Botstein, D., *et al.*, Gene Ontology: tool for the unification of biology. *Nature Genetics*, 2000. **25**(1): p. 25-29.<https://doi.org/10.1038/75556>.
42. QIAGEN. QIAGEN Ingenuity Pathway Analysis (IPA). 2020 [Last accessed 2020 July]; Available from: <https://digitalinsights.qiagen.com/products-overview/discovery-insights-portfolio/analysis-and-visualization/qiagen-ipa/>.
43. Mi, H., Muruganujan, A., and Thomas, P.D., PANTHER in 2013: modeling the evolution of gene function, and other gene attributes, in the context of phylogenetic trees. *Nucleic Acids Research*, 2012. **41**(D1): p. D377-D386.<https://doi.org/10.1093/nar/gks1118>.
44. Kamburov, A., Wierling, C., Lehrach, H., and Herwig, R., ConsensusPathDB—a database for integrating human functional interaction networks. *Nucleic Acids Research*, 2008. **37**(suppl\_1): p. D623-D628.<https://doi.org/10.1093/nar/gkn698>.
45. Kamburov, A., Pentchev, K., Galicka, H., Wierling, C., *et al.*, ConsensusPathDB: toward a more complete picture of cell biology. *Nucleic Acids Research*, 2010. **39**(suppl\_1): p. D712-D717.<https://doi.org/10.1093/nar/gkq1156>.
46. Janky, R.s., Verfaillie, A., Imrichová, H., Van de Sande, B., *et al.*, iRegulon: From a Gene List to a Gene Regulatory Network Using Large Motif and Track Collections. *PLOS Computational Biology*, 2014. **10**(7): p. e1003731.<https://doi.org/10.1371/journal.pcbi.1003731>.
47. Huang da, W., Sherman, B.T., and Lempicki, R.A., Systematic and integrative analysis of large gene lists using DAVID bioinformatics resources. *Nature Protocols*, 2009. **4**(1): p. 44-57.<https://doi.org/10.1038/nprot.2008.211>.

48. Raudvere, U., Kolberg, L., Kuzmin, I., Arak, T., *et al.*, g:Profiler: a web server for functional enrichment analysis and conversions of gene lists (2019 update). *Nucleic Acids Research*, 2019. **47**(W1): p. W191-W198.<https://doi.org/10.1093/nar/gkz369>.
49. Holdorf, A.D., Higgins, D.P., Hart, A.C., Boag, P.R., *et al.*, WormCat: An Online Tool for Annotation and Visualization of *Caenorhabditis elegans* Genome-Scale Data. *Genetics*, 2020. **214**(2): p. 279-294.<https://doi.org/10.1534/genetics.119.302919>.
50. Angeles-Albores, D., N. Lee, R.Y., Chan, J., and Sternberg, P.W., Tissue enrichment analysis for *C. elegans* genomics. *BMC Bioinformatics*, 2016. **17**(1): p. 366.<https://doi.org/10.1186/s12859-016-1229-9>.
51. Angeles-Albores, D., Lee, R.Y.N., Chan, J., and Sternberg, P.W., Two new functions in the WormBase Enrichment Suite. *microPublication Biology*, 2018.<https://doi.org/10.17912/W2502N>.
52. Coordinators, N.R., Database resources of the National Center for Biotechnology Information. *Nucleic Acids Research*, 2012. **41**(D1): p. D8-D20.<https://doi.org/10.1093/nar/gks1189>.
53. Kinsella, R.J., Kähäri, A., Haider, S., Zamora, J., *et al.*, Ensembl BioMarts: a hub for data retrieval across taxonomic space. *Database*, 2011. **2011**.<https://doi.org/10.1093/database/bar030>.
54. Kim, W., Underwood, R.S., Greenwald, I., and Shaye, D.D., OrthoList 2: A New Comparative Genomic Analysis of Human and *Caenorhabditis elegans* Genes. *Genetics*, 2018. **210**(2): p. 445-461.<https://doi.org/10.1534/genetics.118.301307>
55. Hong, G., Zhang, W., Li, H., Shen, X., *et al.*, Separate enrichment analysis of pathways for up- and downregulated genes. *Journal of The Royal Society Interface* 2014. **11**(92): p. 20130950.<https://doi.org/10.1098/rsif.2013.0950>.
56. Vogel, C., de Sousa Abreu, R., Ko, D., Le, S.-Y., *et al.*, Sequence signatures and mRNA concentration can explain two-thirds of protein abundance variation in a human cell line. *Molecular Systems Biology*, 2010. **6**(1): p. 400.<https://doi.org/10.1038/msb.2010.59>.
57. Brawand, D., Soumillon, M., Necsulea, A., Julien, P., *et al.*, The evolution of gene expression levels in mammalian organs. *Nature*, 2011. **478**(7369): p. 343-348.<https://doi.org/10.1038/nature10532>.
58. Sandberg, R., Yasuda, R., Pankratz, D.G., Carter, T.A., *et al.*, Regional and strain-specific gene expression mapping in the adult mouse brain. *Proceedings of the National Academy of Sciences*, 2000. **97**(20): p. 11038-11043.<https://doi.org/10.1073/pnas.97.20.11038>.
59. Stark, R., Grzelak, M., and Hadfield, J., RNA sequencing: the teenage years. *Nature Reviews Genetics*, 2019. **20**(11): p. 631-656.<https://doi.org/10.1038/s41576-019-0150-2>.
60. Ouchi, Y., Yoshikawa, E., Futatsubashi, M., Yagi, S., *et al.*, Altered Brain Serotonin Transporter and Associated Glucose Metabolism in Alzheimer Disease. *Journal of Nuclear Medicine*, 2009. **50**(8): p. 1260-1266.<https://doi.org/10.2967/jnumed.109.063008>.

61. Doder, M., Rabiner, E.A., Turjanski, N., Lees, A.J., *et al.*, Tremor in Parkinson's disease and serotonergic dysfunction. *Neurology*, 2003. **60**(4): p. 601-605.<https://doi.org/10.1212/01.Wnl.0000031424.51127.2b>.
62. Jahanshahi, A., Vlamings, R., van Roon-Mom, W.M.C., Faull, R.L.M., *et al.*, Changes in brainstem serotonergic and dopaminergic cell populations in experimental and clinical Huntington's disease. *Neuroscience*, 2013. **238**: p. 71-81.<https://doi.org/10.1016/j.neuroscience.2013.01.071>.
63. Trouillas, P., The Cerebellar Serotonergic System and its Possible Involvement in Cerebellar Ataxia. *Canadian Journal of Neurological Sciences / Journal Canadien des Sciences Neurologiques*, 1993. **20**(S3): p. S78-S82.<https://doi.org/10.1017/S0317167100048575>.
64. Jacobs, B.L. and Fornal, C.A., Serotonin and motor activity. *Current Opinion in Neurobiology*, 1997. **7**(6): p. 820-825.[https://doi.org/10.1016/S0959-4388\(97\)80141-9](https://doi.org/10.1016/S0959-4388(97)80141-9).
65. Schmidt, B.J. and Jordan, L.M., The role of serotonin in reflex modulation and locomotor rhythm production in the mammalian spinal cord. *Brain Research Bulletin*, 2000. **53**(5): p. 689-710.[https://doi.org/10.1016/S0361-9230\(00\)00402-0](https://doi.org/10.1016/S0361-9230(00)00402-0).
66. Kawashima, T., The role of the serotonergic system in motor control. *Neuroscience Research*, 2018. **129**: p. 32-39.<https://doi.org/10.1016/j.neures.2017.07.005>.
67. Lou, J.-S., Goldfarb, L., McShane, L., Gatev, P., *et al.*, Use of Buspirone for Treatment of Cerebellar Ataxia: An Open-Label Study. *Archives of Neurology*, 1995. **52**(10): p. 982-988.<https://doi.org/10.1001/archneur.1995.00540340074015>.
68. Yang, Z.-h., Shi, C.-h., Zhou, L.-n., Li, Y.-s., *et al.*, Metabolic Profiling Reveals Biochemical Pathways and Potential Biomarkers of Spinocerebellar Ataxia 3. *Frontiers in Molecular Neuroscience*, 2019. **12**(159).<https://doi.org/10.3389/fnmol.2019.00159>.
69. Gershon, M.D. and Tack, J., The Serotonin Signaling System: From Basic Understanding To Drug Development for Functional GI Disorders. *Gastroenterology*, 2007. **132**(1): p. 397-414.<https://doi.org/10.1053/j.gastro.2006.11.002>.
70. Pardridge, W.M., Brain metabolism: a perspective from the blood-brain barrier. *Physiological Reviews*, 1983. **63**(4): p. 1481-1535.<https://doi.org/10.1152/physrev.1983.63.4.1481>.
71. Boado, R.J., Li, J.Y., Nagaya, M., Zhang, C., *et al.*, Selective expression of the large neutral amino acid transporter at the blood-brain barrier. *Proceedings of the National Academy of Sciences*, 1999. **96**(21): p. 12079-12084.<https://doi.org/10.1073/pnas.96.21.12079>.
72. Kayser, V., Elfassi, I.E., Aubel, B., Melfort, M., *et al.*, Mechanical, thermal and formalin-induced nociception is differentially altered in 5-HT<sub>1A</sub><sup>-/-</sup>, 5-HT<sub>1B</sub><sup>-/-</sup>, 5-HT<sub>2A</sub><sup>-/-</sup>, 5-HT<sub>3A</sub><sup>-/-</sup> and 5-HTT<sup>-/-</sup> knock-out male mice. *PAIN*, 2007. **130**(3): p. 235-248.<https://doi.org/10.1016/j.pain.2006.11.015>.
73. Friedman, J.H., Machado-Joseph disease/spinocerebellar ataxia 3 responsive to buspirone. *Movement Disorders*, 1997. **12**(4): p. 613-614.<https://doi.org/10.1002/mds.870120426>.



74. Takei, A., Fukazawa, T., Hamada, T., Sohma, H., *et al.*, Effects of Tansospirone on “5-HT1A Receptor-Associated Symptoms” in Patients with Machado-Joseph Disease: An Open-Label Study. *Clinical Neuropharmacology*, 2004. **27**(1): p. 9-13.<https://doi.org/10.1097/00002826-200401000-00005>.
75. Takei, A., Honma, S., Kawashima, A., Yabe, I., *et al.*, Beneficial effects of tandospirone on ataxia of a patient with Machado-Joseph disease. *Psychiatry and Clinical Neurosciences*, 2002. **56**(2): p. 181-185.<https://doi.org/10.1046/j.1440-1819.2002.00952.x>.
76. Cecchin, C.R., Pires, A.P., Rieder, C.R., Monte, T.L., *et al.*, Depressive Symptoms in Machado-Joseph Disease (SCA3) Patients and Their Relatives. *Public Health Genomics*, 2007. **10**(1): p. 19-26.<https://doi.org/10.1159/000096276>.
77. Ma, J., Gao, Y., Jiang, L., Chao, F.-I., *et al.*, Fluoxetine attenuates the impairment of spatial learning ability and prevents neuron loss in middle-aged APP<sup>swe</sup>/PSEN1<sup>dE9</sup> double transgenic Alzheimer’s disease mice. *Oncotarget*, 2017. **8**(17).<https://doi.org/10.18632/oncotarget.15398>.
78. Zhang, Q., Yang, C., Liu, T., Liu, L., *et al.*, Citalopram restores short-term memory deficit and non-cognitive behaviors in APP/PS1 mice while halting the advance of Alzheimer's disease-like pathology. *Neuropharmacology*, 2018. **131**: p. 475-486.<https://doi.org/10.1016/j.neuropharm.2017.12.021>.
79. Sheline, Y.I., West, T., Yarasheski, K., Swarm, R., *et al.*, An Antidepressant Decreases CSF A $\beta$  Production in Healthy Individuals and in Transgenic AD Mice. *Science Translational Medicine*, 2014. **6**(236): p. 236re4-236re4.<https://doi.org/10.1126/scitranslmed.3008169>.
80. Chung, Y.C., Kim, S.R., Park, J.-Y., Chung, E.S., *et al.*, Fluoxetine prevents MPTP-induced loss of dopaminergic neurons by inhibiting microglial activation. *Neuropharmacology*, 2011. **60**(6): p. 963-974.<https://doi.org/10.1016/j.neuropharm.2011.01.043>.
81. Duan, W., Guo, Z., Jiang, H., Ladenheim, B., *et al.*, Paroxetine retards disease onset and progression in Huntington mutant mice. *Annals of Neurology*, 2004. **55**(4): p. 590-594.<https://doi.org/10.1002/ana.20075>.
82. Duan, W., Peng, Q., Masuda, N., Ford, E., *et al.*, Sertraline slows disease progression and increases neurogenesis in N171-82Q mouse model of Huntington's disease. *Neurobiology of Disease*, 2008. **30**(3): p. 312-322.<https://doi.org/10.1016/j.nbd.2008.01.015>.
83. Ng, L., Bernard, A., Lau, C., Overly, C.C., *et al.*, An anatomic gene expression atlas of the adult mouse brain. *Nature Neuroscience*, 2009. **12**(3): p. 356-362.<https://doi.org/10.1038/nn.2281>.
84. Allen Institute for Brain Science. Allen Mouse Brain Atlas - Htr1a ISH experiment. ©2004 [Last accessed 2020; Available from: <http://mouse.brain-map.org/experiment/show/79394355>].
85. Allen Institute for Brain Science. Allen Mouse Brain Atlas - Htr2a ISH experiment. ©2004 [Last accessed 2020; Available from: <http://mouse.brain-map.org/experiment/show/81671344>].

86. Vilaró, M.T., Cortés, R., Mengod, G., and Hoyer, D., Chapter 6 - Distribution of 5-HT receptors in the central nervous system: an update, in *Handbook of Behavioral Neuroscience*, C.P. Müller and K.A. Cunningham, Editors. 2020, Elsevier. p. 121-146.<https://doi.org/10.1016/B978-0-444-64125-0.00006-2>.
87. Sakamoto, K., Karelina, K., and Obrietan, K., CREB: a multifaceted regulator of neuronal plasticity and protection. *Journal of Neurochemistry*, 2011. **116**(1): p. 1-9.<https://doi.org/10.1111/j.1471-4159.2010.07080.x>.
88. Nibuya, M., Nestler, E., and Duman, R., Chronic antidepressant administration increases the expression of cAMP response element binding protein (CREB) in rat hippocampus. *The Journal of Neuroscience*, 1996. **16**(7): p. 2365-2372.<https://doi.org/10.1523/JNEUROSCI.16-07-02365.1996>
89. Tiraboschi, E., Tardito, D., Kasahara, J., Moraschi, S., *et al.*, Selective Phosphorylation of Nuclear CREB by Fluoxetine is Linked to Activation of CaM Kinase IV and MAP Kinase Cascades. *Neuropsychopharmacology*, 2004. **29**(10): p. 1831-1840.<https://doi.org/10.1038/sj.npp.1300488>.
90. Toonen, L.J.A., Overzier, M., Evers, M.M., Leon, L.G., *et al.*, Transcriptional profiling and biomarker identification reveal tissue specific effects of expanded ataxin-3 in a spinocerebellar ataxia type 3 mouse model. *Molecular Neurodegeneration*, 2018. **13**(1): p. 31.<https://doi.org/10.1186/s13024-018-0261-9>.
91. Costa, M.d.C., Ashraf, N.S., Fischer, S., Yang, Y., *et al.*, Unbiased screen identifies aripiprazole as a modulator of abundance of the polyglutamine disease protein, ataxin-3. *Brain*, 2016. **139**(11): p. 2891-2908.<https://doi.org/10.1093/brain/aww228>.
92. Pereira-Sousa, J., Ferreira-Lomba, B., Bellver-Sanchis, A., Vilasboas-Campos, D., *et al.*, Identification of the 5-HT<sub>1A</sub> serotonin receptor as a novel therapeutic target in a *C. elegans* model of Machado-Joseph disease. *Neurobiology of Disease*, 2021. **152**: p. 105278.<https://doi.org/10.1016/j.nbd.2021.105278>.
93. Cemal, C.K., Carroll, C.J., Lawrence, L., Lowrie, M.B., *et al.*, YAC transgenic mice carrying pathological alleles of the *MJD1* locus exhibit a mild and slowly progressive cerebellar deficit. *Human Molecular Genetics*, 2002. **11**(9): p. 1075-1094.<https://doi.org/10.1093/hmg/11.9.1075>.
94. Zschocke, J., Zimmermann, N., Berning, B., Ganal, V., *et al.*, Antidepressant Drugs Diversely Affect Autophagy Pathways in Astrocytes and Neurons—Dissociation from Cholesterol Homeostasis. *Neuropsychopharmacology*, 2011. **36**(8): p. 1754-1768.<https://doi.org/10.1038/npp.2011.57>.
95. Berendzen, K.M., Durieux, J., Shao, L.-W., Tian, Y., *et al.*, Neuroendocrine Coordination of Mitochondrial Stress Signaling and Proteostasis. *Cell*, 2016. **166**(6): p. 1553-1563.e10.<https://doi.org/10.1016/j.cell.2016.08.042>.
96. de Assis, A.M., Saute, J.A.M., Longoni, A., Haas, C.B., *et al.*, Peripheral Oxidative Stress Biomarkers in Spinocerebellar Ataxia Type 3/Machado–Joseph Disease. *Frontiers in Neurology*, 2017. **8**(485).<https://doi.org/10.3389/fneur.2017.00485>.



97. Khanzode, S.D., Dakhale, G.N., Khanzode, S.S., Saoji, A., *et al.*, Oxidative damage and major depression: the potential antioxidant action of selective serotonin re-uptake inhibitors. *Redox Report*, 2003. **8**(6): p. 365-370.<https://doi.org/10.1179/135100003225003393>.
98. Hyttel, J., Pharmacological characterization of selective serotonin reuptake inhibitors (SSRIs). *International Clinical Psychopharmacology*, 1994. **9**: p. 19-26.<https://doi.org/10.1097/00004850-199403001-00004>.
99. Jaako-Movits, K., Zharkovsky, T., Pedersen, M., and Zharkovsky, A., Decreased Hippocampal Neurogenesis Following Olfactory Bulbectomy is Reversed by Repeated Citalopram Administration. *Cellular and Molecular Neurobiology*, 2006. **26**(7): p. 1557.<https://doi.org/10.1007/s10571-006-9090-4>.
100. Jurkowski, M.P., Bettio, L., K. Woo, E., Patten, A., *et al.*, Beyond the Hippocampus and the SVZ: Adult Neurogenesis Throughout the Brain. *Frontiers in Cellular Neuroscience*, 2020. **14**(293).<https://doi.org/10.3389/fncel.2020.576444>.
101. Becker, G., Streichenberger, N., Billard, T., Newman-Tancredi, A., *et al.*, A Postmortem Study to Compare Agonist and Antagonist 5-HT<sub>1A</sub> Receptor-binding Sites in Alzheimer's Disease. *CNS Neuroscience & Therapeutics*, 2014. **20**(10): p. 930-934.<https://doi.org/10.1111/cns.12306>.
102. Vidal, B., Sebti, J., Verdurand, M., Fieux, S., *et al.*, Agonist and antagonist bind differently to 5-HT<sub>1A</sub> receptors during Alzheimer's disease: A *post-mortem* study with PET radiopharmaceuticals. *Neuropharmacology*, 2016. **109**: p. 88-95.<https://doi.org/10.1016/j.neuropharm.2016.05.009>.

## **Annexes**

---

## **Annex I: Ethical approval for the use of animal models in research by the University of Minho (Parecer da Subcomissão de Ética para as Ciências da Vida e da Saúde)**



Universidade do Minho

SECVS

### **Subcomissão de Ética para as Ciências da Vida e da Saúde**

Identificação do documento: SECVS 120/2014

Título do Projeto: *Desenvolvimento de estratégias terapêuticas para a doença de Machado-Joseph*

Investigador Principal: Patrícia Maciel

Investigador responsável pela experimentação animal: Patrícia Maciel

Subunidade orgânica: Instituto de Investigação em Ciências da Vida e da Saúde (ICVS)

### **PARECER**

A Subcomissão de Ética para as Ciências da Vida e da Saúde (SECVS) analisou o processo relativo ao projeto de investigação com recurso a modelos animais intitulado *Desenvolvimento de estratégias terapêuticas para a doença de Machado-Joseph*.

Os documentos apresentados revelam que o projeto obedece aos requisitos exigidos para as boas práticas na experimentação com recurso à utilização de modelos animais, considerando a aplicação dos 3 Rs de Russel e Burch e a aplicação de limites críticos de sofrimento - *humane endpoints*.

Face ao exposto, a SECVS não tem nada a opor à realização do projeto, emitindo o seu parecer favorável.

A SECVS salienta ainda que:

- Todas as pessoas envolvidas no projeto de experimentação animal devem ter formação adequada e a correspondente creditação legal atribuída pela Direção Geral de Alimentação e Veterinária (DGAV);
- A aprovação legal de projetos de investigação/ experimentação animal é feita pela DGAV a quem deverá submeter o respetivo formulário e o resumo não-técnico do projeto.

Braga, 11 de setembro de 2014.

A Presidente

(Maria Cecília de Lemos Pinto Estrela Leão)